HUMAN MACHINE INTERFACE-BASED NEUROMODULATION SOLUTIONS FOR NEUROREHABILITATION

EDITED BY: Jing Wang, Haoyong Yu and Jinhua Zhang
PUBLISHED IN: Frontiers in Neuroscience

frontiers Research Topics

ISSN 1664-8714
ISBN 978-2-83250-172-6
DOI 10.3389/978-2-83250-172-6

About Frontiers

Frontiers is more than just an open-access publisher of scholarly articles: it is a pioneering approach to the world of academia, radically improving the way scholarly research is managed. The grand vision of Frontiers is a world where all people have an equal opportunity to seek, share and generate knowledge. Frontiers provides immediate and permanent online open access to all its publications, but this alone is not enough to realize our grand goals.

Frontiers Journal Series

The Frontiers Journal Series is a multi-tier and interdisciplinary set of open-access, online journals, promising a paradigm shift from the current review, selection and dissemination processes in academic publishing. All Frontiers journals are driven by researchers for researchers; therefore, they constitute a service to the scholarly community. At the same time, the Frontiers Journal Series operates on a revolutionary invention, the tiered publishing system, initially addressing specific communities of scholars, and gradually climbing up to broader public understanding, thus serving the interests of the lay society, too.

Dedication to Quality

Each Frontiers article is a landmark of the highest quality, thanks to genuinely collaborative interactions between authors and review editors, who include some of the world's best academicians. Research must be certified by peers before entering a stream of knowledge that may eventually reach the public - and shape society; therefore, Frontiers only applies the most rigorous and unbiased reviews.
Frontiers revolutionizes research publishing by freely delivering the most outstanding research, evaluated with no bias from both the academic and social point of view. By applying the most advanced information technologies, Frontiers is catapulting scholarly publishing into a new generation.

What are Frontiers Research Topics?

Frontiers Research Topics are very popular trademarks of the Frontiers Journals Series: they are collections of at least ten articles, all centered on a particular subject. With their unique mix of varied contributions from Original Research to Review Articles, Frontiers Research Topics unify the most influential researchers, the latest key findings and historical advances in a hot research area! Find out more on how to host your own Frontiers Research Topic or contribute to one as an author by contacting the Frontiers Editorial Office: frontiersin.org/about/contact

HUMAN MACHINE INTERFACE-BASED NEUROMODULATION SOLUTIONS FOR NEUROREHABILITATION

Topic Editors:
Jing Wang, Xi'an Jiaotong University, China
Haoyong Yu, National University of Singapore, Singapore
Jinhua Zhang, Xi'an Jiaotong University, China

Citation: Wang, J., Yu, H., Zhang, J., eds. (2022). Human Machine Interface-Based Neuromodulation Solutions for Neurorehabilitation. Lausanne: Frontiers Media SA. doi: 10.3389/978-2-83250-172-6

Table of Contents

frontiers | Frontiers in Neuroscience

TYPE Editorial
PUBLISHED 25 August 2022
DOI 10.3389/fnins.2022.987455

OPEN ACCESS

EDITED AND REVIEWED BY
Michela Chiappalone,
University of Genoa, Italy

*CORRESPONDENCE
Jing Wang
wangpele@gmail.com
Jinhua Zhang
jjshua@mail.xjtu.edu.cn
Haoyong Yu
bieyhy@nus.edu.sg
Bin Shi
sb902580@stu.xjtu.edu.cn

SPECIALTY SECTION
This article was submitted to Neuroprosthetics, a section of the journal Frontiers in Neuroscience

RECEIVED 06 July 2022
ACCEPTED 29 July 2022
PUBLISHED 25 August 2022

CITATION
Wang J, Zhang J, Yu H and Shi B (2022) Editorial: Human machine interface-based neuromodulation solutions for neurorehabilitation. *Front. Neurosci.* 16:987455. doi: 10.3389/fnins.2022.987455

Editorial: Human machine interface-based neuromodulation solutions for neurorehabilitation

Jing Wang[1,2]*, Jinhua Zhang[1,2]*, Haoyong Yu[3]* and Bin Shi[1,2]*

[1]School of Mechanical Engineering, Xi'an Jiaotong University, Xi'an, China, [2]Shaanxi Key Laboratory of Intelligent Robots, Xi'an Jiaotong University, Xi'an, China, [3]Department of Biomedical Engineering, National University of Singapore, Singapore, Singapore

KEYWORDS

transcranial magnetic stimulation (TMS), mechanism, neurorehabilitation, brain-computer interface (BCI), intermittent theta burst stimulation (iTBS)

Editorial on the Research Topic
Human machine interface-based neuromodulation solutions for neurorehabilitation

Neurorehabilitation is a complex medical process which aims to aid recovery from a nervous system injury, and to minimize and/or compensate for any functional alterations resulting from nervous system injury disease. These diseases include stroke, spinal cord injury, cerebral palsy, Parkinson's disease, brain injury, and multiple sclerosis. Human-machine interface is a potential neuromodulation scheme for neurorehabilitation. To provide a platform for sharing the latest research findings in human machine interface-based neuromodulation for neurorehabilitation, we organized this Research Topic, in which 18 manuscripts have been accepted for publication, including 12 original research articles, four reviews, and two clinical trials. These articles stated that transcranial magnetic stimulation (TMS), brain–computer interface (BCI) and robots are the current advanced intervention techniques for the treatment of these diseases. In addition, the corresponding neural mechanisms were studied by healthy subjects using these intervention techniques. To a certain extent, these manuscripts have expanded the current understanding of diagnosis, treatment, and prognosis of such nervous system injury diseases.

According to different TMS stimulation pulses, TMS can be divided into three stimulation modes: single TMS (sTMS), double pulse TMS (pTMS), and repetitive TMS (rTMS). A study by Cai et al. explored that brain network activity modulates corticospinal excitability in 32 healthy individuals by recording electroencephalography (EEG) and single TMS measurements. The results suggested that corticospinal excitability can be modulated by the power spectrum of sensorimotor regions and the overall efficiency of functional networks. Thus, EEG network analysis can provide a useful complement to study the relationship between EEG oscillations and corticospinal excitability.

In addition to sTMS, rTMS technology is also widely used in the treatment of stroke, cerebral palsy, and multiple system atrophy (MSA). In studies focusing on recovery of dysphagia post-stroke, Yang, Cao, et al. and Xie Y.-l. et al. systemically evaluated the effect and safety of rTMS on recovery of dysphagia after stroke. They suggested that rTMS improved overall swallowing function and activity of daily living ability and reduced aspiration in post-stroke patients. Moreover, to explore the effect of 5 hz rTMS combined with wrist-ankle acupuncture on improving spasticity and motor function in children with spastic cerebral palsy by measuring electrophysiological parameters and behavior, 25 children with spastic cerebral palsy were enrolled in a single blind and randomized controlled trial. The authors found that wrist-ankle acupuncture combined with 5 Hz rTMS was the best for improving gross motor function and enhancing the conductivity of the corticospinal tract in children with cerebral palsy, but it could not highlight its clinical advantages in improving spasticity. Furthermore, executive dysfunction widely exists in a variety of neuropsychiatric diseases, and is closely related to the decline of daily living ability and function (Li J. et al.). Another study by Liu S. et al. analyzed the effect of low-frequency rTMS on executive function and its neural mechanism by using event-related potential (ERP). Thirty-one healthy subjects were randomly assigned to receive rTMS stimulations (1 Hz rTMS or sham rTMS) to the left dorsolateral prefrontal cortex (DLPFC) twice. They suggested that low-frequency rTMS of the left DLPFC can cause decline of cognitive flexibility in executive function, resulting in the change of N2 amplitude and the decrease of P3 and late positive component (LPC) components during task switching, which is of positive significance for the evaluation and treatment of executive function. In addition, MSA refers to a progressive neurodegenerative disease characterized by autonomic dysfunction, parkinsonism, cerebellar ataxia, as well as cognitive deficits. Zhang et al. systemically assessed the effects of Non-invasive brain stimulation (NIBS) on two subtypes of MSA: parkinsonian-type MSA (MSA-P) and cerebellar-type MSA (MSA-C). They found that NIBS can serve as a useful neurorehabilitation strategy to improve motor and cognitive function in MSA-P and MSA-C patients. However, they suggested that further high-quality articles are required to examine the underlying mechanisms and standardized protocol of rTMS as well as its long-term effect. Meanwhile, the effects of other NIBS subtypes on MSA still need further investigation.

Intermittent theta burst stimulation (iTBS) is a special form of repetitive transcranial magnetic stimulation (rTMS), which effectively increases cortical excitability and has been widely used as a neural modulation approach in stroke rehabilitation. A study by Ding et al. investigated the effects of iTBS on functional brain network through the resting-state EEG of stroke survivors. Thirty stroke survivors with upper limb motor dysfunction were studied. The authors provide evidence that iTBS modulates brain network functioning in stroke survivors. The acute increase in interhemispheric functional connectivity and overall efficiency after iTBS suggests that iTBS has the potential to normalize brain network function after stroke, which can be used for stroke rehabilitation. Furthermore, another study by Xie Y.-J. et al. explored the efficacy of cerebellar iTBS on the walking function of stroke patients. Thirty-six survivors with walking dysfunction who had suffered their first unilateral stroke were recruited. The authors found that applying iTBS over the contralesional cerebellum paired with physical therapy could improve walking performance in patients after stroke, suggesting that cerebellar iTBS intervention might be a non-invasive strategy to improve walking function for stroke survivors. Moreover, a study of Diao et al. investigated whether the individual level of GABA or NMDA receptor-mediated activity before stimulation is correlated with the after-effect in cortical excitability induced by iTBS. They found that that $GABA_A$ receptor-mediated activity measured before stimulation is negatively correlated with the after-effect of cortical excitability induced by iTBS. The short-interval intracortical inhibitory (SICI) might be a good predictor of iTBS-induced LTP-like plasticity for a period lasting 15 min following stimulation.

A brain-computer interface (BCI) is a real-time communication system that connects the brain and external devices. The combination of BCI technology and hand rehabilitation robots is often used for motor function rehabilitation after stroke. In addition, some studies have explored cortical activation and neuroplasticity mechanisms in healthy subjects by BCI technology. Yang, Zhang, et al. provided medical evidence-based support for BCI in the treatment of upper limb dysfunction after stroke by conducting a meta-analysis of relevant clinical studies. A total of 13 randomized controlled trials involving 258 subjects were retrieved. The authors demonstrated that BCI training can effectively promote the recovery of upper limb motor function in stroke survivors, and the effect size was moderate. Moreover, Liu L. et al. evaluated the efficacy of BCI training in chronic stroke patients with moderate or severe paresis. Eighteen hospitalized chronic stroke patients with moderate or severe motor deficits participated. They demonstrated that BCI-based rehabilitation can effectively intervene in the motor performance of post-stroke patients with moderate or severe upper limb paralysis and is a potential strategy for stroke neurorehabilitation. The results shown that the functional connectivity between ipsilesional primary motor cortex (M_1) and frontal cortex might be enhanced after BCI training. Furthermore, Li X. et al. studied the effectiveness of a post-stroke hand rehabilitation system, which is the sensorimotor rhythm (SMR)-based BCI with audio-cue, motor observation and multisensory feedback. Twenty-four stroke survivors with severe upper limb motor deficits were studied. The authors found that the hand rehabilitation system combined with conventional therapy may promote long-lasting upper limb motor improvement. In addition to BCI training

for stroke subjects, Lin et al. analyzed effects of frequency of motor imagery (MI) BCI training on the central nervous system. Sixteen young healthy subjects were randomly assigned to a high frequency group with performed MI-BCI training once per day and low frequency group which performed once every other day. The results revealed that compared to the low frequency group, the high frequency group presents more cortical activation and better BCI performance. Meanwhile, the authors suggested that 30 min per day for five consecutive days may be the lowest effective dose of MI-BCI training to activate modulation of cortical activation in healthy subjects, which can be extrapolated in the future to stroke patients. Similarly, another study by Qiu et al. used synchronous functional near infrared spectroscopy (fNIRS) to analyze whether mirror visual feedback (MVF) and a soft robotic bilateral hand rehabilitation system have synergistic effects on cortical activation. Twenty healthy subjects were recruited to perform four different visual feedback tasks with simultaneous fNIRS monitoring. Four different visual feedback tasks include the real visual feedback (RVF) task, mirror visual feedback (MVF) task, bilateral robotic movement (BRM) task, and MVF + BRM task. The results found that the synergistic gain effect on cortical activation from mirror visual feedback combined with a soft robotic bilateral hand rehabilitation system for the first time, which could be utilized to guide the clinical application and the future studies. Furthermore, Liu Y. et al. conducted 4-week BCI-controlled supernumerary robotic finger (SRF) training in 10 right-handed subjects to study the neuroplasticity mechanisms. The results shown that cerebellar compensatory and inhibitory mechanisms exist during BCI-controlled SRF training, and this result provides evidence for the neuroplasticity mechanism brought about by BCI-controlled motor-augmentation devices.

Muscle synergies have been largely used in many application fields, including motor control studies, prosthesis control, movement classification, rehabilitation, and clinical studies. Zhao et al. analyzed the performance of five methods for the extraction of spatial muscle synergy, namely, principal component analysis (PCA), independent component analysis (ICA), factor analysis (FA), non-negative matrix factorization (NMF), and AEs using simulated data and a publicly available database. The results showed that the performance of synergy extraction methods was affected by the noise and the number of channels, and classification algorithms were sensitive to the extraction methods. Moreover, the effect and mechanism of underlying enriched rehabilitation as a potentially effective strategy to improve gait and cognitive performance in patients with early Parkinson's disease (PD) were explored (Wang et al.). The enriched rehabilitation represents that the enriched sensorimotor environmental stimulation paired with different types of sensory and motor exercises was applied to improve gait disorder and cognitive function in PD. The authors found that enriched rehabilitation could serve as a potentially effective therapy for early-stage PD for improving gait performance and cognitive function. The underlying mechanism based on functional magnetic resonance imaging (fMRI) involved strengthened resting-state functional connectivity (RSFC) between the left dorsolateral prefrontal cortex (DLPFC) and other brain regions.

After the analysis of 18 manuscripts in this Research Topic, we can draw the following conclusions. The rTMS could improve overall swallowing function and activity of daily living ability in post-stroke patients. Furthermore, rTMS can serve as a useful neurorehabilitation strategy to improve motor and cognitive function in MSA-P and MSA-C patients. However, further studies are performed to examine the underlying mechanisms and standardized protocol of rTMS as well as its long-term effect. The iTBS has the potential to normalize brain network function after stroke and also might be a noninvasive strategy to improve walking function for stroke survivors. The BCI-based rehabilitation can effectively intervene in the motor performance of post-stroke patients with moderate or severe upper limb paralysis and is a potential strategy for stroke neurorehabilitation.

Author contributions

BS was responsible for drafting the manuscript. JW revised the manuscript. JZ and HY analyzed and discussed the results. All authors read and approved the final manuscript.

Acknowledgments

We thank the authors for their valuable work for this Research Topic and the reviewers for their constructive comments. We are also grateful to the editorial board for approving this topic and we hope this issue will promote the research on Human machine interface-based neuromodulation solutions for neurorehabilitation.

Conflict of interest

The authors declare that the research was conducted in the absence of any commercial or financial relationships that could be construed as a potential conflict of interest.

Publisher's note

frontiers in Neuroscience

ORIGINAL RESEARCH
published: 23 August 2021
doi: 10.3389/fnins.2021.722231

The Corticospinal Excitability Can Be Predicted by Spontaneous Electroencephalography Oscillations

Guiyuan Cai[1,2†], Manfeng Wu[1,2†], Qian Ding[1,3†], Tuo Lin[1,3], Wanqi Li[1,3], Yinghua Jing[1,3], Hongying Chen[1,2], Huiting Cai[4], Tifei Yuan[4,5,6], Guangqing Xu[7]* and Yue Lan[1,3]**

[1] Department of Rehabilitation Medicine, The Second Affiliated Hospital of South China University of Technology, Guangzhou, China, [2] Department of Rehabilitation Medicine, School of Medicine, South China University of Technology, Guangzhou, China, [3] Department of Rehabilitation Medicine, Guangzhou First People's Hospital, Guangzhou, China, [4] Shanghai Key Laboratory of Psychotic Disorders, Shanghai Mental Health Center, Shanghai Jiao Tong University School of Medicine, Shanghai, China, [5] Co-innovation Center of Neuroregeneration, Nantong University, Nantong, China, [6] Translational Research Institute of Brain and Brain-Like Intelligence, Shanghai Fourth People's Hospital Affiliated to Tongji University School of Medicine, Shanghai, China, [7] Department of Rehabilitation Medicine, Guangdong Provincial People's Hospital, Guangdong Academy of Medical Sciences, Guangzhou, China

OPEN ACCESS

Edited by:
Jing Wang,
Xi'an Jiaotong University, China

Reviewed by:
Bin Hu,
University of Calgary, Canada
Sean K. Meehan,
University of Waterloo, Canada
Xiquan Hu,
Third Affiliated Hospital of Sun Yat-sen University, China

***Correspondence:**
Tifei Yuan
ytf0707@126.com
Guangqing Xu
guangchingx@163.com
Yue Lan
bluemooning@163.com

† These authors have contributed equally to this work

Specialty section:
This article was submitted to Neuroprosthetics, a section of the journal Frontiers in Neuroscience

Received: *08 June 2021*
Accepted: *31 July 2021*
Published: *23 August 2021*

Citation:
Cai G, Wu M, Ding Q, Lin T, Li W, Jing Y, Chen H, Cai H, Yuan T, Xu G and Lan Y (2021) The Corticospinal Excitability Can Be Predicted by Spontaneous Electroencephalography Oscillations. Front. Neurosci. 15:722231. doi: 10.3389/fnins.2021.722231

Transcranial magnetic stimulation (TMS) has a wide range of clinical applications, and there is growing interest in neural oscillations and corticospinal excitability determined by TMS. Previous studies have shown that corticospinal excitability is influenced by fluctuations of brain oscillations in the sensorimotor region, but it is unclear whether brain network activity modulates corticospinal excitability. Here, we addressed this question by recording electroencephalography (EEG) and TMS measurements in 32 healthy individuals. The resting motor threshold (RMT) and active motor threshold (AMT) were determined as markers of corticospinal excitability. The least absolute shrinkage and selection operator (LASSO) was used to identify significant EEG metrics and then correlation analysis was performed. The analysis revealed that alpha2 power in the sensorimotor region was inversely correlated with RMT and AMT. Innovatively, graph theory was used to construct a brain network, and the relationship between the brain network and corticospinal excitability was explored. It was found that the global efficiency in the theta band was positively correlated with RMT. Additionally, the global efficiency in the alpha2 band was negatively correlated with RMT and AMT. These findings indicated that corticospinal excitability can be modulated by the power spectrum in sensorimotor regions and the global efficiency of functional networks. EEG network analysis can provide a useful supplement for studying the association between EEG oscillations and corticospinal excitability.

Keywords: electroencephalography, transcranial magnetic stimulation, corticospinal excitability, network, power spectrum

INTRODUCTION

Transcranial Magnetic Stimulation (TMS) induces an electric field through a time-varying magnetic field, resulting in induced electric currents and changing the action potential of nerve cells in the cerebral cortex, thus affecting blood circulation, metabolism, and nerve excitability in the brain (Wanalee et al., 2015). As an effective non-invasive nerve stimulation technology,

TMS is widely used in clinical practice and can be used to improve motor function in stroke patients, improve individual cognitive function, and reduce depression (Myczkowski et al., 2018; Chen et al., 2019).

Neuron oscillatory activity plays an important role in the cortical response to TMS. To clarify the interaction between neural activity and TMS, researchers explored the association between electroencephalography (EEG) and corticospinal excitability, defined as the cortical output in response to TMS. It was found that the fluctuation of EEG oscillations selectively affects corticospinal excitability (Berger et al., 2014; Bergmann et al., 2019; Ogata et al., 2019). Although EEG oscillations were assumed to regulate cortical excitability, the findings in previous studies were inconsistent. Some studies reported a correlation between corticospinal excitability and pre-stimulation alpha oscillation power (Sauseng et al., 2009) as well as beta oscillation power (Maki and Ilmoniemi, 2010; Hussain et al., 2019b) while others found no correlations between various EEG frequencies (Iscan et al., 2016). There are contradictions in these studies. Sauseng et al. (2009) found that the amplitude of motor evoked potentials (MEPs) is negatively correlated with the pre-stimulation alpha oscillation power, while Ogata et al. (2019) reported the opposite results. These conflicting results have evoked the need for further investigation of the relationship between EEG oscillations and corticospinal excitability to obtain reliable results.

Interestingly, previous studies focused on how EEG oscillations in sensorimotor regions modulated corticospinal excitability, while ignoring the effects of brain global network activity. Early neuroscience research focused on the function of single brain regions, while modern approaches tend to use complex network methods to analyze the structure and dynamic behavior of neural networks. Brain regions such as the frontal and parietal lobes regulate corticospinal excitability (Cattaneo and Barchiesi, 2011). A previous study showed that corticospinal excitability was regulated by the attention network, providing another perspective for understanding the association between corticospinal excitability and brain networks (Avenanti et al., 2018). A recent study indicated that TMS efficacy was modulated by the functional state of the target brain network (Schiena et al., 2020), suggesting that researchers should pay more attention to the impact of brain networks on corticospinal excitability rather than a single brain region.

In the field of brain networks, techniques for the construction and analysis of brain networks are still evolving. As a branch of scientific computing, graph theory involves the construction of a network by defining a series of nodes and connecting edges. This model fits the pattern of brain activity, which makes it a great tool for brain functional segmentation and integration (Sporns, 2018). The global efficiency and the clustering coefficient can be calculated using graph theory to measure the features of the brain network. Graph theory analysis of EEG has been gradually applied to describe neural electrophysiological activity (Rubinov and Sporns, 2010). A previous study showed that adjusting brain excitability through transcranial direct current stimulation can change the small-world propensity in brain networks (Vecchio et al., 2018), suggesting that graph theory can be a useful approach to study the interactions between brain networks and neural regulation technology.

For the purpose of this study, we aimed to explore the association between corticospinal excitability and EEG oscillations. The resting motor threshold (RMT) and active motor threshold (AMT) were identified as markers of corticospinal excitability according to previous study (Stefanou et al., 2020). Innovatively, we used graph theory analysis methods to construct brain networks to explore the relationship between the network properties and corticospinal excitability. Considering the factors mentioned above, we assumed that corticospinal excitability depends not only on the neural activity of the motor region, but also on the functional activity of the brain network. Clarifying the mechanism by which oscillating brain activity modulates corticospinal excitability will help elucidate how TMS works, which is conducive to enhancing the effect of TMS by stimulating the brain based on the current neural state.

MATERIALS AND METHODS

Participants

A total of 32 right-handed individuals (mean age: 21.53 ± 1.46; 7 men), all college students, were included in this study. The participants did not take psychotropic drugs and had no history of central nervous system diseases or head trauma. Individuals with contraindications to TMS were excluded (Rossi et al., 2021). Before the experiment, the participants were required to get enough sleep to maintain a good mental state during the experiment. All participants were informed of the purpose and content of the experiment and signed informed consent forms before the experiment. This study was approved by the Ethics Committee of Guangzhou First People's Hospital.

EEG Acquisition and Processing

EEG Acquisition

Resting-state EEG were recorded before application of TMS. The EEG data collection was performed in the electrophysiological laboratory and the room was quiet during EEG recording. The participants sat in a comfortable chair and their resting EEG was recorded for 10 min while their eyes were closed. They were required to remain awake throughout the recording. EEG data were recorded by using 128-channel HydroCel Geodesic Sensor Net (Electrical Geodesics, Inc., Eugene, OR, United States), and the Cz electrodes were used as the online reference. The impedances of all electrodes were kept below 10 kΩ by input impedance amplifiers (Geodesic EEG system 400). The signal was amplified at a sampling rate of 2,048 Hz and filtered through a 0.1–100 Hz band-pass filter. Data were processed offline after continuous EEG acquisition.

EEG Processing

*E*lectroencephalography processing was conducted with Matlab R2013a (The MathWorks, Natick, M*A*, United States) and eeglab12.0.[1] After reducing the sampling rate to 1,000 Hz, the

[1]http://www.sccn.ucsd.edu/eeglab/

data were filtered through 0.1–40 Hz with a finite impulse response (FIR) filter. Continuous data were segmented into 2 s for each epoch. Bad data were defined when the amplitude exceeded ± 100 μV. Independent components analysis (ICA) was conducted to eliminate electro-oculograms after removing bad epochs and interpolating electrodes with high noise.

To obtain spectrum information for the EEG data, Fast Fourier Transform (FFT) was used to decompose the data. We calculated the power of the four frequency bands: delta (1–4 Hz), theta (4–8 Hz), alpha1 (8–10 Hz), alpha2 (10–13 Hz), beta1 (13–20 Hz), and beta2 (20–30 Hz). In accordance with previous research, data collected from the cluster of EEG electrodes around C4 were averaged to represent the activity of the sensorimotor region (Bayram et al., 2015).

As for functional connectivity, the phase lag index (PLI) was applied to characterize the connections between the electrode pairs because it can eliminate the volumetric conduction effect. Band-pass filtering was performed on the electrode signal, and Hilbert Transform was performed on the filtered electrical signal to extract the phase at each time point. Afterward, the PLI of each electrode pair in the six frequency bands was calculated. PLI was calculated using the following formula (Su et al., 2017).

$$\mathrm{PLI} = \left|\left\langle \mathrm{sign}\left[\sin\left(\triangle\varphi\left(t_k\right)\right)\right]\right\rangle\right| \quad (1)$$

The range of the PLI value was 0–1; 0 indicated that the two signals did not have a linear dependence in this frequency band, while 1 indicated complete synchronization.

In this study, the GRETNA toolbox[2] was used for graph theoretical network analysis (Wang et al., 2015). The undirected weighted network was set up using electrical poles as nodes and the PLI value as the edge weight (de Waal et al., 2014). Based on previous studies, the clustering coefficient and efficiency, which are the most commonly used metrics, were selected to characterize the complex networks (Zomorrodi et al., 2019). Since there was no definite method for selecting a single threshold, referring to previous studies, we integrated the metrics over the entire threshold range to obtain the area under the curve (AUC) to characterize the brain network (Wang et al., 2015; Yan et al., 2017).

The clustering coefficient is defined as the ratio of the actual number of edges between a given node and its neighbors and the total number of possible edges between these nodes, and is used to measure the tightness between a node and its neighbor nodes in a network.

$$C_i = \frac{2l_i}{k_i(k_i-1)} \quad (2)$$

The clustering coefficient of the whole network is the average of all nodes in the network.

$$C_{global} = \frac{1}{n}\sum_{i\in N} C_i \quad (3)$$

Efficiency refers to the reciprocal of the harmonic average distance between all nodes in the network. The efficiency of a node is used to measure the information transmission capacity of the given node in the network.

$$E_i = \frac{\sum_{j\in N,\, j\neq i}\left(d_{ij}\right)^{-1}}{n-1} \quad (4)$$

The global efficiency is the average of all nodes in the network.

$$E_{global} = \frac{1}{n}\sum_{i\in N} E_i \quad (5)$$

For the formula and interpretation of these metrics, see Rubinov and Sporns (2010). The clustering coefficient and node efficiency of the motor cortex are the average values from the electrodes in the motor region.

TMS Procedure

Resting motor threshold and AMT was recorded immediately after EEG acquisition. Stimulation was applied using a figure-eight coil connected to the NS5000 Magnetic Stimulator (YIRUIDE Medical Co., Wuhan, China) with a maximum magnetic field intensity of 2.5 T. The participants assumed a sitting position with the body relaxed. The coil was placed in the projection of the primary motor cortex on the body surface of the right hemisphere, tangent to the scalp with the handle points facing backward and 45° away from the midline. This orientation induced a posterolateral to anteromedial current in the brain that preferentially activated the cortical-spinal system through horizontal cortical–cortical connections (Premoli et al., 2014). A single TMS pulse was applied to the M1 region, and MEPs from the left first digital interosseous (FDI) muscle were recorded with surface electromyography. The resting motion threshold was determined using the relative frequency method, defined as the minimum intensity that was sufficient for the MEPs to reach an amplitude > 50 μV in at least five out of ten of the subsequent stimuli. AMT was determined during muscle contraction (approximately 20% of maximum muscle strength) and was defined as the minimum intensity able to elicit MEPs (peak amplitude > 200 μV) in 50% of the subsequent stimuli. Furthermore, we used the neuro-navigation system (Visor2, ANT Neuro, Hengelo, Netherlands) to record the FDI hot spots to ensure that the coil would not deviate from the stimulus target throughout the experiment.

Statistical Analysis

To confirm the relationship between spontaneous EEG oscillations and corticospinal excitability, the least absolute shrinkage and selection operator (LASSO) was used to identify significant features and correlation analysis was conducted for these features. The basic idea of LASSO is that it compresses the coefficient of variables by adding penalty functions to the model and eliminates variables with a regression coefficient of 0 to facilitate the selection of variables (Li et al., 2017). The R 4.0.5 software[3] and glmnet package (Friedman et al., 2010) were used to perform LASSO. The parameter Lambda (λ) was tuned by 10-fold cross-validation based on the minimum criteria.

[2]http://www.nitrc.org/projects/gretna/

[3]http://www.R-project.org

To obtain the best fitting effect, the model with minimum λ was chosen. Correlations between significant features extracted by LASSO and corticospinal excitability were then evaluated. Statistical analysis was conducted using SPSS 25.0 (SPSS Inc., Chicago, IL, United States). The Shapiro-Wilk normality test was performed on all variables, and Pearson correlation analysis was used for variables with normal distribution; otherwise, Spearman correlation analysis was applied. $p < 0.05$ was considered statistically significant.

RESULTS

Descriptive Results

The range of RMT was from 21 to 73% MSO and the mean value was 46.25% MSO [standard deviation (SD) = 13.579]. AMT ranged from 12 to 57% MSO and the mean value was 32.31% MSO (SD = 11.183). The descriptive results for other variables are shown in **Table 1**.

Extraction of Features

Least absolute shrinkage and selection operator was used to construct the regression model for EEG parameters to predict RMT, and the regression model with the minimum λ value was selected because it had the best prediction. The minimum λ was 1.548, and eight potential predictors were identified, including alpha2 and beta1 oscillations power in the sensorimotor region, nodal efficiency in the alpha1 and alpha2 bands, global efficiency in the delta, theta, and alpha2 bands, and global clustering coefficient in the theta band. In the model used to predict AMT, the minimum λ was 1.844. Alpha2 oscillations power in the sensorimotor region, nodal efficiency in the theta and alpha1 bands, global efficiency in the theta and alpha2 bands, and global clustering coefficient in the beta2 band were selected as predictors. All significant factors were included in the subsequent correlation analysis. See **Figure 1**.

Correlation Analysis

Correlation analysis showed that the power of alpha2 oscillations in the sensorimotor region was negatively correlated with RMT ($\rho = -0.376$, $p = 0.034$). Similarly, alpha2 power in the sensorimotor region showed an inverse correlation with AMT ($\rho = -0.432$, $p = 0.014$). The strength of the correlation between beta1 and RMT did not reach a statistically significant level ($\rho = -0.328$, $p = 0.066$), similar to that between beta1 and AMT ($\rho = -0.314$, $p = 0.080$). See **Figure 2**.

When exploring the relationship between the nodal metrics and RMT, we found that RMT was negatively correlated with nodal efficiency in the alpha2 band, but the correlation did not reach statistical significance ($r = -0.347$, $p = 0.051$). Nodal efficiency in the theta band had no correlation with RMT ($r = 0.023$, $p = 0.900$) and AMT ($r = 0.336$, $p = 0.060$) and there was no correlation between nodal efficiency in the alpha1 band and RMT ($r = -0.247$, $p = 0.173$) or AMT ($r = -0.210$, $p = 0.249$). See **Figure 3**.

As for global metrics, we found that the global efficiency in the theta band was positively correlated with RMT ($r = 0.374$, $p = 0.035$), while the global efficiency in the alpha2 band was negatively correlated with RMT ($\rho = -0.363$, $p = 0.041$), showing the opposite trend. Similarly, the global efficiency in the alpha2 band was negatively correlated with the AMT ($\rho = -0.427$, $p = 0.015$) and the correlation strength between the global efficiency in the theta band and AMT did not reach the statistically significant level ($r = 0.291$, $p = 0.106$). There was no correlation between global efficiency in the delta band and RMT ($r = 0.074$, $p = 0.688$) as well as AMT ($r = -0.281$, $p = 0.119$). Further, the global clustering coefficient in the theta and beta2 band had no significant correlation with RMT or AMT. See **Figures 4**, **5**.

DISCUSSION

In this study, we explored the relationship between EEG oscillations and corticospinal excitability. Analysis revealed that the alpha2 power in the sensorimotor region showed an inverse correlation with RMT and AMT. Innovatively, we explored the relationship between brain activity and corticospinal excitability from the perspective of the functional network and found that the global efficiency in the theta band was positively correlated with RMT. Additionally, the global efficiency in the alpha2 band was negatively correlated with RMT and AMT. These findings indicated that the power spectrum in sensorimotor regions and the global efficiency of functional networks modulate corticospinal excitability, which provides an important basis for understanding the interactions between neural electrical activity and TMS.

TABLE 1 | Descriptive results of electroencephalography (EEG) metrics.

	Delta	Theta	Alpha1	Alpha2	Beta1	Beta2
Power spectrum	2.062 ± 1.030	1.247 ± 0.493	1.412 ± 0.672	1.359 ± 0.697	0.736 ± 0.338	0.497 ± 0.193
Global metric						
CC	0.163 ± 0.016	0.160 ± 0.017	0.140 ± 0.023	0.143 ± 0.026	0.156 ± 0.028	0.136 ± 0.028
Efficiency	0.089 ± 0.003	0.079 ± 0.002	0.077 ± 0.008	0.076 ± 0.012	0.053 ± 0.004	0.045 ± 0.003
Nodal metric						
CC	0.165 ± 0.030	0.161 ± 0.026	0.130 ± 0.050	0.133 ± 0.056	0.170 ± 0.043	0.143 ± 0.037
Efficiency	0.084 ± 0.007	0.080 ± 0.007	0.072 ± 0.024	0.070 ± 0.022	0.053 ± 0.007	0.048 ± 0.006

Data are presented as mean ± standard deviation. CC, clustering coefficient.

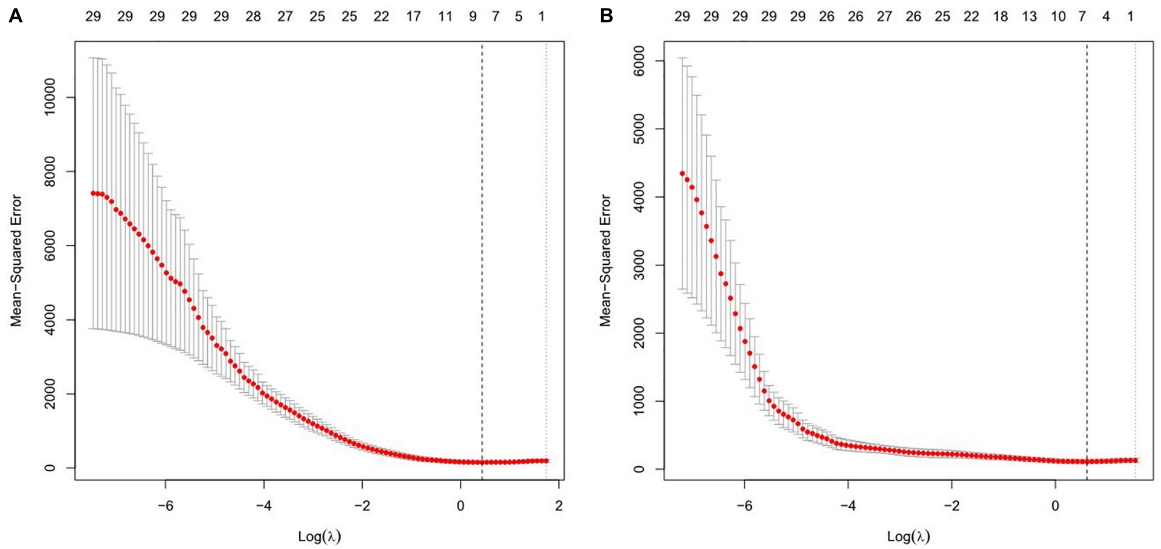

FIGURE 1 | Features selection using the least absolute shrinkage and selection operator (LASSO) regression model for resting motor threshold (RMT) **(A)** and active motor threshold (AMT) **(B)**. The horizontal axis plotted value of log λ and the vertical axis plotted mean squared error. The dotted vertical line was plotted at the optimal λ values based on minimum criteria.

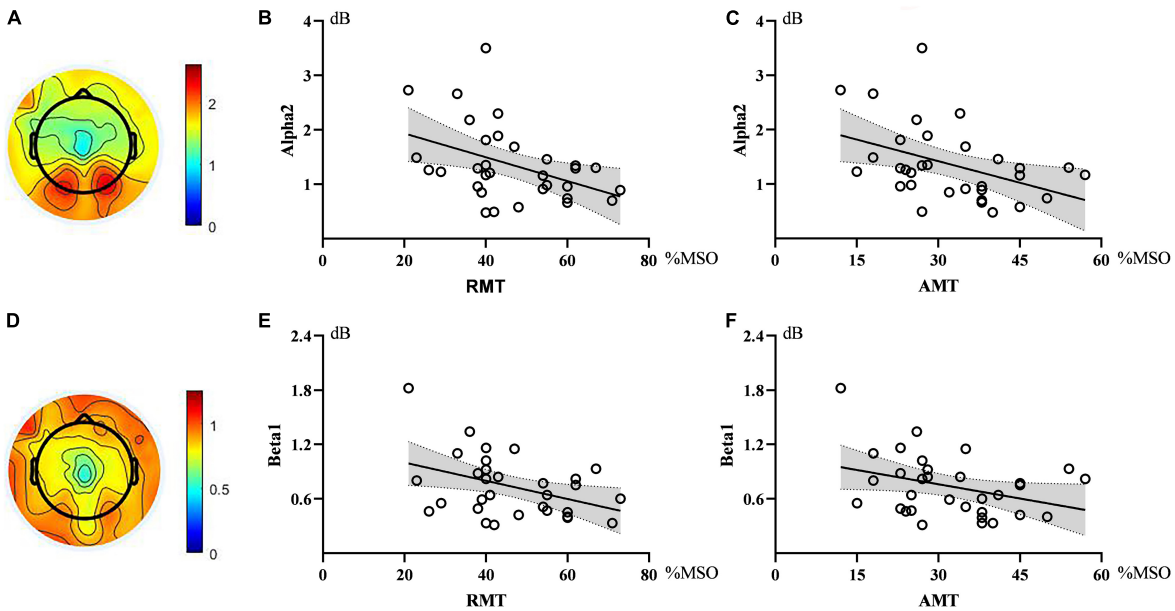

FIGURE 2 | Topographic maps and scatter diagrams. Topographic maps showed the power of alpha2 oscillations and beta1 oscillations. The color bar represents the value of power **(A,D)**. Scatter diagrams showed the correlation between electroencephalography (EEG) oscillations and motor threshold **(B,C,E,F)**. There were significant negative correlations between alpha2 and RMT as well as AMT.

The Correlation Between Power Spectrum in Sensorimotor Regions and Corticospinal Excitability

The spontaneous oscillation of EEG reflects the rhythmic changes in the membrane potential of neurons and thus reflects the current excitatory–inhibitory balance of underlying neuronal cell assemblies (Klimesch et al., 2007; Jensen and Mazaheri, 2010; Schulz et al., 2014). Each EEG band is associated with different cognitive and behavioral functions. Low-frequency EEG oscillations are associated with responsible motivation, emotion, and reward processing, while high-frequency EEG oscillations may reflect cognitive processes such as attention control, memory encoding, and recognition (MacLean et al., 2012; Sandler et al., 2016; De Pascalis et al., 2020). Alpha oscillations are the most significant phenomenon in human EEG recordings, and

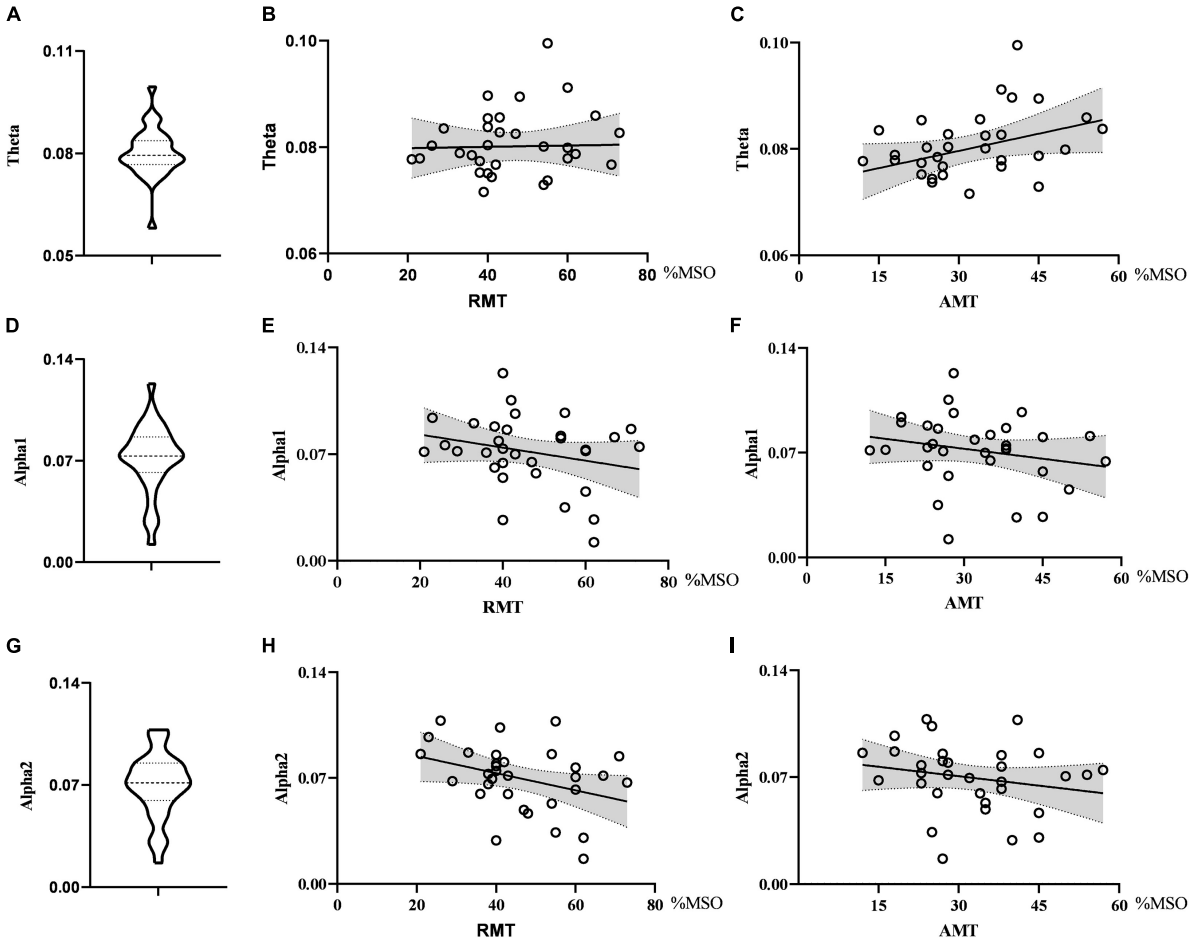

FIGURE 3 | Violin diagrams and scatter diagrams. Violin diagrams showed the distribution of nodal efficiency in theta, alpha1, and alpha2 band **(A,D,G)**. Scatter diagrams showed the correlation between nodal efficiency and motor threshold **(B,C,E,F,H,I)**.

their occurrence and function are some of the basic research topics in neuroscience. At first, researchers believed that the alpha activity reflected the idle state of the brain, but the current leading interpretation of alpha oscillations is that alpha oscillations causally determine excitability and modulate signal processing instead of passively respond to stimulus. Converging evidence suggests that alpha oscillations are related to the cyclic regulation of neuronal excitability and can affect the response of neurons to sensory stimuli (Palva and Palva, 2011). Currently, researchers recognize that the alpha oscillations contain at least two sub-components. The first is lower alpha or alpha1, which is endogenous and independent of any internal or external stimuli. The second is upper alpha or alpha2, mainly exists in the sensorimotor cortex, and is related to the function of the sensorimotor system (Vecchio et al., 2018).

In this study, RMT and AMT decreased when the alpha2 oscillation power increased, indicating an inverse correlation between alpha2 oscillations and corticospinal excitability. A number of studies support the view that the alpha rhythm reflects cortical excitability. Previous studies have shown that central alpha oscillations (mu rhythms) are associated with the resting state of the primary sensory and motor cortex by correlating the rhythm strength with fMRI blood signals (Ritter et al., 2009). Alpha oscillations in the central region are suppressed during movement and return to the baseline when the movement ends (Hao et al., 2019). According to the pulsed inhibition hypothesis, alpha oscillations are associated with the underlying localized global suppression of neuronal activity in cortical circuits, with high alpha power representing the suppressed state and low alpha power representing the excited state (Palva and Palva, 2011; Schulz et al., 2014). Since RMT and AMT are inversely associated with cortical excitability, similar to alpha oscillations, there should be a positive correlation between RMT, AMT, and alpha oscillations. However, in this study, alpha2 oscillations were negatively correlated with corticospinal excitability, which seems controversial. A recent study explored the relationship between pre-stimulus EEG oscillations and MEPs, and the results showed that high alpha and low beta power before stimulation could lead to high MEP amplitudes (Ogata et al., 2019). In a real-time TMS-EEG study, researchers explored the relationship between the phase of the alpha oscillations in the sensory motor area and MEPs. They found that the MEP

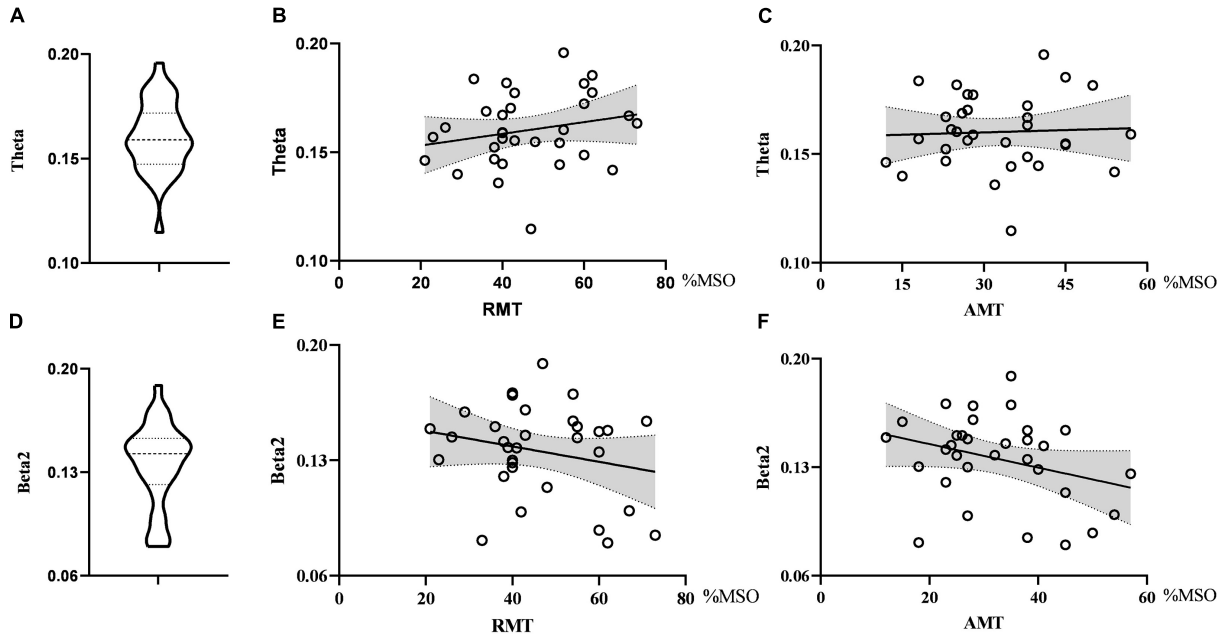

FIGURE 4 | Violin diagrams and scatter diagrams. Violin diagrams showed the distribution of clustering coefficient in theta and beta2 band **(A,D)**. Scatter diagrams showed the correlation between clustering coefficient and motor threshold **(B,C,E,F)**.

amplitude increased during the high alpha power, indicating that the alpha oscillations could promote corticospinal excitability (Bergmann et al., 2019). These results were consistent with our findings. The discrepancies between studies may be caused by different experimental designs. Previous studies proved the negative correlation between alpha oscillations and cortical excitability mainly by exploring the changes of alpha rhythm during motor tasks, such as voluntary movement and motor imagery, whereas our study recorded EEG and motor threshold at rest and the task state would contribute to the relationship between EEG oscillations and corticospinal excitability. Our results suggested that alpha oscillations can modulate the cortical response to TMS.

The relationship between beta oscillations and cortical excitability has been studied using different modalities. Generally, beta oscillations in the motor cortex decrease in amplitude during movement and increase in amplitude when movement stops (Darch et al., 2020). Hussain et al. (2019a) found that the beta rhythm power before TMS stimulation can be used to predict the amplitude of MEPs. The stronger the beta rhythm power is, the larger the MEP amplitude will be, indicating that the beta rhythm is positively correlated with corticospinal excitability. These findings may be because beta activity reflects the activity of the II/III interlayer neurons, which could regulate the excitability of the spinal cord by activating descending corticospinal neurons (Hussain et al., 2019b). In this study, beta1 oscillation was a significant feature in the regression model, and correlation analysis showed no significant correlation between beta oscillations and corticospinal excitability. This may be due to the small sample size. Nevertheless, the results of this study are valuable, because previous studies focused on how alpha oscillations regulate corticospinal excitability and beta oscillations were used to be ignored. Future studies can further explore the relationship between beta oscillations and corticospinal excitability.

The Correlation Between Efficiency of Network and Corticospinal Excitability

With the advancement of neuroscience, the network connection pattern formed by the cooperation of multiple brain regions has been identified as the physiological foundation for information processing in the brain. The small-world network is the most commonly studied complex network which has both a large clustering coefficient and a small path length (Bassett and Bullmore, 2006). It examines the brain's functional connectivity architecture, focusing on the brain's ability to integrate and transmit information between different regions. Efficiency is an important metric to measure the ability of network information exchange, and its contribution to cortical excitability has attracted the attention of researchers. Blain-Moraes et al. (2017) investigated the neural activity of subjects under general anesthesia and found that while the subjects were unconscious, the alpha network efficiency decreased and the alpha network clustering coefficient increased significantly. This showed that the efficiency of the alpha network is positively correlated with cortical excitability. Previous studies have shown that the efficiency of the alpha network increased during exercise, possibly due to increased metabolism and cortical arousal during exercise (Tamburro et al., 2020). High global efficiency corresponds to fast information transmission. Our study showed that RMT decreased with the elevation of alpha network efficiency,

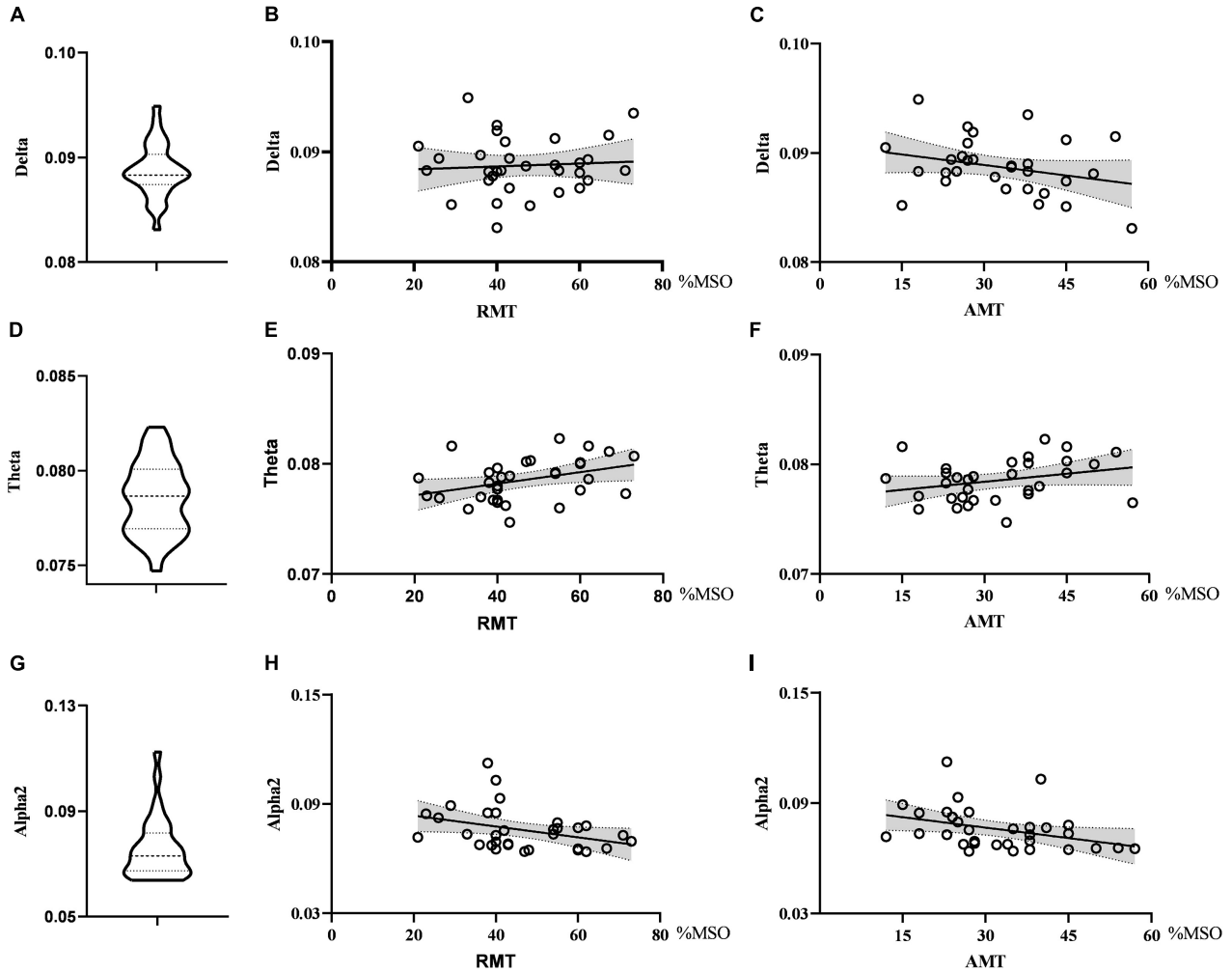

FIGURE 5 | Violin diagrams and scatter diagrams. Violin diagrams showed the distribution of global efficiency in delta, theta, and alpha2 band **(A,D,G)**. Scatter diagrams showed the correlation between global efficiency and motor threshold **(B,C,E,F,H,I)**. There was significant positive correlation between global efficiency in theta and RMT. And there were significant negative correlations between global efficiency in alpha2 and RMT as well as AMT.

indicating that brain activity increased with the enhancement of the alpha network information processing capacity, making it easier to respond to TMS.

Theta oscillations are often considered to be related to cognitive functions such as memory and emotion (Wang et al., 2018), and a few studies show that the theta rhythm contributes to the movement process. Popovych et al. (2016) reported that a significant phase-locking effect in the delta-theta frequency band could be observed in the M1 area when individuals completed an exercise task, suggesting that the theta oscillations were related to movement and indirectly showing that the theta rhythm contributes to the excitability of the motor cortex. Storti et al. (2016) used graph theory to analyze the brain network characteristics of individuals during movement and found that the betweenness in the theta band of the motor cortex increased significantly, providing a new perspective for exploring the theta network and the excitability of the motor cortex. Interestingly, in this study, the modulating effects of the global efficiency of the theta band and alpha band on RMT were in the opposite direction, which may indicate that different rhythm networks regulate cortical excitability in different directions and coordinate with each other to regulate brain activities.

In this study, the LASSO regression showed that the clustering coefficient in the theta and beta2 bands was the predictor of the motion threshold, but the correlation analysis results indicated that there was no correlation. This may result from the differences of statistical methods. Correlation analysis is univariate analysis, while LASSO is a multivariate analysis method and the results would be affected by the interaction between variables. The combination of clustering coefficients and other parameters can provide more comprehensive information about corticospinal excitability.

Strengths and Limitations

The strength of this study is that it explored the relationship between TMS and neural oscillation from a network perspective

using graph theory analysis. In the application of graph theory, a network is constructed by defining a series of nodes and connecting edges and the model can fit the pattern of brain activity, which makes it a great tool for brain functional segmentation and integration. In this study, graph theory was used to construct a brain network, and the relationship between neural oscillatory activities and TMS was explained from the perspective of the global network, which can help to explore the electrophysiological mechanism of TMS.

There are some limitations to this study. Firstly, we studied the association between EEG oscillation and TMS in non-dominant hemisphere, and the generalizability of the results to dominant hemisphere can be explored in future study. Besides, EEG were recorded before application of TMS in this study. Future study can record them simultaneously to provide stronger evidences. We chose the EEG spectrum and graph theory to analyze the relationship between EEG oscillation and cortical excitability because these are the classic metrics used to describe the characteristics of EEG. In future studies, other metrics such as entropy and complexity which quantifies the non-linear dynamic characteristics of EEG and reflect cortical functional state can be selected to explore the relationship between EEG oscillation and corticospinal excitability comprehensively.

CONCLUSION

In conclusion, we found that the alpha2 power in the sensorimotor region showed an inverse correlation with RMT and AMT. And the global efficiency in the theta band was positively correlated with RMT. Additionally, the global efficiency in the alpha2 band was negatively correlated with RMT and AMT. It is crucial to understand the mechanisms of TMS from the perspective of neurophysiology. The findings of this study indicate that the effect of TMS on the cortex is dependent on the activity of local neurons and global network activity, which provides an important basis for uncovering the regulatory effect of TMS on neural electrical activity. The network analysis of EEG can provide a useful supplement for studying the brain response to TMS.

DATA AVAILABILITY STATEMENT

The raw data supporting the conclusion of this article will be made available by the authors, without undue reservation.

ETHICS STATEMENT

The studies involving human participants were reviewed and approved by the Ethics Committee of Guangzhou First People's Hospital. The patients/participants provided their written informed consent to participate in this study.

AUTHOR CONTRIBUTIONS

YL, GX, and TY: study design. QD, GC, MW, HCh, and HCa: data acquisition and processing. TL: statistical analysis. GC and MW: drafting of the manuscript. QD: critical revision of the manuscript. YJ and WL: technical assistance. All authors contributed to the article and approved the submitted version.

FUNDING

This work was supported by the National Science Foundation of China [Grant Numbers 81772438 (YL), 81974357 (YL), 82072548 (GX), and 81802227 (TL)]; the Guangzhou Municipal Science and Technology Program [Grant Number 201803010083 (YL)]; the Fundamental Research Funds for the Central University [Grant Number 2018PY03 (YL)]; National Key R&D Program of China [Grant Number 2017YFB1303200 (YL)]; Guangdong Basic and Applied Basic Research Foundation [Grant Number 2020A1515110761 (QD)]; and Guangzhou Postdoctoral Science Foundation (QD).

ACKNOWLEDGMENTS

We sincerely thank all the subjects for their support and cooperation in our experiment.

REFERENCES

Avenanti, A., Wright, D. J., Wood, G., Franklin, Z. C., Marshall, B., Riach, M., et al. (2018). Directing visual attention during action observation modulates corticospinal excitability. *PLoS One* 13:e0190165. doi: 10.1371/journal.pone.0190165

Bassett, D. S., and Bullmore, E. (2006). Small-world brain networks. *Neuroscientist* 12, 512–523. doi: 10.1177/1073858406293182

Bayram, M. B., Siemionow, V., and Yue, G. H. (2015). Weakening of corticomuscular signal coupling during voluntary motor action in aging. *J. Gerontol.* 70, 1037–1043. doi: 10.1093/gerona/glv014

Berger, B., Minarik, T., Liuzzi, G., Hummel, F. C., and Sauseng, P. (2014). EEG oscillatory phase-dependent markers of corticospinal excitability in the resting brain. *Biomed. Res. Int.* 2014:936096.

Bergmann, T. O., Lieb, A., Zrenner, C., and Ziemann, U. (2019). Pulsed facilitation of corticospinal excitability by the sensorimotor mu-alpha rhythm. *J. Neurosci.* 39, 10034–10043. doi: 10.1523/jneurosci.1730-19.2019

Blain-Moraes, S., Tarnal, V., Vanini, G., Bel-Behar, T., Janke, E., Picton, P., et al. (2017). Network efficiency and posterior alpha patterns are markers of recovery from general anesthesia: a high-density electroencephalography study in healthy volunteers. *Front. Hum. Neurosci.* 11:328. doi: 10.3389/fnhum.2017.00328

Cattaneo, L., and Barchiesi, G. (2011). Transcranial magnetic mapping of the short-latency modulations of corticospinal activity from the ipsilateral hemisphere during rest. *Front. Neural Circuits* 5:14. doi: 10.3389/fncir.2011.00014

Chen, Y.-J., Huang, Y.-Z., Chen, C.-Y., Chen, C.-L., Chen, H.-C., Wu, C.-Y., et al. (2019). Intermittent theta burst stimulation enhances upper limb motor function in patients with chronic stroke: a pilot randomized controlled trial. *BMC Neurol.* 19:69. doi: 10.1186/s12883-019-1302-x

Darch, H. T., Cerminara, N. L., Gilchrist, I. D., and Apps, R. (2020). Pre-movement changes in sensorimotor beta oscillations predict motor adaptation drive. *Sci. Rep.* 10:17946.

De Pascalis, V., Vecchio, A., and Cirillo, G. (2020). Resting anxiety increases EEG delta–beta correlation: relationships with the reinforcement sensitivity

theory personality traits. *Pers. Indiv. Differ.* 156:109796. doi: 10.1016/j.paid.2019.109796

de Waal, H., Stam, C. J., Lansbergen, M. M., Wieggers, R. L., Kamphuis, P. J., Scheltens, P., et al. (2014). The effect of souvenaid on functional brain network organisation in patients with mild Alzheimer's disease: a randomised controlled study. *PLoS One* 9:e86558. doi: 10.1371/journal.pone.0086558

Friedman, J., Hastie, T., and Tibshirani, R. (2010). Regularization paths for generalized linear models via coordinate descent. *J. Stat. Softw.* 33, 1–22.

Hao, J., Feng, W., Zhang, L., and Liao, Y. (2019). The post-movement beta rebound and motor-related Mu suppression in children. *J. Motor Behav.* 52, 590–600. doi: 10.1080/00222895.2019.1662762

Hussain, S. J., Claudino, L., Bonstrup, M., Norato, G., Cruciani, G., Thompson, R., et al. (2019a). Sensorimotor oscillatory phase-power interaction gates resting human corticospinal output. *Cereb. Cortex* 29, 3766–3777. doi: 10.1093/cercor/bhy255

Hussain, S. J., Cohen, L. G., and Bonstrup, M. (2019b). Beta rhythm events predict corticospinal motor output. *Sci. Rep.* 9:18305.

Iscan, Z., Nazarova, M., Fedele, T., Blagovechtchenski, E., and Nikulin, V. V. (2016). Pre-stimulus alpha oscillations and inter-subject variability of motor evoked potentials in single- and paired-pulse TMS paradigms. *Front. Hum. Neurosci.* 10:504. doi: 10.3389/fnhum.2016.00504

Jensen, O., and Mazaheri, A. (2010). Shaping functional architecture by oscillatory alpha activity: gating by inhibition. *Front. Hum. Neurosci.* 4:186. doi: 10.3389/fnhum.2010.00186

Klimesch, W., Sauseng, P., and Hanslmayr, S. (2007). EEG alpha oscillations: the inhibition-timing hypothesis. *Brain Res. Rev.* 53, 63–88. doi: 10.1016/j.brainresrev.2006.06.003

Li, J., Wang, J., Chen, Y., Yang, L., and Chen, S. (2017). A prognostic 4-gene expression signature for squamous cell lung carcinoma. *J. Cell Physiol.* 232, 3702–3713. doi: 10.1002/jcp.25846

MacLean, M. H., Arnell, K. M., and Cote, K. A. (2012). Resting EEG in alpha and beta bands predicts individual differences in attentional blink magnitude. *Brain Cogn.* 78, 218–229.

Maki, H., and Ilmoniemi, R. J. (2010). EEG oscillations and magnetically evoked motor potentials reflect motor system excitability in overlapping neuronal populations. *Clin. Neurophysiol.* 121, 492–501. doi: 10.1016/j.clinph.2009.11.078

Myczkowski, M. L., Fernandes, A., Moreno, M., Valiengo, L., Lafer, B., Moreno, R. A., et al. (2018). Cognitive outcomes of TMS treatment in bipolar depression: Safety data from a randomized controlled trial. *J. Affect. Disord.* 235, 20–26.

Ogata, K., Nakazono, H., Uehara, T., and Tobimatsu, S. (2019). Prestimulus cortical EEG oscillations can predict the excitability of the primary motor cortex. *Brain Stimul.* 12, 1508–1516. doi: 10.1016/j.brs.2019.06.013

Palva, S., and Palva, J. M. (2011). Functional roles of alpha-band phase synchronization in local and large-scale cortical networks. *Front. Psychol.* 2:204. doi: 10.3389/fpsyg.2011.00204

Popovych, S., Rosjat, N., Toth, T. I., Wang, B. A., Liu, L., Abdollahi, R. O., et al. (2016). Movement-related phase locking in the delta-theta frequency band. *Neuroimage* 139, 439–449. doi: 10.1016/j.neuroimage.2016.06.052

Premoli, I., Castellanos, N., Rivolta, D., Belardinelli, P., Bajo, R., Zipser, C., et al. (2014). TMS-EEG signatures of GABAergic neurotransmission in the human cortex. *J. Neurosci.* 34, 5603–5612. doi: 10.1523/jneurosci.5089-13.2014

Ritter, P., Moosmann, M., and Villringer, A. (2009). Rolandic alpha and beta EEG rhythms' strengths are inversely related to fMRI-BOLD signal in primary somatosensory and motor cortex. *Hum. Brain Mapp.* 30, 1168–1187. doi: 10.1002/hbm.20585

Rossi, S., Antal, A., Bestmann, S., Bikson, M., Brewer, C., Brockmoller, J., et al. (2021). Safety and recommendations for TMS use in healthy subjects and patient populations, with updates on training, ethical and regulatory issues: expert guidelines. *Clin. Neurophysiol.* 132, 269–306. doi: 10.1016/j.clinph.2020.10.003

Rubinov, M., and Sporns, O. (2010). Complex network measures of brain connectivity: uses and interpretations. *Neuroimage* 52, 1059–1069. doi: 10.1016/j.neuroimage.2009.10.003

Sandler, H., Tamm, S., Fendel, U., Rose, M., Klapp, B. F., and Bosel, R. (2016). Positive emotional experience: induced by vibroacoustic stimulation using a body monochord in patients with psychosomatic disorders: is associated with an increase in EEG-theta and a decrease in EEG-alpha power. *Brain Topogr.* 29, 524–538. doi: 10.1007/s10548-016-0480-8

Sauseng, P., Klimesch, W., Gerloff, C., and Hummel, F. C. (2009). Spontaneous locally restricted EEG alpha activity determines cortical excitability in the motor cortex. *Neuropsychologia* 47, 284–288. doi: 10.1016/j.neuropsychologia.2008.07.021

Schiena, G., Maggioni, E., Pozzoli, S., and Brambilla, P. (2020). Transcranial magnetic stimulation in major depressive disorder: response modulation and state dependency. *J. Affect. Disord.* 266, 793–801. doi: 10.1016/j.jad.2020.02.006

Schulz, H., Ubelacker, T., Keil, J., Muller, N., and Weisz, N. (2014). Now I am ready-now i am not: the influence of pre-TMS oscillations and corticomuscular coherence on motor-evoked potentials. *Cereb. Cortex* 24, 1708–1719. doi: 10.1093/cercor/bht024

Sporns, O. (2018). Graph theory methods: applications in brain networks. *Dial. Clin. Neurosci.* 20, 111–121. doi: 10.31887/dcns.2018.20.2/osporns

Stefanou, M. I., Galevska, D., Zrenner, C., Ziemann, U., and Nieminen, J. O. (2020). Interhemispheric symmetry of micro-rhythm phase-dependency of corticospinal excitability. *Sci. Rep.* 10:7853.

Storti, S. F., Formaggio, E., Manganotti, P., and Menegaz, G. (2016). Brain network connectivity and topological analysis during voluntary arm movements. *Clin. EEG Neurosci.* 47, 276–290. doi: 10.1177/1550059415598905

Su, S., Yu, D., Cheng, J., Chen, Y., Zhang, X., Guan, Y., et al. (2017). Decreased global network efficiency in young male smoker: an EEG study during the resting state. *Front. Psychol.* 8:1605. doi: 10.3389/fpsyg.2017.01605

Tamburro, G., Di Fronso, S., Robazza, C., Bertollo, M., and Comani, S. (2020). Modulation of brain functional connectivity and efficiency during an endurance cycling task: a source-level EEG and graph theory approach. *Front. Hum. Neurosci.* 14:243. doi: 10.3389/fnhum.2020.00243

Vecchio, F., Di Iorio, R., Miraglia, F., Granata, G., Romanello, R., Bramanti, P., et al. (2018). Transcranial direct current stimulation generates a transient increase of small-world in brain connectivity: an EEG graph theoretical analysis. *Exp. Brain Res.* 236, 1117–1127. doi: 10.1007/s00221-018-5200-z

Wanalee, K., Rose, K., and Alexandra, L. V. (2015). Basic principles of transcranial magnetic stimulation (TMS) and repetitive TMS (rTMS). *Ann. Phys. Rehabil. Med.* 58, 208–213. doi: 10.1016/j.rehab.2015.05.005

Wang, B., Li, P., Li, D., Niu, Y., Yan, T., Li, T., et al. (2018). Increased functional brain network efficiency during audiovisual temporal asynchrony integration task in aging. *Front. Aging Neurosci.* 10:316. doi: 10.3389/fnagi.2018.00316

Wang, J., Wang, X., Xia, M., Liao, X., Evans, A., and He, Y. (2015). GRETNA: a graph theoretical network analysis toolbox for imaging connectomics. *Front. Hum. Neurosci.* 9:386. doi: 10.3389/fnhum.2015.00386

Yan, T., Wang, W., Liu, T., Chen, D., Wang, C., Li, Y., et al. (2017). Increased local connectivity of brain functional networks during facial processing in schizophrenia: evidence from EEG data. *Oncotarget* 8, 107312–107322. doi: 10.18632/oncotarget.20598

Zomorrodi, R., Loheswaran, G., Pushparaj, A., and Lim, L. (2019). Pulsed near infrared transcranial and intranasal photobiomodulation significantly modulates neural oscillations: a pilot exploratory study. *Sci. Rep.* 9:6309.

Conflict of Interest: The authors declare that the research was conducted in the absence of any commercial or financial relationships that could be construed as a potential conflict of interest.

Publisher's Note: All claims expressed in this article are solely those of the authors and do not necessarily represent those of their affiliated organizations, or those of the publisher, the editors and the reviewers. Any product that may be evaluated in this article, or claim that may be made by its manufacturer, is not guaranteed or endorsed by the publisher.

frontiers in Neuroscience

ORIGINAL RESEARCH
published: 22 October 2021
doi: 10.3389/fnins.2021.755709

The Effects of Intermittent Theta Burst Stimulation on Functional Brain Network Following Stroke: An Electroencephalography Study

Qian Ding[1†], Shunxi Zhang[1†], Songbin Chen[1], Jixiang Chen[1], Xiaotong Li[1], Junhui Chen[1], Yuan Peng[1], Yujie Chen[1], Kang Chen[1], Guiyuan Cai[1], Guangqing Xu[2] and Yue Lan[1]**

[1] Department of Rehabilitation Medicine, Guangzhou First People's Hospital, School of Medicine, South China University of Technology, Guangzhou, China, [2] Department of Rehabilitation Medicine, Guangdong Provincial People's Hospital, Guangdong Academy of Medical Sciences, Guangzhou, China

OPEN ACCESS

Edited by:
Jing Wang,
Xi'an Jiaotong University, China

Reviewed by:
Pratik Yashvant Chhatbar,
Duke University, United States
Fabricio Lima Brasil,
Santos Dumont Institute (ISD), Brazil

***Correspondence:**
Guangqing Xu
guangchingx@163.com
Yue Lan
bluemooning@163.com

[†] These authors have contributed equally to this work

Specialty section:
This article was submitted to Neuroprosthetics, a section of the journal Frontiers in Neuroscience

Received: 09 August 2021
Accepted: 05 October 2021
Published: 22 October 2021

Citation:
Ding Q, Zhang S, Chen S, Chen J, Li X, Chen J, Peng Y, Chen Y, Chen K, Cai G, Xu G and Lan Y (2021) The Effects of Intermittent Theta Burst Stimulation on Functional Brain Network Following Stroke: An Electroencephalography Study. Front. Neurosci. 15:755709. doi: 10.3389/fnins.2021.755709

Objective: Intermittent theta burst stimulation (iTBS) is a special form of repetitive transcranial magnetic stimulation (rTMS), which effectively increases cortical excitability and has been widely used as a neural modulation approach in stroke rehabilitation. As effects of iTBS are typically investigated by motor evoked potentials, how iTBS influences functional brain network following stroke remains unclear. Resting-state electroencephalography (EEG) has been suggested to be a sensitive measure for evaluating effects of rTMS on brain functional activity and network. Here, we used resting-state EEG to investigate the effects of iTBS on functional brain network in stroke survivors.

Methods: We studied thirty stroke survivors (age: 63.1 ± 12.1 years; chronicity: 4.0 ± 3.8 months; UE FMA: 26.6 ± 19.4/66) with upper limb motor dysfunction. Stroke survivors were randomly divided into two groups receiving either Active or Sham iTBS over the ipsilesional primary motor cortex. Resting-state EEG was recorded at baseline and immediately after iTBS to assess the effects of iTBS on functional brain network.

Results: Delta and theta bands interhemispheric functional connectivity were significantly increased after Active iTBS (P = 0.038 and 0.011, respectively), but were not significantly changed after Sham iTBS (P = 0.327 and 0.342, respectively). Delta and beta bands global efficiency were also significantly increased after Active iTBS (P = 0.013 and 0.0003, respectively), but not after Sham iTBS (P = 0.586 and 0.954, respectively).

Conclusion: This is the first study that used EEG to investigate the acute neuroplastic changes after iTBS following stroke. Our findings for the first time provide evidence that iTBS modulates brain network functioning in stroke survivors. Acute increase in interhemispheric functional connectivity and global efficiency after iTBS suggest that iTBS has the potential to normalize brain network functioning following stroke, which can be utilized in stroke rehabilitation.

Keywords: intermittent theta burst stimulation (iTBS), electroencephalography (EEG), stroke, functional connectivity, graph theory

INTRODUCTION

Stroke is one of the main causes of adult disability worldwide (Hankey, 2013). Upper extremity motor impairment is a common clinical representation following stroke. More than half of individuals experience upper extremity motor impairment acutely after stroke, and the motor deficits persist to the chronic phase in approximately two thirds of stroke survivors who initially had upper extremity motor impairment (Kwakkel et al., 2004; Tedesco Triccas et al., 2019). The persistent motor deficits following stroke may result from altered cortical activity and brain network functioning (Desowska and Turner, 2019; Vecchio et al., 2019). As one of the non-invasive brain stimulation techniques, repetitive transcranial magnetic stimulation (rTMS) offers a chance to modulate cortical excitability and correct abnormal cortical activity following stroke (Suppa et al., 2016), which has been suggested to be a promising approach for stroke rehabilitation (Corti et al., 2012).

Intermittent theta burst stimulation (iTBS) is a specific form of rTMS that effectively elevates cortical excitability of the stimulated brain regions for at least 20 min (Huang et al., 2005). As iTBS employs a shorter stimulation period and a lower stimulation intensity compared with traditional rTMS, iTBS could be a good rTMS option in clinical practice (Talelli et al., 2007). Neural effects of iTBS are typically investigated by motor evoked potentials (MEP), which are muscular responses elicited by single-pulse TMS (Huang et al., 2005; Talelli et al., 2007; Di Lazzaro et al., 2008; Ackerley et al., 2010; Hinder et al., 2014; Ding et al., 2021b). However, this approach is not applicable to stroke survivors in whom MEPs in the paretic limb cannot be elicited. In addition, it has been suggested that iTBS has impact on functional brain network in remote regions from the stimulated site (Suppa et al., 2016). As MEPs only reflect corticospinal excitability of primary motor cortex (M1), other neuroimaging tools are needed to complement with MEPs and investigate neurophysiological effects induced by iTBS from other aspects.

Electroencephalography (EEG) is a neuroimaging approach that records cortical electrical activity along the scalp. Resting-state EEG has been suggested to be a sensitive measure for evaluating effects of rTMS on brain functional activity (e.g., functional connectivity) (Casarotto et al., 2010). Functional connectivity refers to synchrony of cortical activity in anatomically distinct but functionally collaborating brain regions (Vecchio et al., 2019), which forms the basis of functional brain network. Graph theory analysis is an approach for characterizing functional brain network (Park et al., 2014). Based on graph theory, the average of interregional efficiency between every pair of brain region over the entire brain is called global efficiency, which measures the efficiency in transporting information at a global scale (Park et al., 2014). EEG-based functional brain network analysis could provide additional valuable information on the neural effects induced by iTBS.

Following stroke, focal brain lesions could cause alteration in the dynamics of functional brain network, which involves not only the damaged brain areas but also extending to remote areas (Vecchio et al., 2019). It has been reported that interhemispheric functional connectivity was reduced acutely after stroke, and increased gradually in parallel with motor improvements in stroke survivors, indicating a supportive role of interhemispheric functional connectivity in motor recovery following stroke (Golestani et al., 2013; Desowska and Turner, 2019; Hoshino et al., 2020; Li et al., 2020). Global efficiency has also been suggested to be reduced following stroke, and individuals with worse motor performance tend to have lower global efficiency (Philips et al., 2017). Therefore, brain network functioning can be considered as a potential biomarker indicating stroke recovery and has been frequently used as an outcome assessment in stroke studies (Caliandro et al., 2017; Philips et al., 2017; Vecchio et al., 2019). However, to our knowledge, no published study has applied EEG to evaluate the aftereffects of rTMS (including iTBS) on the functional brain network in stroke survivors.

van Meer et al. (2010) reported that impaired motor function acutely after experimental stroke in rats was related to partial loss of interhemispheric functional connectivity, and interhemispheric functional connectivity was increased subsequently concomitant to motor recovery. In humans, reduced interhemispheric functional connectivity was also observed acutely after stroke (Philips et al., 2017; Desowska and Turner, 2019; Hoshino et al., 2020; Li et al., 2020). It has been reported that the increase in interhemispheric functional connectivity was associated with motor improvements in stroke survivors, and restoration of interhemispheric functional connectivity was noted only in well recovered individuals, but not in the poorly recovered stroke survivors (Golestani et al., 2013; Desowska and Turner, 2019; Hoshino et al., 2020; Li et al., 2020), suggesting that interhemispheric functional connectivity is possibly a potential biomarker indicating stroke recovery (Caliandro et al., 2017; Philips et al., 2017; Vecchio et al., 2019).

The effects of iTBS or high frequency rTMS on functional brain network have been previously investigated in healthy adults (Nettekoven et al., 2014; Park et al., 2014; Hoy et al., 2016). Interhemispheric functional connectivity has been reported to be increased after iTBS in both EEG (Hoy et al., 2016) and functional magnetic resonance imaging (fMRI) (Nettekoven et al., 2014) studies. Park et al. (2014) used resting-state EEG to investigate the effects of high frequency rTMS on global efficiency in healthy adults, and an increase in global efficiency was observed in individuals with behavioral facilitation after rTMS. Due to the differences between healthy adults and stroke survivors, it is still unclear whether iTBS would produce similar effects on interhemispheric functional connectivity and global efficiency in stroke survivors.

In present study, we used resting-state EEG to investigate the effects of iTBS on functional brain network in stroke survivors. We anticipated that interhemispheric functional connectivity and global efficiency would be increased after

Abbreviations: rTMS, repetitive transcranial magnetic stimulation; iTBS, intermittent theta burst stimulation; MEP, motor evoked potential; M1, primary motor cortex; EEG, electroencephalography; fMRI, functional magnetic resonance imaging; FMA, Fugl-Meyer assessment; ARAT, action research arm test; IH, ipsilesional hemisphere; RMT, resting motor threshold; EMG, electromyography; FDI, first dorsal interosseous; MSO, maximum stimulator output; ICA, independent component analysis; AUC, area under the curve; LME, linear mixed effects; LTP, long-term potentiation.

iTBS. These results would have potential implications for understanding the influences of iTBS on functional brain network in stroke survivors.

MATERIALS AND METHODS

Participants

Thirty stroke survivors participated in this study. Stroke survivors were included into this study if they had a single stroke less than 18 months prior to enrollment. All stroke survivors were screened for eligibility to receive iTBS and excluded if they were using medications that reduce seizure threshold or had history of seizure disorder; pregnant; or any implanted devices or metal that might be affected by iTBS (Rossi et al., 2009). Stroke survivors were also excluded if there was a presence of cognitive impairment as defined by inability to comprehend and follow three step commands (Ding et al., 2018). Upper-extremity component of the Fugl-Meyer motor function assessment (FMA) and action research arm test (ARAT) were used to assess motor impairment and upper extremity motor performance, respectively. Demographic characteristics are reported in **Tables 1**, **2**.

Subjects gave their written informed consent for the experimental procedures that were approved by the Guangzhou First People's Hospital Human Research Ethics Committee. The study was performed in accordance with the Declaration of Helsinki.

Study Design

We used a sham-controlled, randomized single-blinded design. Stroke survivors were randomly assigned to the experimental (Active iTBS) and control (Sham iTBS) groups, with fifteen subjects in each group. Stroke survivors were blinded with respect to the group they were assigned to, that is, whether the subject received Active or Sham iTBS.

Intermittent Theta Burst Stimulation

Intermittent theta burst stimulation was applied over the M1 in the ipsilesional hemisphere (IH) using a NS5000 Magnetic Stimulator (YIRUIDE Medical Co., Wuhan, China). The iTBS pattern consists of bursts containing three pulses at 50 Hz repeated at 5 Hz. A 2 s train of TBS was repeated every 10 s for a total of 192 s (600 pulses in total) (Huang et al., 2005). Of note, the stimulation intensity was set at 70% resting motor threshold (RMT) instead of 80% active motor threshold (AMT) in the original iTBS protocol (Volz et al., 2016). The reason for setting stimulation intensity based on RMT rather than AMT is that the latter would require stroke survivors to perform constant submaximal contractions of the target muscle which is often impossible for the paretic hand, especially in low-functioning stroke survivors (Volz et al., 2016). Furthermore, previous studies have shown similar aftereffects of iTBS with a stimulation intensity of 70% RMT or 80% AMT (Gentner et al., 2008; Cardenas-Morales et al., 2014). Therefore, a stimulation intensity of 70% RMT can be considered as an effective variant for increasing cortical excitability after iTBS (Volz et al., 2016; Yu et al., 2021).

Resting motor threshold determination was performed prior to the application of iTBS. Surface electromyography (EMG) was recorded from the first dorsal interosseous (FDI) in the paretic hand. Stroke survivors were seated in a comfortable chair with back support (Ding et al., 2018). TMS was applied over M1 using a figure-of-eight-shaped coil (70 mm diameter) positioned tangentially 45° from midline. Stroke survivors were asked to remain static while determining the optimal scalp position (i.e., "hotspot") for eliciting maximal responses in the FDI (Ding et al., 2018). RMT was determined experimentally as the lowest stimulation intensity that produced MEP greater than 50 μV in at least 50% of consecutive stimulations at rest (Chen et al., 1998). A neuronavigation system (Visor2, ANT Neuro, Hengelo, Netherlands) was used to ensure reliable and consistent coil positioning over the "hotspot" throughout the experiment (Ding et al., 2021a).

Intermittent theta burst stimulation was applied over the "hotspot." During the application of iTBS, stroke survivors were asked to remain static. As 40% maximum stimulator output (MSO) is the upper limit for iTBS with the NS5000 Magnetic Stimulator, stimulation intensity was set at 40% MSO for iTBS if the calculated stimulation intensity was greater than 40% MSO (i.e., for those whose RMT was greater than 57% MSO). For sham stimulation, the same stimulation intensity was used as for iTBS, and the TMS coil was held perpendicular to the

TABLE 1 | Patients' demographic and clinical characteristics.

	Age, years	Sex	Paretic side	Type of stroke	Months after stroke onset	UE FMA (0–66)	ARAT (0–57)
	Mean ± SD (range)	Male/ Female	Right/ Left	Ischemic/ Hemorrhagic	Mean ± SD (range)	Mean ± SD (range)	Mean ± SD (range)
Active iTBS group (*N* = 15)	65.1 ± 11.9 (35–85)	12/3	5/10	12/3	3.9 ± 3.0 (1–11)	28.0 ± 19.8 (4–62)	26.1 ± 20.9 (0–56)
Sham iTBS group (*N* = 15)	61.1 ± 12.1 (35–79)	9/6	7/8	12/3	4.0 ± 4.4 (1–18)	25.1 ± 18.8 (4–64)	21.8 ± 22.2 (0–57)

UE FMA refers to upper-extremity component of the Fugl-Meyer Motor Function Assessment, indicating motor impairments in stroke survivors (Fugl-Meyer et al., 1975). ARAT refers to Action Research Arm Test, indicating upper extremity performance (i.e., coordination and dexterity) in neurological populations (Lang et al., 2006). SD refers to standard deviation. No significant difference in chronicity, UE FMA, or ARAT was revealed between subjects in Active and Sham iTBS groups.

TABLE 2 | Stroke characteristics.

Subject number	Sex	Age (years)	Paretic hand	Chronicity (months)	Type of stroke	Lesion location	UE FMA	RMT (%MSO)
Stroke 01	M	62	R	4	Ischemic	Basal ganglia	10	100
Stroke 02	M	70	L	8	Ischemic	Pons	37	70
Stroke 03	M	57	R	8	Hemorrhagic	Frontal/parietal lobe	47	55
Stroke 04	M	70	L	2	Ischemic	Basal ganglia, corona radiata	14	100
Stroke 05	F	85	L	1	Ischemic	Basal ganglia	62	55
Stroke 06	F	66	R	1	Ischemic	Frontal/temporal/parietal lobe	4	100
Stroke 07	M	77	L	1	Ischemic	Centrum semiovale, corona radiata, basal ganglia	58	70
Stroke 08	F	35	L	5	Ischemic	Frontal/parietal lobe	49	100
Stroke 09	M	69	R	11	Ischemic	Corona radiata	18	100
Stroke 10	M	46	L	5	Hemorrhagic	Posterior horn of lateral ventricle	27	100
Stroke 11	M	72	R	1	Hemorrhagic	Parietal/temporal lobe	47	40
Stroke 12	M	62	L	2	Ischemic	Pons	26	50
Stroke 13	M	63	L	6	Ischemic	Basal ganglia, corona radiata, centrum semiovale	12	100
Stroke 14	M	75	L	4	Ischemic	Pons	5	100
Stroke 15	M	67	L	2	Ischemic	Frontal/temporal/parietal lobe	4	100
Stroke C01	F	65	R	7	Ischemic	Basal ganglia, corona radiata	8	100
Stroke C02	M	69	R	2	Ischemic	Basal ganglia	28	80
Stroke C03	F	70	L	2	Ischemic	Basal ganglia, corona radiata, frontal lobe	45	100
Stroke C04	M	42	L	6	Hemorrhagic	Pons	21	100
Stroke C05	F	79	R	2	Ischemic	Thalamus/occipital lobe	36	40
Stroke C06	M	60	R	9	Ischemic	Frontal/parietal/temporal lobe	4	100
Stroke C07	M	43	L	1	Ischemic	Frontal/parietal lobe, basal ganglia, corona radiata	64	20
Stroke C08	M	67	L	2	Ischemic	Frontal/parietal/temporal lobe	4	100
Stroke C09	F	64	R	2	Hemorrhagic	Basal ganglia	12	50
Stroke C10	M	64	L	1	Ischemic	Corona radiata, basal ganglia, thalamus	49	78
Stroke C11	M	72	L	2	Ischemic	Basal ganglia, periventricular white matter	46	80
Stroke C12	F	64	R	3	Ischemic	Frontal/temporal/parietal lobe	4	100
Stroke C13	M	70	R	3	Ischemic	Basal ganglia	28	75
Stroke C14	M	35	L	18	Hemorrhagic	Basal ganglia	24	100
Stroke C15	F	52	L	1	Ischemic	Corona radiata	4	100

UE FMA refers to upper-extremity component of the Fugl-Meyer Motor Function Assessment. M refers to male, and F refers to female. L refers to left, and R refers to right. RMT refers to resting motor thresholds in the ipsilesional hemisphere. MSO refers to maximum stimulator output. "RMT = 100" indicates that MEPs were unable to be elicited in the paretic hand. Stroke 1–15 indicate subjects in the Active iTBS group. Stroke C1-15 indicate subjects in the Sham iTBS group.

skull, touching the skull with the rim opposite the handle (Nettekoven et al., 2014).

Electroencephalography (EEG)

Electroencephalography Acquisition

Resting-state EEG was recorded at baseline and immediately after iTBS. During EEG recording, participants were seated comfortably in a sound-shielded, dimly lit room with eyes closed, which lasted for 6 min. EEG signals were recorded using a TMS-compatible EEG cap (ANT Neuro, Enschede, Netherlands) with 64 Ag/AgCl electrodes in a layout based on the extended international 10–20 system for electrodes placement (Jurcak et al., 2007; Tamburro et al., 2020). All channels were referenced online to CPz and amplified with an eego amplifier (ANT Neuro, Enschede, Netherlands). Data were sampled at 2,048 Hz with impedances kept below 10 kΩ for all channels throughout data collection.

Electroencephalography Analysis

Acquired EEG signals were analyzed off-line using MATLAB2019b (MathWorks, Inc., Natick, MA, United States). EEGLAB toolbox (version 14.1.2b) was used for EEG data preprocessing (Delorme and Makeig, 2004). After the raw data were imported into EEGLAB, the signals were sampled down to 1,000 Hz. Then, the EEG signals were filtered with a band-pass filter with cut-off values ranging from 0.1 to 40 Hz and segmented in epochs lasting 2,000 ms. The independent component analysis (ICA) was then performed to exclude components endowing eye (blink and movement), cardiac, and muscular artifacts. The resulting data was inspected to exclude remaining "bad trials" (i.e., amplitudes >100 μV) and re-referenced using the average signals of every scalp electrode as reference.

Power and functional connectivity analyses were conducted using customed MATLAB scripts. Absolute power (μV^2) was calculated by fast Fourier transform and averaged in four frequency bands: delta (1–4 Hz), theta (4–8 Hz), alpha (8–13 Hz), beta (13–30 Hz). As we were interested in assessing cortical activity in bilateral sensorimotor cortices, the averaged power of the electrodes in the cluster of EEG electrodes around C3 and C4 (Left sensorimotor cortex: C1, C3, C5, CP1, CP3, CP5, FC1, FC3, FC5; Right sensorimotor cortex: C2, C4, C6, CP2,

CP4, CP6, FC2, FC4, FC6) was calculated for statistical analysis (Bayram et al., 2015).

Coherence was calculated using customed MATLAB scripts to indicate functional connectivity between bilateral sensorimotor cortices. The Welch's averaged, modified periodogram method (Welch, 1967), was performed to calculate the squared coherence between each pair of electrodes in four frequency bands. All connectivity matrices were Fisher's z-transformed (Arun et al., 2020) to the set of Gaussian distributed values and the z scores were used for further analysis. As we were interested in assessing interhemispheric functional connectivity, the averaged z-scores of each pair of electrodes between sensorimotor cortices were calculated for statistical analysis.

GRaph thEoretical Network Analysis (GRETNA) toolbox was used for graph theory analysis (Wang et al., 2015). In general, a graph is based on a set of nodes. The connections between these nodes are edges, which form the brain network. In present study, weighted and undirected networks were built based on coherence (Vecchio et al., 2019). Since there was no definite method for selecting a single threshold, we integrated the metrics over the entire threshold range (i.e., 0.1–0.4, with an interval of 0.05) to obtain the area under the curve (AUC) to characterize the brain network (Wang et al., 2015; Yan et al., 2017). Global efficiency is the average of interregional efficiency between every pair of brain region over the entire brain, which characterizes information transferring ability in the entire brain network (G) (Park et al., 2014). It can be computed as the average of nodal efficiency across all nodes of the brain network:

$$E_{global}(G) = \frac{1}{N(N-1)} \sum_{j \neq i \in G} \frac{1}{D(i,j)}$$

where D(i, j) is the shortest path length between node i and node j, and N is the number of nodes in the brain network.

Statistical Analysis

All statistical analyses were performed in JMP Pro Version 13.2 (SAS Institute Inc., Cary, NC, United States). Linear mixed effects (LME) modeling was performed to test differential changes in EEG power, coherence and global efficiency after iTBS between groups. Group, Timepoint, and Group×Timepoint interaction were included as fixed effects, and subject was included as a random effect. Timepoint was set as repeated covariance structure. Normality of the residuals was visually assessed for each model with conditional residual quantile-quantile plots, and all were found to reasonably conform to the assumption of normality. *Post hoc* tests were performed when *F*-tests were significant. Multiple comparisons between Timepoints or Groups were performed with Tukey-Kramer adjustment.

Data were found to meet the normality assumption using the Kolmogorov-Smirnov test. Pearson correlations were performed to investigate the relationship between baseline and changes in neurophysiological measures (e.g., EEG power, coherence, and global efficiency) and patients characteristics (e.g., age, chronicity, FMA, and ARAT). For all analyses, the statistical significance was set at $P < 0.05$.

RESULTS

All subjects tolerated iTBS well with no adverse events reported. Individual values of RMT in the ipsilesional hemisphere were presented in **Table 2**. Of note, RMT was presented as 100% MSO for the individuals in whom MEP was not elicitable in the paretic hand. The averaged RMT in the Active and Sham iTBS groups was 82.7% MSO (SD = 22.3) and 81.5% MSO (SD = 24.9), respectively. The averaged stimulation intensity for iTBS in the Active and Sham iTBS groups was 38.7% MSO (SD = 3.1) and 37.1% MSO (SD = 6.9), respectively. There was no significant difference in RMT or stimulation intensity for iTBS between groups ($P = 0.900$ and 0.457, respectively).

Electroencephalography Power

The LME modeling did not reveal any significant Group×Timepoint interaction in EEG power in the ipsilesional [$F_{(1,28)} = 0.02$, $P = 0.893$; $F_{(1,28)} = 1.59$, $P = 0.218$; $F_{(1,28)} = 0.64$, $P = 0.429$; $F_{(1,28)} = 0.70$, $P = 0.409$] or contralesional [$F_{(1,28)} = 0.40$, $P = 0.534$; $F_{(1,28)} = 1.79$, $P = 0.192$; $F_{(1,28)} = 0.10$, $P = 0.753$; $F_{(1,28)} = 0.14$, $P = 0.707$] hemisphere in the delta, theta, alpha or beta band, respectively.

Coherence

In the delta band, results of LME modeling revealed significant Group×Timepoint interaction [$F_{(1,28)} = 5.03$, $P = 0.033$]. *Post hoc* revealed that in the Active iTBS group, coherence was significantly increased after iTBS compared with baseline ($P = 0.038$), while there was no significant change in coherence over time in the Sham iTBS group ($P = 0.327$) (**Figure 1**).

In the theta band, results of LME modeling revealed significant Group×Timepoint interaction [$F_{(1,28)} = 6.75$, $P = 0.015$]. *Post hoc* revealed that in the Active iTBS group, coherence was significantly increased after iTBS compared with baseline ($P = 0.011$), while there was no significant change in coherence over time in the Sham iTBS group ($P = 0.342$) (**Figure 2**).

In the beta band, results of LME modeling revealed significant main effect of Timepoint [$F_{(1,28)} = 6.38$, $P = 0.018$], but there was no significant Group×Timepoint interaction [$F_{(1,28)} = 3.25$, $P = 0.082$], suggesting coherence was increased after iTBS in both groups without group differences (**Figure 3**).

In the alpha band, the LME modeling did not reveal significant Group×Timepoint interaction [$F_{(1,28)} = 0.38$, $P = 0.544$].

Global Efficiency

In the delta band, results of LME modeling revealed significant Group×Timepoint interaction [$F_{(1,28)} = 5.11$, $P = 0.032$]. *Post hoc* revealed that in the Active iTBS group, global efficiency was significantly increased after iTBS compared with baseline ($P = 0.013$), while there was no significant change in global efficiency over time in the Sham iTBS group ($P = 0.586$) (**Figures 4A–C**).

In the beta band, results of LME modeling revealed significant main effect of Timepoint [$F_{(1,28)} = 8.54$, $P = 0.007$] and Group×Timepoint interaction [$F_{(1,28)} = 8.06$, $P = 0.008$]. *Post hoc* revealed that global efficiency was significantly increased after iTBS compared with baseline in the Active iTBS group

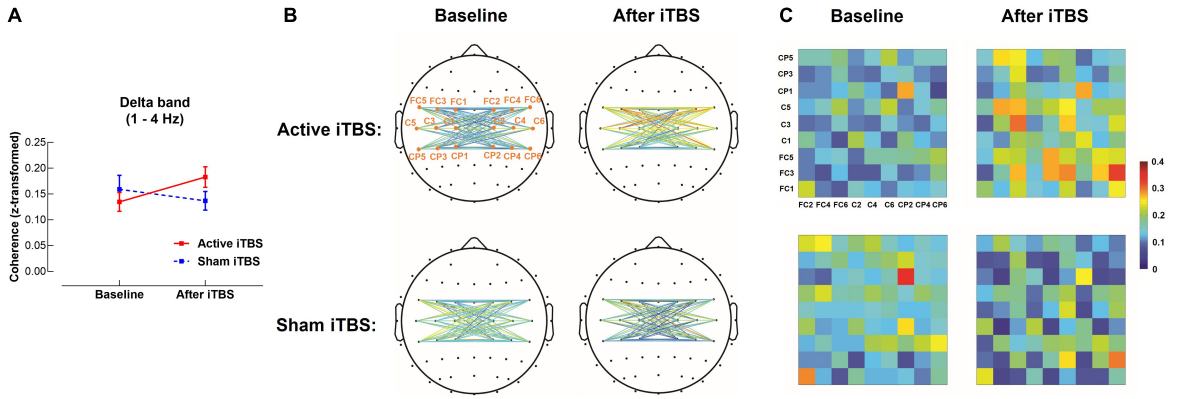

FIGURE 1 | Delta band interhemispheric functional connectivity change after iTBS. Delta band coherence between left and right sensorimotor cortices was significantly increased in the Active iTBS group, but not in the Sham iTBS group after iTBS **(A)**. The topographies **(B)** and matrixes **(C)** represent z-scores of coherences between pairs of electrodes in the left and right sensorimotor cortices before and after iTBS in the Active and Sham iTBS groups. Warmer colors indicate greater coherence, while cooler colors indicate less coherence.

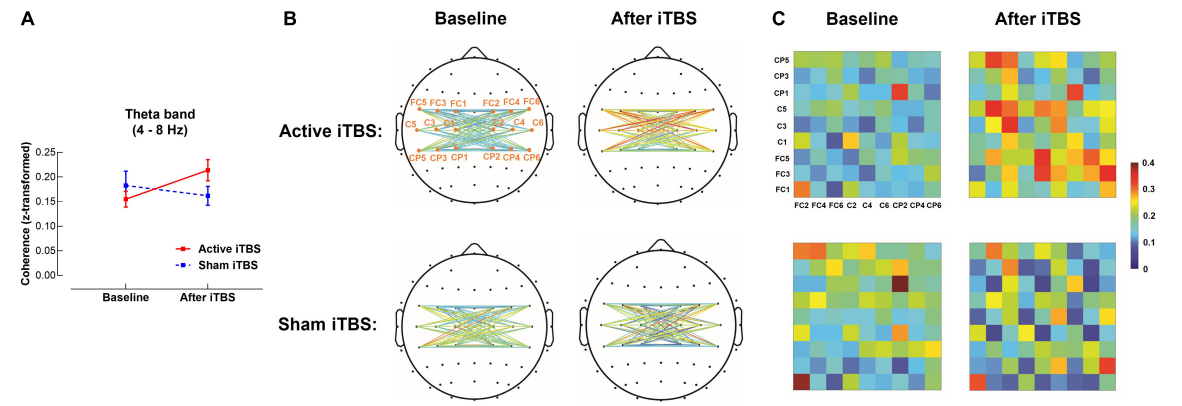

FIGURE 2 | Theta band interhemispheric functional connectivity change after iTBS. Theta band coherence between left and right sensorimotor cortices was significantly increased in the Active iTBS group, but not in the Sham iTBS group after iTBS **(A)**. The topographies **(B)** and matrixes **(C)** represent z-scores of coherences between pairs of electrodes in the left and right sensorimotor cortices before and after iTBS in the Active and Sham iTBS groups. Warmer colors indicate greater coherence, while cooler colors indicate less coherence.

($P < 0.001$), while there was no significant change in global efficiency over time in the Sham iTBS group ($P = 0.954$) (**Figures 4D–F**).

In the theta and alpha band, the LME modeling did not reveal any significant Group×Timepoint interaction [$F_{(1,28)} = 3.08$, $P = 0.090$; $F_{(1,28)} = 2.19$, $P = 0.150$, respectively].

Correlation Analysis

No significant correlation was observed between neurophysiological measures (i.e., EEG power, coherence and global efficiency) and subject characteristics (i.e., age, chronicity, FMA, and ARAT).

DISCUSSION

In this study, we measured resting-state EEG at baseline and immediately after iTBS applied over ipsilesional M1 in stroke survivors. To the best of our knowledge, this is the first study that used resting-state EEG to investigate the aftereffects of iTBS in stroke survivors. Our primary findings are: (1) interhemispheric functional connectivity was significantly increased after iTBS; (2) global efficiency was significantly increased after iTBS; and (3) no significant change in EEG power was observed after iTBS.

Interhemispheric Functional Connectivity

We observed an increase in delta and theta bands coherence between bilateral sensorimotor cortices after iTBS, indicating increased interhemispheric functional connectivity after iTBS. The acute effects of iTBS on functional connectivity have not been investigated in stroke survivors, but it has been investigated in healthy adults (Nettekoven et al., 2014; Hoy et al., 2016). Our results are in line with Hoy et al.'s (2016) study that reported increased interhemispheric functional connectivity in theta band after iTBS in healthy adults. Similarly, an fMRI study (Nettekoven et al., 2014) also reported an increase in functional connectivity

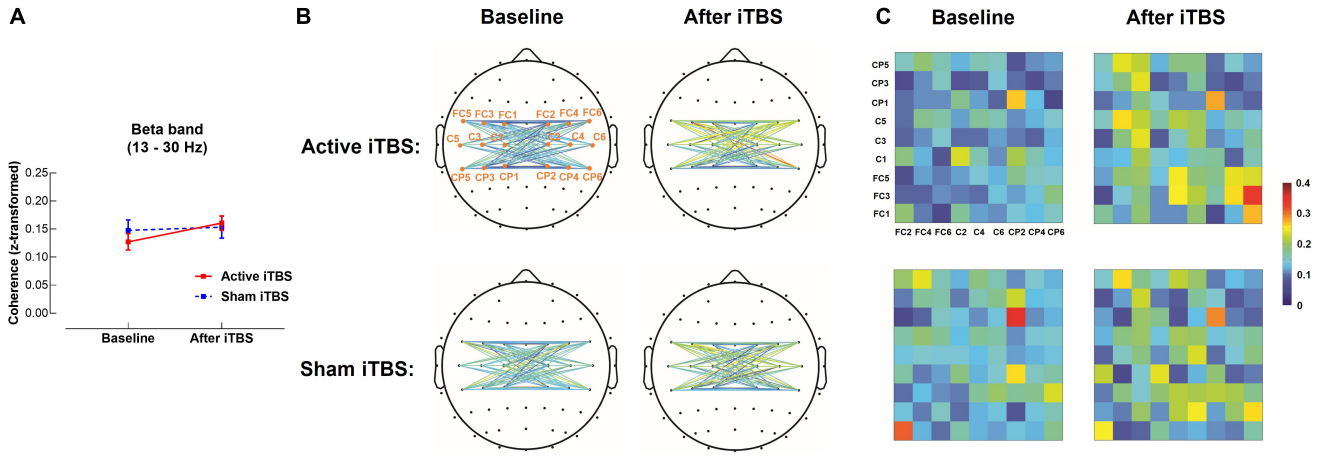

FIGURE 3 | Beta band interhemispheric functional connectivity change after iTBS. Beta band coherence between left and right sensorimotor cortices was significantly increased after Active or Sham iTBS in all subjects without significant group differences **(A)**. The topographies **(B)** and matrixes **(C)** represent z-scores of coherences between pairs of electrodes in the left and right sensorimotor cortices before and after iTBS in the Active and Sham iTBS groups. Warmer colors indicate greater coherence, while cooler colors indicate less coherence.

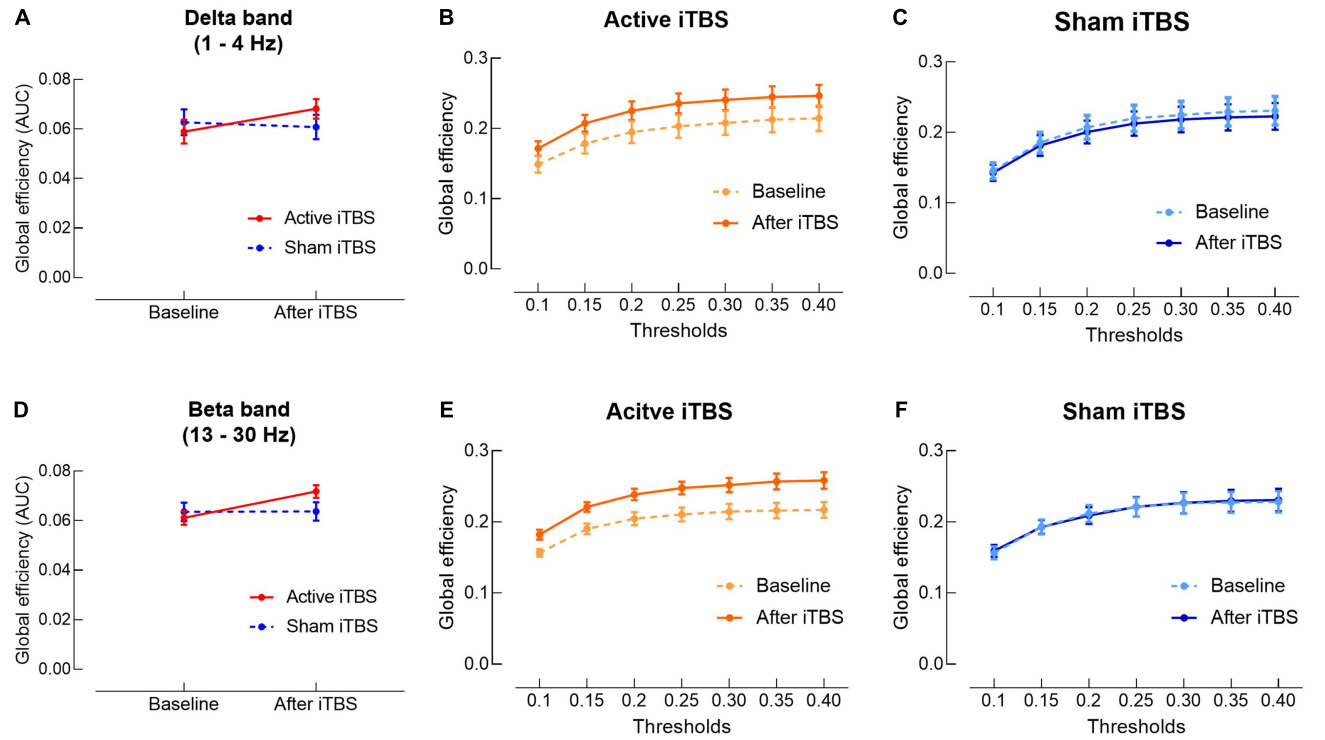

FIGURE 4 | Delta and beta bands global efficiency change after iTBS. Delta **(A)** and beta **(D)** bands global efficiency (area under the curves) were significantly increased in the Active iTBS group, but not in the Sham iTBS group after iTBS. **(B,C)** Delta band global efficiency at each threshold in the Active and Sham iTBS groups, respectively. **(E,F)** Beta band global efficiency at each threshold in the Active and Sham iTBS groups, respectively.

between bilateral sensorimotor areas after the application of iTBS on M1 in healthy adults. Despite different methodology among studies, our current study for the first time extends these findings from healthy adults to stroke population, suggesting that iTBS produces similar effects on interhemispheric functional connectivity in stroke survivors and healthy adults.

Neural mechanisms underlying the increase in interhemispheric functional connectivity after iTBS in stroke survivors remain unclear, which possibly relates to the simultaneous induction of neural activity in the whole motor network during the application of iTBS (Nettekoven et al., 2014). It has been reported that rTMS-induced changes

in cortical activity are not exclusively local, but also extending to remote, interconnected regions (Bestmann et al., 2004; Suppa et al., 2008; Cardenas-Morales et al., 2014). As bilateral sensorimotor cortices are interconnected by transcallosal fibers, iTBS applied on ipsilesional M1 would induce simultaneous activation in the contralesional sensorimotor cortex (Nettekoven et al., 2014). The simultaneous activation of bilateral sensorimotor cortices would contribute to an increase in the coherence of brain activity that represents an important neurophysiological mechanism enforcing communication between the interconnected brain regions via transcallosal connections, and thus increases interhemispheric functional connectivity (Fries, 2005; Di Lazzaro et al., 2008).

Interestingly, beta band coherence was increased in both Active and Sham iTBS groups without significant group difference, suggesting changes in beta band coherence might not relate to neural effects of iTBS but result from other confounding factors such as the noise of iTBS click (Fuggetta et al., 2008). An increase in beta band coherence was also reported after sham rTMS in healthy adults (Fuggetta et al., 2008). The increased beta band coherence after sham rTMS may be caused by a cumulative effect of the rapid sequency of auditory TMS-click sounds produced during the application of rTMS (Fuggetta et al., 2008). Some neuroimaging studies (Bestmann et al., 2004; Takano et al., 2004) suggested that TMS clicks induce activations of the auditory systems and influence cerebral blood flow and synaptic activity in the brain regions interconnected with the auditory systems, which possibly influences beta band coherence between bilateral sensorimotor cortices. Collectively, external influences on cortical oscillations due to concomitant auditory stimulation need to be carefully controlled in TMS studies (Fuggetta et al., 2008).

Global Efficiency

We observed an increase in delta and beta bands global efficiency after iTBS. Acute changes in global efficiency induced by iTBS or high frequency rTMS have not been investigated in stroke survivors. Park et al. (2014) investigated acute changes in global efficiency after high frequency rTMS in healthy adults. No significant change in global efficiency was observed in the whole sample, but the authors reported an increase in global efficiency in individuals with behavioral facilitation after rTMS (Park et al., 2014). In our current study, we observed an increase in global efficiency after iTBS in the whole sample. The inconsistent results between Park et al.'s (2014) and our study may result from differences in subjects' characteristics (i.e., healthy adults in Park et al.'s (2014) study vs. stroke survivors in ours) and experimental methodology. For example, Park et al. (2014) used 10 Hz rTMS, while we used iTBS in the present study. As the neural effects produced by iTBS have been suggested to be stronger than traditional rTMS (Fuggetta et al., 2008), it is reasonable to speculate that increase in global efficiency is possibly more robust after iTBS compared with 10 Hz rTMS.

The mechanisms for the increase in global efficiency after iTBS has not been fully elucidated. It has been suggested that iTBS induces long-term potentiation (LTP)-like changes at synaptic connections (Huang et al., 2007), and would increase efficiency of synaptic transmission in both local and remote brain regions from the stimulation site (Philips et al., 2017). Furthermore, iTBS causes simultaneous activation in the interconnected brain regions which increases neural synchrony in the global brain network (Di Lazzaro et al., 2008). Therefore, iTBS possibly facilitates global information exchange and thus increases global efficiency.

Electroencephalography Power

We did not observe any change in EEG power after iTBS. Although there was no stroke study investigating aftereffects of rTMS (including iTBS) on EEG power, our results are in line with studies conducted in healthy adults, which reported no change in EEG power after iTBS (Hoy et al., 2016) or high frequency rTMS (Oliviero et al., 2003; Fuggetta et al., 2008); however, increased EEG power after high frequency rTMS has also been reported (Azila Noh and Fuggetta, 2012). These conflicting results may be due to the different methodological details among studies. For example, 10 Hz rTMS was applied in Azila Noh and Fuggetta (2012) study, while 5 Hz rTMS was applied in Oliviero et al.'s (2003) and Fuggetta et al.'s (2008) studies. These results suggest that different types of rTMS might influence its effect on EEG power.

Clinical Implications

This study for the first time used EEG to investigate the aftereffects of iTBS following stroke. Our results revealed increased interhemispheric functional connectivity and global efficiency after iTBS in stroke survivors. Dynamics of functional brain network has been suggested to be altered following stroke due to focal brain lesions (Vecchio et al., 2019). Normal functioning of brain network (i.e., interhemispheric functional connectivity and global efficiency) plays an important role in recovery of motor performance following stroke.

Interhemispheric functional connectivity has been suggested to play a supportive role in motor recovery following stroke (Rehme et al., 2011). van Meer et al. (2010) reported that impaired motor function acutely after experimental stroke in rats was related to partial loss of interhemispheric functional connectivity, and interhemispheric functional connectivity was increased subsequently concomitant to motor recovery. In humans, reduced interhemispheric functional connectivity was also observed acutely after stroke (Philips et al., 2017; Desowska and Turner, 2019; Hoshino et al., 2020; Li et al., 2020). It has been reported that the increase in interhemispheric functional connectivity was associated with motor improvements in stroke survivors, and restoration of interhemispheric functional connectivity was noted only in well recovered individuals, but not in the poorly recovered stroke survivors (Golestani et al., 2013; Desowska and Turner, 2019; Hoshino et al., 2020; Li et al., 2020), suggesting that interhemispheric functional connectivity is a potential biomarker indicating stroke recovery (Caliandro et al., 2017; Philips et al., 2017; Vecchio et al., 2019). Increase in interhemispheric functional connectivity after iTBS observed in our current study provides evidence that iTBS could normalize brain network functioning in stroke survivors.

Global efficiency exhibits the efficiency in transporting information at a global scale between genetic brain areas (Vecchio et al., 2019). Increased global efficiency after iTBS suggests alterations in how efficiently information is transferred over the brain, reflecting an acute shift of the brain state induced by iTBS (Park et al., 2014). Reduced global efficiency indicates lower efficiency in global information flow, which has been suggested to be related to motor deficits associated with aging (Park et al., 2012) or neurological conditions such as stroke (Philips et al., 2017). Contrary to the brain state of motor deficits, increased efficiency in global information flow could reflect the brain state of intact or enhanced motor function (Park et al., 2014). Therefore, the shift of brain state toward an emphasis on global information exchange after iTBS suggests that iTBS has the potential to be utilized in stroke rehabilitation.

The influence of stroke characteristics (e.g., chronicity, motor impairment, age, etc.) on the effects of iTBS is less clear. In present study, no significant correlation observed between clinical characteristics and neurophysiological measures was observed. Our results suggest that the effects of iTBS on functional brain network were not influenced by stroke characteristics. As our sample size is small (N = 30), cautions are needed when interpreting these results. Further studies with larger sample sizes are still needed to investigate how the heterogeneity of stroke survivors influences the effects of iTBS.

Limitations

As a pilot study, the sample size of current study is small (N = 30). Chronicity of stroke survivors in current study ranged from 1 to 18 months, so cautions are needed when generalizing our findings to more chronic stroke survivors. Chronicity of stroke survivors was not evenly distributed in our sample, and most subjects were within 3 months post-stroke. Therefore, we did not perform subgroup analysis for chronicity. Further research is required to test our results in stroke survivors with a wider range of chronicity with larger sample sizes and to perform subgroup analysis for individuals in acute, subacute and chronic phases of stroke.

Our current study only measured resting-state EEG for 6 min immediately after iTBS without a follow-up. We understand that it would be more meaningful to measure EEG at multiple time points after iTBS. However, it has already been a long experiment for stroke survivors, and many subjects could not tolerate for a longer time of data collection. Further studies are needed to monitor changes in EEG at multiple time points after iTBS.

Another limitation is that sex of stroke survivors was not very balanced between groups with 12 males in the Active iTBS group vs. 9 males in the Sham iTBS group. To the best of our knowledge, no previous study has reported sex difference in the aftereffects of TBS. There was a tDCS study (Kuo et al., 2006) reporting sex differences in the aftereffects of cathodal (i.e., inhibitory) but not anodal (i.e., excitatory) tDCS due to changes in ovarian hormones over the menstrual cycle. In current study, most female subjects (8 out of 9) were postmenopausal women. Those postmenopausal women did not have a menstrual cycle, so they were less likely to be influenced by changes in ovarian hormones. Although it is still unclear whether sex influences aftereffects of iTBS, our results are unlikely to be attributed to sex difference. Further studies are still needed to investigate sex difference in the aftereffects of iTBS.

In this study, 40% MSO was the upper limit for iTBS with the TMS machine. We set the stimulation intensity of iTBS at 40% MSO if the calculated stimulation intensity (i.e., 70% RMT) was greater than 40% MSO. Therefore, the actual stimulation intensity of iTBS was lower than the calculated stimulation intensity for those whose RMT was greater than 57% MSO. In 11 out of 15 subjects in the Active iTBS group, RMT was greater than 57% MSO. We acknowledge that the relatively lower stimulation intensity of iTBS for subjects with high RMT is a limitation of current study. However, as higher stimulation intensity may produce stronger neurophysiological effects, neuroplastic changes observed in current study were induced by relatively lower stimulation intensity, suggesting that the neuroplastic changes observed in current study were robust.

Conclusion

Ours is the first study that used EEG to investigate the aftereffects of iTBS on functional brain network in stroke survivors. This study for the first time provides evidence that iTBS modulates functional brain network in stroke survivors. Our results revealed an increase in interhemispheric functional connectivity and global efficiency after iTBS, suggesting that iTBS has the potential to normalize brain network functioning following stroke, which can be utilized in stroke rehabilitation.

DATA AVAILABILITY STATEMENT

The raw data supporting the conclusions of this article will be made available by the authors, without undue reservation.

ETHICS STATEMENT

The studies involving human participants were reviewed and approved by the Guangzhou First People's Hospital Human Research Ethics Committee. The patients/participants provided their written informed consent to participate in this study.

AUTHOR CONTRIBUTIONS

YL, GX, and QD designed the experiment. JiC and YP recruited the participants. QD, SZ, SC, XL, JuC, YC, and KC conducted the experiments. QD, SZ, GC, and JiC reduced and analyzed the data. QD and SZ interpreted the data. QD, SZ, and YL wrote the manuscript. All authors contributed to the article and approved the submitted version.

FUNDING

This work was supported by the National Key R&D Program of China [grant number 2017YFB1303200 (YL)]; National Natural Science Foundation of China [grant numbers 81772438 (YL), 81974357 (YL), 82072548 (GX), and 82102678 (QD)]; the Guangzhou Municipal Science and Technology

Program [grant number 201803010083 (YL)]; Guangdong Basic and Applied Basic Research Foundation [grant number 2020A1515110761 (QD)]; and Guangzhou Postdoctoral Science Foundation (QD).

ACKNOWLEDGMENTS

We would like to thank all our participants for their interest and time investment.

REFERENCES

Ackerley, S. J., Stinear, C. M., Barber, P. A., and Byblow, W. D. (2010). Combining theta burst stimulation with training after subcortical stroke. *Stroke* 41, 1568–1572. doi: 10.1161/STROKEAHA.110.583278

Arun, K. M., Smitha, K. A., Sylaja, P. N., and Kesavadas, C. (2020). Identifying resting-state functional connectivity changes in the motor cortex using fNIRS during recovery from stroke. *Brain Topogr.* 33, 710–719. doi: 10.1007/s10548-020-00785-2

Azila Noh, N., and Fuggetta, G. (2012). Human cortical theta reactivity to high-frequency repetitive transcranial magnetic stimulation. *Hum. Brain Mapp.* 33, 2224–2237. doi: 10.1002/hbm.21355

Bayram, M. B., Siemionow, V., and Yue, G. H. (2015). Weakening of corticomuscular signal coupling during voluntary motor action in aging. *J. Gerontol. A Biol. Sci. Med. Sci.* 70, 1037–1043. doi: 10.1093/gerona/glv014

Bestmann, S., Baudewig, J., Siebner, H. R., Rothwell, J. C., and Frahm, J. (2004). Functional MRI of the immediate impact of transcranial magnetic stimulation on cortical and subcortical motor circuits. *Eur. J. Neurosci.* 19, 1950–1962. doi: 10.1111/j.1460-9568.2004.03277.x

Caliandro, P., Vecchio, F., Miraglia, F., Reale, G., Della Marca, G., La Torre, G., et al. (2017). Small-World characteristics of cortical connectivity changes in acute stroke. *Neurorehabil. Neural Repair* 31, 81–94. doi: 10.1177/1545968316662525

Cardenas-Morales, L., Volz, L. J., Michely, J., Rehme, A. K., Pool, E. M., Nettekoven, C., et al. (2014). Network connectivity and individual responses to brain stimulation in the human motor system. *Cereb. Cortex* 24, 1697–1707. doi: 10.1093/cercor/bht023

Casarotto, S., Romero Lauro, L. J., Bellina, V., Casali, A. G., Rosanova, M., Pigorini, A., et al. (2010). EEG responses to TMS are sensitive to changes in the perturbation parameters and repeatable over time. *PLoS One* 5:e10281. doi: 10.1371/journal.pone.0010281

Chen, R., Tam, A., Butefisch, C., Corwell, B., Ziemann, U., Rothwell, J. C., et al. (1998). Intracortical inhibition and facilitation in different representations of the human motor cortex. *J. Neurophysiol.* 80, 2870–2881. doi: 10.1152/jn.1998.80.6.2870

Corti, M., Patten, C., and Triggs, W. (2012). Repetitive transcranial magnetic stimulation of motor cortex after stroke: a focused review. *Am. J. Phys. Med. Rehabil.* 91, 254–270. doi: 10.1097/PHM.0b013e318228bf0c

Delorme, A., and Makeig, S. (2004). EEGLAB: an open source toolbox for analysis of single-trial EEG dynamics including independent component analysis. *J. Neurosci. Methods* 134, 9–21. doi: 10.1016/j.jneumeth.2003.10.009

Desowska, A., and Turner, D. L. (2019). Dynamics of brain connectivity after stroke. *Rev. Neurosci.* 30, 605–623. doi: 10.1515/revneuro-2018-0082

Di Lazzaro, V., Pilato, F., Dileone, M., Profice, P., Oliviero, A., Mazzone, P., et al. (2008). The physiological basis of the effects of intermittent theta burst stimulation of the human motor cortex. *J. Physiol.* 586, 3871–3879. doi: 10.1113/jphysiol.2008.152736

Ding, Q., Lin, T., Wu, M., Yang, W., Li, W., Jing, Y., et al. (2021b). Influence of iTBS on the acute neuroplastic change after BCI training. *Front. Cell. Neurosci.* 15:653487. doi: 10.3389/fncel.2021.653487

Ding, Q., Cai, H., Wu, M., Cai, G., Chen, H., Li, W., et al. (2021a). Short intracortical facilitation associates with motor-inhibitory control. *Behav. Brain Res.* 407:113266, doi: 10.1016/j.bbr.2021.113266

Ding, Q., Triggs, W. J., Kamath, S. M., and Patten, C. (2018). Short intracortical inhibition during voluntary movement reveals persistent impairment post-stroke. *Front. Neurol.* 9:1105. doi: 10.3389/fneur.2018.01105

Fries, P. (2005). A mechanism for cognitive dynamics: neuronal communication through neuronal coherence. *Trends. Cogn. Sci.* 9, 474–480. doi: 10.1016/j.tics.2005.08.011

Fuggetta, G., Pavone, E. F., Fiaschi, A., and Manganotti, P. (2008). Acute modulation of cortical oscillatory activities during short trains of high-frequency repetitive transcranial magnetic stimulation of the human motor cortex: a combined EEG and TMS study. *Hum. Brain Mapp.* 29, 1–13. doi: 10.1002/hbm.20371

Fugl-Meyer, A. R., Jaasko, L., Leyman, I., Olsson, S., and Steglind, S. (1975). The post-stroke hemiplegic patient. 1. A method for evaluation of physical performance. *Scand. J. Rehabil. Med.* 7, 13–31.

Gentner, R., Wankerl, K., Reinsberger, C., Zeller, D., and Classen, J. (2008). Depression of human corticospinal excitability induced by magnetic theta-burst stimulation: evidence of rapid polarity-reversing metaplasticity. *Cereb. Cortex* 18, 2046–2053. doi: 10.1093/cercor/bhm239

Golestani, A. M., Tymchuk, S., Demchuk, A., Goodyear, B. G., and Group, V.-S. (2013). Longitudinal evaluation of resting-state FMRI after acute stroke with hemiparesis. *Neurorehabil. Neural Repair* 27, 153–163. doi: 10.1177/1545968312457827

Hankey, G. J. (2013). The global and regional burden of stroke. *Lancet Glob. Health* 1, e239–e240. doi: 10.1016/S2214-109X(13)70095-0

Hinder, M. R., Goss, E. L., Fujiyama, H., Canty, A. J., Garry, M. I., Rodger, J., et al. (2014). Inter- and Intra-individual variability following intermittent theta burst stimulation: implications for rehabilitation and recovery. *Brain Stimul.* 7, 365–371. doi: 10.1016/j.brs.2014.01.004

Hoshino, T., Oguchi, K., Inoue, K., Hoshino, A., and Hoshiyama, M. (2020). Relationship between lower limb function and functional connectivity assessed by EEG among motor-related areas after stroke. *Top. Stroke Rehabil.* 28, 614–623. doi: 10.1080/10749357.2020.1864986

Hoy, K. E., Bailey, N., Michael, M., Fitzgibbon, B., Rogasch, N. C., Saeki, T., et al. (2016). Enhancement of working memory and task-related oscillatory activity following intermittent theta burst stimulation in healthy controls. *Cereb. Cortex* 26, 4563–4573. doi: 10.1093/cercor/bhv193

Huang, Y. Z., Chen, R. S., Rothwell, J. C., and Wen, H. Y. (2007). The after-effect of human theta burst stimulation is NMDA receptor dependent. *Clin. Neurophysiol.* 118, 1028–1032. doi: 10.1016/j.clinph.2007.01.021

Huang, Y. Z., Edwards, M. J., Rounis, E., Bhatia, K. P., and Rothwell, J. C. (2005). Theta burst stimulation of the human motor cortex. *Neuron* 45, 201–206. doi: 10.1016/j.neuron.2004.12.033

Jurcak, V., Tsuzuki, D., and Dan, I. (2007). 10/20, 10/10, and 10/5 systems revisited: their validity as relative head-surface-based positioning systems. *Neuroimage* 34, 1600–1611. doi: 10.1016/j.neuroimage.2006.09.024

Kuo, M. F., Paulus, W., and Nitsche, M. A. (2006). Sex differences in cortical neuroplasticity in humans. *Neuroreport* 17, 1703–1707. doi: 10.1097/01.wnr.0000239955.68319.c2

Kwakkel, G., Kollen, B., and Lindeman, E. (2004). Understanding the pattern of functional recovery after stroke: facts and theories. *Restor. Neurol. Neurosci.* 22, 281–299.

Lang, C. E., Wagner, J. M., Dromerick, A. W., and Edwards, D. F. (2006). Measurement of upper-extremity function early after stroke: properties of the action research arm test. *Arch. Phys. Med. Rehabil.* 87, 1605–1610. doi: 10.1016/j.apmr.2006.09.003

Li, R., Li, S., Roh, J., Wang, C., and Zhang, Y. (2020). Multimodal neuroimaging using concurrent EEG/fNIRS for poststroke recovery assessment: an exploratory study. *Neurorehabil. Neural Repair* 34, 1099–1110. doi: 10.1177/1545968320969937

Nettekoven, C., Volz, L. J., Kutscha, M., Pool, E. M., Rehme, A. K., Eickhoff, S. B., et al. (2014). Dose-dependent effects of theta burst rTMS on cortical excitability and resting-state connectivity of the human motor system. *J. Neurosci.* 34, 6849–6859. doi: 10.1523/JNEUROSCI.4993-13.2014

Oliviero, A., Strens, L. H., Di Lazzaro, V., Tonali, P. A., and Brown, P. (2003). Persistent effects of high frequency repetitive TMS on the coupling between motor areas in the human. *Exp. Brain Res.* 149, 107–113. doi: 10.1007/s00221-002-1344-x

Park, C. H., Boudrias, M. H., Rossiter, H., and Ward, N. S. (2012). Age-related changes in the topological architecture of the brain during hand grip. *Neurobiol. Aging* 33, e827–e837. doi: 10.1016/j.neurobiolaging.2011.08.003

Park, C. H., Chang, W. H., Yoo, W. K., Shin, Y. I., Kim, S. T., and Kim, Y. H. (2014). Brain topological correlates of motor performance changes after repetitive transcranial magnetic stimulation. *Brain Connect.* 4, 265–272. doi: 10.1089/brain.2013.0187

Philips, G. R., Daly, J. J., and Principe, J. C. (2017). Topographical measures of functional connectivity as biomarkers for post-stroke motor recovery. *J. Neuroeng. Rehabil.* 14:67. doi: 10.1186/s12984-017-0277-3

Rehme, A. K., Eickhoff, S. B., Wang, L. E., Fink, G. R., and Grefkes, C. (2011). Dynamic causal modeling of cortical activity from the acute to the chronic stage after stroke. *Neuroimage* 55, 1147–1158. doi: 10.1016/j.neuroimage.2011.01.014

Rossi, S., Hallett, M., Rossini, P. M., Pascual-Leone, A., and Safety Of, T. M. S. C. G. (2009). Safety, ethical considerations, and application guidelines for the use of transcranial magnetic stimulation in clinical practice and research. *Clin. Neurophysiol.* 120, 2008–2039. doi: 10.1016/j.clinph.2009.08.016

Suppa, A., Huang, Y. Z., Funke, K., Ridding, M. C., Cheeran, B., Di Lazzaro, V., et al. (2016). Ten years of theta burst stimulation in humans: established knowledge, unknowns and prospects. *Brain Stimul.* 9, 323–335. doi: 10.1016/j.brs.2016.01.006

Suppa, A., Ortu, E., Zafar, N., Deriu, F., Paulus, W., Berardelli, A., et al. (2008). Theta burst stimulation induces after-effects on contralateral primary motor cortex excitability in humans. *J. Physiol.* 586, 4489–4500. doi: 10.1113/jphysiol.2008.156596

Takano, B., Drzezga, A., Peller, M., Sax, I., Schwaiger, M., Lee, L., et al. (2004). Short-term modulation of regional excitability and blood flow in human motor cortex following rapid-rate transcranial magnetic stimulation. *Neuroimage* 23, 849–859. doi: 10.1016/j.neuroimage.2004.06.032

Talelli, P., Greenwood, R. J., and Rothwell, J. C. (2007). Exploring theta burst stimulation as an intervention to improve motor recovery in chronic stroke. *Clin. Neurophysiol.* 118, 333–342. doi: 10.1016/j.clinph.2006.10.014

Tamburro, G., Di Fronso, S., Robazza, C., Bertollo, M., and Comani, S. (2020). Modulation of brain functional connectivity and efficiency during an endurance cycling task: a source-level eeg and graph theory approach. *Front. Hum. Neurosci.* 14:243. doi: 10.3389/fnhum.2020.00243

Tedesco Triccas, L., Meyer, S., Mantini, D., Camilleri, K., Falzon, O., Camilleri, T., et al. (2019). A systematic review investigating the relationship of electroencephalography and magnetoencephalography measurements with sensorimotor upper limb impairments after stroke. *J. Neurosci. Methods* 311, 318–330. doi: 10.1016/j.jneumeth.2018.08.009

van Meer, M. P., Van Der Marel, K., Wang, K., Otte, W. M., El Bouazati, S., Roeling, T. A., et al. (2010). Recovery of sensorimotor function after experimental stroke correlates with restoration of resting-state interhemispheric functional connectivity. *J. Neurosci.* 30, 3964–3972. doi: 10.1523/JNEUROSCI.5709-09.2010

Vecchio, F., Tomino, C., Miraglia, F., Iodice, F., Erra, C., Di Iorio, R., et al. (2019). Cortical connectivity from EEG data in acute stroke: a study via graph theory as a potential biomarker for functional recovery. *Int. J. Psychophysiol.* 146, 133–138. doi: 10.1016/j.ijpsycho.2019.09.012

Volz, L. J., Rehme, A. K., Michely, J., Nettekoven, C., Eickhoff, S. B., Fink, G. R., et al. (2016). shaping early reorganization of neural networks promotes motor function after stroke. *Cereb. Cortex* 26, 2882–2894. doi: 10.1093/cercor/bhw034

Wang, J., Wang, X., Xia, M., Liao, X., Evans, A., and He, Y. (2015). GRETNA: a graph theoretical network analysis toolbox for imaging connectomics. *Front. Hum. Neurosci.* 9:386. doi: 10.3389/fnhum.2015.00458

Welch, P. D. (1967). Use of fast fourier transform for estimation of power spectra–a method based on time averaging over short modified periodograms. *IEEE Trans. Audio Electroacoust.* 15, 70-73. doi: 10.1109/TAU.1967.1161901

Yan, T., Wang, W., Liu, T., Chen, D., Wang, C., Li, Y., et al. (2017). Increased local connectivity of brain functional networks during facial processing in schizophrenia: evidence from EEG data. *Oncotarget* 8, 107312–107322. doi: 10.18632/oncotarget.20598

Yu, F., Tang, X., Hu, R., Liang, S., Wang, W., Tian, S., et al. (2021). Corrigendum: the after-effect of accelerated intermittent theta burst stimulation at different session intervals. *Front. Neurosci.* 15:687972. doi: 10.3389/fnins.2021.687972

Conflict of Interest: The authors declare that the research was conducted in the absence of any commercial or financial relationships that could be construed as a potential conflict of interest.

Publisher's Note: All claims expressed in this article are solely those of the authors and do not necessarily represent those of their affiliated organizations, or those of the publisher, the editors and the reviewers. Any product that may be evaluated in this article, or claim that may be made by its manufacturer, is not guaranteed or endorsed by the publisher.

frontiers in Neuroscience

ORIGINAL RESEARCH
published: 26 October 2021
doi: 10.3389/fnins.2021.688569

Cerebellar Theta Burst Stimulation on Walking Function in Stroke Patients: A Randomized Clinical Trial

Yun-Juan Xie[1,2,3†], Qing-Chuan Wei[1,3†], Yi Chen[1,3], Ling-Yi Liao[1,3,4], Bao-Jin Li[1,3], Hui-Xin Tan[1,3], Han-Hong Jiang[1,3], Qi-Fan Guo[1,3] and Qiang Gao[1,3]*

[1] Department of Rehabilitation Medicine, West China Hospital, Sichuan University, Chengdu, China, [2] Department of Rehabilitation Medicine, The Third Affiliated Hospital, Sun Yat-sen University, Guangzhou, China, [3] Key Laboratory of Rehabilitation Medicine in Sichuan Province, West China Hospital, Sichuan University, Chengdu, China, [4] Daping Hospital, Third Military Medical University, Chongqing, China

Objectives: The objective of this study was to explore the efficacy of cerebellar intermittent theta burst stimulation (iTBS) on the walking function of stroke patients.

Methods: Stroke patients with walking dysfunction aged 25–80 years who had suffered their first unilateral stroke were included. A total of 36 patients [mean (SD) age, 53 (7.93) years; 10 women (28%)] were enrolled in the study. All participants received the same conventional physical therapy, including transfer, balance, and ambulation training, during admission for 50 min per day during 2 weeks (10 sessions). Every session was preceded by 3 min procedure of cerebellar iTBS applyed over the contralesional cerebellum in the intervention group or by a similar sham iTBS in control group. The groups were formed randomly and the baseline characteristics showed no significant difference. The primary outcome measure was Fugl–Meyer Assessment–Lower Extremity scores. Secondary outcomes included walking performance and corticospinal excitability. Measures were performed before the intervention beginning (T0), after the first (T1) and the second (T2) weeks.

Results: The Fugl–Meyer Assessment for lower extremity scores slightly improved with time in both groups with no significant difference between the groups and over the time. The walking performance significantly improved with time and between group. Two-way mixed measures ANOVA showed that there was significant interaction between time and group in comfortable walking time ($F_{2,68} = 6.5242$, $P = 0.0080$, $\eta^2_{partial} = 0.276$, $\varepsilon = 0.641$), between-group comparisons revealed significant differences at T1 ($P = 0.0072$) and T2 ($P = 0.0133$). The statistical analysis of maximum walking time showed that there was significant interaction between time and groups ($F_{2,68} = 5.4354$, $P = 0.0115$, $\eta^2_{partial} = 0.198$, $\varepsilon = 0.734$). Compared with T0, the differences of maximum walking time between the two groups at T1 ($P = 0.0227$) and T2 ($P = 0.0127$) were statistically significant. However, both the Timed up and go test and functional ambulation category scale did not yield significant differences between groups ($P > 0.05$).

Conclusion: Our results revealed that applying iTBS over the contralesional cerebellum paired with physical therapy could improve walking performance in patients after stroke,

OPEN ACCESS

Edited by:
Haoyong Yu,
National University of Singapore, Singapore

Reviewed by:
Elena Yu. Shapkova,
St. Petersburg Research Institute of Phthisiopulmonology, Russia
Pratik Yashvant Chhatbar,
Duke University, United States

****Correspondence:***
Qiang Gao
gaoqiang_hxkf@163.com

† These authors have contributed equally to this work

Specialty section:
This article was submitted to Neuroprosthetics, a section of the journal Frontiers in Neuroscience

Received: *31 March 2021*
Accepted: *05 October 2021*
Published: *26 October 2021*

Citation:
Xie YJ, Wei QC, Chen Y, Liao LY, Li BJ, Tan HX, Jiang HH, Guo QF and Gao Q (2021) Cerebellar Theta Burst Stimulation on Walking Function in Stroke Patients: A Randomized Clinical Trial. Front. Neurosci. 15:688569. doi: 10.3389/fnins.2021.688569

implying that cerebellar iTBS intervention may be a noninvasive strategy to promote walking function in these patients. This study was registered at ChiCTR, number ChiCTR1900026450.

Keywords: walking function, intermittent theta burst stimulation, stroke, cerebellum, neurotherapeutic

INTRODUCTION

Stroke is the second most common cause of death worldwide and one of the leading causes of disability (Wang et al., 2014; Feigin et al., 2016). According to the Global Burden of Disease study of 2019, China is the country with the highest risk of stroke in the world (Langhorne et al., 2018). Even if patients are treated in time, they may still have disabilities, such as balance and walking limitations, spasms, dysphagia, and aphasia, which limit patients' ability to carry out their daily activities and affect their quality of life (Winstein et al., 2016). Walking dysfunction is one of the most serious consequences of stroke, nearly 30% of stroke patients are unable to walk even in the chronic stage (Park et al., 2011). Therefore, recovery of walking function is strongly demanded in stroke patients.

Repetitive transcranial magnetic stimulation (rTMS) has been increasingly used to treat many neurological and neuropsychiatric disorders (Chen et al., 2019). Theta burst stimulation (TBS), a novel pattern of rTMS, saves time in the rehabilitation of motor function after stroke (Huang et al., 2005). There are two types of TBS: intermittent TBS (iTBS) and continuous TBS (cTBS) generating excitatory and inhibitory effects, respective (Larson et al., 1986; Huang et al., 2011). Compared with conventional rTMS protocols, TBS provides major advantages due to its reduced administration time (Chung et al., 2015) and long-lasting effects with lower intensity stimulation (Cárdenas-Morales et al., 2010).

Stimulation with rTMS at different sites exerts different effects depending on the impairment (Lefaucheur, 2006). The cerebellum, one of the main neural control centers for walking, plays a substantial role in movement execution and motor function, including balance, postural stability, and gait control (Bastian, 2011; Witter and De Zeeuw, 2015). Cerebellar stimulation in healthy individuals can modulate primary motor cortex excitability by altering cerebello-cerebral inhibition (Fierro et al., 2007; Langguth et al., 2008). One study demonstrated that changes in cerebellar excitability are associated with human locomotor adaptive learning, suggesting a potential role for cerebellar stimulation in stroke patients (Jayaram et al., 2011). Kim et al. (2014) reported that low frequency rTMS over the cerebellum has a curative effect on balance and walking functions in patients with ataxia following a posterior circulation stroke, further suggesting the promising therapeutic effects of cerebellar stimulation.

The research on the impact of iTBS over the cerebellum on walking performance in stroke patients is increasing. A study involving 36 patients with hemiparesis resulting from chronic ischemic strokes demonstrated that cerebellar iTBS could affect the plasticity of the cerebellar cortex and improve gait and balance function in stroke patients (Koch et al., 2018). Our previous research showed that cerebellar iTBS could improve balance function in stroke patients (Liao et al., 2021). However, the effect of cerebellar iTBS on walking function in subacute stroke patients has been rarely reported. Therefore, the purpose of this randomized, double-blind, sham-controlled study was to explore the impact of cerebellar iTBS on the walking function of stroke patients and to determine its effect on corticospinal excitability.

MATERIALS AND METHODS

Study Design and Participants

The study was designed as a randomized, double-blind, parallel-group trial. Participants were recruited after referral to the hospital from September 2019 to September 2021. The inclusion criteria were stroke patients with walking dysfunction, which was diagnosed according to the stroke diagnostic criteria. We recruited patients aged 25–80 years (Feigin et al., 2018) who had suffered their first unilateral stroke within 6 months (Bütefisch et al., 2008), as confirmed by brain Computed Tomography (CT) or Magnetic Resonance Imaging (MRI). Exclusion criteria were having neurological disease(s) other than that the first stroke or a serious medical comorbidity (cardiac, renal or respiratory failure; active neoplasia), cerebellar or brainstem stroke, severe vision or hearing impairments, or the presence of a cardiac pacemaker, intracranial implant, or metal in the cranium. Patients with a history of seizures or who were pregnant were also excluded. The study was approved by the West China Hospital Clinical Trials and Biomedical Ethics Committee of Sichuan University. All participants were fully informed of the purpose and procedures of the study and gave written informed consent before participating in the trial.

Randomization and Blinding

Participants were randomly assigned by a computer-generated, blockwise random sequence to either the intervention group (cerebellar iTBS coupled with physical therapy) or the control group (sham iTBS with physical therapy) with a 1:1 allocation ratio. The randomization identification number and treatment allocation code were kept in sealed opaque envelopes. Assessments were performed by two study assessors (Y-JX and L-YL) who were not otherwise involved in the study. Both assessors were trained how to administer and score the outcome measures. Participants, physical therapists, and study assessor were unaware of the group assignment. Physiotherapists who performed the cerebellar iTBS and sham iTBS were aware of the treatment condition. Participants were instructed not to discuss their treatment allocation with the treatment technicians or other participants.

Transcranial Magnetic Stimulation Procedure

During the examination, the participants were seated in a chair and were asked to relax their arms in a comfortable position. A bathing cap with brain regions was placed on each participant's head in order to conveniently mark the primary motor cortex. Surface electromyography was recorded from the contralateral abductor pollicis brevis (APB) muscle, using Ag-Cl electrodes and a muscle belly tendon configuration (Berger et al., 2011). The active electrode was placed over the APB muscle belly, and the reference electrode was placed on the arm, 10 cm from the wrist.

Abductor pollicis brevis muscle motor-evoked potentials (MEPs) were evoked by TMS delivered using a CCY-I magnetic stimulator (YIRUIDE medical, Wuhan, China) with a 70 mm diameter figure-of-eight coil over the contralateral primary motor cortex (M1). The intensity was initially set at 100% of the machine output to determine the optimal stimulation site (hotspot). The initial TMS coil was placed over M1 with the handle directed backward and laterally and at an angle of approximately 45° to the mid-sagittal line of the head. We determined the hot spot by moving the coil over the scalp to find the location where TMS produced the largest MEP from the target muscle during muscle activation. The hot spot was then marked on the scalp. Subsequently, we decreased the intensity in a stepwise manner while stimulating the hotspot. The resting motor threshold (RMT), which was defined as the lowest stimulus intensity to produce MEPs of at least 50 μV in at least 5 of the 10 consecutive trials, of the contralateral abductor pollicis brevis muscle was measured over the M1 of the unaffected hemisphere (Rossini et al., 2015). The active motor threshold (AMT) was defined as the lowest intensity required to evoke MEPs of greater than 200 μV in at least five out of ten trials while the subject performed a 10% of maximum voluntary contraction using visual feedback from a dynamometer (Terao et al., 1998). The AMT was only assessed once before the cerebellar stimulation to determinate the stimulation intensity of each patient.

Interventions

Cerebellar iTBS was performed using a CCY-I magnetic stimulator (YIRUIDE medical, Wuhan, China) with a standard 70 mm diameter figure-of-eight flat coil. The stimulus intensity was set at 80% of the AMT. Each session of iTBS consisted of bursts of three pulses at 50 Hz applied at a rate of 5 Hz, with 20 trains of 10 bursts delivered at 8-s intervals, achieving 600 pulses in total. iTBS was applied over the contralesional cerebellum, 1 cm inferior to and 3 cm lateral to the inion (Del Olmo et al., 2007). Cerebellar iTBS was performed daily for 10 consecutive weekdays. The coil was positioned tangentially to the scalp, with the handle pointing upward (Pinto and Chen, 2001). Sham iTBS was delivered with the coil applied perpendicular to the scalp (Shin et al., 2019). The parameters, including noise, time, and frequency, of the sham iTBS were the same as those of the real iTBS to minimize current flow into the skull (Machado et al., 2008). After receiving cerebellar iTBS, all participants received conventional physical therapy, including motor function, transfer, balance, and ambulation training, during admission for 50 min per day. Interventions were initiated on the weekday following the pretest and were performed daily for 10 consecutive weekdays. iTBS and conventional physical therapy were conducted and supervised by well-trained and qualified physical therapist.

Outcomes

The primary outcome measure was the Fugl–Meyer Assessment–Lower Extremity (FMA-LE), which was reported to have good reliability for evaluating lower extremity motor control in stroke patients (Sanford et al., 1993). It was scored on a 3-point ordinal scale (0–2), with a maximum score of 34. Higher scores indicated better control of the lower extremities. Secondary outcome measures included walking performance and corticospinal excitability. The assessment was performed at treatment sites before the intervention (T0), after 1 week of the intervention (T1) and after 2 weeks of the intervention (T2) by physical therapist who was unaware of the intervention assignment. Any adverse effects or discomfort reported during the iTBS sessions were investigated and recorded. The baseline assessment of stroke severity was conducted using the National Institutes of Health Stroke Scale (NIHSS) (Gandhi and Sharma, 2020).

Walking Performance

The ten-meter walking test (10 MWT) is a valid and reliable measure of walking ability in stroke patients (van Bloemendaal et al., 2012) that assesses the time it takes for subjects to walk 10 m at a self-selected speed and maximum speed with or without a gait aid. The Timed Up and Go test (TUG) evaluates dynamic balance and mobility function, and is reported to have excellent test-retest reliability and to correlate well with other measures of gait and balance in stroke patients (Lin et al., 2004; Flansbjer et al., 2005). TUG assesses the time taken to complete a series of actions, including standing up from a chair, walking forward three meters, turning, and walking back to the chair. The functional ambulation category scale (FAC) is a quick and cost-effective visual measurement of walking (Wade, 1992), that correlates the walking speed with the step length. The FAC has been proven to possess excellent reliability, predictive validity, and good responsiveness in stroke patients (Mehrholz et al., 2007).

Corticospinal Excitability

The peak-peak amplitude of MEPs were recorded by delivering a pulse at an intensity of 120% of the RMT through a figure-of-eight coil placed on the contralateral motor cortex. The average RMT, MEP amplitude were used to measure corticospinal excitability (Boylan and Sackeim, 2000). MEP measurement is a sensitive approach for detecting residual corticospinal function and is predictive of motor recovery after stroke (Peinemann et al., 2004).

Statistical Analyses

The sample size calculation was based on data from Koch et al. (2018) showing an estimated effect size of 0.28 on the Fugl–Meyer Assessment score when comparing cerebellar iTBS with sham stimulation. To detect a significant increase from the baseline in

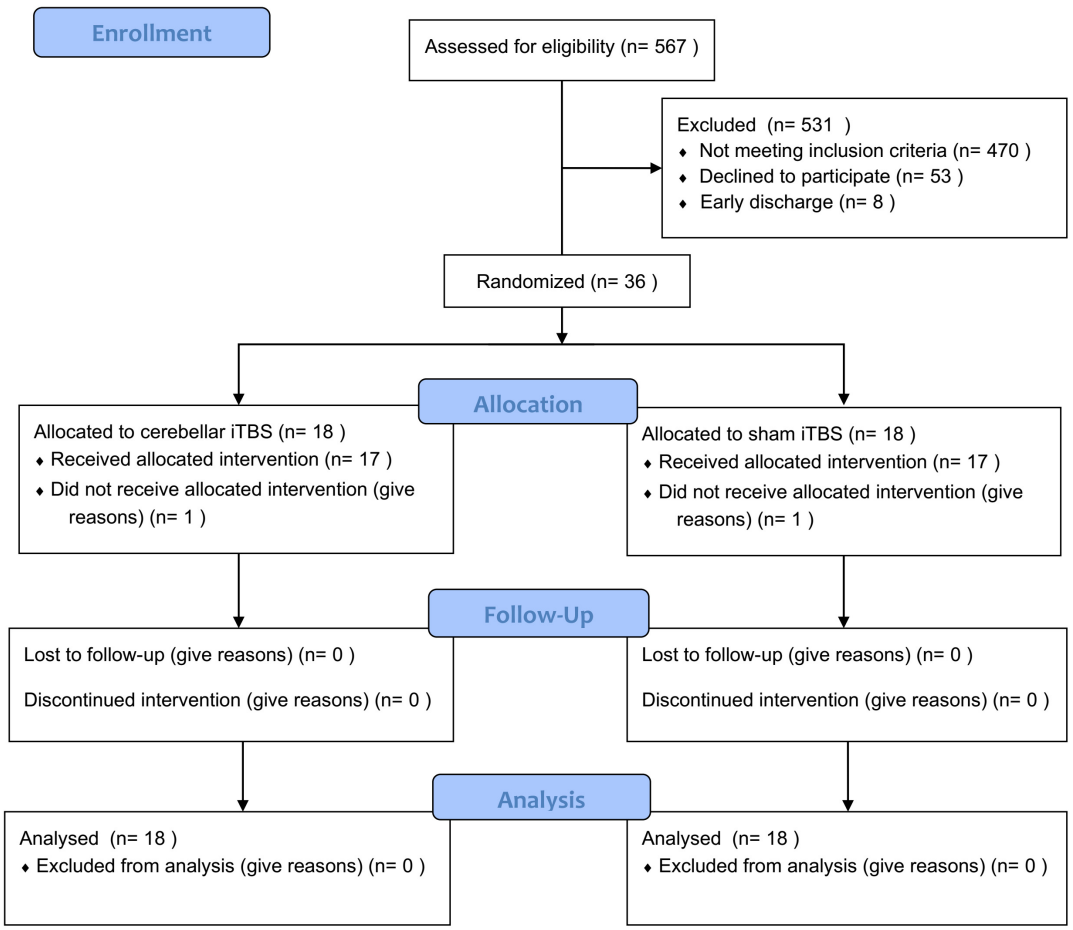

FIGURE 1 | Flow diagram of patients through the study.

the primary outcome measure after the 2-week iTBS intervention, it was estimated that at least 15 patients per group were needed to ensure a statistical power of 0.90 and a two-sided α significance level of 0.05. The dropout rate was expected to be 20%, on the basis of clinical experience during the study design period, so 18 patients were enrolled in each group.

The intention-to-treat population, which included all randomized patients who received at least 1 day of therapy, was used to analyze the primary and secondary outcomes. Missing outcomes data were imputed using the last observation carried forward approach. The means [standard deviation (SD)] or medians [interquartile range (IQR)] of the outcome measures are reported as appropriate. For continuous measures, the normality of the data was tested using the D'Agostino-Pearson normality test. Parametric methods were used for normally distributed data. For nonparametric data, the Mann–Whitney *U* test was used for between-group comparisons and the Wilcoxon signed-rank test was used for pairwise intrasubject comparisons. The primary outcome was analyzed by two-way mixed measures analysis of variance (ANOVA) with a between-individual factor group (iTBS and sham iTBS), and a within-individual factor time (T0, T1, and T2). The Greenhouse-Geisser correction was used when necessary to correct for nonsphericity. Tukey's *post hoc* multiple comparison test was applied to explore the significant interactions within the groups, and Student's *t*-test was used to examine differences between the groups. The secondary outcomes were both evaluated by two-way mixed measures ANOVA. Statistical significance was maintained at $p < 0.05$, and 95% confidence intervals were calculated. All statistical analyses and graph generations were performed using SPSS version 22.0 and GraphPad Prism version 7.0 (GraphPad Inc., San Diego, CA, United States). This study was registered at ChiCTR, number ChiCTR1900026450.

RESULTS

A total of 36 patients [mean (SD) age, 53 (7.93) years; 10 women (28%)] were enrolled in the study between September 1, 2019, and August 31, 2020 and were randomly assigned to the intervention or control group at a 1:1 ratio. However, two patients (one from each group) withdrew for personal reasons after undergoing their first evaluation but before receiving treatment. Seventeen patients in the intervention group and 17 patients in the control

group completed 2 weeks of treatment and had their outcomes evaluated (**Figure 1**). Among those 36 patients, 20 had suffered (59%) ischemic strokes, and most participants were 1 to 6 months poststroke. There were no significant differences in age, gender, disease duration, or lesion side between the intervention and control groups. The baseline characteristics of the participants did not differ between the two groups (**Table 1**) and the outcome measure did not exist difference before intervention (**Table 2**). The mean baseline NIHSS was 4.7, with no significant difference between groups. No participants reported any adverse events.

TABLE 1 | Baseline characteristics (n = 36).

Characteristic	Intervention group (n = 18)	Control group (n = 18)	P value
Age, mean (SD), y	52.35 (8.62)	54.41 (7.01)	0.375[a]
Sex, No. (%)			
Male	13 (72%)	11 (61%)	0.480[b]
Female	5 (28%)	7 (39%)	
Weight, median (IQR), kg	69 (64 ∼ 72)	65 (58 ∼ 72)	0.437[a]
Height, median (IQR), cm	165 (159 ∼ 171)	168 (160 ∼ 174)	0.752[a]
Stroke subtype, No. (%)			
Ischemic	10 (56%)	10 (56%)	1.000[b]
Hemorrhagic	8 (44%)	8 (44%)	
Affected side, No. (%)			
Left	7 (39%)	6 (33%)	0.729[b]
Right	11 (61%)	12 (77%)	
Right-handed, No. (%)	18 (100%)	16 (89%)	0.146[b]
Time since onset, mean (SD), mo	2.22 (1.70)	2.91 (1.96)	0.233[a]
NIHSS score, No. (%)			
Mild (1–7)	14 (78%)	15 (83%)	0.674[b]
Moderate (8–16)	4 (22%)	3 (17%)	
Severe (> 16)	0	0	

[a]*Assessed using t-test;* [b]*assessed using chi-square test.*
y, year; IQR, interquartile range; mo, month; NIHSS, National Institutes of Health Stroke Scale.

TABLE 2 | Comparisons of outcome measures before intervention.

	Intervention group (n = 18)	Control group (n = 18)	P value
FMA-LE (score)	24.94 (5.98)	23.17 (4.99)	0.339
10 MWT(s)			
Comfortable walking time	18.41 (9.81)	19.90 (12.53)	0.693
Maximum walking time	13.64 (6.96)	16.53 (10.95)	0.352
TUG (s)	30.25 (18.17)	36.18 (24.73)	0.418
FAC, (score), median (IQR)	3 (2 ∼ 3)	3 (2 ∼ 4)	0.713*
RMT (%)	45.33 (11.23)	44.00 (12.14)	0.734
MEP latency (ms)	21.12 (2.13)	21.26 (2.30)	0.857
MEP amplitude (μV)	220.89 (136.27)	197.63 (88.88)	0.548

Data are expressed as mean (SD) unless otherwise indicated.
**Assessed using Mann–Whitney U-test.*
FMA-LE, Fugl–Meyer Assessment–Lower Extremity; 10 MWT, ten-meter walking test; TUG, timed up and go test; FAC, functional ambulation category scale; IQR, interquartile range; RMT, resting motor threshold; MEP, motor evoked potential.

FMA-LE

The FMA-LE scores slightly improved with time in both groups with no significant difference between the groups and over the time [mean (SD), intervention group, T0: 24.94 (5.98); T1: 26.94 (5.05); T2: 27.67 (4.69); control group, T0: 23.17 (4.99); T1: 25.06 (6.31); T2: 25.50 (6.22)]. The analysis of the Fugl–Meyer Assessment–Lower Extremity scores showed that there was nonsphericity, and therefore the Greenhouse-Geisser correction was employed to correct the degree of freedom. The corrected results revealed a significant difference over time ($F_{2,68}$ = 31.1172, $P < 0.0001$, $\eta^2_{partial}$ = 0.645, ε = 0.630), but no interaction between group and time ($F_{2,68}$ = 0.1782, P = 0.7255, $\eta^2_{partial}$ = 0.010, ε = 0.594). The improvement trend of the experimental group was consistent with that of the control group. There was no significant difference in the main effect between the groups (F = 1.1440, P = 0.2923, $\eta^2_{partial}$ = 0.089) (**Figure 2A**).

Walking Performance

10 MWT-Comfortable Walking Time

The comfortable walking time decreased in the intervention group [mean (SD), T0: 18.41 (9.81); T1: 15.33 (7.92); T2: 14.08 (7.63)] but not for the control group [mean (SD), T0: 19.90 (12.53); T1: 20.20 (12.03); T2: 19.18 (10.83)]. The two-way mixed measures ANOVA showed an effect for the time factors ($F_{2,68}$ = 10.2376, P = 0.0010, $\eta^2_{partial}$ = 0.378, ε = 0.719) and time × group ($F_{2,68}$ = 6.5242, P = 0.0080, $\eta^2_{partial}$ = 0.276, ε = 0.641) interaction but not for the groups (F = 1.2851, P = 0.2649, $\eta^2_{partial}$ = 0.068).

The comfortable walking time decreased in the intervention group, but *post hoc* analysis revealed that the decrease within group did not reach statistical significance. The between-group comparisons revealed significant differences in the comfortable walking time at T1 (−3.37; 95% CI, −5.77 to −0.98; P = 0.0072) and T2 (−3.61; 95% CI, −6.42 to −0.80; P = 0.0133), compared to T0 (**Figure 2B**).

10 MWT-Maximum Walking Time

The maximum walking time decreased in the intervention group [mean (SD), T0: 13.64 (6.96); T1: 11.93 (6.04); T2: 11.28 (5.63)] and the control group [mean (SD), T0: 16.53 (10.95); T1: 16.24 (10.17); T2: 16.08 (10.42)]. The corrected results using the Greenhouse-Geisser correction revealed a significant difference over time ($F_{2,68}$ = 11.6524, P = 0.0002, $\eta^2_{partial}$ = 0.494) and interaction between group and time ($F_{2,68}$ = 5.4354, P = 0.0115, $\eta^2_{partial}$ = 0.198, ε = 0.734) (**Figure 2C**).

Post hoc analysis showed that the mean maximum walking time differed substantially between the groups at T1 [mean (SD), 11.93 (6.04) in the intervention group and 16.24 (10.17) in the control group; mean difference, −1.41; 95% CI, −2.62 to −0.21; P = 0.0227] and T2 [mean (SD), 11.28 (5.63) in the intervention group and 16.08 (10.42) in the control group; mean difference, −1.91; 95% CI, −3.38 to −0.43; P = 0.0127] (**Figure 2C**) but did not differ within the groups.

TUG

Both patients receiving real iTBS and sham iTBS showed an improvement on the TUG [mean (SD), intervention group, T0: 30.25 (18.17); T1: 25.23 (10.37); T2: 26.09 (11.01);

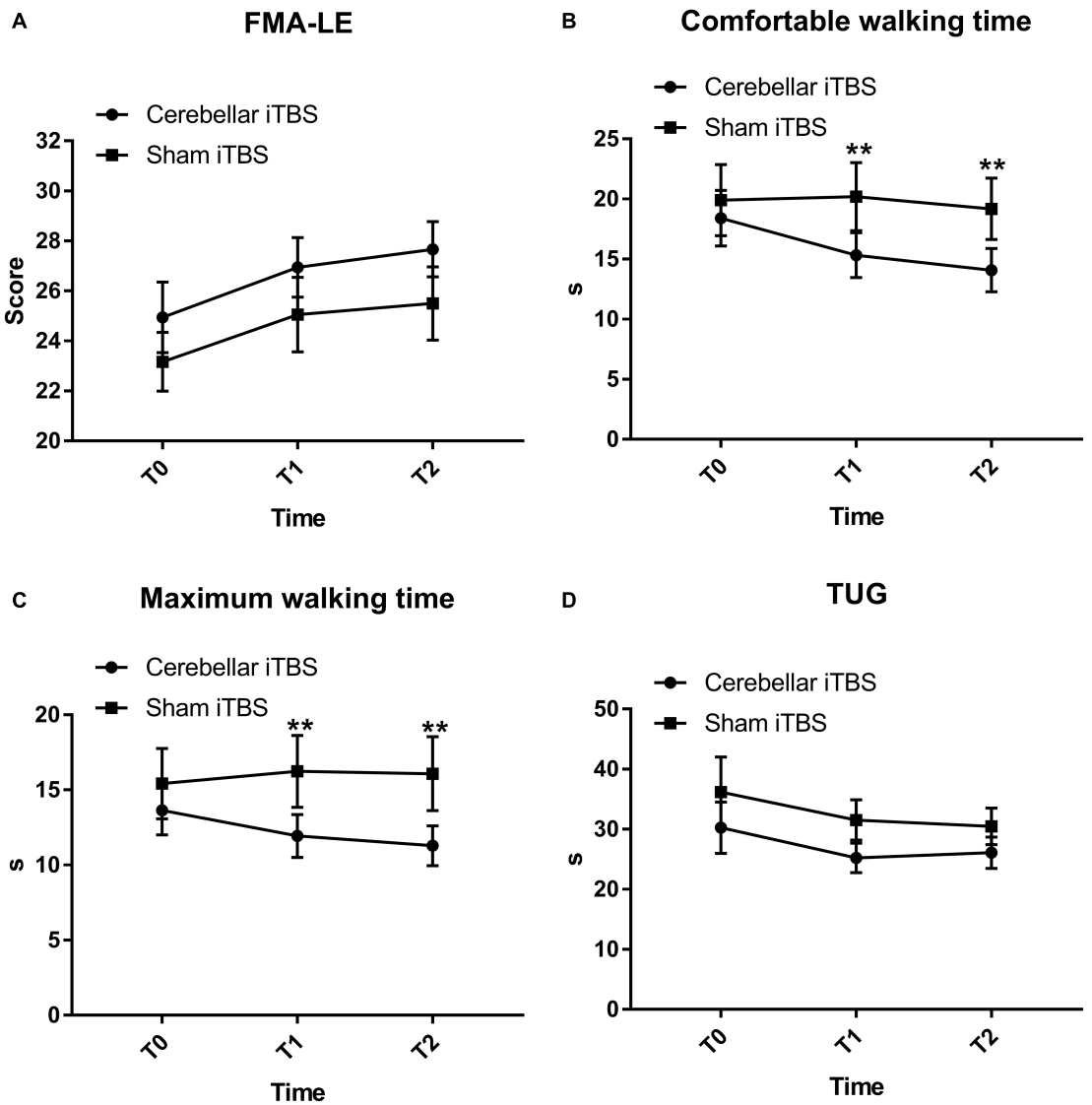

FIGURE 2 | Fugl-Mayer Assessment–Lower Extremity (FMA-LE) **(A)**, comfortable **(B)** and maximum walking time **(C)** measured by ten-meter walking test, Time up and go test (TUG) **(D)** mean scores and effectiveness for the cerebellar intermittent theta burst stimulation (iTBS) and sham iTBS group at baseline (T0), 1 week after intervention (T1), and 2 weeks after intervention (T2). Error bars represent standard error of the mean (SEM). $^{**}P < 0.05$.

control group, T0: 36.18 (24.73); T1: 31.54 (14.20); T2: 30.49 (12.95), $F_{2,68} = 5.119$, $P = 0.034$, $\eta^2_{partial} = 0.231$, $\varepsilon = 0.532$] (**Figure 2D**). However, the TUG did not display significant results time × group ($F_{2,68} = 0.1593$, $P = 0.7163$, $\eta^2_{partial} = 0.009$, $\varepsilon = 0.567$) interaction or between-group differences ($F = 1.2692$, $P = 0.2678$, $\eta^2_{partial} = 0.078$).

FAC

Mann–Whitney *U*-test displayed that the median FAC scores at T1 were 3 (IQR, 3 to 4) in the intervention group and 3 (IQR, 2 to 4) in the control group, but the difference between the groups was not statistically significant (0; 95% CI, −1 to 0; $P = 0.5030$). Furthermore, no significant between-group differences were found in FAC score when assessed at T2 (−1; 95% CI, −1 to 0; $P = 0.3590$). Similarly, there were no significant within-group differences.

Corticospinal Excitability

The results of RMT showed that there was no significant interaction between time and group ($F_{2,68} = 2.1638$, $P = 0.1227$, $\eta^2_{partial} = 0.101$). Over 2 weeks, the RMT in the intervention group improved from baseline in a repeated measures analysis of variance model [mean (SD), T0: 45.33 (11.23); T1: 41.83 (11.75); T2: 39.17 (11.79)], but was not statistically different compared to the control group ($F = 0.0728$, $P = 0.7889$, $\eta^2_{partial} = 0.007$). The time difference was statistically significant ($F_{2,68} = 9.3479$, $P = 0.0003$, $\eta^2_{partial} = 0.387$) (**Figure 3A**).

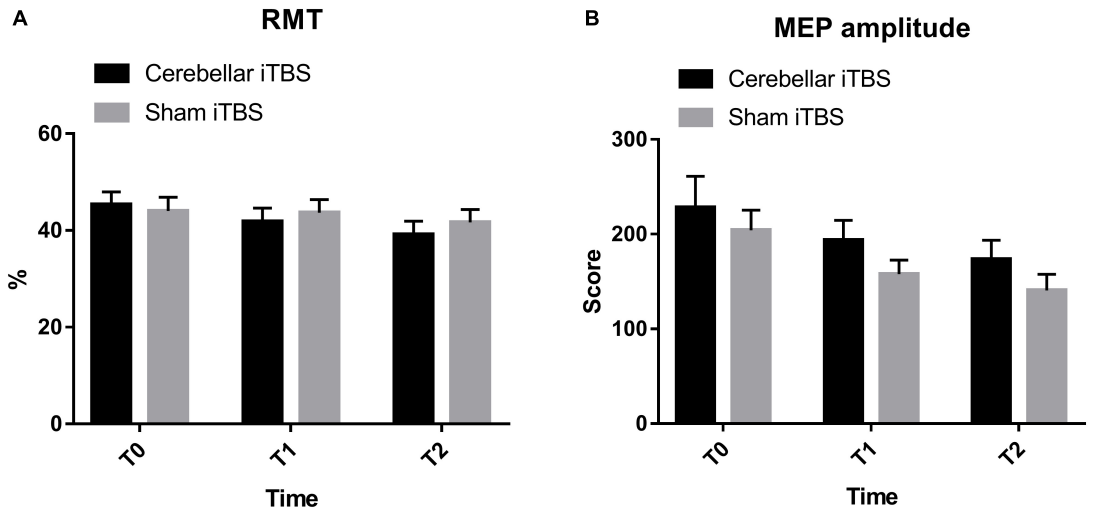

FIGURE 3 | Resting motor threshold **(A)** and motor evoked potential amplitude **(B)** cerebellar intermittent theta burst stimulation (iTBS) and sham iTBS group at baseline (T0), 1 week after intervention (T1), and 2 weeks after intervention (T2). Error bars represent standard error of the mean (SEM).

No increase in MEP amplitude and individual changes were found within the intervention or control group ($F_{2,68} = 204.8659$, $P = 0.0106$, $\eta^2_{partial} = 0.218$). Besides, none of the differences between the groups were statistically significant ($F = 1.8745$, $P = 0.1799$, $\eta^2_{partial} = 0.129$) (**Figure 3B**).

DISCUSSION

The results of this randomized, double-blind, sham-controlled clinical trial showed that in patients recovering from stroke, cerebellar intermittent theta burst stimulation plus physical therapy, compared to physical therapy alone, significantly improved walking performance, as reflected by the ten-meter walking test, comfortable walking time and maximum walking time after 1 and 2 weeks of stimulation.

These findings indicate that this 3 min cerebellar iTBS protocol, with a shorter treatment duration than the conventional rTMS protocol, improved walking function in stroke patients, a finding that is in accordance with the results of Koch et al. (2018). In our previous study, lower extremity motor function measured by FMA-LE did not improve, which was consistent with our result (Liao et al., 2021). Our research group also found that cerebellar iTBS could improve balance in subacute stroke patients (Liao et al., 2021). From a clinical perspective, cerebellar iTBS can be advantageous for designing rapid protocols for gait rehabilitation, as these improvements were achieved with a relatively short treatment duration.

Moreover, comfortable and maximum walking time decreased with cerebellar iTBS, confirming improved gait speed after intervention. Limited walking ability after stroke limits a patient's independence in their home and community, and gait speed is the most accurate method for predicting walking classification (Perry et al., 1995). An increase in gait speed promotes a transition to improved walking, resulting in better function and quality of life, especially for those who can walk in the home (Schmid et al., 2007).

The results of the TUG revealed encouraging but nonsignificant findings suggesting better dynamic balance and mobility function following cerebellar iTBS stimulation. A study by Tramontano et al. (2020) indicated that patients receiving cerebellar iTBS showed a significant improvement in balance function. A potential explanation for the lack of positive effect on dynamic balance and mobility function in our study could be that cerebellar iTBS was applied for only 2 weeks during hospitalization.

The cerebellum is known to play a crucial role in movement execution and motor control (Manto et al., 2012). Anatomically, Purkinje cells in the cerebellar cortex inhibit the dentate nucleus, which regulates the motor cortex through the ventrolateral motor thalamus. Therefore, cerebellar brain inhibition (CBI) refers to an inhibition of the motor cortex due to activation of Purkinje cells (Ugawa et al., 1995; Daskalakis et al., 2004). It has been observed that cerebellar stimulation can modulate CBI by altering the activity of Purkinje cells, resulting in continuous and polarity-related bidirectional regulation of cerebellar excitability (Koch, 2010; Strzalkowski et al., 2019). Cerebellar iTBS could indirectly regulate the dentate nucleus by activating local low-threshold interneurons. Synapse transmission can be controlled using noninvasive brain stimulation, which results in lasting changes in synaptic connection strength. iTBS applied over the motor cortex is known to result in lasting MEP facilitation, termed long-term potentiation (LTP). The induction of LTP generates changes in activity in interconnected cortical motor networks (Koch et al., 2020).

There were no discernible differences in MEP amplitude following iTBS treatment. One possible explanation for these changes is that when the TMS-induced excitation phase is reached, that forced motor neuron excitation is more likely

to result in subthreshold motor neuron discharges (Aminoff, 1986). Different intensities of 1 Hz rTMS applied over the motor cortex exert different effects (Berger et al., 2011). The MEP amplitude decreased significantly with low intensity stimulation, while high intensity stimulation increased the MEP amplitude. Additionally, an 80% motor threshold intensity resulted in less inhibition, although that decrease was not statistically significant, a finding that may also hold true in cerebellar iTBS given that no discernible differences in MEP amplitude were observed between groups.

There were several limitations to our study. First, the small sample size may affect the results of the outcome measures and did not allow for a more refined stratified analysis of the findings. Besides, only the excitability of unaffected hand M1 was assessed, which may be nonspecific for the changes. When eliminating difficulties in equipment testing, the cortical excitability of the affected hand M1, as well as the responses in the leg muscles would be more specific for the changes of corticospinal excitability. Another limitation is the lack of follow-up assessment, as we were not able to determine the long-term effects of cerebellar iTBS.

CONCLUSION

Importantly, this study revealed that applying iTBS over the contralesional cerebellum paired with physical therapy could improve walking performance in stroke patients, implying that cerebellar iTBS may be a cost-effective and noninvasive strategy to promote recovery of walking function in stroke patients. More high-quality studies are needed to examine changes in corticospinal excitability.

DATA AVAILABILITY STATEMENT

The raw data supporting the conclusions of this article will be made available by the authors, without undue reservation.

ETHICS STATEMENT

The studies involving human participants were reviewed and approved by West China Hospital Clinical Trials and Biomedical Ethics Committee of Sichuan University. The patients/participants provided their written informed consent to participate in this study.

AUTHOR CONTRIBUTIONS

Y-JX: conceptualization, visualization, software, validation, formal analysis, and writing—original draft. Q-CW: conceptualization, visualization, software, and validation. YC: methodology, visualization, and software. L-YL: methodology, investigation, visualization, software, writing—review and editing. B-JL and H-HJ: investigation. H-XT and Q-FG: methodology, investigation, and visualization. QG: resources, visualization, writing—review and editing, supervision, and project administration. All authors contributed to the article and approved the submitted version.

REFERENCES

Aminoff, M. J. (1986). Evoked potentials in clinical medicine. *Q. J. Med.* 59, 345–362.

Bastian, A. J. (2011). Moving, sensing and learning with cerebellar damage. *Curr. Opin. Neurobiol.* 21, 596–601. doi: 10.1016/j.conb.2011.06.007

Berger, U., Korngreen, A., Bar-Gad, I., Friedman, A., Wolfus, S., Yeshurun, Y., et al. (2011). Magnetic stimulation intensity modulates motor inhibition. *Neurosci. Lett.* 504, 93–97. doi: 10.1016/j.neulet.2011.09.004

Boylan, L. S., and Sackeim, H. A. (2000). Magnetoelectric brain stimulation in the assessment of brain physiology and pathophysiology. *Clin. Neurophysiol.* 111, 504–512. doi: 10.1016/S1388-2457(99)00280-1

Bütefisch, C. M., Wessling, M., Netz, J., Seitz, R. J., and Hömberg, V. (2008). Relationship between interhemispheric inhibition and motor cortex excitability in subacute stroke patients. *Neurorehabil. Neural Repair.* 22, 4–21. doi: 10.1177/1545968307301769

Cárdenas-Morales, L., Nowak, D. A., Kammer, T., Wolf, R. C., and Schönfeldt-Lecuona, C. (2010). Mechanisms and applications of theta-burst rTMS on the human motor cortex. *Brain Topogr.* 22, 294–306. doi: 10.1007/s10548-009-0084-7

Chen, Y., Cha, Y. H., Li, C., Shou, G., Gleghorn, D., Ding, L., et al. (2019). Multimodal imaging of repetitive transcranial magnetic stimulation effect on brain network: a combined electroencephalogram and functional magnetic resonance imaging study. *Brain Connect.* 9, 311–321. doi: 10.1089/brain.2018.0647

Chung, S. W., Hoy, K. E., and Fitzgerald, P. B. (2015). Theta-burst stimulation: a new form of TMS treatment for depression? *Depress. Anxiety* 32, 182–192. doi: 10.1002/da.22335

Daskalakis, Z. J., Paradiso, G. O., Christensen, B. K., Fitzgerald, P. B., Gunraj, C., and Chen, R. (2004). Exploring the connectivity between the cerebellum and motor cortex in humans. *J. Physiol.* 557, 689–700. doi: 10.1113/jphysiol.2003.059808

Del Olmo, M. F., Cheeran, B., Koch, G., and Rothwell, J. C. (2007). Role of the cerebellum in externally paced rhythmic finger movements. *J. Neurophysiol.* 98, 145–152. doi: 10.1152/jn.01088.2006

Feigin, V. L., Nguyen, G., Cercy, K., Johnson, C. O., Alam, T., Parmar, P. G., et al. (2018). Global, regional, and country-specific lifetime risks of stroke, 1990 and 2016. *New Engl. J. Med.* 379, 2429–2437. doi: 10.1056/NEJMoa1804492

Feigin, V. L., Roth, G. A., Naghavi, M., Parmar, P., Krishnamurthi, R., Chugh, S., et al. (2016). Global burden of stroke and risk factors in 188 countries, during 1990-2013: a systematic analysis for the Global Burden of Disease Study 2013. *Lancet. Neurol.* 15, 913–924. doi: 10.1016/S1474-4422(16)30073-4

Fierro, B., Giglia, G., Palermo, A., Pecoraro, C., Scalia, S., and Brighina, F. (2007). Modulatory effects of 1 Hz rTMS over the cerebellum on motor cortex excitability. *Exp. Brain Res.* 176, 440–447. doi: 10.1007/s00221-006-0628-y

Flansbjer, U.-B., Holmbäck, A. M., Downham, D., Patten, C., and Lexell, J. (2005). Reliability of gait performance tests in men and women with hemiparesis after stroke. *J. Rehabil. Med.* 37, 75–82. doi: 10.1080/16501970410017215

Gandhi, N., and Sharma, D. (2020). Role of platelet indices in predicting severity of disease in patients of acute ischemic stroke and its correlation with NIHSS (National Institute Of Health Stroke Scale) score. *J. Assoc. Phys. India* 68, 66–66.

Huang, Y.-Z., Edwards, M. J., Rounis, E., Bhatia, K. P., and Rothwell, J. C. (2005). Theta burst stimulation of the human motor cortex. *Neuron* 45, 201–206. doi: 10.1016/j.neuron.2004.12.033

Huang, Y. Z., Rothwell, J. C., Chen, R. S., Lu, C. S., and Chuang, W. L. (2011). The theoretical model of theta burst form of repetitive transcranial magnetic

stimulation. *Clin. Neurophysiol.* 122, 1011–1018. doi: 10.1016/j.clinph.2010.08.016

Jayaram, G., Galea, J. M., Bastian, A. J., and Celnik, P. (2011). Human locomotor adaptive learning is proportional to depression of cerebellar excitability. *Cereb. Cortex* 21, 1901–1909. doi: 10.1093/cercor/bhq263

Kim, W. S., Jung, S. H., Oh, M. K., Min, Y. S., Lim, J. Y., and Paik, N. J. (2014). Effect of repetitive transcranial magnetic stimulation over the cerebellum on patients with ataxia after posterior circulation stroke: a pilot study. *J. Rehabil. Med.* 46, 418–423. doi: 10.2340/16501977-1802

Koch, G. (2010). Repetitive transcranial magnetic stimulation: a tool for human cerebellar plasticity. *Funct. Neurol.* 25, 159–163.

Koch, G., Bonni, S., Casula, E. P., Iosa, M., Paolucci, S., Pellicciari, M. C., et al. (2018). Effect of cerebellar stimulation on gait and balance recovery in patients with hemiparetic stroke: a randomized clinical trial. *JAMA Neurol.* 76, 170–178. doi: 10.1001/jamaneurol.2018.3639

Koch, G., Esposito, R., Motta, C., Casula, E. P., Di Lorenzo, F., Bonnì, S., et al. (2020). Improving visuo-motor learning with cerebellar theta burst stimulation: behavioral and neurophysiological evidence. *Neuroimage* 208:116424. doi: 10.1016/j.neuroimage.2019.116424

Langguth, B., Eichhammer, P., Zowe, M., Landgrebe, M., Binder, H., Sand, P., et al. (2008). Modulating cerebello-thalamocortical pathways by neuronavigated cerebellar repetitive transcranial stimulation (rTMS). *Neurophysiol. Clin.* 38, 289–295. doi: 10.1016/j.neucli.2008.08.003

Langhorne, P., O'Donnell, M. J., Chin, S. L., Zhang, H., Xavier, D., Avezum, A., et al. (2018). Practice patterns and outcomes after stroke across countries at different economic levels (INTERSTROKE): an international observational study. *Lancet (London, England)* 391, 2019–2027. doi: 10.1016/S0140-6736(18)30802-X

Larson, J., Wong, D., and Lynch, G. (1986). Patterned stimulation at the theta frequency is optimal for the induction of hippocampal long-term potentiation. *Brain Res.* 368, 347–350. doi: 10.1016/0006-8993(86)90579-2

Lefaucheur, J. P. (2006). Stroke recovery can be enhanced by using repetitive transcranial magnetic stimulation (rTMS). *Neurophysiol. Clin.* 36, 105–115. doi: 10.1016/j.neucli.2006.08.011

Liao, L. Y., Xie, Y. J., Chen, Y., and Gao, Q. (2021). Cerebellar theta-burst stimulation combined with physiotherapy in subacute and chronic stroke patients: a pilot randomized controlled trial. *Neurorehabil. Neural Repair* 35, 23–32. doi: 10.1177/1545968320971735

Lin, M.-R., Hwang, H.-F., Hu, M.-H., Wu, H.-D. I., Wang, Y.-W., and Huang, F.-C. (2004). Psychometric comparisons of the timed up and go, one-leg stand, functional reach, and Tinetti balance measures in community-dwelling older people. *J. Am. Geriatr. Soc.* 52, 1343–1348. doi: 10.1111/j.1532-5415.2004.52366.x

Machado, S., Bittencourt, J., Minc, D., Portella, C. E., Velasques, B., Cunha, M., et al. (2008). Therapeutic applications of repetitive transcranial magnetic stimulation in clinical neurorehabilitation. *Funct. Neurol.* 23, 113–122.

Manto, M., Bower, J. M., Conforto, A. B., Delgado-García, J. M., da Guarda, S. N., Gerwig, M., et al. (2012). Consensus paper: roles of the cerebellum in motor control–the diversity of ideas on cerebellar involvement in movement. *Cerebellum* 11, 457–487. doi: 10.1007/s12311-011-0331-9

Mehrholz, J., Wagner, K., Rutte, K., Meissner, D., and Pohl, M. (2007). Predictive validity and responsiveness of the functional ambulation category in hemiparetic patients after stroke. *Arch. Phys. Med. Rehabil.* 88, 1314–1319. doi: 10.1016/j.apmr.2007.06.764

Park, H. J., Oh, D. W., Kim, S. Y., and Choi, J. D. (2011). Effectiveness of community-based ambulation training for walking function of post-stroke hemiparesis: a randomized controlled pilot trial. *Clin. Rehabil.* 25, 451–459. doi: 10.1177/0269215510389200

Peinemann, A., Reimer, B., Löer, C., Quartarone, A., Münchau, A., Conrad, B., et al. (2004). Long-lasting increase in corticospinal excitability after 1800 pulses of subthreshold 5 Hz repetitive TMS to the primary motor cortex. *Clin. Neurophysiol.* 115, 1519–1526. doi: 10.1016/j.clinph.2004.02.005

Perry, J., Garrett, M., Gronley, J. K., and Mulroy, S. J. (1995). Classification of walking handicap in the stroke population. *Stroke* 26, 982–989. doi: 10.1161/01.STR.26.6.982

Pinto, A. D., and Chen, R. (2001). Suppression of the motor cortex by magnetic stimulation of the cerebellum. *Exp. Brain Res.* 140, 505–510. doi: 10.1007/s002210100862

Rossini, P. M., Burke, D., Chen, R., Cohen, L. G., Daskalakis, Z., Di Iorio, R., et al. (2015). Non-invasive electrical and magnetic stimulation of the brain, spinal cord, roots and peripheral nerves: basic principles and procedures for routine clinical and research application. an updated report from an I.F.C.N. Committee. *Clin. Neurophysiol.* 126, 1071–1107. doi: 10.1016/j.clinph.2015.02.001

Sanford, J., Moreland, J., Swanson, L. R., Stratford, P. W., and Gowland, C. (1993). Reliability of the Fugl-Meyer assessment for testing motor performance in patients following stroke. *Phys. Ther.* 73, 447–454. doi: 10.1093/ptj/73.7.447

Schmid, A., Duncan, P. W., Studenski, S., Lai, S. M., Richards, L., Perera, S., et al. (2007). Improvements in speed-based gait classifications are meaningful. *Stroke* 38, 2096–2100. doi: 10.1161/STROKEAHA.106.475921

Shin, H. W., Hallett, M., and Sohn, Y. H. (2019). Cerebellar repetitive transcranial magnetic stimulation for patients with essential tremor. *Parkinsonism Related Disord.* 64, 304–307. doi: 10.1016/j.parkreldis.2019.03.019

Strzalkowski, N. D. J., Chau, A. D., Gan, L. S., and Kiss, Z. H. T. (2019). Both 50 and 30 Hz continuous theta burst transcranial magnetic stimulation depresses the cerebellum. *Cerebellum* 18, 157–165. doi: 10.1007/s12311-018-0971-0

Terao, Y., Ugawa, Y., Sakai, K., Miyauchi, S., Fukuda, H., Sasaki, Y., et al. (1998). Localizing the site of magnetic brain stimulation by functional MRI. *Exp. Brain Res.* 121, 145–152. doi: 10.1007/s002210050446

Tramontano, M., Grasso, M. G., Soldi, S., Casula, E. P., Bonnì, S., Mastrogiacomo, S., et al. (2020). Cerebellar intermittent theta-burst stimulation combined with vestibular rehabilitation improves gait and balance in patients with multiple sclerosis: a preliminary double-blind randomized controlled trial. *Cerebellum* 19, 897–901. doi: 10.1007/s12311-020-01166-y

Ugawa, Y., Uesaka, Y., Terao, Y., Hanajima, R., and Kanazawa, I. (1995). Magnetic stimulation over the cerebellum in humans. *Ann. Neurol.* 37, 703–713. doi: 10.1002/ana.410370603

van Bloemendaal, M., van de Water, A. T. M., and van de Port, I. G. L. (2012). Walking tests for stroke survivors: a systematic review of their measurement properties. *Disabil. Rehabil.* 34, 2207–2221. doi: 10.3109/09638288.2012.680649

Wade, D. T. (1992). Measurement in neurological rehabilitation. *Curr. Opin. Neurol. Neurosurg.* 5, 682–686.

Wang, H., Liddell, C. A., Coates, M. M., Mooney, M. D., Levitz, C. E., Schumacher, A. E., et al. (2014). Global, regional, and national levels of neonatal, infant, and under-5 mortality during 1990-2013: a systematic analysis for the Global Burden of Disease Study 2013. *Lancet (London, England)* 384, 957–979. doi: 10.1016/S0140-6736(14)60497-9

Winstein, C. J., Stein, J., Arena, R., Bates, B., Cherney, L. R., Cramer, S. C., et al. (2016). Guidelines for adult stroke rehabilitation and recovery: a guideline for healthcare professionals from the american heart association/american stroke association. *Stroke* 47, e98–e169. doi: 10.1161/STR.0000000000000098

Witter, L., and De Zeeuw, C. I. (2015). Regional functionality of the cerebellum. *Curr. Opin. Neurobiol.* 33, 150–155. doi: 10.1016/j.conb.2015.03.017

Conflict of Interest: The authors declare that the research was conducted in the absence of any commercial or financial relationships that could be construed as a potential conflict of interest.

frontiers in Neuroscience

ORIGINAL RESEARCH
published: 27 October 2021
doi: 10.3389/fnins.2021.701560

Effect of Low-Frequency Repetitive Transcranial Magnetic Stimulation on Executive Function and Its Neural Mechanism: An Event-Related Potential Study

*Sishi Liu[1,2], Xianglong Wang[1,2], Junqin Ma[1], Kangling Wang[1], Zhengtao Wang[1], Jie Li[1], Jiali Chen[1], Hongrui Zhan[3] and Wen Wu[1,2]**

[1] Department of Rehabilitation, Zhujiang Hospital, Southern Medical University, Guangzhou, China, [2] Rehabilitation Medical School, Southern Medical University, Guangzhou, China, [3] Department of Rehabilitation, The Fifth Affiliated Hospital of Sun Yat-sen University, Zhuhai, China

OPEN ACCESS

Edited by:
Jinhua Zhang,
Xi'an Jiaotong University, China

Reviewed by:
Sean K. Meehan,
University of Waterloo, Canada
Yue Lan,
Guangzhou First People's Hospital, China

***Correspondence:**
Wen Wu
wuwen66@163.com

Specialty section:
This article was submitted to Neuroprosthetics, a section of the journal Frontiers in Neuroscience

Received: *28 April 2021*
Accepted: *29 September 2021*
Published: *27 October 2021*

Citation:
Liu S, Wang X, Ma J, Wang K, Wang Z, Li J, Chen J, Zhan H and Wu W (2021) Effect of Low-Frequency Repetitive Transcranial Magnetic Stimulation on Executive Function and Its Neural Mechanism: An Event-Related Potential Study. Front. Neurosci. 15:701560. doi: 10.3389/fnins.2021.701560

Objective: Executive function refers to the conscious control of thinking and behavior in psychological process. Executive dysfunction widely exists in a variety of neuropsychiatric diseases, and is closely related to the decline of daily living ability and function. This study intends to explore the effect of low-frequency repetitive transcranial magnetic stimulation (rTMS) on executive function and its neural mechanism by using event-related potential (ERP), so as to provide basis for further study on the relationship between cerebral cortex and executive function.

Methods: Task switching paradigm was used to study the cognitive flexibility in executive function. Thirty-one healthy subjects were randomly assigned to receive rTMS stimulations (1 Hz rTMS or sham rTMS) to the left dorsolateral prefrontal cortex (DLPFC) twice. The switching task and the electroencephalography (EEG) recordings were performed before (pre-rTMS/pre-sham rTMS) and immediately after the end of the rTMS application (post-rTMS/ post-sham rTMS).

Results: The analysis of RTs showed that the main effects of switching and time were statistically significant. Further analysis revealed that the RT of rTMS stimulation was longer than sham rTMS at post-stimulation. ERP analysis showed that there was a significant switching effect in frontal and central scalp location, and the P2 amplitude in switch trials was greater than that in non-switch trials. At post-stimulation, the N2 amplitude of rTMS is more negative than that of sham rTMS at non-switch trials, whereas no such difference was found at switch trials. The P3 amplitude and LPC amplitude are significantly reduced by rTMS at post-stimulation.

Conclusion: Low-frequency rTMS of the left DLPFC can cause decline of cognitive flexibility in executive function, resulting in the change of N2 amplitude and the decrease of P3 and LPC components during task switching, which is of positive significance for the evaluation and treatment of executive function.

Keywords: rTMS, executive function, DLPFC, P3, task switching, ERP

INTRODUCTION

Executive function refers to conscious control related to thinking and behavior in psychological process, including decision-making, planning, cognitive flexibility, attention, working memory, and other cognitive processes (Guo et al., 2017; Ozga et al., 2018). These important thinking abilities can help people adapt to the complex and changeable environment. When the executive function is impaired, patients cannot make plans and cannot adjust themselves according to the rules, which is a great obstacle for patients to return to society. Although the concept of executive function was first discovered and perfected in the study of frontal lobe syndrome (DeRight, 2019), it has been recognized that executive function involves the precise network of frontal cortex and other brain regions, including parietal cortex, basal ganglia, and colliculus. A previous study (Niendam et al., 2012) has shown that the frontal cingulate parietal subcortical cognitive control network supports a wide range of executive functions. Executive dysfunction is caused by the damage of white matter connection or neurotransmitter system in related brain regions (Rabinovici et al., 2015). Therefore, executive dysfunction widely exists in a variety of neurological, mental, and systemic diseases, and is closely related to the decline of daily living ability and function.

It is well known that the DLPFC plays an important role in various higher-order cognitive functions, such as executive control, planning, working memory, and so on. In elderly subjects, the regulatory effect of DLPFC-SAI (short-latency afferent inhibition) paradigm on N100 was related to the experimental executive function (Noda et al., 2017), and in schizophrenia, the decrease of N100 modulation of TMS-evoked potentials (TEPS) by DLPFC was significantly correlated with executive function (Noda et al., 2018). These studies indicate that DLPFC plays an important role in executive function, and executive function shows asymmetry in left and right DLPFC, showing obvious left hemisphere dominance. A study Ko et al. (2008) showed that continuous theta pulse stimulation (cTBS) was applied to left and right DLPFC, compared with cTBS at the vertex (control). Only cTBS of the left DLPFC impaired Montreal card sorting task (MCST) performance and striatal dopamine neurotransmission.

Cognitive flexibility is one of the core components of executive function and plays an important role in executive control. Task switching program is usually used to study cognitive flexibility, which requires participants to switch between two tasks with different rules (Vanderhasselt et al., 2006). When participants switch between tasks, they shift their attention between one task and another, and activate a new task set in working memory. This process is usually accompanied by an increase in reaction time (RT) and error rate (ER) (Bahlmann et al., 2015). Switching cost represents the performance difference between repeated tasks and switching tasks (Strobach et al., 2018). The behavioral research of task switching paradigm (Swainson et al., 2019) is very mature, but the research on its electrophysiology is limited.

TMS is a non-invasive, safe, and reliable method for cortical (and peripheral) stimulation (He et al., 2020). Because of its painless, non-invasive physical characteristics, it can achieve virtual damage of brain regions to explore brain function and advanced cognitive function. It enables researchers to infer the causal relationship between cortical function and potential cognitive and behavioral processes, while avoiding inconsistencies in the location, volume, and nature of brain damage in clinical models (Lowe and Hall, 2018). However, the physiological mechanism of rTMS induced action is not clear. At present, some studies have confirmed that stimulation of local blood flow and metabolism (Lin et al., 2018), upregulation of brain-derived nerve growth factor, improvement of synaptic plasticity, or change of cortical excitability may be the effective mechanisms of rTMS. So far, there are few studies on the mechanism of rTMS affecting executive function by using ERP.

Event-related potential is a technology with high temporal resolution, reaching the millisecond level, which can record, analyze, and characterize the dynamic electrophysiological activities of living brain (Raz et al., 2016). ERP makes up for the low time resolution of PET and fMRI methods, and has important value in the study of the relationship between cognitive function and neural process. As for task switching, three main ERP components are particularly relevant: P200, N200, and P300 (Massa et al., 2020). P200 is a positive waveform, which reaches its peak about 200 ms after stimulation, and its amplitude is the largest at the frontal electrode. In the paradigm of task switching, some literatures show that P200 is the first component to distinguish switching and non-switching trials. The second useful component of execution process is N200, which is a negative waveform and reaches its peak between 200 and 350 ms after stimulation. N200 is related to attention system and cognitive control, reflecting the cognition of conflict or suppression of dominant responses (Ruberry et al., 2017). P300 is a typical positive waveform in the time window of 250–800 ms after stimulation. P300 components are generated in the neural network composed of frontal lobe, anterior cingulate cortex, inferior temporal lobe, and parietal cortex. The distribution of P3b in parietal lobe is related to working memory and task cognitive resource allocation, and the decrease of P3b is related to lower task performance (Hawkes et al., 2014).

In this study, we intend to investigate the effects of low-frequency rTMS on the left DLPFC to explore the effect on executive function and its neural mechanism by using ERP.

Through the operation of complex task switching paradigm, the ERP components related to executive function of midline frontal, central, and parietal channels were analyzed to provide basis for further study on the relationship between cerebral cortex and executive function. Assuming that the low-frequency rTMS on the left DLPFC could cause decline of executive function during task switching, we expected an increase of RTs and decline of accuracy following rTMS as compared to sham rTMS.

EXPERIMENTAL PROCEDURES

Participants

Thirty-one college students (mean age 23.84 ± 0.344 years old, 12 males and 19 females) were recruited. The subjects were healthy and right-handed with normal or corrected-to-normal vision. Exclusion criteria are as follows: people with metal or electronic device implantation, such as cochlear implant, pulse generator, and medical pump; color blindness or color weakness; organic or functional nervous system diseases; history of taking antipsychotics and drug abuse; and having contact with similar related experimenters. Before the experiment, subjects gave their informed consent. They were able to complete the tests intensively and conscientiously. All procedures complied with guidelines as described in the Declaration of Helsinki. The experiment was approved by the Ethical Committee of the Zhujang Hospital of Southern Medical University. The data from two females and one male were excluded from the analyses due to excessive electroencephalography (EEG) artifacts and baseline drifts that were difficult to correct. The remaining 28 participants (17 females, 23.89 ± 1.99 years old) were included in the analyses.

Switching Task

The task was performed with E-prime 3.0 software (Psychology Software Tools Inc., Pittsburgh, United States), using numbers between 1 and 9 (except 5) as stimulus. The stimuli were presented on a 21-inch CRT monitor (60-Hz refresh rate), with a white background at a distance of approximately 100 cm from the participant. The task included 216 trials; in half of the trials, the numbers were shown in black and the other half in blue. In each experiment, in the center of the computer screen, the fixation was presented for 1,000 ms, a single black or blue number was presented for 500 ms, and then a blank screen was presented for 2,000 ms. Participants switch between tasks based on the color of the number. When the screen shows black numbers, judge the size of the number, press the "Q" key when it is less than 5, and press the "P" key if it is larger than 5. When the blue number is displayed, judge whether the number is odd or even. Press "Q" for odd number and "P" for even number. Instruct participants to answer as quickly and accurately as possible. Participants pressed the button with their left or right index finger and response mapping was counter-balanced across them. The number presentation is random, and the number of switch and non-switch (repeated) trials is the same. The color of the number is the same as the previous experiment, which is a repeated experiment, while the color of the number is different from the previous experiment, which is a switch experiment. Record the RT and accuracy of switch and repeated test. There is a short exercise before the experiment, and the correct rate of reaction needs to reach 80% to enter the formal test.

Transcranial Magnetic Stimulation Parameters

rTMS pulses were delivered using a YRD CCY-I TMS stimulator (YRD, Wuhan, China) with a figure-of-eight focal coil (external diameter of each loop, 9 cm), which produced a maximum stimulator output (MSO) of 3.0 T. The subjects relaxed naturally and sat in a comfortable armchair. Stimulation was applied over the hand representation within primary motor cortex, and the EMG recording electrode was placed in the abdomen of the abductor pollicis brevis (APB) to record the motor-evoked potentials (MEPs). In the resting state, we localized the thumb area of the left motor cortex by eliciting a robust MEP, and then gradually decreased the output intensity to stimulate until the motor threshold (MT) is found, so that at least 5 out of 10 consecutive stimuli can trigger the right APB motion. The intensity of stimulation used for different subjects ranged between 44 and 75% (mean ± SD, 58.93 ± 8.42%) of maximal stimulator output with wearing EEG cap. TMS was then applied 20 min stimulus (1,040 impulses) at a frequency of 1 Hz and an amplitude of 90% of the MT at a distance of 5 cm anterior to the located left primary motor cortex. For 1 Hz stimulation, the stimulating coil was held tangentially to the skull with the coil handle pointing backward and laterally 45°away from the anterior–posterior axis, while for sham stimulation, the coil was placed vertically (at a 90° angle) to the scalp.

Procedure

The experiment was designed as a single-blind crossover design. The subjects sat in a comfortable chair and received 20 min of treatment with 1 Hz rTMS or sham rTMS on the left DLPFC. In each session, the switching task and the EEG recordings were performed before (pre-rTMS/pre-sham rTMS) and immediately after the end of the rTMS application (post-rTMS/post-sham rTMS), which lasted approximately 12 min, respectively. All subjects were wearing the 32-channel EEG cap during the whole session (Levit-Binnun et al., 2010). The interval between rTMS stimulation and task should be as short as possible (interval range 7–11 min). Each subject received two experiments (including 1 Hz rTMS and sham rTMS stimulation) with an average interval of 1 week to eliminate possible carry-over effects. The sequence of low-frequency and sham rTMS stimuli was balanced among participants to minimize possible sequence effects.

Electroencephalography Recording and Data Acquisition

The incorrect response trials were excluded from analysis. EEG was recorded with the 64-channel BIOSEMI Active Two system, which used an electrode cap with 32 Ag/AgCl electrodes mounted according to the international 10–20 system. We used the average value of bilateral mastoid as the reference when recoding EEG online. The sampling rate of EEG was 2,048 Hz, and the bandpass filtered from 0.1 to 100 Hz. The electrode impedance was kept below 5 kΩ.

We used EEGLAB (version 13_0_0b) for offline analysis of EEG data. EEGLAB is a MATLAB (R2013b, MathWorks, Natick, MA, United States) open source toolbox. Data were bandpass filtered at 0.1–50 Hz while notch filtering (49–51 Hz). Change the sampling rate to 500 Hz. EEG recordings were segmented into epochs from -100 to 800 ms relative to the onset of stimulus. A baseline correction (pre-stimulus interval) and automatic artifact rejection (±100 μV) were executed. Remove EOG and EMG activities using independent component analysis (ICA). We observed ERP waveforms and found that the basic characteristics of the ERP curve in the frontal channels (F3, Fz, F4) were consistent, as were the three electrodes in the central channels (C3, Cz, C4) and the parietal channels (P3, Pz, P4). According to previous studies (Küper et al., 2017; Pestalozzi et al., 2020) and the characteristics of this experiment, the average amplitudes of P2 (140–240 ms), N2 (260–340 ms), P3 (360–450 ms), and late components (500–800 ms) were measured across the three brain regions, including frontal (F3, Fz, F4), central (C3, Cz, C4), and parietal (P3, Pz, P4) electrodes.

Data Analysis

SPSS Statistics 22 (IBM Corp, Armonk, NY, United States) was implemented for statistical analysis. The statistical threshold was set at $p < 0.05$.

Data corresponding to correct responses were analyzed. Repeated measurement ANOVA of 2 (stimulation factors: low-frequency rTMS, sham rTMS) × 2 (time factors: pre-stimulation, post-stimulation) × 2 (switching factors: switch, non-switch) was performed with response time and accuracy as dependent variables.

Multiple channel ERP data were analyzed by repeated measurement ANOVA of 2 (stimulation factors: low-frequency rTMS, sham rTMS) × 2 (time factors: pre-stimulation, post-stimulation) × 2 (switching factors: switch, non-switch). Significant ANOVA effects were further analyzed with pairwise *t*-test comparisons.

RESULTS

The subjects did not report side effects during or after the experiment. All data were checked the Q-Q plots to meet the assumption of normality.

Behavioral Data

Results of RTs and accuracy rates on switch and non-switch conditions for different stimulation conditions are presented in **Figure 1**.

The results of ANOVA of response time showed that the main effects of switching [$F_{(1,\ 27)} = 58.819$, $p < 0.001$] and time [$F_{(1,\ 27)} = 9.729$, $p = 0.004$] were statistically significant. The main effect of stimulation was not significant [$F_{(1,\ 27)} = 2.169$, $p = 0.152$]. The interaction "stimulation" × "time" was significant [$F_{(1,\ 27)} = 5.084$, $p = 0.032$]. Further analysis revealed that the RT of rTMS stimulation was longer than sham rTMS at post-stimulation [$F_{(1,\ 27)} = 4.192$, $p = 0.05$], whereas no significant difference was found at pre-stimulation [$F_{(1,\ 27)} = 0.009$, $p = 0.926$]. The interactions stimulation × switching type, time × switching type, and stimulation × time × switching type were not significant [$F_{(1,\ 27)} = 1.408$, $p = 0.246$; $F_{(1,\ 27)} = 3.87$, $p = 0.06$; and $F_{(1,\ 27)} = 1.318$, $p = 0.261$, respectively].

The results of ANOVA of the accuracy showed that the main effect of switching [$F_{(1,\ 27)} = 10.403$, $p = 0.003$] was significant, whereas stimulation [$F_{(1,\ 27)} = 0.623$, $p = 0.437$] and time [$F_{(1,\ 27)} = 0.101$, $p = 0.753$] were not significant. The interactions stimulation × time, stimulation × switching, time × switching type, and stimulation × time × switching type were not significant [$F_{(1,\ 27)} = 2.448$, $p = 0.129$; $F_{(1,\ 27)} = 1.513$, $p = 0.229$; $F_{(1,\ 27)} = 0.612$, $p = 0.441$; and $F_{(1,\ 27)} = 0.275$, $p = 0.604$, respectively].

Event-Related Potential Data

Figure 2 depicts the grand averaged ERPs to switch and non-switch conditions at frontal, central, and parietal channels for 1 Hz rTMS and sham rTMS stimulations, including post-stimulation and pre-stimulation. **Figure 3** presents voltage distribution of P2, N2, P3, and LPC to switch and non-switch conditions for 1 Hz rTMS and sham rTMS stimulations.

P2 (140–240 ms Post-stimulus)

Analysis of the P2 component in the frontal channels revealed a significant main effect of time [$F_{(1,\ 27)} = 5.481$, $p = 0.027$], indicating a larger P2 at post-stimulation (5.074 ± 0.573 μV) than at pre-stimulation (4.31 ± 0.604 μV). The main effect of switching type was also significant [$F_{(1,\ 27)} = 4.671$, $p = 0.04$]. The amplitude of the switch trials (4.989 ± 0.56 μV) was greater than the non-switch trials (4.395 ± 0.604 μV). No other main effect or interaction effects were found [$F_{(1,\ 27)} = 0.531$, $p = 0.472$; stimulation × time $F_{(1,\ 27)} = 0.826$, $p = 0.371$; stimulation × switching $F_{(1,\ 27)} = 1.735$, $p = 0.199$; time × switching $F_{(1,\ 27)} = 0.749$, $p = 0.395$; and stimulation × time × switching $F_{(1,\ 27)} = 0.103$, $p = 0.751$, respectively].

Analysis of the P2 component in the central channels revealed a marginally significant main effect of time [$F_{(1,\ 27)} = 4.075$, $p = 0.054$], indicating a larger P2 at post-stimulation (4.779 ± 0.519 μV) than at pre-stimulation (4.148 ± 0.519 μV). The main effect of switching type was also significant [$F_{(1,\ 27)} = 7.196$, $p = 0.012$]. The amplitude of the switch trials (4.736 ± 0.488 μV) was greater than the non-switch trials (4.191 ± 0.522 μV). No other main effect or interaction effects were found [$F_{(1,\ 27)} = 0.087$, $p = 0.771$; stimulation × time $F_{(1,\ 27)} = 0.151$, $p = 0.701$; stimulation × switching $F_{(1,\ 27)} = 0.712$, $p = 0.406$; time × switching $F_{(1,\ 27)} = 1.022$, $p = 0.321$; and stimulation × time × switching $F_{(1,\ 27)} = 0.129$, $p = 0.722$, respectively]. There were no main effects or interactions in the parietal channels.

N2 (260–340 ms Post-stimulus)

Analysis of the N2 in the frontal channels revealed a marginally significant main effect of time [$F_{(1,\ 27)} = 2.992$, $p = 0.095$]. There was a marginally significant interaction between stimulation × switching [$F_{(1,\ 27)} = 3.954$, $p = 0.057$]. Through further analysis, we found a significant main effect of

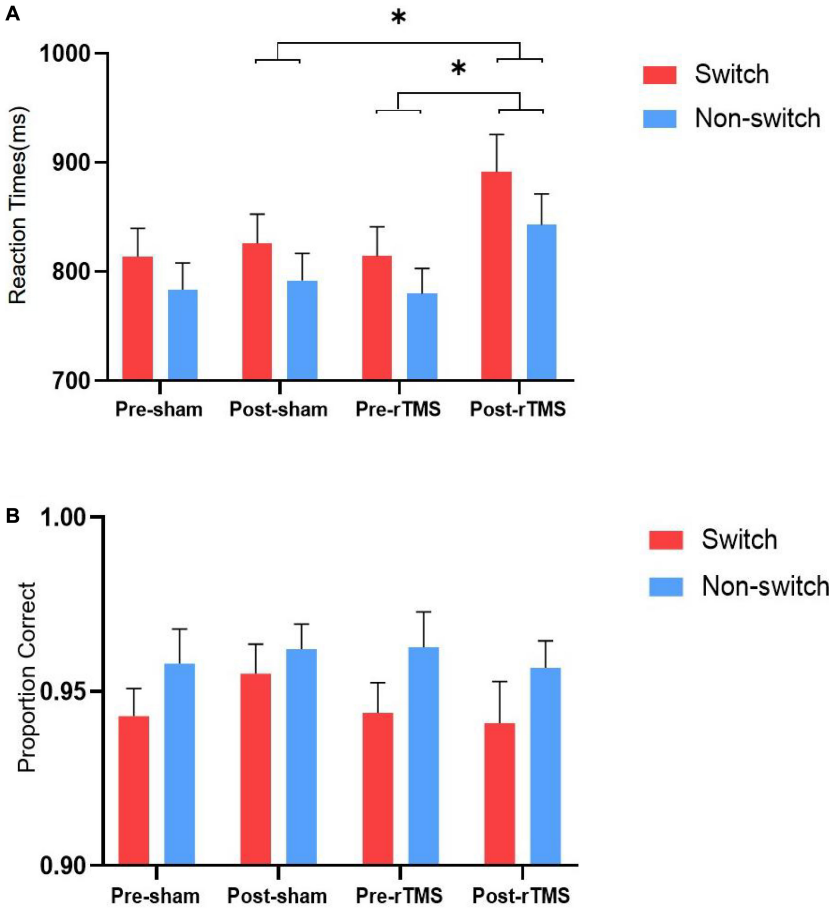

FIGURE 1 | Reaction times **(A)** and accuracy rates **(B)** on switch and non-switch conditions for different stimulation conditions. * Significant difference between stimulation conditions, $p < 0.05$. Error bars represent SEM.

switching type [$t(27) = -2.199$, $p = 0.037$] with sham rTMS, whereas no such difference was found within rTMS stimulation [$t(27) = 1.109$, $p = 0.277$]. The N2 amplitude of switch trials (0.533 ± 0.628 μV) was more pronounced (more negative) than non-switch trials (1.031 ± 0.544 μV) with sham rTMS. The main effects of stimulation [$F_{(1,\ 27)} = 0.084$, $p = 0.774$] and switching [$F_{(1,\ 27)} = 0.119$, $p = 0.733$] were not significant. The interactions stimulation × time, time × switching, and stimulation × time × switching [$F_{(1,\ 27)} = 0.408$, $p = 0.528$; $F_{(1,\ 27)} = 0.053$, $p = 0.819$; $F_{(1,\ 27)} = 0.031$, $p = 0.862$] were not significant.

Analysis of the N2 in the central channels revealed a marginally significant main effect of time [$F_{(1,\ 27)} = 3.121$, $p = 0.089$]. The main effects of stimulation [$F_{(1,\ 27)} = 0.268$, $p = 0.609$] and switching [$F_{(1,\ 27)} = 0.924$, $p = 0.345$] were not significant. The interactions stimulation × time, stimulation × switching, time × switching, and stimulation × time × switching were not significant [$F_{(1,\ 27)} = 0.007$, $p = 0.936$; $F_{(1,\ 27)} = 2.176$, $p = 0.152$; $F_{(1,\ 27)} = 0.176$, $p = 0.678$; $F_{(1,\ 27)} = 0.025$, $p = 0.876$, respectively].

Analysis of the N2 in the parietal channels revealed a three-way interaction between stimulation × time × switching [$F_{(1,\ 27)} = 4.702$, $p = 0.039$]. At non-switch trials, further analysis revealed that there was a significant main effect of stimulation [$F_{(1,\ 27)} = 4.62$, $p = 0.041$]. The interaction between the stimulation × time was also significant [$F_{(1,\ 27)} = 11.974$, $p = 0.002$]. Further analysis revealed a significant main effect of stimulation [$t(27) = 3.08$, $p = 0.005$] at post-stimulation, whereas no such difference was found at pre-stimulation [$t(27) = -0.965$, $p = 0.343$]. The N2 amplitude of rTMS (4.615 ± 0.681 μV) was more pronounced (more negative) than sham rTMS (6.006 ± 0.55 μV) at post-stimulation. There were no main effects or interaction effects at switch trials.

P3 (360–450 ms Post-stimulus)

There were no main effects or interactions in the frontal and central channels. Analysis of the P3 in the parietal channels revealed a significant main effect of stimulation [$F_{(1,\ 27)} = 7.876$, $p = 0.009$], which revealed significant decreased P3 amplitude in rTMS (7.128 ± 0.588 μV) in contrast to sham rTMS (8.091 ± 0.694 μV). There was a significant interaction between stimulation × time [$F_{(1,\ 27)} = 6.736$, $p = 0.015$]. Through further analysis, we found a significant main effect of stimulation [$t(27) = 2.84$, $p = 0.008$] at post-stimulation, whereas no such difference was found at pre-stimulation [$t(27) = 0.562$, $p = 0.579$].

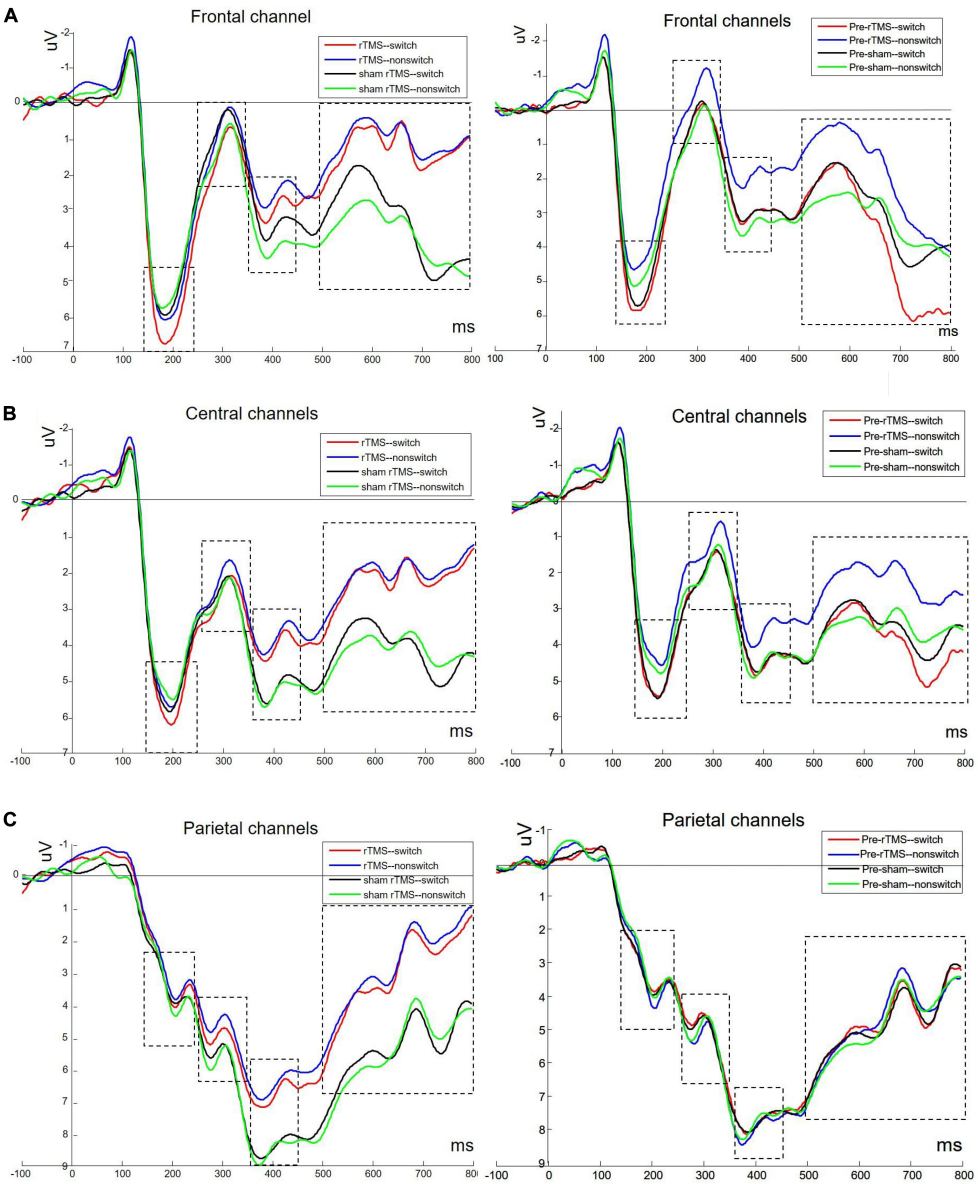

FIGURE 2 | Grand averaged ERPs to switch and non-switch conditions at frontal (**A**: average of channels 4, 27, and 31), central (**B**: average of channels 8, 23, and 32), and parietal channels (**C**: average of channels 12, 13, and 19) for 1 Hz rTMS and sham rTMS stimulations, including post-stimulation and pre-stimulation.

There was a significant decreased P3 amplitude in rTMS ($6.665 \pm 0.649\ \mu V$) in contrast to sham rTMS ($8.474 \pm 0.707\ \mu V$) at post-stimulation. The main effects of time [$F_{(1,\ 27)} = 0.032$, $p = 0.86$] and switching [$F_{(1,\ 27)} < 0.001$, $p = 0.985$] were not significant. The interactions stimulation × switching, time × switching, and stimulation × time × switching [$F_{(1,\ 27)} = 0.822$, $p = 0.373$; $F_{(1,\ 27)} = 0.793$, $p = 0.381$; $F_{(1,\ 27)} = 1.601$, $p = 0.217$, respectively] were not significant.

Late Positive Component (LPC, 500–800 ms Post-stimulus)

Analysis of the LPC in the frontal channels revealed a significant main effect of stimulation [$F_{(1,\ 27)} = 7.019$, $p = 0.013$], which revealed significant decreased LPC amplitude in rTMS ($1.999 \pm 0.503\ \mu V$) in contrast to sham rTMS ($3.316 \pm 0.736\ \mu V$). There was a marginally significant interaction between stimulation × time [$F_{(1,\ 27)} = 4.136$, $p = 0.052$]. Through further analysis, we found a significant main effect of stimulation [$t(27) = 2.631$, $p = 0.014$] at post-stimulation, whereas no such difference was found at pre-stimulation [$t(27) = 0.648$, $p = 0.522$]. There was a significant decreased LPC amplitude in rTMS ($1.205 \pm 0.643\ \mu V$) in contrast to sham rTMS ($3.543 \pm 0.736\ \mu V$) at post-stimulation. No other main effects or interaction effects were found.

Analysis of the LPC in the central channels revealed a significant main effect of stimulation [$F_{(1,\ 27)} = 7.436$, $p = 0.011$],

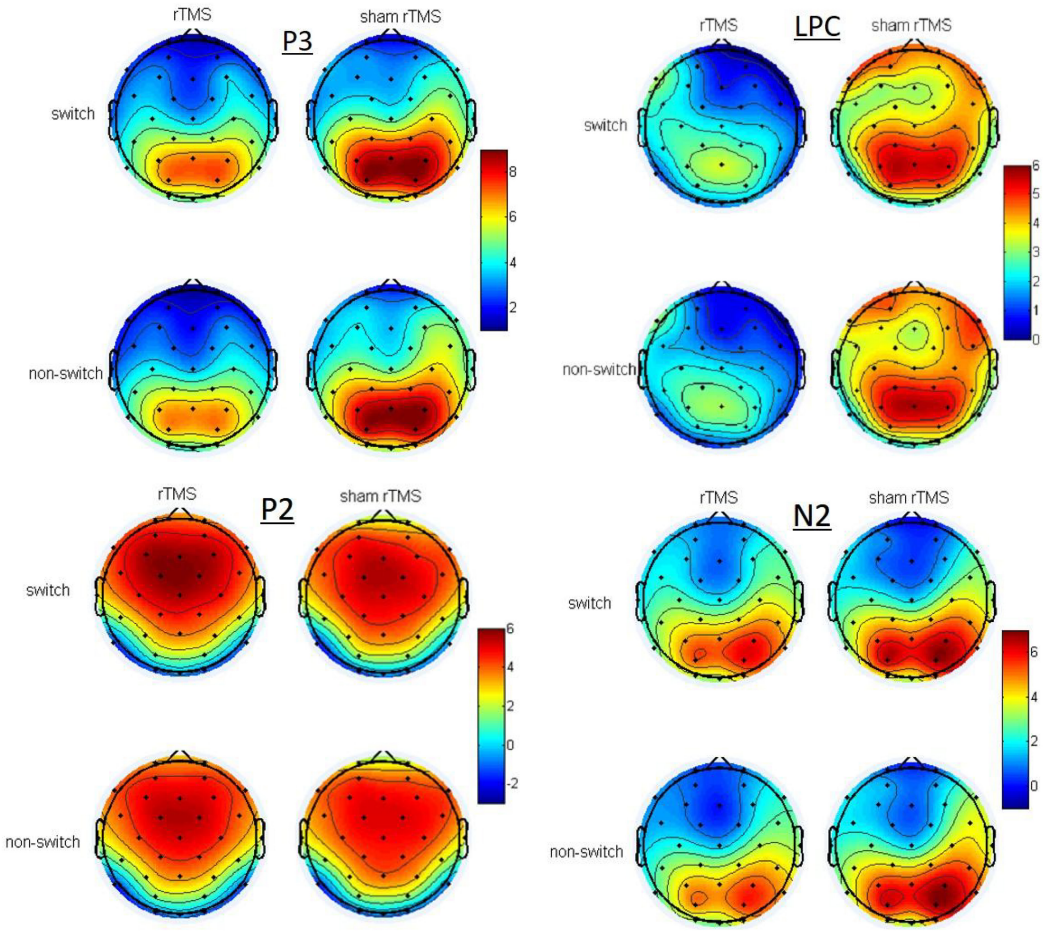

FIGURE 3 | Topographic maps of the voltage distribution of P2, N2, P3, and LPC to switch and non-switch conditions for 1 Hz rTMS and sham rTMS stimulations at post-stimulation.

which revealed significant decreased LPC amplitude in rTMS (2.51 ± 0.398 μV) in contrast to sham rTMS (3.829 ± 0.622 μV). No other main effects or interaction effects were found.

Analysis of the LPC in the parietal channels revealed a significant main effect of stimulation [$F_{(1,\ 27)}$ = 14.767, p = 0.001], which revealed significant decreased LPC amplitude in rTMS (3.731 ± 0.449 μV) in contrast to sham rTMS (5.079 ± 0.667 μV). There was a significant interaction between stimulation × time [$F_{(1,\ 27)}$ = 9.804, p = 0.004]. Through further analysis, we found a significant main effect of stimulation [$t(27)$ = 3.742, p = 0.001] at post-stimulation, whereas no such difference was found at pre-stimulation [$t(27)$ = 0.848, p = 0.404]. There was a significant decreased LPC amplitude in rTMS (2.93 ± 0.443 μV) in contrast to sham rTMS (5.404 ± 0.714 μV) at post-stimulation. No other main effects or interaction effects were found.

DISCUSSION

We investigated behavioral and ERP results of executive function in healthy subjects with rTMS stimulation compared with sham rTMS. At the behavioral level, we found poorer performance of subjects with rTMS stimulation, resulting in longer RTs. The average response time of switch trials was significantly longer than that of non-switch trials. On an electrophysiological level, there is an obvious switching effect of P2 amplitude in frontal and central channels. At post-stimulation, the N2 amplitude of rTMS is more negative than that of sham rTMS at non-switch trials, whereas no such difference was found at switch trials. The P3 amplitude and LPC amplitude are significantly reduced by rTMS at post-stimulation, whereas no such difference was found at pre-stimulation. These results indicate that rTMS of the left DLPFC resulted in significant impairments in the task switching of executive function.

Many studies have found that the change of executive function is closely related to the changes of ERP components, which shows the substantial change of event-related brain electrical activities. For example, in the study of the executive function of dyslexic adolescents, it was found that (Horowitz-Kraus, 2012) in the implementation task of the Wisconsin Card Sorting Test (WCST), ERP differences were found under the condition of "target-locked," and the ERP components (N100, P300) of dyslexics were lower than those of skilled readers.

In this study, for the P2 component, it is found that there is a significant switching effect in frontal and central scalp locations, and the P2 amplitude in switch trials was greater than that in non-switch trials. This shows that the impact of task switching on P2 component reflects the recruitment of processes related to the switch of task sets, which is consistent with other research results (Raz et al., 2016). An additional active reconfiguration process is supposed to be needed in switch trials in order to activate the task set of the current trial and to inhibit the task set of the previous trial (Fiedler et al., 2009). Higher cognitive control resources, reflected by larger P2 amplitude, are needed during switch trials (Massa et al., 2020). P2 is believed to originate from the visual association cortex and is related to the task relevance of evaluating stimuli. A study (Choi et al., 2014) has found that the increase of P200 amplitude of auditory oddball task after 3 weeks of rTMS treatment is related to the improvement of depression symptoms in drug-resistant depression patients, which may play a role by suppressing irrelevant features (negative stimuli) or enhancing related features (positive stimuli). In this study, rTMS stimulation had no effect on the switch effect of P2 components, indicating that rTMS stimulation of the left DLPFC had little effect on the early perception stage of task switching in healthy people.

In the parietal scalp locations, at post-stimulation, the N2 amplitude of rTMS is more negative than that of sham rTMS at non-switch trials, whereas no such difference was found at switch trials. N2 is considered to reflect the successful inhibition control, and its neural sources include frontal lobe and superior temporal cortex, as well as anterior cingulate cortex. The frontal cortex is a key area for sensory information integration, and also a key area for controlling and allocating attention resources (Nathou et al., 2018). Some results suggested that the difference between switch and repeat trials is due primarily to differences in the strength of responses within a statistically indistinguishable frontoparietal brain network, which indicated that the activity on switch trials is not qualitatively different from that on repeat trials (Wylie et al., 2009). The difference between switch and non-switch N2 suggests that during implementation of task sets (i.e., stimulus–response sets), interference from the currently irrelevant S–R set has to be overcome (inhibited) (Gajewski et al., 2018). However, the switch-N2 effect was not found in this study, which is consistent with another relevant study (Zhuo et al., 2021). The current study found that N2 was less sensitive to task switching, but more sensitive to rTMS stimulation. The N2 amplitude of rTMS stimulation was more negative than that of sham rTMS for non-switch trials at post-stimulation, which indicated that inhibition control of rTMS stimulation was more effective for non-switch trials. The low-frequency rTMS stimulation inhibited the cortical excitability, changing the N2 amplitude of task switching, which may reflect the active "top-down" suppression of dominant response.

Analysis of the P3 in the parietal channels showed a significant effect of rTMS stimulation at post-stimulation, whereas no such difference was found at pre-stimulation. The amplitude of P3 induced by low-frequency rTMS stimulation was smaller than that induced by sham stimulation. The study gave evidence that prefrontal areas of the left hemisphere play a major role in eliciting the P3 component (Evers et al., 2001). It seems to be a consensus that P3 has become a neurophysiological indicator for information processing and updating in working memory (Gu et al., 2019). In many studies, P3 amplitude is associated with the success of task performance, including attention and memory (Downes et al., 2017). Studies have found that the P3 amplitude was larger for those trials that responded faster (Jost et al., 2008). The amplitude of P300, MMN, and N400 increased after 10 Hz high-frequency rTMS stimulation in schizophrenic patients (Lin et al., 2018), which can be used as a valuable electrophysiological reference for evaluating the therapeutic effect of rTMS in schizophrenia. In this study, low-frequency rTMS stimulation of the left DLPFC reduced the amplitude of P3, which may damage the information processing and updating process in task switching, and this is consistent with our behavioral results of impaired performance. There were significant changes of P3 amplitude stimulated by rTMS in the parietal areas far away from the stimulation, which showed that rTMS could affect the function of the surrounding cortex in relatively distant areas (Nathou et al., 2018), and the affected areas were related to the functional state of the brain, which was also confirmed in the relevant fMRI experiment (van den Heuvel et al., 2013).

Analysis of the LPC in frontal and parietal channels showed that there was a significant effect of rTMS stimulation at post-stimulation, whereas no such difference was found at pre-stimulation. The amplitude of low-frequency rTMS stimulation was smaller than that of sham stimulation. In the previous task switching paradigm study, healthy controls induced a more positive posterior switch positivity (PSP) (Elchlepp et al., 2012) waveform under the switch cues than the non-switch cues, while the amyotrophic lateral sclerosis (ALS) patients lacked switch-related ERP modulations due to executive dysfunction (Lange et al., 2016). The reason why there is no PSP waveform in the results of this study may be the different switching paradigms used. In this study, there was no cue before the stimulus was presented, but the switch or non-switch stimulus was directly presented. Therefore, there was no process of identifying clues in advance and preparing for anticipation, and there were differences in cognitive processing. This component of time window of 500–800 ms is usually called the LPC, which is found to be related to the cognitive process of conflict resolution and self-monitoring in speech production in language switching study (Pestalozzi et al., 2020). The LPC was decreased in frontal and parietal channels, suggesting the involvement of the frontoparietal network in task-switch processes. The LPC may reflect the activity of a neural mechanism that supports processes of the task set reconfiguration involved in the task-switch processes (Bisiacchi et al., 2009). Low-frequency rTMS stimulation of the left DLPFC reduces the amplitude of LPC, which may indicate that the task set reconfiguration efficiency in the process of task execution is affected and the frontal lobe's recruitment of cognitive resources is reduced.

In this study, the effect of low-frequency rTMS on behavior results is significant, which is consistent with some research results (Lowe et al., 2018). As there was no significant stimulation × time × switching interaction in behavior, it seems that rTMS did not cause behavioral changes in switching

tasks; however, the significant interaction was found in ERP results, which indicates that the change of brain activity in these executive control areas following stimulation seems to be related to task switching. In healthy bilinguals who have a high level of attentional control, the effects of prefrontal cTBS stimulation on language control showed no behavioral changes, but ERP changes (Pestalozzi et al., 2020), which were different from patients with lesions in the DLPFC. Many studies have shown that ERP measurement may be more sensitive to the impact of rTMS than behavioral data. Gottesman and Gould (2003) and Grossheinrich et al. (2013) introduced the concept of endophenotype, that is, "measurable components that are invisible to the naked eye along the pathway between disease and distal genotype." Compared with behavioral measures such as RT and accuracy, ERP measurement is an invisible component. The concept of endophenotype explains the interaction change in endogenous cognitive ERP components without behavioral changes.

There are still some deficiencies in this study. Firstly, the limitations of the sham rTMS approach used in this paper do exist. In recent years, new progress has been made in the study of TMS, and the research on sham TMS approaches has become more and more in-depth. Turning the coil on its side is not really and effective sham condition. It is rather difficult to determine whether or not there is residual brain stimulation in such cases (Duecker and Sack, 2015). Therefore, more appropriate TMS control conditions should be used in the future. Secondly, executive function includes multiple sub-components, including inhibitory control, working memory, and decision-making, but this study only studied one of them, cognitive flexibility through task switching. In the future, we plan to study other sub-components of executive function.

CONCLUSION

In conclusion, we present a novel investigation of cognitive function and associated brain mechanisms and dynamics in rTMS stimulation. Our results clearly indicate impairments in executive function in the rTMS condition, accompanied by significant alterations in neural activation. Low-frequency rTMS of the left DLPFC can cause decline of executive function, resulting in the change of N2 amplitude and the decrease of amplitude of P3 component and LPC component during the performance of task switching. Low-frequency rTMS has an effect on many stages of cognitive time course of executive function in healthy subjects. The influence of early perception stage is not significant, and the effect is obvious in parietal area, which has positive significance for the evaluation and treatment of executive function.

DATA AVAILABILITY STATEMENT

The raw data supporting the conclusions of this article will be made available by the authors, without undue reservation.

ETHICS STATEMENT

The studies involving human participants were reviewed and approved by the Ethical Committee of the Zhujang Hospital of Southern Medical University. The patients/participants provided their written informed consent to participate in this study.

AUTHOR CONTRIBUTIONS

XW contributed to the experimental operation and data processing. SL, JM, KW, ZW, JL, JC, HZ, and WW contributed to the experimental design. WW was helpful in the whole process of the experiment and the writing of the manuscript. All authors contributed to the article and approved the submitted version.

FUNDING

This work was supported by the Zhujiang Hospital of Southern Medical University. This study was also supported by the National Natural Science Foundation of China (No. 81772430).

REFERENCES

Bahlmann, J., Beckmann, I., Kuhlemann, I., Schweikard, A., and Münte, T. F. (2015). Transcranial magnetic stimulation reveals complex cognitive control representations in the rostral frontal cortex. *Neuroscience* 300, 425–431. doi: 10.1016/j.neuroscience.2015.05.058

Bisiacchi, P. S., Schiff, S., Ciccola, A., and Kliegel, M. (2009). The role of dual-task and task-switch in prospective memory: behavioural data and neural correlates. *Neuropsychologia* 47, 1362–1373. doi: 10.1016/j.neuropsychologia.2009.01.034

Choi, K. M., Jang, K. M., Jang, K. I., Um, Y. H., Kim, M. S., Kim, D. W., et al. (2014). The effects of 3 weeks of rTMS treatment on P200 amplitude in patients with depression. *Neurosci. Lett.* 577, 22–27.

DeRight, J. (2019). History of "Frontal" syndromes and executive dysfunction. *Front. Neurol. Neurosci.* 44:100–107. doi: 10.1159/000494957

Downes, M., Bathelt, J., and De Haan, M. (2017). Event-related potential measures of executive functioning from preschool to adolescence. *Dev. Med. Child Neurol.* 59, 581–590. doi: 10.1111/dmcn.13395

Duecker, F., and Sack, A. T. (2015). Rethinking the role of sham TMS. *Front. Psychol.* 6:210. doi: 10.3389/fpsyg.2015.00210

Elchlepp, H., Lavric, A., Mizon, G. A., and Monsell, S. (2012). A brain-potential study of preparation for and execution of a task-switch with stimuli that afford only the relevant task. *Hum. Brain Mapp.* 33, 1137–1154. doi: 10.1002/hbm.21277

Evers, S., Bockermann, I., and Nyhuis, P. W. (2001). The impact of transcranial magnetic stimulation on cognitive processing: an event-related potential study. *Neuroreport* 12, 2915–2918. doi: 10.1097/00001756-200109170-00032

Fiedler, A., Schröter, H., and Ulrich, R. (2009). No evidence for a late locus of task switch effects. *Brain Res.* 1253, 74–80. doi: 10.1016/j.brainres.2008.11.091

Gajewski, P. D., Ferdinand, N. K., Kray, J., and Falkenstein, M. (2018). Understanding sources of adult age differences in task switching: evidence from behavioral and ERP studies. *Neurosci. Biobehav. Rev.* 92, 255–275. doi: 10.1016/j.neubiorev.2018.05.029

Gottesman, I. I., and Gould, T. D. (2003). The endophenotype concept in psychiatry: etymology and strategic intentions. *Am. J. Psychiatry* 160, 636–645. doi: 10.1176/appi.ajp.160.4.636

Grossheinrich, N., Reinl, M., Pogarell, O., Karch, S., Mulert, C., Brueckl, M., et al. (2013). Effects of low frequency prefrontal repetitive transcranial magnetic stimulation on the N2 amplitude in a GoNogo task. *PLoS One* 8:e67136. doi: 10.1371/journal.pone.0067136

Gu, L., Chen, J., Gao, L., Shu, H., Wang, Z., Liu, D., et al. (2019). Deficits of visuospatial working memory and executive function in single- versus multiple-domain amnestic mild cognitive impairment: a combined ERP and sLORETA study. *Clin. Neurophysiol.* 130, 739–751. doi: 10.1016/j.clinph.2019.01.025

Guo, Q., Zhou, T., Li, W., Dong, L., Wang, S., and Zou, L. (2017). Single-trial EEG-informed fMRI analysis of emotional decision problems in hot executive function. *Brain Behav.* 7:e728. doi: 10.1002/brb3.728

Hawkes, T. D., Manselle, W., and Woollacott, M. H. (2014). Tai Chi and meditation-plus-exercise benefit neural substrates of executive function: a cross-sectional, controlled study. *J Complement. Integr. Med.* 11, 279–288. doi: 10.1515/jcim-2013-0031

He, R., Fan, J., Wang, H., Zhong, Y., and Ma, J. (2020). Differentiating responders and non-responders to rTMS treatment for disorder of consciousness using EEG after-effects. *Front. Neurol.* 11:583268. doi: 10.3389/fneur.2020.583268

Horowitz-Kraus, T. (2012). Pinpointing the deficit in executive functions in adolescents with dyslexia performing the wisconsin card sorting test. *J. Learn. Disabil.* 47, 208–223. doi: 10.1177/0022219412453084

Jost, K., Mayr, U., and Rosler, F. (2008). Is task switching nothing but cue priming? Evidence from ERPs. *Cogn. Affect. Behav. Neurosci.* 8, 74–84. doi: 10.3758/CABN.8.1.74

Ko, J. H., Monchi, O., Ptito, A., Bloomfield, P., Houle, S., and Strafella, A. P. (2008). Theta burst stimulation-induced inhibition of dorsolateral prefrontal cortex reveals hemispheric asymmetry in striatal dopamine release during a set-shifting task - a TMS-[(11)C]raclopride PET study. *Eur. J. Neurosci.* 28, 2147–2155. doi: 10.1111/j.1460-9568.2008.06501.x

Küper, K., Gajewski, P. D., Frieg, C., and Falkenstein, M. (2017). A randomized controlled ERP study on the effects of multi-domain cognitive training and task difficulty on task switching performance in older adults. *Front. Hum. Neurosci.* 11:184. doi: 10.3389/fnhum.2017.00184

Lange, F., Vogts, M., Seer, C., Fürkötter, S., Abdulla, S., Dengler, R., et al. (2016). Impaired set-shifting in amyotrophic lateral sclerosis: an event-related potential study of executive function. *Neuropsychology* 30, 120–134. doi: 10.1037/neu0000218

Levit-Binnun, N., Litvak, V., Pratt, H., Moses, E., Zaroor, M., and Peled, A. (2010). Differences in TMS-evoked responses between schizophrenia patients and healthy controls can be observed without a dedicated EEG system. *Clin. Neurophysiol.* 121, 332–339. doi: 10.1016/j.clinph.2009.10.035

Lin, X. D., Chen, X. S., Chen, C., Zhang, L. J., Xie, Z. L., Huang, Z. Y., et al. (2018). Effects of repetitive transcranial magnetic stimulation treatment on event - related potentials in Schizophrenia. *Chin. Med. J.* 131, 301–306. doi: 10.4103/0366

Lowe, C. J., and Hall, P. A. (2018). Reproducibility and sources of interindividual variability in the responsiveness to prefrontal continuous theta burst stimulation (cTBS). *Neurosci. Lett.* 687, 280–284. doi: 10.1016/j.neulet.2018.09.039

Lowe, C. J., Manocchio, F., Safati, A. B., and Hall, P. A. (2018). The effects of theta burst stimulation (TBS) targeting the prefrontal cortex on executive functioning: a systematic review and meta-analysis. *Neuropsychologia* 111, 344–359. doi: 10.1016/j.neuropsychologia.2018.02.004

Massa, E., Köpke, B., and El Yagoubi, R. (2020). Age-related effect on language control and executive control in bilingual and monolingual speakers: Behavioral and electrophysiological evidence. *Neuropsychologia* 138, 107336. doi: 10.1016/j.neuropsychologia.2020.107336

Nathou, C., Duprey, E., Simon, G., Razafimandimby, A., Razafimandimby, A., Dollfus, S., et al. (2018). Effects of low- and high-frequency repetitive transcranial magnetic stimulation on long-latency auditory evoked potentials. *Neurosci. Lett.* 686, 198–204.

Niendam, T. A., Laird, A. R., Ray, K. L., Dean, Y. M., Glahn, D. C., and Carter, C. S. (2012). Meta-analytic evidence for a superordinate cognitive control network subserving diverse executive functions. *Cogn. Affect. Behav. Neurosci.* 12, 241–268. doi: 10.3758/s13415-011-0083-5

Noda, Y., Barr, M. S., Zomorrodi, R., Cash, R. F. H., Rajji, T. K., Farzan, F., et al. (2018). Reduced short-latency afferent inhibition in prefrontal but not motor cortex and its association with executive function in schizophrenia: a combined TMS-EEG study. *Schizophr. Bull.* 44, 193–202. doi: 10.1093/schbul/sbx041

Noda, Y., Zomorrodi, R., Backhouse, F., Cash, R. F. H., Barr, M. S., Rajji, T. K., et al. (2017). Reduced prefrontal short—latency afferent inhibition in older adults and its relation to executive function: a TMS-EEG study. *Front. Aging Neurosci.* 9:119. doi: 10.3389/fnagi.2017.00119

Ozga, J. E., Povroznik, J. M., Engler-Chiurazzi, E. B., and Haar, C. V. (2018). Executive (dys)function after traumatic brain injury. *Behav. Pharmacol.* 29, 617–637. doi: 10.1097/FBP.0000000000000430

Pestalozzi, M. I., Annoni, J., Müri, R. M., and Jost, L. B. (2020). Effects of theta burst stimulation over the dorsolateral prefrontal cortex on language switching – a behavioral and ERP study. *Brain Lang.* 205:104775. doi: 10.1016/j.bandl.2020.104775

Rabinovici, G. D., Stephens, M. L., and Possin, K. L. (2015). Executive dysfunction. *Continuum (Minneap Minn)* 21, 646–659.

Raz, S., Koren, A., Dan, O., and Levin, C. (2016). Executive function and neural activation in adults with β-thalassemia major: an event-related potentials study. *Ann. N. Y. Acad. Sci.* 1386, 16–29. doi: 10.1111/nyas.13279

Ruberry, E. J., Lengua, L. J., Crocker, L. H., Bruce, J., Upshaw, M. B., and Sommerville, J. A. (2017). Income, neural executive processes, and preschool children's executive control. *Dev. Psychopathol.* 29, 143–154. doi: 10.1017/S095457941600002X

Strobach, T., Wendt, M., and Janczyk, M. (2018). Editorial: multitasking: executive functioning in dual-task and task switching situations. *Front. Psychol.* 9:108. doi: 10.3389/fpsyg.2018.00108

Swainson, R., Prosser, L., Karavasilev, K., and Romanczuk, A. (2019). The effect of performing versus preparing a task on the subsequent switch cost. *Psychol. Res.* 85, 364–383.

van den Heuvel, O. A., Van Gorsel, H. C., Veltman, D. J., and Van Der Werf, Y. D. (2013). Impairment of executive performance after transcranial magnetic modulation of the left dorsal frontal-striatal circuit. *Hum. Brain Mapp.* 34, 347–355. doi: 10.1002/hbm.21443

Vanderhasselt, M., De Raedt, R., Baeken, C., Leyman, L., and D'haenen, H. (2006). The influence of rTMS over the right dorsolateral prefrontal cortex on intentional set switching. *Exp. Brain Res.* 172, 561–565. doi: 10.1007/s00221-006-0540-5

Wylie, G. R., Murray, M. M., Javitt, D. C., and Foxe, J. J. (2009). Distinct neurophysiological mechanisms mediate mixing costs and switch costs. *J. Cogn. Neurosci.* 21, 105–118. doi: 10.1162/jocn.2009.21009

Zhuo, B., Chen, Y., Zhu, M., Cao, B., and Li, F. (2021). Response variations can promote the efficiency of task switching: electrophysiological evidence. *Neuropsychologia* 156:107828. doi: 10.1016/j.neuropsychologia.2021.107828

Conflict of Interest: The authors declare that the research was conducted in the absence of any commercial or financial relationships that could be construed as a potential conflict of interest.

frontiers in Neuroscience

SYSTEMATIC REVIEW
published: 15 November 2021
doi: 10.3389/fnins.2021.769848

The Effect of Repetitive Transcranial Magnetic Stimulation on Dysphagia After Stroke: A Systematic Review and Meta-Analysis

Weiwei Yang[1], *Xiongbin Cao*[2], *Xiaoyun Zhang*[1], *Xuebing Wang*[1], *Xiaowen Li*[1] *and Yaping Huai*[1]*

[1] Rehabilitation Department, Shenzhen Longhua District Central Hospital, Shenzhen, China, [2] Neurology Department, Shenzhen Longhua District Central Hospital, Shenzhen, China

Objective: The primary purpose of our study is to systemically evaluate the effect of repetitive transcranial magnetic stimulation (rTMS) on recovery of dysphagia after stroke.

Search Methods: We searched randomized controlled trials (RCTs) and non-RCTs published by PubMed, the Cochrane Library, ScienceDirect, MEDLINE, and Web of Science from inception until April 24, 2021. Language is limited to English. After screening and extracting the data, and evaluating the quality of the selected literature, we carried out the meta-analysis with software RevMan 5.3 and summarized available evidence from non-RCTs.

Results: Among 205 potentially relevant articles, 189 participants (from 10 RCTs) were recruited in the meta-analysis, and six non-RCTs were qualitatively described. The random-effects model analysis revealed a pooled effect size of SMD = 0.65 (95% CI = 0.04–1.26, $p = 0.04$), which indicated that rTMS therapy has a better effect than conventional therapy. However, the subgroup analysis showed that there was no significant difference between low-frequency and high-frequency groups. Even more surprisingly, there were no statistically significant differences between the two groups and the conventional training group in the subgroup analysis, but the combined effect was positive.

Conclusion: Our study suggests that rTMS might be effective in treating patients with dysphagia after stroke.

Keywords: deglutition disorders, transcranial magnetic stimulation, stroke, meta-analysis, systematic review

OPEN ACCESS

Edited by:
Jinhua Zhang,
Xi'an Jiaotong University, China

Reviewed by:
Giuseppe Lanza,
University of Catania, Italy
Taher Omari,
Flinders University, Australia

***Correspondence:**
Yaping Huai
huaiyaping@163.com

Specialty section:
This article was submitted to Neuroprosthetics, a section of the journal Frontiers in Neuroscience

Received: *02 September 2021*
Accepted: *07 October 2021*
Published: *15 November 2021*

Citation:
Yang W, Cao X, Zhang X, Wang X, Li X and Huai Y (2021) The Effect of Repetitive Transcranial Magnetic Stimulation on Dysphagia After Stroke: A Systematic Review and Meta-Analysis. Front. Neurosci. 15:769848. doi: 10.3389/fnins.2021.769848

INTRODUCTION

Dysphagia is one of the common complications after stroke, with a high incidence of 37–78% (Cola et al., 2010). Dysphagia can cause malnutrition, pneumonia, dehydration, etc., which will significantly increase the death rate of patients. Edmiaston et al. (2010) found that the mortality rate of patients with dysphagia after stroke was three times as high as stroke patients with normal deglutitive function. Therefore, rehabilitation training for dysphagia after stroke is still an urgent problem to be solved in clinical practice.

At present, repetitive transcranial magnetic stimulation (rTMS) is a non-invasive brain stimulation method for use in treating post-stroke dysphagia. In general, rTMS can be divided into two primary treatment regimes: low-frequency rTMS (<1 Hz) and high-frequency rTMS (≥1 Hz) according to its stimulation frequencies. Low-frequency rTMS (LF-rTMS) inhibits cortical excitability, while high-frequency rTMS (HF-rTMS) activates cortical excitability. It can modulate human cortical and subcortical structures both at the site of stimulation and in remote areas (Bestmann et al., 2004; Valero-Cabré et al., 2017). The repeated electrical stimulation could produce a cumulative effect, which causes nerve cells to produce action potential, promote the release of neurotransmitters and regulation of synaptic plasticity to improve neurological outcome (Michou et al., 2014). Moreover, rTMS can modify excitability of the cerebral cortex at the stimulated site and also at remote areas along functional anatomical connections (Kobayashi and Pascual-Leone, 2003). Up to now, it has been recognized that rTMS can inhibit maladaptive cortical plasticity and improve adaptive cortical activity to promote neurological rehabilitation in stroke patients. According to the latest TMS guidelines (Rossini et al., 2015), rTMS has demonstrated level "A" efficacy in the rehabilitation of depression and neuropathic pain.

As a non-pharmacological strategy, rTMS could explore cortical circuits by the measurement of motor evoked potential and cortical silent period. On the other hand, it can search the related neurochemical pathways in neurological disorders and induce cortical plasticity to achieve the purpose of treatment (Bordet et al., 2017). Some experiments and reviews have shown that the mechanism of action of rTMS mainly depends on the long-term depression (LTD) and long-term potentiation (LTP) (Ziemann, 2004; Lanza and Ferri, 2019). Additionally, the change of synaptic plasticity and neurotransmitter release are also the way for therapeutic role (Ziemann, 2004; Lanza and Ferri, 2019).

In recent years, increasing number of clinical studies and reviews have shown that rTMS can be new diagnostic and therapeutic tools for assessment and rehabilitation in motor and cognitive impairments (Fisicaro et al., 2019; Di Lazzaro et al., 2021). However, since the nerve conduction pathways of dysphagia are complex, the effects of rTMS on the improvement of dysphagia after stroke varies according to the stimulation on site, frequency, time, and other parameters. Currently, there are no detailed uniform standards for the clinical practice of rTMS on post-stroke dysphagia. Therefore, we conducted qualitative systematic review and quantitative meta-analysis of relevant clinical trials, aiming to provide objective evidence-based medical evidence for the effect of rTMS on post-stroke dysphagia.

MATERIALS AND METHODS

Search Strategy

We systematically searched five databases including PubMed, Cochrane Library, ScienceDirect, MEDLINE, and Web of Science for relevant studies, which were published through April 24, 2021. The retrieval language was limited to English, and the search strategy was designed by the combination of MeSH words and free words. MeSH words include deglutition disorders, stroke, and transcranial magnetic stimulation, and free words include swallowing disorders, dysphagia, cerebrovascular accident, apoplexy, cerebrovascular apoplexy, repetitive transcranial magnetic stimulation, and rTMS.

Inclusion and Exclusion Criteria

Two reviewers (Weiwei Yang and Xiaoyun Zhang) independently screened the titles and abstracts by applying the same inclusion and exclusion criteria. Any disagreements were resolved by consensus with the third (Yaping Huai).

Inclusion Criteria

The inclusion criteria of this meta-analysis were as follows: (1) all patients with ischemic or hemorrhagic stroke displayed definitive radiographic evidence of relevant pathology on magnetic resonance imaging (MRI) or computed tomography (CT); (2) dysphagia symptoms were investigated in all patients; (3) no participants had other neurological diseases or other swallowing disorders; and (4) the experimental group received rTMS training, and the control group received routine rehabilitation training or other rehabilitation training.

Exclusion Criteria

Exclusion criteria were as follows: (1) patients with unstable tachyarrhythmia, fever, infection, seizures, and sedative use; (2) patients had severe cognitive impairment or aphasia; (3) non-English publications; (4) papers that do not provide data of interest; (5) reduplicated articles; and (6) reviews, abstracts, case reports, and non-clinical studies.

Data Extraction and Quality Assessment

After screening the titles and abstracts, two evaluators (Weiwei Yang and Xiaoyun Zhang) independently assessed eligibility for inclusion in the analysis and extracted the relevant material according to predefined inclusion and exclusion criteria. We retrieved full-text articles for references for which a decision on eligibility could not be made based on title and abstract alone. Another two researchers (Xiongbin Cao and Xuebing Wang) then performed quality evaluation of the selected articles according to the Cochrane Handbook for Systematic Reviews of Interventions 5.1.0. The criteria consist of seven parts: random sequence generation, allocation concealment, blinding of participants and personnel, blinding of outcome assessment, incomplete outcome data, selective reporting, and other sources of bias. If the above quality standards are fully met, which indicates that the overall risk of bias is low and the study quality is high and the studies are rated as Grade A, while one or more of the standards are met, the risk of bias is moderate and the studies are defined as Grade B, and if the above standards are not met, the risk of bias is high and the quality of the studies is rated as Grade C. In cases of disagreement, a third person (Xiaowen Li) was consulted to reach a consensus.

Outcome Indicators

For the included RCTs, we calculated the mean scores (Mean) and standards deviations (SDs) before and after interventions according to guidance in the Cochrane Handbook for Systematic Reviews of Intervention. Outcome measures for the efficacy

of therapy were as follows: (1) PAS (Penetration–Aspiration Scale) and (2) DD (Dysphagia Grade). The PAS is an eight-point scale that measures selected aspects such as penetration and inhalation, depth of invasion into the delivery airway, and whether substances entering the airway are expelled (Rosenbek et al., 1996; Borders and Brates, 2020). The DD is a four-level score for the swallowing function of patients according to their clinical manifestations; the higher the grade is, the worse the swallowing function of the patients is (Ertekin et al., 2000; Khedr and Abo-Elfetoh, 2010).

Statistical Analysis

Meta-analysis was performed using Review Manager version 5.3 and heterogeneity was investigated using I^2. If $p > 0.05$ and $I^2 \leq 50\%$, heterogeneity was not significant and a fixed-effects model was used; otherwise, a random-effects model was used. If heterogeneity existed, we conducted sensitivity analysis and subgroup analysis to find the source of heterogeneity. As for subgroup analysis (frequency), random-effects model was used. A pooled standardized mean difference (SMD) together with 95% confidence interval (CI) were calculated. $p < 0.05$ was regarded as statistically significant.

RESULTS

Literature Search Results

A total of 193 articles were retrieved from PubMed (65), Cochrane Library (32), Science Direct (25), MEDLINE (17), and Web of Science (54), and 12 were retrieved through references. After reading titles and abstracts, 81 duplicated studies and 68 irrelevant studies were excluded. After reading the full text, 30 articles without available full-text visions or outcomes data and 13 literature including complex experimental scheme were excluded. Finally, we included seven literature (Khedr et al., 2009; Khedr and Abo-Elfetoh, 2010; Kim et al., 2011; Park et al., 2013, 2017; Lim et al., 2014; Ünlüer et al., 2019), with a total of 186

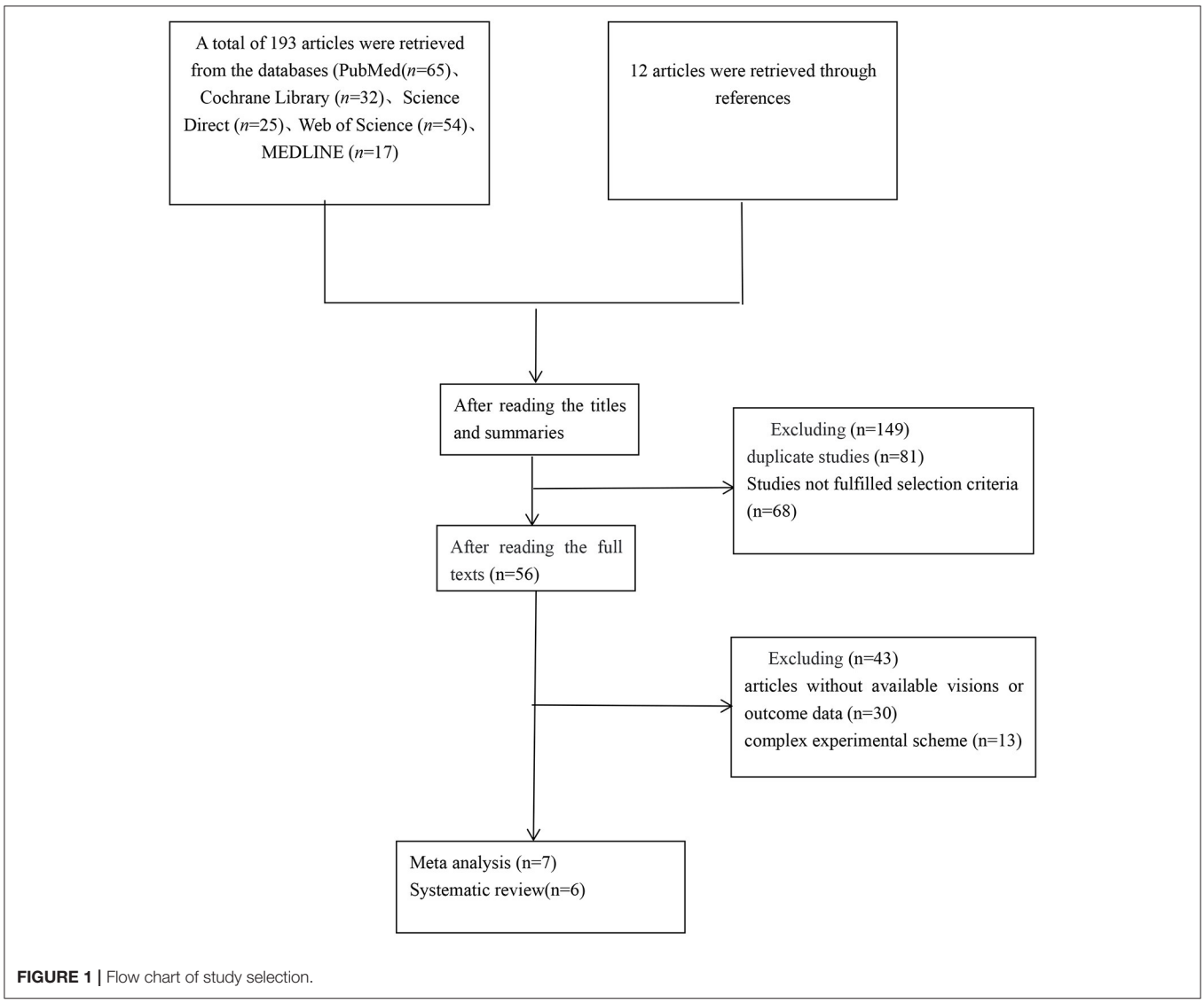

FIGURE 1 | Flow chart of study selection.

participants from 14 groups of patients in our meta-analysis, and a qualitative systematic review of six studies (Verin and Leroi, 2009; Cheng et al., 2015, 2017; Du et al., 2016; Tarameshlu et al., 2019; Zhang et al., 2019). The literature screening process and detailed characteristics of included studies are shown in **Figure 1** and **Table 1**.

Quality Assessment of the Included Studies

In our included literature, individual articles designed two experimental groups according to the lesion site, stimulation frequency, and other parameters. According to our audit, it was found that both two experimental groups in the same literature did not interfere with each other. Therefore, we treated each study in these three literatures (Khedr and Abo-Elfetoh, 2010; Kim et al., 2011; Park et al., 2017) as a randomized controlled experiment. So, we got 10 studies from seven articles. Two researchers evaluated the reporting quality of 10 included studies. The integrity of the data was guaranteed to a great extent, but the experimental scheme of Khedr and Abo-Elfetoh (2010), Kim et al. (2011), and Lim et al. (2014) had a risk of selection bias. Researches of Park et al. (2017) and Ünlüer et al. (2019) had an implementation bias (complete blindness of subjects was not achieved). Out of the 10 studies, 2 studies (Khedr et al., 2009; Park et al., 2013) were rated as Grade A, while others were rated as Grade B. The results were presented in **Figures 2**, **3** and **Table 2**.

Additionally, the outcome indicators in recruited articles were different; we have to use a random-effects model and SMD to reduce the inevitable heterogeneity. In future experiments and studies, we will try to select the same standard for unified data analysis of randomized controlled trials.

Results of Systematic Review

A total of six studies with a small sample size or non-randomized controlled trial studies (Verin and Leroi, 2009; Cheng et al., 2015, 2017; Du et al., 2016; Tarameshlu et al., 2019; Zhang et al., 2019) were included in the systematic review. They investigated the efficacy of rTMS on patients with dysphagia after stroke from different perspectives. Tarameshlu et al. (2019), Zhang et al. (2019), Du et al. (2016), and Verin and Leroi (2009) all supported that rTMS treatment over the tongue area of the motor cortex may facilitate the recovery of dysphagia after stroke. However, not all studies proved the efficacy of rTMS for the treatment of dysphagia. The research group of Cheng et al. published

TABLE 1 | Characteristics of the randomized controlled studies.

References	*N*		Age (years)		Intervention		Time	Outcome measures
	E	C	E	C	E	C		
Kim et al., 2011	10	10	69.8 ± 8.0	68.2 ± 12.6	5 Hz, 100% MT, ipsilesional mylohyoid muscle	Sham stimulation	20 min/day, 5 days/week, 2 weeks	FDS, PAS
Kim et al., 2011	10	10	66.4 ± 12.3	68.2 ± 12.6	1 Hz, 100% MT, contralesional mylohyoid muscle	Sham stimulation	20 min/day, 5 days/week, 2 weeks	FDS, PAS
Khedr et al., 2009	14	12	58.9 ± 11.7	56.2 ± 13.4	3 Hz, 120% MT, ipsilesional esophagus area	Sham stimulation	10 min/day, 5 days	DD
Khedr and Abo-Elfetoh, 2010	6	5	56.7 ± 16	58.0 ± 17.5	3 Hz, 130% MT, both hemisphere esophagus area	Sham stimulation	10 min/day, 5 days	DD
Khedr and Abo-Elfetoh, 2010	5	6	55.4 ± 9.7	60.5 ± 11.0	3 Hz, 130% MT, both hemisphere esophagus area	Sham stimulation	10 min/day, 5 days	DD
Park et al., 2013	9	9	73.7 ± 3.8	68.9 ± 9.3	5 Hz, 90% MT, contralesional pharyngeal	Sham stimulation	10 min/day, 5 days/week, 2 weeks	VDS, PAS
Ünlüer et al., 2019	15	13	67.8 ± 11.9	69.3 ± 12.9	1 Hz, 90% MT, unaffected hemisphere mylohyoid muscle	Conventional therapy	20 min/day, 5 days	PAS
Lim et al., 2014	14	15	59.8 ± 11.8	62.5 ± 8.2	1 Hz, 100% MT, contralesional hemisphere pharyngeal	Conventional therapy	20 min/day, 5 days/week, 2 weeks	FDS, PTT, PAS
Park et al., 2017	11	11	67.5 ± 13.4	69.6 ± 8.6	10 Hz, 90% MT, ipsilesional hemisphere mylohyoid	Sham stimulation	20 min/day, 5 days/week, 2 weeks	DOSS, PAS, VDS
Park et al., 2017	11	11	60.2 ± 13.8	69.6 ± 8.6	10 Hz, 90% MT, bilateral hemisphere mylohyoid	Sham stimulation	20 min/day, 5 days/weeks, 2 weeks	DOSS, PAS, VDS

T, experimental group; C, control group; Hz, hertz; MT, motor threshold; FDS, functional dysphagia scale; PAS, penetration-aspiration scale; VDS, videofluoroscopic dysphagia scale; DD, dysphagic grade; PTT, pharyngeal transit time; ASHA NOMS, American speech-language hearing association national outcomes measurements system swallowing scale.

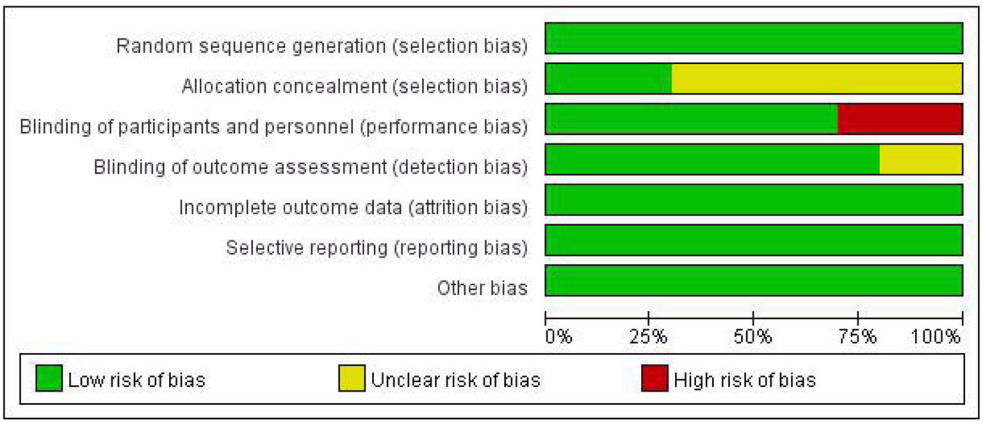

FIGURE 2 | Risk of bias graph.

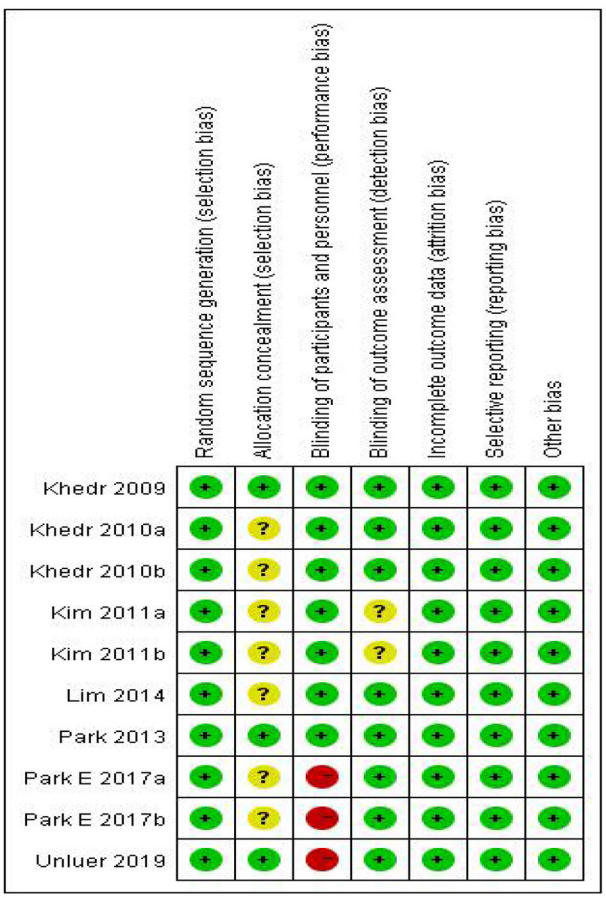

FIGURE 3 | Risk of bias summary.

relevant studies of rTMS on swallowing disorders in chronic post-stroke patients in 2015 and 2017, respectively (Cheng et al., 2015, 2017). In the previous study, they pointed out that 5-Hz rTMS might improve swallowing flexibility and promote the recovery of swallowing function *via* improving tongue muscle function, but the latter study showed that the efficacy retention time of rTMS was relatively short, and the long-term therapeutic effect could not be observed. The two studies were conducted by the same authors and design, but the result was different, which probably resulted from the small sample size. It was found that the theoretical basis of these studies was based on the hypothesis of transcallosal imbalance for bilateral hemisphere, which also suggested that functional recovery of dysphagia after stroke critically depends on neural plasticity.

Results of Meta-Analysis

Effects on Deglutition Disorders

Ultimately, 10 studies involving 186 subjects were included in the meta-analysis. The pooled results indicated that rTMS had a significant effect on the improvement of swallowing function after stroke compared with the control group [SMD = 0.65, 95% CI (0.04, 1.26), $p = 0.04$, fixed-effects model]. However, there was great heterogeneity among studies ($p = 0.0004$, $I^2 = 74\%$). Due to the small number of included control groups, funnel plot analysis was deemed not useful and hence not conducted. We attempted to conduct sensitivity analysis to find out the main sources of heterogeneity, but none of the included studies could explain the main causes of heterogeneity after removing each study one by one. Therefore, we can only reduce the heterogeneity statistically using a random-effects model. The results showed that rTMS may significantly improve swallowing function [SMD = 0.65, 95% CI (0.04, 1.26), $p = 0.04$, random-effects model]. The results are presented in **Figure 4**.

Subgroup Analysis of the Effects of rTMS for Swallowing Function (Frequency)

In clinical practice, rTMS mainly acts on the brain in two modes of stimulation: LF-rTMS and HF-rTMS. Low-frequency cortical stimulation can inhibit cortical excitability and might play a role in long-term inhibition. However, high-frequency stimulation can increase the excitability of the site of stimulation and achieve long-term effect. In our study, subgroup analysis was conducted

TABLE 2 | Methodological quality assessment of the controlled studies.

References	Random sequence generation	Allocation concealment	Blinding of participants and personnel	Blinding of outcome assessment	Incomplete outcome data	Selective reporting	Other bias	Grade
Khedr et al., 2009	Low risk	Low risk	Unclear	Low risk	Low risk	Low risk	Low risk	A
Khedr and Abo-Elfetoh, 2010	Low risk	Unclear	Low risk	Low risk	Low risk	Low risk	Low risk	B
Khedr and Abo-Elfetoh, 2010	Low risk	Unclear	Low risk	Low risk	Low risk	Low risk	Low risk	B
Kim et al., 2011	Low risk	Unclear	Low risk	Unclear	Low risk	Low risk	Low risk	B
Kim et al., 2011	Low risk	Unclear	Low risk	Unclear	Low risk	Low risk	Low risk	B
Lim et al., 2014	Low risk	Unclear	Low risk	Low risk	Low risk	Low risk	Low risk	B
Park et al., 2013	Low risk	Low risk	Low risk	Low risk	Low risk	Low risk	Low risk	A
Park et al., 2017	Low risk	Unclear	High risk	Low risk	Low risk	Low risk	Low risk	B
Park et al., 2017	Low risk	Unclear	High risk	Low risk	Low risk	Low risk	Low risk	B
Ünlüer et al., 2019	Low risk	Low risk	High risk	Low risk	Low risk	Low risk	Low risk	B

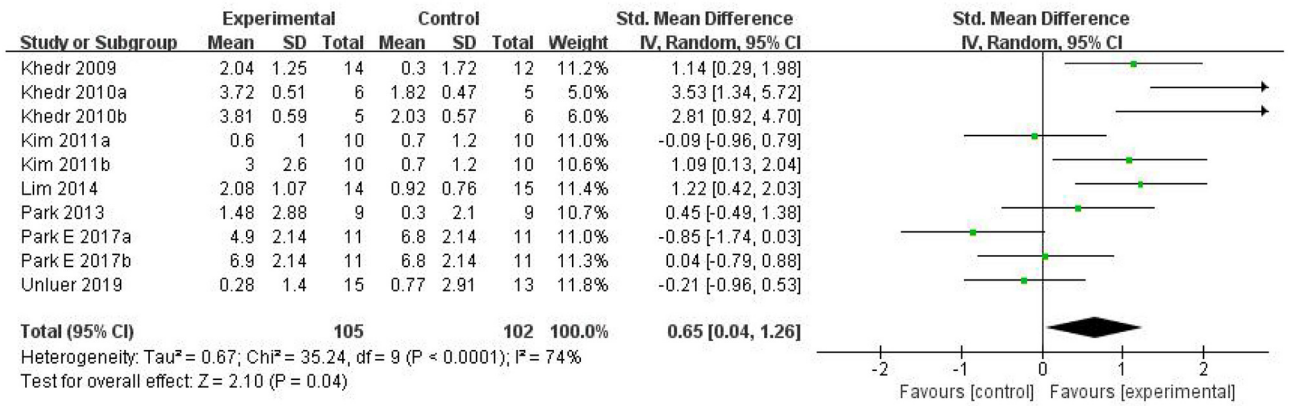

FIGURE 4 | The effects of rTMS on deglutition disorders.

according to different frequencies. The combined results showed that rTMS was superior to conventional rehabilitation training in treating dysphagia after stroke. However, both the low-frequency stimulation group [SMD = 0.68, 95% CI (−0.28, 1.63), $p = 0.16$] and high-frequency stimulation group [SMD = 0.69, 95% CI (−0.15, 1.53), $p = 0.11$] had the same efficacy as conventional rehabilitation for dysphagia after stroke. The differences between the two subgroups were not statistically significant, which may stem from the fact that the number of studied patients was too small. Although the combined result generated positive outcomes, the dominant effect was not significant. Specific results are shown in **Figure 5**.

Adverse Events

In our included studies, four studies reported that no adverse effects occurred after rTMS treatment, and eight studies showed no adverse effects during or after rTMS treatment. Only two studies (Lim et al., 2014; Ünlüer et al., 2019) reported mild noise sensation, headache, and dizziness during treatment, but the above sensations would disappear spontaneously shortly after treatment without further interventions. Although it has been reported that high-frequency stimulation may cause the occurrence of epilepsy, none of the participants in the included studies experienced epilepsy. However, for safety concerns, therapeutic protocols of rTMS to treat dysphagia should be developed to avoid various side effects.

DISCUSSION

Our study suggested that rTMS treatment may improve the swallowing function of patients with dysphagia after stroke, but the efficacy of either the LF-rTMS or HF-rTMS group was not significantly different from that of the conventional treatment group. This observation differed from what was reported by Liao et al. (2017). The possible reasons were speculated as follows. First of all, the number of included participants was small in our analysis, and the combination of LF-rTMS and HF-rTMS was with a slight advantage over conventional treatment for treating dysphagia. Thus, further subgroup analysis led to a smaller number of included patients and had an overall high risk

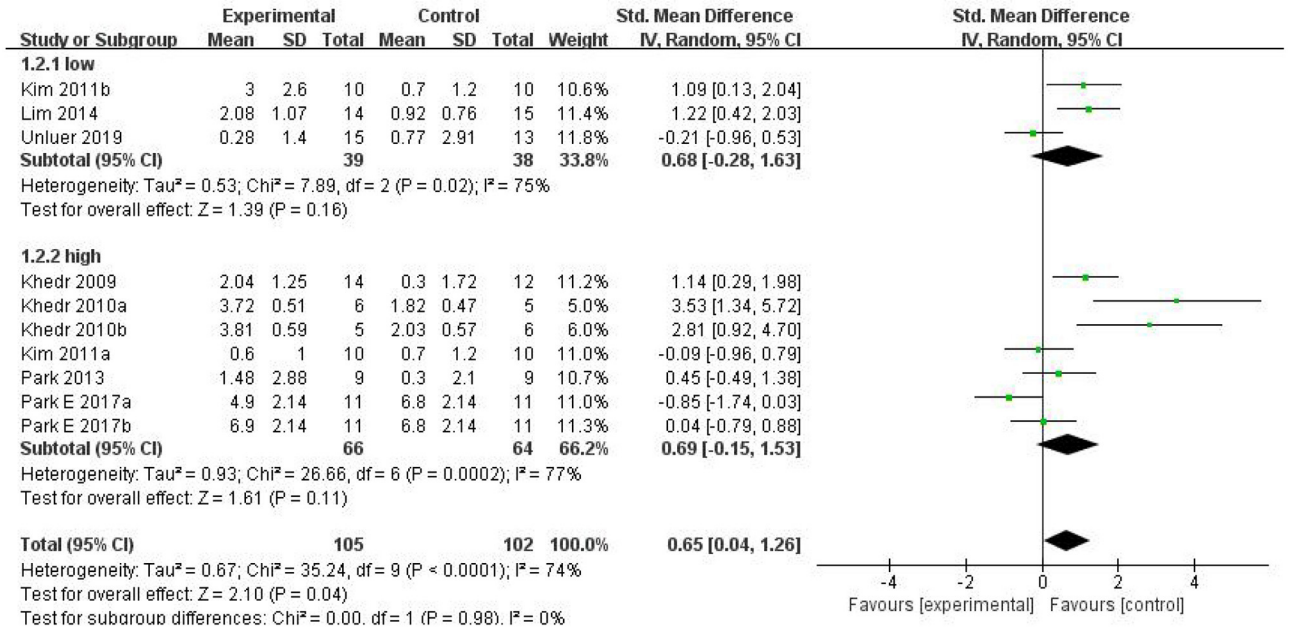

FIGURE 5 | Subgroup analysis of the effects of rTMS for swallowing function (frequency).

of bias. Secondly, after careful observation of the studies by Khedr and Abo-Elfetoh (2010), and Khedr et al. (2009), it was found that the patients selected by their research group all had dysphagia caused by brain stem or medulla oblongata lesions, while other studies were dominated by cortical lesions. This leads us to speculate that rTMS has different results for different lesion sites, especially cortical and subcortical lesions. In a word, combined analysis confirmed the advantage of rTMS, which was consistent with the results of Yang et al. (2015) and Pisegna et al. (2016). Distinct from the analyses of Yang et al. (2015) and Pisegna et al. (2016) we evaluated the effect of rTMS as the only intervention methods for patients without using other non-invasive central stimulation techniques (rTMS and tDCS) concurrently to avoid the interference.

Review of the included studies found that most of the studies were based on the interhemispheric inhibition theory and investigated two kinds of treatment methods—LF-rTMS and HF-rTMS. LF-rTMS is supposed to suppress the cortical excitability of healthy hemisphere while HF-rTMS activates excitability of stroked hemisphere. The combination of two methods helps improve bilateral imbalance of the brain so as to improve patients' swallowing functions. Interhemispheric inhibition theory is now commonly used in clinic. However, a few studies (Park et al., 2013, 2017) used the hypothesis of compensatory model to explain the effect of high-frequency stimulation on healthy hemispheres for the improvement of deglutition. Hamdy et al. (1996, 1998) used TMS to study the mechanisms of post-stroke deglutition disorders and found that the swallowing muscle group represents asymmetrical cortical functional areas in bilateral hemispheres. Swallowing function requires the common input information from bilateral cortices. This means that the recovery of post-stroke deglutition may probably depend on functional compensation of the healthy hemisphere. Therefore, the compensation model is also a strong argument for the therapeutic effect of rTMS on swallowing function recovery. In recent years, researchers have further developed the "bimodal balance recovery model" (Di Pino et al., 2014; Sankarasubramanian et al., 2017), arguing that the previous two models are no longer opposite, but are integrated with each other to achieve brain neuroplasticity. So, maybe rTMS stimulated the plasticity involved in swallowing control by acting on different circuits (Cantone et al., 2021). The above assumptions attempt to explain the complex mechanisms of rTMS on dysphagia. The review of Cantone et al. has shown that rTMS could modify cortical excitability, plasticity, and connectivity interacting in the pathophysiology of the impairment (Cantone et al., 2020). Additionally, restoration of maladaptive plasticity is another mechanism for the effect of rTMS (Hulme et al., 2013; Cantone et al., 2018, 2020; Vinciguerra et al., 2020). All these can promote the plasticity of neurons in the brain and achieve functional recovery.

However, there are still certain limitations with our analyses. First of all, the main limitations of the review are the small number of studies and participants included in our review. Secondly, only subgroup analysis for frequency was performed in our paper, whereas heterogeneity was observed in both subgroups. The efficacy of rTMS could also be affected by other parameters such as stimulation sites and locations of lesions. Thirdly, we chose PAS and DD as evaluation criteria, but did not include other evaluation criteria, which also resulted in a certain bias in the inclusion process of the article. In order to better serve the clinical practice, we will sort out all commonly used

clinical evaluation criteria and collect relevant literature for data analysis in the later stage. Further clinical controlled trials should be conducted to explore the influence factors on the efficacy and mechanism of rTMS in treating post-stroke dysphagia.

CONCLUSION

We conducted a systematic review and meta-analysis of rTMS for dysphagia after stroke, and the results showed that rTMS is more effective than conventional training for the recovery of dysphagia. However, subgroup analysis of HF-rTMS and LF-rTMS did not show significant efficacy for post-stroke dysphagia when compared with conventional rehabilitation, which was probably due to a small number of included studies. Thus, more large trials were needed for further study. Our study also found that both interhemispheric inhibition theory and compensatory model may play a role in the therapeutic effect of rTMS in treating dysphagia. More clinical studies are needed to help develop better treatment plans for these patients.

DATA AVAILABILITY STATEMENT

The original contributions presented in the study are included in the article, further inquiries can be directed to the corresponding author/s.

AUTHOR CONTRIBUTIONS

XC, XZ, XW, and XL assisted in literature review, quality assessment, and data analysis for our review. All authors contributed to the article and approved the submitted version.

FUNDING

The research was supported by the 2020 District Level Scientific Research Project of Longhua District Medical (ID:2020040) and Health Institutions and Shenzhen Longhua District Rehabilitation Medical Equipment Development and Transformation Joint Key Laboratory.

REFERENCES

Bestmann, S., Baudewig, J., Siebner, H. R., Rothwell, J. C., and Frahm, J. (2004). Functional MRI of the immediate impact of transcranial magnetic stimulation on cortical and subcortical motor circuits. *Eur. J. Neurosci*. 19, 1950–1962. doi: 10.1111/j.1460-9568.2004.03277.x

Borders, J. C., and Brates, D. (2020). Use of the penetration-aspiration scale in dysphagia research: a systematic review. *Dysphagia* 35, 583–597. doi: 10.1007/s00455-019-10064-3

Bordet, R., Ihl, R., Korczyn, A. D., Lanza, G., Jansa, J., Hoerr, R., et al. (2017). Towards the concept of disease-modifier in post-stroke or vascular cognitive impairment: a consensus report. *BMC Med.* 15:107. doi: 10.1186/s12916-017-0869-6

Cantone, M., Catalano, M. A., Lanza, G., La Delfa, G., Ferri, R., Pennisi, M., et al. (2018). Motor and perceptual recovery in adult patients with mild intellectual disability. *Neural Plast*. 2018:3273246. doi: 10.1155/2018/3273246

Cantone, M., Lanza, G., Fisicaro, F., Pennisi, M., Bella, R., Di Lazzaro, V., et al. (2020). Evaluation and treatment of vascular cognitive impairment by transcranial magnetic stimulation. *Neural Plast*. 2020:8820881. doi: 10.1155/2020/8820881

Cantone, M., Lanza, G., Ranieri, F., Opie, G. M., and Terranova, C. (2021). Editorial: non-invasive brain stimulation in the study and modulation of metaplasticity in neurological disorders. *Front. Neurol*. 12:721906. doi: 10.3389/fneur.2021.721906

Cheng, I. K., Chan, K. M., Wong, C. S., and Cheung, R. T. (2015). Preliminary evidence of the effects of high-frequency repetitive transcranial magnetic stimulation (rTMS) on swallowing functions in post-stroke individuals with chronic dysphagia. *Int. J. Lang. Commun. Disord*. 50, 389–396. doi: 10.1111/1460-6984.12144

Cheng, I. K. Y., Chan, K. M. K., Wong, C. S., Li, L. S. W., Chiu, K. M. Y., Cheung, R. T. F., et al. (2017). Neuronavigated high-frequency repetitive transcranial magnetic stimulation for chronic post-stroke dysphagia: a randomized controlled study. *J. Rehabil. Med*. 49, 475–481. doi: 10.2340/16501977-2235

Cola, M. G., Daniels, S. K., Corey, D. M., Lemen, L. C., Romero, M., and Foundas, A. L. (2010). Relevance of subcortical stroke in dysphagia. *Stroke* 41, 482–486. doi: 10.1161/STROKEAHA.109.566133

Di Lazzaro, V., Bella, R., Benussi, A., Bologna, M., Borroni, B., Capone, F., et al. (2021). Diagnostic contribution and therapeutic perspectives of transcranial magnetic stimulation in dementia. *Clin. Neurophysiol*. 132, 2568–2607. doi: 10.1016/j.clinph.2021.05.035

Di Pino, G., Pellegrino, G., Assenza, G., Capone, F., Ferreri, F., Formica, D., et al. (2014). Modulation of brain plasticity in stroke: a novel model for neurorehabilitation. *Nat. Rev. Neurol*. 10, 597–608. doi: 10.1038/nrneurol.2014.162

Du, J., Yang, F., Liu, L., Hu, J., Cai, B., Liu, W., et al. (2016). Repetitive transcranial magnetic stimulation for rehabilitation of poststroke dysphagia: a randomized, double-blind clinical trial. *Clin. Neurophysiol*. 127, 1907–1913. doi: 10.1016/j.clinph.2015.11.045

Edmiaston, J., Connor, L. T., Loehr, L., and Nassief, A. (2010). Validation of a dysphagia screening tool in acute stroke patients. *Am. J. Crit. Care* 19, 357–364. doi: 10.4037/ajcc2009961

Ertekin, C., Aydogdu, I., Yüceyar, N., Kiylioglu, N., Tarlaci, S., and Uludag, B. (2000). Pathophysiological mechanisms of oropharyngeal dysphagia in amyotrophic lateral sclerosis. *Brain* 123 (Pt. 1), 125–140. doi: 10.1093/brain/123.1.125

Fisicaro, F., Lanza, G., Grasso, A. A., Pennisi, G., Bella, R., Paulus, W., et al. (2019). Repetitive transcranial magnetic stimulation in stroke rehabilitation: review of the current evidence and pitfalls. *Ther. Adv. Neurol. Disord*. 12:1756286419878317. doi: 10.1177/1756286419878317

Hamdy, S., Aziz, Q., Rothwell, J. C., Power, M., Singh, K. D., Nicholson, D. A., et al. (1998). Recovery of swallowing after dysphagic stroke relates to functional reorganization in the intact motor cortex. *Gastroenterology* 115, 1104–1112. doi: 10.1016/S0016-5085(98)70081-2

Hamdy, S., Aziz, Q., Rothwell, J. C., Singh, K. D., Barlow, J., Hughes, D. G., et al. (1996). The cortical topography of human swallowing musculature in health and disease. *Nat. Med*. 2, 1217–1224. doi: 10.1038/nm1196-1217

Hulme, S. R., Jones, O. D., and Abraham, W. C. (2013). Emerging roles of metaplasticity in behaviour and disease. *Trends Neurosci*. 36, 353–362. doi: 10.1016/j.tins.2013.03.007

Khedr, E. M., and Abo-Elfetoh, N. (2010). Therapeutic role of rTMS on recovery of dysphagia in patients with lateral medullary syndrome and brainstem infarction. *J Neurol. Neurosurg. Psychiatry* 81, 495–499. doi: 10.1136/jnnp.2009.188482

Khedr, E. M., Abo-Elfetoh, N., and Rothwell, J. C. (2009). Treatment of post-stroke dysphagia with repetitive transcranial magnetic stimulation. *Acta Neurol. Scand*. 119, 155–161. doi: 10.1111/j.1600-0404.2008.01093.x

Kim, L., Chun, M. H., Kim, B. R., and Lee, S. J. (2011). Effect of repetitive transcranial magnetic stimulation on patients with brain injury and dysphagia. *Ann. Rehabil. Med*. 35, 765–771. doi: 10.5535/arm.2011.35.6.765

Kobayashi, M., and Pascual-Leone, A. (2003). Transcranial magnetic stimulation in neurology. *Lancet Neurol*. 2, 145–156. doi: 10.1016/S1474-4422(03)00321-1

Lanza, G., and Ferri, R. (2019). The neurophysiology of hyperarousal in restless legs syndrome: hints for a role of glutamate/GABA. *Adv Pharmacol*. 84, 101–119. doi: 10.1016/bs.apha.2018.12.002

Liao, X., Xing, G., Guo, Z., Jin, Y., Tang, Q., He, B., et al. (2017). Repetitive transcranial magnetic stimulation as an alternative therapy for dysphagia after stroke: a systematic review and meta-analysis. *Clin. Rehabil.* 31, 289–298. doi: 10.1177/0269215516644771

Lim, K. B., Lee, H. J., Yoo, J., and Kwon, Y. G. (2014). Effect of low-frequency rTMS and NMES on subacute unilateral hemispheric stroke with dysphagia. *Ann. Rehabil. Med.* 38, 592–602. doi: 10.5535/arm.2014.38.5.592

Michou, E., Mistry, S., Jefferson, S., Tyrrell, P., and Hamdy, S. (2014). Characterizing the mechanisms of central and peripheral forms of neurostimulation in chronic dysphagic stroke patients. *Brain Stimul.* 7, 66–73. doi: 10.1016/j.brs.2013.09.005

Park, E., Kim, M. S., Chang, W. H., Oh, S. M., Kim, Y. K., Lee, A., et al. (2017). Effects of bilateral repetitive transcranial magnetic stimulation on post-stroke dysphagia. *Brain Stimul.* 10, 75–82. doi: 10.1016/j.brs.2016.08.005

Park, J. W., Oh, J. C., Lee, J. W., Yeo, J. S., and Ryu, K. H. (2013). The effect of 5Hz high-frequency rTMS over contralesional pharyngeal motor cortex in post-stroke oropharyngeal dysphagia: a randomized controlled study. *Neurogastroenterol. Motil.* 25, 324–e250. doi: 10.1111/nmo.12063

Pisegna, J. M., Kaneoka, A., Pearson, W. G. Jr, Kumar, S., and Langmore, S. E. (2016). Effects of non-invasive brain stimulation on post-stroke dysphagia: a systematic review and meta-analysis of randomized controlled trials. *Clin. Neurophysiol.* 127, 956–968. doi: 10.1016/j.clinph.2015.04.069

Rosenbek, J. C., Robbins, J. A., Roecker, E. B., Coyle, J. L., and Wood, J. L. (1996). A penetration-aspiration scale. *Dysphagia* 11, 93–98. doi: 10.1007/BF00417897

Rossini, P. M., Burke, D., Chen, R., Cohen, L. G., Daskalakis, Z., Di Iorio, R., et al. (2015). Non-invasive electrical and magnetic stimulation of the brain, spinal cord, roots and peripheral nerves: basic principles and procedures for routine clinical and research application. An updated report from an I.F.C.N. committee. *Clin. Neurophysiol.* 126, 1071–1107. doi: 10.1016/j.clinph.2015.02.001

Sankarasubramanian, V., Machado, A. G., Conforto, A. B., Potter-Baker, K. A., Cunningham, D. A., Varnerin, N. M., et al. (2017). Inhibition versus facilitation of contralesional motor cortices in stroke: deriving a model to tailor brain stimulation. *Clin. Neurophysiol.* 128, 892–902. doi: 10.1016/j.clinph.2017.03.030

Tarameshlu, M., Ansari, N. N., Ghelichi, L., and Jalaei, S. (2019). The effect of repetitive transcranial magnetic stimulation combined with traditional dysphagia therapy on poststroke dysphagia: a pilot double-blinded randomized-controlled trial. *Int. J. Rehabil. Res.* 42, 133–138. doi: 10.1097/MRR.0000000000000336

Ünlüer, N. Ö., Temuçin ÇM, Demir, N., Serel Arslan, S., and Karaduman, A. A. (2019). Effects of low-frequency repetitive transcranial magnetic stimulation on swallowing function and quality of life of post-stroke patients. *Dysphagia* 34, 360–371. doi: 10.1007/s00455-018-09965-6

Valero-Cabré, A., Amengual, J. L., Stengel, C., Pascual-Leone, A., and Coubard, O. A. (2017). Transcranial magnetic stimulation in basic and clinical neuroscience: a comprehensive review of fundamental principles and novel insights. *Neurosci. Biobehav. Rev.* 83, 381–404. doi: 10.1016/j.neubiorev.2017.10.006

Verin, E., and Leroi, A. M. (2009). Poststroke dysphagia rehabilitation by repetitive transcranial magnetic stimulation: a noncontrolled pilot study. *Dysphagia* 24, 204–210. doi: 10.1007/s00455-008-9195-7

Vinciguerra, L., Lanza, G., Puglisi, V., Fisicaro, F., Pennisi, M., Bella, R., et al. (2020). Update on the neurobiology of vascular cognitive impairment: from lab to clinic. *Int. J. Mol. Sci.* 21:2977. doi: 10.3390/ijms21082977

Yang, S. N., Pyun, S. B., Kim, H. J., Ahn, H. S., and Rhyu, B. J. (2015). Effectiveness of non-invasive brain stimulation in dysphagia subsequent to stroke: a systemic review and meta-analysis. *Dysphagia* 30, 383–391. doi: 10.1007/s00455-015-9619-0

Zhang, C., Zheng, X., Lu, R., Yun, W., Yun, H., and Zhou, X. (2019). Repetitive transcranial magnetic stimulation in combination with neuromuscular electrical stimulation for treatment of post-stroke dysphagia. *J. Int. Med. Res.* 47, 662–672. doi: 10.1177/0300060518807340

Ziemann, U. (2004). TMS and drugs. *Clin. Neurophysiol.* 115, 1717–1729. doi: 10.1016/j.clinph.2004.03.006

Conflict of Interest: The authors declare that the research was conducted in the absence of any commercial or financial relationships that could be construed as a potential conflict of interest.

Publisher's Note: All claims expressed in this article are solely those of the authors and do not necessarily represent those of their affiliated organizations, or those of the publisher, the editors and the reviewers. Any product that may be evaluated in this article, or claim that may be made by its manufacturer, is not guaranteed or endorsed by the publisher.

frontiers in Neuroscience

ORIGINAL RESEARCH
published: 02 December 2021
doi: 10.3389/fnins.2021.733311

Enriched Rehabilitation Improves Gait Disorder and Cognitive Function in Parkinson's Disease: A Randomized Clinical Trial

Xin Wang[1]†, LanLan Chen[2†], Hongyu Zhou[1], Yao Xu[2], Hongying Zhang[3], Wenrui Yang[4], XiaoJia Tang[1], Junya Wang[5], Yichen Lv[6], Ping Yan[7] and Yuan Peng[8]**

[1] Department of Rehabilitation Medicine, Clinical Medical College, Yangzhou University, Yangzhou, China, [2] Department of Neurology, Clinical Medical College, Yangzhou University, Yangzhou, China, [3] Department of Medical Imaging, Clinical Medical College, Yangzhou University, Yangzhou, China, [4] Graduate School, Dalian Medical University, Dalian, China, [5] Medical College, Yangzhou University, Yangzhou, China, [6] School of Rehabilitation Medicine, Binzhou Medical University, Yantai, China, [7] School of Nursing, Yangzhou University, Yangzhou, China, [8] Department of Rehabilitation Medicine, Guangzhou First People's Hospital, Guangzhou, China

OPEN ACCESS

Edited by:
Jinhua Zhang,
Xi'an Jiaotong University, China

Reviewed by:
Riccardo Bravi,
Università degli Studi di Firenze, Italy
Paola Feraco,
University of Bologna, Italy

***Correspondence:**
Xin Wang
wx000805qm@yeah.net
Yuan Peng
eyyuanpeng@scut.edu.cn

†These authors share first authorship

Specialty section:
This article was submitted to Neuroprosthetics, a section of the journal Frontiers in Neuroscience

Received: 30 June 2021
Accepted: 03 November 2021
Published: 02 December 2021

Citation:
Wang X, Chen L, Zhou H, Xu Y, Zhang H, Yang W, Tang X, Wang J, Lv Y, Yan P and Peng Y (2021) Enriched Rehabilitation Improves Gait Disorder and Cognitive Function in Parkinson's Disease: A Randomized Clinical Trial. Front. Neurosci. 15:733311. doi: 10.3389/fnins.2021.733311

Background: Studies on non-pharmacological strategies for improving gait performance and cognition in Parkinson's disease (PD) are of great significance. We aimed to investigate the effect of and mechanism underlying enriched rehabilitation as a potentially effective strategy for improving gait performance and cognition in early-stage PD.

Methods: Forty participants with early-stage PD were randomly assigned to receive 12 weeks (2 h/day, 6 days/week) of enriched rehabilitation (ER; n = 20; mean age, 66.14 ± 4.15 years; 45% men) or conventional rehabilitation (CR; n = 20; mean age 65.32 ± 4.23 years; 50% men). In addition, 20 age-matched healthy volunteers were enrolled as a control (HC) group. We assessed the general motor function using the Unified PD Rating Scale—Part III (UPDRS-III) and gait performance during single-task (ST) and dual-task (DT) conditions pre- and post-intervention. Cognitive function assessments included the Montreal Cognitive Assessment (MoCA), the Symbol Digit Modalities Test (SDMT), and the Trail Making Test (TMT), which were conducted pre- and post-intervention. We also investigated alteration in positive resting-state functional connectivity (RSFC) of the left dorsolateral prefrontal cortex (DLPFC) in participants with PD, mediated by ER, using functional magnetic resonance imaging (fMRI).

Results: Compared with the HC group, PD participants in both ER and CR groups performed consistently poorer on cognitive and motor assessments. Significant improvements were observed in general motor function as assessed by the UPDRS-III in both ER and CR groups post-intervention. However, only the ER group showed improvements in gait parameters under ST and DT conditions post-intervention. Moreover, ER had a significant effect on cognition, which was reflected in increased MoCA, SDMT, and TMT scores post-intervention. MoCA, SDMT, and TMT scores were significantly different between ER and CR groups post-intervention. The RSFC analysis

showed strengthened positive functional connectivity between the left DLPFC and other brain areas including the left insula and left inferior frontal gyrus (LIFG) post-ER.

Conclusion: Our findings indicated that ER could serve as a potentially effective therapy for early-stage PD for improving gait performance and cognitive function. The underlying mechanism based on fMRI involved strengthened RSFC between the left DLPFC and other brain areas (e.g., the left insula and LIFG).

Keywords: enriched rehabilitation, cognitive function, gait disorder, Parkinson's disease, left dorsolateral prefrontal cortex

INTRODUCTION

Parkinson's disease (PD) is the second most common neurodegenerative disorder in older adults, which is typically characterized by motor and non-motor impairments that lead to increasingly serious physical disability (Homayoun, 2018; Armstrong and Okun, 2020). Gait impairments remain the most common motor symptoms and are characterized by abnormal spatiotemporal variables, such as gait speed, stride length, and cadence (Creaby and Cole, 2018; Islam et al., 2020). Furthermore, cognitive deficits are prominently exhibited non-motor symptoms as the disease progresses (Goldman et al., 2018). However, the early onset of cognitive deficits can exacerbate gait disorder because cognition is vital for controlling both bilateral coordination and dynamic posture during walking (Lord et al., 2014; Morris et al., 2019). Clinical evidence has shown that gait deficits in PD patients are more obvious during dual-task (DT) conditions, which are more cognitively demanding owing to the simultaneous performance of cognitive and motor tasks, than during single-task (ST) conditions (Salazar et al., 2017). Despite emerging clinical targets for enhancing motor and cognitive functions simultaneously, pharmacological strategies, such as dopamine replacement therapy, usually only resolve motor symptoms while barely improving cognitive function (Armstrong and Okun, 2020). Therefore, research on non-pharmacological strategies for improving motor and cognitive outcomes in PD is highly warranted (Petzinger et al., 2013; Dagan et al., 2018; Ni et al., 2018).

Environmental enrichment is a viable non-pharmacological strategy in which participants are permitted to explore and interact with each other in a multistimuli environment to participate in highly social, physical, and cognitive activities simultaneously. Clinical and animal studies have shown that environmental enrichment has the potential to improve functional outcomes by triggering neuroplasticity in participants with neurological diseases, such as stroke and traumatic brain injury (Bondi et al., 2014; Wang et al., 2016, 2020). Although cognitive deficits have been shown to attenuate, motor impairments do not always show improvement by simple immersion in an enriched environment (McDonald et al., 2018). Therefore, conducting comprehensive training batteries is vital to synergistically improve behavioral outcomes in patients with neurological diseases (Schuch et al., 2016). A more effective paradigm that could dramatically promote overall function is enriched rehabilitation (ER), which is an integrated strategy that combines environmental enrichment with task-oriented training (Schuch et al., 2016; Vive et al., 2020). Evidence from animal studies has demonstrated that ER restores limb function better than does environment enrichment alone in patients with stroke (Schuch et al., 2016). Moreover, a recent clinical study reported a marked improvement in motor and cognitive function mediated by ER in chronic stroke patients (Vive et al., 2020). However, few studies have explored the effect of ER on PD gait disorders and cognitive function (Shah et al., 2016; Fujiwara et al., 2019). Furthermore, the specific mechanism by which ER enhances cognitive function remains unclear.

Resting-state functional magnetic resonance imaging (rs-fMRI) is an extensively used method for exploring neuro-rehabilitation mechanisms by detecting changes in blood oxygenation level-dependent intensity (Lv et al., 2018). To date, resting-state functional connectivity (RSFC) assessed by rs-fMRI has enabled the identification of the functional interaction between brain regions to understand the pathophysiological mechanisms underlying PD (Chen et al., 2020). Rs-fMRI studies have demonstrated that the left dorsolateral prefrontal cortex (DLPFC), one of the vital regions in the central executive network (CEN) that mediates cognitive function, has decreased functional connectivity with other brain areas in PD compared with healthy controls (Prodoehl et al., 2014; Caspers et al., 2017). Furthermore, studies on global connectivity have shown that improved cognition is related to stronger functional connectivity of the DLPFC with specific brain areas, such as the frontal, parietal, occipital, and limbic regions (Trujillo et al., 2015). Thus, we hypothesized that ER would improve gait disorder and cognitive function in early-stage PD patients by inducing neuroplasticity in the form of brain network changes. Therefore, the current study explored the effect of and mechanisms underlying ER in early-stage PD patients with gait disorder to assess its viability as a non-pharmacological strategy for PD rehabilitation.

MATERIALS AND METHODS

Study Population

All participants were enrolled from the outpatient center at the Clinical College of Yangzhou University between September 2019 and October 2020. Participants with PD were recruited from the Department of Neurology and Rehabilitation. Inclusion criteria were as follows: (1) aged 50–75 years; (2) met diagnostic criteria for PD based on the United Kingdom Parkinson's Disease Society

Brain Bank, with confirmation made by two neurologists; (3) able to walk independently for at least 6 min (with rest intervals) without an assistive device; (4) an educational level higher than junior high school and a Montreal Cognitive Assessment (MoCA) score between 20 and 25 points; (5) severity of PD between grade 1 and 2 as assessed by the revised Hoehn–Yahr scale; (6) on a stable drug regimen for more than 2 weeks; and (7) volunteered to accept rehabilitative training. Exclusion criteria were as follows: (1) secondary or acquired parkinsonism; (2) other neurological disorders, such as stroke or previous traumatic brain injury; (3) severe cognitive impairment based on a MoCA score of < 20 points; (4) alcohol or drug abuse; (5) poor compliance with prescribed treatment; and (6) medical complications, such as severe lung and heart disease based on clinical symptoms and medical history. Based on these inclusion and exclusion criteria, 40 participants with PD were enrolled and randomly assigned into the enrichment rehabilitation (ER; $n = 20$) or conventional rehabilitation (CR; $n = 20$) group. In addition, 20 age-matched healthy volunteers were recruited from the Department of Physical Examination Center as the healthy control (HC) group. This study was approved by the Ethical Review Board of the Clinical Medical College in Yangzhou University, China (No. 2019070). All participants provided informed consent preintervention. **Figure 1** describes the process of the study.

Intervention

Participants in the ER and CR groups (i.e., PD groups) received ER and CR for 2 h/day, 6 days/week, for 12 consecutive weeks. Rehabilitative activities in the ER and CR groups were implemented by the same physical therapy team without knowing the aim of the study. A total of 65 therapists participated in the study. All rehabilitative activities were in mild to moderate intensity monitored by a wristwatch (Apple Watch Series 5) during the rehabilitation sessions, which induced a target heart rate below 65–70% of the maximum heart rate (Garber et al., 2011; Marusiak et al., 2019). Participants in the HC group received no intervention. We stopped other additional rehabilitation to avoid interferences with the treatment effect from the interventions used in this study.

Enriched rehabilitation was conceived and developed by combining environmental enrichment with repetitive and meaningful individual functional training during everyday tasks (Bondi et al., 2014; Vive et al., 2020). Participants in the ER group were unaware that the ER was not CR. The ER group was exposed to an enriched environment with easy access to both communal and individual equipment and activities for individual intensive rehabilitation (Vive et al., 2020). The rehabilitation training contents focused on three key areas, which are summarized below:

1. Enriched sensorimotor environmental stimulation paired with different types of sensory and motor exercises: to simulate the effect of an enriched environment, ER was carried out in a space with periodically changing light, sound, aroma, and lawn using multimedia equipment (**Supplementary Figure 1**). In addition, varied tactile textures and diverse thermal, visual, and auditory stimulation were provided as previous studies reported (Janssen et al., 2014). Integrated sensory and balance training was provided through playing games in virtual reality scenarios during 10-min exercise sessions to improve balance and coordination. Dynamic cycling training under different intensities and rhythms of music was also provided to improve motor function. Detailed information is listed in **Supplementary Table 1**.
2. Cognition-related activities integrated with specific tasks: participants were able to access interesting web pages by using an internet-connected computer and summarize the content in the ER area. Participants were also encouraged to read and recite their favorite books or articles in the electronic library. Simple board games and recreational activities (i.e., bingo) were made available throughout the intervention period, which need only single-player experiences on the tabletop to improve cognition. We provided individual enrichment by including music, audiobooks, and number puzzles.
3. Social interactions and therapeutic rehabilitation support: participants were encouraged to communicate with their family members about a particular topic with the guidance therapists. Participants in the ER group also interacted socially by participating in different activities together, such as playing board games (i.e., mahjong) and table tennis, which were cooperative and competitive activities to improve cognition and social skills in the meanwhile.

Participants in the CR group participated in standard physical therapy, which included balance and gait training (Ni et al., 2018). Balance training referred to usual static and dynamic balance activities, such as standing with one leg on stable or unstable surfaces and tilting the body in different directions to maximum angles in a seated or standing position. Gait training included bearing weight on the affected leg, walking on a treadmill, stepping onto a step, and walking on various types of surfaces. Detailed information on CR is provided in **Supplementary Table 2**.

Outcomes and Measurement Procedures

Detailed demographic and medical characteristics, including age, sex, length of lower limbs, Hoehn–Yahr stage, symptom-dominant side, daily levodopa dosage, and disease duration, were recorded. For the PD groups, general motor function, gait performance, and cognition were assessed at two time points: (1) 72 h before the first rehabilitation training (pre-intervention) and (2) 24 h after the 12-week rehabilitation process (post-intervention). General motor function of participants with PD was assessed using the Unified PD Rating Scale—Part III (UPDRS-III; no disability 0, severe disability 108) and Hoehn–Yahr stage (minimal functional disability, confinement to wheelchair/bed) (Opara et al., 2017). To evaluate cognitive function, we administered the validated Chinese versions of the following scales: (1) the MoCA, which is used to assess general cognitive function, (2) the Symbol Digit Modalities Test (SDMT) to evaluate processing speed and attention, and (3) the

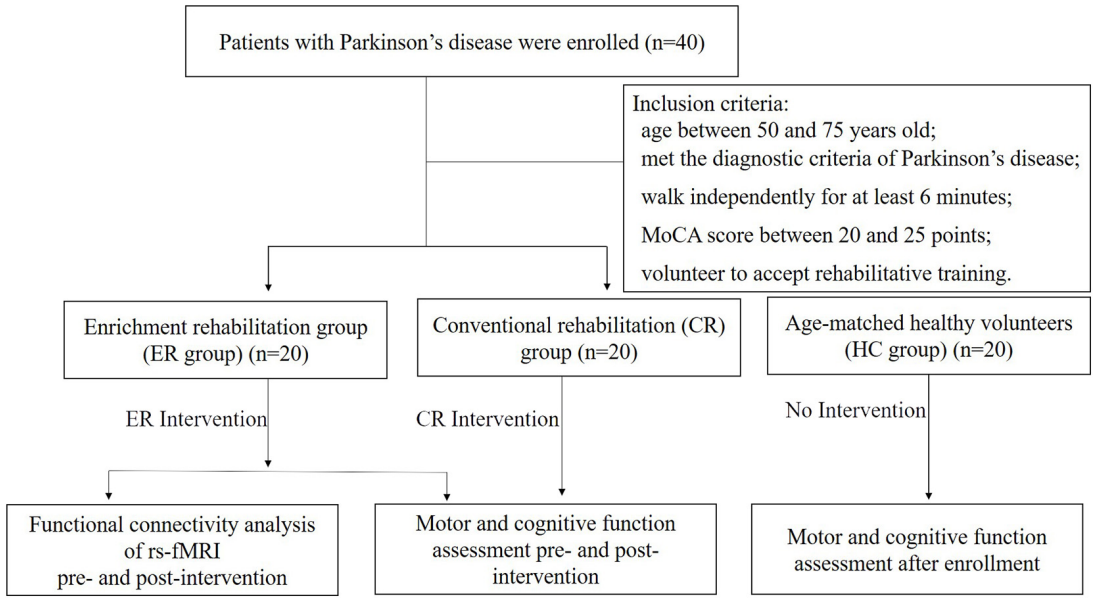

FIGURE 1 | Flowchart illustrating the process for the study. MoCA, montreal cognitive assessment.

TABLE 1 | Characteristics of the patients in the study groups.

Characteristics	ER group (*n* = 20)	CR group (*n* = 20)	HC group (*n* = 20)	*p*
Age (year)	65.25 ± 4.15	64.95 ± 3.99	66.15 ± 3.58	0.52
Sex, male/female	9/11	10/10	11/9	0.819
Hoehn and Yahr	1.37 ± 0.41	1.32 ± 0.36	–	0.395
Disease duration (year)	2.23 ± 1.69	2.28 ± 1.53	–	0.095
Symptom-dominant side (R/L)	12/8	12/8	–	1
Daily levodopa dosage (mg/day)	227 ± 116	230 ± 113	–	0.102
Length of lower limbs (cm)	83.76 ± 4.45	84.75 ± 4.82	83.99 ± 4.75	0.232

ER, enriched rehabilitation; CR, conventional rehabilitation; HC, healthy control.

Trail Making Test (TMT), which assesses the executive function (Federico et al., 2015). Motor and cognitive functions of the HC group were assessed within 24 h of enrollment. All assessments were carried out by a trained neuropsychologist who was blinded to patient group assignment.

Gait analysis of all participants was examined under ST and DT conditions. For both ST and DT, participants walked the length of a 20-m straight corridor that was free of obstacles at their preferred speed. In the DT condition, participants continuously performed a serial seven-subtraction task (i.e., 100−7 = 93, 93−7 = 86) while walking at their usual pace. Spatiotemporal gait parameters were acquired using wearable sensors of inertial measurement units (GYENNO Science, Shenzhen, China) (Brognara et al., 2019). Each participant was equipped with 10 sensors on the lower back, chest, bilateral feet, ankles, thighs, and wrists using elastic belts, which recorded the overall gait posture during walking (Cao et al., 2020). Each sensor collected real-time spatial and temporal gait information of the participants while walking, and the information was transmitted to a host computer *via* a Bluetooth link for further processing and storage. Gait parameters, including speed and stride length, were recorded. For each walking condition, repetitions were performed to ensure that three complete 10-s walking processes were recorded; the average values of the gait parameters were used for subsequent analyses. The first and last meters of the walking process were not included in the analysis of gait parameters to eliminate the effects of the acceleration and deceleration phases (Stuck et al., 2020).

Magnetic Resonance Imaging Data Acquisition

To compare changes in functional connectivity mediated by ER, each patient in the ER group underwent brain magnetic resonance imaging (MRI), which included T1-weighted and rs-fMRI acquisitions, within 24 h pre- and post-intervention. T1-weighted images were used for reconstructing individual structural brain anatomy and were acquired using the following parameters: pulse repetition time/echo time = 1,900 ms/3.39 ms, field of view (FOV) = 240 × 176 mm, matrix = 256 × 176, slice thickness = 0.9375 mm, flip angle = 7°, reverse time = 1,100 ms, scan time = 4 min, and number of layers = 32. T2*-weighted

rs-fMRI volumes were used for functional connectivity analyses and were acquired using the following parameters: echo-planar imaging sequence = 31 slices, pulse repetition time/echo time = 2,000/30 ms, slice thickness = 4 mm, matrix = 64 × 64 mm, FOV = 240 × 240 mm, flip angle = 90°, number of layers = 31, and scanning time = 8 min. Each patient was asked to keep their eyes closed and stay as still as possible during the scan.

Functional Connectivity Analysis

To qualitatively and quantitatively compare left DLPFC functional connectivity between post- and pre-ER, we preprocessed data using the Statistical Parametric Mapping 8 (SPM8) software (Wellcome Centre for Human Neuroimaging, London, United Kingdom) in MATLAB to prepare the rs-fMRI data. To exclude motion-related signals from the data, images with a maximum displacement of 3.0 mm in the x-, y-, or z-direction or 3° in any angle direction were discarded. All images were time shifted so that the slices were temporally aligned before slices were segmented into gray and white matter by co-registering with anatomical images. The Montreal Neurological Institute (MNI) template was applied to normalize the anatomical images, and the normalized parameters were used for the functional images. The linear trend was removed, and a temporal band-pass filter (0.01–0.08 Hz) was applied for regional homogeneity.

For the RSFC analysis, the Resting-state fMRI Data Analysis Toolkit was used for processing. Functional connectivity was measured using the seed-based correlation method using the CONN-fMRI functional connectivity toolbox. We measured the connectivity between the left DLPFC (MNI coordinates: $x = -42$, $y = 33$, $z = 21$) and each voxel of the brain. Correlations maps were calculated for each subject by extracting the mean signal time course from the seed and computing Pearson's correlations coefficients with the time courses of all other voxels of the brain. These correlation coefficients were converted into normally distributed z-scores using the Fisher transformation to allow for linear model analyses.

Statistical Analysis

Statistical analysis was performed using SPSS 22.0 (IBM Corp., Armonk, NY, United States). Data were described as means ± standard deviations (SDs). As coefficients of variation (CV) was considered a better indicator of gait performance, we calculated CV of gait performance for analysis as follows: CV = (standard deviation/mean) × 100%. A chi-square test was used to analyze the between-group differences for categorical variables, such as gender and symptom-dominant side. A one-way repeated-measures analysis of variance was performed to detect between-group differences (ER, CR, and HC groups) for continuous variables, which included motor and cognitive performance, and a least significant difference test was performed for multiple comparison correction. Independent t-test was conducted to compare the between-group differences post-intervention (ER and CR group) in continuous variables including motor and cognitive performance. Paired t-tests were used to detect within-group differences (pre- vs. post-intervention in the PD groups) for motor and cognitive performance. A statistical significance was set at $p < 0.05$.

Group-level statistical analyses of the fMRI data were performed using a random-effects model in SPM8. A two-sample t-test between groups (pre- vs. post-ER) was applied to the individual z-maps of the two groups, using small volume correction for the one-sample results masks. Multiple comparison correction was implemented using Monte Carlo simulation[1]. Significant between-group differences met the criteria of an uncorrected $p < 0.01$ at the voxel level and a cluster size of > 17 voxels, which corresponded to a corrected $p < 0.05$. To examine differences in alterations in functional connectivity, one-sample t-tests were used to compare individual within-group peak voxel z-maps, using a significance criterion of $p < 0.05$ in the SPSS 22.0 software package. Dissociable anomalies in functional connectivity patterns between groups (pre- vs. post-ER) were explored in the whole brain using a criterion of corrected $p < 0.05$ at the voxel level and a cluster size of > 228 voxels. The alpha for all significant results was two-tailed, except where noted.

RESULTS

Demographics

There were no significant differences in baseline characteristics between the HC group and the PD groups, including age, sex, and length of lower limbs (**Table 1**, $p > 0.05$). Demographic characteristics, including age, gender, length of lower limbs, Hoehn–Yahr stage, symptom-dominant side, daily levodopa dosage, and disease duration were comparable between the ER and CR groups (**Table 1**, $p > 0.05$).

Behavioral Performance

Gait Parameters in the Single-Task and Dual-Task Conditions

As shown in **Table 2**, there were no significant differences in gait speed or stride length between the PD groups and the HC group pre-intervention under the ST condition ($p > 0.05$), whereas CVs of gait speed and stride length were significantly different ($p < 0.05$). Before the intervention, there were no significant differences in gait parameters between the PD groups under the ST condition ($p > 0.05$). The CVs of gait speed and stride length significantly improved in the ER group post-intervention ($p < 0.05$). In addition, significant differences were observed in the CVs of gait speed and stride length between the ER and CR groups in the ST condition post-intervention ($p < 0.05$).

As indicated in **Table 2**, under the DT condition, gait parameters of the ER and CR groups were significantly different from those of the HC group pre-intervention ($p < 0.05$). There were no significant differences in gait parameters between the PD groups pre-intervention under the DT condition ($p > 0.05$). No significant changes in gait parameters were observed in the CR group post-intervention ($p > 0.05$). However, the gait parameters of gait speed, stride length, CV of gait speed, and CV of stride

[1] http://afni.nimh.nih.gov/pub/dist/doc/manual/AlphaSim.pdf

TABLE 2 | Gait characteristics for all participants pre- and post-intervention.

	ST					DT				
	ER group (*n* = 20)	**CR group (*n* = 20)**	**HC group (*n* = 20)**	**F^**	***p^***	**ER group (*n* = 20)**	**CR group (*n* = 20)**	**HC group (*n* = 20)**	**F^**	***p^***
Gait speed (m/s)										
Pre-intervention	1.17 ± 0.08	1.16 ± 0.10	1.19 ± 0.05	0.56	0.53	0.79 ± 0.11*	0.76 ± 0.16*	1.09 ± 0.08[&]	46.67	0.40
Post-intervention	1.18 ± 0.07	1.17 ± 0.08		0.91	0.37	0.91 ± 0.15[*#$]	0.78 ± 0.11*		3.17	0.00
CV of gait speed (%)										
Pre-intervention	6.67 ± 1.58*	6.65 ± 1.23*	4.42 ± 1.19[&]	17.66	0.96	15.46 ± 3.33*	15.62 ± 3.71*	8.24 ± 1.01[&]	39.11	0.87
Post-intervention	5.13 ± 0.92[*#$]	6.76 ± 1.13*		−4.87	0.00	12.81 ± 3.14[*#$]	15.48 ± 3.69*		−2.41	0.00
Stride length (m)										
Pre-intervention	1.13 ± 0.13	1.11 ± 0.13	1.11 ± 0.07	0.15	0.72	0.82 ± 0.11*	0.83 ± 0.18*	1.03 ± 0.09[&]	14.24	0.87
Post-intervention	1.14 ± 0.09	1.09 ± 0.13		1.46	0.15	0.92 ± 0.08[*#$]	0.84 ± 0.14*		2.46	0.01
CV of stride length (%)										
Pre-intervention	9.74 ± 2.14*	9.94 ± 2.53*	6.12 ± 1.93[&]	17.99	0.77	15.06 ± 4.78*	15.29 ± 4.16*	7.79 ± 1.05[&]	25.15	0.85
Post-intervention	7.11 ± 1.99[*#$]	9.92 ± 2.31*		−4.03	0.00	11.33 ± 3.58[*#$]	15.32 ± 4.20*		−3.15	0.00

ST, single-task; DT, dual-task; ER, enriched rehabilitation; CR, conventional rehabilitation; HC, healthy control.
**Compared with HC group pre-intervention, $p < 0.05$.*
[&]Compared with CR group pre-intervention, $p < 0.05$.
[#]Compared with CR group post-intervention, $p < 0.05$.
[$]Compared with pre-intervention, $p < 0.05$.
F^, the F-value of ER group compared with CR group; p^, the p-value of ER group compared with CR group.

TABLE 3 | Motor and cognitive assessments for all participants pre- and post-intervention.

	ER group (n = 20)	CR group (n = 20)	HC group (n = 20)	F^	p^
UPDRS-III					
Pre-intervention	15.35 ± 2.83	15.25 ± 2.12		0.12	0.90
Post-intervention	10.95 ± 2.56$^{\$}$	11.15 ± 1.65$^{\$}$		−0.29	0.78
MoCA					
Pre-intervention	23.05 ± 1.28*	23.15 ± 1.24*	29.15 ± 0.48$^{\&}$	204.44	0.77
Post-intervention	26.15 ± 1.93$^{*\#\$}$	23.55 ± 1.56*		4.56	0.00
SDMT					
Pre-intervention	48.85 ± 10.25*	48.15 ± 10.29*	73.25 ± 7.48$^{\&}$	63.64	0.82
Post-intervention	64.15 ± 10.03$^{*\#\$}$	47.55 ± 11.86*		4.66	0.00
TMT-A (s)					
Pre-intervention	73.68 ± 18.75*	72.54 ± 18.22*	48.12 ± 12.09$^{\&}$	14.33	0.83
Post-intervention	72.72 ± 18.36*	72.85 ± 12.78*		−0.02	0.98
TMT-B (s)					
Pre-intervention	148.60 ± 34.44*	148.67 ± 33.57*	99.17 ± 19.95$^{\&}$	17.15	0.99
Post-intervention	125.80 ± 29.65$^{*\#\$}$	150.62 ± 37.14*		−2.28	0.03

ER, enriched rehabilitation; CR, conventional rehabilitation; HC, healthy control.
**Compared with HC group pre-intervention, $p < 0.05$.*
$^{\&}$Compared with CR group pre-intervention, $p < 0.05$.
$^{\#}$Compared with CR group post-intervention, $p < 0.05$.
$^{\$}$Compared with pre-intervention, $p < 0.05$.
F^, the F-value of ER group compared with CR group; p^, the p-value of ER group compared with CR group.

length under the DT condition of the ER group improved post-intervention ($p < 0.05$). Moreover, significant differences were observed in gait parameters under the DT condition between the ER and CR groups post-intervention ($p < 0.05$).

Motor and Cognitive Outcomes

There was a significant change from pre- to post-intervention in both PD groups for UPDRS-III scores (**Table 3**; $p < 0.05$), which indicated that the PD groups performed consistently better overall during motor assessments following the interventions. There was no significant difference in UPDRS-III score between the PD groups post-intervention ($p > 0.05$), which indicated that there were no differential effects of the interventions on general motor function.

The cognitive assessment results of each PD group pre- and post-intervention are summarized in **Table 3**. Cognitive function scores of the MoCA, SDMT, and TMT were significantly different between the PD groups and HC group pre-intervention ($p < 0.05$); however, they did not differ significantly between the PD groups ($p > 0.05$), which indicated that PD participants performed consistently poorer on the cognitive assessments than did the HC group at baseline. No changes were observed in cognitive scores from pre- to post-intervention in the CR group ($p > 0.05$), which indicated that CR had no effect on cognition. In contrast, there was a significant therapeutic effect of ER on cognition, which was shown by increased MoCA, SDMT, and TMT scores from pre- to post-intervention ($p < 0.05$). Moreover, these cognitive function scores were significantly different between the PD groups post-intervention ($p < 0.05$).

Functional Connectivity Analysis

As shown in **Figure 2A** and **Supplementary Table 5**, the left inferior temporal gyrus, bilateral middle frontal gyrus, right lenticular putamen, and right precentral gyrus showed positive functional connectivity with the left DLPFC pre-ER ($p < 0.05$, cluster size > 228 voxels). **Supplementary Table 6** and **Figure 2B** show that the left inferior temporal gyrus, left middle frontal gyrus, right triangular inferior frontal gyrus (IFG), left parietal inferior marginal angular gyrus, and right superior marginal gyrus exhibited positive RSFC with the left DLPFC post-ER ($p < 0.05$, cluster size > 228 voxels). As shown in **Figure 2C** and **Table 4**, RSFC between the left DLPFC and deep brain regions, including the left insula and left IFG (LIFG), was stronger post-ER compared with pre-ER ($p < 0.05$, Alphasim corrected, cluster size > 228 voxels).

DISCUSSION

In this study, we investigated the effect of ER on gait performance and cognitive function in patients with PD. We compared the differentially positive RSFC of the left DLPFC before and after ER. The study yielded three main results: first, ER induced significant improvements in motor and walking function, as indexed by gait parameters in the ST and DT conditions. Second, ER training led to an improvement in cognitive function, which was shown by increases in MoCA, SDMT, and TMT scores following the intervention. ER had obvious advantage to improve cognition compared with CR. Third, we found a strengthened positive RSFC between the left DLPFC and the left insula and LIFG after ER, which suggested that ER induced neuroplasticity to restore cognitive and walking function in early-stage PD.

Walking is a complex task, whereby gait performance relies on the interplay between motor control and cognition (Forte et al., 2019; Wollesen et al., 2019). However, both motor and cognitive function are impaired even in the early stages of PD

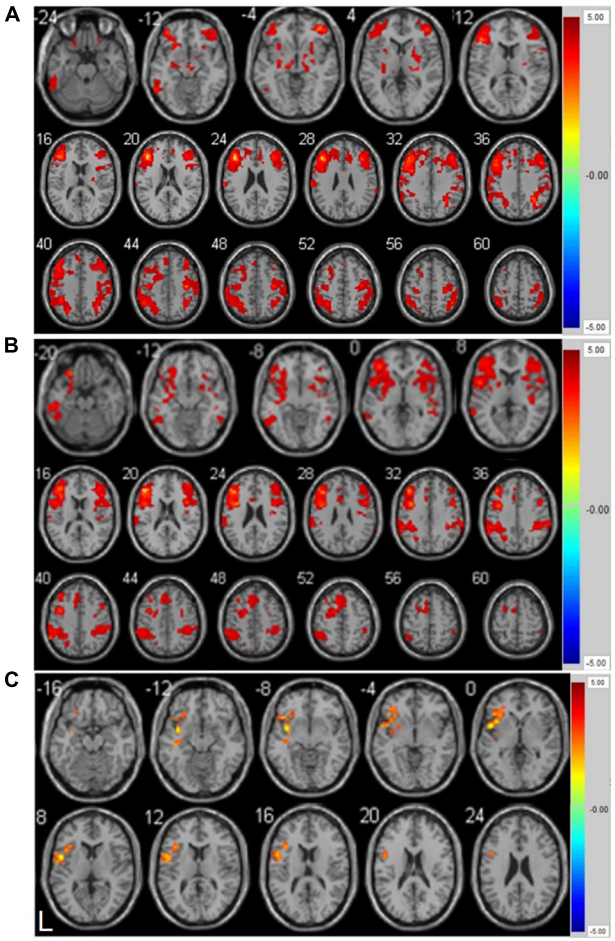

FIGURE 2 | (A) Positive resting-state functional connectivity with left DLPFC pre-ER intervention in PD patients. **(B)** Positive resting-state functional connectivity with left DLPFC post-ER intervention in PD patients. **(C)** Differential positive resting-state functional connectivity with left DLPFC between pre- and post-ER intervention in PD patients ($p < 0.05$, Alphasim corrected, cluster size > 228 voxels). Abbreviation: ER, enriched rehabilitation.

TABLE 4 | Strengthened positive resting-state functional connectivity (RSFC) of left DLPFC post- compared with pre-ER intervention in PD patients.

Region	BA	MNI coordinate (mm)	Peak *T* value	Cluster size
		(X Y Z)		
Left insular cortex	13	−48 6 3	6.0982	216
Left inferior frontal gyrus	13/47	−32 20 6	8.0220	164

BA, Brodman's area; cluster size, the number of voxels; MNI, Montreal Neurological Institute.
$p < 0.05$, Alphasim corrected, cluster size > 228 voxels.

due to dopaminergic neuronal loss in the basal ganglia (San Martín Valenzuela et al., 2020). Consistent with previous studies, the PD groups in our study performed consistently poorer on cognitive and motor assessments than did the HC group (Opara et al., 2017; Szeto et al., 2020). The early onset of cognitive deficits exacerbates gait impairments in PD because attention and executive function are indispensable for maintaining gait performance, which includes bilateral coordination and dynamic posture (Ehgoetz Martens et al., 2018). Deleterious changes in the gait parameters of speed, stride width, and gait variability have been reported in DT studies of PD (Penko et al., 2018). As expected, lower gait speed and stride length were observed in the PD groups than in the HC group during the DT condition. However, no significant differences were seen in gait speed and stride length between the PD groups and the HC group during the ST condition. Previous studies have shown that the increased CV of gait parameters was related with a decrease in postural control ability, which is a strong predictor of fall (Hausdorff, 2009). Notably, we observed greater gait variability, including CV of gait speed and stride length, in the PD groups compared with that of the HC during ST and DT conditions. CV is likely more sensitive than gait speed and stride length for detecting gait disorder in relatively early stages of PD (Noh et al., 2020).

Neurorehabilitation is a potent intervention for improving motor function in patients with PD (Ekker et al., 2016; Ferrazzoli et al., 2020). A few studies have reported the potential of CR for PD, which include exercise and physical therapy, to alleviate motor deficits in muscle strength, balance, and endurance by targeting neuroplasticity (Mak et al., 2017; van der Kolk et al., 2019). It is also encouraging that rehabilitation (both the ER and CR groups) showed consistent improvement in general motor function as assessed by the UPDRS-III. However, our gait analysis showed that CR did not improve walking function in early-stage PD, especially during the DT condition, which is likely due to its lack of impact on cognitive function and, in turn, the lack of interaction between gait and cognition. Few studies have focused on rehabilitation strategies to simultaneously improve cognitive and motor functions, which would offer a better treatment protocol for PD patients in early-stage PD.

Environmental rehabilitation is a novel strategy to simultaneously ameliorate motor and cognitive deficits by combining environmental enrichment with task-specific therapy (Vive et al., 2020). Studies have confirmed the effect of ER on the improvement of motor-cognitive function in patients with stroke and neonatal hypoxia–ischemia (Schuch et al., 2016; Vive et al., 2020). In the present study, significant improvement was observed in walking function as assessed by gait parameters, accompanied by enhanced cognition post-ER in early-stage PD patients. Moreover, we revealed that ER was favorable over CR for improving walking function, especially under the DT condition, which was primarily related to the significant effect of ER on cognition. This conclusion is consistent with previous evidence, which reported a possible mechanism whereby brain cognitive framework changes caused by ER mediates neuroplasticity. We speculated that task-oriented exercise training in ER requires the activation of motor control and the attention-executive network simultaneously, which could strengthen the integration of motor and cognitive resources in turn. Besides, attention-executive function of

PD patients was also enhanced by activities in ER including multisensory and social interactive stimulations, such as supermarket shopping and chess. However, the specific mechanism by which ER enhances cognitive function remains to be elucidated.

Our rs-fMRI analysis provided a quantitative metric of RSFC, which reflects the neural activity and functional integrity of the brain frameworks related to cognition (Lv et al., 2018). The left DLPFC is one of the vital regions within the CEN that mediates cognitive function including attention, working memory, and decision-making (Dong et al., 2020). Neuroimaging studies in participants with early-stage PD have demonstrated that the left DLPFC has decreased connectivity with the left insula (de Bondt et al., 2016), which is a vital regulatory brain area required for performing cognitive tasks (Fu et al., 2021). The involvement of the insula in cognitive tasks is primarily reflected in the flexible switching of attention, the regulation of goal-directed behavior, and the inhibition of irrelevant stimuli (Varjačić et al., 2018). Our data confirmed a strengthened positive RSFC between the left DLPFC and left insula in participants with PD, which was brought about by an enriched sensorimotor environmental stimulation paired with different types of sensory and motor exercises, alongside cognition-related activities and social interaction. In addition, the left IFG is pivotal for successfully exercising inhibitory control over motor responses (Leite et al., 2018). Studies showed that DLPFC and IFG play a complementary and dissociable role in the settlement of decision conflict (Mitchell et al., 2009). Moreover, our FC analysis demonstrated a strengthened positive FC between the left DLPFC and IFG after ER. We inferred from these findings that ER induces neuroplasticity in participants with early-stage PD through strengthening the FC between the left DLPFC and deep brain regions, including the left insular cortex and IFG, which resulted in a positive executive functional network to improve cognitive and walking function. Our findings demonstrated that ER has potential in the improvement of motor function and cognition in early-stage PD patients.

This study has several strengths. We analyzed gait parameters in both the ST and DT walking conditions in early-stage PD patients. Additionally, we investigated RSFC between the left DLPFC and other brain areas pre- and post-ER. However, there are also several limitations. First, the sample size in our study was small, and participants were recruited from only one hospital, which may have introduced bias. In addition, we did not stratify participants based on different clinical classifications of PD, which would likely impact the effect of ER. Furthermore, we only observed the RSFC alteration of PD patients induced by ER; the differential functional connectivity induced by ER and CR would be explored in our future study.

CONCLUSION

Our findings indicated that ER has potential as a potent therapy for participants with early-stage PD for improving cognitive function and gait disorder. The underlying mechanism deduced from rs-fMRI was related to the intervention-induced neuroplasticity whereby the functional connectivity between the left DLPFC and the left insula and IFG was strengthened.

DATA AVAILABILITY STATEMENT

The original contributions presented in the study are included in the article/**Supplementary Material**, further inquiries can be directed to the corresponding authors.

ETHICS STATEMENT

The studies involving human participants were reviewed and approved by Ethical Review Board of Clinical Medical College of Yangzhou University, China (No. 2019070). All study subjects were recruited by the Clinical Medical College of Yangzhou University. The patients/participants provided their written informed consent to participate in this study.

AUTHOR CONTRIBUTIONS

XW, LC, and YP designed the study. XW, LC, HZo, YX, HZa, and WY performed the experiments. XW, XT, JW, YL, PY, and YP analyzed the data. XW, LC, and YP wrote the manuscript. All authors contributed to the article and approved the submitted version.

FUNDING

This work was supported by the National Natural Science Foundation of China (82072533), the "Six One Project" Scientific Research Project for High-Level Health Talents of Jiangsu Province (Nos. LGY2017028 and LGY2018027), the Key Young Medical Talents in Jiangsu Province (No. QNRC2016339), Yangzhou Science and Technology Development Plan Project (YZ2020201), Huxin fund of Jiangsu Key Laboratory of Zoonosis (HX2003), and the Science Foundation of Guangzhou First People's Hospital (M2019009).

ACKNOWLEDGMENTS

All the participants in this study are greatly appreciated.

SUPPLEMENTARY MATERIAL

The Supplementary Material for this article can be found online at: https://www.frontiersin.org/articles/10.3389/fnins.2021.733311/full#supplementary-material

REFERENCES

Armstrong, M. J., and Okun, M. S. (2020). Diagnosis and treatment of Parkinson disease: a review. *JAMA* 323, 548–560. doi: 10.1001/jama.2019.22360

Bondi, C. O., Klitsch, K. C., Leary, J. B., and Kline, A. E. (2014). Environmental enrichment as a viable neurorehabilitation strategy for experimental traumatic brain injury. *J. Neurotrauma* 31, 873–888. doi: 10.1089/neu.2014.3328

Brognara, L., Palumbo, P., Grimm, B., and Palmerini, L. (2019). Assessing gait in Parkinson's disease using wearable motion sensors: a systematic review. *Diseases* 7:18. doi: 10.3390/diseases7010018

Cao, S. S., Yuan, X. Z., Wang, S. H., Taximaimaiti, R., and Wang, X. P. (2020). Transverse strips instead of wearable laser lights alleviate the sequence effect toward a destination in Parkinson's disease patients with freezing of gait. *Front. Neurol.* 11:838. doi: 10.3389/fneur.2020.00838

Caspers, J., Mathys, C., Hoffstaedter, F., Südmeyer, M., Cieslik, E. C., Rubbert, C., et al. (2017). Differential functional connectivity alterations of two subdivisions within the right dlPFC in Parkinson's disease. *Front. Hum. Neurosci.* 11:288. doi: 10.3389/fnhum.2017.00288

Chen, K., Azeez, A., Chen, D. Y., and Biswal, B. B. (2020). Resting-State functional connectivity: signal origins and analytic methods. *Neuroimaging Clin. N. Am.* 30, 15–23. doi: 10.1016/j.nic.2019.09.012

Creaby, M. W., and Cole, M. H. (2018). Gait characteristics and falls in Parkinson's disease: a systematic review and meta-analysis. *Parkinsonism Relat. Disord.* 57, 1–8. doi: 10.1016/j.parkreldis.2018.07.008

Dagan, M., Herman, T., Harrison, R., Zhou, J., Giladi, N., Ruffini, G., et al. (2018). Multitarget transcranial direct current stimulation for freezing of gait in Parkinson's disease. *Mov. Disord.* 33, 642–646. doi: 10.1002/mds.27300

de Bondt, C. C., Gerrits, N. J., Veltman, D. J., Berendse, H. W., van den Heuvel, O. A., and van der Werf, Y. D. (2016). Reduced task-related functional connectivity during a set-shifting task in unmedicated early-stage Parkinson's disease patients. *BMC Neurosci.* 17:20. doi: 10.1186/s12868-016-0254-y

Dong, W., Qiu, C., Jiang, X., Shen, B., Zhang, L., Liu, W., et al. (2020). Can the executive control network be used to diagnose Parkinson's disease and as an efficacy indicator of deep brain stimulation? *Parkinsons Dis.* 2020:6348102. doi: 10.1155/2020/6348102

Ehgoetz Martens, K. A., Hall, J. M., Georgiades, M. J., Gilat, M., Walton, C. C., Matar, E., et al. (2018). The functional network signature of heterogeneity in freezing of gait. *Brain* 141, 1145–1160. doi: 10.1093/brain/awy019

Ekker, M. S., Janssen, S., Nonnekes, J., Bloem, B. R., and de Vries, N. M. (2016). Neurorehabilitation for Parkinson's disease: future perspectives for behavioural adaptation. *Parkinsonism Relat. Disord.* 22(Suppl. 1), S73–S77. doi: 10.1016/j.parkreldis.2015.08.031

Federico, A., Maier, A., Vianello, G., Mapelli, D., Trentin, M., Zanette, G., et al. (2015). Screening for mild cognitive impairment in parkinson's disease: comparison of the italian versions of three neuropsychological tests. *Parkinsons Dis.* 2015:681976. doi: 10.1155/2015/681976

Ferrazzoli, D., Ortelli, P., Cucca, A., Bakdounes, L., Canesi, M., and Volpe, D. (2020). Motor-cognitive approach and aerobic training: a synergism for rehabilitative intervention in Parkinson's disease. *Neurodegener. Dis. Manag.* 10, 41–55. doi: 10.2217/nmt-2019-2025

Forte, R., Pesce, C., Di Baldassarre, A., Shea, J., Voelcker-Rehage, C., Capranica, L., et al. (2019). How older adults cope with cognitive complexity and environmental constraints during dual-task walking: the role of executive function involvement. *Int. J. Environ. Res. Public Health* 16:1835. doi: 10.3390/ijerph16101835

Fu, Y., Long, Z., Luo, Q., Xu, Z., Xiang, Y., Du, W., et al. (2021). Functional and structural connectivity between the left dorsolateral prefrontal cortex and insula could predict the antidepressant effects of repetitive transcranial magnetic stimulation. *Front. Neurosci.* 15:645936. doi: 10.3389/fnins.2021.645936

Fujiwara, T., Ushiba, J., and Soekadar, S. R. (2019). Neurorehabilitation: neural plasticity and functional recovery 2018. *Neural Plast.* 2019:7812148. doi: 10.1155/2019/7812148

Garber, C. E., Blissmer, B., Deschenes, M. R., Franklin, B. A., Lamonte, M. J., Lee, I. M., et al. (2011). American college of sports medicine position stand. quantity and quality of exercise for developing and maintaining cardiorespiratory, musculoskeletal, and neuromotor fitness in apparently healthy adults: guidance for prescribing exercise. *Med. Sci. Sports Exerc.* 43, 1334–1359. doi: 10.1249/MSS.0b013e318213fefb

Goldman, J. G., Vernaleo, B. A., Camicioli, R., Dahodwala, N., Dobkin, R. D., Ellis, T., et al. (2018). Cognitive impairment in Parkinson's disease: a report from a multidisciplinary symposium on unmet needs and future directions to maintain cognitive health. *NPJ Parkinsons Dis.* 4:19. doi: 10.1038/s41531-018-0055-53

Hausdorff, J. M. (2009). Gait dynamics in Parkinson's disease: common and distinct behavior among stride length, gait variability, and fractal-like scaling. *Chaos* 19:026113. doi: 10.1063/1.3147408

Homayoun, H. (2018). Parkinson disease. *Ann. Intern. Med.* 169, Itc33–Itc48. doi: 10.7326/aitc201809040

Islam, A., Alcock, L., Nazarpour, K., Rochester, L., and Pantall, A. (2020). Effect of Parkinson's disease and two therapeutic interventions on muscle activity during walking: a systematic review. *NPJ Parkinsons Dis.* 6:22. doi: 10.1038/s41531-020-00119-w

Janssen, H., Ada, L., Bernhardt, J., McElduff, P., Pollack, M., Nilsson, M., et al. (2014). An enriched environment increases activity in stroke patients undergoing rehabilitation in a mixed rehabilitation unit: a pilot non-randomized controlled trial. *Disabil. Rehabil.* 36, 255–262. doi: 10.3109/09638288.2013.788218

Leite, J., Gonçalves, ÓF., Pereira, P., Khadka, N., Bikson, M., Fregni, F., et al. (2018). The differential effects of unihemispheric and bihemispheric tDCS over the inferior frontal gyrus on proactive control. *Neurosci. Res.* 130, 39–46. doi: 10.1016/j.neures.2017.08.005

Lord, S., Galna, B., Coleman, S., Yarnall, A., Burn, D., and Rochester, L. (2014). Cognition and gait show a selective pattern of association dominated by phenotype in incident Parkinson's disease. *Front. Aging Neurosci.* 6:249. doi: 10.3389/fnagi.2014.00249

Lv, H., Wang, Z., Tong, E., Williams, L. M., Zaharchuk, G., Zeineh, M., et al. (2018). Resting-State functional MRI: everything that nonexperts have always wanted to know. *AJNR Am. J. Neuroradiol.* 39, 1390–1399. doi: 10.3174/ajnr.A5527

Mak, M. K., Wong-Yu, I. S., Shen, X., and Chung, C. L. (2017). Long-term effects of exercise and physical therapy in people with Parkinson disease. *Nat. Rev. Neurol.* 13, 689–703. doi: 10.1038/nrneurol.2017.128

Marusiak, J., Fisher, B. E., Jaskolska, A., Slotwinski, K., Budrewicz, S., Koszewicz, M., et al. (2019). Eight weeks of aerobic interval training improves psychomotor function in patients with Parkinson's disease-randomized controlled trial. *Int. J. Environ. Res. Public Health* 16:880. doi: 10.3390/ijerph16050880

McDonald, M. W., Hayward, K. S., Rosbergen, I. C. M., Jeffers, M. S., and Corbett, D. (2018). Is environmental enrichment ready for clinical application in human post-stroke rehabilitation? *Front. Behav. Neurosci.* 12:135. doi: 10.3389/fnbeh.2018.00135

Mitchell, D. G., Luo, Q., Avny, S. B., Kasprzycki, T., Gupta, K., Chen, G., et al. (2009). Adapting to dynamic stimulus-response values: differential contributions of inferior frontal, dorsomedial, and dorsolateral regions of prefrontal cortex to decision making. *J. Neurosci.* 29, 10827–10834. doi: 10.1523/JNEUROSCI.0963-09.2009

Morris, R., Martini, D. N., Smulders, K., Kelly, V. E., Zabetian, C. P., Poston, K., et al. (2019). Cognitive associations with comprehensive gait and static balance measures in Parkinson's disease. *Parkinsonism Relat. Disord.* 69, 104–110. doi: 10.1016/j.parkreldis.2019.06.014

Ni, M., Hazzard, J. B., Signorile, J. F., and Luca, C. (2018). Exercise guidelines for gait function in parkinson's disease: a systematic review and meta-analysis. *Neurorehabil. Neural Repair* 32, 872–886. doi: 10.1177/1545968318801558

Noh, B., Youm, C., Lee, M., and Cheon, S. M. (2020). Gait characteristics in individuals with Parkinson's disease during 1-minute treadmill walking. *PeerJ* 8:e9463. doi: 10.7717/peerj.9463

Opara, J., Małecki, A., Małecka, E., and Socha, T. (2017). Motor assessment in Parkinson's disease. *Ann. Agric. Environ. Med.* 24, 411–415. doi: 10.5604/12321966.1232774

Penko, A. L., Streicher, M. C., Koop, M. M., Dey, T., Rosenfeldt, A. B., Bazyk, A. S., et al. (2018). Dual-task interference disrupts Parkinson's gait across multiple cognitive domains. *Neuroscience* 379, 375–382. doi: 10.1016/j.neuroscience.2018.03.021

Petzinger, G. M., Fisher, B. E., McEwen, S., Beeler, J. A., Walsh, J. P., and Jakowec, M. W. (2013). Exercise-enhanced neuroplasticity targeting motor and cognitive circuitry in Parkinson's disease. *Lancet Neurol.* 12, 716–726. doi: 10.1016/s1474-4422(13)70123-70126

Prodoehl, J., Burciu, R. G., and Vaillancourt, D. E. (2014). Resting state functional magnetic resonance imaging in Parkinson's disease. *Curr. Neurol. Neurosci. Rep.* 14:448. doi: 10.1007/s11910-014-0448-446

Salazar, R. D., Ren, X., Ellis, T. D., Toraif, N., Barthelemy, O. J., Neargarder, S., et al. (2017). Dual tasking in Parkinson's disease: cognitive consequences while walking. *Neuropsychology* 31, 613–623. doi: 10.1037/neu0000331

San Martín Valenzuela, C., Dueñas Moscardó, L., López-Pascual, J., Serra-Añó, P., and Tomás, J. M. (2020). Interference of functional dual-tasks on gait in untrained people with Parkinson's disease and healthy controls: a cross-sectional study. *BMC Musculoskelet. Disord.* 21:396. doi: 10.1186/s12891-020-03431-x

Schuch, C. P., Jeffers, M. S., Antonescu, S., Nguemeni, C., Gomez-Smith, M., Pereira, L. O., et al. (2016). Enriched rehabilitation promotes motor recovery in rats exposed to neonatal hypoxia-ischemia. *Behav. Brain Res.* 304, 42–50. doi: 10.1016/j.bbr.2016.02.010

Shah, C., Beall, E. B., Frankemolle, A. M., Penko, A., Phillips, M. D., Lowe, M. J., et al. (2016). Exercise therapy for Parkinson's disease: pedaling rate is related to changes in motor connectivity. *Brain Connect* 6, 25–36. doi: 10.1089/brain.2014.0328

Stuck, A. K., Bachmann, M., Fullemann, P., Josephson, K. R., and Stuck, A. E. (2020). Effect of testing procedures on gait speed measurement: a systematic review. *PLoS One* 15:e0234200. doi: 10.1371/journal.pone.0234200

Szeto, J. Y. Y., Walton, C. C., Rizos, A., Martinez-Martin, P., Halliday, G. M., Naismith, S. L., et al. (2020). Dementia in long-term Parkinson's disease patients: a multicentre retrospective study. *NPJ Parkinsons Dis.* 6:2. doi: 10.1038/s41531-019-0106-104

Trujillo, J. P., Gerrits, N. J., Veltman, D. J., Berendse, H. W., van der Werf, Y. D., and van den Heuvel, O. A. (2015). Reduced neural connectivity but increased task-related activity during working memory in de novo Parkinson patients. *Hum. Brain Mapp.* 36, 1554–1566. doi: 10.1002/hbm.22723

van der Kolk, N. M., de Vries, N. M., Kessels, R. P. C., Joosten, H., Zwinderman, A. H., Post, B., et al. (2019). Effectiveness of home-based and remotely supervised aerobic exercise in Parkinson's disease: a double-blind, randomised controlled trial. *Lancet Neurol.* 18, 998–1008. doi: 10.1016/s1474-4422(19)30285-30286

Varjačić, A., Mantini, D., Levenstein, J., Slavkova, E. D., Demeyere, N., and Gillebert, C. R. (2018). The role of left insula in executive set-switching: lesion evidence from an acute stroke cohort. *Cortex* 107, 92–101. doi: 10.1016/j.cortex.2017.11.009

Vive, S., Bunketorp-Käll, L., and Carlsson, G. (2020). Experience of enriched rehabilitation in the chronic phase of stroke. *Disabil. Rehabil.* doi: 10.1080/09638288.2020.1768598 Online ahead of print.

Wang, X., Chen, A., Wu, H., Ye, M., Cheng, H., Jiang, X., et al. (2016). Enriched environment improves post-stroke cognitive impairment in mice by potential regulation of acetylation homeostasis in cholinergic circuits. *Brain Res.* 1650, 232–242. doi: 10.1016/j.brainres.2016.09.018

Wang, X., Meng, Z. X., Chen, Y. Z., Li, Y. P., Zhou, H. Y., Yang, M., et al. (2020). Enriched environment enhances histone acetylation of NMDA receptor in the hippocampus and improves cognitive dysfunction in aged mice. *Neural Regen. Res.* 15, 2327–2334. doi: 10.4103/1673-5374.285005

Wollesen, B., Wanstrath, M., van Schooten, K. S., and Delbaere, K. (2019). A taxonomy of cognitive tasks to evaluate cognitive-motor interference on spatiotemporal gait parameters in older people: a systematic review and meta-analysis. *Eur. Rev. Aging Phys. Act* 16:12. doi: 10.1186/s11556-019-0218-211

Conflict of Interest: The authors declare that the research was conducted in the absence of any commercial or financial relationships that could be construed as a potential conflict of interest.

Publisher's Note: All claims expressed in this article are solely those of the authors and do not necessarily represent those of their affiliated organizations, or those of the publisher, the editors and the reviewers. Any product that may be evaluated in this article, or claim that may be made by its manufacturer, is not guaranteed or endorsed by the publisher.

frontiers in Neuroscience

SYSTEMATIC REVIEW
published: 13 December 2021
doi: 10.3389/fnins.2021.771090

Effects of Non-invasive Brain Stimulation on Multiple System Atrophy: A Systematic Review

Mengjie Zhang[1,2†], *Ting He*[1,2†] *and Quan Wang*[1,2*]

[1] *Department of Occupational Therapy, Shanghai Yangzhi Rehabilitation Hospital (Shanghai Sunshine Rehabilitation Center), School of Medicine, Tongji University, Shanghai, China,* [2] *Department of Rehabilitation Sciences, School of Medicine, Tongji University, Shanghai, China*

Background/Objective: Multiple system atrophy (MSA) refers to a progressive neurodegenerative disease characterized by autonomic dysfunction, parkinsonism, cerebellar ataxia, as well as cognitive deficits. Non-invasive brain stimulation (NIBS) has recently served as a therapeutic technique for MSA by personalized stimulation. The primary aim of this systematic review is to assess the effects of NIBS on two subtypes of MSA: parkinsonian-type MSA (MSA-P) and cerebellar-type MSA (MSA-C).

Methods: A literature search for English articles was conducted from PubMed, Embase, Web of Science, Cochrane Library, CENTRAL, CINAHL, and PsycINFO up to August 2021. Original articles investigating the therapeutics application of NIBS in MSA were screened and analyzed by two independent reviewers. Moreover, a customized form was adopted to extract data, and the quality of articles was assessed based on the PEDro scale for clinical articles.

Results: On the whole, nine articles were included, i.e., five for repetitive transcranial magnetic stimulation (rTMS), two for transcranial direct current stimulation (tDCS), one for paired associative stimulation, with 123 patients recruited. The mentioned articles comprised three randomized controlled trials, two controlled trials, two non-controlled trials, and two case reports which assessed NIBS effects on motor function, cognitive function, and brain modulatory effects. The majority of articles demonstrated significant motor symptoms improvement and increased cerebellar activation in the short term after active rTMS. Furthermore, short-term and long-term effects on improvement of motor performance were significant for tDCS. As opposed to the mentioned, no significant change of motor cortical excitability was reported after paired associative stimulation.

Conclusion: NIBS can serve as a useful neurorehabilitation strategy to improve motor and cognitive function in MSA-P and MSA-C patients. However, further high-quality articles are required to examine the underlying mechanisms and standardized protocol of rTMS as well as its long-term effect. Furthermore, the effects of other NIBS subtypes on MSA still need further investigation.

Keywords: non-invasive brain stimulation (NIBS), repetitive transcranial magnetic stimulation, transcranial direct current stimulation, multiple system atrophy, motor function, cognitive function

OPEN ACCESS

Edited by:
Jinhua Zhang,
Xi'an Jiaotong University, China

Reviewed by:
Giuseppe Lanza,
University of Catania, Italy
Jinyoung Youn,
Sungkyunkwan University School of Medicine, South Korea

****Correspondence:***
Quan Wang
wangquan813@163.com

† These authors have contributed equally to this work

Specialty section:
This article was submitted to Neuroprosthetics, a section of the journal Frontiers in Neuroscience

Received: *05 September 2021*
Accepted: *22 November 2021*
Published: *13 December 2021*

Citation:
Zhang M, He T and Wang Q (2021) Effects of Non-invasive Brain Stimulation on Multiple System Atrophy: A Systematic Review. Front. Neurosci. 15:771090. doi: 10.3389/fnins.2021.771090

BACKGROUND

Multiple system atrophy (MSA) refers to an adult-onset, fatal, progressive neurodegenerative disease characterized by autonomics dysfunction, parkinsonism, cerebellar ataxia, as well as cognitive deficits (Gilman et al., 2008; Fanciulli et al., 2019). The significant neuropathology characteristics exhibited by MSA contain degeneration of striatonigral and olivopontocerebellar structures, accompanied by distinctive glial cytoplasmic inclusions formed by fibrillated a-synuclein proteins (Koga and Dickson, 2018; Schweighauser et al., 2020).

MSA can fall into two main types either with parkinsonian-type MSA (MSA-P) or cerebellar-type MSA (MSA-C) based on the predominant clinical phenotype during assessment, and the predominant characteristic can vary over time (Gilman et al., 2008). MSA-P patients exhibit more parkinsonian signs (e.g., bradykinesia with rigidity, postural instability, tremor, and freezing of gait). In addition, the mentioned parkinsonian symptoms are observed in most MSA-C patients (Köllensperger et al., 2010; Low et al., 2015). The most frequent cerebellar characteristics in MSA-C patients are gait ataxia, accompanied by ataxic dysarthria and limb ataxia. The mentioned cerebellar signs are also present in around half of MSA-P patients (Köllensperger et al., 2010; Low et al., 2015).

Beyond the core clinical phenotype, autonomic failure (e.g., orthostatic hypotension, neurogenic lower urinary tract dysfunction, and constipation) and rapid eye movement sleep behavior disorder (RBD) are common pre-motor characteristics of MSA (Ito et al., 2006; Iodice et al., 2012; Figueroa et al., 2014; Lin et al., 2020). Besides, ∼30% of MSA patients were diagnosed with several cognitive deficits, primarily as executive functions and verbal memory (Eschlböck et al., 2020).

However, there have been no effective treatments for MSA thus far. Existing pharmacological treatment of MSA is purely symptomatic (Rohrer et al., 2018; Mészáros et al., 2020). Only 30% of MSA patients benefit from levodopa therapy targeting parkinsonism, whereas the efficacy is limited and usually diminishes over time (Rohrer et al., 2018). Furthermore, long-term use of the mentioned medications often exerts adverse effects (e.g., hypotension, cognitive impairments, and hypersomnia) (Meissner et al., 2020).

Non-pharmacological approaches including physiotherapy and occupational therapy aim at improving symptoms and patient's quality of life. However, the evidence regarding physiotherapy or occupational therapy in MSA patients is limited (Jain et al., 2004; Raccagni et al., 2019; Coon and Ahlskog, 2021). Thus, non-invasive brain stimulation (NIBS) has recently become an alternative non-pharmacological therapeutic technique for MSA by personalized stimulation (Liu et al., 2018; Alexoudi et al., 2020). Transcranial magnetic stimulation (TMS) and transcranial direct current stimulation (tDCS) have been two extensively applied NIBS techniques.

TMS is a non-invasive, well-tolerated neurophysiological technique based on electro- magnetic induction. TMS has played a prominent role in the functional evaluation to characterize distinctive pattern of change at the final motor output stage between Parkinson's disease (PD) and atypical parkinsonian syndromes (e.g., MSA, progressive supranuclear palsy, and as well as corticobasal-ganglionic degeneration) (Kuhn et al., 2004). MSA patients showed abnormal motor cortex excitability upon TMS, with the reduction of short interval intracortical inhibition (SICI) following the increased motor thresholds and prolongation of ipsilateral and contralateral silent periods (Kuhn et al., 2004; Morita et al., 2008; Suppa et al., 2014). Moreover, inter-hemispheric inhibition measured by TMS could act as a possible neurophysiological correlate of cognitive dysfunction among MSA patients, since abnormal inter-hemispheric inhibition was correlated with cognitive impairment in MSA (Hara et al., 2018). Although the pathophysiological processes can be complex, the TMS articles suggest that dysfunction within the corticobasal ganglia-thalamocortical circuits form an important pathogenic basis for MSA. Additionally, intracortical facilitation and SICI have been shown significantly decreased in patients with RBD which suggests that through identifying subtle changes in the pathophysiology of the motor cortex, TMS can be a useful tool in the detection of very early stages of MSA (Lanza et al., 2020).

Several articles investigated the use of repetitive TMS (rTMS) for treating movement disorder [e.g., Parkinson's disease (PD), Tourette syndrome, dystonia, as well as essential tremor] (Lefaucheur et al., 2017; Tschöpe et al., 2021). The published data suggest that rTMS may mitigate motor symptoms in PD, whereas the evidence in other movement disorders remains unclear.

tDCS refers to another safe, cost-effective NIBS method, offering promise in mitigating motor impairment and improving cognitive and executive function in advanced PD (Lattari et al., 2017; Dagan et al., 2018; Lau et al., 2019). Given the possible regulatory effects of tDCS on cortical excitability, there have been numerous articles over the last decade applying tDCS technique for promoting cognitive and executive function (Doruk et al., 2014; Broeder et al., 2015; Manenti et al., 2018). Besides, existing articles have highlighted the therapeutic potential of tDCS in patients with cerebellar ataxias and the MSA-C (Ferrucci et al., 2016; Barretto et al., 2019; Chen et al., 2021).

There have been several systematic review and meta-analyses that investigating the effect of NIBS in Parkinson's disease and cerebellar ataxia (Goodwill et al., 2017; Kim et al., 2019; Chen et al., 2021). In the mentioned articles, MSA was regarded as one of atypical parkinsonism or degenerative ataxia. Up to present, there is no review has systematically assessed the effect of NIBS on MSA-P and MSA-C. This review hypothesized that NIBS can improve motor function and cognitive function in patients with MSA, and it can serve as an effective adjuvant therapy in MSA treatment. As a consequence, this systematic review aimed to summarize current interventions of NIBS in MSA-P and MSA-C and to examine the effects and safety of NIBS technique applied in the management of MSA-P and MSA-C.

METHODS

Search Strategy

Seven electronic databases (e.g., PubMed, Embase, Cochrane Library, PsycINFO, CINAHL, CENTRAL, and Web of Science) were searched from inception to August 2021. The search strategy

below was applied: (multiple system atrophy OR MSA-P OR MSA-C OR MSA) AND (transcranial magnetic stimulation OR TMS OR transcranial direct current stimulation OR tDCS OR transcranial alternating current stimulation OR tACS OR theta burst stimulation OR TBS OR non-invasive brain stimulation OR NIBS). Related systematic reviews and meta-analyses were identified, and the reference lists of them were checked. Two authors (MZ and TH) identified the potential articles independently by complying with the uniform screening criteria and any disagreements were settled through discussion.

Eligibility Criteria

Articles meeting the criteria were included: adult participants diagnosed with MSA (e.g., probable MSA or possible MSA) in accordance with the clinically diagnostic criteria (Gilman et al., 2008); interventions were NIBS (e.g., TMS or tDCS), and NIBS was employed for therapeutic purposes; outcomes of interest consisted of symptoms, motor function, cognitive function and brain modulatory effects and others; controlled or exploratory articles; peer-reviewed articles and published in English. Articles were excluded if: NIBS was intended for assessing neurophysiological measures; conference papers, abstracts and other articles whose full text is not available; reviews, editorials, commentaries, and other non-clinical trials.

Study Selection

First, the Endnote software was adopted to remove duplications after completing the search process. Second, the author screened relevant articles through reading titles and abstracts. Third, the full-text of the remaining articles were read for in-depth screening.

Data Extraction and Methodological Quality Assessment

A customized form was adopted to collect data of the included articles. The data (i.e., study characteristics, characteristics of study subjects, intervention details, and outcome measures of included articles) were extracted. The Physiotherapy Evidence Database (PEDro) scale was used to assess the methodological quality of included articles (de Morton, 2009). By complying with this criterion, those with a score below three were classified as low quality, while those with a score between 4 and 6 were classified as moderate quality, and those with score above seven were classified as high quality. Two independent reviewers conducted the data extraction and quality assessment. Any discrepancies were resolved through face-to-face discussions.

RESULTS

Study Selection

The study selection is illustrated in **Figure 1**. Initially, 210 records were identified by searching electronic databases and hand searching. After removing duplications, 101 records were retained, of which 50 records were excluded after screening the titles and abstracts. Of the other 51 articles, 42 were removed after reading the full text. Lastly, 9 articles were eligible for qualitative analysis.

Methodological Quality of Reviewed Articles

The results of methodological quality assessment of the included articles were presented in **Table 1**. Nine included articles were published between 2013 and 2020, of which three were randomized controlled trials (Benussi et al., 2015; Chou et al., 2015; Wang et al., 2016; Song et al., 2020), two were controlled trials (Kawashima et al., 2013; Yildiz et al., 2018), two were case report (Wang et al., 2017; Alexoudi et al., 2020) and one was non-controlled trial (Liu et al., 2018).

Except for two case reports, only three articles were classified as high quality (Benussi et al., 2015; Chou et al., 2015; Song et al., 2020), and four were moderate quality (Kawashima et al., 2013; Wang et al., 2016; Liu et al., 2018; Yildiz et al., 2018). All articles did not describe allocation concealment, and only three articles (Benussi et al., 2015; Chou et al., 2015; Song et al., 2020) blinded subjects and therapists. Regarding the comparison on baseline characteristics, five articles (Kawashima et al., 2013; Benussi et al., 2015; Chou et al., 2015; Wang et al., 2016; Song et al., 2020) reported a comparable level between the intervention group and the control group. Besides, intention to treat analysis was performed in six articles (Kawashima et al., 2013; Benussi et al., 2015; Wang et al., 2016; Liu et al., 2018; Yildiz et al., 2018; Song et al., 2020).

Participants

The demographic characteristics of the included articles were presented in **Table 2**. The number of participants was 123 in total, and the number of sample sizes ranged from 1 to 50. The mean age of participants ranged from 52.71 (Wang et al., 2016) to 67.8 (Benussi et al., 2015) years. All articles, except for the two case reports, included participants of both genders, with a higher proportion of men overall. The mean duration of symptoms ranged from 2.18 (Wang et al., 2016) to 5.7 (Benussi et al., 2015) years. Only three articles (Chou et al., 2015; Wang et al., 2016; Alexoudi et al., 2020) used the Hoehn and Yahr scale (H&Y) to describe the severity of recruited samples, and the mean of H&Y scores ranged from 3.2 to 4.

Intervention Characteristics

The characteristics of interventions of the included studies were shown in **Table 2**.

Among the nine articles explored the therapeutic effect of NIBS on MSA, rTMS was applied in six articles (Chou et al., 2015; Wang et al., 2016, 2017; Liu et al., 2018; Yildiz et al., 2018; Song et al., 2020), and tDCS was applied in two studies (Benussi et al., 2015; Alexoudi et al., 2020), the paired associative stimulation (PAS) was used in the remaining one (Kawashima et al., 2013). Stimulation site was left primary motor cortex (M1) in four articles (Kawashima et al., 2013; Chou et al., 2015; Wang et al., 2016, 2017), cerebellum in two articles (Yildiz et al., 2018; Song et al., 2020), and one study simulated both cerebellum and bilateral M1 (Liu et al., 2018). High frequency stimulation ranged from 5 to 50 hz was performed in five articles (Chou et al., 2015; Wang et al., 2016, 2017; Liu et al., 2018; Song et al., 2020), and low frequency stimulation between 0.2 and 1 hz was performed in two articles (Kawashima et al., 2013; Yildiz et al., 2018). The

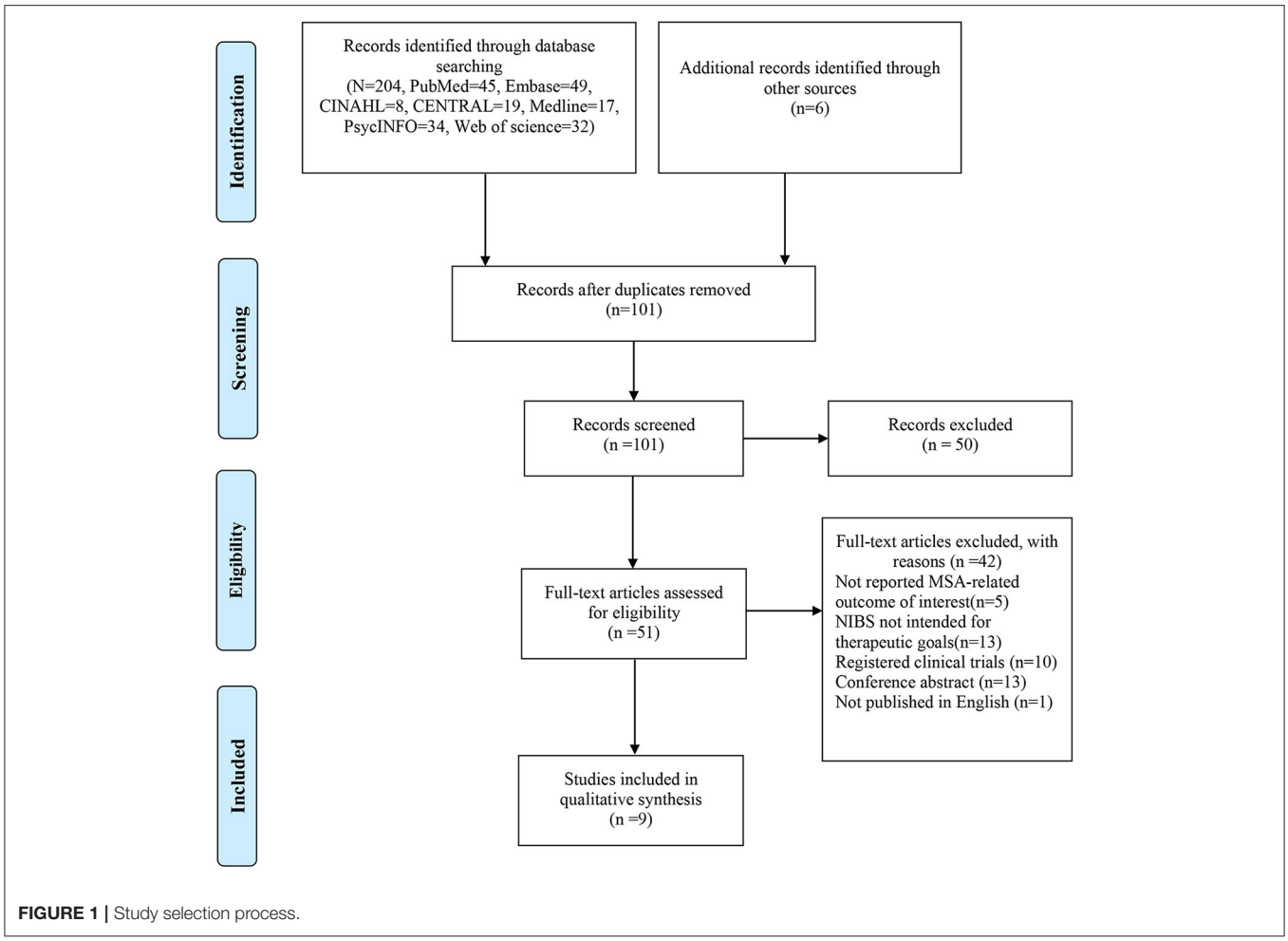

FIGURE 1 | Study selection process.

duration of intervention varied from single session to 2 weeks. Only one study reported follow up period, which was 3 months after first stimulation (Alexoudi et al., 2020).

Outcomes

Description of outcomes of the included articles was grouped by complying with the NIBS employed and the subtypes of MSA.

NIBS in MSA-P

There were five articles explored the effects of NIBS in MSA-P patients.

rTMS Articles

Three articles employed rTMS in MSA-P. Chou et al. (2015) performed a randomized sham-controlled study on 19 MSA-P patients using 10 sessions of high frequency (5 hz) rTMS over the left M1 and reported a significant improvement of motor symptoms, as measured by UMSARS-II, in comparison with sham stimulation (Chou et al., 2015). The authors exploited functional magnetic resonance imaging (fMRI) to measure brain resting-state functional connectivity. They found that positive changes in functional connectivity of functional links involving the DMN, cerebellar network, and limbic network were only identified in the active rTMS group. Moreover, the amelioration of motor symptoms was correlated with positive changes in functional connectivity after active rTMS stimulation.

Wang et al. (2016, 2017) adopted an intervention protocol that was almost identical to Chou et al. (2015). The case report of Wang et al. (2017) showed a significant improvement in UPDRS-III and finger tapping, hand alternating, and heel tapping performance (Wang et al., 2017). Additionally, central motor conduct time of both sides were shortened after rTMS stimulation in comparison with baseline.

Likewise, Wang et al. (2016) conducted a randomized-sham controlled study on 15 MSA-P patients and reported improved motor function and promoted activation of bilateral cerebellum in the real rTMS group other than the sham one (Wang et al., 2016). However, different from the finding of Chou et al. (2015), no correlation was identified between improvement of motor function and increase of cerebellum activation.

PAS Article

Kawashima et al. (2013) employed a single session of low frequency (0.2 hz) TMS over left M1 and electrical stimulation in the right median nerve at the wrist in 10 MSA-P patients.

TABLE 1 | The PEDro scale scores of included studies.

References	Eligibility criteria	Random allocation	Concealed allocation	Baseline comparability	Blind subjects	Blind therapists	Blind assessors	Adequate follow-up	Intention-to-treat analysis	Between-group comparisons	Point estimates and variability	Scores
Kawashima et al. (2013)	✓	×	×	✓	×	×	×	✓	✓	✓	✓	5
Benussi et al. (2015)	✓	✓	×	✓	✓	×	✓	✓	✓	✓	✓	8
Chou et al. (2015)	✓	✓	×	✓	✓	×	✓	✓	×	✓	✓	7
Wang et al. (2016)	✓	✓	×	✓	✓	×	×	✓	✓	✓	✓	6
Liu et al. (2018)	✓	×	×	×	×	×	×	✓	✓	✓	✓	4
Yildiz et al. (2018)	✓	×	×	×	×	×	×	✓	✓	✓	✓	4
Song et al. (2020)	✓	✓	×	✓	✓	×	✓	✓	✓	✓	✓	8

The variations of motor-evoked potential (MEP) amplitudes were determined to reveal the effect of PAS on motor cortex excitability. Furthermore, no significant difference was reported in M1 function before and after stimulation (Kawashima et al., 2013).

tDCS Article

Alexoudi et al. (2020) employed 10 sessions (30 min per session) of anodal tDCS over motor and pre-motor cortices in a 66-year-old woman. Improvements were reported in motor function after tDCS, as well as in activities of daily living, visuomotor activity and processing speed, and working memory. Importantly, the treatment effect lasted for 3 months (Alexoudi et al., 2020).

NIBS in MSA-C

There were three articles explored the effects of NIBS in MSA-C patients.

rTMS Articles

In the randomized controlled trial conducted by Song et al. (2020), the effects of 10 sessions of high frequency (50 hz) intermittent theta-burst stimulation (iTBS) on bilateral cerebellum in 50 MSA-C patients were examined. According to the results, in the active iTBS group, a significant of improvement of motor imbalance and cerebello-frontal connectivity was reported, as revealed by the Scale for Assessment and Rating of Ataxia (SARA) scores and TMS-EEG, respectively. Furthermore, the SARA scores were significantly and negatively correlated with the neural activity of frontal connectivity from 80 to 100 ms after iTBS intervention (Song et al., 2020).

Different from the above articles, Yildiz et al. (2018) performed a controlled clinical trial using single session of low frequency (1 hz) rTMS stimulation over cerebellum in 12 MSA-C patients and found impaired short-latency afferent inhibition (SAI), attention and the spatial working memory, as measured by reaction time, were significantly improved, in comparison with baseline (Yildiz et al., 2018).

tDCS Article

Benussi et al. (2015) performed a randomized sham-controlled trial to examine the effect of a single session cerebellar anodal tDCS that lasts 20 min in six MSA-C patients. The authors reported significant improvement in severity of ataxia, finger dexterity and upper limb coordination, as assessed by SARA, International cooperative ataxia rating scale (ICARS) and the nine-hole peg test (9HPT), respectively, in real tDCS group, in comparison with sham one. However, no significant difference was identified in gait speed, as measured by the 8-Meter Walking Time (8MW), between the two groups (Benussi et al., 2015).

NIBS in MSA-P and MSA-C

Liu et al. (2018) performed a non-controlled trail to explore the effects of high-frequency rTMS over bilateral M1 and cerebellum in three MSA-P patients and six MSA-C patients. Although only five sessions stimulation were applied, the authors found a significant improvement in motor function and an increase in resting-state complexity within the motor network, as recorded by UMSARS-II and blood-oxygen-level

TABLE 2 | Clinical and demographic characteristics of the patients and technical aspects of the reviewed studies.

References	Design	*N*, G (F/M)	Age (y)	DD (y)	Severity (HY)	Intervention	Outcome measures	Main results
NIBS in MSA-P								
Kawashima et al. (2013)	Controlled	MSA-P: 10 (6/4) PD: 10 (6:4)	MSA-P: 59.5 (11.2) PD: 66 (7.7)	MSA-P: 2.76 (0.9) PD: 2.76 (0.7)	NR	PAS Stimulation site: right median nerve (ES); left M1 (TMS) Key parameters ES: Intensity = 110% RMT; TMS: Intensity = SI1 mV; Frequency = 0.2 Hz; Total = 240 pairs of stimuli; Duration = 20 min with an interstimulus interval of 25 ms; F8c; single session	UPDRS; MEP	No change in the averaged amplitude of MEPs
Chou et al. (2015)	RCT, double blinded	Active: 9(3/6) Sham:10(6/4)	Active: 55 (7) Sham: 54 (2)	Active: 2.5 (1.58) Sham: 2 (1)	Active: 3.2 (0.9) Sham: 3.2 (0.7)	rTMS Stimulation site: left M1 Key parameters Frequency = 5 Hz Intensity = 110% RMT 10 trains of 100 pulses with an intertrain interval of 40 s)/session; F8c;10 sessions	UMSARS- II and resting-state functional connectivity	Significant rTMS-related changes in motor symptoms and functional connectivity in active rTMS group
Wang et al. (2016)	RCT, single blinded	MSA-P: 15 (8/7) HC: 18 (9/9)	MSA-P: 53.40 (4.69) HC: 55.17 (3.20)	MSA-P: 2.18 (1.33)	MSA-P: 3.23 (0.70)	rTMS Stimulation site: left M1 Key parameters: Frequency = 5 Hz Intensity = 110% RMT 10 trains of 100 pulses/session F8c;10 sessions	UMSARS- II	Significant decreased UMSARS-II scores in active rTMS group
Wang et al. (2017)	Case report	1, Female	61	4	NR	rTMS Stimulation site: left M1 Key parameters: Frequency = 5 Hz Intensity = 110% RMT 10 trains of 100 pulses/session F8c;10 sessions	UPDRS-III; CMCT	Significant improvement in UPDRS-III and specific task performance; shortened CMCT
Alexoudi et al. (2020)	Case report	1, Female	66	5	4	tDCS Stimulation site: motor and pre-motor cortices (anodal), mastoids (cathodal) Key parameters: 2 mA; 30 min 10 sessions	UPDRS III, TUG; RAVLT; DSST-WAIS-III, TMT-A	Improvement in UPDRS III and the TUG test; positive effect in RAVLT, the DSST-WAIS-III and the TMT-A
NIBS in MSA-C								
Benussi et al. (2015)	RCT, double blinded	4/2	67.8 (8.3)	5.7(2.7)	NR	tDCS Stimulation site: cerebellum (anodal), right deltoid muscle (cathodal) Key parameters: 2 mA; 20 min single session	SARA; ICARS; 8MW; 9HPT	Significant improvement in SARA, ICARS, 8MW and 9HPT.

(Continued)

TABLE 2 | Continued

References	Design	*N*, G (F/M)	Age (y)	DD (y)	Severity (HY)	Intervention	Outcome measures	Main results
Yildiz et al. (2018)	Controlled	MSA-C: (12, 4/8) AD: (5, 2/3) HC: (9, 4/5)	MSA-C: 56.7 (6.9) AD: 80 (4.2) HC: 53.4 (7.7)	MSA-C: 2.94 (1.5) AD: 2.4 (0.49)	NR	rTMS Stimulation site: cerebellum Key parameters: Frequency = 1 Hz Intensity = 90% RMT 600 pulses/session F8c; single session	SAI Reaction Time	SAI responses got improved in MSA-C group
Song et al. (2020)	RCT, double blinded	Active: 25 (11/14) Sham: 25 (10/15)	Active: 53.1 (8.1) Sham: 53.2 ± 9.4	Active: 2.7 (1.1) Sham: 2.5 (0.9)	NR	rTMS Stimulation site: cerebellum Key parameters: iTBS Frequency = 50 Hz Intensity = 80% RMT Total pulse = 1,800 F8c;10 sessions	Dynamic cerebello- fronto connectivity; SARA	Improvement of cerebello-frontal connectivity and balance functions
NIBS in MSA-P and MSA-C								
Liu et al. (2018)	Non-controlled	9 (5/4)	58.0 (7.0)	2.39 (0.78)	NR	Stimulation site: cerebellum AND bilateral M1 Key parameters: Frequency = 5 Hz Intensity = 100% RMT 2,000 pulses and 50 trains Round coil; 5 sessions	UMSARS-II; resting-state brain activity	Increased motor network resting-state complexity

Nr, number; F, female; M, male; DD, disease duration; rTMS, repetitive transcranial magnetic stimulation; MSA-P, Multiple system atrophy- predominant Parkinsonism; MSA-C, Multiple system atrophy-predominant cerebellar ataxia; PD, Parkinson's disease; NR, not reported; F8c, figure eight-shaped coil; ES, electric stimulation; TMS, transcranial magnetic stimulation; M1, primary motor cortex; PAS, Paired Associative Stimulation; RMT, resting motor threshold; UMSARS, Unified Multiple System Atrophy Rating Scale; MEP, motor-evoked potential; RCT, randomized controlled trial; HY, Hoehn and Yahr scale; HC, healthy control group; CMCT, Central motor conduction time; SAI, short-latency afferent inhibition; iTBS, intermittent theta burst stimulation; SARA, Scale for Assessment and Rating of Ataxia scores; ICARS, International Cooperative Ataxia Rating Scale; 8MW, 8-Meter Walking Time; 9HPT, Nine-Hole Peg Test; TUG, Timed Up and Go test; RAVLT, Rey's Auditory Verbal Learning Test; DSST-WAIS-III, Digit Symbol Substitution Test-Wechsler Adult Intelligence; TMT-A, Trail Making Test.

dependency (BOLD) functional magnetic resonance imaging, separately. Consistent with previously achieved results, the improvement in motor function was positively correlated with the increase in motor network resting-state complexity. However, the authors did not report the efficacy of rTMS in MSA-P and MSA-C respectively by complying with disease types (Liu et al., 2018).

DISCUSSION

To the best of the author's knowledge, this review has been the first review that systematically investigated the existing evidence of the use of NIBS (e.g., rTMS, tDCS, and PAS) for treating MSA-P and MSA-C. The recruited articles were reported with significant heterogeneity and variability of study population, study designs and interventional protocols, thereby increasing difficulty in drawing a definite conclusion of the prospect of NIBS techniques. However, most of the included articles reported improving effects of NIBS on the motor function, cognitive function and cortical function of MSA patients. As impacted by the low number of included articles and the low quality of articles, there is no sufficient confidence in mentioned findings, and the estimates should be interpreted cautiously.

Over the past few years, the effects of NIBS on MSA have been increasingly studied, whereas the exact mechanisms remain unclear. rTMS uses repeated magnetic pulses *via* a stimulation coil placed over the scalp to generate electromagnetic fields that are capable of inducing action potential in the brain (Valero-Cabré et al., 2017). To be specific, cortical excitability is enhanced by high-frequency rTMS (≥5 Hz), while it is inhibited by low-frequency rTMS (≤1 Hz) (Pascual-Leone et al., 1994). tDCS delivers weak direct currents to the cortex *via* two electrodes attached to the scalp. The stimulation consists of two types, i.e., anodal stimulation excites neuronal activity and while cathodal stimulation can suppress neuronal activity. rTMS and tDCS regulate cortex excitability in different manners. Specifically, rTMS can induce direct and trans-synaptic neuronal activation, while tDCS can lead to subthreshold neuronal membrane polarization. However, the long-term potentiation or depression (LTP/LTD)-like synaptic plasticity was found to be induced by both methods (Nitsche et al., 2003; Esser et al., 2006; Monte-Silva et al., 2013).

According to all the included articles examining the role of NIBS in treating MSA-P, the targeted area of stimulation was the M1. Nevertheless, in the MSA-C articles, the cerebellum was selected for stimulation. Existing articles exploited theta-burst stimulation to examine M1 excitability in MSA and

reported reduced short-interval intracortical facilitation in MSA-P and MSA-C patients, thereby demonstrating impaired M1 plasticity (Suppa et al., 2014). Moreover, in the longitudinal study conducted by Burciu et al. (2016), the authors reported decreased functional activity presented by task-related fMRI signal in M1, supplementary motor area and superior cerebellum in MSA over a 1-year period. All the mentioned revealed that the role of brain plasticity is of pivotal importance in the treatment of MSA.

Motor impairments in MSA are considered to be attributed to dysfunction of the cerebellum and the neural networks it connects to Lu et al. (2013). Through the cerebello-thalamo-cortical circuit, the cerebellum and the bilateral M1, a connected network of the cerebellum, are critical to motor control (Grimaldi et al., 2014). Pukinje cells within the cerebellum have physiological inhibitory effects on the M1 by inhibiting the dentate nucleus (Spampinato et al., 2020), which is termed cerebellar brain inhibition (CBI) (Galea et al., 2009) MSA impairs the regulation of the dentate nucleus and Purkinje cells, thereby decreasing the excitability of M1 and ultimately leading to motor control dysfunction (Yang et al., 2019a).

Liu et al. (2018) applied rTMS over cerebellum and bilateral M1, and the beneficial effect of rTMS might be correlated with the direct activation of M1 and the reduction of M1 inhibition by the cerebellum (Liu et al., 2018). Since the cerebellum and M1 are functionally connected, in-depth research should be conducted to verify whether stimulating the two regions is better than targeting either region separately.

In the included articles of high-frequency rTMS in MSA-P, its regulatory effect on the brain was found, which was manifested as the improved default mode network (DMN) plasticity and cerebellar activation. The underlying mechanisms of DMN modulation remain unclear, DMN plasticity may show sensitivity to rTMS treatment and facilitate the consolidation and maintenance of brain function *via* DMN plasticity (Fjell et al., 2014; Chou et al., 2015). Wang et al. (2016) hypothesized that the increase in cerebellar activation was correlated with the motor effect in MSA, which is probably attributed due to cerebellar loop compensation induced by high-frequency rTMS treatment. DMN is closely correlated with the cerebellar and limbic networks (Catani et al., 2013; Halko et al., 2014). DMN exhibits the maximal activation during rest, which is correlated with a high degree of neuroplasticity (Shulman et al., 1997; Fjell et al., 2014). Accordingly, it can be speculated that rTMS may change the excitability of the motor cortex by regulating the brain plasticity in MSA patients.

Furthermore, central motor conduction time (CMCT) was reported to be prolonged in MSA patients (Abbruzzese et al., 1997). CMCT is the time it takes for nerve impulses to reach the target muscles based on the central nervous system. Since the CMCT decreased after the high-frequency rTMS treatment, the improvement in trans-synaptic efficiency might be reflected (Wang et al., 2017).

Inconsistent with high-frequency rTMS, low-frequency rTMS can temporarily inhibit cortical excitability (Kobayashi and Pascual-Leone, 2003). Articles reported that low-frequency rTMS on the lateral cerebellum impacted the excitability of the motor cortex for 30 min (Chen et al., 1997; Heide et al., 2006). As indicated from articles, rTMS targeting the cerebellum could inhibit the excitability of Purkinje cells, thereby inhibiting the dentate nucleus and in turn the contralateral M1 (Ugawa et al., 1995). Besides, the possible mechanism underlying the therapeutic benefits of rTMS was found as the neuroprotective effect of rTMS. According to May et al. (2007), the gray matter volume at the left superior temporal gyrus increased significantly after 1 Hz rTMS was applied for 5 days in the identical site (May et al., 2007). Cerebral cortex and cerebellum atrophy is evident in MSA-P and MSA-C. Yang et al. (2019b) identified gray matter loss in anterior and posterior cerebellar lobes. Moreover, they found the negative correlation between the extent of atrophy involving left lobule IX and motor performance. Next, they observed a negative correlation between the extent of cerebellar volume loss and cognitive impairments (Yang et al., 2019b), and the mentioned findings comply with those of others (Kim et al., 2015). It can be therefore speculated that rTMS may increase gray matter of cerebellum, which can improve motor and cognitive function in MSA patients.

Likewise, the exact mechanisms of cognitive impairment in MSA remain unclear. As demonstrated from neuroimaging, neuropsychological and neuropathologic articles the cognitive decline in MSA may originate from the atrophy of the cerebral cortex (especially the frontal lobes), the subcortical structure, as well as the cerebellum (Stankovic et al., 2014; Lee et al., 2016; Barcelos et al., 2018; Santangelo et al., 2018; Caso et al., 2020). To be specific, the lesions of subcortical circuit loop (i.e., the cerebral cortex-basal gangliathalamus-cerebral cortex circuit and the cerebral cortex-pons-cerebellumthalamus-cerebral cortical circuit) may cause essential signals conduction impairment (Miyachi, 2009; Zhang et al., 2018).

Although cognitive deficits are significantly common in MSA patients, only one of the recruited articles examined the effects of rTMS on the treatment of cognitive impairment (Yildiz et al., 2018). The effects of rTMS on cognitive enhancement have been reported in mild cognitive impairment and Alzheimer's disease. Executive performance can be significantly improved by high-frequency rTMS over the right inferior frontal gyrus, and memory functions can be noticeably improved by low-frequency rTMS targeting on the left dorsolateral prefrontal cortex (DLPFC) (Chou et al., 2020). According to Minnerop et al., significant hypoperfusion was reported in the frontal and dorsolateral prefrontal cortex and in MSA-P patients and the severity of cognitive impairment correlated with hypoperfusion in the DLPFC. Compared with MSA-P, visuospatial cognitive and construction impairment was more significant in MSA-C patients, and it was correlated with hypoperfusion in the prefrontal and cerebellar cortex, thereby indicating the different mechanisms of cognitive impairments in two types of MSA (Minnerop et al., 2007). The underlying mechanisms of the effect of rTMS on cognitive function may consist of increasing LTP (Thickbroom, 2007), enhancing synaptic function (Shang et al., 2016), increasing hippocampal neurogenesis in the dentate gyrus (Ueyama et al., 2011) and leading to network level changes in brain function (Bangen et al., 2012). High-quality research should be further conducted to clarify whether rTMS can

improve cognitive function in MSA patients and elucidate the underlying mechanisms.

Cerebellar tDCS were shown to modulate cerebellar excitability in polar-specific manners, as highlighted by the modulation of CBI. Cerebellar anodal stimulation was reported to improve the excitability of the cerebellar cortex, thereby promoting CBI, while cathodal stimulation could reduce excitability, thereby causing CBI to decrease (Galea et al., 2009). Cerebellar tDCS are suggested to work by polarizing Purkinje cells and alternating activity patterns in the deep cerebellar output nuclei (Galea et al., 2009; Grimaldi et al., 2016). Moreover, anodal cerebellar tDCS was reported to reduce the amplitudes of long-latency stretch reflexes in patients with ataxia by increasing the inhibitory effect exerted by the cerebellar cortex on the cerebellar nuclei (Grimaldi and Manto, 2013).

This systematic review shows the advantages that only peer-reviewed articles were recruited, and that the methodological quality was assessed. However, some limitations remain in this review. First, the total numbers of recruited articles and participants were small. In addition, some articles did not elaborate on the diagnosis of the enrolled subjects, so the authors have no way to distinguish whether the subjects belong to probable MSA or possible MSA. Therefore, the generalization of the conclusion of this review is limited. Second, because of the heterogeneity of interventional protocol and outcome measures among the mentioned articles and an insufficient number of articles in each subgroup, we did not conduct a meta-analysis. Third, gray literature was not searched, and only articles published in English were included, thereby probably causing published bias.

CONCLUSIONS

NIBS can be a useful neurorehabilitation strategy to improve motor and cognitive function in MSA-P and MSA-C patients. However, the effects of other NIBS subtypes on MSA should be investigated more specifically. Further high-quality articles are required to examine the underlying mechanisms of NIBS, to determine the long-term effects of NIBS on motor and cognitive function in MSA patients, as well as to clarify the optimal stimulation protocol (e.g., stimulation site, intensity, duration, and number of sessions).

DATA AVAILABILITY STATEMENT

The original contributions presented in the study are included in the article/supplementary material, further inquiries can be directed to the corresponding author.

AUTHOR CONTRIBUTIONS

The study has been designed by MZ, TH, and QW. Data have been gathered by MZ and TH under the supervision of QW. Data have been analyzed and the manuscript has been drafted by MZ and TH. QW revised the manuscript for important intellectual content. All authors approved the final version of the manuscript.

FUNDING

The funding was supported by grants from Rehabilitation Research Project for the disabled of Shanghai (K2018036).

REFERENCES

Abbruzzese, G., Marchese, R., and Trompetto, C. (1997). Sensory and motor evoked potentials in multiple system atrophy: a comparative study with Parkinson's disease. *Mov. Disord.* 12, 315–321. doi: 10.1002/mds.870120309

Alexoudi, A., Patrikelis, P., Fasilis, T., Deftereos, S., Sakas, D., and Gatzonis, S. (2020). Effects of anodal tDCS on motor and cognitive function in a patient with multiple system atrophy. *Disabil. Rehabil.* 42, 887–891. doi: 10.1080/09638288.2018.1510043

Bangen, K. J., Kaup, A. R., Mirzakhanian, H., Wierenga, C. E., Jeste, D. V., and Eyler, L. T. (2012). Compensatory brain activity during encoding among older adults with better recognition memory for face-name pairs: an integrative functional, structural, and perfusion imaging study. *J. Int. Neuropsychol. Soc.* 18, 402–413. doi: 10.1017/S1355617712000197

Barcelos, L. B., Saad, F., Giacominelli, C., Saba, R. A., de Carvalho Aguiar, P. M., Silva, S. M. A., et al. (2018). Neuropsychological and clinical heterogeneity of cognitive impairment in patients with multiple system atrophy. *Clin. Neurol Neurosurg.* 164, 121–126. doi: 10.1016/j.clineuro.2017.10.039

Barretto, T. L., Bandeira, I. D., Jagersbacher, J. G., Barretto, B. L., de Oliveira, E. T. Â., Peña, N., et al. (2019). Transcranial direct current stimulation in the treatment of cerebellar ataxia: a two-phase, double-blind, auto-matched, pilot study. *Clin. Neurol. Neurosurg.* 182, 123–129. doi: 10.1016/j.clineuro.2019.05.009

Benussi, A., Koch, G., Cotelli, M., Padovani, A., and Borroni, B. (2015). Cerebellar transcranial direct current stimulation in patients with ataxia: a double-blind, randomized, sham-controlled study. *Mov. Disord.* 30, 1701–1705. doi: 10.1002/mds.26356

Broeder, S., Nackaerts, E., Heremans, E., Vervoort, G., Meesen, R., Verheyden, G., et al. (2015). Transcranial direct current stimulation in Parkinson's disease: neurophysiological mechanisms and behavioral effects. *Neurosci. Biobehav. Rev.* 57, 105–117. doi: 10.1016/j.neubiorev.2015.08.010

Burciu, R. G., Chung, J. W., Shukla, P., Ofori, E., Li, H., McFarland, N. R., et al. (2016). Functional MRI of disease progression in Parkinson's disease and atypical parkinsonian syndromes. *Neurology* 87, 709–717. doi: 10.1212/WNL.0000000000002985

Caso, F., Canu, E., Lukic, M. J., Petrovic, I. N., Fontana, A., Nikolic, I., et al. (2020). Cognitive impairment and structural brain damage in multiple system atrophy-parkinsonian variant. *J. Neurol.* 267, 87–94. doi: 10.1007/s00415-019-09555-y

Catani, M., Dell'acqua, F., and Thiebaut de Schotten, M. (2013). A revised limbic system model for memory, emotion and behaviour. *Neurosci. Biobehav. Rev.* 37, 1724–1737. doi: 10.1016/j.neubiorev.2013.07.001

Chen, R., Classen, J., Gerloff, C., Celnik, P., Wassermann, E. M., Hallett, M., et al. (1997). Depression of motor cortex excitability by low-frequency transcranial magnetic stimulation. *Neurology* 48, 1398–1403. doi: 10.1212/WNL.48.5.1398

Chen, T. X., Yang, C. Y., Willson, G., Lin, C. C., and Kuo, S. H. (2021). The efficacy and safety of transcranial direct current stimulation for cerebellar ataxia: a systematic review and meta-analysis. *Cerebellum* 20, 124–133. doi: 10.1007/s12311-020-01181-z

Chou, Y.-h., You, H., Wang, H., Zhao, Y.-p., Hou, B., Chen, N.-k., et al. (2015). Effect of repetitive transcranial magnetic stimulation on fMRI resting-state connectivity in multiple system atrophy. *Brain Connect.* 5, 451–459. doi: 10.1089/brain.2014.0325

Chou, Y. H., Ton That, V., and Sundman, M. (2020). A systematic review and meta-analysis of rTMS effects on cognitive enhancement in mild cognitive impairment and Alzheimer's disease. *Neurobiol. Aging* 86, 1–10. doi: 10.1016/j.neurobiolaging.2019.08.020

Coon, E. A., and Ahlskog, J. E. (2021). My treatment approach to multiple system atrophy. *Mayo Clin. Proc.* 96, 708–719. doi: 10.1016/j.mayocp.2020.10.005

Dagan, M., Herman, T., Harrison, R., Zhou, J., Giladi, N., Ruffini, G., et al. (2018). Multitarget transcranial direct current stimulation for freezing of gait in Parkinson's disease. *Mov. Disord.* 33, 642–646. doi: 10.1002/mds.27300

de Morton, N. A. (2009). The PEDro scale is a valid measure of the methodological quality of clinical trials: a demographic study. *Aust. J. Physiother.* 55, 129–133. doi: 10.1016/S0004-9514(09)70043-1

Doruk, D., Gray, Z., Bravo, G. L., Pascual-Leone, A., and Fregni, F. (2014). Effects of tDCS on executive function in Parkinson's disease. *Neurosci. Lett.* 582, 27–31. doi: 10.1016/j.neulet.2014.08.043

Eschlböck, S., Delazer, M., Krismer, F., Bodner, T., Fanciulli, A., Heim, B., et al. (2020). Cognition in multiple system atrophy: a single-center cohort study. *Ann. Clin. Transl. Neurol.* 7, 219–228. doi: 10.1002/acn3.50987

Esser, S. K., Huber, R., Massimini, M., Peterson, M. J., Ferrarelli, F., and Tononi, G. (2006). A direct demonstration of cortical LTP in humans: a combined TMS/EEG study. *Brain Res. Bull.* 69, 86–94. doi: 10.1016/j.brainresbull.2005.11.003

Fanciulli, A., Stankovic, I., Krismer, F., Seppi, K., Levin, J., and Wenning, G. K. (2019). Multiple system atrophy. *Int. Rev. Neurobiol.* 149, 137–192. doi: 10.1016/bs.irn.2019.10.004

Ferrucci, R., Bocci, T., Cortese, F., Ruggiero, F., and Priori, A. (2016). Cerebellar transcranial direct current stimulation in neurological disease. *Cerebellum Ataxias* 3:16. doi: 10.1186/s40673-016-0054-2

Figueroa, J. J., Singer, W., Parsaik, A., Benarroch, E. E., Ahlskog, J. E., Fealey, R. D., et al. (2014). Multiple system atrophy: prognostic indicators of survival. *Mov. Disord.* 29, 1151–1157. doi: 10.1002/mds.25927

Fjell, A. M., McEvoy, L., Holland, D., Dale, A. M., and Walhovd, K. B. (2014). What is normal in normal aging? Effects of aging, amyloid and Alzheimer's disease on the cerebral cortex and the hippocampus. *Prog. Neurobiol.* 117, 20–40. doi: 10.1016/j.pneurobio.2014.02.004

Galea, J. M., Jayaram, G., Ajagbe, L., and Celnik, P. (2009). Modulation of cerebellar excitability by polarity-specific noninvasive direct current stimulation. *J. Neurosci.* 29, 9115–9122. doi: 10.1523/JNEUROSCI.2184-09.2009

Gilman, S., Wenning, G. K., Low, P. A., Brooks, D. J., Mathias, C. J., Trojanowski, J. Q., et al. (2008). Second consensus statement on the diagnosis of multiple system atrophy. *Neurology* 71:670. doi: 10.1212/01.wnl.0000324625.00404.15

Goodwill, A. M., Lum, J. A. G., Hendy, A. M., Muthalib, M., Johnson, L., Albein-Urios, N., et al. (2017). Using non-invasive transcranial stimulation to improve motor and cognitive function in Parkinson's disease: a systematic review and meta-analysis. *Sci. Rep.* 7:14840. doi: 10.1038/s41598-017-13260-z

Grimaldi, G., Argyropoulos, G. P., Bastian, A., Cortes, M., Davis, N. J., Edwards, D. J., et al. (2016). Cerebellar transcranial direct current stimulation (ctDCS): a novel approach to understanding cerebellar function in health and disease. *Neuroscientist* 22, 83–97. doi: 10.1177/1073858414559409

Grimaldi, G., Argyropoulos, G. P., Boehringer, A., Celnik, P., Edwards, M. J., Ferrucci, R., et al. (2014). Non-invasive cerebellar stimulation–a consensus paper. *Cerebellum* 13, 121–138. doi: 10.1007/s12311-013-0514-7

Grimaldi, G., and Manto, M. (2013). Anodal transcranial direct current stimulation (tDCS) decreases the amplitudes of long-latency stretch reflexes in cerebellar ataxia. *Ann. Biomed. Eng.* 41, 2437–2447. doi: 10.1007/s10439-013-0846-y

Halko, M. A., Farzan, F., Eldaief, M. C., Schmahmann, J. D., and Pascual-Leone, A. (2014). Intermittent theta-burst stimulation of the lateral cerebellum increases functional connectivity of the default network. *J. Neurosci.* 34, 12049–12056. doi: 10.1523/JNEUROSCI.1776-14.2014

Hara, K., Watanabe, H., Bagarinao, E., Kawabata, K., Yoneyama, N., Ohdake, R., et al. (2018). Corpus callosal involvement is correlated with cognitive impairment in multiple system atrophy. *J. Neurol.* 265, 2079–2087. doi: 10.1007/s00415-018-8923-7

Heide, G., Witte, O. W., and Ziemann, U. (2006). Physiology of modulation of motor cortex excitability by low-frequency suprathreshold repetitive transcranial magnetic stimulation. *Exp. Brain Res.* 171, 26–34. doi: 10.1007/s00221-005-0262-0

Iodice, V., Lipp, A., Ahlskog, J. E., Sandroni, P., Fealey, R. D., Parisi, J. E., et al. (2012). Autopsy confirmed multiple system atrophy cases: mayo experience and role of autonomic function tests. *J. Neurol. Neurosurg. Psychiatry* 83, 453–459. doi: 10.1136/jnnp-2011-301068

Ito, T., Sakakibara, R., Yasuda, K., Yamamoto, T., Uchiyama, T., Liu, Z., et al. (2006). Incomplete emptying and urinary retention in multiple-system atrophy: when does it occur and how do we manage it? *Mov. Disord.* 21, 816–823. doi: 10.1002/mds.20815

Jain, S., Dawson, J., Quinn, N. P., and Playford, E. D. (2004). Occupational therapy in multiple system atrophy: a pilot randomized controlled trial. *Mov. Disord.* 19, 1360–1364. doi: 10.1002/mds.20211

Kawashima, S., Ueki, Y., Mima, T., Fukuyama, H., Ojika, K., and Matsukawa, N. (2013). Differences in dopaminergic modulation to motor cortical plasticity between Parkinson's disease and multiple system atrophy. *PLoS ONE.* 8:e0062515. doi: 10.1371/journal.pone.0062515

Kim, J. S., Yang, J. J., Lee, D. K., Lee, J. M., Youn, J., and Cho, J. W. (2015). Cognitive impairment and its structural correlates in the Parkinsonian subtype of multiple system atrophy. *Neurodegener. Dis.* 15, 294–300. doi: 10.1159/000430953

Kim, Y. W., Shin, I. S., Moon, H. I., Lee, S. C., and Yoon, S. Y. (2019). Effects of non-invasive brain stimulation on freezing of gait in parkinsonism: a systematic review with meta-analysis. *Parkinsonism Relat. Disord.* 64, 82–89. doi: 10.1016/j.parkreldis.2019.02.029

Kobayashi, M., and Pascual-Leone, A. (2003). Transcranial magnetic stimulation in neurology. *Lancet Neurol.* 2, 145–156. doi: 10.1016/S1474-4422(03)00321-1

Koga, S., and Dickson, D. W. (2018). Recent advances in neuropathology, biomarkers and therapeutic approach of multiple system atrophy. *J. Neurol. Neurosurg. Psychiatry* 89, 175–184. doi: 10.1136/jnnp-2017-315813

Köllensperger, M., Geser, F., Ndayisaba, J.-P., Boesch, S., Seppi, K., Ostergaard, K., et al. (2010). Presentation, diagnosis, and management of multiple system atrophy in Europe: final analysis of the European multiple system atrophy registry. *Mov. Disord.* 25, 2604–2612. doi: 10.1002/mds.23192

Kuhn, A. A., Grosse, P., Holtz, K., Brown, P., Meyer, B. U., and Kupsch, A. (2004). Patterns of abnormal motor cortex excitability in atypical parkinsonian syndromes. *Clin. Neurophysiol.* 115, 1786–1795. doi: 10.1016/j.clinph.2004.03.020

Lanza, G., Arico, D., Lanuzza, B., Cosentino, F. I. I., Tripodi, M., Giardina, F., et al. (2020). Facilitatory/inhibitory intracortical imbalance in REM sleep behavior disorder: early electrophysiological marker of neurodegeneration? *Sleep* 43:zsz242. doi: 10.1093/sleep/zsz242

Lattari, E., Costa, S. S., Campos, C., de Oliveira, A. J., Machado, S., and Maranhao Neto, G. A. (2017). Can transcranial direct current stimulation on the dorsolateral prefrontal cortex improves balance and functional mobility in Parkinson's disease? *Neurosci. Lett.* 636, 165–169. doi: 10.1016/j.neulet.2016.11.019

Lau, C. I., Liu, M. N., Chang, K. C., Chang, A., Bai, C. H., Tseng, C. S., et al. (2019). Effect of single-session transcranial direct current stimulation on cognition in Parkinson's disease. *CNS Neurosci. Ther.* 25, 1237–1243. doi: 10.1111/cns.13210

Lee, M. J., Shin, J. H., Seoung, J. K., Lee, J. H., Yoon, U., Oh, J. H., et al. (2016). Cognitive impairments associated with morphological changes in cortical and subcortical structures in multiple system atrophy of the cerebellar type. *Eur. J. Neurol.* 23, 92–100. doi: 10.1111/ene.12796

Lefaucheur, J. P., Antal, A., Ayache, S. S., Benninger, D. H., Brunelin, J., Cogiamanian, F., et al. (2017). Evidence-based guidelines on the therapeutic use of transcranial direct current stimulation (tDCS). *Clin. Neurophysiol.* 128, 56–92. doi: 10.1016/j.clinph.2016.10.087

Lin, J. Y., Zhang, L. Y., Cao, B., Wei, Q. Q., Ou, R. W., Hou, Y. B., et al. (2020). Sleep-related symptoms in multiple system atrophy: determinants and impact on disease severity. *Chin. Med. J. (Engl).* 134, 690–698. doi: 10.1097/CM9.0000000000001211

Liu, Z., Ma, H., Poole, V., Wang, X., Wang, Z., Yang, Y., et al. (2018). Effects of multi-session repetitive transcranial magnetic stimulation on motor control and spontaneous brain activity in multiple system atrophy: a pilot study. *Front. Behav. Neurosci.* 12:e00090. doi: 10.3389/fnbeh.2018.00090

Low, P. A., Reich, S. G., Jankovic, J., Shults, C. W., Stern, M. B., Novak, P., et al. (2015). Natural history of multiple system atrophy in the USA: a prospective cohort study. *Lancet Neurol.* 14, 710–719. doi: 10.1016/S1474-4422(15)00058-7

Lu, C. F., Soong, B. W., Wu, H. M., Teng, S., Wang, P. S., and Wu, Y. T. (2013). Disrupted cerebellar connectivity reduces whole-brain network efficiency in multiple system atrophy. *Mov. Disord.* 28, 362–369. doi: 10.1002/mds.25314

Manenti, R., Cotelli, M. S., Cobelli, C., Gobbi, E., Brambilla, M., Rusich, D., et al. (2018). Transcranial direct current stimulation combined with cognitive

training for the treatment of Parkinson Disease: a randomized, placebo-controlled study. *Brain Stimul.* 11, 1251–1262. doi: 10.1016/j.brs.2018.07.046

May, A., Hajak, G., Gänssbauer, S., Steffens, T., Langguth, B., Kleinjung, T., et al. (2007). Structural brain alterations following 5 days of intervention: dynamic aspects of neuroplasticity. *Cereb. Cortex.* 17, 205–210. doi: 10.1093/cercor/bhj138

Meissner, W. G., Traon, A. P., Foubert-Samier, A., Galabova, G., Galitzky, M., Kutzelnigg, A., et al. (2020). A phase 1 randomized trial of specific active α-synuclein immunotherapies PD01A and PD03A in multiple system atrophy. *Mov. Disord.* 35, 1957–1965. doi: 10.1002/mds.28218

Mészáros, L., Hoffmann, A., Wihan, J., and Winkler, J. (2020). Current symptomatic and disease-modifying treatments in multiple system atrophy. *Int. J. Mol. Sci.* 21:2775. doi: 10.3390/ijms21082775

Minnerop, M., Specht, K., Ruhlmann, J., Schimke, N., Abele, M., Weyer, A., et al. (2007). Voxel-based morphometry and voxel-based relaxometry in multiple system atrophy-a comparison between clinical subtypes and correlations with clinical parameters. *Neuroimage* 36, 1086–1095. doi: 10.1016/j.neuroimage.2007.04.028

Miyachi, S. (2009). Cortico-basal ganglia circuits–parallel closed loops and convergent/divergent connections. *Brain Nerve* 61, 351–359. doi: 10.11477/mf.1416100459

Monte-Silva, K., Kuo, M. F., Hessenthaler, S., Fresnoza, S., Liebetanz, D., Paulus, W., et al. (2013). Induction of late LTP-like plasticity in the human motor cortex by repeated non-invasive brain stimulation. *Brain Stimul.* 6, 424–432. doi: 10.1016/j.brs.2012.04.011

Morita, Y., Osaki, Y., and Doi, Y. (2008). Transcranial magnetic stimulation for differential diagnostics in patients with parkinsonism. *Acta Neurol. Scand.* 118, 159–163. doi: 10.1111/j.1600-0404.2007.00988.x

Nitsche, M. A., Fricke, K., Henschke, U., Schlitterlau, A., Liebetanz, D., Lang, N., et al. (2003). Pharmacological modulation of cortical excitability shifts induced by transcranial direct current stimulation in humans. *J. Physiol.* 553, 293–301. doi: 10.1113/jphysiol.2003.049916

Pascual-Leone, A., Grafman, J., and Hallett, M. (1994). Modulation of cortical motor output maps during development of implicit and explicit knowledge. *Science* 263, 1287–1289. doi: 10.1126/science.8122113

Raccagni, C., Goebel, G., Gaßner, H., Granata, R., Ndayisaba, J. P., Seebacher, B., et al. (2019). Physiotherapy improves motor function in patients with the Parkinson variant of multiple system atrophy: a prospective trial. *Parkinsonism Relat. Disord.* 67, 60–65. doi: 10.1016/j.parkreldis.2019.09.026

Rohrer, G., Höglinger, G. U., and Levin, J. (2018). Symptomatic therapy of multiple system atrophy. *Autonomic Neurosci. Basic Clin.* 211, 26–30. doi: 10.1016/j.autneu.2017.10.006

Santangelo, G., Cuoco, S., Pellecchia, M. T., Erro, R., Barone, P., and Picillo, M. (2018). Comparative cognitive and neuropsychiatric profiles between Parkinson's disease, multiple system atrophy and progressive supranuclear palsy. *J. Neurol.* 265, 2602–2613. doi: 10.1007/s00415-018-9038-x

Schweighauser, M., Shi, Y., Tarutani, A., Kametani, F., Murzin, A. G., Ghetti, B., et al. (2020). Structures of α-synuclein filaments from multiple system atrophy. *Nature* 585, 464–469. doi: 10.1038/s41586-020-2317-6

Shang, Y., Wang, X., Shang, X., Zhang, H., Liu, Z., Yin, T., et al. (2016). Repetitive transcranial magnetic stimulation effectively facilitates spatial cognition and synaptic plasticity associated with increasing the levels of BDNF and synaptic proteins in Wistar rats. *Neurobiol. Learn. Mem.* 134, 369–378. doi: 10.1016/j.nlm.2016.08.016

Shulman, G. L., Fiez, J. A., Corbetta, M., Buckner, R. L., Miezin, F. M., Raichle, M. E., et al. (1997). Common blood flow changes across visual tasks: II. Decreases in cerebral cortex. *J. Cogn. Neurosci.* 9, 648–663. doi: 10.1162/jocn.1997.9.5.648

Song, P., Li, S., Wang, S., Wei, H., Lin, H., and Wang, Y. (2020). Repetitive transcranial magnetic stimulation of the cerebellum improves ataxia and cerebello-fronto plasticity in multiple system atrophy: a randomized, double-blind, sham-controlled and TMS-EEG study. *Aging* 12, 20611–20622. doi: 10.18632/aging.103946

Spampinato, D. A., Celnik, P. A., and Rothwell, J. C. (2020). Cerebellar-motor cortex connectivity: one or two different networks? *J. Neurosci.* 40, 4230–4239. doi: 10.1523/JNEUROSCI.2397-19.2020

Stankovic, I., Krismer, F., Jesic, A., Antonini, A., Benke, T., Brown, R. G., et al. (2014). Cognitive impairment in multiple system atrophy: a position statement by the Neuropsychology Task Force of the MDS Multiple System Atrophy (MODIMSA) study group. *Mov. Disord.* 29, 857–867. doi: 10.1002/mds.25880

Suppa, A., Marsili, L., Di Stasio, F., Latorre, A., Parvez, A. K., Colosimo, C., et al. (2014). Primary motor cortex long-term plasticity in multiple system atrophy. *Mov. Disord.* 29, 97–104. doi: 10.1002/mds.25668

Thickbroom, G. W. (2007). Transcranial magnetic stimulation and synaptic plasticity: experimental framework and human models. *Exp. Brain Res.* 180, 583–593. doi: 10.1007/s00221-007-0991-3

Tschöpe, C., Sherif, M., Anker, M. S., Geisel, D., Kuehne, T., and Kelle, S. (2021). COVID-19-convalescence phase unmasks a silent myocardial infarction due to coronary plaque rupture. *ESC Heart Fail.* 8, 971–973. doi: 10.1002/ehf2.13186

Ueyama, E., Ukai, S., Ogawa, A., Yamamoto, M., Kawaguchi, S., Ishii, R., et al. (2011). Chronic repetitive transcranial magnetic stimulation increases hippocampal neurogenesis in rats. *Psychiatry Clin. Neurosci.* 65, 77–81. doi: 10.1111/j.1440-1819.2010.02170.x

Ugawa, Y., Uesaka, Y., Terao, Y., Hanajima, R., and Kanazawa, I. (1995). Magnetic stimulation over the cerebellum in humans. *Ann. Neurol.* 37, 703–713. doi: 10.1002/ana.410370603

Valero-Cabré, A., Amengual, J. L., Stengel, C., Pascual-Leone, A., and Coubard, O. A. (2017). Transcranial magnetic stimulation in basic and clinical neuroscience: a comprehensive review of fundamental principles and novel insights. *Neurosci. Biobehav. Rev.* 83, 381–404. doi: 10.1016/j.neubiorev.2017.10.006

Wang, H., Li, L., Wu, T., Hou, B., Wu, S., Qiu, Y., et al. (2016). Increased cerebellar activation after repetitive transcranial magnetic stimulation over the primary motor cortex in patients with multiple system atrophy. *Ann. Transl. Med.* 4:103. doi: 10.21037/atm.2016.03.24

Wang, H., Zhao, Y. P., Wu, S., Feng, F., and Yinga, C. L. (2017). Long term repetitive transcranial magnetic stimulation improve task performance in a patient with multiple system atrophy. *Int. J. Phys. Med. Rehabil.* 5:e1000425. doi: 10.4172/2329-9096.1000425

Yang, H., Wang, N., Luo, X., Lv, H., Liu, H., and Fan, G. (2019a). Altered functional connectivity of dentate nucleus in parkinsonian and cerebellar variants of multiple system atrophy. *Brain Imaging Behav.* 13, 1733–1745. doi: 10.1007/s11682-019-00097-5

Yang, H., Wang, N., Luo, X., Lv, H., Liu, H., Li, Y., et al. (2019b). Cerebellar atrophy and its contribution to motor and cognitive performance in multiple system atrophy. *Neuroimage Clin.* 23:101891. doi: 10.1016/j.nicl.2019.101891

Yildiz, F. G., Saka, E., Elibol, B., and Temucin, C. M. (2018). Modulation of cerebellar-cortical connections in multiple system atrophy type C by cerebellar repetitive transcranial magnetic stimulation. *Neuromodulation* 21, 402–408. doi: 10.1111/ner.12589

Zhang, L., Zhang, L., Xue, F., Yue, K., Peng, H., Wu, Y., et al. (2018). Brain morphological alteration and cognitive dysfunction in multiple system atrophy. *Quant. Imaging Med. Surg.* 8, 1030–1038. doi: 10.21037/qims.2018.11.02

Conflict of Interest: The authors declare that the research was conducted in the absence of any commercial or financial relationships that could be construed as a potential conflict of interest.

frontiers in Neuroscience

CLINICAL TRIAL
published: 15 December 2021
doi: 10.3389/fnins.2021.771064

Evaluating the Effects of 5-Hz Repetitive Transcranial Magnetic Stimulation With and Without Wrist-Ankle Acupuncture on Improving Spasticity and Motor Function in Children With Cerebral Palsy: A Randomized Controlled Trial

Jiamin Li[1,2,3†], Cen Chen[1†], Shenyu Zhu[4†], Xiulian Niu[1], Xidan Yu[1], Jie Ren[2] and Min Shen[1,2]*

[1] Shanghai YangZhi Rehabilitation Hospital (Shanghai Sunshine Rehabilitation Center), School of Medicine, Tongji University, Shanghai, China, [2] School of Rehabilitation Science, Shanghai University of Traditional Chinese Medicine, Shanghai, China, [3] Shanghai Taiping Rehabilitation Hospital, Shanghai, China, [4] Nuffield Department of Women's & Reproductive Health, University of Oxford, Oxford, United Kingdom

OPEN ACCESS

Edited by:
Jinhua Zhang,
Xi'an Jiaotong University, China

Reviewed by:
Jorge Hugo Villafañe,
Fondazione Don Carlo Gnocchi Onlus, Scientific Institute for Research, Hospitalization and Healthcare (IRCCS), Italy
Marcello Romano,
Azienda Ospedaliera Ospedali Riuniti Villa Sofia Cervello, Italy

***Correspondence:**
Min Shen
minshen223@tongji.edu.cn

† These authors have contributed equally to this work

Specialty section:
This article was submitted to Neuroprosthetics, a section of the journal Frontiers in Neuroscience

Received: *05 September 2021*
Accepted: *03 November 2021*
Published: *15 December 2021*

Citation:
Li J, Chen C, Zhu S, Niu X, Yu X, Ren J and Shen M (2021) Evaluating the Effects of 5-Hz Repetitive Transcranial Magnetic Stimulation With and Without Wrist-Ankle Acupuncture on Improving Spasticity and Motor Function in Children With Cerebral Palsy: A Randomized Controlled Trial. Front. Neurosci. 15:771064. doi: 10.3389/fnins.2021.771064

Objective: The goal of this study is to explore the effect of wrist-ankle acupuncture combined with 5-Hz repetitive transcranial magnetic stimulation (rTMS) on improving spastic state and motor function of children with spastic cerebral palsy by measuring electrophysiological parameters and behaviors.

Methods: Twenty-five children with spastic cerebral palsy were enrolled in a single-blind and randomized controlled trial. The control group received 20 sessions of 5-Hz rTMS over the affected hemisphere with 1,000 pulses. The experimental group was given wrist-ankle acupuncture on the basis of the control group. Gross motor function measure (GMFM-66), muscle tension, and electrophysiological parameters of the two groups were assessed at baseline and after intervention.

Results: After treatment, the GMFM-66 scores in the same groups were significantly improved ($p < 0.001$). Besides, the *R*-value of soleus, gastrocnemius, and hamstring muscle decreased ($p < 0.05$), and the results showed a trend of shortening MEP latency, increasing amplitude and duration ($p < 0.05$). Compared to the controlled group, the experimental group displayed more excellent changes in the GMFM-66 scores and motor evoked potential (MEP) latency. The statistical results showed that the increase of GMFM-66 score and the shortening of MEP latency in the experimental group were greater than that in the control group ($p < 0.05$). However, no significant differences were found in the assessment of muscle tension, amplitude, and duration of MEPs between two groups ($p > 0.05$).

Conclusion: Wrist-ankle acupuncture combined with 5-Hz rTMS is optimal to improve gross motor function and enhance the conductivity of corticospinal tract in children with cerebral palsy but cannot highlight its clinical superiority in improving spasticity.

Clinical Trial Registration: [http://www.chictr.org.cn/index.aspx], identifier [chictr2000039495].

Keywords: repetative transcranial magnetic stimulation, wrist-ankle acupuncture, corticospinal tract (CST), motor evoked potential (MEP), spasm

INTRODUCTION

Cerebral palsy (CP) is considered to be a group of persistent central and postural developmental disorders and activity limitation syndrome caused by non-progressive brain injury in fetus or infants, occurring in 1–3 per 1,000 live births (Sellier et al., 2016). Children with spastic CP mainly have motor dysfunction due to different degrees of increased muscle tension and persistent primitive reflex. It is generally believed that the higher central nervous system is damaged, which leads to the obstacle of the central nervous system in the regulation of spinal cord stretch reflex, making the stretch reflex stronger (Kesar et al., 2012). Traditional Chinese medicine believes that the etiology of infantile CP is mostly Yin deficiency, less fluid, and loss of nourishment of muscles, bones, muscles, and joints (Wang Xuefeng, 2005).

Wrist-ankle acupuncture refers to the method of selecting specific needle entry points at the wrist and ankle and using filiform needles to treat diseases by subcutaneous shallow needling along the longitudinal axis of the limb (Zhao et al., 2011). Compared with other acupuncture therapies, it has the characteristics of relative safety, convenient operation, and rapid pain relief and has the function of promoting Qi and blood circulation and mobilizing Wei Qi to regulate the metabolism of human body fluid. The study suggests (Qinghui, 2017) that one of the mechanisms of wrist-ankle acupuncture may be due to the existence of nerve conduction function activities. When the nerve endings are stimulated, it will trigger a series of nerve conduction activities of connecting nerves in the reflex arc and play a complex adjustment role.

Transcranial magnetic stimulation (TMS) is a non-invasive form of brain stimulation that assesses cortical excitability and corticospinal tract conduction through depolarization of corticospinal neurons (Rossini et al., 2015). In many psychiatric and neurological cases, such as depression, the use of 10-Hz frequency, 120% motor threshold, and 3,000 pulses can achieve therapeutic goals (Guse et al., 2010). Besides, it is a valuable supplementary treatment for motor dysfunction, by effectively activating cortical neurons, directly regulating the neurophysiological functions of cortical spinal cord and motor cortex, thus promoting the improvement of motor function (Kamble et al., 2014). According to different parameters, stimulation with frequency $\leq$ 1 Hz is called low-frequency TMS, whereas stimulation with frequency $>$ 1 Hz is called high-frequency TMS (Kamble et al., 2014). Various studies have shown that high-frequency stimulation increases cortical excitability, whereas low-frequency stimulation suppresses cortical excitability (Marzbani et al., 2018). Children with spastic diplegia and quadriplegia often show bilateral and diffuse brain damage. According to the model of interhemispheric competition inhibition, high-frequency repetitive TMS (rTMS) is often used to increase cortical excitability at the M1 site of the ipsilateral cerebral hemisphere (Valle et al., 2007).

Besides, the security of TMS has been paid more attention (Valle et al., 2007). Krishnan et al. (2015) reviewed the literature on the use of TMS in people under 18 years of age to understand the safety and tolerance ability of non-invasive brain stimulation in children and adolescents, and data from 48 studies in 513 children and adolescents (2.5–17.8 years old) showed that the side effects of non-invasive brain stimulation were generally mild and transient. The side effects after TMS were headache (11.5%) and scalp discomfort (2.5%), convulsions (1.2%), mood changes (1.2%), fatigue (0.9%), tinnitus (0.6%), etc. There are few serious side effects (Krishnan et al., 2015).

In recent years, several studies (Ji et al., 2019) have confirmed that traditional acupuncture combined with rTMS can improve motor function, relieve spasticity and neurotransmitter indexes in children with CP, and promote the improvement of hemodynamics. It can be seen that acupuncture combined with rTMS can further enhance the clinical efficacy compared with a single treatment. Wrist-ankle acupuncture, as one of the means of acupuncture, is a more simplified version compared with traditional acupuncture therapy, and it has the merit of high tolerance for children. This study attempts to use peripheral-central integration model, to further strengthen the clinical effect of children with CP to provide a new way of treatment.

MATERIALS AND METHODS

Participants

Twenty-eight children with spastic CP who received treatment at Shanghai Yangzhi Rehabilitation Hospital between June 2020 and January 2021 were recruited into this trial by an attending physician. However, during the course of treatment and follow-up, there were three cases of rejection and abscission due to personal factors. Finally, 25 cases completed the clinical trial and included the results. The inclusion criteria are as follows: (1) Confirmed diagnosis of spastic CP; (2) aged 3–7 years old; (3) Gross Motor Function Classification System (GMFCS) of CP grading from I to III; and (4) sufficient understanding and cooperation to complete this trial. The exclusion criteria are as follows: (1) The absence of either hemisphere motor evoked potential (MEP); (2) children with organ dysfunction, history of severe epilepsy, cognitive impairment, and other serious diseases; (3) children with CP accompanied by involuntary

TABLE 1 | Descriptive characteristics of participants.

	Experimental Group	Control Group	*p*-value	t/Z/x^2
	N **= 14**	***N*** **= 14**		
Gender				
Male, N(%)	9(64.3)	10(71.4)	0.686	0.164
Female, N(%)	5(35.7)	4(28.6)		
Age (m)	64.42 ± 21.10	69.28 ± 18.15	0.198	0.653
Height (cm)	116.42 ± 14.37	119.28 ± 12.82	0.638	0.555
Weight (kg)	21.14 ± 6.16	21.92 ± 6.53	0.747	0.323
Classification of cerebral palsy				
Hemiplegia, N(%)	5(35.7)	6(42.9)	0.699	0.150
Diplegia, N(%)	9(64.3)	8(57.1)		
Gross motor function classification system				
Level I, N(%)	8(57.1)	5(35.7)	0.429	1.692
Level II, N(%)	3(21.4)	6(42.9)		
Level III, N(%)	3(21.4)	3(21.4)		

Continuous variables were presented as mean ±SD.

movements, ataxia, or mixed type; (4) children with artificial pacemaker, cochlear implant, and metal implants; and (5) taken or injected with anti-spasmodic drugs in the past 6 months. The clinical characteristics of participants are shown in **Table 1**.

Study Design

This was a randomized, controlled, single-blind, and parallel-designed prospective clinical trial that was implemented comparing 5-Hz rTMS with and without wrist-ankle acupuncture on motor function and spastic state in children with CP. Ethical approval was obtained by the Medical Ethics Committee of Shanghai Yangzhi Rehabilitation Hospital (YZ2020-066). In addition, the project was registered in Chinese Clinical Trial Registry (no. ChiCTR20000039495). All parents or caregivers have signed informed consent and children verbally agreed to participate in the trial. Participants who met the criteria were randomly assigned (1:1) to two groups (Group A and Group B). The experimental group (Group A) received 20 daily sessions of 5-Hz rTMS over the affected hemisphere with 1,000 pulses. The control group (Group B) was given wrist-ankle acupuncture on the basis of the control group. Assessments were performed at T0 (baseline, 1 week before the intervention onset) and T1 (within 5 days after the intervention). A detailed description of the experimental design is shown in **Figure 1**.

Randomization

Randomization was performed by an independent researcher who is not involved in the recruitment procedure, intervention, or evaluation. Participants were randomly assigned into two groups using a random number table in accordance with the 1:1 ratio.

Sample Size

According to previous study report (Yan-fen, 2015), we selected the scores of GMFM-88 after intervention as a similar reference index. On the basis of the GMFM-88 scores, a margin of 0, an alpha-level of 0.025, a statistical power of 0.90, and a drop rate of 10%, 14 children per group were calculated as the minimum sample size by the formula (Wu et al., 2013; Zhang et al., 2016).

Blinding

Evaluators and statisticians were all blinded.

Intervention

The control and experimental groups were conducted in the process of routine rehabilitation, including routine stretch training and strength training. The control used the method of 5-Hz rTMS and the experimental group incorporated wrist-ankle acupuncture treatment in addition to the control. To reduce random error and contingency of the clinical result, wrist-ankle acupuncture was performed first followed by rTMS in the experimental group.

Repetitive Transcranial Magnetic Stimulation

We utilized TMS devices (made in Denmark with MCF-125 8-shaped coil, model: MagPro × 100) to perform rehabilitation therapy and utilized a neurological diagnosis system (made in Denmark, model: KEYPOINT) to monitor the MEP.

(1) Resting motor threshold (RMT) measurement: RMT refers to the minimum stimulation that induces target muscle, typically abductor pollicis brevis (APB) muscle to generate MEP over 50 μV in at least five of the 10 single-pulse stimulation (Groppa et al., 2012a; Rossini et al., 2015). Because of individual differences, RMT varies among populations. To monitor the real-time MEP of APB, the patient was placed recumbent or semi-recumbent position and was told to relax. The ground electrode was placed 2-cm proximal to the wrist crease of the forearm. The detection electrode and reference electrode were placed at the muscle belly and the tendon (base of the proximal side of the first phalanx) of APB, respectively. The coil was placed tangent to the surface of the skull and rotated 45° along the sagittal plane. Single-pulse TMS was used to stimulate the corresponding sites of M1 of the head. The output power was first set at 50–60%. If the MEP is not detected after three to five attempts at each site, then the output is increased by 5%. If it reaches 90% of maximum output power and no MEP is induced, then the coil is relocated 0.5 cm front, back, left, and right to the original position, and the same procedure is repeated. Thus, the best site to induce MEP is recorded, and the corresponding RMT is measured and recorded.

(2) Treatment parameters: Subjects were stimulated for 15 min at a frequency of 5-Hz, for a total of 20 sessions (5 days a week, for 4 weeks). The stimulation intensity was set at 90% relative to the observed RMT of the patient, with a stimulus train duration of 5 s and an inter-train interval of 5 s. A total of 40 successive stimulation and 1,000 pulses were performed every time. As the RMT maybe changeable

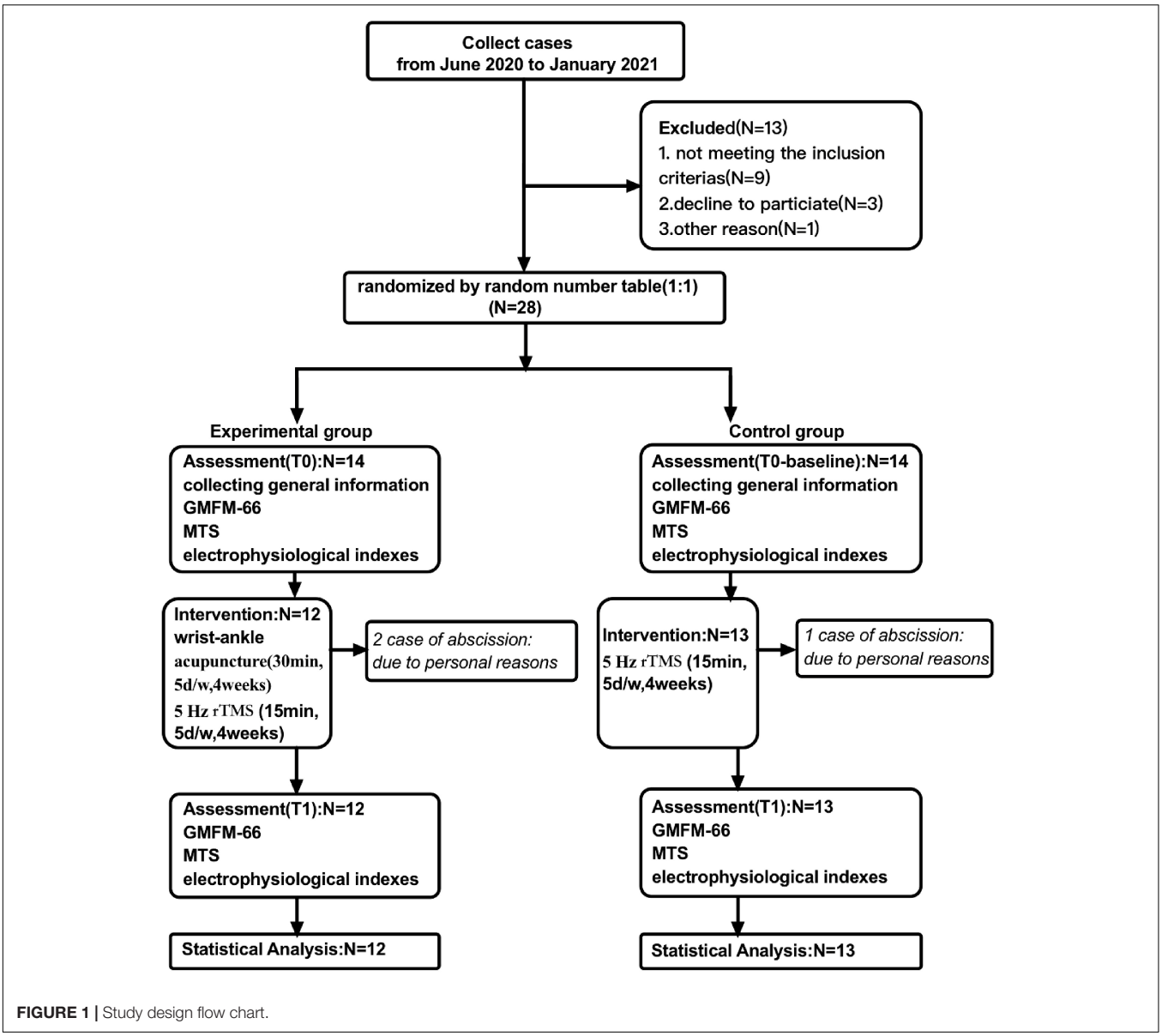

FIGURE 1 | Study design flow chart.

during the whole trial, we would remeasure RMT before daily treatment.

(3) Stimulation site: According to the inter-hemispheric competition inhibition model, a high-frequency stimulation of 5 Hz was performed on the M1 site of the affected hemisphere. If there was no detection of MEP from the ipsilateral M1, the optimal stimulus site is the symmetrical location of the contralateral M1.

(4) Location of M1 (the primary motor cortex): C3 and C4 were located in line with the international 10–20 electroencephalogram (EEG) system on the corresponding sites of the primary motor cortices (Silva et al., 2020). First, the length from nasion to inion was measure and set as 100%. Then, the length between preauricular points was measured and set as 100%. The intersection of the two lines was the point Cz. Four points on the connecting line between the two preauricular points were labeled T3, T4, C3, and C4. T3 and T4 were 10% of the total length between the preauricular points, and the remaining points (including Cz) were all separated by 20% of the total length (**Figure 2**). Because of anatomical differences, the actual effective stimulation site may differ from the C3 and C4 points. Thus, the exact location of M1 can be determined by moving the coil slightly around the two electrode points to see if there are MEPs.

Wrist-Ankle Acupuncture Treatment

(1) Acupuncture sites: As stated by Prof. Xinshu Zhang and his summary of acupuncture sites and treatment, the needle insertion

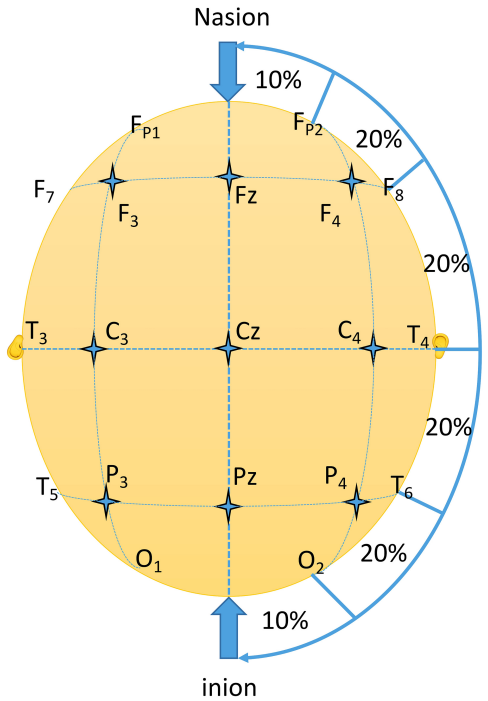

FIGURE 2 | International 10-20 EEG electrode location map.

points were determined at sections of upper 4, upper 5, lower 1, and lower 4 on the lesion side of the body (Yang et al., 2019).

(2) Method and parameters: Filiform acupuncture needles (Brand: HUATUO, 0.30 × 40 mm) were used. After routine skin disinfection, the site was selected by the criteria. Acupuncture was performed with subcutaneous superficial puncture to avoid feelings of swelling and pain. The insertion was 30° of angle and was performed with single-handed fast insertion and no needle twisting. Then, the needle tail was fixed with medical tape on the skin surface. The patient was told to stay at rest and reduce wrist and ankle movement. The needle insertion lasted for 30 min, once every day, for a total of 20 sessions (5 days a week, for 4 weeks).

Assessment

Gross Motor Function Measure-66

The GMFM-66 consists of 66 items; each item is scored 0–3 points. The final score value is converted by software. On the basis of the original GMFM-88, the GMFM-66 scale was modified and optimized to measure the gross motor function of children with CP in different postures and reflect their motor development level. Compared with GMFM-88, GMFM-66 showed good reliability, validity, and reactivity (Avery et al., 2013).

Modified Tardieu Scale—*R*-value

The scale has good reliability and validity in evaluating the degree of spasticity of upper and lower limbs in children with CP. First, move the joint slowly to the "point of sticking" and record the joint angle at this time as R2. Then, move the joint quickly to the "point of sticking" and record the joint angle at this time as R1. Calculate the difference between the two and mark it as R(R = R2-R1). The improvement of muscle spasm was evaluated by the change of R-value before and after treatment (Numanoğlu and Günel, 2012).

Latency of Motor Evoked Potentials (MEP LAT)

When the muscle is stimulated, an action potential will be generated, resulting in a negative wave (upward wave). The latency refers to the period from the beginning of the stimulation artifact to the departure of the negative wave from the baseline. It is usually expressed in milliseconds, which represents the excitability of motor cortex and the integrity of corticospinal tract pathway (Kowalski et al., 2019). We recorded the latency five times per subject and calculated the mean of the latency as the measurement of cortical excitability.

Amplitude of Motor Evoked Potentials (MEP AMP)

The amplitude refers to the distance between the negative wave peaks and the baseline. It is usually expressed in millivolts. The amplitude of MEP reflects the structural and functional integrity of the corticospinal tract and the excitability of the motor cortex (Van Den Bos et al., 2017).

Duration of Motor Evoked Potentials (MEP DUR)

Duration refers to the period from the beginning of the negative wave of action potential deviated from the baseline to returning to the baseline again. Usually, it is expressed in milliseconds. These data can indicate the level of discharge of a single muscle fiber at the same time.

Data and Statistical Analysis

Statistical analysis was performed using SPSS version 25.0 (Property of IBM Corp, New York, America) and completed by an independent researcher who is not involved in the recruitment procedure, intervention, or evaluation. If measurement data conforms to normal distribution, the Independent Sample T-test and Paired Samples T-test are used. If it does not conform to normal distribution, then non-parametric test is used. Pearson chi square test was used for counting data. Wilcoxon rank sum test was used for grading data. Continuous variables were presented as mean ± standard deviation, and $p < 0.05$ was considered statistically significant.

RESULTS

The subjects of this study were children with spastic CP who received rehabilitation treatment in the outpatient Department of Shanghai Sunshine Rehabilitation Center from June 2020 to January 2021. A total of 28 subjects were included and signed informed consent voluntarily after screening according to diagnosis and to inclusion and exclusion criteria. During the study, two cases were removed from the experimental group, and one case was removed from the control group. They are unable to continue to receive treatment in accordance with the regulations due to personal reasons, such as heavy homework and transfer to other hospitals. Therefore, a total of 25 patients completed the study and were included in the outcome index for

TABLE 2 | Outcome scores at baseline (mean ± SD).

	Experimental Group	Control Group	*p*-value
	n = 12	*n* = 13	
GMFM-66 MTS (*R*-value)	79.34 ± 11.37	72.46 ± 9.44	0.428
Hamstring	16.17 ± 8.87	14.08 ± 4.91	0.956
Gastrocnemius	13.33 ± 4.92	10.46 ± 4.62	0.561
Soleus	12.50 ± 5.84	12.62 ± 5.49	0.905
MEP LAT	32.49 ± 10.36	29.64 ± 9.48	0.414
MEP AMP	0.07 ± 0.02	0.08 ± 0.02	0.536
MEP DUR	6.03 ± 1.34	6.56 ± 1.32	0.606

TABLE 3 | Changes of outcome scores (mean ± SD).

	Experimental Group	Control Group	*p*-value
	n = 12	*n* = 13	
GMFM-66 MTS (*R*-value)	5.75 ± 2.66	2.81 ± 1.65	0.026
Hamstring	8.25 ± 7.98	5.53 ± 4.96	0.435
Gastrocnemius	3.41 ± 4.79	1.61 ± 2.25	0.434
Soleus	3.66 ± 4.71	3.07 ± 3.81	0.648
MEP LAT	8.65 ± 8.41	2.31 ± 1.67	0.026
MEP AMP	0.07 ± 0.06	0.03 ± 0.04	0.051
MEP DUR	1.23 ± 1.06	1.07 ± 0.76	0.462

statistical analysis, including 12 in the experimental group and 13 in the control group. The clinical characteristics of participants are shown in **Table 1**.

As can be seen from **Table 1**, before treatment, there was no statistical significance in gender, age, height, weight, CP classification, GMFCS, and other general data between the two groups ($p > 0.05$), and the data between the two groups were comparable.

As can be seen from **Table 2**, before treatment, GMFM-66 scores between the two groups were in line with normal distribution, and there was no statistically difference between two groups by independent-samples *t*-test ($p>0.05$), indicating that the data were comparable. At the same time, there was no significant difference in the *R*-values of hamstring muscle, gastrocnemius muscle, and soleus muscle tension between the two groups before treatment ($p > 0.05$). MEP LAT, MEP AMP, and MEP DUR were also compared between the experimental group and the control group before treatment, and there was no significant difference between the two groups ($p > 0.05$). Overall, the data of the two groups were comparable.

As can be seen from **Table 3**, after treatment, there was significant difference in GMFM-66 scores between the two groups ($p = 0.026$), the increase of score in the experimental group was greater than that in the control group, however there was no significant difference in the *R*-values of hamstring muscle, gastrocnemius muscle, and soleus muscle tension between the two groups ($p>0.05$). Besides, there was significant difference in MEP LAT between experimental group and control group ($p = 0.026$), whereas there was no significance in MEP AMP and MEP DUR ($p>0.05$).

As can be seen from **Figures 3–9**, we can see a change trend of the value. After two courses of treatment, the GMFM-66 scores in the same group were significantly higher than that before, and the difference was statistically significant ($p_A<0.001$, $p_B<0.001$). The *R*-values of hamstring muscle, gastrocnemius muscle, and soleus muscle tension in the same group were lower than that before treatment, indicating significant difference (hamstring: $p_A = 0.005$, $p_B = 0.002$; gastrocnemius: $p_A = 0.027$, $p_B = 0.039$; soleus: $p_A = 0.011$, $p_B = 0.027$). The latency of MEP in the same group was significantly shorter than that before treatment ($p_A = 0.002$, $p_B = 0.002$). The amplitude of MEP in the same group was significantly higher than that before treatment ($p_A = 0.003$, $p_B = 0.016$). The duration of MEP in the same group was significantly increased compared with that before treatment ($p_A = 0.002$, $p_B<0.001$).

DISCUSSION

This study explored the superiority of wrist-ankle acupuncture combined with 5-Hz rTMS in improving motor function and spasticity in children with CP. From the statistical results, it was found that through the mode of peripheral-central combination, the scores of GMFM-66 and the conductivity of corticospinal tract could be improved. However, it cannot be proved that it has a significant effect on improving spasticity in children with CP in this study. Next, we further discuss the effect and mechanism of wrist-ankle acupuncture combined with 5-Hz rTMS according to previous research reports.

Effect on Corticospinal Conduction Tract

This study compared the changes of corticospinal tract conductivity between two groups before and after treatment by detecting the electrophysiological indexes such as MEP LAT, MEP AMP, and MEP DUR. The results showed that, after two courses of treatment, both experimental group and control group showed the trend of shortening MEP LAT, expanding MEP AMP and increasing MEP DUR. The difference was statistically significant ($p < 0.05$). At the same time, the decrease of latency in experimental group after treatment was significantly greater than that in control group ($p < 0.05$), but there was no significant statistical difference between two groups on MEP AMP and MEP DUR ($p > 0.05$). The results showed that the conductivity of corticospinal tract was improved in both groups after treatment, but the clinical effect of combined wrist-ankle acupuncture group was better than that of single 5-Hz rTMS group. It can be seen that wrist-ankle acupuncture, as a derivative of traditional acupuncture, plays a certain role and significance in improving neurophysiological function.

The corticospinal tract is the descending nerve conduction tract that controls the voluntary movement of skeletal muscles. The development of pyramidal tracts in bilateral cerebral hemispheres of children with CP is slower than that of normal children; it reflects the disruption of the myelination and axonal integrity of the pyramidal tract during perinatal period, which leads to the dysfunction of motor function (Papadelis et al., 2019). Through single-pulse TMS evaluation, corresponding

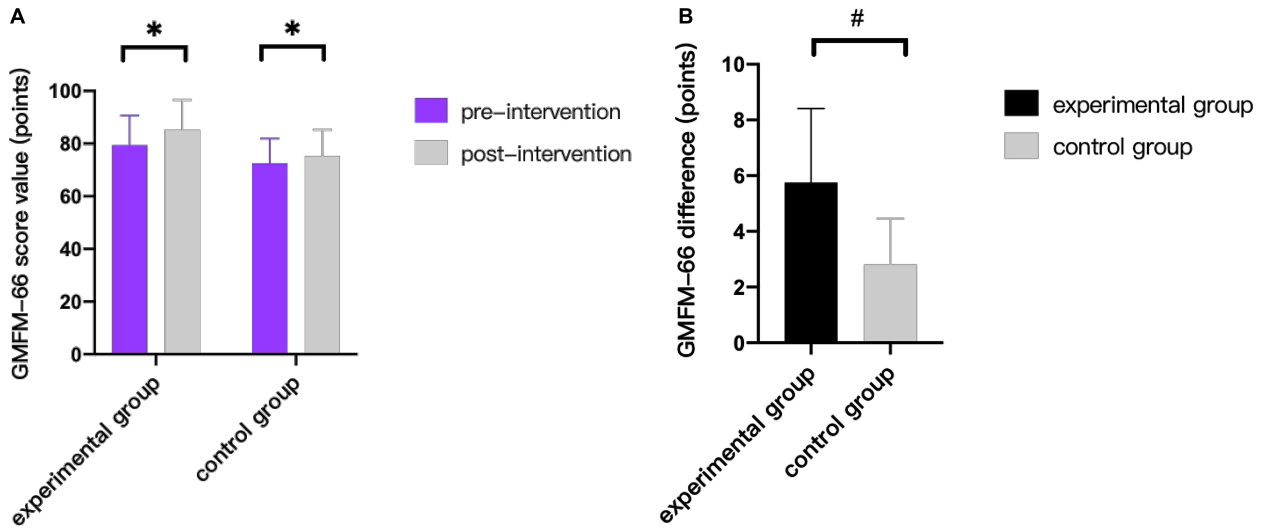

FIGURE 3 | Comparison of GMFM-66 scores. **(A)** Comparison of score value in the same group before and after treatment. **(B)** Comparison of differences between the two groups before and after treatment. * indicates intra-group $p < 0.05$, and # indicates inter-group $p < 0.05$.

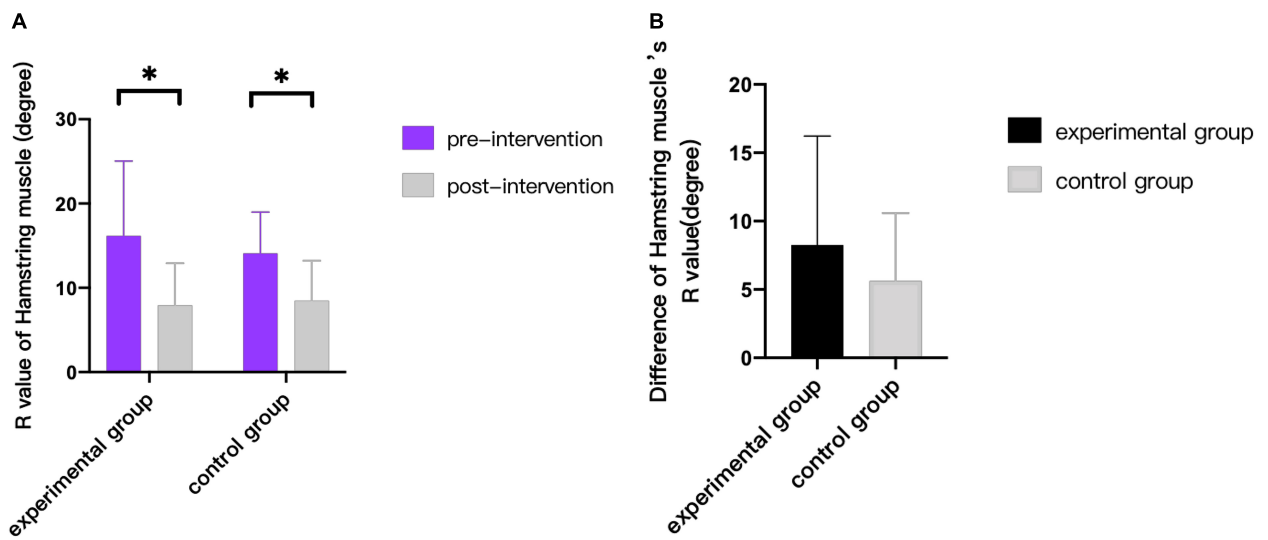

FIGURE 4 | Comparison of R value of hamstring Muscle. * indicates intra-group $p < 0.05$.

neurophysiological indexes can be obtained, which can be used as functional biomarkers of brain neuroplasticity and potential therapeutic targets, and further reflect the changes of brain function after non-traumatic brain stimulation intervention (Kirton, 2017). The MEP detected by TMS can be used as a neurobiological marker for the early development of pyramidal tracts in perinatal stroke patients (Kowalski et al., 2019). There is a mechanism that suggests that the shortening of MEP LAT and the widening of amplitude are due to the excitability of α motor neurons and corticospinal tracts (Van Den Bos et al., 2017). The action mechanism of the increase of MEP DUR is explained through research (Brum et al., 2016). It is considered that, during the descending conduction of corticospinal tract, the I α inhibitory interneurons were activated, which further activated the excitatory activity of α motor neurons, and then, MEP DUR increased.

Although the action mechanism of wrist-ankle acupuncture combined with 5-Hz rTMS has not been further studied in this trial, literature studies have found that acupuncture is a bottom-up mode of regulation, specific activation of different brain regions, and there are potential neurochemical mechanisms. By using functional magnetic resonance imaging techniques, researcher found that acupuncture at "Taichong" can trigger increased or decreased signal intensity in several areas of the brain in children with CP (Wu et al., 2008). By exploring the effect of acupuncture on rats with hypoxic-ischemic brain

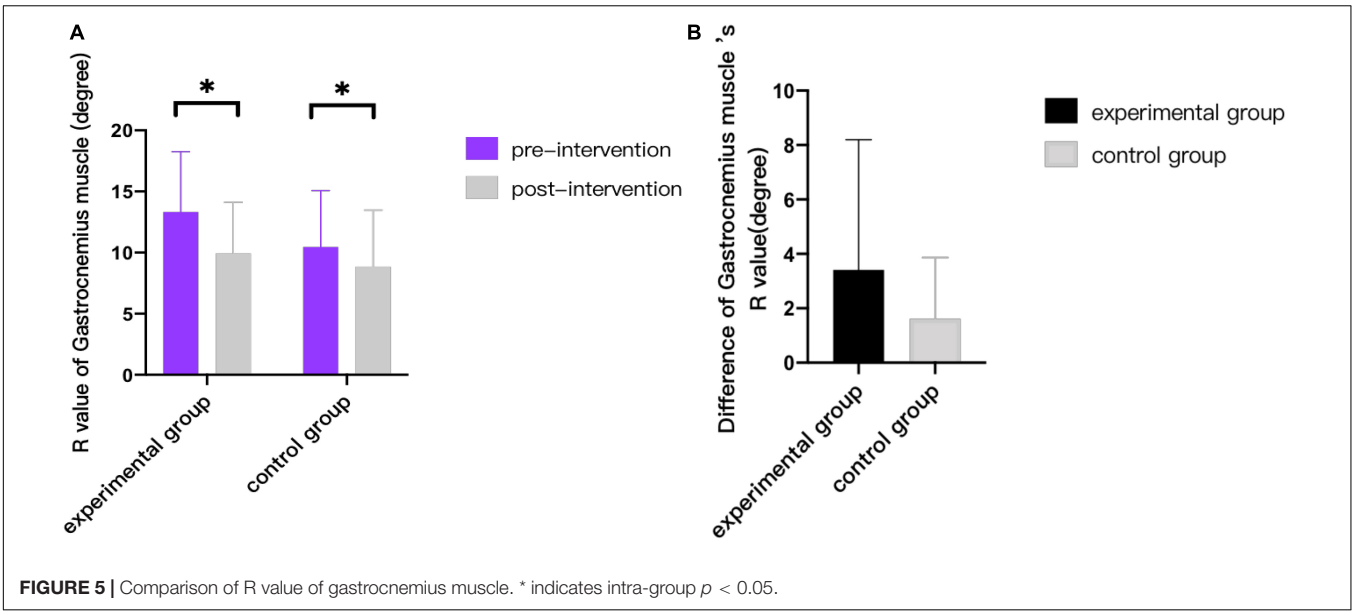

FIGURE 5 | Comparison of R value of gastrocnemius muscle. * indicates intra-group $p < 0.05$.

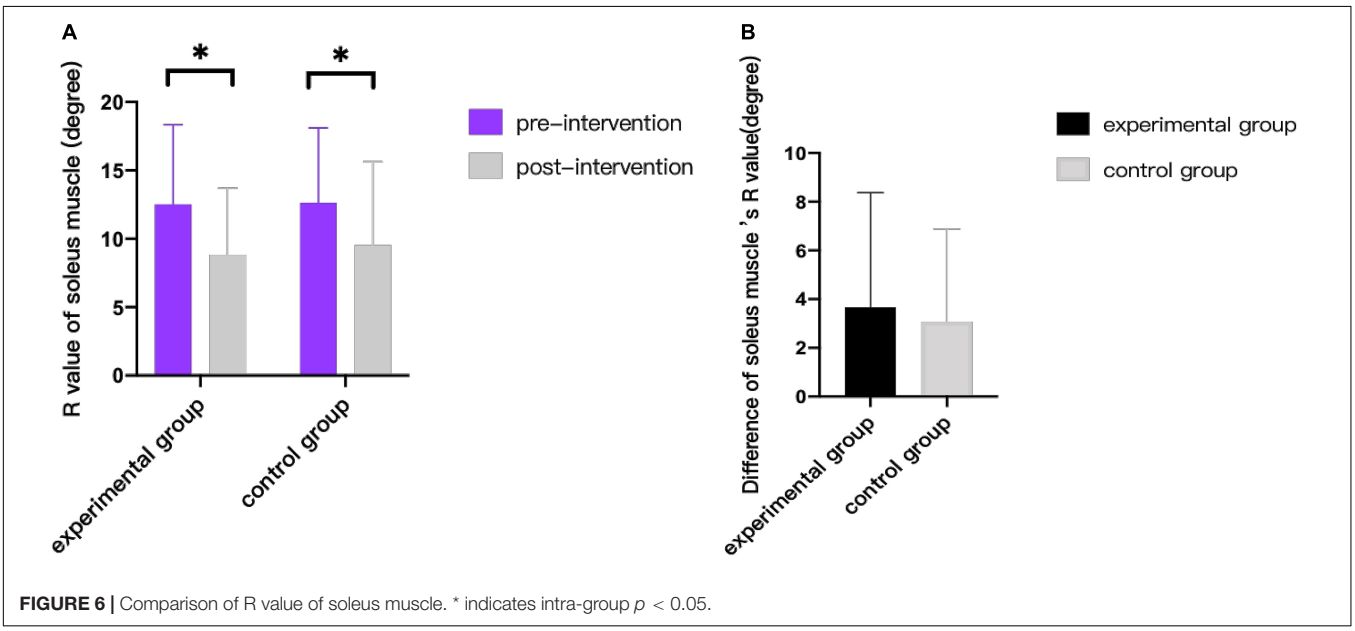

FIGURE 6 | Comparison of R value of soleus muscle. * indicates intra-group $p < 0.05$.

injury, it is found that acupuncture may reduce the degree of neuronal injury after ischemia by inhibiting apoptosis and increasing the expression of glial cell derived neurotrophie factor (GDNF) and brain-derived neurotrophic factor (BDNF), further promote the growth and development, and improve the function of ethology (Zhang et al., 2015). When TMS is applied to the head, it induces action potentials in the cortical axons and spreads across synapses to other neurons, resulting in neuronal activation and spreading of excitation to the adjacent cortical and subcortical regions (Groppa et al., 2012b). At present, there is no specific literature report on the joint action mechanism of wrist-ankle acupuncture combined with 5-Hz rTMS at home and abroad, which can be used as an exploration direction in the future of this study to explore the superiority of the central peripheral closed-loop stimulation mode formed by the combination of the two treatment methods for improving neural electrophysiological function.

Effect on Spasticity

Through this trial, it is found, that after two courses of intervention, the *R*-value tends to decrease, and muscle tension of the subjects in both groups have been improved to a certain extent ($p<0.05$). It can be concluded that the treatment methods of the two groups have a positive effect on reducing the degree of spasm.

Animal studies have found that (Qi et al., 2014) acupuncture can inhibit the release of inflammatory cells after brain injury, reduce immune response, significantly reduce the muscle tension of spastic CP rats, and increase the activity of spastic limbs. At

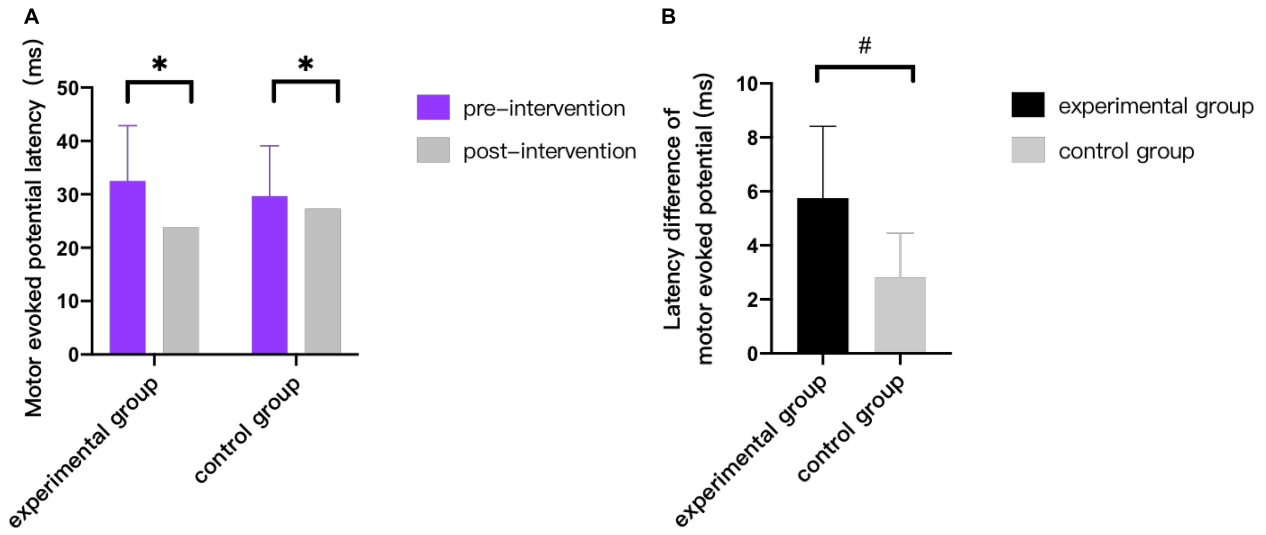

FIGURE 7 | Comparison of latency of motor evoked potentials. * indicates intra-group $p < 0.05$, and # indicates inter-group $p < 0.05$.

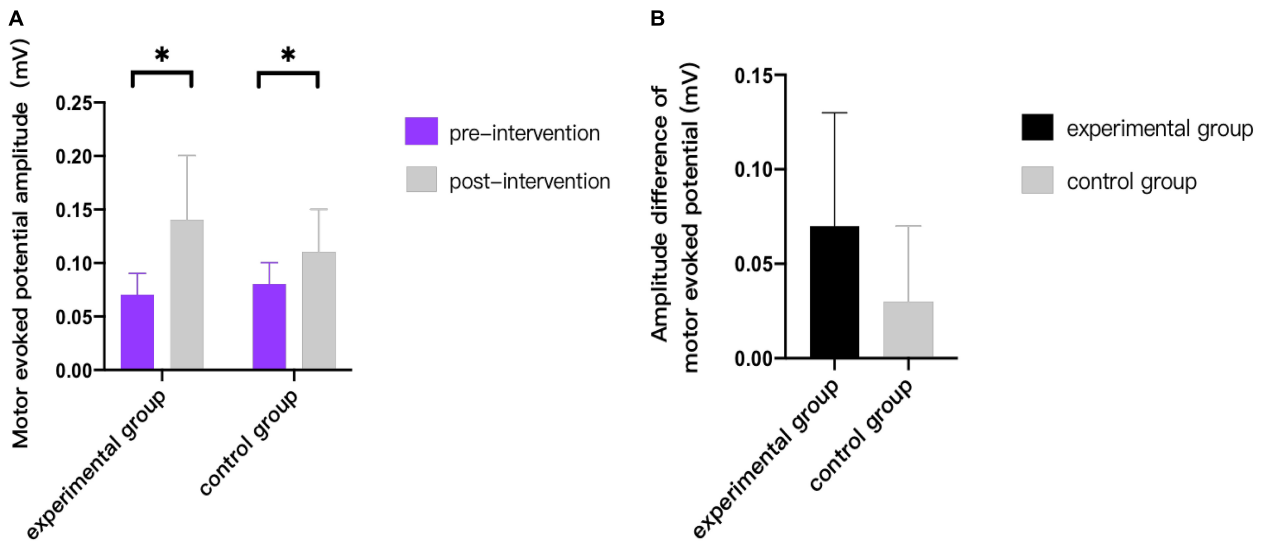

FIGURE 8 | Comparison of amplitude of motor evoked potentials. * indicates intra-group $p < 0.05$.

the same time, the clinical study also found that (Qianfang, 2018) the use of wrist-ankle acupuncture technology in the treatment of children with spastic CP can significantly reduce the muscle tension of the affected side of the upper limb and improve its grasping and visual motor integration ability, and the effect is better than that of traditional acupuncture. It is speculated that the good antispasmodic effect of wrist-ankle acupuncture may be closely related to its analgesic ability.

Pain is common in children with CP (Poirot et al., 2017). Long-term muscle spasticity and skeletal deformity caused by spasm often cause pain (Smith and Field, 2020). The analgesic effect of wrist-ankle acupuncture has been confirmed by many studies. Animal trials have shown that (Liu et al., 2015) wrist-ankle acupuncture can significantly increase the level of nitric oxide in rat tissues and inhibit the production of prostaglandin F2α that causes hyperalgesia and relieves pain. In addition, wrist-ankle acupuncture can activate an endogenous pain regulation mechanism that increases the secretion of β-endorphins and substance P to block the transmission of pain signals.

Besides, Rajak et al. (2019) treated children with spastic CP by rTMS with 10 Hz and 2,500 pulse sequences. The results showed that, after treatment, the degree of upper limb muscle spasm was significantly reduced (Rajak et al., 2019). However, the role of rTMS at different frequencies is also different. Valle et al. (2007) studied the therapeutic effects of low frequency and

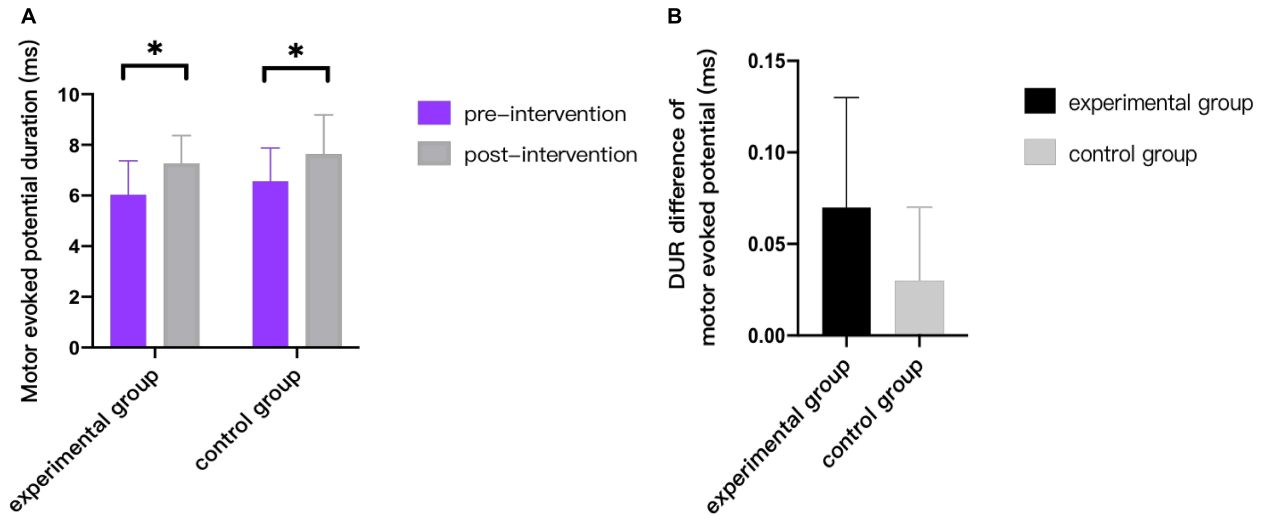

FIGURE 9 | Comparison of duration of motor evoked potentials. * indicates intra-group $p < 0.05$.

high frequency on spasticity in children with CP. The results showed that the 5-Hz group had more obvious relief of upper limb spasticity and significantly improved elbow movement than the 1-Hz and sham stimulation groups, and the safety evaluation showed that 1-Hz or 5-Hz stimulation did not cause any side effects in children.

However, there is no significant statistical difference between the experimental group and the control group before and after treatment (p>0.05), so the evidence does not support the assumptions that the effect of combined wrist-ankle acupuncture group on improving spasticity in children with CP is better than that in the single 5-Hz rTMS group. The small sample size or low treatment frequency might be the reason. Further experiments are still needed to verify whether this hypothesis is correct.

Effect on Motor Function

Recent years, acupuncture combined with rTMS were reported to have a more effective impact on motor function when compared to single rTMS (Yan-fen, 2015; Ji et al., 2019. In addition, our statistical results showed that the increase of GMFM-66 scores in the experimental group was greater than that in the control group (p<0.05), which revealed the evident superiority of rTMS and wrist-ankle acupuncture combination therapy during motor function recovery.

From the perspective of traditional Chinese medicine, the division of wrist-ankle acupuncture is similar to the 12 skin meridians. The 12 skin meridians are the distribution of the 12 meridians on the body surface. Some theoretical studies refer that the upper 4 areas belong to the hand Yangming large intestine meridian, the upper 5 areas belong to the hand Shaoyang Sanjiao meridian, the lower 1 area belongs to the foot Shaoyin kidney meridian, and the lower 4 areas belong to the Foot Yangming stomach meridian (Qinghui, 2017). The meridians scattered on the skin are adjusted through the selection of needle entry parts at the wrist and ankle, so as to achieve the goal of regulating the viscera, making the Qi and blood sufficient and nourishing the joints.

Several clinical studies investigating the efficacy of wrist-ankle acupuncture in children with spastic CP have reported a large improvement in motor function. These studies (Qianfang, 2018) have suggested that wrist-ankle acupuncture can effectively improve the fine motor ability of both hands of children with spastic CP, and the curative effect is better than traditional acupuncture. Besides, the research results found that (Wenjie, 2019) wrist-ankle acupuncture can significantly improve the pointy foot gait of children with spastic CP and increase the ankle range of motion.

At the same time, rTMS also has a positive effect on the treatment of children with CP. A large number of studies have proved that (Valle et al., 2007; Feng et al., 2013; Rajak et al., 2019) rTMS can improve motor dysfunction in children with CP. Studies showed that (Tan et al., 2014) rTMS can improve cerebral blood flow, improve the metabolic environment of brain cells, delay the cell death cycle, and promote the recovery of brain function. A randomized controlled trial (Feng et al., 2013) discussed the therapeutic effect of rTMS on children with spastic CP. The results showed that, after 1 month of treatment, the sitting ability was significantly improved. After 3 months of treatment, the gross motor functions, such as sitting, kneeling, and climbing, and the fine motor functions, such as range of motion, grasping, and operating objects of limb joints, were significantly improved compared with that in the control group.

This trial found that rTMS combined with wrist-ankle acupuncture has obvious advantages in improving motor function of children with cerebral palsy. In the future, we can also expand the sample size to further explore the persistence of its effect.

CONCLUSION

From a clinical point of view, 5-Hz rTMS alone or combined wrist-ankle acupuncture are both of positive significance in improving gross motor function, reducing tension of soleus, gastrocnemius, and hamstring muscles; shortening latency of MEP; increasing amplitude of MEP and prolonging duration of MEP in children with CP; and promoting recovery of motor function by regulating nerve function of corticospinal pathway. However, from a statistical point of view, it can be found that the clinical efficacy of high-frequency rTMS combined with wristankle acupuncture in improving gross motor function and enhancing the conductivity of corticospinal tract in children with CP is better than that of simple high-frequency rTMS, and there is no significant difference in the improvement of spasticity.

LIMITATIONS

Through the results of this study, it could be found that the clinical efficacy of 5-Hz rTMS combined with wrist-ankle acupuncture in improving gross motor function and enhancing the conductivity of corticospinal tract in children with CP was better than that of 5-Hz rTMS alone. In addition, there was no statistical difference in the improvement of spasticity, which may be related to insufficient sample size and low treatment frequency. However, the degree of spasticity was improved according to the change trend of clinical data. Because the influence of COVID-19, recruiting patients during this period was more difficult and time consuming. In the future, it is still necessary to further expand the sample size to increase the reliability of the conclusions. In addition, because the research object is children, there was a problem of compliance in the treatment process. It is necessary to further strengthen the communication with children and parents, so as to obtain better cooperation. At the same time, there is no research report on the joint action mechanism of wrist-ankle acupuncture combined with rTMS, which can be used as an exploration direction in the future to explore the superiority of the central peripheral closed-loop stimulation mode to improve the neurophysiological function. It can also be combined with functional MRI and other imaging methods to explore its mechanism.

DATA AVAILABILITY STATEMENT

The original contributions presented in the study are included in the article/**Supplementary Material**, further inquiries can be directed to the corresponding author/s.

ETHICS STATEMENT

The studies involving human participants were reviewed and approved by the Medical Ethics Committee of Shanghai YangZhi Rehabilitation Hospital (YZ2020-066). In addition, the project was registered in Chinese Clinical Trial Registry (No. ChiCTR20000039495). Written informed consent to participate in this study was provided by the participants' legal guardian/next of kin. Written informed consent was obtained from the individual(s), and minor(s)' legal guardian/next of kin, for the publication of any potentially identifiable images or data included in this article.

AUTHOR CONTRIBUTIONS

JL, CC, SZ, and MS contributed to the design and conception of the study. All authors contributed to the acquisition of data, analysis, and interpretation of the results. JL, CC, and SZ drafted the first version of the manuscript. All authors revised it critically for important intellectual content and approved the final version.

SUPPLEMENTARY MATERIAL

The Supplementary Material for this article can be found online at: https://www.frontiersin.org/articles/10.3389/fnins.2021.771064/full#supplementary-material

REFERENCES

Avery, L. M., Russell, D. J., and Rosenbaum, P. L. (2013). Criterion validity of the GMFM-66 item set and the GMFM-66 basal and ceiling approaches for estimating GMFM-66 scores. *Dev. Med. Child Neurol.* 55, 534–538. doi: 10.1111/dmcn.12120

Brum, M., Cabib, C., and Valls-Solé, J. (2016). Clinical value of the assessment of changes in MEP duration with voluntary contraction. *Front. Neurosci.* 9:505. doi: 10.3389/fnins.2015.00505

Feng, J. Y., Jia, F. Y., Jiang, H. Y., Li, N., Li, H. H., and Du, L. (2013). Effect of infra-low-frequency transcranial magnetic stimulation on motor function in children with spastic cerebral palsy. *Chin. J. Contemp. Pediatr.* 15, 187–191. doi: 10.7499/j.issn.1008-8830.2013.03.006

Groppa, S., Oliviero, A., Eisen, A., Quartarone, A., Cohen, L. G., Mall, V., et al. (2012a). A practical guide to diagnostic transcranial magnetic stimulation: report of an IFCN committee. *Clin. Neurophysiol.* 123, 858–882. doi: 10.1016/j.clinph.2012.01.010

Groppa, S., Schlaak, B. H., Münchau, A., Werner-Petroll, N., Dünnweber, J., Bäumer, T., et al. (2012b). The human dorsal premotor cortex facilitates the excitability of ipsilateral primary motor cortex via a short latency cortico-cortical route. *Hum. Brain Mapp.* 33, 419–430. doi: 10.1002/hbm.21221

Guse, B., Falkai, P., and Wobrock, T. (2010). Cognitive effects of high-frequency repetitive transcranial magnetic stimulation: a systematic review. *J. Neural Transm.* 117, 105–122. doi: 10.1007/s00702-009-0333-7

Ji, Y.-H., Ji, Y.-H., and Sun, B.-D. (2019). Effect of acupuncture combined with repetitive transcranial magnetic stimulation on motorfunction and cerebral hemodynamics in children with spastic cerebral palsy with spleen-kidney deficiency. *Acupunct. Res.* 44, 757–761. doi: 10.13702/j.1000-0607.190154

Kamble, N., Netravathi, M., and Pal, P. K. (2014). Therapeutic applications of repetitive transcranial magnetic stimulation (rTMS) in movement disorders: a review. *Parkinsonism Relat. Disord.* 20, 695–707. doi: 10.1016/j.parkreldis.2014.03.018

Kesar, T. M., Sawaki, L., Burdette, J. H., Cabrera, M. N., Kolaski, K., Smith, B. P., et al. (2012). Motor cortical functional geometry in cerebral palsy and its

relationship to disability. *Clin. Neurophysiol.* 123, 1383–1390. doi: 10.1016/j.clinph.2011.11.005

Kirton, A. (2017). Advancing non-invasive neuromodulation clinical trials in children: lessons from perinatal stroke. *Eur. J. Paediatr. Neurol.* 21, 75–103. doi: 10.1016/j.ejpn.2016.07.002

Kowalski, J. L., Nemanich, S. T., Nawshin, T., Chen, M., Peyton, C., Zorn, E., et al. (2019). Motor evoked potentials as potential biomarkers of early atypical corticospinal tract development in infants with perinatal stroke. *J. Clin. Med.* 8:1208. doi: 10.3390/jcm8081208

Krishnan, C., Santos, L., Peterson, M. D., and Ehinger, M. (2015). Safety of noninvasive brain stimulation in children and adolescents. *Brain Stimul.* 8, 76–87. doi: 10.1016/j.brs.2014.10.012

Liu, W. X., Zhao, Y., and Yu, Y. Y. (2015). Effects of wrist-ankle acupuncture on associated factors in uterus tissue and serum in rats with primary dysmenorrhea. *J. Acupunct. Tuina Sci.* 13, 146–149. doi: 10.1007/s11726-015-0839-5

Marzbani, H., Shahrokhi, A., Irani, A., Mehdinezhad, M., Kohanpour, M., and Mirbagheri, M. M. (2018). "The effects of low frequency repetitive transcranial magnetic stimulation on white matter structural connectivity in children with cerebral palsy," in *Proceedings of the 2018 40th Annual International Conference of the IEEE Engineering in Medicine and Biology Society (EMBC)*, Honolulu, HI, 2491–2494. doi: 10.1109/EMBC.2018.8512866

Numanoğlu, A., and Günel, M. K. (2012). Intraobserver reliability of modified Ashworth scale and modified Tardieu scale in the assessment of spasticity in children with cerebral palsy. *Acta Orthop. Traumatol. Turc.* 46, 196–200. doi: 10.3944/AOTT.2012.2697

Papadelis, C., Kaye, H., Shore, B., Snyder, B., Grant, P. E., and Rotenberg, A. (2019). Maturation of corticospinal tracts in children with hemiplegic cerebral palsy assessed by diffusion tensor imaging and transcranial magnetic stimulation. *Front. Hum. Neurosci.* 13:254. doi: 10.3389/fnhum.2019.00254

Poirot, I., Laudy, V., Rabilloud, M., Roche, S., Ginhoux, T., Kassaï, B., et al. (2017). Prevalence of pain in 240 non-ambulatory children with severe cerebral palsy. *Ann. Phys. Rehabil. Med.* 60, 371–375. doi: 10.1016/j.rehab.2017.03.011

Qi, Y. C., Xiao, X. J., Duan, R. S., Yue, Y. H., Zhang, X. L., Li, J. T., et al. (2014). Effect of acupuncture on inflammatory cytokines expression of spastic cerebral palsy rats. *Asian Pac. J. Trop. Med.* 7, 492–495. doi: 10.1016/S1995-7645(14)60081-X

Qianfang, J. I. A. (2018). Clinical observation on wrist-ankle acupuncture for upper extremity function disorder in children with spastic cerebral palsy. *New Trad. Chin. Med.* 50, 198–200. doi: 10.13457/j.cnki.jncm.2018.07.060

Qinghui, W. Q. Z. (2017). Theoretical origin and clinical application of wrist-ankle acupuncture therapy. *Chin. Acupunct.* 37, 509–512. doi: 10.13703/j.0255-2930.2017.05.016

Rajak, B. L., Gupta, M., Bhatia, D., and Mukherjee, A. (2019). Increasing number of therapy sessions of repetitive transcranial magnetic stimulation improves motor development by reducing muscle spasticity in cerebral palsy children. *Ann. Indian Acad. Neurol.* 22, 302–307. doi: 10.4103/aian.AIAN_102_18

Rossini, P. M., Burke, D., Chen, R., Cohen, L. G., Daskalakis, Z., Di Iorio, R., et al. (2015). Non-invasive electrical and magnetic stimulation of the brain, spinal cord, roots and peripheral nerves: basic principles and procedures for routine clinical and research application. An updated report from an I.F.C.N. Committee. *Clin. Neurophysiol.* 126, 1071–1107. doi: 10.1016/j.clinph.2015.02.001

Sellier, E., Platt, M. J., Andersen, G. L., Krägeloh-Mann, I., De La Cruz, J., Cans, C., et al. (2016). Decreasing prevalence in cerebral palsy: a multi-site European population-based study, 1980 to 2003. *Dev. Med. Child Neurol.* 58, 85–92. doi: 10.1111/dmcn.12865

Silva, L. M., Silva, K. M. S., Lira-Bandeira, W. G., Costa-Ribeiro, A. C., and Araújo-Neto, S. A. (2020). Localizing the primary motor cortex of the hand by the 10-5 and 10-20 systems for neurostimulation: an MRI Study. *Clin. EEG Neurosci.* 52, 427–435. doi: 10.1177/1550059420934590

Smith, J. M. C., and Field, T. S. (2020). Pain in adults with cerebral palsy: measuring the contribution of spasticity. *Dev. Med. Child Neurol.* 62:271. doi: 10.1111/dmcn.14396

Tan, X.-Q., Wu, W.-H., Zeng, F.-Y., et al. (2014). Effect of ultra- low frequency transcranial magnetic stimulation on cerebral blood flow in children with cerebral palsy. *Chin. J. Rehabil. Theory Pract.* 20, 675–678. doi: 10.3969/j.issn.1006-9771.2014.07.017

Valle, A. C., Dionisio, K., Pitskel, N. B., Pascual-Leone, A., Orsati, F., Ferreira, M. J., et al. (2007). Low and high frequency repetitive transcranial magnetic stimulation for the treatment of spasticity. *Dev. Med. Child Neurol.* 49, 534–538. doi: 10.1111/j.1469-8749.2007.00534.x

Van Den Bos, M. A. J., Geevasinga, N., Menon, P., Burke, D., Kiernan, M. C., and Vucic, S. (2017). Physiological processes influencing motor-evoked potential duration with voluntary contraction. *J. Neurophysiol.* 117, 1156–1162. doi: 10.1152/jn.00832.2016

Wang Xuefeng, H. X. (2005). The analysis of spastic cerebral palsy of children (stagnation of the liverqi and deficiency of the spleen) in TCM. *J. Pediatr. Trad. Chin. Med.* 01, 27–30.

Wenjie, F. (2019). "Effect of Wrist Ankle on relieving spasticity of distal lower limb muscles in children with spastic cerebral palsy," in *Pediatric Professional Committee of Chinese Society of Integrated Traditional and Western Medicine: Chinese Society of Integrated Traditional and Western Medicine*, 294–295. doi: 10.26914/c.cnkihy.2019.014285

Wu, X., Li, J., Chen, C., and Zhu, S. (2013). Sample size estimation in superiority clinical trials for two means comparison. *J. Math. Med.* 26, 517–519. doi: 10.3969/j.issn.1004-4337.2013.05.005

Wu, Y., Jin, Z., Li, K., Lu, Z. L., Wong, V., Han, T. L., et al. (2008). Effect of acupuncture on the brain in children with spastic cerebral palsy using functional neuroimaging (fMRI). *J. Child Neurol.* 23, 1267–1274. doi: 10.1177/0883073808318049

Yan-fen, C. (2015). Clinical effects of infra-low-frequency transcranial magnetic stimulation (ILF-TMS) combined with acupuncture on the gross motor function of children with cerebral palsy. *J. Trop. Med.* 15, 1507–1510.

Yang, K., Du, Y. Z., Shi, J., Wang, J. L., Sun, Y. H., Xing, H. J., et al. (2019). Exploration of dominant diseases and clinical application characteristics of wrist-ankle acupuncture therapy based on data mining technology. *Chin. Acupunct.* 39, 673–678. doi: 10.13703/j.0255-2930.2019.06.029

Zhang, B., Kang, J., and Chen, X. M. (2016). Methods to combine standard deviations of different subgroups in meta-analysis. *Chin. J. Evid. Based Med.* 16, 851–854. doi: 10.7507/1672-2531.20160130

Zhang, Y., Lan, R., Wang, J., Li, X. Y., Zhu, D. N., Ma, Y. Z., et al. (2015). Acupuncture reduced apoptosis and up-regulated BDNF and GDNF expression in hippocampus following hypoxia-ischemia in neonatal rats. *J. Ethnopharmacol.* 172, 124–132. doi: 10.1016/j.jep.2015.06.032

Zhao, X., Guo, Y., Chen, Z.-L., and Li, G.-L. (2011). Discussion on Some Problems of National Standard "Standardized Manipulation of Acupuncture and Moxibustion Part 19 Wrist-ankle Acupuncture.". *Clin. J. Acupunct. Moxibustion* 27, 1–3. doi: 10.1016/s1003-5257(13)60054-9

Conflict of Interest: The authors declare that the research was conducted in the absence of any commercial or financial relationships that could be construed as a potential conflict of interest.

frontiers in Neuroscience

ORIGINAL RESEARCH
published: 04 February 2022
doi: 10.3389/fnins.2022.807045

Synergistic Immediate Cortical Activation on Mirror Visual Feedback Combined With a Soft Robotic Bilateral Hand Rehabilitation System: A Functional Near Infrared Spectroscopy Study

Yaxian Qiu[1†], Yuxin Zheng[1†], Yawen Liu[2], Wenxi Luo[2], Rongwei Du[2], Junjie Liang[1], Anniwaer Yilifate[1], Yaoyao You[1], Yongchun Jiang[2], Jiahui Zhang[2], Aijia Chen[2], Yanni Zhang[1], Siqi Huang[2], Benguo Wang[3,4], Haining Ou[1] and Qiang Lin[1]**

[1] Department of Rehabilitation, The Fifth Affiliated Hospital of Guangzhou Medical University, Guangzhou, China, [2] Department of Rehabilitation, Guangzhou Medical University, Guangzhou, China, [3] Department of Rehabilitation, Longgang District People's Hospital of Shenzhen, Shenzhen, China, [4] Department of Rehabilitation, The Third Affiliated Hospital of The Chinese University of Hong Kong, Shenzhen, China

Background: Mirror visual feedback (MVF) has been widely used in neurological rehabilitation. Due to the potential gain effect of the MVF combination therapy, the related mechanisms still need be further analyzed.

Methods: Our self-controlled study recruited 20 healthy subjects (age 22.150 ± 2.661 years) were asked to perform four different visual feedback tasks with simultaneous functional near infrared spectroscopy (fNIRS) monitoring. The right hand of the subjects was set as the active hand (performing active movement), and the left hand was set as the observation hand (static or performing passive movement under soft robotic bilateral hand rehabilitation system). The four VF tasks were designed as RVF Task (real visual feedback task), MVF task (mirror visual feedback task), BRM task (bilateral robotic movement task), and MVF + BRM task (Mirror visual feedback combined with bilateral robotic movement task).

Results: The beta value of the right pre-motor cortex (PMC) of MVF task was significantly higher than the RVF task (RVF task: -0.015 ± 0.029, MVF task: 0.011 ± 0.033, $P = 0.033$). The beta value right primary sensorimotor cortex (SM1) in MVF + BRM task was significantly higher than MVF task (MVF task: 0.006 ± 0.040, MVF + BRM task: 0.037 ± 0.036, $P = 0.016$).

Conclusion: Our study used the synchronous fNIRS to compare the immediate hemodynamics cortical activation of four visual feedback tasks in healthy subjects. The results showed the synergistic gain effect on cortical activation from MVF combined with a soft robotic bilateral hand rehabilitation system for the first time, which could be used to guide the clinical application and the future studies.

Keywords: mirror visual feedback, soft robotic bilateral hand rehabilitation system, functional near infrared spectroscopy, cortical activation, synergistic gain effect

OPEN ACCESS

Edited by:
Jing Wang,
Xi'an Jiaotong University, China

Reviewed by:
Bin Liu,
Sun Yat-sen University, China
Hua Zhou,
NYU Langone Health, United States
Xingang Zhao,
Shenyang Institute of Automation, Chinese Academy of Sciences (CAS), China

***Correspondence:**
Qiang Lin
qianglin0925@gzhmu.edu.cn
Haining Ou
ouhaining@gzhmu.edu.cn

†These authors share first authorship

Specialty section:
This article was submitted to Neuroprosthetics, a section of the journal Frontiers in Neuroscience

Received: *01 November 2021*
Accepted: *12 January 2022*
Published: *04 February 2022*

Citation:
Qiu Y, Zheng Y, Liu Y, Luo W, Du R, Liang J, Yilifate A, You Y, Jiang Y, Zhang J, Chen A, Zhang Y, Huang S, Wang B, Ou H and Lin Q (2022) Synergistic Immediate Cortical Activation on Mirror Visual Feedback Combined With a Soft Robotic Bilateral Hand Rehabilitation System: A Functional Near Infrared Spectroscopy Study. Front. Neurosci. 16:807045. doi: 10.3389/fnins.2022.807045

INTRODUCTION

Mirror therapy or mirror visual feedback (MVF) was first proposed by Ramachandran et al. (1995) and applied to the treatment of limb phantom pain. It was found that the input of a mirrored visual illusion could activate brain plasticity of the affected limb and thus inhibit the abnormal displacement of the central functional area of the brain and in turn alleviate pain (Ramachandran and Altschuler, 2009; Herrador Colmenero et al., 2018). Subsequently, MVF has been widely used in neurological rehabilitation. Thieme et al. (2018) meta-analysis found moderate quality of evidence that MVF was beneficial in improving motor dysfunction and activities of daily living. Until now, the relevant mechanistic hypotheses involved in MVF mainly include the following three aspects: MVF can activate the mirror neuron system, thus inducing or enhancing motor imagery (Grèzes and Decety, 2001); MVF might also conducive to the recruitment of ipsilateral cortical spinal cord bundles (Zheng and Hu, 2011) and can enhance attention in affected sides via a mirror illusion, thus activating the motor network in the brain region of the affected side (Deconinck et al., 2015). However, due to the small sample size and large heterogeneity of patients (including the locations and side of brain injury, motor and cognitive impairment levels, sensory function, and even age, etc.) (Luo et al., 2020), the clinical efficacy and related mechanisms of MVF still needs further analysis. More recently, the Central-Peripheral-Central closed-loop regulation mode, formed by the combination of MVF as a central intervention method with other peripheral interventions, has become a research hotspot to further improve the technique. In recent years, some MVF studies have combined it with electromyographic biofeedback (Kim and Lee, 2015; Liu et al., 2021), EMG-triggered electrical stimulation (Schick et al., 2017), electrical stimulation (Lee and Lee, 2019), robot-assisted therapy (Ji-feng et al., 2019), and other intervention methods. These results suggest that combination therapy has potential for improving moderate to severe upper limb dysfunction after stroke. In the past some studies simply superimposed MVF and other interventions in order [such as MVF combined with acupuncture (Yin et al., 2020), robot-assisted therapy (Thakkar et al., 2020; Rong et al., 2021)], and failed to form MVF synchronized with other peripheral interventions to achieve central-peripheral-central closed-loop measures. Additionally, although some studies (such as MVF synchronous electromyographic biofeedback, EMG-induced electrical stimulation) have achieved closed-loop intervention formally, the muscle electrical stimulation given by the electrode could not accurately induce hand movement resulting in a significant difference between the passive movement of the affected side and the mirror movement leading to the poor effect of the closed-loop regulation mode. Therefore, it is necessary to explore a better MVF synchronous intervention mode to further improve the effect of closed-loop regulation.

In our study we use a soft robotic bilateral hand rehabilitation system. The soft robotic bilateral hand rehabilitation system is a pneumatically driven soft robot based on bilateral hand movement intervention for patients with hand dysfunction after stroke. In this method, the unaffected hand is fitted with an inductive glove for normal hand movement, while the affected hand is fitted with an exoskeleton robotic glove for passive hand movement, imitating the unaffected hand. The principle is to have the inductive glove record normal hand movements of the unaffected hand and input data into the exoskeleton robotic glove to guide the affected hand to simulate movement. Therefore, it is also defined as robot – mediated bilateral therapy (Haghshenas-Jaryani et al., 2020). This intervention method may be related to three potential principles of nerve remodeling. First, soft robotic gloves can not only activate the primary motor cortex of the affected side by driving the affected hand through the unaffected hand, but also trigger the proprioceptive input by moving the affected hand, so as to activate the corresponding primary sensory cortex (Haghshenas-Jaryani et al., 2019), and establish effective "peripheral" stimulation feedback to "central." Second, soft robotic gloves realize bilateral exercise training mode through the joint action of the unaffected hand, which is conducive to the normalization of inter-cortical inhibition between cerebral hemispheres. Previous studies have shown that the mechanism of bilateral movement pattern was that the simultaneous movement of the same muscle groups on both sides was beneficial to the activation of similar neural networks in bilateral hemispheres, thereby reducing inter-hemispheric inhibition and improving the functional performance of paralytic hand (Renner et al., 2020). Several studies showed that bilateral training was superior to neurodevelopment treatment and unilateral robot-assisted training in improving upper limb motor function after stroke (Chen et al., 2019; Straudi et al., 2020). Finally, the linkage device of the robotic glove make it easy to realize the repeated movement of the affected hand, which can continuously provide positive feedback to the central nervous system through the peripheral movement and strengthen the neuronal circuit (Mane et al., 2020), thus facilitating the neural remodeling of the brain on the affected side. Moderate-quality evidence showed a beneficial effect of high repetitive task practice is considered to be an effective intervention method (Pollock et al., 2014). Repeated exercise is considered to be the physiological basis for motor learning, and motor and sensory coupling contributes to the adaptation and recovery of neural pathways (French et al., 2007). Overall, soft robotic gloves can provide positive and effective "peripheral" stimulation, and MVF is based on the mechanism of motor imagery and mirror neurons to produce central regulation. If they are combined with synchronous intervention, a complete and strong "central-peripheral-central" closed-loop regulation can be theoretically formed. However, whether it can bring a better clinical effect and its mechanism remain unclear.

Previous studies on central nervous regulation based on MVF mostly used functional magnetic resonance imaging (fMRI) (Rjosk et al., 2017; Manuweera et al., 2018), electroencephalography (EEG) (Al-Wasity et al., 2019; Luo et al., 2020; Fong et al., 2021) and functional near infrared spectroscopy (fNIRS) (Inagaki et al., 2019; Bai et al., 2020), but these studies are limited by the high cost of fMRI examination, spatial limitations, and low spatial resolution of EEG. fNIRS is portable, environmentally friendly, and has relatively high spatial resolution. This study included healthy young subjects to minimize the differences between individuals, such as part of

brain damage, degree of surviving motor function and cognitive function, and used synchronous fNIRS to determine whether MVF and a soft robotic bilateral hand rehabilitation system have synergistic effects on cortical activation. The results can guide future clinical treatments and mechanistic research.

MATERIALS AND METHODS

Participants

Our self-controlled study recruited 20 healthy subjects from Guangzhou Medical University who met the following criteria: (a) 18–35 years old; (b) right hand dominant according to the Edinburgh Handedness Inventory; (c) no previous affected vision field or vision diseases; (d) no central nervous system diseases; and (e) no upper limb fracture history and upper limb deformity. The study was approved by the Ethics Review Committee of the Fifth Affiliated Hospital of Guangzhou Medical University (No. GYWY-L2021-74). All subjects signed informed consent forms. This study was also approved by the China Clinical Registration Center (No. ChiCTR2100052042)[1].

Procedure and Experimental Tasks

All recruited subjects were asked to perform four different visual feedback tasks with simultaneous fNIRS monitoring. The order of tasks was random and based on random computer software. The right hand of the subjects was set as the active hand (performing active movement), and the left hand was set as the observation hand (static or performing passive movement under soft robotic bilateral hand rehabilitation system). The active hand followed the preset sound prompt to grasp or extend at a frequency of 0.5 Hz.

Mirror visual feedback used a three-dimensional triangular mirror box with an area of 30 cm × 30 cm. The soft robotic bilateral hand rehabilitation system contains soft-robotic bilateral gloves (SY-HR06, Siyi Intelligent Technology Co., Ltd., Shanghai, China) including one for the motion-command glove on the right hand (active side) and the other for the motion-actuator glove on the left hand (slave side). Through this master-slave configuration, the motion trajectory of the active hand (right, master) provides input instructions for robotic glove that drive the passive limb (left, slave) to perform synchronous motion. All subjects were asked to wear soft-robotic bilateral gloves to maintain the same cortex activation from glove itself during four tasks. Before testing, the robotic gloves should be calibrated to confirm correct mirror motion.

According to whether the observed hand was in static or passive movement through linkage, the VF tasks could be divided into a non-linkage state (real visual feedback task, RVF task; mirror visual feedback task, MVF task) and linkage state (bilateral robotic movement, BRM task; MVF + BRM task). They could also be divided based whether the mirror image was involved: real visual feedback from the observed hand (real visual feedback task, RVF task; bilateral robotic movement, BRM task) and mirror visual feedback from active hand (mirror visual feedback task, MVF task; MVF + BRM task). The four VF tasks were designed as follows (**Figure 1**):

(1) RVF task: The active hand performed grasping/extension without mirror visual feedback; the observed hand remained static, and visual feedback was from the observed hand (**Figure 1A**).
(2) MVF task: The active hand performed grasping/extension with mirror visual feedback; the observed hand remained static, and visual feedback was from the mirror illusion of the active hand (**Figure 1B**).
(3) BRM task: The active hand performed grasping/extension without mirror visual feedback; the observed hand performed passive movement in the soft robotic bilateral hand rehabilitation system; visual feedback was from the observed hand (**Figure 1C**).
(4) MVF + BRM task: The active hand performed grasping/extension with mirror visual feedback; the observed hand performed passive movement under soft robotic bilateral hand rehabilitation system, and visual feedback was from the mirror illusion of the active hand (**Figure 1D**).

Functional Near Infrared Spectroscopy Measurement

Data Acquisition

Synchronized fNIRS (NirSmart, Danyang Huichuang Medical Equipment Co., Ltd., Beijing, China) was used to monitor hemodynamic responses during different visual feedback tasks. 12 source probes and 10 detectors were integrated into a custom head cap that was fixed on the subjects' heads and adjusted according to size and shape. Two infrared wavelengths (730 and 850 nm) emitted by the transmitter were received by a pair of adjacent detectors with an interval of 30 mm, and were collected at a sampling rate of 10 Hz. The source probe and detector could form 24 channels according to the placement of the 10–20 systems (Chatrian et al., 1988; Oostenveld and Praamstra, 2001; Fornia et al., 2020a). The position of the source probe and detector in this study were shown in **Figure 2**. After subject preparation ready, a fNIRS gain quality check was performed before the test to ensure that the data acquisition was neither under-gained nor over-gained.

The fNIRS testing was divided into a baseline phase (240 s) and a random task phase (960 s). The random task phase contains four visual feedback tasks, and each task included one 60-s resting stage and three 60-s blocks (40 s for grasp and 20 s for rest over three blocks for a total of 1,200 s; **Figure 3**).

When the subjects performed different tasks, the corresponding cerebral cortex was activated. The increase in neuronal activity was accompanied by the increase in cerebral oxygen metabolism, and blood oxygen was consumed resulting in the changes in the concentrations of oxygenated hemoglobin (HbO_2) and deoxygenated hemoglobin (HbR). The relative concentration change of the fNIRS data was calculated according to the modified Beer-Lambert law and then filtered by a Butterworth band-pass filter with a frequency band of 0.01-0.2 Hz. Previous studies have demonstrated that HbO_2 was

[1]https://www.chictr.org.cn

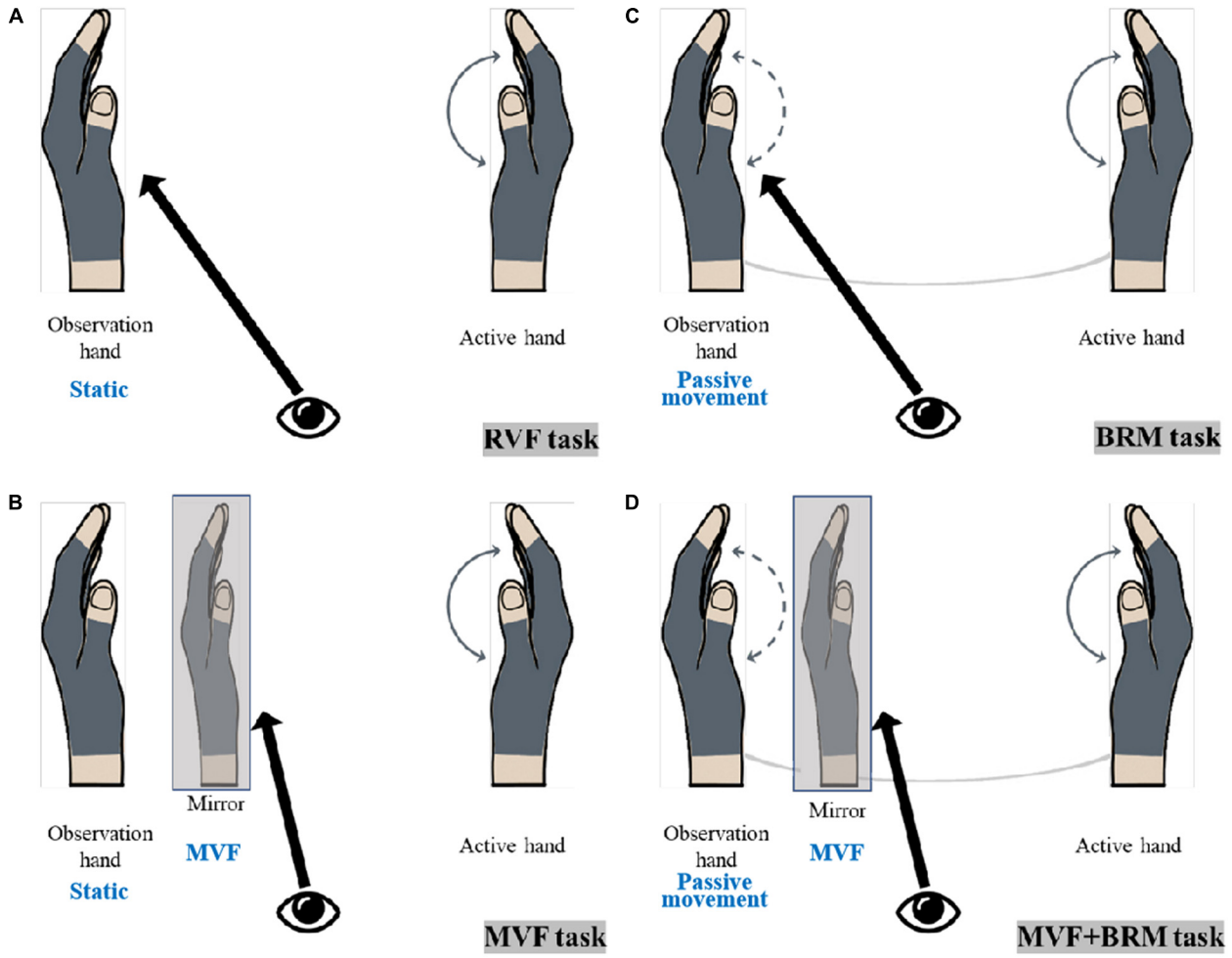

FIGURE 1 | The diagram of visual feedback tasks. **(A)** RVF Task (real visual feedback task); **(B)** MVF task (mirror visual feedback task); **(C)** BRM task (bilateral robotic movement task); **(D)** MVF + BRM task (Mirror visual feedback combined with bilateral robotic movement task).

a reliable and sensitive indicator of movement-related changes in brain activation (Chen et al., 2020). Therefore, this study selected the concentration change of HbO_2 (ΔHbO_2) as the outcome measurement for analysis.

Regions of Interests

Regions of interest were set on bilateral primary sensorimotor cortex (SM1), pre-motor cortex (PMC), and dorsolateral prefrontal cortex (DLPFC) as shown in **Figure 3**. According to the results of MRIcro registration, the average value of all channels in the regions of interests greater than 50% was used as the activation value of the brain area (Ye et al., 2009; Wan et al., 2018). Performing the general linear model (GLM) and average beta values were obtained in the channel of the regions of interest (ROIs).

Statistical Analysis

SPSS 25.0 software was used for statistical analysis. The measurement data conform to normal distribution and were expressed as the mean ± standard deviation; enumeration data were expressed as the rate or composition ratio. One-way analysis of variance was used to compare to measurement data between multiple groups in line with normal distribution and homogeneity of variance, and the Least Significant Difference method was used for pairwise comparisons between groups. The Kruskal–Wallis H method was used to compare the measurement data among multiple groups that did not meet the application conditions.

RESULTS

Twenty healthy subjects included in our study (nine males and eleven females; age: 22.150 ± 2.661 years). The statistical results showed that compared with RVF task, the beta value of the right PMC of MVF task (RVF task: -0.015 ± 0.029, MVF task: 0.011 ± 0.033, P = 0.033) was higher, and the difference was statistically significant. Compared with BRM task, the beta value of left SM1 in RVF task was higher (RVF task: 0.023 ± 0.042, BRM task: -0.001 ± 0.049, P = 0.047), and

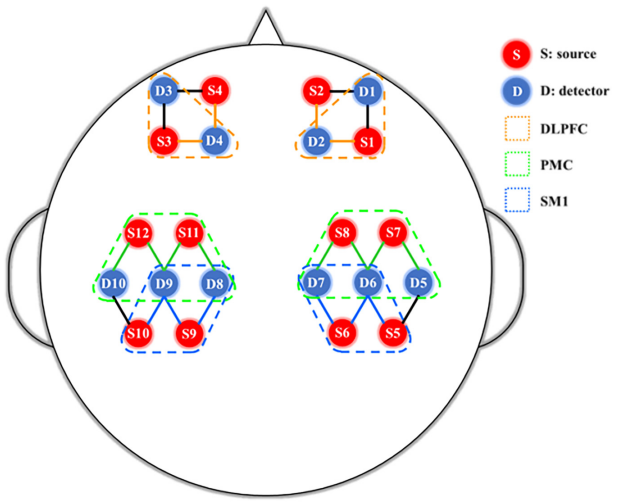

FIGURE 2 | fNIRS 24-channel placement. SM1, primary sensorimotor cortex; PMC, pre-motor cortex; DLPFC, dorsolateral prefrontal cortex.

the difference was statistically significant. Compared with MVF task, the beta value right SM1 in MVF + BRM task was higher (MVF task: 0.006 ± 0.040, MVF + BRM task: 0.037 ± 0.036, P = 0.016), and the difference was statistically significant. Compared with BRM task, the beta values of right DLPFC (BRM task: −0.031 ± 0.057, MVF + BRM task: 0.018 ± 0.057, P = 0.009), right PMC (BRM task: −0.018 ± 0.050, MVF + BRM task: 0.024 ± 0.036, P = 0.001), right SM1 (BRM task: −0.008 ± 0.049, MVF + BRM task: 0.037 ± 0.036, P = 0.001), left DLPFC (BRM task: −0.033 ± 0.067, MVF + BRM task: 0.014 ± 0.058, P = 0.029), left PMC (BRM task: −0.013 ± 0.038, MVF + BRM task: 0.021 ± 0.042, P = 0.012), and left SM1 (BRM task: −0.009 ± 0.049, MVF + BRM task: 0.028 ± 0.047, P = 0.021) in MVF + BRM task were higher, and the difference was statistically significant (**Figures 4**, **5**).

DISCUSSION

Our study used the synchronous fNIRS to compare the immediate hemodynamics cortical activation of four MVF tasks in healthy subjects. We explored the synergistic gain effect on cortical activation from MVF combined with a soft robotic bilateral hand rehabilitation system for the first time. Specifically, the combination of MVF and the robotic bilateral hand rehabilitation system was more conducive for cortical activation than either approach alone.

We first compared the RVF and MVF tasks. The results showed that MVF activated PMC on the mirror side. Its potential mechanism might be related to the key role of PMC in the mirror neuron network. MVF training is a rehabilitation method derived from the mirror neuron system (MNS) (Zhang et al., 2018). Mirror neurons both fire when an individual observes an action and when he/she performs a similar action (Ruggiero and Catmur, 2018).

Mirror visual feedback is a more vivid observation of movement mediated by mirrors. It promotes motor imagery and is further related to the rehabilitation of motor function (Ding et al., 2018). Meanwhile, the frontal-parietal MNS system is constructed by the parietal lobe, PMC, and the tail of the inferior frontal gyrus. It is an important neural network with mirror features (Rizzolatti and Craighero, 2004; Frenkel-Toledo et al., 2016). As one of the main components of the mirror neurons system, the activation of PMC could be seen both in action observation and action execution (Sun et al., 2018; Xu et al., 2019). Studies have shown that PMC is composed of interconnected regions in the primary motor cortex located in the frontal lobe of the brain (Fornia et al., 2020a). The upper motor neurons in the PMC can directly affect motor behavior

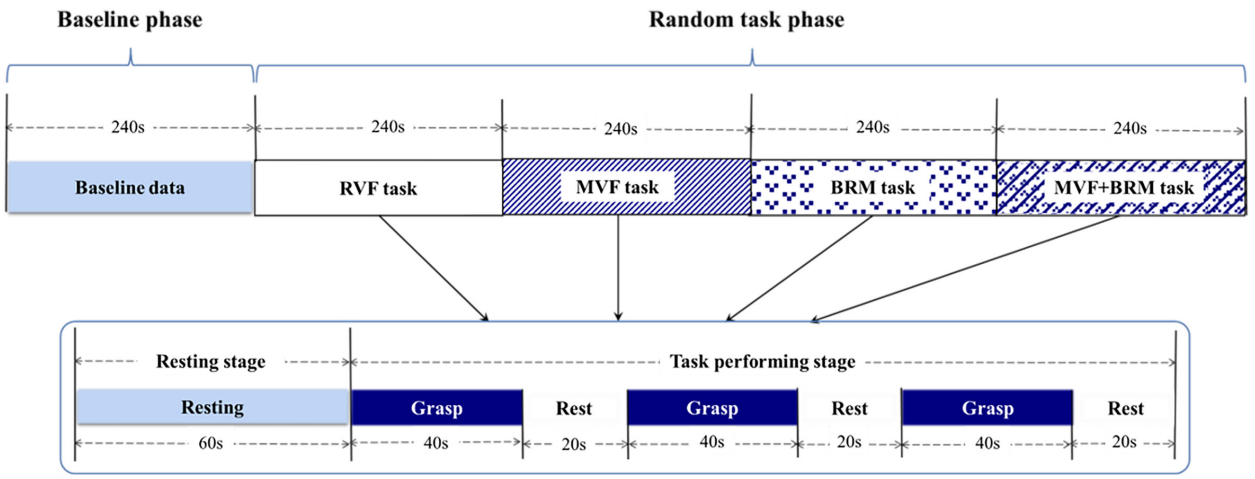

FIGURE 3 | fNIRS testing procedure including baseline phase and visual feedback task phase. The order of four tasks were randomized. Each visual feedback task consists of three trials. RVF task, real visual feedback task; MVF task, mirror visual feedback task; BRM task, bilateral robotic movement task; MVF + BRM task, Mirror visual feedback combined with bilateral robotic movement task.

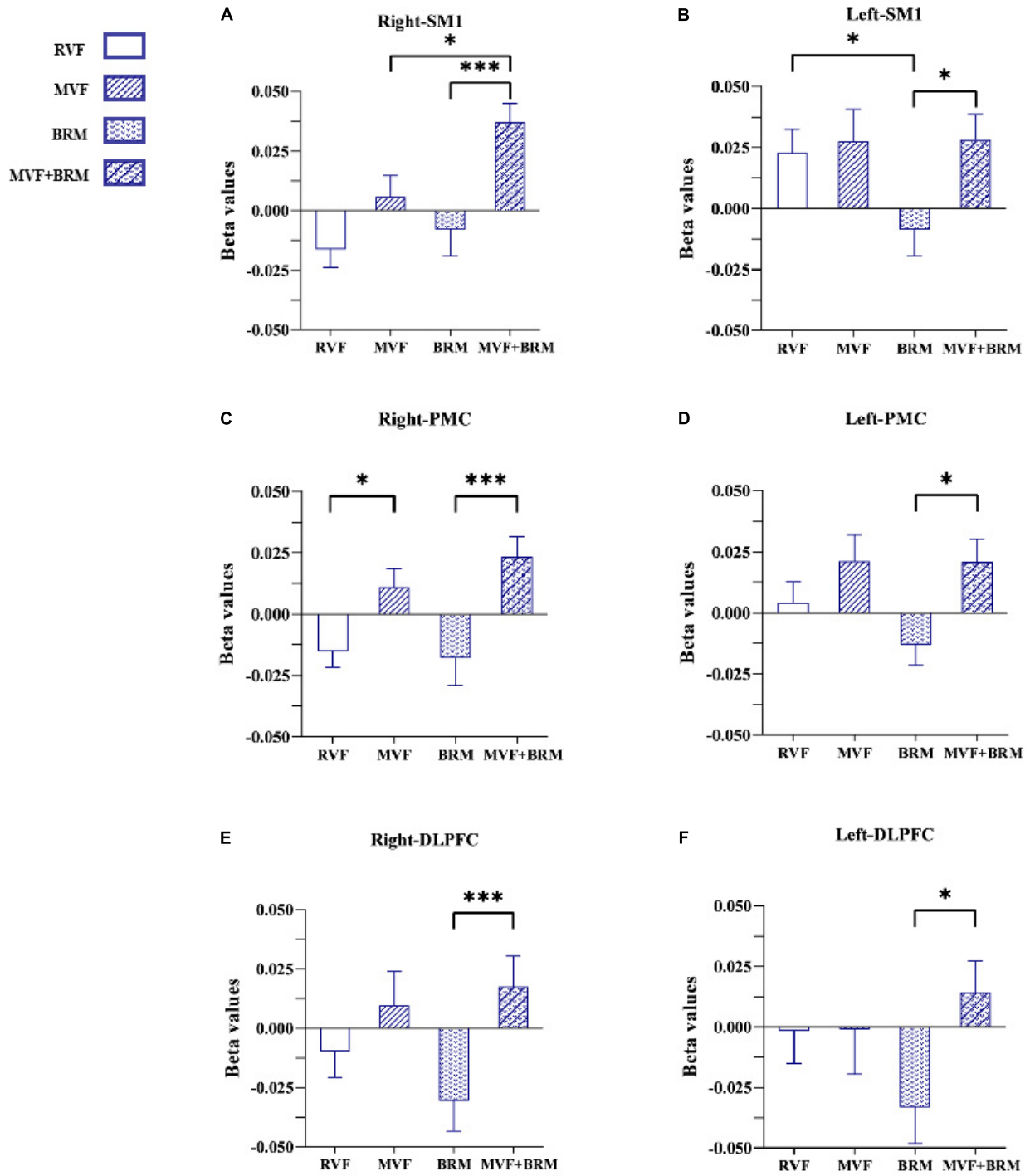

FIGURE 4 | The comparisons of average beta values of ROIs in different four visual feedback tasks. **(A)** Right-SM1; **(B)** Left-SM1; **(C)** Right-PMC; **(D)** Left-PMC; **(E)** Right-DLPFC; **(F)** Left-DLPFC. Error bars represent standard error. *$P < 0.05$ and ***$P < 0.001$. RVF task, real visual feedback task; MVF task, mirror visual feedback task; BRM task, bilateral robotic movement task; MVF + BRM task, Mirror visual feedback combined with bilateral robotic movement task. SM1, primary sensorimotor cortex; PMC, pre-motor cortex; DLPFC, dorsolateral prefrontal cortex.

via axons due to the extensive mutual connections with the primary motor cortex (Fornia et al., 2020b). Studies related to fMRI have also shown that motor imagery could enhance exercise preparation by increasing the activation of the premotor cortex (Bajaj et al., 2015a,b). Accordingly, MVF induced by a MVF task activated PMC through the components of motor imagery.

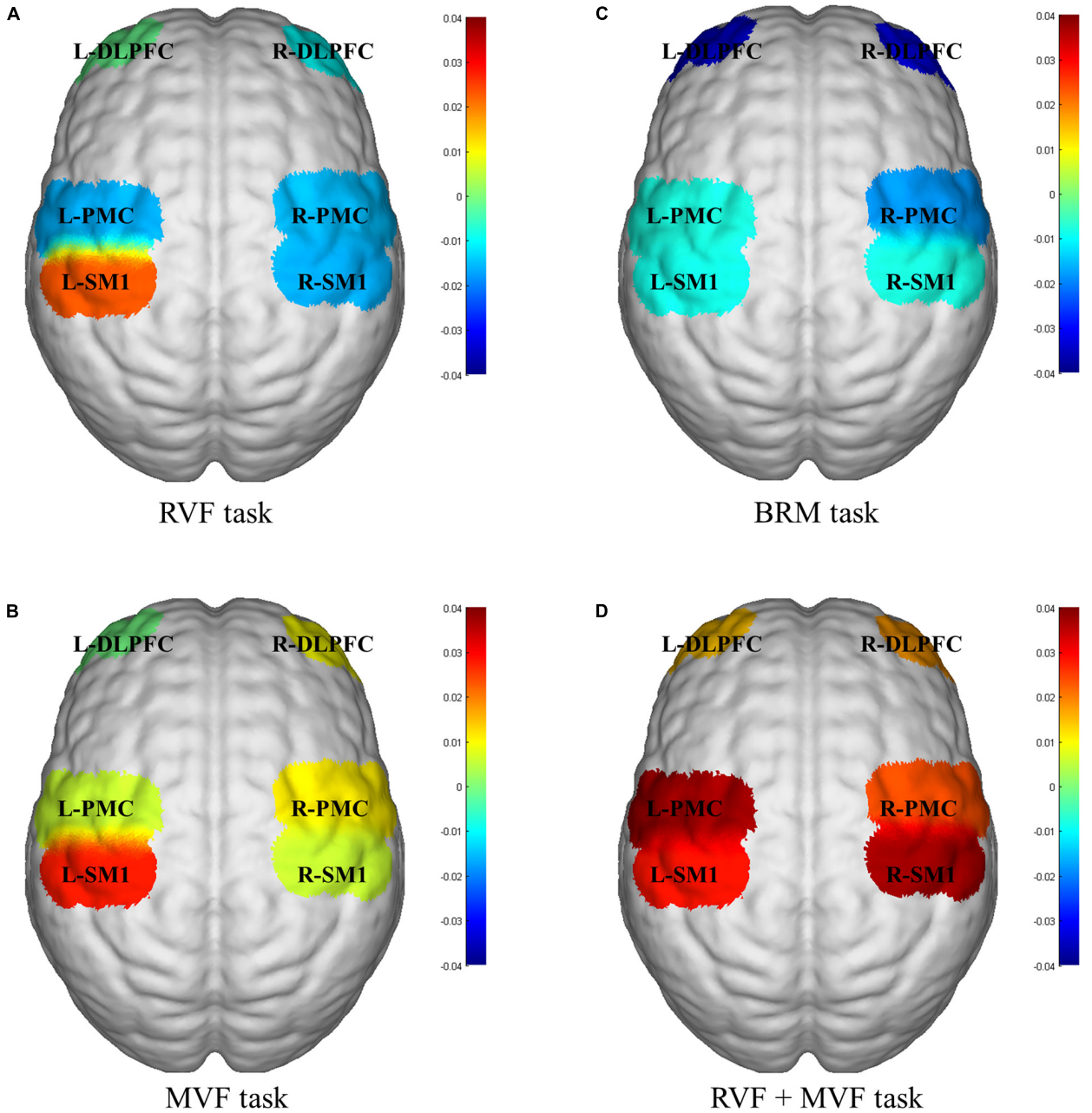

FIGURE 5 | fNIRS activation maps for four visual feedback tasks. **(A)** RVF task; **(B)** MVF task; **(C)** BRM task; **(D)** RVF+MVF task. The beta values are indicated by color. RVF task, real visual feedback task; MVF task, mirror visual feedback task; BRM task, bilateral robotic movement task; MVF + BRM task, Mirror visual feedback combined with bilateral robotic movement task; SM1, primary sensorimotor cortex; PMC, pre-motor cortex; DLPFC, dorsolateral prefrontal cortex; L, left; R, right.

These may be used as a key node in exercise preparation and can improve the neuroplasticity of the motor-related cortical areas on the mirror side.

The results also showed that the MVF + BRM task was more significantly activated in the SM1 region of mirror side than MVF task. The MVF + BRM task could significantly activate bilateral SM1, PMC, and DLPFC regions versus the BRM task. This suggests that MVF combined with BRM was more conducive to the activation of brain functional regions than MVF only or BRM only. The combination of these two strategies could lead to a synergistic gain effect. Previous studies showed that MVF induced the patient's embodiment of the feedback limb images through mirror illusion (Ding et al., 2020). Combined visual and proprioception feedback could enhance the perception of embodiment (Wittkopf et al., 2017). MVF only emphasizes the embodied perception caused by visual feedback: The limited feedback on proprioception might limit the clinical utility of MVF (Feys et al., 2004). Thus, this study combined

MVF and robotic bilateral hand movement to synchronize visual feedback and proprioceptive feedback, thus enhancing the overall embodied experience of the subjects. Moreover, about 40% of people with an acute right hemispheric and 20% of people with a left hemispheric stroke present a unilateral neglect (Ringman et al., 2004). In clinical applications, the increased attention of the affected limbs mediated by the illusion image from MVF may be beneficial to activate the movement network of the affected side.

Finally, we compared the RVF and BRM tasks. The results showed that robotic bilateral hand movement reduced activation of the left SM1. Clinical experiments also confirmed the effectiveness of bilateral training in improving upper limb motor function. Lee et al. (2017) included thirty stroke patients and found that the bilateral upper limb exercise training was more effective than conventional occupational therapy in improving upper limb function of stroke patients. Previous studies have also reported that MVF can be regarded as a special type of bilateral movement (Deconinck et al., 2015), however, compared with conventional bilateral exercise, MVF uses visual illusions to replace the actual movement of the affected side. The combination of MVF and robot linkage device just makes up for this shortcoming. The simultaneous movement of bilateral upper limbs generated by the robotic linkage device could reduce the interhemispheric inhibition, and the proprioceptive feedback of the affected side due to simultaneous movement of the bilateral upper limbs was also conducive to connections between motion control and primary motor cortex. This led to integration of interhemispheric sensory movements. This mechanism was critical for post-stroke patients especially for patients with moderate to severe upper limb motor dysfunction who might experience more brain activation inhibition from the healthy side.

Past meta-analysis of mirror therapy suggests that mirror therapy can be at least as an adjunct to conventional rehabilitation for post-stroke patients with upper limb motor dysfunction and activities of daily living (Thieme et al., 2018). However, there was lack of relevant mechanism research. In our study, the different tasks of the MVF combined robot glove showed a synergistic gain effect on the activation of the sensory motor zone. It might be a perfect combination with the bilateral movement caused by the linkage device of the robot glove and the MVF optical illusion to achieve the "central-peripheral-central" closed-loop central control is related. At the same time, the same direction bilateral upper limb movement under the linkage device can be used to improve the inhibition of the hemisphere after stroke, and the repetitive training of the contralateral side to drive the affected side is conducive to the remodeling of the cranial nerves. It is the "MVF combined with upper limb robot training" mediating the rehabilitation of upper limb motor function of patients after stroke and providing theoretical support, which can be further clinically studied in the future.

Limitation

This was a pilot study of healthy young subjects. The heterogeneity between subjects was carefully controlled. The differences in the results might largely be due to the different settings used for the experiments. Future work will test this in diseased subjects. Neuroimaging is also needed to study activation of the whole brain of MVF combined with other rehabilitation strategies.

CONCLUSION

Our study used the synchronous fNIRS to compare the immediate hemodynamics cortical activation of four visual feedback tasks in healthy subjects. The results showed the synergistic gain effect on cortical activation from MVF combined with a soft robotic bilateral hand rehabilitation system for the first time, which could be used to guide the clinical application and the future studies.

DATA AVAILABILITY STATEMENT

The raw data supporting the conclusions of this article will be made available by the authors, without undue reservation.

ETHICS STATEMENT

The studies involving human participants were reviewed and approved by the Ethics Review Committee of The Fifth Affiliated Hospital of Guangzhou Medical University. The patients/participants provided their written informed consent to participate in this study.

AUTHOR CONTRIBUTIONS

QL, HO, and YQ designed the study. QL, YQ, and YXZ drafted the manuscript. YL, WL, and RD performed the data analysis. JL, AY, YY, and YJ collected the data. JZ, AC, YNZ, SH, and BW wrote sections of the manuscript. QL and HO approved the final version of the manuscript. All authors contributed to manuscript revision, read, and approved the submitted version.

FUNDING

This study was supported by the National Science Foundation of China [Grant Number: 81902281]; the General Guidance Program of Guangzhou Municipal Health and Family Planning [Grant Numbers: 20221A011106, 20221A011109, 20211A011106, and 20211A010079]; and the National Innovation and Entrepreneurship Training Program for College Students [Grant Numbers: 202110570018 and 202110570016].

ACKNOWLEDGMENTS

We would like to thank the undergraduates of Guangzhou Medical University (Biyi Zhao, Yajie Zhang, and Xiaomin Ke), and employees of The Fifth Affiliated Hospital of Guangzhou Medical University (Wenjing Xiong, Shijuan Lang, and Wei Liao) for data collection.

REFERENCES

Al-Wasity, S. M. H., Pollick, F., Sosnowska, A., and Vuckovic, A. (2019). Cortical functional domains show distinctive oscillatory dynamic in bimanual and mirror visual feedback tasks. *Front. Computat. Neurosci.* 13:30. doi: 10.3389/fncom.2019.00030

Bai, Z., Fong, K. N. K., Zhang, J., and Hu, Z. (2020). Cortical mapping of mirror visual feedback training for unilateral upper extremity: a functional near-infrared spectroscopy study. *Brain Behav.* 10:e01489. doi: 10.1002/brb3.1489

Bajaj, S., Butler, A. J., Drake, D., and Dhamala, M. (2015a). Brain effective connectivity during motor-imagery and execution following stroke and rehabilitation. *Neuroimage Clin.* 8, 572–582. doi: 10.1016/j.nicl.2015.06.006

Bajaj, S., Butler, A. J., Drake, D., and Dhamala, M. (2015b). Functional organization and restoration of the brain motor-execution network after stroke and rehabilitation. *Front. Hum. Neurosci.* 9:173. doi: 10.3389/fnhum.2015.00173

Chatrian, G. E., Lettich, E., and Nelson, P. L. (1988). Modified nomenclature for the "10%" electrode system. *J. Clin. Neurophysiol. : Off. Publ. Am. Electroencephalogr. Soc.* 5:183. doi: 10.1097/00004691-198804000-00005

Chen, P. M., Kwong, P. W. H., Lai, C. K. Y., and Ng, S. S. M. (2019). Comparison of bilateral and unilateral upper limb training in people with stroke: a systematic review and meta-analysis. *PLoS One* 14:e0216357. doi: 10.1371/journal.pone.0216357

Chen, W.-L., Wagner, J., Heugel, N., Sugar, J., Lee, Y.-W., Conant, L., et al. (2020). Functional near-infrared spectroscopy and its clinical application in the field of neuroscience: advances and future directions. *Front. Neurosci.* 14:724. doi: 10.3389/fnins.2020.00724

Deconinck, F. J., Smorenburg, A. R., Benham, A., Ledebt, A., Feltham, M. G., and Savelsbergh, G. J. (2015). Reflections on mirror therapy: a systematic review of the effect of mirror visual feedback on the brain. *Neurorehabil. Neural Repair* 29, 349–361. doi: 10.1177/1545968314546134

Ding, L., He, J., Yao, L., Zhuang, J., Chen, S., Wang, H., et al. (2020). Mirror visual feedback combining vibrotactile stimulation promotes embodiment perception: an Electroencephalogram (EEG) pilot study. *Front. Bioeng. Biotechnol.* 8:553270. doi: 10.3389/fbioe.2020.553270

Ding, L., Wang, X., Guo, X., Chen, S., Wang, H., Jiang, N., et al. (2018). Camera-based mirror visual feedback: potential to improve motor preparation in stroke patients. *IEEE Trans. Neural Syst. Rehabil. Eng.* 26, 1897–1905. doi: 10.1109/TNSRE.2018.2864990

Feys, H., De Weerdt, W., Verbeke, G., Steck, G. C., Capiau, C., Kiekens, C., et al. (2004). Early and repetitive stimulation of the arm can substantially improve the long-term outcome after stroke: a 5-year follow-up study of a randomized trial. *Stroke* 35, 924–929. doi: 10.1161/01.STR.0000121645.44752.f7

Fong, K. N. K., Ting, K. H., Zhang, J. J. Q., Yau, C. S. F., and Li, L. S. W. (2021). Event-Related desynchronization during mirror visual feedback: a comparison of older adults and people after stroke. *Front. Hum. Neurosci.* 15:629592. doi: 10.3389/fnhum.2021.629592

Fornia, L., Puglisi, G., Leonetti, A., Bello, L., Berti, A., Cerri, G., et al. (2020a). Direct electrical stimulation of the premotor cortex shuts down awareness of voluntary actions. *Nat. Commun.* 11:705. doi: 10.1038/s41467-020-14517-4

Fornia, L., Rossi, M., Rabuffetti, M., Leonetti, A., Puglisi, G., Viganò, L., et al. (2020b). Direct electrical stimulation of premotor areas: different effects on hand muscle activity during object manipulation. *Cereb Cortex* 30, 391–405. doi: 10.1093/cercor/bhz139

French, B., Thomas, L. H., Leathley, M. J., Sutton, C. J., and Watkins, C. L. (2007). Repetitive task training for improving functional ability after stroke. Cochrane Database Syst. Rev. 4, CD006073. doi: 10.1002/14651858

Frenkel-Toledo, S., Liebermann, D. G., Bentin, S., and Soroker, N. (2016). Dysfunction of the human mirror neuron system in ideomotor apraxia: evidence from Mu suppression. *J. Cogn. Neurosci.* 28, 775–791. doi: 10.1162/jocn_a_00936

Grèzes, J., and Decety, J. (2001). Functional anatomy of execution, mental simulation, observation, and verb generation of actions: a meta-analysis. *Hum. Brain Mapp.* 12, 1–19. doi: 10.1002/1097-0193(200101)12:1<1::aid-hbm10<3.0.co;2-v

Haghshenas-Jaryani, M., Pande, C., and Muthu Wijesundara, B. J. (2019). "Soft robotic bilateral hand rehabilitation system for fine motor learning," in *Proceeding of the IEEE International Conference on Rehabilitation Robotics*, (IEEE), 337–342. doi: 10.1109/ICORR.2019.8779510

Haghshenas-Jaryani, M., Patterson, R. M., Bugnariu, N., and Wijesundara, M. B. J. (2020). A pilot study on the design and validation of a hybrid exoskeleton robotic device for hand rehabilitation. *J. Hand Ther.* 33, 198–208. doi: 10.1016/j.jht.2020.03.024

Herrador Colmenero, L., Perez Marmol, J. M., Martí-García, C., Querol Zaldivar, M. D. L. Á, Tapia Haro, R. M., Castro Sánchez, A. M., et al. (2018). Effectiveness of mirror therapy, motor imagery, and virtual feedback on phantom limb pain following amputation: a systematic review. *Prosthetics Orthotics Int.* 42, 288–298. doi: 10.1177/0309364617740230

Inagaki, Y., Seki, K., Makino, H., Matsuo, Y., Miyamoto, T., and Ikoma, K. (2019). Exploring hemodynamic responses using mirror visual feedback with electromyogram-triggered stimulation and functional near-infrared spectroscopy. *Front. Hum. Neurosci.* 13:60. doi: 10.3389/fnhum.2019.00060

Ji-feng, R., Li, D., Wen, Z., Wei-ning, W., Mei-kui, D., Li, X., et al. (2019). Effects of robot-assisted therapy combined with mirror therapy on upper limbs rehabilitation in patients with hemiplegia after stroke. *Chin. J. Rehabil. Theory Pract.* 25:709.

Kim, J. H., and Lee, B. H. (2015). Mirror therapy combined with biofeedback functional electrical stimulation for motor recovery of upper extremities after stroke: a pilot randomized controlled trial. *Occup. Ther. Int.* 22, 51–60. doi: 10.1002/oti.1384

Lee, D., and Lee, G. (2019). Effect of afferent electrical stimulation with mirror therapy on motor function, balance, and gait in chronic stroke survivors: a randomized controlled trial. *Eur. J. Phys. Rehabil. Med.* 55, 442–449. doi: 10.23736/s1973-9087.19.05334-6

Lee, M. J., Lee, J. H., Koo, H. M., and Lee, S. M. (2017). Effectiveness of bilateral arm training for improving extremity function and activities of daily living performance in hemiplegic patients. *J. Stroke Cerebrovasc. Dis.* 26, 1020–1025. doi: 10.1016/j.jstrokecerebrovasdis.2016.12.008

Liu, M., Xu, L., Li, H., Chen, S., and Chen, B. (2021). Morphological and functional changes of the tibialis anterior muscle after combined mirror visual feedback and electromyographic biofeedback in poststroke patients: a randomized trial. *Am. J. Phys. Med. Rehabil.* 100, 766–773. doi: 10.1097/phm.0000000000001628

Luo, Z., Zhou, Y., He, H., Lin, S., Zhu, R., Liu, Z., et al. (2020). Synergistic effect of combined mirror therapy on upper extremity in patients with stroke: a systematic review and meta-analysis. *Front. Neurol.* 11:155. doi: 10.3389/fneur.2020.00155

Mane, R., Chouhan, T., and Guan, C. (2020). BCI for stroke rehabilitation: motor and beyond. *J. Neural. Eng.* 17:041001. doi: 10.1088/1741-2552/aba162

Manuweera, T., Yarossi, M., Adamovich, S., and Tunik, E. (2018). Parietal activation associated with target-directed right hand movement is lateralized by mirror feedback to the ipsilateral hemisphere. *Front. Hum. Neurosci.* 12:531. doi: 10.3389/fnhum.2018.00531

Oostenveld, R., and Praamstra, P. (2001). The five percent electrode system for high-resolution EEG and ERP measurements. *Clin. Neurophysiol.* 112, 713–719. doi: 10.1016/s1388-2457(00)00527-7

Pollock, A., Farmer, S. E., Brady, M. C., Langhorne, P., Mead, G. E., Mehrholz, J., et al. (2014). Interventions for improving upper limb function after stroke. *Cochrane Database Syst. Rev.* 2014:Cd010820. doi: 10.1002/14651858.CD010820.pub2

Ramachandran, V. S., and Altschuler, E. L. (2009). The use of visual feedback, in particular mirror visual feedback, in restoring brain function. *Brain: J. Neurol.* 132(Pt 7), 1693–1710. doi: 10.1093/brain/awp135

Ramachandran, V. S., Rogers-Ramachandran, D., and Cobb, S. (1995). Touching the phantom limb. *Nature* 377, 489–490. doi: 10.1038/377489a0

Renner, C. I. E., Brendel, C., and Hummelsheim, H. (2020). Bilateral arm training vs unilateral arm training for severely affected patients with stroke: exploratory single-blinded randomized controlled trial. *Arch. Phys. Med. Rehabil.* 101, 1120–1130. doi: 10.1016/j.apmr.2020.02.007

Ringman, J. M., Saver, J. L., Woolson, R. F., Clarke, W. R., and Adams, H. P. (2004). Frequency, risk factors, anatomy, and course of unilateral neglect in an acute stroke cohort. *Neurology* 63, 468–474. doi: 10.1212/01.wnl.0000133011.10689.ce

Rizzolatti, G., and Craighero, L. (2004). The mirror-neuron system. *Annu. Rev. Neurosci.* 27, 169–192. doi: 10.1146/annurev.neuro.27.070203.144230

Rjosk, V., Lepsien, J., Kaminski, E., Hoff, M., Sehm, B., Steele, C. J., et al. (2017). Neural correlates of mirror visual feedback-induced performance improvements: a resting-state fMRI study. *Front. Hum. Neurosci.* 11:54. doi: 10.3389/fnhum.2017.00054

Rong, J., Ding, L., Xiong, L., Zhang, W., Wang, W., Deng, M., et al. (2021). Mirror visual feedback prior to robot-assisted training facilitates rehabilitation after stroke: a randomized controlled study. *Front. Neurol.* 12:683703. doi: 10.3389/fneur.2021.683703

Ruggiero, M., and Catmur, C. (2018). Mirror neurons and intention understanding: dissociating the contribution of object type and intention to mirror responses using electromyography. *Psychophysiology* 55:e13061. doi: 10.1111/psyp.13061

Schick, T., Schlake, H. P., Kallusky, J., Hohlfeld, G., Steinmetz, M., Tripp, F., et al. (2017). Synergy effects of combined multichannel EMG-triggered electrical stimulation and mirror therapy in subacute stroke patients with severe or very severe arm/hand paresis. *Restor. Neurol. Neurosci.* 35, 319–332. doi: 10.3233/rnn-160710

Straudi, S., Baroni, A., Mele, S., Craighero, L., Manfredini, F., Lamberti, N., et al. (2020). Effects of a robot-assisted arm training plus hand functional electrical stimulation on recovery after stroke: a randomized clinical trial. *Arch. Phys. Med. Rehabil.* 101, 309–316. doi: 10.1016/j.apmr.2019.09.016

Sun, P. P., Tan, F. L., Zhang, Z., Jiang, Y. H., Zhao, Y., and Zhu, C. Z. (2018). Feasibility of Functional Near-Infrared Spectroscopy (fNIRS) to investigate the mirror neuron system: an experimental study in a real-life situation. *Front. Hum. Neurosci.* 12:86. doi: 10.3389/fnhum.2018.00086

Thakkar, H. K., Liao, W. W., Wu, C. Y., Hsieh, Y. W., and Lee, T. H. (2020). Predicting clinically significant motor function improvement after contemporary task-oriented interventions using machine learning approaches. *J. Neuroeng. Rehabil.* 17:131. doi: 10.1186/s12984-020-00758-3

Thieme, H., Morkisch, N., Mehrholz, J., Pohl, M., Behrens, J., Borgetto, B., et al. (2018). Mirror therapy for improving motor function after stroke. *Cochrane Database Syst. Rev.* 7:Cd008449. doi: 10.1002/14651858.CD008449.pub3

Wan, N., Hancock, A. S., Moon, T. K., and Gillam, R. B. (2018). A functional near-infrared spectroscopic investigation of speech production during reading. *Hum. Brain Mapp.* 39, 1428–1437. doi: 10.1002/hbm.23932

Wittkopf, P. G., Lloyd, D. M., and Johnson, M. I. (2017). Changing the size of a mirror-reflected hand moderates the experience of embodiment but not proprioceptive drift: a repeated measures study on healthy human participants. *Exp. Brain Res.* 235, 1933–1944. doi: 10.1007/s00221-017-4930-7

Xu, Z., Hu, M., Wang, Z. R., Li, J., Hou, X. H., and Xiang, M. Q. (2019). The positive effect of moderate-intensity exercise on the mirror neuron system: an fNIRS study. *Front. Psychol.* 10:986. doi: 10.3389/fpsyg.2019.00986

Ye, J. C., Tak, S., Jang, K. E., Jung, J., and Jang, J. (2009). NIRS-SPM: statistical parametric mapping for near-infrared spectroscopy. *NeuroImage* 44, 428–447. doi: 10.1016/j.neuroimage.2008.08.036

Yin, Z.-L., Meng, Z.-X., Ge, S., Zhang, M.-J., and Huang, L.-H. (2020). [Clinical observation of dynamic scalp acupuncture combined with task-oriented mirror therapy for upper limbs function impairment in patients with hemiplegia after ischemic stroke]. *Zhongguo Zhen Jiu = Chinese Acupuncture Moxibustion* 40, 918–922. doi: 10.13703/j.0255-2930.20190819-0001

Zhang, J. J. Q., Fong, K. N. K., Welage, N., and Liu, K. P. Y. (2018). The activation of the mirror neuron system during action observation and action execution with mirror visual feedback in stroke: a systematic review. *Neural Plast* 2018:2321045. doi: 10.1155/2018/2321045

Zheng, Y., and Hu, X. (2011). Research progress of bilateral upper limb training in rehabilitation of stroke patients. *Chin. J. Rehabil. Med.* 26, 296–299. doi: 10.3969/j.issn.1001-1242.2011.03.027

Conflict of Interest: The authors declare that the research was conducted in the absence of any commercial or financial relationships that could be construed as a potential conflict of interest.

Publisher's Note: All claims expressed in this article are solely those of the authors and do not necessarily represent those of their affiliated organizations, or those of the publisher, the editors and the reviewers. Any product that may be evaluated in this article, or claim that may be made by its manufacturer, is not guaranteed or endorsed by the publisher.

frontiers in Neuroscience

SYSTEMATIC REVIEW
published: 07 February 2022
doi: 10.3389/fnins.2021.766879

The Effect of Brain–Computer Interface Training on Rehabilitation of Upper Limb Dysfunction After Stroke: A Meta-Analysis of Randomized Controlled Trials

*Weiwei Yang, Xiaoyun Zhang, Zhenjing Li, Qiongfang Zhang, Chunhua Xue and Yaping Huai**

Rehabilitation Department, Shenzhen Longhua District Central Hospital, Shenzhen, China

OPEN ACCESS

Edited by:
Jinhua Zhang,
Xi'an Jiaotong University, China

Reviewed by:
Rupert Ortner,
g.tec Medical Engineering Spain S.L., Spain
Hongmei Wen,
Third Affiliated Hospital of Sun Yat-sen University, China
Lei Jiang,
Hannover Medical School, Germany

****Correspondence:***
Yaping Huai
huaiyaping@163.com

Specialty section:
This article was submitted to Neuroprosthetics, a section of the journal Frontiers in Neuroscience

Received: *30 August 2021*
Accepted: *13 December 2021*
Published: *07 February 2022*

Citation:
Yang W, Zhang X, Li Z, Zhang Q, Xue C and Huai Y (2022) The Effect of Brain–Computer Interface Training on Rehabilitation of Upper Limb Dysfunction After Stroke: A Meta-Analysis of Randomized Controlled Trials. Front. Neurosci. 15:766879. doi: 10.3389/fnins.2021.766879

Background: Upper limb motor dysfunction caused by stroke greatly affects the daily life of patients, significantly reduces their quality of life, and places serious burdens on society. As an emerging rehabilitation training method, brain–computer interface (BCI)–based training can provide closed-loop rehabilitation and is currently being applied to the restoration of upper limb function following stroke. However, because of the differences in the type of experimental clinical research, the quality of the literature varies greatly, and debate around the efficacy of BCI for the rehabilitation of upper limb dysfunction after stroke has continued.

Objective: We aimed to provide medical evidence-based support for BCI in the treatment of upper limb dysfunction after stroke by conducting a meta-analysis of relevant clinical studies.

Methods: The search terms used to retrieve related articles included "brain-computer interface," "stroke," and "upper extremity." A total of 13 randomized controlled trials involving 258 participants were retrieved from five databases (PubMed, Cochrane Library, Science Direct, MEDLINE, and Web of Science), and RevMan 5.3 was used for data analysis.

Results: The total effect size for BCI training on upper limb motor function of post-stroke patients was 0.56 (95% CI: 0.29–0.83). Subgroup analysis indicated that the standard mean differences of BCI training on upper limb motor function of subacute stroke patients and chronic stroke patients were 1.10 (95% CI: 0.20–2.01) and 0.51 (95% CI: 0.09–0.92), respectively ($p = 0.24$).

Conclusion: Brain–computer interface training was shown to be effective in promoting upper limb motor function recovery in post-stroke patients, and the effect size was moderate.

Keywords: brain-computer interface, upper extremity, rehabilitation, stroke, meta-analysis

INTRODUCTION

Stroke is the leading cause of death and disability worldwide, and the 2016 Global Burden of Disease (GBD) study highlighted that Chinese people have a lifetime risk of stroke of up to 39.3%, which is the highest in the world (GBD 2016, 2018). Furthermore, persistent impairment of upper limb movement is one of the most common disabilities for patients following stroke, which seriously impact patients' daily lives (Broeks et al., 1999; Bhatnagar et al., 2020); two-thirds of patients have upper limb dysfunction 6 months after the onset of stroke (Dobkin, 2005).

To date, various rehabilitation techniques have been proposed for the rehabilitation of post-stroke patients, which include physical therapy, occupational therapy, constraint-induced motor therapy, neuromuscular electrical stimulation, and task-oriented training (Veerbeek et al., 2014; Lin et al., 2019). Most rehabilitation strategies focus mainly on behavioral training and not directly on the brain. Moreover, the effect of conventional rehabilitation on the sequelae of cerebral infarction, such as hypokinesia and poor coordination, is usually unsatisfactory. Therefore, strategies that allow direct stimulation of the brain, such as transcranial magnetic stimulation and transcranial direct current stimulation, show promise for achieving more effective outcomes.

Recent developments in the field of biomedical engineering and rehabilitation robots have led to the introduction of brain–computer interfaces (BCIs) for stroke rehabilitation. Typically, BCI systems allow the completion of specific actions independent of cerebral electricity outputs to peripheral nerves and skeletal muscles (Wolpaw et al., 2000). BCI training is composed of three modules: signal acquisition, signal processing, and interactive control. Through BCI training, patients can directly control external devices with their brain and produce corresponding movements. According to the signal source, common control modes of BCIs can be categorized into steady-state visual evoked potential, motor imagined rhythm signal, P300 potential, and mixed BCI (Yu, 2017). Furthermore, they can be classified into two general categories: auxiliary and rehabilitative BCI, depending on the forms of use. Auxiliary BCI is a commonly used paradigm in clinical work, which involves the application of BCIs to rehabilitation robots, artificial limbs, and other devices to help patients carry out daily living activities to improve their quality of life. In contrast, rehabilitative BCI acquires patients' neural signals in real time through the BCI and provides feedback training according to the signal processing results, which provides the closed-loop rehabilitation training mode from the central to the peripheral. In general, BCI training requires patients to maintain a high level of concentration during training, which enhances neural plasticity owing to the numerous repeated central stimulus feedback (Yulian and Sijie, 2020). Thus, BCI allows patients to engage in safe, standard, and repeatable rehabilitation training with maximum participation.

The clinical practice of neural rehabilitation is based on the hypothesis that motor learning promotes motor recovery after stroke (Kitago and Krakauer, 2013; Maier et al., 2019). BCI activates neural recovery through motor imagination and motion observation (da Silva et al., 2020) and ensures that patients' motor intention is well-matched with the auxiliary means during the training process to complete the "central-peripheral-central" closed-loop pathway and achieve an effective training effect (Mengya et al., 2019). Recently, several studies reported that BCI training is beneficial to the recovery of upper limb function after stroke (Baniqued et al., 2021). However, the results of these experiments vary and have limited significance for clinical applications. Therefore, we analyzed several randomized clinical trials (limited to clinical trials involving non-invasive BCI) to provide evidence-based support for BCI for the rehabilitation of upper limb dysfunction in post-stroke patients.

MATERIALS AND METHODS

Search Strategy

The review included randomized controlled trials (RCTs) that investigated the effect of BCI-based training on the rehabilitation of upper limb function in post-stroke patients. Search terms that included "upper extremity," "stroke," and "brain-computer interface" were used to query several databases, including PubMed, Cochrane Library, Science Direct, MEDLINE, and Web of Science to retrieve relevant articles. Only English articles published up until March 26, 2021, were included. We also checked the reference lists of the articles to retrieve additional relevant articles for the analysis.

Inclusion and Exclusion Criteria

The retrieved articles were independently screened by two researchers (WY and YH) by reviewing the titles and abstracts using the same inclusion and exclusion criteria. After eliminating repetitive articles using the Endnote software, we reviewed the titles and abstracts of each article to exclude review articles, non-English articles, case reports, conference minutes, and books. If we could not clearly understand the type of study by the abstract, we read the article in its entirety to avoid missing relevant research. Discrepancies were resolved by consensus with a third reviewer (CX).

The inclusion criteria for selecting the articles were as follows: (1) all stroke patients were diagnosed with confirmation by CT or MRI; (2) stroke patients had sequelae of upper limb dysfunctions; (3) control group also underwent evaluation of the effects of the BCI group and other routine rehabilitation; (4) none of the patients had cognitive impairment; (5) study design was an RCT.

The exclusion criteria were as follows: (1) studies that included patients with comorbidities of unstable tachyarrhythmia, fever, infection, seizures, or sedative use; (2) reviews, abstracts, case reports, or non-clinical studies; (3) studies that were not written in English; (4) insufficient data reported even after attempting to contact the corresponding author; (5) duplicated articles.

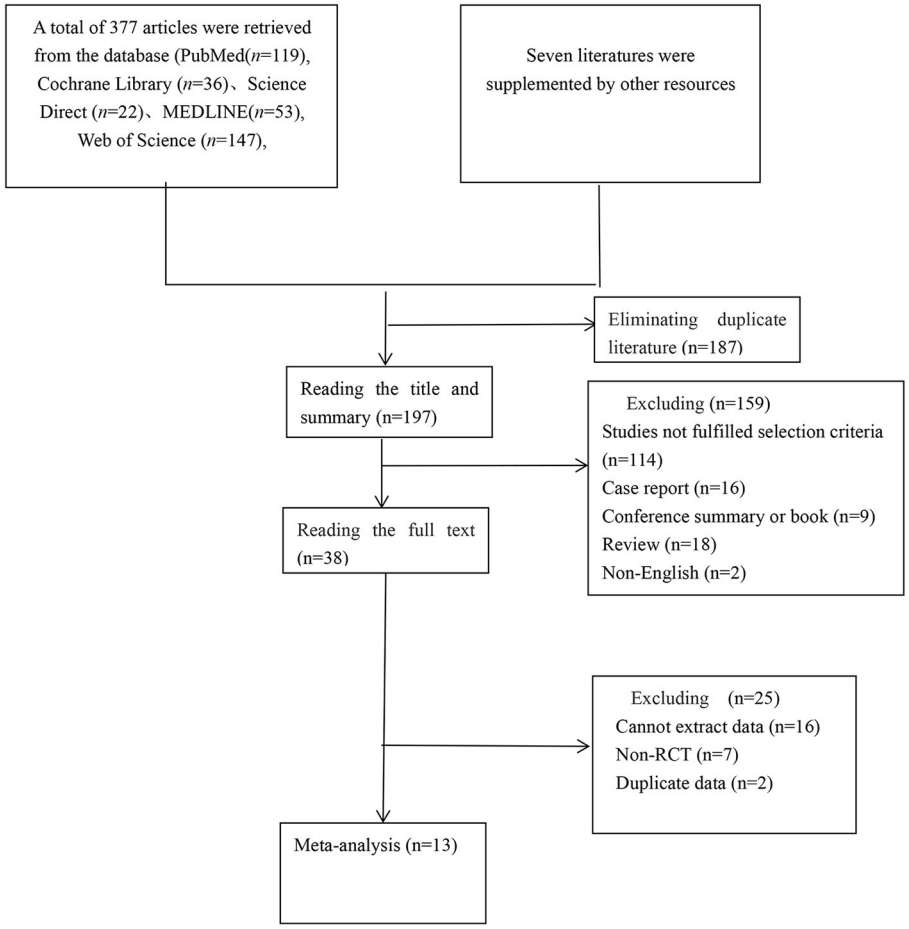

FIGURE 1 | Flow chart of study selection.

Data Extraction and Quality Assessment

The extracted information included first author name, publication year, number of participants, participant characteristics (age and sex), intervention received and time of intervention, and outcome indicators [Fugl–Meyer Assessment Scale of Upper Extremity (FMA-UE) and Modified Function Test (MFT)]. Articles that could not be classified according to the title and abstract alone were retrieved as full texts. If there were disagreements, the two authors (XZ and ZL) discussed the article with a third party (QZ) to reach a consensus. Because all the studies were RCTs, the Cochrane Handbook for Systematic Reviews of Interventions was used to assess the quality of the included studies. The criteria comprise seven elements: random sequence generation, allocation concealment, blinding of participants and personnel, blinding of outcome assessment, incomplete outcome data, selective reporting, and other sources of bias. Two researchers (CX and QZ) independently read the full text of the article to assess the quality based on the seven elements. If the study met all of the conditions, it was considered "Grade A"; if it only met some of the conditions, it was classified as "Grade B"; if the study met none of the conditions, it was considered "Grade C." If there was a conflict in grade, the quality of the article was decided following a discussion.

Outcome Indicators

Outcome indicators used in our study were FMA-UE and MFT. FMA-UE is now widely used in the clinical assessment of motor function. Previous studies have shown that FMA-UE is reliable, effective, and feasible for the evaluation of post-stroke upper limb function (Platz et al., 2005; Amano et al., 2018; Hijikata et al., 2020). However, several studies (Jang et al., 2016) used MFT as the primary evaluation standard instead of FMA-UE. Therefore, we used both the FMA-UE and MFT to calculate the pooled effect size.

Statistical Analysis

Data analysis was performed using the Review Manager software version 5.3 (a software from Cochrane Informatics and Knowledge Management Department). The data analyzed were the changes in patients from baseline to after treatment. For data collection, we calculated the mean differences between pre-

TABLE 1 | Characteristics of the RCTs.

References	Subjects		Age (years)		Type of interventions		Time of interventions	Outcome measures
	T	C	T	C	T	C		
Ang et al. (2014)	6	7	54.0 ± 8.9	58 ± 19.3	EEG-BCI + routine rehabilitation	Routine rehabilitation	1.5 h/d, 3 d/wk, 6 wk	FMA-UE
Ang et al. (2015)	11	14	48.5 ± 13.5	53.6 ± 9.5	BCI	Routine rehabilitation	1.5 h/d, 3 d/wk, 4 wk	FMA-UE
Biasiucci et al. (2018)	14	13	56.4 ± 9.9	59.0 ± 12.4	EEG-BCI + FES	Sham stimulation	1 h/d, 2 d/wk, 5 wk	FMA-UE, MFT, MRC
Jang et al. (2016)	10	10	61.10 ± 13.77	61.70 ± 12.09	BCI+FES	FES	20 min/d, 5 d/wk, 6 wk	MFT, MAS
Lee et al. (2020)	13	13	55.15 ± 11.57	58.30 ± 9.19	EEG-BCI-FES + routine rehabilitation	Routine rehabilitation	30 min/d, 5 d/wk, 4 wk	FMA-UE, MAL, MBI, ROM
Ramos-Murguialday et al. (2013)	16	14	49.3 ± 12.5	50.3 ± 12.2	EEG-BCI	Routine rehabilitation	40 min/d, 5 d/wk, 20 d	FMA-UE, MAS, GAS
Wu et al. (2020)	14	11	62.93 ± 10.56	64.82 ± 7.22	BCI	Routine rehabilitation	1 h/d, 5 d/wk, 4 wk	FMA-UE, ARAT, WMFT
Miao et al. (2020)	8	8	48.80 ± 16.70	50.3 ± 17.1	BCI + routine rehabilitation	Routine rehabilitation	3 sessions/wk, 4 wk	FMA-UE
Lin et al. (2018)	5	5	45.0 ± 11.2	49.0 ± 10.8	BCI + MTD-VR	MTD-VR	35 min/d, 3 d/wk, 4 wk	FMA-UE
Chen et al. (2020)	7	7	41.6 ± 12.0	52.0 ± 11.1	MI-BCI	MI	3 sessions/wk, 4 wk	FMA-UE
Li et al. (2014)	7	7	66.29 ± 4.89	66.00 ± 6.30	BCI + routine rehabilitation	Routine rehabilitation	1.5 h/d, 3 d/w, 8 wk	FMA-UE, ARAT
Cheng et al. (2020)	5	5	62.4 ± 4.7	61.4 ± 4.5	BCI + soft robotic	Soft robotic	90 min/session, 3 sessions/wk, 6 wk	FMA-UE, ARAT
Pichiorri et al. (2015)	14	14	64.1 ± 8.4	59.6 ± 12.7	MI-BCI	MI	30 min/d, 3 d/wk, 4 wk	FMA-UE, MAS, MRC

T, experimental group; C, control group; FMA-UE, Fugl–Meyer Assessment Scale of Upper Extremity; MFT, Modified Function Test; MRC, Medical Research Council Scale; MAS, Modified Ashworth Scale; MBI, Modified Barthel Index; ROM, range of motion; GAS, Goal Attainment Scale; ARAT, Action Research Arm Test; WMFT, Wolf Motor Function Test.

TABLE 2 | Methodological quality assessment of the RCTs.

References	Random sequence generation	Allocation concealment	Blinding of participants and personnel	Blinding of outcome assessment	Incomplete outcome data	Selective reporting	Other bias	Grade
Ang et al. (2014)	Low risk	Low risk	Unclear	Low risk	Low risk	Low risk	Low risk	B
Ang et al. (2015)	Low risk	Low risk	Unclear	Low risk	Low risk	Low risk	Low risk	B
Biasiucci et al. (2018)	Low risk	Low risk	Unclear	Low risk	Low risk	Low risk	Low risk	B
Jang et al. (2016)	Low risk	Unclear	Unclear	Low risk	Low risk	Low risk	Low risk	B
Lee et al. (2020)	Low risk	Low risk	Unclear	Low risk	Low risk	Low risk	Unclear	B
Ramos-Murguialday et al. (2013)	Low risk	Low risk	Low risk	Low risk	Low risk	Low risk	Low risk	A
Wu et al. (2020)	Low risk	Low risk	Unclear	Low risk	Low risk	Low risk	Low risk	B
Miao et al. (2020)	Low risk	Unclear	Unclear	Low risk	Low risk	Low risk	Low risk	B
Lin et al. (2018)	Low risk	Low risk	Unclear	Unclear	Low risk	Low risk	Low risk	B
Chen et al. (2020)	Low risk	Unclear	Low risk	Low risk	Low risk	Low risk	Low risk	B
Li et al. (2014)	Low risk	Low risk	Unclear	Low risk	Low risk	Low risk	Low risk	B
Cheng et al. (2020)	Low risk	Unclear	Low risk	Low risk	Low risk	Low risk	Low risk	B
Pichiorri et al. (2015)	Low risk	Low risk	Unclear	Low risk	Low risk	High risk	Low risk	B

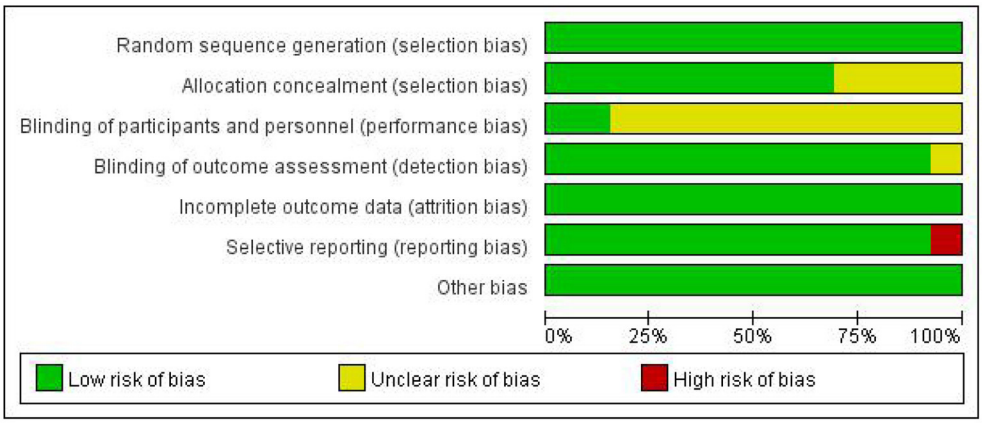

FIGURE 2 | Risk of bias graph.

and post-intervention for each study according to the Cochrane Handbook for Systematic Reviews of Interventions guidelines. The I^2 statistic was used to test the heterogeneity of the studies. If $p > 0.05$ and $I^2 \leq 50\%$, this indicated no heterogeneity among studies, and a fixed-effect model was selected for further analysis. If $p \leq 0.05$ and $I^2 > 50\%$, this indicated significant heterogeneity among studies, and a random-effects model was used for statistical analysis. If heterogeneity could not be ignored, we conducted a sensitivity analysis to determine the source of the heterogeneity. In our study, all data were continuous variables; thus, we used the standard mean difference (SMD) method. Moreover, because the included studies used different evaluation criteria, we used random-effects models for the analysis. For the subgroup analysis of intervention time, we used a random-effects model. A p-value <0.05 was considered statistically significant.

RESULTS

Search Results

A total of 384 articles were reviewed: 119 studies from PubMed, 36 studies from Cochrane Library, 22 studies from ScienceDirect, 53 studies from MEDLINE, 147 studies from Web of Science, and 7 studies from other sources. We eliminated 187 duplicate studies. The independent screening of titles and abstracts resulted in the exclusion of 18 review articles, two non-English studies, 16 case reports, and nine conference summaries or book chapters. Seventy-two studies were excluded because they compared BCI systems rather than investigating the clinical effect or were not BCI training interventions. Another 52 studies did not meet our requirements or included healthy subjects as controls. Some experiments included in the 23 articles were excluded because the data or full text could not be extracted or the study was a cross-control trial. In addition, two studies were excluded because they utilized the same data. Finally, 13 studies that comprised 258 patients were included in our meta-analysis based on the Preferred Reporting Items for Systematic Reviews and Meta-Analyses (PRISMA) protocol. The detailed literature retrieval process is shown in **Figure 1** and **Table 1** (Ramos-Murguialday et al., 2013; Ang et al., 2014, 2015; Li et al., 2014; Pichiorri et al., 2015; Jang et al., 2016; Biasiucci et al., 2018; Lin et al., 2018; Chen et al., 2020; Cheng et al., 2020; Lee et al., 2020; Miao et al., 2020; Wu et al., 2020).

Quality Assessment

The quality assessment of the included RCTs is shown in **Table 2** and **Figures 2**, **3**. A total of 130 BCI subjects and 128 patients receiving traditional treatments from 13 studies were included in the final analysis. Among the 13 studies, one was considered to have an evidence level of "Grade A," and the other 12 studies were considered to have an evidence level of "Grade B." The studies that were categorized as "Grade B" involved selective reporting, an unrigorous design, and a non-blind method. The study with the highest evidence level was that by Ramos-Murguialday et al. (2013), and the study with the lowest was by Pichiorri et al. (2015). Consistency analysis was conducted on the basic information of patients across all studies, and the differences were not significant.

Efficacy of BCI

Efficacy of BCI on Upper Limb Motor Function

Most studies (Ramos-Murguialday et al., 2013; Ang et al., 2014, 2015; Li et al., 2014; Pichiorri et al., 2015; Biasiucci et al., 2018; Lin et al., 2018; Chen et al., 2020; Cheng et al., 2020; Lee et al., 2020; Miao et al., 2020; Wu et al., 2020) used FMA-UE as the outcome measure, and one study (Jang et al., 2016) used MFT as the outcome measure. Because MFT and FMA-UE are continuous variables, we used SMD with 95% CIs to evaluate the pooled results. Results showed that BCI training significantly improved upper limb motor function [SMD = 0.70, 95% CI (0.28, 1.11), $p < 0.001$, random-effects model] (**Figure 4**). In addition, the studies had significant heterogeneity ($p < 0.001$, $I^2 = 59\%$), and the funnel plot showed an asymmetric state (**Figure 5**). For the sensitivity analysis, the meta-analysis was conducted again after removing one study at a time to investigate whether the results

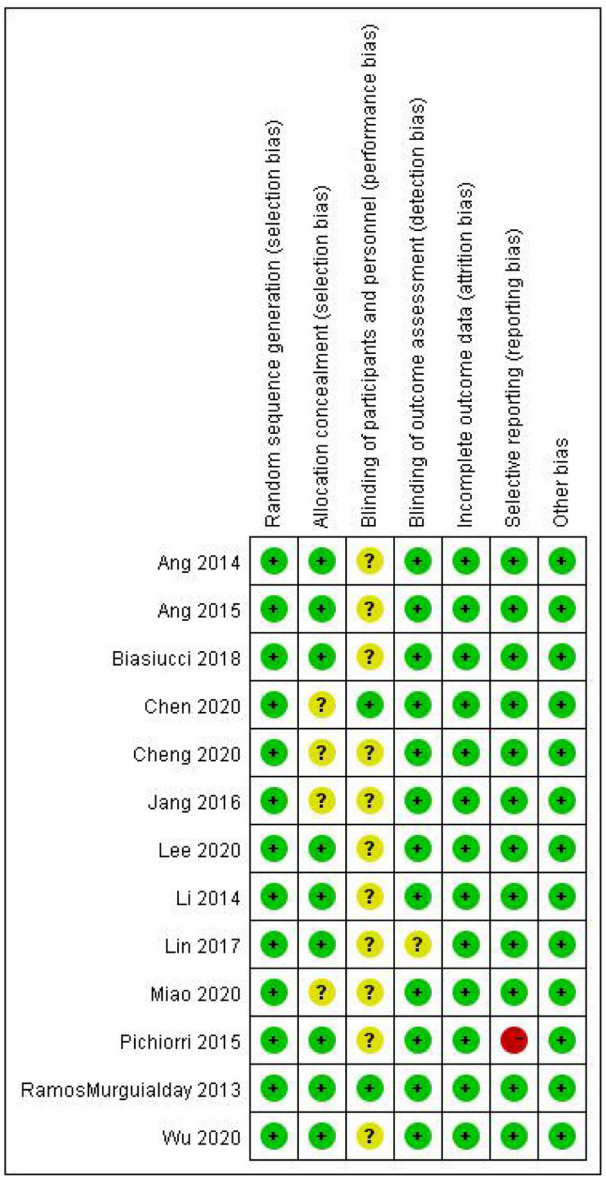

FIGURE 3 | Risk of bias summary.

changed. The sensitivity analysis revealed that the main source of heterogeneity was the study by Wu et al. (2020); after excluding this study, the heterogeneity was reduced significantly ($I^2 = 0\%$). The results of the fixed-effects model showed that BCI training significantly improves upper limb motor function [SMD = 0.56, 95% CI (0.29, 0.83), $p < 0.001$; **Figure 6**], and the funnel plot became more symmetrical (**Figure 7**).

Subgroup Analysis of the Efficacy of BCI for Different Intervention Durations

For the subgroup analysis, we used acute or subacute stroke stage as the criterion. For the intervention period following stroke, the duration of onset was limited to 6 months; longer than 6 months was considered the chronic phase, and up to 6 months was considered the subacute phase. The studies by Li et al. (2014), Pichiorri et al. (2015), Jang et al. (2016), Chen et al. (2020), and Wu et al. (2020) were included in the subacute group, and the studies by Ramos-Murguialday et al. (2013), Ang et al. (2014, 2015), Biasiucci et al. (2018), Lin et al. (2018), Cheng et al. (2020), Lee et al. (2020), and Miao et al. (2020) were included in the chronic group. As shown in **Figure 8**, the results of the subgroup analysis revealed that both the subacute [SMD = 1.10, 95% CI (0.20, 2.01), $p = 0.02$] and chronic groups exhibited a superior effect of BCI on upper limb motor function than that of the control group [SMD = 0.51, 95% CI (0.09, 0.92), $p = 0.02$]. However, the difference between the two subgroups was not significant ($p = 0.24$).

DISCUSSION

BCI training has recently emerged as a novel method to improve upper limb motor function in stroke patients. Here, we conducted a meta-analysis to investigate the efficacy of BCI training on the limb function of stroke patients.

Our meta-analysis included 258 stroke patients from 13 studies, and results showed that BCI training significantly promotes the recovery of upper limb motor function. Based on our evidence-based medical analysis of relevant studies, we found that BCI is beneficial to the recovery of upper limb function following stroke, which provides support for its clinical application. Our meta-analysis included additional studies to those conducted previously (Cervera et al., 2018; Bai et al., 2020). Because the evaluation time for limb motor function varied from 6 weeks (Ang et al., 2015) to 12–24 weeks (Cheng et al., 2020) across various studies, we investigated immediate evaluation shortly after training rather than follow-up evaluation. In addition to evaluation time, we considered intervention time as another influencing factor for treatment effects. The reviews by Cervera et al. (2018) and Bai et al. (2020) also showed that BCI training improves hand function in stroke patients. However, neither review stated whether intervention time affected efficacy. Here, we performed a subgroup analysis of intervention time, and the results suggested that both the subacute and chronic groups showed significant improvement in upper limb motor function, with the subacute group showing the greatest improvement.

The source of heterogeneity in our study came from the study conducted by Wu et al. (2020), which investigated the clinical efficacy of BCI training and the changes in brain functional networks. In contrast to other studies, patients in this study received more intense training with a total of 20 BCI training sessions (lasting for 1 h per day, 5 days per week, over 4 weeks) and shorter training time intervals between each session, which ensured that patients received sufficient treatment time. This study yielded the best efficacy.

Our findings clearly indicate that BCI training can improve patients' recovery. However, the use of external auxiliary equipment requires patients to focus and cooperate with therapists; the more that patients focus on the training, the greater the effectiveness. The BCI training system acquires,

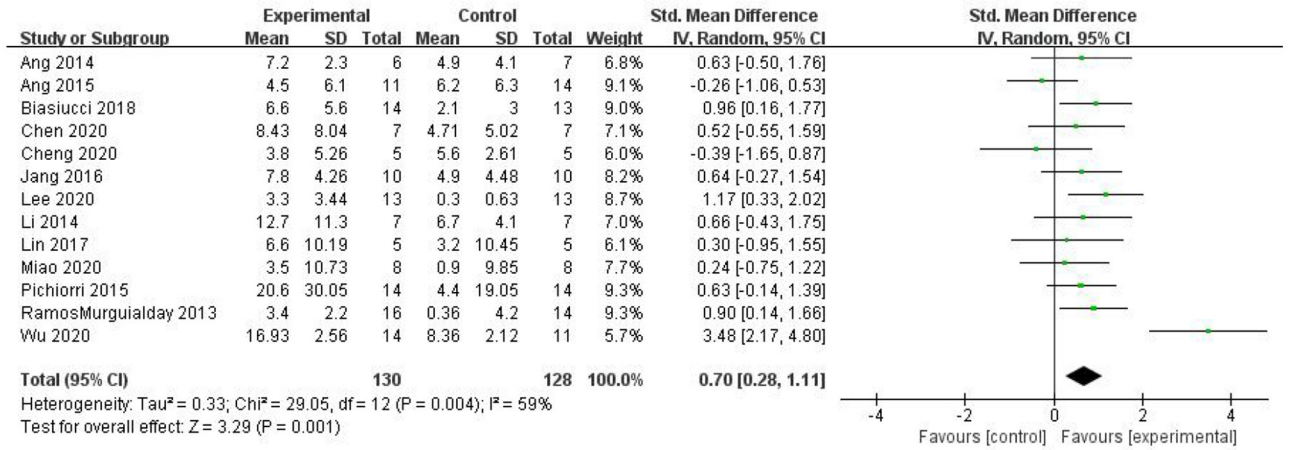

FIGURE 4 | Comparison of the effects of BCI interventions and control interventions on upper limb dysfunction before sensitivity analysis.

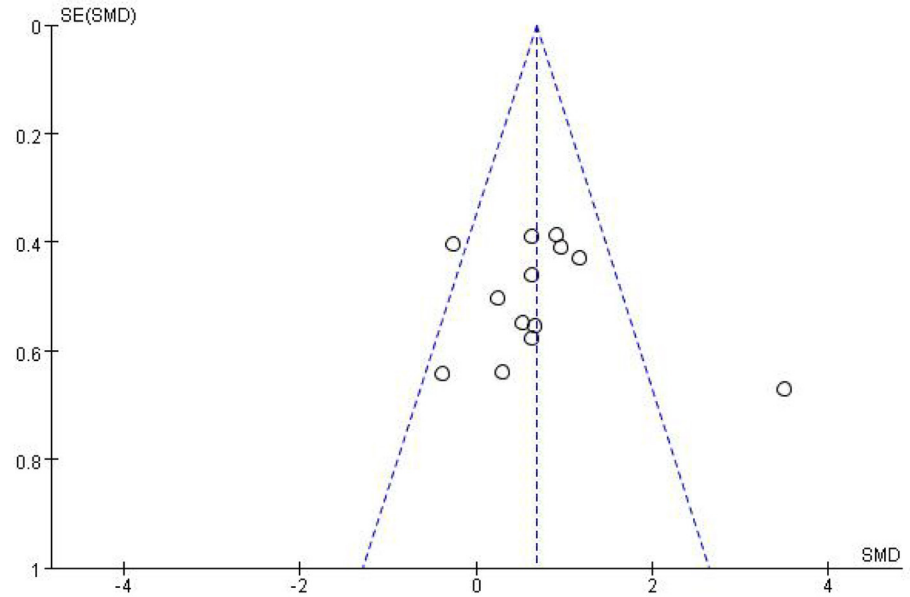

FIGURE 5 | Funnel plot of comparison of the effects of BCI interventions and control interventions on upper limb dysfunction before sensitivity analysis.

analyzes, and translates brain signals into control commands for output devices when the motor cortex of the brain sends signals indicating the intention to move (Wolpaw et al., 2002; Kim et al., 2016). The neural mechanism of BCI training is mainly attributed to changes in neuroplasticity, which may be reflected by changes in the functional connections and structure of the brain. The studies (Ramos-Murguialday et al., 2013; Li et al., 2014; Pichiorri et al., 2015; Biasiucci et al., 2018; Chen et al., 2020; Wu et al., 2020) included in our meta-analysis used electroencephalography and MRI to analyze the functional connections between hemispheres (including the temporal, parietal, occipital, and subcortical regions), which may partly explain the mechanisms. In addition to changes in brain structure, changes in the integrity of the corticospinal tract may be another contributor to the improvement in motor function. The study by Halder et al. (2013) used magnetic resonance diffusion tensor imaging to visualize structural changes and discovered that changes in the integrity (fractional anisotropy value) of the corticospinal tract of the regions of interest (e.g., the right cingulate, left fronto-occipital tract, corpus callosum, left cerebral infarction, and right posterior coronal radiation) were positively correlated with changes in motor function, which suggested that BCI training improves the integrity of the corticospinal tract to regulate neuroplasticity, and thus facilitates the improvement of motor function.

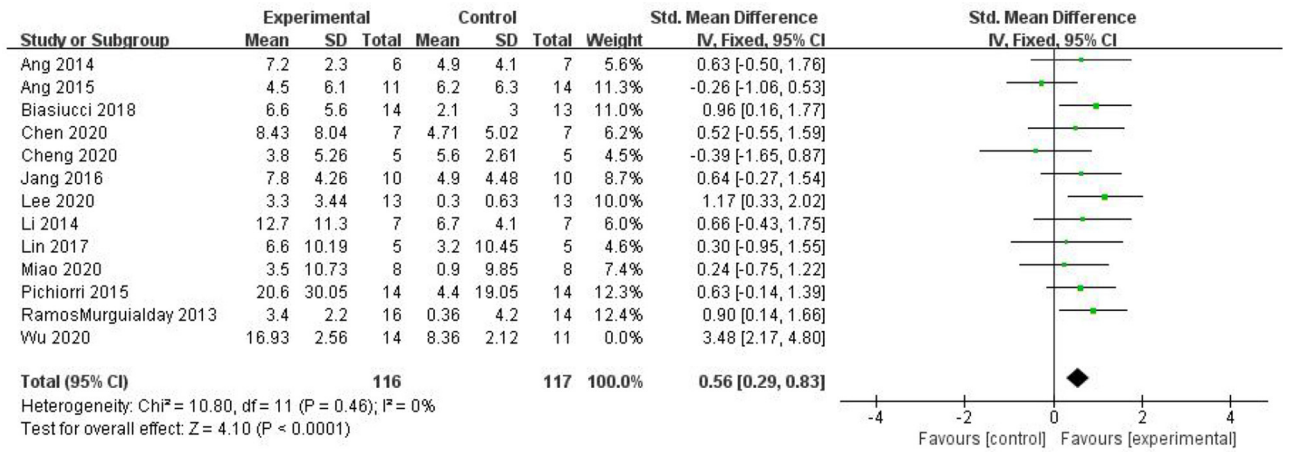

FIGURE 6 | Comparison of the effects of BCI interventions and control interventions on upper limb dysfunction before sensitivity analysis and after sensitivity analysis.

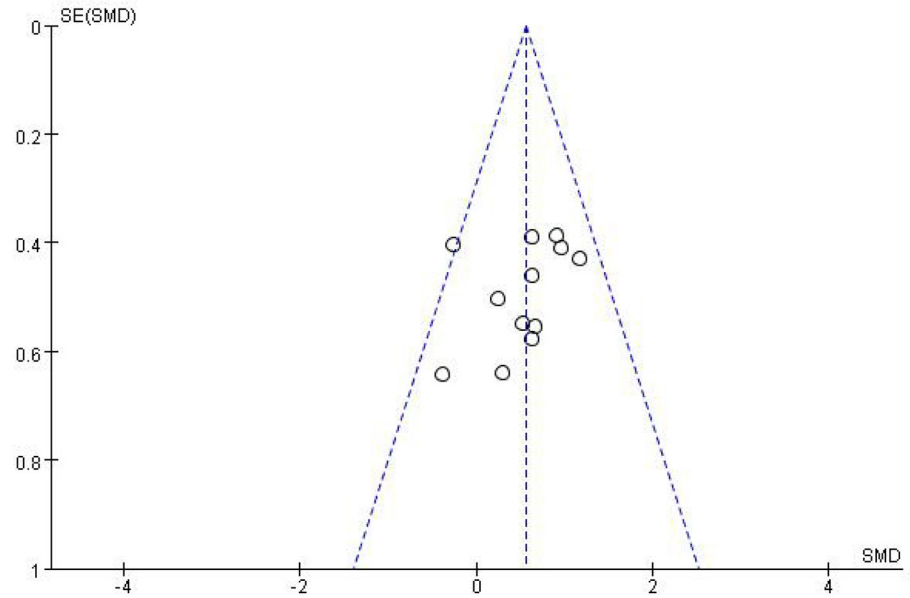

FIGURE 7 | Funnel plot of comparison of the effects of BCI interventions and control interventions on upper limb dysfunction after sensitivity analysis.

We chose FMA-UE as the evaluation indicator for motor function. FMA is a quantitative score of patient motor function based on Brunnstrom staging. In addition to FMA-UE, Modified Barthel Index (MBI) and the Modified Ashworth Scale (MAS) were also used as evaluation tools for post-stroke patients. A study conducted by Lee et al. found that MBI changed (7.07 ± 6.31) after BCI training (Lee et al., 2020), whereas another study showed no significant differences between the BCI and control groups (Jang et al., 2016) based on the MAS metric.

A limitation of our analysis is that the number of included patients was small, which may affect the quality of the review results. Because there are considerable variations in the model and implementation methods (especially treatment time) of BCI in clinical use, the efficacy of BCI training varies between individuals. Previous clinical trials seldom mention the follow-up efficacy of BCI training; thus, future studies may investigate the optimal training time to achieve favorable immediate and long-term improvements in hand function in post-stroke patients.

CONCLUSIONS

Our analysis revealed that BCI training significantly improves upper limb motor function in both subacute and chronic stroke patients. Existing studies revealed that the mechanisms of BCI are primarily related to improvements in the functional connectivity

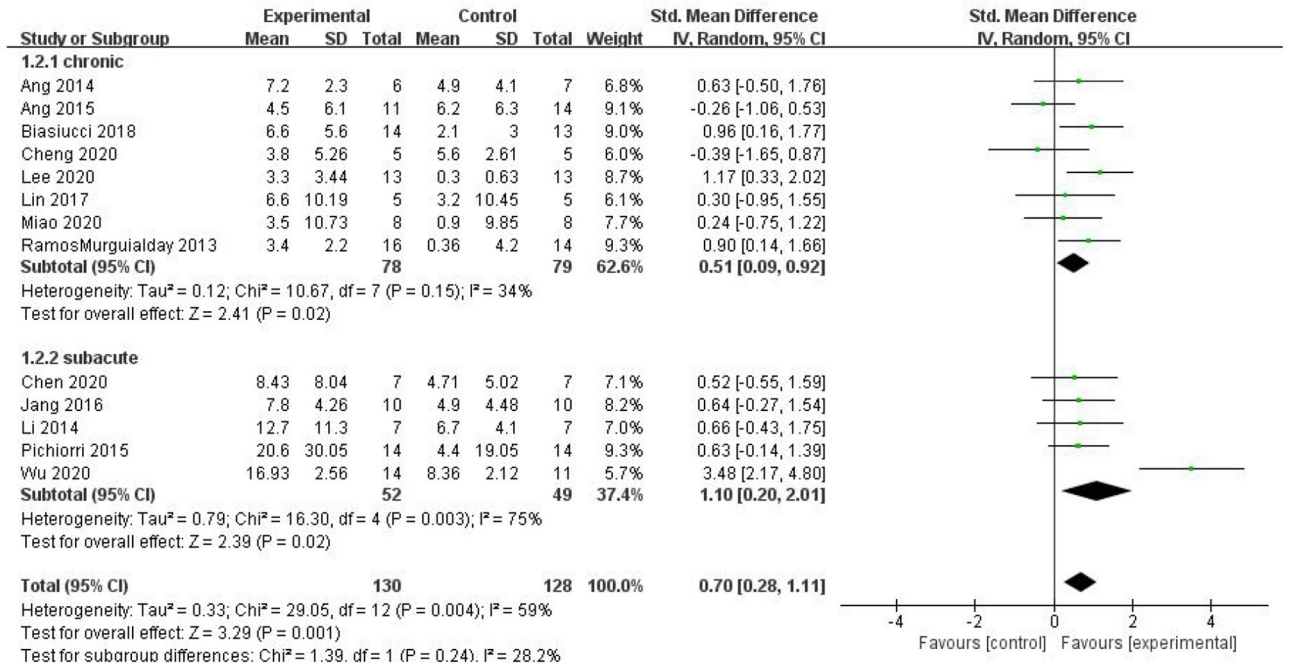

FIGURE 8 | A subgroup analysis of the effects of BCI on upper limb motor function in different intervention periods.

and structural integrity of the brain. Further studies are needed to explore optimal training and evaluation times for BCI training.

DATA AVAILABILITY STATEMENT

The original contributions presented in the study are included in the article, further inquiries can be directed to the corresponding author/s.

AUTHOR CONTRIBUTIONS

WY, YH, and XZ contributed to the typographical logic of the article. CX, QZ, and ZL provided help for the data collection of the article. All authors contributed to the article and approved the submitted version.

FUNDING

This work was supported by the Longhua District High-level Medical Team Project, the 2021 Basic Research Project of Shenzhen Science, Technology and Innovation Commission (ID: JCYJ20210324123414039), and the Shenzhen Longhua District Rehabilitation Medical Equipment Development and Transformation Joint Key Laboratory in 2021.

REFERENCES

Amano, S., Umeji, A., Uchita, A., Hashimoto, Y., Takebayashi, T., Takahashi, K., et al. (2018). Clinimetric properties of the Fugl-Meyer assessment with adapted guidelines for the assessment of arm function in hemiparetic patients after stroke. *Top. Stroke Rehabil.* 25, 500–508. doi: 10.1080/10749357.2018.1484987

Ang, K. K., Chua, K. S., Phua, K. S., Wang, C., Chin, Z. Y., Kuah, C. W., et al. (2015). of EEG-Based Motor Imagery Brain-Computer Interface Robotic Rehabilitation for Stroke. *Clin. EEG Neurosci.* 46, 310–320. doi: 10.1177/1550059414522229

Ang, K. K., Guan, C., Phua, K. S., Wang, C., Zhou, L., Tang, K. Y., et al. (2014). Brain-computer interface-based robotic end effector system for wrist and hand rehabilitation: results of a three-armed randomized controlled trial for chronic stroke. *Front. Neuroeng.* 7:30. doi: 10.3389/fneng.2014.00030

Bai, Z., Fong, K. N. K., Zhang, J. J., Chan, J., and Ting, K. H. (2020). Immediate and long-term effects of BCI-based rehabilitation of the upper extremity after stroke: a systematic review and meta-analysis. *J. Neuroeng. Rehabil.* 17:57. doi: 10.1186/s12984-020-00686-2

Baniqued, P. D. E., Stanyer, E. C., Awais, M., Alazmani, A., Jackson, A. E., Mon-Williams, M. A., et al. (2021). Brain-computer interface robotics for hand rehabilitation after stroke: a systematic review. *J. Neuroeng. Rehabil.* 18:15. doi: 10.1186/s12984-021-00820-8

Bhatnagar, K., Bever, C. T., Tian, J., Zhan, M., and Conroy, S. S. (2020). Comparing home upper extremity activity with clinical evaluations of arm function in chronic stroke. *Arch. Rehabil. Res. Clin. Transl.* 2:100048. doi: 10.1016/j.arrct.2020.100048

Biasiucci, A., Leeb, R., Iturrate, I., Perdikis, S., Al-Khodairy, A., Corbet, T., et al. (2018). Brain-actuated functional electrical stimulation elicits lasting arm motor recovery after stroke. *Nat. Commun.* 9:2421. doi: 10.1038/s41467-018-04673-z

Broeks, J. G., Lankhorst, G. J., Rumping, K., and Prevo, A. J. (1999). The long-term outcome of arm function after stroke: results of a follow-up study. *Disabil. Rehabil.* 21, 357–364. doi: 10.1080/096382899297459

Cervera, M. A., Soekadar, S. R., Ushiba, J., Millán, J. D. R., Liu, M., Birbaumer, N., et al. (2018). Brain-computer interfaces for post-stroke motor rehabilitation: a meta-analysis. *Ann. Clin. Transl. Neurol.* 5, 651–663. doi: 10.1002/acn3.544

Chen, S., Cao, L., Shu, X., Wang, H., Ding, L., Wang, S. H., et al. (2020). Longitudinal electroencephalography analysis in subacute stroke patients during intervention of brain-computer interface with exoskeleton feedback. *Front Neurosci*. 14:809. doi: 10.3389/fnins.2020.00809

Cheng, N., Phua, K. S., Lai, H. S., Tam, P. K., Tang, K. Y., Cheng, K. K., et al. (2020). Brain-computer interface-based soft robotic glove rehabilitation for stroke. *IEEE Trans. Biomed. Eng.* 67, 3339–3351. doi: 10.1109/TBME.2020.2984003

da Silva, E. S. M., Ocamoto, G. N., Santos-Maia, G. L. D., de Fátima Carreira Moreira Padovez, R., Trevisan, C., de Noronha. M. A. et al. (2020). The effect of priming on outcomes of task-oriented training for the upper extremity in chronic stroke: a systematic review and meta-analysis. *Neurorehabil. Neural. Repair*. 34, 479–504. doi: 10.1177/1545968320912760

Dobkin, B. H. (2005). Clinical practice. Rehabilitation after stroke. *N. Engl. J. Med.* 352, 1677–1684. doi: 10.1056/NEJMcp043511

GBD 2016 (2018). Lifetime risk of stroke collaborators. global, regional, and country-specific lifetime risks of stroke, 1990 and 2016. *N. Engl. J. Med*. 379, 2429–2437. doi: 10.1056/NEJMoa1804492

Halder, S., Varkuti, B., Bogdan, M., Kübler, A., Rosenstiel, W., Sitaram, R., et al. (2013). Prediction of brain-computer interface aptitude from individual brain structure. *Front. Hum. Neurosci.* 7:105. doi: 10.3389/fnhum.2013.00105

Hijikata, N., Kawakami, M., Ishii, R., Tsuzuki, K., Nakamura, T., Okuyama, K., et al. (2020). Item difficulty of fugl-meyer assessment for upper extremity in persons with chronic stroke with moderate-to-severe upper limb impairment. *Front. Neurol.* 11:577855. doi: 10.3389/fneur.2020.577855

Jang, Y. Y., Kim, T. H., and Lee, B. H. (2016). Effects of brain-computer interface-controlled functional electrical stimulation training on shoulder subluxation for patients with stroke: a randomized controlled trial. *Occup. Ther. Int*. 23, 175–185. doi: 10.1002/oti.1422

Kim, T., Kim, S., and Lee, B. (2016). Effects of action observational training plus brain-computer interface-based functional electrical stimulation on paretic arm motor recovery in patient with stroke: a randomized controlled trial. *Occup. Ther. Int*. 23, 39–47. doi: 10.1002/oti.1403

Kitago, T., and Krakauer, J. W. (2013). Motor learning principles for neurorehabilitation. *Handb. Clin. Neurol.* 110, 93–103. doi: 10.1016/B978-0-444-52901-5.00008-3

Lee, S. H., Kim, S. S., and Lee, B. H. (2020). Action observation training and brain-computer interface controlled functional electrical stimulation enhance upper extremity performance and cortical activation in patients with stroke: a randomized controlled trial. *Physiother. Theory Pract*. 7, 1–9. doi: 10.1080/09593985.2020.1831114

Li, M., Liu, Y., Wu, Y., Liu, S., Jia, J., and Zhang, L. (2014). Neurophysiological substrates of stroke patients with motor imagery-based Brain-Computer Interface training. *Int. J. Neurosci*. 124, 403–415. doi: 10.3109/00207454.2013.850082

Lin, B., Chen, J., and Hsu, H. (2018). Novel upper-limb rehabilitation system based on attention technology for post-stroke patients: a preliminary study. *IEEE Access*. 6, 2720–2731. doi: 10.1109/ACCESS.2017.2785122

Lin, I. H., Tsai, H. T., Wang, C. Y., Hsu, C. Y., Liou, T. H., and Lin, Y. N. (2019). Effectiveness and superiority of rehabilitative treatments in enhancing motor recovery within 6 months poststroke: a systemic review. *Arch. Phys. Med. Rehabil.* 100, 366–378. doi: 10.1016/j.apmr.2018.09.123

Maier, M., Ballester, B. R., and Verschure, P. F. M. J. (2019). Principles of neurorehabilitation after stroke based on motor learning and brain plasticity mechanisms. *Front. Syst. Neurosci*. 13:74. doi: 10.3389/fnsys.2019.00074

Mengya, W., Zhongpeng, W., Long, C., Baikun, W., Xiaosong, G., and Dong, M. (2019). Research progress and prospects of motor neurofeedback rehabilitation training after stroke. *Chin. J. Biomed. Eng.* 38, 742–752. doi: 10.3969/j.issn.0258-8021.2019.06.013

Miao, Y., Chen, S., Zhang, X., Jin, J., Xu, R., Daly, I., et al. (2020). BCI-based rehabilitation on the stroke in sequela stage. *Neural. Plast*. 2020:8882764. doi: 10.1155/2020/8882764

Pichiorri, F., Morone, G., Petti, M., Toppi, J., Pisotta, I., Molinari, M., et al. (2015). Brain-computer interface boosts motor imagery practice during stroke recovery. *Ann. Neurol*. 77, 851–865. doi: 10.1002/ana.24390

Platz, T., Pinkowski, C., van Wijck, F., Kim, I. H., di Bella, P., and Johnson, G. (2005). Reliability and validity of arm function assessment with standardized guidelines for the Fugl-Meyer Test, action research arm test and box and block test: a multicentre study. *Clin. Rehabil*. 19, 404–411. doi: 10.1191/0269215505cr832oa

Ramos-Murguialday, A., Broetz, D., Rea, M., Läer, L., Yilmaz, O., Brasil, F. L., et al. (2013). Brain-machine interface in chronic stroke rehabilitation: a controlled study. *Ann. Neurol*. 74, 100–108. doi: 10.1002/ana.23879

Veerbeek, J. M., van Wegen, E., van Peppen, R., van der Wees, P. J., Hendriks, E., Rietberg, M., et al. (2014). What is the evidence for physical therapy poststroke? A systematic review and meta-analysis. *PLoS ONE*. 9:e87987. doi: 10.1371/journal.pone.0087987

Wolpaw, J. R., Birbaumer, N., Heetderks, W. J., McFarland, D. J., Peckham, P. H., Schalk, G., et al. (2000). Brain-computer interface technology: a review of the first international meeting. *IEEE Trans. Rehabil. Eng.* 8, 164–173. doi: 10.1109/TRE.2000.847807

Wolpaw, J. R., and Birbaumer, N., McFarland, D. J., Pfurtscheller, G., Vaughan, T. M. (2002). Brain-computer interfaces for communication and control. *Clin. Neurophysiol*. 113, 767–791. doi: 10.1016/S1388-2457(02)00057-3

Wu, Q., Yue, Z., Ge, Y., Ma, D., Yin, H., Zhao, H., et al. (2020). Brain functional networks study of subacute stroke patients with upper limb dysfunction after comprehensive rehabilitation including BCI training. *Front. Neurol*. 10:1419. doi: 10.3389/fneur.2019.01419

Yu, L. (2017). Progress in technology and application of brain-computer interface. *Chin. J. Pharmacol. Toxicol*. 31, 1068–1074. doi: 10.3867/j.issn.1000-3002.2017.11.006

Yulian, Z., and Sijie, L. (2020). Review of brain computer interface technology in the treatment of motor dysfunction after stroke. *Rehabil. Med*. 30, 162–166. doi: 10.3724/SP.J.1329.2020.02015

Conflict of Interest: The authors declare that the research was conducted in the absence of any commercial or financial relationships that could be construed as a potential conflict of interest.

Publisher's Note: All claims expressed in this article are solely those of the authors and do not necessarily represent those of their affiliated organizations, or those of the publisher, the editors and the reviewers. Any product that may be evaluated in this article, or claim that may be made by its manufacturer, is not guaranteed or endorsed by the publisher.

frontiers in Neuroscience

ORIGINAL RESEARCH
published: 11 February 2022
doi: 10.3389/fnins.2021.766648

Functional Reorganization After Four-Week Brain–Computer Interface-Controlled Supernumerary Robotic Finger Training: A Pilot Study of Longitudinal Resting-State fMRI

*Yuan Liu, Shuaifei Huang, Zhuang Wang, Fengrui Ji and Dong Ming**

Academy of Medical Engineering and Translational Medicine (AMT), Tianjin University, Tianjin, China

OPEN ACCESS

Edited by:
Jing Wang,
Xi'an Jiaotong University, China

Reviewed by:
Gionata Salvietti,
University of Siena, Italy
Hewei Wang,
Fudan University, China
Shuichi Nishio,
Advanced Telecommunications Research Institute International (ATR), Japan

***Correspondence:**
Dong Ming
richardming@tju.edu.cn

Specialty section:
This article was submitted to Neuroprosthetics, a section of the journal Frontiers in Neuroscience

Received: *29 August 2021*
Accepted: *21 December 2021*
Published: *11 February 2022*

Citation:
Liu Y, Huang S, Wang Z, Ji F and Ming D (2022) Functional Reorganization After Four-Week Brain–Computer Interface-Controlled Supernumerary Robotic Finger Training: A Pilot Study of Longitudinal Resting-State fMRI. Front. Neurosci. 15:766648. doi: 10.3389/fnins.2021.766648

Humans have long been fascinated by the opportunities afforded through motor augmentation provided by the supernumerary robotic fingers (SRFs) and limbs (SRLs). However, the neuroplasticity mechanism induced by the motor augmentation equipment still needs further investigation. This study focused on the resting-state brain functional reorganization during longitudinal brain–computer interface (BCI)-controlled SRF training in using the fractional amplitude of low-frequency fluctuation (fALFF), regional homogeneity (ReHo), and degree centrality (DC) metrics. Ten right-handed subjects were enrolled for 4 weeks of BCI-controlled SRF training. The behavioral data and the neurological changes were recorded at baseline, training for 2 weeks, training for 4 weeks immediately after, and 2 weeks after the end of training. One-way repeated-measure ANOVA was used to investigate long-term motor improvement [$F(2.805,25.24) = 43.94$, $p < 0.0001$] and neurological changes. The fALFF values were significantly modulated in Cerebelum_6_R and correlated with motor function improvement ($r = 0.6887$, $p < 0.0402$) from t0 to t2. Besides, Cerebelum_9_R and Vermis_3 were also significantly modulated and showed different trends in longitudinal SRF training in using ReHo metric. At the same time, ReHo values that changed from t0 to t1 in Vermis_3 was significantly correlated with motor function improvement ($r = 0.7038$, $p < 0.0344$). We conclude that the compensation and suppression mechanism of the cerebellum existed during BCI-controlled SRF training, and this current result provided evidence to the neuroplasticity mechanism brought by the BCI-controlled motor-augmentation devices.

Keywords: supernumerary robotic finger, resting-state fMRI, fALFF, ReHo, DC, neuroplasticity

INTRODUCTION

The hands and fingers are the important mediums for humans to interact with the outside world and have a well-established functional representation in the brain (Jones and Lederman, 2006; Dall'Orso et al., 2018; Arcaro et al., 2019). Scientists are currently focusing on the hand or arm motor augmentation device like the supernumerary robotic fingers (SRF) and

even the entire limbs (SRL) (Llorens-Bonilla et al., 2012; Parietti and Asada, 2013; Parietti et al., 2014; Prattichizzo et al., 2014; Wu and Asada, 2015; Hussain et al., 2017a,b,c; Kieliba et al., 2021). These devices have changed the way our inherent limbs interact with the external environment and bring some effects on the brain and the corticospinal motor synergies (Kieliba et al., 2021; Rossi et al., 2021). However, despite motor augmentation caused by these devices can be clearly observed in behavioral experiments, little notice is given to the brain neuroplasticity mechanism. Here, we used the brain–computer interface (BCI)-controlled SRF system to investigate longitudinal neuroplasticity changes in 4 weeks by using resting-state fMRI (rs-fMRI) local metrics like ALFF, ReHo, and DC.

In the present research on the SRF, the motor augmentation effects were clearly investigated in behavior measurement. For normal people, the extra robotic finger can enhance manipulation dexterity and enlarge the workspace of humans, like grasping a larger-sized object using one hand or completing two-handed collaboration tasks using one hand (Prattichizzo et al., 2014; Wu and Asada, 2015; Kieliba et al., 2021). For patients, the extra robotic finger can compensate missing grasping abilities and help rehabilitation training, like assistance in grasping the cup or manipulation dexterity training for the paretic hand (Hussain et al., 2017a,b,c). However, there was only some preliminary research focus on the brain neuroplasticity effect caused by SRF. From task-based fMRI analysis, it was clearly found that the bilateral cingulate cortex, bilateral superior parietal lobule, left inferior parietal lobule, and right middle frontal gyrus have greater neural representation in the finger opposition task after 2 days of SRF training (Hussain et al., 2017b). The biological hand neural representation in the sensorimotor cortex will generate a shrinkage after 5 days of third thumb wearing training (Kieliba et al., 2021). In addition, healthy humans wearing the SRF will rapidly reshape the pattern of corticospinal outputs toward the forearm and hand muscles governing imagined grasping actions of different objects after a few minutes of training (Rossi et al., 2021) and suggesting that human beings are open to very quick welcoming emerging augmentative bioartificial corticospinal grasping strategies. However, these studies did not pay attention to the long duration training effect on the resting state neuroplasticity of the brain, and these results are affected by the control method of the SRF.

Different from the EMG control (Kieliba et al., 2021) or toe switch control (Hussain et al., 2017b) that required residual motor function, the brain–computer interface (BCI) has been developed to transmit autonomous control intentions to corresponding external execution devices such as robots, orthosis, and functional electrical stimulation (Yuan et al., 2020). A previous study has proven that the human brain has the ability to bear the load of the supernumerary finger from the research of polydactyly subjects (Mehring et al., 2019) and the six-finger illusory perception creation (Newport et al., 2016; Cadete and Longo, 2020). The motor imagery (MI) technology based on BCI has great advantages of transmitting human intentions into the control of the external devices proven in the research of the third arm (Penaloza and Nishio, 2018). From task-based fMRI analysis, MI consistently recruits the frontoparietal network and the subcortical and cerebellar regions (Hetu et al., 2013). As for the reason that MI possesses a similar activation of the motor area during the motor execution, it has been widely used in clinical rehabilitation (Eaves et al., 2014). Clinical studies have found that functional connectivity between sensorimotor regions was significantly modulated after motor imagery training of the own inherent inborn limbs of stroke patients (Zhang et al., 2016). In addition, the rehabilitation neuroplasticity effect has also been fully proved in combination with MI and rehabilitation equipment (Kim et al., 2016; Biasiucci et al., 2018; Wang et al., 2018; Yuan et al., 2021). A study has found that the MI-guided robot-hand training robot has significantly modulated the time variability of the sensory–motor areas, attention network, auditory network, and default mode network in stroke patients than the no MI-guided training group (Wang et al., 2018), and training promotes the recruitment of selected brain areas and facilitates neuroplasticity by providing feedback on the intended movement (Cervera et al., 2018). However, there is currently no neuroplasticity research on the MI-controlled supernumerary robotic limb training. Here, we used the BCI-controlled SRF system based on MI mechanism to investigate the resting state changes of the human brain.

Resting-state functional magnetic resonance imaging (rs-fMRI) is a promising tool to investigate functional alterations in the human brain, which takes into account the advantages of both spatial resolution and time resolution, and also has unique advantages in clinical conditions because it does not require participants to engage in cognitive activities (Biswal et al., 1995; Fox and Raichle, 2007). Although the majority of analytic techniques [functional connectivity (FC) (Friston, 1994), graph theory, independent component analysis (ICA), etc.] for rs-fMRI data characterize the function of the brain network, the local dynamics cannot be fully addressed with these approaches (Lv et al., 2019). Several methods have been proposed to characterize the local dynamic properties of the rs-fMRI signal: fractional amplitude of low-frequency fluctuation (fALFF) (Zou et al., 2008), regional homogeneity (ReHo) (Zang et al., 2004), and degree centrality (DC) (Buckner et al., 2009). The fALFF measures the relative predominance of low-frequency amplitude to the amplitude of all oscillations across the entire power spectrum (Zou et al., 2008). ReHo was proposed to measure the synchronization of the voxel time courses with the neighboring voxels based on the hypothesis that voxels within a functional brain area synchronize their metabolic activity depending on specific conditions (Zang et al., 2004). DC mapped the degree of intrinsic FC across the brain in order to reflect a stable property of cortical network architecture at the voxel level (Buckner et al., 2009). These three voxel-wise metrics define brain functional characteristics from different perspectives (single voxel, neighboring voxels, and whole brain) and present the progressive relationship (Lv et al., 2019).

This current study aims to fill this gap by investigating the functional reorganization of 4 weeks of BCI-controlled SRF training based on the new supernumerary robotic finger imagery paradigm. Specifically, we sought to determine how SRF training influence the local function by using three local metrics (fALFF, ReHo, and DC) and whether those local changes (if observed)

are associated with behavioral performance of the participants. These findings in this study may bring some insights into the mechanism of neuroplasticity brought by the BCI-controlled augmentative device.

MATERIALS AND METHODS

Participants

Ten participants (4 females; aged 21.5 years; range 20–23 years) were recruited from Tianjin University. Participants were all right handed (laterality quotient 0.89 ± 0.09; range 0.60–1.0) as assessed by the Edinburgh Handedness questionnaire. Participants gave informed consent, and the study was approved by the Tianjin University Human Research Ethics Committee.

Training System and Intervention Protocols

A self-designed brain control supernumerary robotic finger (SRF) system was used in this training (**Figure 1A**; Liu et al., 2021a,b). The whole system contained six modules: EEG acquisition, EEG control, SRF control, SRF finger, TENS feedback, and status information module. The EEG acquisition module uses the module OPENBCI to collect the eight channels of EEG signals of FC1, FC2, FCZ, etc., with a sampling frequency of 250 Hz. Then the EEG signal is resampled, filtered (8- to 13-Hz bandpass, 50-Hz notch), re-referenced, ICA, and time-frequency features extracted. Finally, the preprocessed EEG signal is imported into the convolutional neural network (CNN) to obtain the training model. The CNN was formed by two convolutional layers, a pooling layer and two fully connected layers. The first layer of convolution kernel was to extract the time characteristics of each channel and frequency band of EEG signal. The second layer of convolution kernel was to integrate the eight channel features and extract the signal spatial features. Finally, the two fully connected layers were used to realize the training of the two-feature classification model of MI state and resting state (Dose et al., 2018). A novel "sixth-finger" motor imaginary (MI) paradigm is performed to provide the SRF natural control. Participants wear the SRF and imagined the SRF finger opposing with the inborn inherent finger from the first-person perspective. Based on the developed "sixth-finger" MI decoding algorithm, the difference between the MI and resting (rest) state of the EEG signal can be classified, and the training model of the MI state is used for online classification. The EEG characteristic investigation interrelated with the new MI paradigm is investigated in detail in another paper of our team (Liu et al., 2021b).

The SRF finger module is driven by a single actuator and has one DOF (degree of freedom) to perform the flexion and extension. When the system captures the MI signal, the SRF finger module will flex, and participants will move their inborn inherent finger to cooperate with the SRF finger. In the SRF fingertip, a capacitive sensor detects the finger force signal and give the feedback to the system to make the SRF finger extend. At the same time, the TENS feedback module will release a 0.2-s electrical stimulation (duty factor: 50%, frequency: 5 Hz, voltage: 10 V) to the median nerve of the forearm wearing the SRF.

The SRF finger was worn on the left hand, and the reason for using subdominant hands (left hand) instead of dominant (right hand) is the better anti-interference ability for daily life activities (**Figure 1C**). During the training, participants were asked to sit in front of a table to keep their bodies relaxed. All participants received a 20-session BCI-controlled SRF training in 4 weeks with an intensity of five sessions per week and 1 h per session. During each training session, the subject was required to imagine the MI paradigm. When the system completes one MI trigger, the SRF finger will bend four times and cooperate with the inherent four fingers to complete a round of SRF-finger opposition task. The training opposition sequence is little, middle, ring, index (Sale et al., 2017; **Figure 1B**), and the intermittent breaks every 10 repetitions were given to avoid fatigue.

Data Acquisition

Behavioral and rs-fMRI measures were obtained in four time periods: before training (t0), training for 2 weeks (t1), immediately after 4 weeks of training (t2), and 2 weeks after the intervention (t3).

Behavioral Measure

The performance of participants on the SRF-finger opposition tasks was evaluated by the number of correct sequences completed in 30 s. The performance was documented online with a handheld video camera and quantified offline. Participants performed both trained and control sequences (Sale et al., 2017) using their left hand with SRF, as shown in the opposition sequence figure of **Figure 1B**. The trained sequence (order: little, middle, ring, index) was used for every day training and collected in data acquisition periods. The control sequence (order: little, index, ring, middle) was only acquired in data acquisition periods to investigate whether training induced any spill-over of effects to a novel sequence. This method has been used in other finger training tasks (Sale et al., 2017). Furthermore, prior to the quantification of baseline performance of the sequences (before training), participants were given a brief period of time (two to three sequences) to practice the two sequences.

Image Data Acquisition

All participants were scanned with a 3T Siemens MAGNETOM Skyra scanner at Tianjin Huanhu Hospital (Department of Neurosurgery, Tianjin, China). Resting-state fMRI images were acquired using T2-weighted gradient-echo planner imaging (EPI) sequence (TR = 2,000 ms, TE = 30 ms, flip angle = 90°, FOV = 220 × 220 mm^2, matrix = 64 × 64, slice thickness = 3 mm, gap = 0 mm, voxel size = 3.5 × 3.5 × 4 mm^3, acquisition time = 8:06 min). During the scanning, participants were instructed to stay still and keep their eyes closed without falling asleep. In addition, a T1-weighted structural image was acquired for each participant using the MPRAGE sequence (TR = 2,000 ms, TE = 2.98 ms, flip angle = 9°, FOV = 256 × 256 mm^2, matrix = 256 × 256, slice thickness = 1 mm, voxel size 1 × 1 × 1 mm^3, acquisition time = 4:26 min).

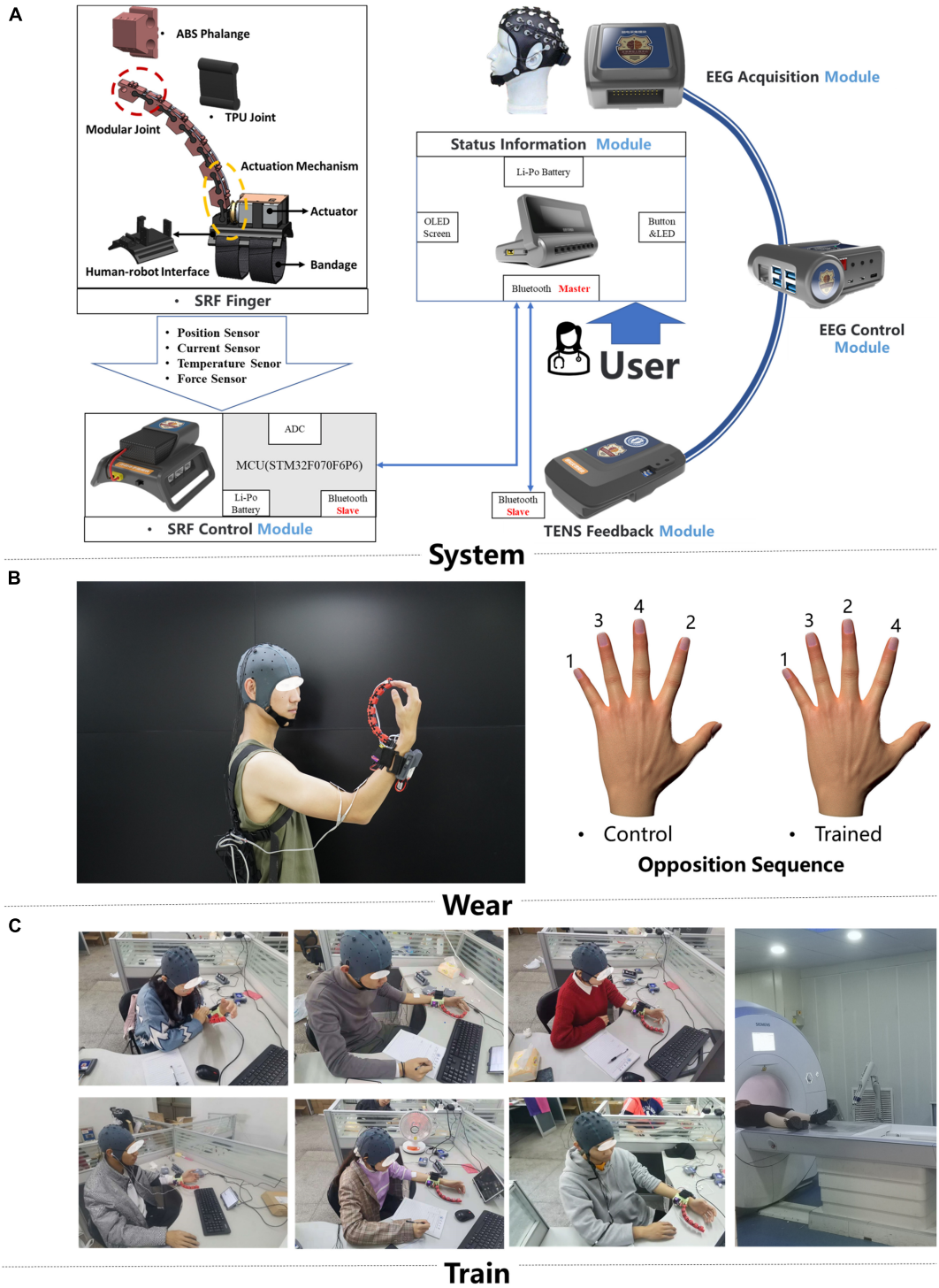

FIGURE 1 | Training system and intervention protocols. **(A)** The hardware design of the brain computer interface (BCI)-controlled supernumerary robotic finger (SRF) system and the signal transmission diagram **(B)**. The display of the portable SRF and behavioral measure paradigm. **(C)** Scene of subjects wearing SRF training.

Image Processing

Resting-State fMRI Data Preprocessing

Resting-state fMRI data were processed using SPM12 and RestPlus (Jia et al., 2019) including (1) removing the first 10 time points to make the longitudinal magnetization reach steady state and to let the participant get used to the scanning environment, (2) slice timing to correct the differences in image acquisition time between slices, (3) head motion correction,

(4) spatial normalization to the Montreal Neurological Institute (MNI) space via the deformation fields derived from tissue segmentation of structural images (resampling voxel size = 3 mm × 3 mm × 3 mm), (5) spatial smoothing with an isotropic Gaussian kernel with a full width at half maximum (FWHM) of 6 mm, (6) removing linear trend of the time course, (7) regressing out the head motion effect (using Friston 24 parameter) from the fMRI data (Friston et al., 1996), and (8) band-pass filtering (0.01–0.08 Hz). One participant was excluded from further analysis due to large head motion (more than 3.0 mm of maximal translation in any direction of x, y, or z or 3.0° of maximal rotation throughout the course of scanning).

Fractional Amplitude of Low-Frequency Fluctuation Calculation

After data preprocessing (exclude preprocessing part 8: band-pass filtering), the time series for each voxel was transformed into the frequency domain using a fast Fourier transform, and the power spectrum was then obtained. The averaged square root was obtained across 0.01–0.08 Hz at each voxel, and this value was regarded as the power and then a ratio of the power of each frequency at the low-frequency range (0.01–0.08 Hz) to that of the entire frequency range (0–0.25 Hz) as the fALFF value (Zou et al., 2008).

Regional Homogeneity Calculation

After preprocessing (exclude preprocessing part 5: spatial smoothing), ReHo maps were produced by the Kendall's coefficient of concordance (KCC) of the given voxel time series with its nearest 26 neighbors. The formula is as follows:

$$W = \frac{\sum (R_i)^2 - n\left(\bar{R}\right)^2}{\frac{1}{12}K^2\left(n^3 - n\right)} \quad (1)$$

where W is the KCC among the given voxels, ranging from 0 to 1; R_i is the sum rank of the ith time point; $\overline{R}$ = [(n+1)K]/2 is the mean of R_i′s; K is the number of the time series within a measured cluster (K = 7, 19, and 27, respectively. 27 in the current study); and n is the number of ranks. This method measures the local synchronization of the given time series (Zang et al., 2004).

Degree Centrality Calculation

Degree centrality is defined as the sum of weights from edges connecting to a node. After preprocessing (exclude preprocessing part 5: spatial smoothing), Pearson's correlation of time series was performed between each voxel, and the correlation coefficients were summed up for each voxel after taking the threshold ($r \geq 0.25$), and then a weighted DC was obtained for each voxel. The weighted DC of each voxel was further divided by the global mean weighted DC of each individual for group comparison (Zuo et al., 2012). This method is also called the function connectivity strength (FCS).

Statistical Analysis

The performance of SRF-finger opposition sequences was analyzed using one-way repeated measures ANOVA at time level (t0, t1, t2, and t3) and *post-hoc* analyses were performed using Bonferroni's *post-hoc* test. At the same time, the correct number changes of the SRF-finger opposition sequences were counted and used to correlate with the MRI data. Statistical analyses were performed using SPSS 22 (IBM SPSS Statistics, NY, United States) with the significance level set at $p < 0.05$.

For longitudinal comparisons, one-way repeated-measure ANOVA and Bonferroni's *post-hoc* test was used to explore the significance of differences in ALFF, ReHo, and DC changes among various time-related subgroups. In addition, multiple comparisons were corrected using the GRF correction (the voxel-wise, $p < 0.005$; the cluster-wise, $p < 0.05$) in the RestPlus toolbox. For any measure (fALFF, ReHo, and DC) showing training-related alterations, a Pearson correlation analysis was used to assess its associations with behavioral performance of the participant. The correlations were considered significant at a threshold of $p < 0.05$.

RESULTS

Behavioral Performance

Following training, there was a significant improvement in the number of sequences completed in the 30-s period [**Figure 2A**; $F(2.805,25.24) = 43.94$, $p < 0.0001$]. The number of correct sequences completed on the trained sequence significantly increased from t0 to t1 (effect of time $p < 0.0001$), reached to the maximum value at the period of t2, and decreased slightly at the period of t3. At the same time, the control sequence showed the same trend with the trained sequence [$F(2.267,20.40) = 14.01$, $p < 0.0001$].

Longitudinal Analysis Contains Fractional Amplitude of Low-Frequency Fluctuation, Regional Homogeneity, and Degree Centrality

In the result of fALFF, participants exhibited a significantly altered right cerebellum posterior lobe (Cerebelum_6_R) after the repeated-measure ANOVA test (GRF correction, voxel $p < 0.005$, cluster $p < 0.05$, cluster size > 31 voxels) (**Figure 3** and **Table 1**). In addition, the fALFF values in Cerebelum_6_R significantly increased during the training period (t0 to t2), reached to the maximum at t2 period, and decreased significantly in the follow-up period (t3 to t4) (*post-hoc* Bonferroni test, all $p < 0.01$).

In the result of ReHo, participants exhibited a significantly altered right cerebellum posterior lobe IX (Cerebelum_9_R) (GRF correction, voxel $p < 0.005$, cluster $p < 0.05$, cluster size > 39 voxels) and right cerebellum anterior lobe III (Vermis_3) (GRF correction, voxel $p < 0.005$, cluster $p < 0.05$, cluster size > 81 voxels) after the repeated-measure ANOVA test (**Figure 4** and **Table 1**). In Cerebelum_9_R, the ReHo values showed a decreased trend during training (t0 to t2) and reached the minimum at t2 period. Then it increased (not significantly) in the follow-up period (t2 to t3) but still significantly lower than the baseline stage (t0) (*post-hoc* Bonferroni test, all $p < 0.05$). In Vermis_3, the ReHo values significantly increased to the

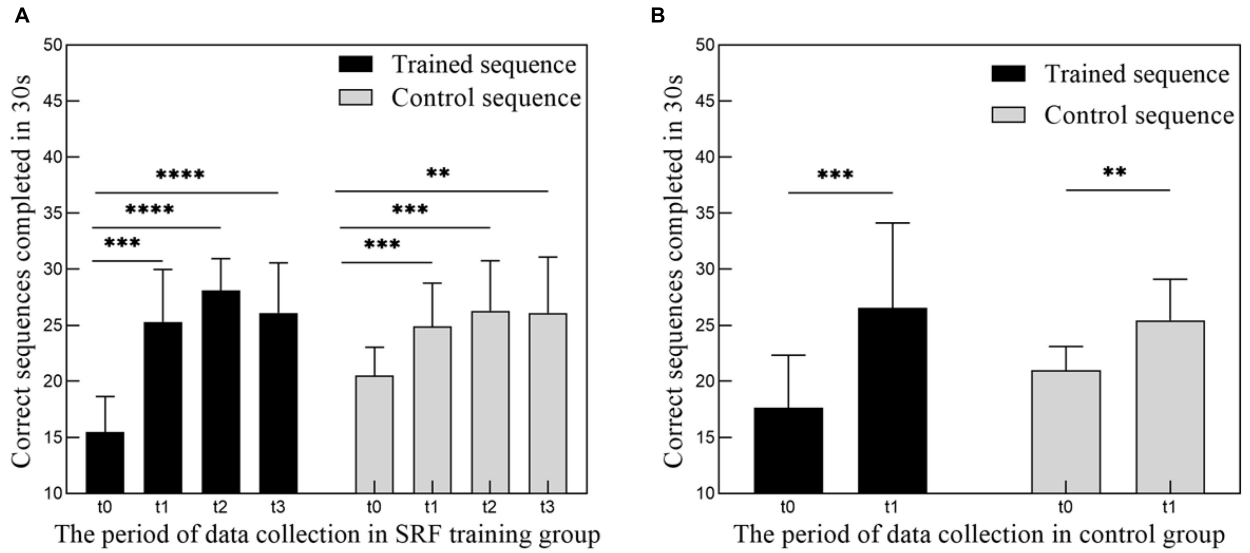

FIGURE 2 | (A) Increase in performance of motor training tasks following 4 weeks of SRF training. Group data (n = 10) showing number of correct sequences (trained and control sequence) performed in 4 periods (t0, t1, t2, t3) of data collection. **(B)** Increase in performance of motor training tasks following 2 weeks of finger movement training. Group data (n = 9) showing number of correct sequences (trained and control sequence) performed in 2 periods (t0, t1) of data collection. Data represent mean ± SEM, * indicates a significant difference in the two groups. $^{**}p < 0.01$, $^{***}p < 0.005$, $^{****}p < 0.001$.

maximum after 2 weeks of training (t0 to t1) and decreased in the next 2 training weeks thought not significantly. In the period of t3, the ReHo values in Vermis_3 kept steady with t2 but were significantly higher than the baseline stage (t0) (*post-hoc* Bonferroni test, all $p < 0.05$).

No regions showed significant differences in DC after the repeated-measure ANOVA test between different time groups (GRF correction, voxel $p < 0.005$, cluster $p < 0.05$, cluster size > 28 voxels).

Correlation With Behavioral Function

The correlations between the metric changes and behavioral improvement are shown in **Figure 5**. We mainly compared the behavioral correlations corresponding to the time periods when the rs-fMRI results changed most significantly. We found a significantly positive correlation between fALFF values change in the Cerebelum_6_R and improvement in the behavioral performance (the change in correct finger opposition number) from t0 to t2 ($r = 0.6887$, $p < 0.0402$). The ReHo values of the Vermis_3 also showed a significantly positive correlation with the improvement in the behavioral performance from t0 to t1 ($r = 0.7038$, $p < 0.0344$).

DISCUSSION

In this study, we investigated the long-term functional reorganization from the rs-fMRI perspective after BCI-controlled supernumerary robotic finger training. The brain regional changes could be identified sensitively from progressive perspectives using these three rs-fMRI analysis metrics: fALFF, ReHo, and DC. Significant changes were observed using fALFF and ReHo analysis, and no changes were found in the DC analysis. The fALFF analysis showed that Cerebelum_6_R was comparatively more active after training, and the fALFF values of Cerebelum_6_R were significantly correlated with motor function improvement. The ReHo analysis showed that Cerebelum_9_R and Vermis_3 were changed comparatively during training, and the ReHo values in Vermis_3 significantly correlated with motor function improvement. To the best of our knowledge, this is the first study to explore BCI-SRF training-induced neural modulation effect from resting state in a longitudinal manner.

Robot-assisted equipment has shown the potential to augment and restore the motor function after training whether in normal people or patients (Yuan et al., 2020; Kieliba et al., 2021). Our results also validated the long-term effect of BCI-controlled robot finger training on normal subjects. It can be clearly found that after 4 weeks of training, not only the operation ability of the training sequence was significantly increased but also the learning ability of the control sequence was significantly increased (as shown in **Figure 2**). Significant improvement in the control sequence may be related with the generalization of learning, which was correlated with the interaction with the primary visual or motor cortices encoding the stimuli or movement memories (Censor, 2013). However, the present study found no significant changes in the motor and visual cortex, which may be related with the closed loop control system, which has sensory feedback, which will reduce the dependence of the brain on visual resources (Kato et al., 2009). It may also be related with the simplicity of the training task. Future research should be detailed in this generalization phenomenon. This significant improvement of the behavioral results also indicated the effectiveness and acceptance of people to the whole SRF system, which integrated

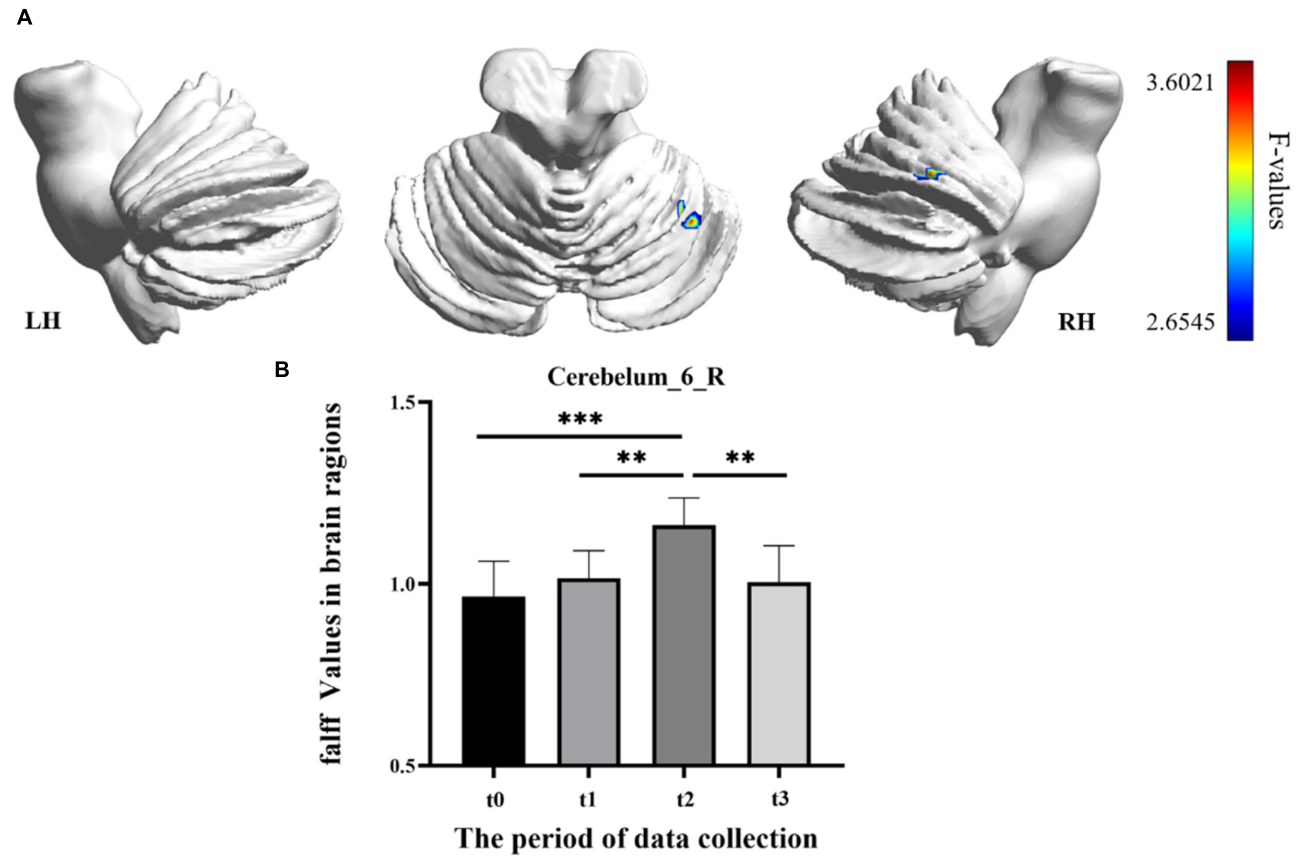

FIGURE 3 | The fractional amplitude of low-frequency fluctuation (fALFF) differences among different time-subgroups. **(A)** One-way repeated-measure ANOVA showed brain regions with fALFF differences among four subgroups in the Cerebelum_6_R. The color bar indicated the F scores. **(B)** Bar plots showed the fALFF values of the Cerebelum_6_R at four different time-subgroups. Cerebelum_6_R, right cerebellum posterior lobe VI; t0, t1, t2, and t3, different time subgroups; LH, left hemisphere; RH, right hemisphere, * indicates a significant difference in the two groups. *p < <0.05, **p < 0.01, ***p < 0.005.

TABLE 1 | Brain regions with longitudinal fALFF and ReHo changes.

			MNI coordinate (mm)		
Regions	**Cluster size**	**Peak *T* value**	**X**	**Y**	**Z**
fALFF					
Cerebelum_6_R	14	3.6021	36	−54	−24
REHO					
Cerebelum_9_R	39	4.1268	15	−54	−30
Vermis_3	81	4.0347	0	−30	−6

the neuroplasticity of the MI (Varkuti et al., 2013; Jeunet et al., 2019) and the effect of the close loop sensory feedback (Kato et al., 2009; van Dokkum et al., 2015).

Resting-state fMRI is widely used in clinical research because of its unique advantages, which require less participants to engage in cognitive activities (Fox and Raichle, 2007). The fALFF, ReHo, and DC, three voxel-wised metrics, define brain functional characteristics from different perspectives and present the progressive relationship (Zang et al., 2004; Zou et al., 2008; Buckner et al., 2009). For a single voxel, fALFF characterizes neural activity intensity of the single voxel, ReHo reveals the importance of this voxel among the nearest voxels, while DC portrays the importance of this voxel in the whole brain (Lv et al., 2019). In this study, fALFF and ReHo had significant results, which indicated that SRF training mainly modulated brain function from single-voxel level and local level. However, the DC metric had no significant results in the longitudinal ANOVA analysis. The reasonable explanation was that SRF training may not lead a certain brain area to take an important position, which has a significant correlation change with all voxels in the whole brain. In addition, we also speculated that some true positive brain regions may not survive the multiple comparison correction when using strict threshold to decrease false positive. In our longitudinal fALFF and ReHo investigation, the values of Cerebelum_6_R (right cerebellum posterior lobe VI) and Vermis_3 (cerebellum anterior lobe III) were significantly increased with the training time. Besides, Cerebelum_6_R and Vermis_3 test values changes were significantly correlated with motor function improvement. Therefore, we speculated that a strong compensatory mechanism existed between the using SRF and changing cerebellum. When the human body adds a supernumerary sixth finger, the brain will undertake greater

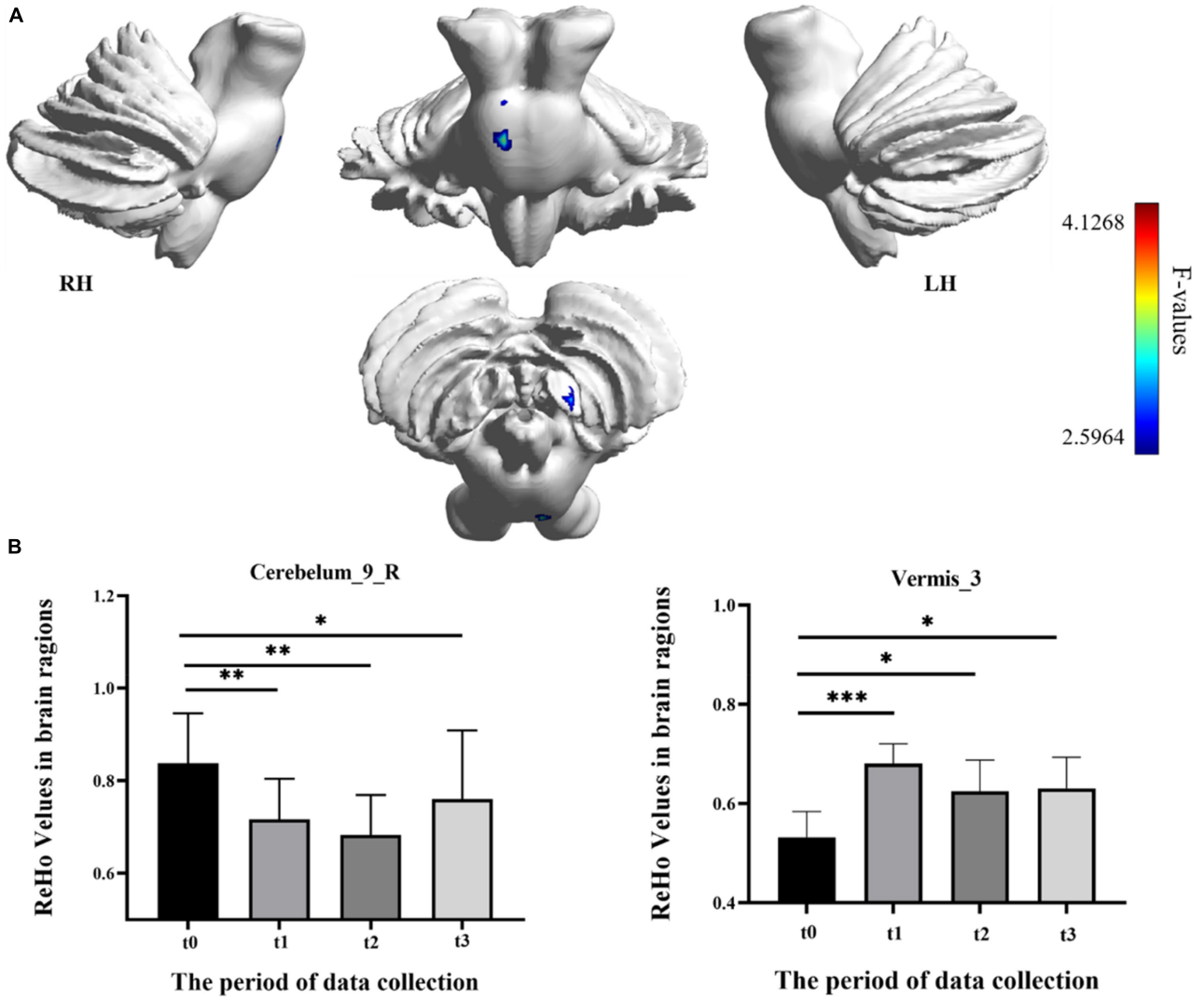

FIGURE 4 | Regional homogeneity (ReHo) differences among different time-subgroups. **(A)** One-way repeated-measure ANOVA showed brain regions with ReHo differences among four subgroups in the Cerebelum_9_R and Vermis_3. The color bar indicated the F scores. **(B)** Bar plots showed the ReHo values of the Cerebelum_9_R at four different time-subgroups. Cerebelum_9_R, right cerebellum posterior lobe IX; Vermis_3, cerebellum anterior lobe III; t0, t1, t2, and t3, different time subgroups; LH, left hemisphere; RH, right hemisphere, * indicates a significant difference in the two groups. *p < <0.05, **p < 0.01, ***p < 0.005.

load and will recruit more somatomotor and sensorimotor networks to participate. Cerebellar lobules IV–VI and VIII were proven to engage in motor processing and activated in the task-based fMRI analysis (Stoodley and Schmahmann, 2009; Stoodley et al., 2010; Keren-Happuch et al., 2014), and the anterior lobe was engaged in overt limb movements (Rijntjes et al., 1999; Bushara et al., 2001). The study of the cerebellum resting-state function connectivity found that cerebellar lobules I–VI have a high correlation with the sensorimotor area (Stoodley et al., 2016; Guell et al., 2018), and then the anterior lobe III was also correlated with the somatomotor networks (Buckner et al., 2011). Therefore, the increased activation in Cerebelum_6_R and Vermis_3 was used to compensate the extra brain load caused by the supernumerary robotic finger. However, activation showed different trends in the two brain areas with the change in training time. The activation in Cerebelum_6_R increased with training time and decreased in the follow-up period (t3), which indicated that the SRF training did not cause long-lasting effects (as shown in **Figure 3B**). This result shows that the compensation effect of the sensorimotor area mapped in the cerebellum will return to the baseline stage with the cessation of training, but in Vermis_3, the activation increased in the early training stage (t0 to t1), decreased in the post-training stage (t1 to t2), and kept steady in the follow-up period (as shown in **Figure 4B**). This result shows that the somatomotor network mapped in the cerebellum plays a compensation role in the early training stage (t0 to t1). With the SRF gradually accepted, the compensation effect decreased by degrees in the post-training stage (t1 to t2), but this effect still maintained a higher level than the baseline (t0) in the post-training stage

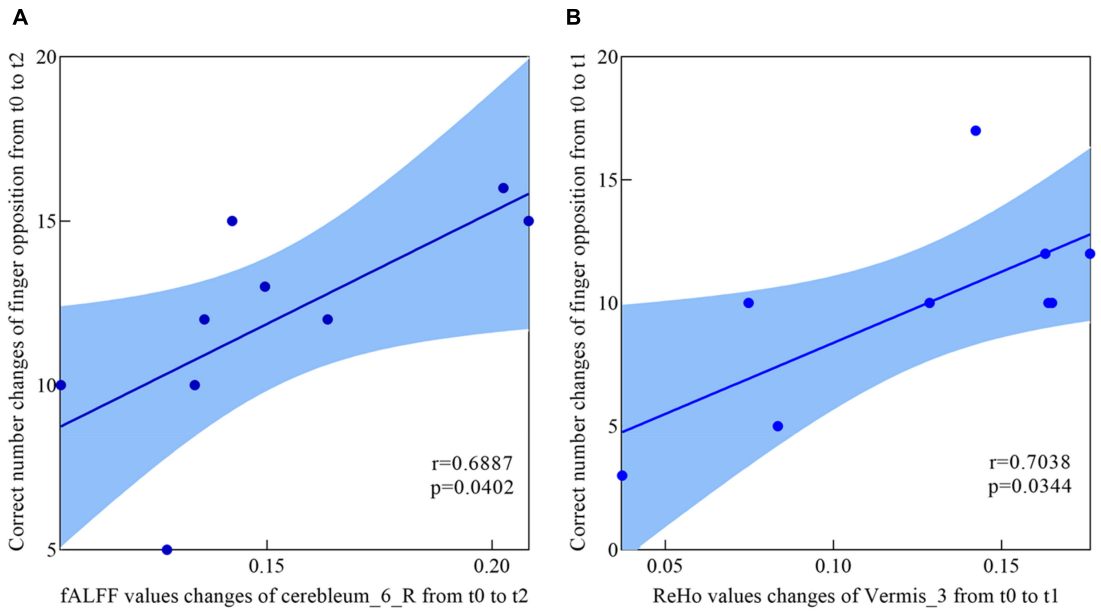

FIGURE 5 | Correlations between fALFF values, ReHo values, and behavioral scores. **(A)** The participants showed a significantly positive correlation between the fALFF values increased in Cerebelum_6_R and the enhancement of behavioral performance (the changes of in correct finger opposition number) from t0 to t2. **(B)** Significantly positive correlation between the ReHo values increased in Vermis_3 and the enhancement of behavioral performance (the changes of in correct finger opposition number) from t0 to t1.

(t2) and follow-up period (t3), which proved that SRF training generated long-lasting effects.

Compared with the increased activation of the cerebellum posterior lobe VI and anterior lobe III, the decreased ReHo values in Cerebelum_9_R (right cerebellum posterior lobe IX) was also a significant result in this research (as shown in **Figure 4A**). Resting-state fMRI found that lobule IX has a high correlation with the default mode network, which was suppressed during tasks that demand external attention and was active during remembering, envisioning the future, and making social inferences (Buckner et al., 2011; Buckner and DiNicola, 2019). Therefore, we speculated that the decreased activation in the default mode network mapped in the cerebellum may be related with the suppression mechanism during tasks that demand external attention. The SRF as the added finger needs additional attention resources of the human brain to control, and Cerebelum_9_R could be inhibited in this active task to achieve the control purpose. As for the suppression mechanism of the default network, the reliable explanation was the significant competition effect that existed between the extensive information processing modes, which were supported by different independent network groups (Stoodley and Schmahmann, 2009). In addition, this suppression mechanism in Cerebelum_9_R was enhanced with training time and recovered in the follow-up period (t3), which indicated that the SRF training did not cause long-lasting effects (as shown in **Figure 4B**).

After 4 weeks of brain-controlled SRF training, this study innovatively found that the changes in the resting state of the human brain were mainly on the cerebellum. Some factors should be taken into account for this innovative result. (1) The present study takes normal people as the subject who have full use of hands in daily life. Such an experimental arrangement can better explore the neuroplasticity effect in motor augmentation of SRF training in the daily lives of normal people. This experiment arrangement may be one of the reasons for this innovative result, which is different from others. (2) The different imaginary paradigm is also one of the reasons for this innovative result. This present paradigm focused on the device of SRF and was different from the previous imaginary paradigm, which mainly focused on inborn inherent limbs (IIL) (Varkuti et al., 2013). Using IIL as the imaginary paradigm has been proven to activate the limb execution network like the somatomotor and sensorimotor network (Hardwick et al., 2018). Besides, the body part involved in the movements and the nature of the MI tasks all seem to influence the consistency of activation within the general MI network (Hetu et al., 2013). However, different from motor imagery of the IIL, using the supernumerary robot limb device, imaginary as the paradigm, was also proven to modulate other brain areas (Penaloza and Nishio, 2018). Therefore, we speculated that the new motor imagery paradigm has the potential to activate the new targeted area of the brain. (3) Unlike motor imagery training, this study mainly explored the neuroplasticity effect of the whole SRF system integrated motor imagery, extra robotic finger, and electrical stimulation feedback. This mixed influence may be different from each effect.

The difference between training with SRF and pure finger movement training on the resting-state neuroplasticity is also a very interesting question. Therefore, we preliminary arranged 2 weeks of pure finger sequence moving training experiment of

nine subjects, and the training dose was matched to the SRF group. Although the behavioral performance has a significant improvement (**Figure 2B**), we have not found any significant changes in this control group after paired *t*-test and GRF correction in the ALFF, ReHo, and DC metrics of resting state in the cerebellum. Therefore, we inferred that the results of the SRF group were produced by the joint effect of the SRF with our body, and pure finger movement training will not cause this similar result. The results of the control group were different from the previous study in Ref. (Sale et al., 2017), and this may be related with the different duration and intensity of training or the different data process methods. In view of the preliminary implementation of this control experiment, the detailed effect needs to be further explored in the future.

Several limitations need to be noted in this study. First of all, the sample size was not large, which may limit the generalization power. More participants should be recruited to validate and extend the findings of this study. Second, it would be better to differentiate the effect caused by the motor imagery and SRF finger training. In the current study, we cannot tell the key part contributing to the neurological changes and functional recovery under the joining of the two components. In further studies, a control group is needed. Third, the effect of different task paradigms and training duration need to be further investigated. Moreover, based on the present results of behavioral performance and cerebellar neuroplasticity, the BCI-controlled SRF can be applied to the rehabilitation of patients with cerebellar stroke or functional impairment in the future.

CONCLUSION

To the best of our knowledge, this is the first study to investigate brain alterations in long-term BCI-controlled supernumerary robotic finger training. Significant changes were found in Cerebelum_6_R, Cerebelum_9_R, and Vermis_3 using fALFF, ReHo, and DC metrics in longitudinal resting-state fMRI study. In addition, fALFF value changes in Cerebelum_6_R and ReHo value changes in Vermis_3 were significantly correlated with motor function improvement. We conclude that the compensation mechanism of the sensorimotor and somatomotor networks mapped in the cerebellum existed during BCI-controlled SRF training. At the same time, the suppression mechanism was also observed in the default mode network mapped in the cerebellum in this study. Our new findings supplement the literature on motor-augmentation neuroplasticity brought by BCI-controlled augmentative device training and may facilitate future research on SRF.

DATA AVAILABILITY STATEMENT

The raw data supporting the conclusions of this article will be made available by the authors, without undue reservation.

ETHICS STATEMENT

The studies involving human participants were reviewed and approved by the Tianjin University Human Research Ethics Committee. The patients/participants provided their written informed consent to participate in this study. Written informed consent was obtained from the individual(s) for the publication of any potentially identifiable images or data included in this article.

AUTHOR CONTRIBUTIONS

YL originally conceptualized the study and drafted the manuscript. SH designed the experiment and analyzed the fMRI data. ZW provided the EEG coding and decoding of the algorithms. FJ designed the hardware system of the SRF. DM gave some advice on hand prehensile taxonomy and helped review the content of the manuscript. All authors contributed to the article and approved the submitted version.

FUNDING

This work was supported by the National Natural Science Foundation of China (51905375 and 81925020), the China Post-Doctoral Science Foundation Funded Project (2019M651033), the Foundation of State Key Laboratory of Robotics and System (HIT) (SKLRS-2019-KF-06), and the Peiyang Elite Scholar Program of Tianjin University (2020XRG-0023).

REFERENCES

Arcaro, M. J., Schade, P. F., and Livingstone, M. S. (2019). Body map proto-organization in newborn macaques. *Proc. Natl. Acad. Sci. U.S.A.* 116, 24861–24871. doi: 10.1073/pnas.1912636116

Biasiucci, A., Leeb, R., Iturrate, I., Perdikis, S., Al-Khodairy, A., Corbet, T., et al. (2018). Brain-actuated functional electrical stimulation elicits lasting arm motor recovery after stroke. *Nat. Commun.* 9:2421. doi: 10.1038/s41467-018-04673-z

Biswal, B., Yetkin, F. Z., Haughton, V. M., and Hyde, J. S. (1995). Functional connectivity in the motor cortex of resting human brain using echo-planar MRI. *Magn. Reson. Med.* 34, 537–541. doi: 10.1002/mrm.1910340409

Buckner, R. L., and DiNicola, L. M. (2019). The brain's default network: updated anatomy, physiology and evolving insights. *Nat. Rev. Neurosci.* 20, 593–608. doi: 10.1038/s41583-019-0212-7

Buckner, R. L., Krienen, F. M., Castellanos, A., Diaz, J. C., and Yeo, B. T. T. (2011). The organization of the human cerebellum estimated by intrinsic functional connectivity. *J. Neurophysiol.* 106, 2322–2345. doi: 10.1152/jn.00339.2011

Buckner, R. L., Sepulcre, J., Talukdar, T., Krienen, F. M., Liu, H., Hedden, T., et al. (2009). Cortical hubs revealed by intrinsic functional connectivity: mapping, assessment of stability, and relation to Alzheimer's disease. *J. Neurosci.* 29, 1860–1873. doi: 10.1523/JNEUROSCI.5062-08.2009

Bushara, K. O., Wheat, J. M., Khan, A., Mock, B. J., Turski, P. A., Sorenson, J., et al. (2001). Multiple tactile maps in the human cerebellum. *Neuroreport* 12, 2483–2486. doi: 10.1097/00001756-200108080-00039

Cadete, D., and Longo, M. R. (2020). A continuous illusion of having a sixth finger. *iPerception* 49, 807–821. doi: 10.1177/0301006620939457

Censor, N. (2013). Generalization of perceptual and motor learning: a causal link with memory encoding and consolidation? *Neuroscience* 250, 201–207. doi: 10.1016/j.neuroscience.2013.06.062

Cervera, M. A., Soekadar, S. R., Ushiba, J., Millan, J. D. R., Liu, M., Birbaumer, N., et al. (2018). Brain-computer interfaces for post-stroke motor rehabilitation: a meta-analysis. *Ann. Clin. Transl. Neurol.* 5, 651–663. doi: 10.1002/acn3.544

Dall'Orso, S., Steinweg, J., Allievi, A. G., Edwards, A. D., Burdet, E., and Arichi, T. (2018). Somatotopic mapping of the developing sensorimotor cortex in the preterm human brain. *Cereb. Cortex* 28, 2507–2515. doi: 10.1093/cercor/bhy050

Dose, H., Moller, J. S., Iversen, H. K., and Puthusserypady, S. (2018). An end-to-end deep learning approach to MI-EEG signal classification for BCIs. *Exp. Syst. Appl.* 114, 532–542. doi: 10.1088/1741-2552/ab3471

Eaves, D. L., Haythornthwaite, L., and Vogt, S. (2014). Motor imagery during action observation modulates automatic imitation effects in rhythmical actions. *Front. Hum. Neurosci.* 8:28. doi: 10.3389/fnhum.2014.00028

Fox, M. D., and Raichle, M. E. (2007). Spontaneous fluctuations in brain activity observed with functional magnetic resonance imaging. *Nat. Rev. Neurosci.* 8, 700–711. doi: 10.1038/nrn2201

Friston, K. J. (1994). Functional and effective connectivity in neuroimaging: a synthesis. *Brain Connect.* 2, 56–78. doi: 10.1002/hbm.460020107

Friston, K. J., Williams, S., Howard, R., Frackowiak, R. S., and Turner, R. (1996). Movement-related effects in fMRI time-series. *Magn. Reson. Med.* 35, 346–355. doi: 10.1002/mrm.1910350312

Guell, X., Gabrieli, J. D. E., and Schmahmann, J. D. (2018). Triple representation of language, working memory, social and emotion processing in the cerebellum: convergent evidence from task and seed-based resting-state fMRI analyses in a single large cohort. *Neuroimage* 172, 437–449. doi: 10.1016/j.neuroimage.2018.01.082

Hardwick, R. M., Caspers, S., Eickhoff, S. B., and Swinnen, S. P. (2018). Neural correlates of action: comparing meta-analyses of imagery, observation, and execution. *Neurosci. Biobehav. Rev.* 94, 31–44. doi: 10.1016/j.neubiorev.2018.08.003

Hetu, S., Gregoire, M., Saimpont, A., Coll, M. P., Eugene, F., Michon, P. E., et al. (2013). The neural network of motor imagery: an ALE meta-analysis. *Neurosci. Biobehav. Rev.* 37, 930–949. doi: 10.1016/j.neubiorev.2013.03.017

Hussain, I., Salvietti, G., Spagnoletti, G., Malvezzi, M., Cioncoloni, D., Rossi, S., et al. (2017a). A soft supernumerary robotic finger and mobile arm support for grasping compensation and hemiparetic upper limb rehabilitation. *Robot. Auton. Syst.* 93, 1–12. doi: 10.1016/j.robot.2017.03.015

Hussain, I., Santarnecchi, E., Leo, A., Ricciardi, E., Rossi, S., and Prattichizzo, D. (2017b). A magnetic compatible supernumerary robotic finger for functional magnetic resonance imaging (fMRI) acquisitions: device description and preliminary results. *IEEE Int. Conf. Rehabil. Robot.* 2017, 1177–1182. doi: 10.1109/ICORR.2017.8009409

Hussain, I., Spagnoletti, G., Salvietti, G., and Prattichizzo, D. (2017c). Toward wearable supernumerary robotic fingers to compensate missing grasping abilities in hemiparetic upper limb. *Int. J. Robot. Res.* 36, 1414–1436. doi: 10.1177/0278364917712433

Jeunet, C., Glize, B., McGonigal, A., Batail, J. M., and Micoulaud-Franchi, J. A. (2019). Using EEG-based brain computer interface and neurofeedback targeting sensorimotor rhythms to improve motor skills: theoretical background, applications and prospects. *Neurophysiol. Clin. Clin. Neurophysiol.* 49, 125–136. doi: 10.1016/j.neucli.2018.10.068

Jia, X. Z., Wang, J., Sun, H. Y., Zhang, H., Liao, W., Wang, Z., et al. (2019). RESTplus: an improved toolkit for resting-state functional magnetic resonance imaging data processing. *Sci. Bull.* 64, 953–954.

Jones, L., and Lederman, S. (2006). *Human Hand Function*. Oxford: Oxford University Press.

Kato, R., Yokoi, H., Hernandez Arieta, A., Yu, W., and Arai, T. (2009). Mutual adaptation among man and machine by using f-MRI analysis. *Robot. Auton. Syst.* 57, 161–166. doi: 10.1016/j.robot.2008.07.005

Keren-Happuch, E., Chen, S. H. A., Ho, M. H. R., and Desmond, J. E. (2014). A meta-analysis of cerebellar contributions to higher cognition from PET and fMRI Studies. *Hum. Brain Mapp.* 35, 593–615. doi: 10.1002/hbm.22194

Kieliba, P., Clode, D., Maimon-Mor, R. O., and Makin, T. R. (2021). Robotic hand augmentation drives changes in neural body representation. *Sci. Robot.* 6:eabd7935. doi: 10.1126/scirobotics.abd7935

Kim, T., Kim, S., and Lee, B. (2016). Effects of action observational training plus brain-computer interface-based functional electrical stimulation on paretic arm motor recovery in patient with stroke: a randomized controlled trial. *Occup. Ther. Int.* 23, 39–47. doi: 10.1002/oti.1403

Liu, Y., Huang, S., Wang, Z., Ji, F., and Ming, D. (2021a). "A novel modular and wearable supernumerary robotic finger via EEG-EMG control with 4-week training assessment," in *Intelligent Robotics and Applications. ICIRA 2021. Lecture Notes in Computer Science*, Vol. 13013, eds X. J. Liu, Z. Nie, J. Yu, F. Xie, and R. Song (Cham: Springer), 748–758. doi: 10.1007/978-3-030-89095-7_71

Liu, Y., Wang, Z., Huang, S., Wei, J., Li, X., and Ming, D. (2021b). EEG Characteristic Investigation of the Sixth-Finger Motor Imagery and optimal channel selection for classification. *J. Neural Eng.* 654–663. doi: 10.1088/1741-2552/ac49a6

Llorens-Bonilla, B., Parietti, F., and Asada, H. H. (2012). "Demonstration-based control of supernumerary robotic limbs," in *Proceedings of the 2012 IEEE/RSJ International Conference on Intelligent Robots and Systems*, (New York, NY: IEEE), 3936–3942.

Lv, Y., Li, L., Song, Y., Han, Y., Zhou, C., Zhou, D., et al. (2019). The local brain abnormalities in patients with transient ischemic attack: a resting-state fMRI study. *Front Neurosci* 13:24. doi: 10.3389/fnins.2019.00024

Mehring, C., Akselrod, M., Bashford, L., Mace, M., Choi, H., Blüher, M., et al. (2019). Augmented manipulation ability in humans with six-fingered hands. *Nat. Commun.* 10, 2401. doi: 10.1038/s41467-019-10306-w

Newport, R., Wong, D. Y., Howard, E. M., and Silver, E. (2016). The anne boleyn illusion is a six-fingered salute to sensory remapping. *Iperception* 7, 1–4. doi: 10.1177/2041669516669732

Parietti, F., and Asada, H. H. (2013). "Dynamic analysis and state estimation for wearable robotic limbs subject to human-induced disturbances," in *Proceedings of the 2013 IEEE International Conference on Robotics and Automation*, (New York, NY: IEEE), 3880–3887.

Parietti, F., Chan, K., and Asada, H. H. (2014). "Bracing the human body with supernumerary robotic limbs for physical assistance and load reduction," in *Proceedings of the 2014 Ieee International Conference on Robotics and Automation*, (New York, NY: IEEE), 141–148.

Penaloza, C. I., and Nishio, S. (2018). BMI control of a third arm for multitasking. *Sci. Robot.* 3:6. doi: 10.1126/scirobotics.aat1228

Prattichizzo, D., Malvezzi, M., Hussain, I., and Salvietti, G. (2014). "The sixth-finger: a modular extra-finger to enhance human hand capabilities," in *Proceedings of the 2014 23rd IEEE International Symposium on Robot and Human Interactive Communication*, (New York, NY: IEEE), 993–998.

Rijntjes, M., Buechel, C., Kiebel, S., and Weiller, C. (1999). Multiple somatotopic representations in the human cerebellum. *Neuroreport* 10, 3653–3658. doi: 10.1097/00001756-199911260-00035

Rossi, S., Salvietti, G., Neri, F., Romanella, S. M., Cinti, A., Sinigaglia, C., et al. (2021). Emerging of new bioartificial corticospinal motor synergies using a robotic additional thumb. *Sci. Rep.* 11:18487. doi: 10.1038/s41598-021-97876-2

Sale, M. V., Reid, L. B., Cocchi, L., Pagnozzi, A. M., Rose, S. E., and Mattingley, J. B. (2017). Brain changes following four weeks of unimanual motor training: evidence from behavior, neural stimulation, cortical thickness, and functional MRI. *Hum. Brain Mapp.* 38, 4773–4787. doi: 10.1002/hbm.23710

Stoodley, C. J., and Schmahmann, J. D. (2009). Functional topography in the human cerebellum: a meta-analysis of neuroimaging studies. *Neuroimage* 44, 489–501. doi: 10.1016/j.neuroimage.2008.08.039

Stoodley, C. J., MacMore, J. P., Makris, N., Sherman, J. C., and Schmahmann, J. D. (2016). Location of lesion determines motor vs. cognitive consequences in patients with cerebellar stroke. *Neuroimage Clin.* 12, 765–775. doi: 10.1016/j.nicl.2016.10.013

Stoodley, C. J., Valera, E. M., and Schmahmann, J. D. (2010). An fMRI study of intra-individual functional topography in the human cerebellum. *Behav. Neurol.* 23, 65–79. doi: 10.3233/BEN-2010-0268

van Dokkum, L. E. H., Ward, T., and Laffont, I. (2015). Brain computer interfaces for neurorehabilitation - its current status as a rehabilitation strategy post-stroke. *Ann. Phys. Rehabil. Med.* 58, 3–8. doi: 10.1016/j.rehab.2014.09.016

Varkuti, B., Guan, C., Pan, Y., Phua, K. S., Ang, K. K., Kuah, C. W., et al. (2013). Resting state changes in functional connectivity correlate with movement recovery for BCI and robot-assisted upper-extremity training after stroke. *Neurorehabil. Neural Repair* 27, 53–62. doi: 10.1177/1545968312445910

Wang, X., Wong, W. W., Sun, R., Chu, W. C., and Tong, K. Y. (2018). Differentiated effects of robot hand training with and without neural guidance

on neuroplasticity patterns in chronic stroke. *Front. Neurol.* 9:810. doi: 10.3389/fneur.2018.00810

Wu, F. Y., and Asada, H. H. (2015). "'Hold-and-manipulate' with a single hand being assisted by wearable extra fingers," in *Proceedings of the 2015 IEEE International Conference on Robotics and Automation (ICRA)*, Vol. 2015, Seattle, WA, 6205–6212.

Yuan, K., Chen, C., Wang, X., Chu, W. C., and Tong, R. K. (2021). BCI training effects on chronic stroke correlate with functional reorganization in motor-related regions: a concurrent EEG and fMRI study. *Brain Sci.* 11:56. doi: 10.3390/brainsci11010056

Yuan, K., Wang, X., Chen, C., Lau, C. C. Y., Chu, W. C. W., and Tong, R. K. Y. (2020). Interhemispheric functional reorganization and its structural base after BCI-guided upper-limb training in chronic stroke. *IEEE Trans. Neural Syst. Rehabil. Eng.* 28, 2525–2536. doi: 10.1109/TNSRE.2020.3027955

Zang, Y. F., Jiang, T. Z., Lu, Y. L., He, Y., and Tian, L. X. (2004). Regional homogeneity approach to fMRI data analysis. *Neuroimage* 22, 394–400. doi: 10.1016/j.neuroimage.2003.12.030

Zhang, Y., Liu, H. L., Wang, L., Yang, J., Yan, R., Zhang, J., et al. (2016). Relationship between functional connectivity and motor function assessment in stroke patients with hemiplegia: a resting-state functional MRI study. *Neuroradiology* 58, 503–511. doi: 10.1007/s00234-016-1646-5

Zou, Q. H., Zhu, C. Z., Yang, Y., Zuo, X. N., Long, X. Y., Cao, Q. J., et al. (2008). An improved approach to detection of amplitude of low-frequency fluctuation (ALFF) for resting-state fMRI: fractional ALFF. *J. Neurosci. Methods* 172, 137–141. doi: 10.1016/j.jneumeth.2008.04.012

Zuo, X. N., Ehmke, R., Mennes, M., Imperati, D., Castellanos, F. X., Sporns, O., et al. (2012). Network centrality in the human functional connectome. *Cereb. Cortex* 22, 1862–1875. doi: 10.1093/cercor/bhr269

Conflict of Interest: The authors declare that the research was conducted in the absence of any commercial or financial relationships that could be construed as a potential conflict of interest.

frontiers in Neuroscience

ORIGINAL RESEARCH
published: 17 February 2022
doi: 10.3389/fnins.2022.788538

Cortical Inhibition State-Dependent iTBS Induced Neural Plasticity

Xiaoying Diao[1,2†], Qian Lu[1†], Lei Qiao[3†], Youhui Gong[1], Xiao Lu[1], Min Feng[1], Panpan Su[1], Ying Shen[4], Ti-Fei Yuan[2,5,6*] and Chuan He[1*]*

[1] Department of Rehabilitation Medicine, The Affiliated Jiangsu Shengze Hospital of Nanjing Medical University, Suzhou, China, [2] Shanghai Key Laboratory of Psychotic Disorders, Shanghai Mental Health Center, Shanghai Jiao Tong University School of Medicine, Shanghai, China, [3] Jiangsu Zhongshan Geriatric Rehabilitation Hospital, Nanjing, China, [4] Rehabilitation Medicine Center, The First Affiliated Hospital of Nanjing Medical University, Nanjing, China, [5] Co-innovation Center of Neuroregeneration, Nantong University, Nantong, China, [6] Translational Research Institute of Brain and Brain-Like Intelligence, Shanghai Fourth People's Hospital Affiliated to Tongji University School of Medicine, Shanghai, China

OPEN ACCESS

Edited by:
Jinhua Zhang,
Xi'an Jiaotong University, China

Reviewed by:
José Vicente Negrete Díaz,
University of Guanajuato, Mexico
Peter J. Fried,
Beth Israel Deaconess Medical Center and Harvard Medical School, United States

***Correspondence:**
Ying Shen
shenying@njmu.edu.cn
Ti-Fei Yuan
ytf0707@126.com
Chuan He
he-chuan@outlook.com

† These authors have contributed equally to this work and share first authorship

Specialty section:
This article was submitted to Neuroprosthetics, a section of the journal Frontiers in Neuroscience

Received: *02 October 2021*
Accepted: *11 January 2022*
Published: *17 February 2022*

Citation:
Diao X, Lu Q, Qiao L, Gong Y, Lu X, Feng M, Su P, Shen Y, Yuan T-F and He C (2022) Cortical Inhibition State-Dependent iTBS Induced Neural Plasticity. Front. Neurosci. 16:788538. doi: 10.3389/fnins.2022.788538

Background: Intermittent theta burst stimulation (iTBS) is an effective stimulus for long-term potentiation (LTP)-like plasticity. However, iTBS-induced effects varied greatly between individuals. Ample evidence suggested that an initial decrease in local γ-aminobutyric acid (GABA) or enhancement in *N*-methyl-D-aspartate (NMDA) facilitation neurotransmission is of vital importance for allowing LTP-like plasticity to occur. Therefore, we aimed to investigate whether the individual level of GABA or NMDA receptor-mediated activity before stimulation is correlated with the after-effect in cortical excitability induced by iTBS.

Methods: Fifteen healthy volunteers were recruited for the present study. We measured short-interval intracortical inhibitory (SICI), long-interval intracortical inhibitory (LICI), and intracortical facilitation (ICF), which index $GABA_A$ receptor-, $GABA_B$ receptor-, and glutamate receptor-mediated activity, respectively, in the cortex before conducting iTBS. After iTBS intervention, the changes of motor-evoked potential (MEP) amplitude were taken as a measure for cortical excitability in response to iTBS protocol.

Results: There was a significant negative correlation between the amount of SICI measured before iTBS and the after-effect of iTBS-induced LTP-like plasticity at the time points of 5, 10, and 15 min after inducing iTBS. A multiple linear regression model indicated that SICI was a good predictor of the after-effect in cortical excitability induced by iTBS at 5, 10, and 15 min following stimulation.

Conclusion: The present study found that $GABA_A$ receptor-mediated activity measured before stimulation is negatively correlated with the after-effect of cortical excitability induced by iTBS. SICI, as the index of $GABA_A$ receptor-mediated activity measured before stimulation, might be a good predictor of iTBS-induced LTP-like plasticity for a period lasting 15 min following stimulation.

Keywords: intermittent theta burst stimulation, LTP-like plasticity, $GABA_A$ receptor-mediated activity, $GABA_B$ receptor-mediated activity, *N*-methyl-D-aspartate receptor-mediated activity

INTRODUCTION

Long-term potentiation (LTP)-like plasticity, defined as the ability of neurons to activity-dependently modify the strength of synaptic transmission, is the most common form of synaptic plasticity (Hebb, 2005; Takeuchi et al., 2014; Llona et al., 2017; Mateos-Aparicio and Rodríguez-Moreno, 2019). It is significant in response to physiological degeneration or brain injury (Wieloch and Nikolich, 2006; Chen et al., 2010; Cramer et al., 2011). LTP has been found to be induced by repetitive electrical stimulation in animal experiments, but recently the introduction of transcranial magnetic stimulation (TMS) with protocols of repetitive TMS (rTMS) presented the possibility of delivering similar LTP-like plasticity in the human brain (Bliss and Lømo, 1973; Wang et al., 1996; Ziemann et al., 1998b; Siebner and Rothwell, 2003; Cooke, 2006). Therefore, these rTMS-induced synaptic changes might have significant implications for therapeutic opportunities after brain damage *via* mechanisms of cortical plasticity (Lefaucheur et al., 2020).

Intermittent theta burst stimulation (iTBS) is one such protocol that can result in increases of cortical excitability persisting beyond the period of stimulation (Huang et al., 2005; Di Lazzaro et al., 2008). Compared with traditional rTMS protocols, iTBS requires lower simulation intensity and less stimulation time for inducing similar after-effects (Todd et al., 2009). Although iTBS may be indicative of an appealing technique for modulating cortical plasticity for clinical or therapeutic applications, recent studies observed that the effect varies greatly between individuals (Hamada et al., 2013; Hinder et al., 2014; Schilberg et al., 2017). Ridding and Ziemann (2010) summarized that the interindividual variability may depend on several different factors such as age, genetics, pharmacological influences, and neural activity in the brain before conducting stimulation. Such variability at present limits the therapeutic effectiveness of iTBS for inducing plastic changes.

The present study aimed at testing one such important factor that contributes to the variation of iTBS-induced plastic changes. Accumulating evidence in animal studies suggested that susceptibility to cortical potential-like plasticity is influenced by the level of cortical NMDAergic excitability and GABAergic inhibition (Kano and Iino, 1991; Schwenkreis et al., 2003; Di Lazzaro et al., 2006; Bachtiar and Stagg, 2014). Hess et al. (1996) suggested that LTP was enhanced by blockade of $GABA_A$ receptors with antagonist bicuculline in the motor cortex; conversely, the *N*-methyl-D-aspartate (NMDA) antagonist 2-amino-5-phosphonovaleric acid blocked LTP induction. LTP has also been found to be induced through iTBS when $GABA_A$ and $GABA_B$ receptors were both blocked (Kotak et al., 2017).

In human studies, paired pulse transcranial magnetic stimulation (ppTMS) can be performed to evaluate the level of GABA or NMDA receptor-mediated activity (Kujirai et al., 1993; Ziemann et al., 1998a; Ilić et al., 2002; McDonnell et al., 2006; Rossini et al., 2015). Therefore, we wished to verify whether the after-effect in cortical excitability induced by iTBS is correlated with the level of GABA or NMDA receptor-mediated activity before stimulation. Here, ppTMS was performed to evaluate short-interval intracortical inhibitory (SICI), long-interval intracortical inhibitory (LICI), and intracortical facilitation (ICF), which index $GABA_A$ receptor-, $GABA_B$ receptor-, and glutamate receptor-mediated activity, respectively.

MATERIALS AND METHODS

Participants

Fifteen healthy volunteers (13 females) were recruited for the present study. Age ranges from 20 to 23 years (M = 21.07, SD = 1.06). All participants were right-handed (assessed by the Edinburgh Handedness Inventory; Oldfield, 1971) and had normal or correlated-with-normal vision. Exclusion criteria included a history of psychiatric or neurologic diseases, epilepsy, cardiovascular complications, taking any medication on a regular basis, and contraindications to TMS (e.g., taking epileptogenic drugs, implants in the brain, pregnant women). Informed consent was obtained from all participants. The study was performed according to the Declaration of Helsinki and approved by the Ethics Committee of Affiliated Jiangsu Shengze Hospital of Nanjing Medical University (JSSZYY-LLSC-202104). The study was registered with the China Clinical Trial Registration Center[1] under the number ChiCTR2100046794.

Transcranial Magnetic Stimulation and Electromyography Recordings

Single monophasic TMS was performed over the hand region of the left primary motor cortex (LM1) using the Neuro-MS/D stimulator (Neurosoft Llc, Ivanovo, Russia) connected with a figure-of-eight coil (external loop diameters, 70 mm; peak magnetic field, 4 Tesla). The optimal coil position was determined by moving the coil in 1-cm steps around the presumed left M1 of hand until the point of the largest motor-evoked potential (MEP) amplitude of the relaxed abductor pollicis brevis (APB) muscle was reached. The stimulating coil was placed tangentially to the scalp with the handle pointing posteriorly and laterally 45° to the sagittal plane over the LM1 region. The stimulation intensity was determined in relation to the resting motor threshold (RMT) which was defined as the minimum TMS intensity eliciting a peak-to-peak MEP-amplitude of 50 μV or more in resting muscle, in at least 5 out or 10 trials (Groppa et al., 2012; Rossini et al., 2015). To assess the motor cortex excitability, motor-evoked potentials (MEPs) were recorded from the right APB muscle at rest (dominant hand in all participants) by use of silver/carbon-backed electrodes Skintact RT-34 (Fannin Ltd., Dublin, Ireland) with the size of 10.5 mm × 25 mm placed 2 cm apart in a belly-tendon montage (see **Figure 1**). The Neuro-MEP-Micro software was used to measure the amplitude of MEPs (Neurosoft Llc, Ivanovo, Russia).

Intermittent Theta Burst Stimulation

iTBS was delivered over the hotspot of the LM1 using the Neuro-MS/D stimulator (Neurosoft Llc, Ivanovo, Russia). The stimulating protocol was conducted in accordance with the

[1]http://www.chictr.org.cn

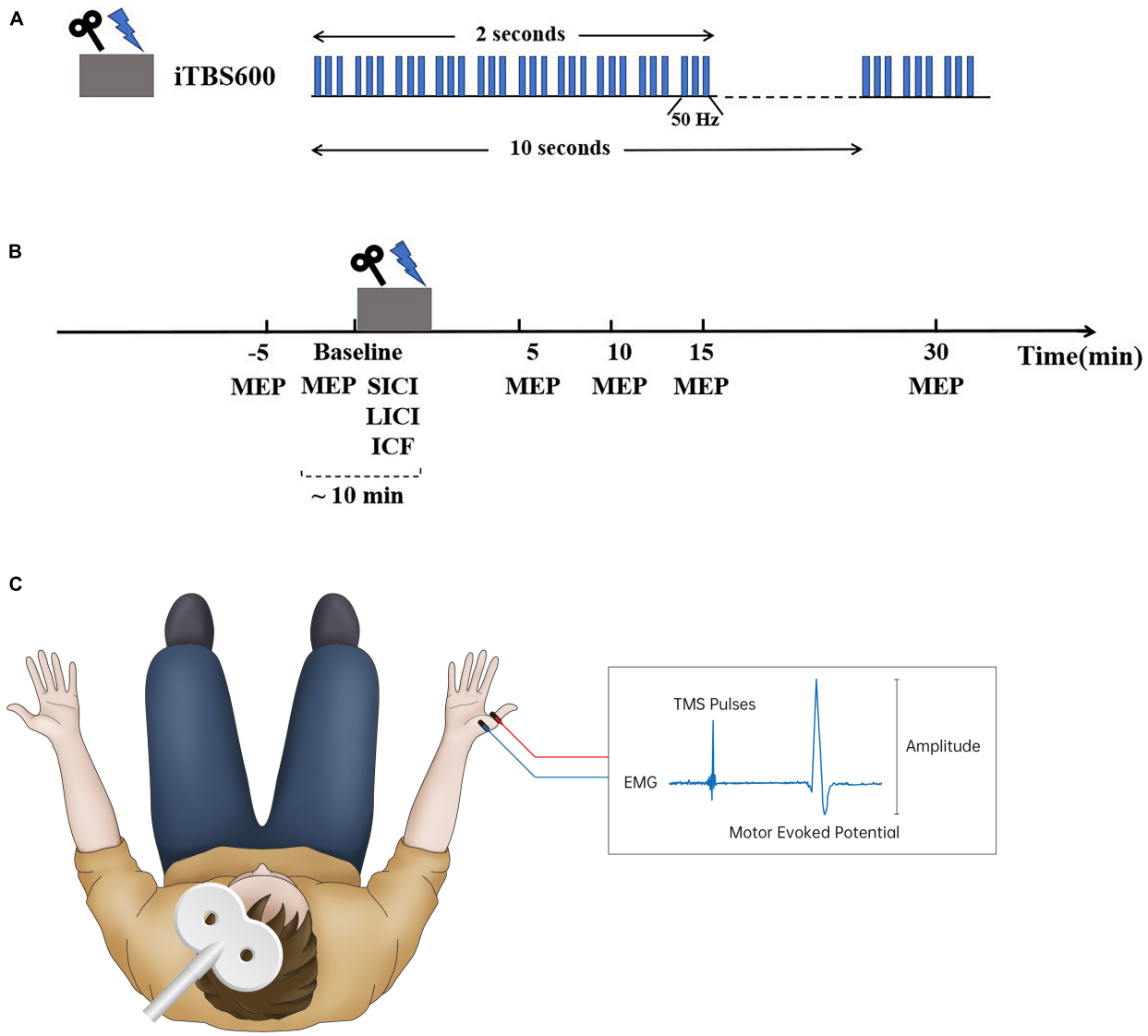

FIGURE 1 | Experimental design. **(A)** Intermittent theta burst stimulation (iTBS) protocol consisted of bursts containing three pulses given at 50 Hz and repeated every 200 ms; a 2-s train of this stimulating pattern was repeated every 10 s for a total of 190 s (600 pulses). **(B)** Each subject was assessed motor-evoked potentials (MEPs) and short-interval intracortical inhibitory (SICI), long-interval intracortical inhibitory (LICI), and intracortical facilitation (ICF) successively before iTBS intervention. Following iTBS, MEPs were assessed at 5, 10, 15, and 30 min after stimulation. **(C)** Transcranial magnetic stimulation (TMS) was performed over the hand region of the left primary motor cortex (LM1) connected with a figure-of-eight coil. The stimulating coil was placed tangentially to the scalp with the handle pointing posteriorly and laterally 45° to the sagittal plane over the LM1 region. MEPs were recorded from the right abductor pollicis brevis (APB) muscle by use of silver/carbon-backed electrodes placed 2 cm apart in a belly-tendon montage to assess cortical excitability.

protocol originally described by Huang et al. (2005), which consisted of bursts containing three pulses given at 50 Hz and repeated every 200 ms (see **Figure 1A**). A 2-s train of this stimulating pattern was repeated every 10 s for a total of 190 s (600 pulses) (Huang et al., 2005). The stimulation intensity was set at 80% of RMT (Bulteau et al., 2017; Fujiki et al., 2020).

Experimental Procedure

Participants were seated in a comfortable chair with a neck support and were asked to relax their right arm entirely. They were also continually reminded to keep their eyes open and fixate forward on throughout each trial. Eyes open and muscle relaxation were observed by visual or electromyography (EMG) monitoring. A hotspot was marked as the optimal coil position where single-pulse TMS produced the largest MEP amplitude of the relaxed APB muscle by moving the coil around the presumed left M1 of hand (Rossini et al., 2015). Single-pulse TMS with intensity of 120% RMT was conducted to assess the excitability of the corticospinal system before and after iTBS. The peak-to-peak amplitude of MEPs evoked by a suprathreshold stimulus with an intensity of 120% RMT was used to probe the excitability of the motor cortex.

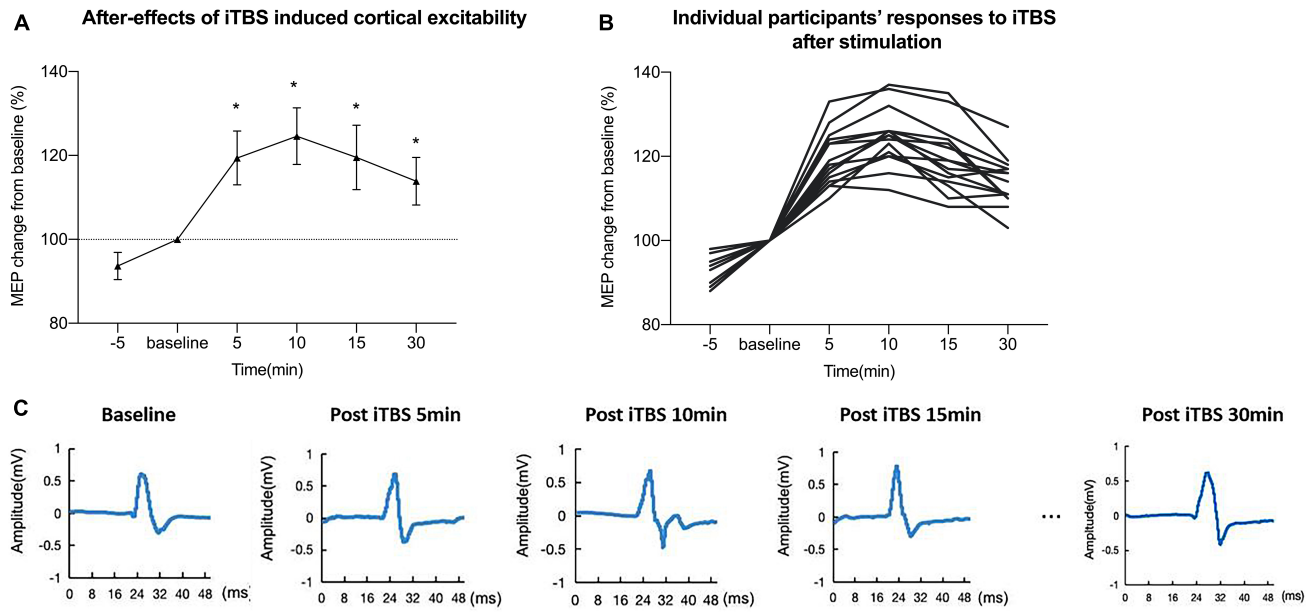

FIGURE 2 | Intermittent theta burst stimulation (iTBS) induced increase in cortical excitability at different time points. **(A)** iTBS induced a mean increase in motor-evoked potential (MEP) amplitude at different time points after intervention. **(B)** Individual responses to iTBS after stimulation of each participant. **(C)** Representative traces in motor-evoked potentials (MEPs) recorded at 5, 10, 15, and 30 min after stimulation. The data indicated that the MEP amplitude began to increase after conducting iTBS.

Before conducting iTBS, each participant received two sessions of single-pulse TMS with 20 consecutive pulses of each with an interval of 5 min at baseline to confirm intraindividual reliability of cortical excitability; the following trials could begin until the difference between average MEPs in two sessions of measurement was no more than 20% (Yu et al., 2020). To quantify the level of GABA or NMDA receptor-mediated activity before stimulation, we measured SICI, LICI, and ICF successively before conducting iTBS using a paired pulse paradigm at rest (Kujirai et al., 1993) (see **Figure 1**). SICI and ICF were delivered with an intensity of 90% RMT for the conditioning stimulus (CS) and 120% RMT for the testing stimulus (TS), with an interstimulus interval (ISI) of 2.5 and 12 ms, respectively, for 10 consecutive trials (Ozdemir et al., 2017; Tran et al., 2020). The CS and TS delivered in LICI were both set at 120% RMT, with an ISI of 150 ms for 10 consecutive trials (Mancheva et al., 2017). Paired pulse TMS results were based on 10 trials with single pulses (unconditioned) and 10 trials with paired pulses (conditioned) as previously recommended (Rossini et al., 2015).

Statistical Analysis

All analyses were performed using IBM SPSS version 22 (Armonk, NY, United States), and statistical significance was set at $p < 0.05$. Data were first tested to evaluate the normal distribution using the Shapiro–Wilk test. The MEPs were normalized to baseline MEP amplitude for each participant to calculate the after-effect of iTBS-induced LTP-like plasticity. Paired-pulse TMS protocols were expressed as the ratio of conditioned MEPs to unconditioned MEPs. A one-way within-subject ANOVA was conducted on the LTP-like after-effect induced by iTBS among different time points (baseline, 5, 10, 15, 30 min). The Mauchly test was used to verify the sphericity. A two-sided Pearson correlation test was used to examine relationships between SICI/LICI/ICF measured before stimulation and the after-effect of iTBS-induced LTP-like plasticity at 5, 10, 15, and 30 min after conducting iTBS, respectively. Multiple tests were corrected using the false discovery rate (FDR) method (Benjamini and Yekutieli, 2001) for ANOVA and Pearson correlation. To examine whether iTBS-induced plasticity can be predicted by SICI, LICI, or ICF, we also performed multiple regression analysis using the stepwise method. The multicollinearity test was performed based on the variance inflation factor (VIF) to examine whether our data met the assumption of collinearity.

RESULTS

Intermittent Theta Burst Stimulation-Induced Plasticity

Figure 2 shows an iTBS-induced increase in cortical excitability at different time points after inducing iTBS and individual participants' responses to iTBS. **Figure 2C** shows representative changes in MEPs recorded at 5, 10, 15, and 30 min after stimulation. The data indicated that the MEP amplitude began to increase after conducting iTBS. A one-way within-subject ANOVA was conducted on the LTP-like after-effect induced by iTBS. There was a significant effect of the after-effect of iTBS-induced LTP-like plasticity among different time points

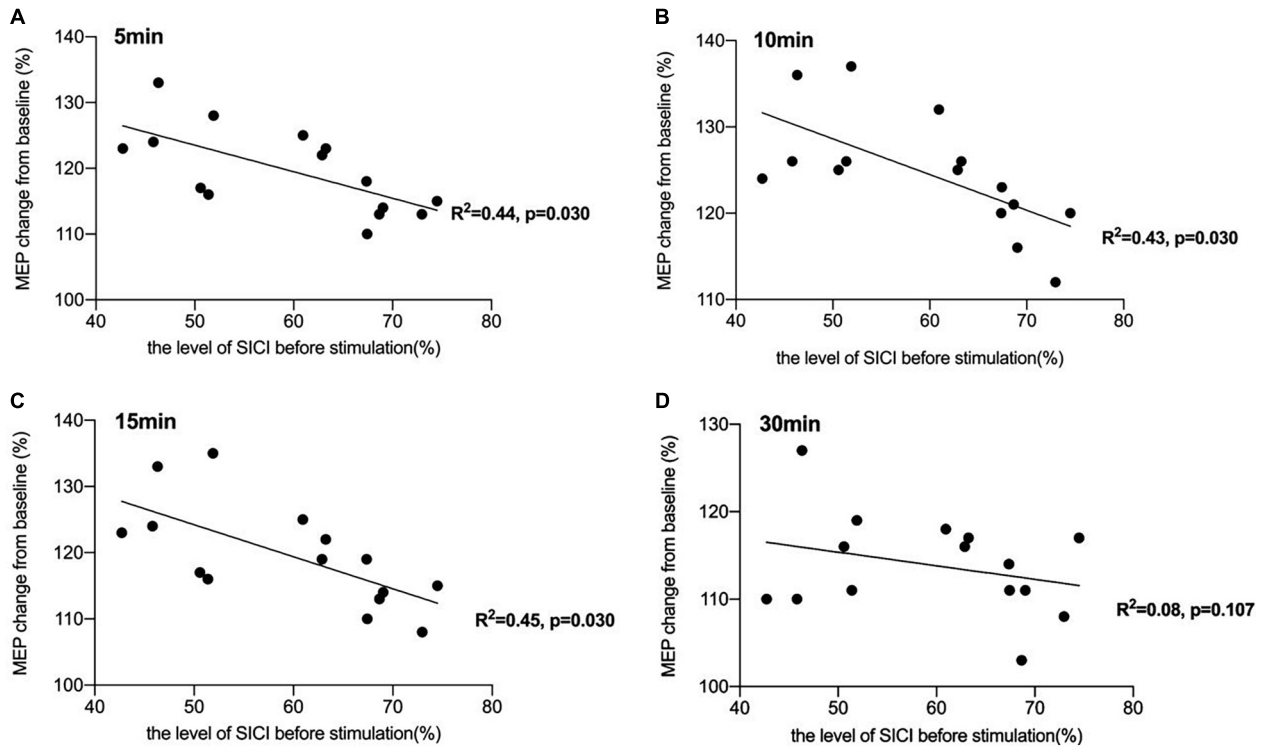

FIGURE 3 | Correlation between short-interval intracortical inhibitory (SICI) and the after-effect of intermittent theta burst stimulation (iTBS)-induced long-term potentiation (LTP)-like plasticity. **(A)** There was a significant negative correlation between the amount of SICI measured before iTBS and the after-effect of iTBS-induced LTP-like plasticity at the time point of 5 min [$R^2 = 0.44$, $p < 0.05$, false discovery rate (FDR) corrected]. **(B)** The correlation between the level of SICI before stimulation and iTBS-induced after-effects at 10 min after conducting iTBS was also significant ($R^2 = 0.43$, $p < 0.05$, FDR corrected). **(C)** A significant negative correlation was also reported between the amount of SICI before stimulation and the iTBS-induced effects at 15 min after stimulation ($R^2 = 0.45$, $p < 0.05$, FDR corrected). **(D)** There was no significant correlation between SICI before stimulation and iTBS effect at 30 min ($R^2 = 0.08$, $p = 0.107$, FDR corrected).

(baseline, 5, 10, 15, 30 min): $F(4,56) = 123.9$, $p < 0.001$ (FDR corrected), $\eta_p 2 = 0.87$.

After-Effect of Intermittent Theta Burst Stimulation-Induced Potential-Like Plasticity Correlates With the Level of Short-Interval Intracortical Inhibitory Before Stimulation

There was a significant negative correlation between the amount of SICI measured before iTBS and the after-effect of iTBS-induced LTP-like plasticity at the time points of 5 min ($R^2 = 0.44$, $p < 0.05$, FDR corrected), 10 min ($R^2 = 0.43$, $p < 0.05$, FDR corrected), and 15 min ($R^2 = 0.45$, $p < 0.05$, FDR corrected) following conduction of iTBS (**Figure 3**). *Post hoc* power analysis indicated that the power to detect the observed effects at the 0.05 level was 0.742, 0.760, and 0.807 at the time points of 5, 10, and 15 min, respectively, while there is no significant correlation between SICI before stimulation and iTBS effect at 30 min ($R^2 = 0.08$, $p = 0.107$, FDR corrected). No correlation between iTBS after-effect and the level of LICI was found at all time points 5, 10, 15, and 30 min after stimulation (**Figure 4**). Similarly, the iTBS after-effect was not correlated with the level of ICF measured before iTBS at all time points (**Figure 5**). **Table 1** shows all R^2 and p-values before and after applying the FDR correction.

Short-Interval Intracortical Inhibitory as a Good Predictor of Effectiveness of Intermittent Theta Burst Stimulation-Induced Cortical Plasticity

To assess predictive values for iTBS-induced cortical plasticity, we performed the multiple linear regression analysis with the levels of SICI, LICI, and ICF before iTBS as independent variables, and the dependent variable the after-effects of iTBS-induced cortical plasticity. Results from multicollinearity tests showed that the data met the assumption of collinearity with VIF = 1. Results from stepwise linear regression indicated that the model, with SICI as the only predictor, was significant at the time point of 5 min following iTBS conduction [$F(1,13) = 10.144$, $p = 0.007$, $R^2 = 0.40$] and with beta coefficient = –0.4 for influence of SICI on the iTBS-induced cortical plasticity. In addition, SICI also remained as the only predictor in the models of 10 min [$F(1,13) = 9.952$, $p = 0.008$, $R^2 = 0.40$] and 15 min [$F(1,13) = 10.733$, $p = 0.006$, $R^2 = 0.41$] after conducting iTBS, with beta coefficients = –0.42 and –0.48 for influence of SICI on the iTBS-induced after-effect at 10 and 15 min after stimulation,

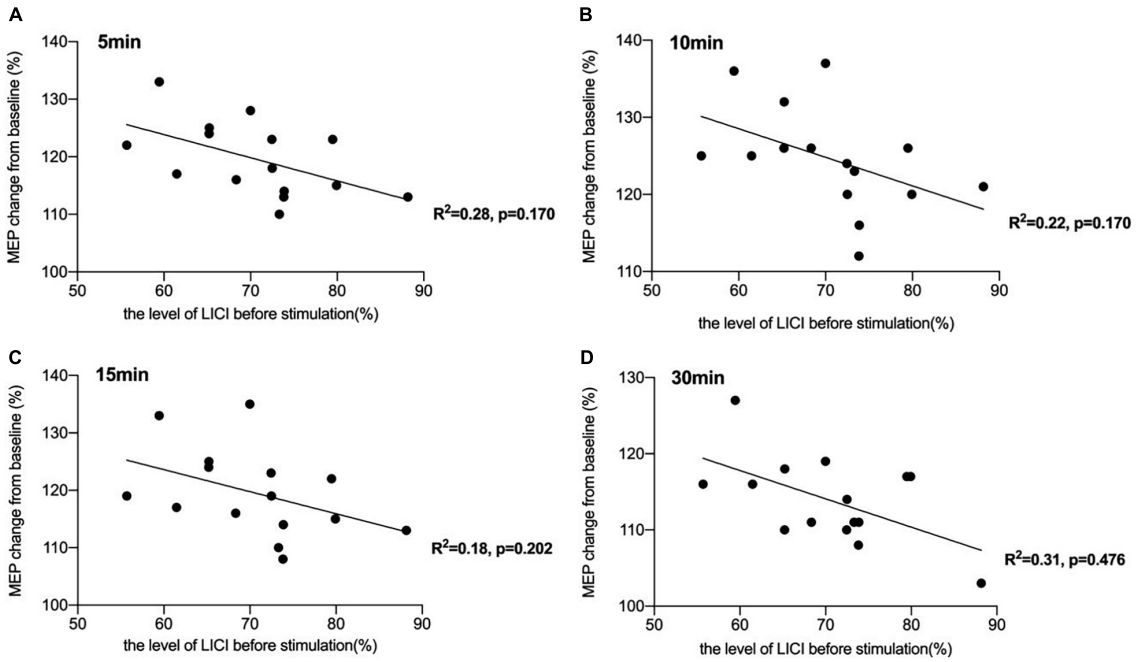

FIGURE 4 | Correlation between long-interval intracortical inhibitory (LICI) and the after-effect of intermittent theta burst stimulation (iTBS)-induced long-term potentiation (LTP)-like plasticity. **(A)** No significant correlation was reported between the amount of LICI measured before iTBS and the iTBS after-effect at the time point of 5 min [R^2 = 0.28, p = 0.170, false discovery rate (FDR) corrected]. **(B)** No significant correlation was also reported between the amount of LICI before stimulation and the iTBS-induced effects at 10 min after stimulation (R^2 = 0.22, p = 0.170, FDR corrected). **(C)** The correlation between the level of LICI before stimulation and iTBS-induced after-effects at 15 min after conducting iTBS was also not significant (R^2 = 0.18, p = 0.202, FDR corrected). **(D)** There was also no significant correlation between the level of LICI and the after-effect of iTBS-induced LTP-like plasticity at the time point of 30 min (R^2 = 0.31, p = 0.476, FDR corrected).

respectively. *Post hoc* power analysis revealed that coefficients of −0.4, −0.42, and −0.48 could be detected at 0.05 at a power of greater than 0.90.

DISCUSSION

The current study aimed at providing a direct investigation of the relationship between LTP-like plasticity induced by iTBS in the human motor cortex and the level of GABA or NMDA receptor-mediated activity before stimulation. We used a series of paired-pulse TMS protocols including SICI, LICI, and ICF to assess $GABA_A$ receptor-, $GABA_B$ receptor-, and glutamate receptor-mediated activity, respectively. Our findings showed that (i) $GABA_A$ receptor-mediated activity assessed before stimulation was significantly negatively correlated with LTP-like plasticity induced by iTBS following 5, 10, and 15 min after conduction of stimulation; (ii) there was no significant correlation between LTP-like plasticity induced by iTBS and $GABA_B$ receptor- or glutamate receptor-mediated activity before stimulation as assessed by the TMS protocol of LICI and ICF; and (iii) SICI, as the index of $GABA_A$ receptor-mediated activity measured before stimulation, is a good predictor of iTBS-induced LTP-like plasticity for a period lasting 15 min following stimulation.

Cortical inhibition is essential for regulating neuronal excitability, and a decrease in local inhibitory signaling is necessary for LTP-like plasticity to occur. In the present study, we found that $GABA_A$ receptor-mediated activity before stimulation was significantly negatively correlated with LTP-like plasticity induced by iTBS. This is consistent with previous evidence indicating that reduced GABAergic inhibition can facilitate induction of LTP-like plasticity (Castro-Alamancos et al., 1995; Trepel and Racine, 2000; Chen et al., 2010; Bachtiar and Stagg, 2014). Similar findings have also been observed in patients during chronic stages of stroke recovery that $GABA_A$ receptor-mediated activity is reduced compared with healthy controls (Blicher et al., 2009). Furthermore, we also found that SICI measured before stimulation is a good predictor of iTBS-induced LTP-like plasticity for a period lasting 15 min. Our findings might add evidence to the suggestion that SICI in the early recovery phase can be a predictor of LTP-like plasticity in the later recovery stage for patients after stroke (McDonnell et al., 2007; Liuzzi et al., 2014).

In addition to $GABA_A$ receptors, $GABA_B$ receptors are also thought to have an important role in induction of LTP (Larson and Munkácsy, 2015). In the present study, $GABA_B$ receptor-mediated activity before stimulation as assessed by LICI was found not significantly correlated with the after-effects of LTP-like plasticity induced by iTBS. This suggested that the interplay between $GABA_B$ receptor-mediated inhibition and plasticity is complex. In addition, metabotropic $GABA_B$ receptors have been found to modulate inhibitory neural circuits

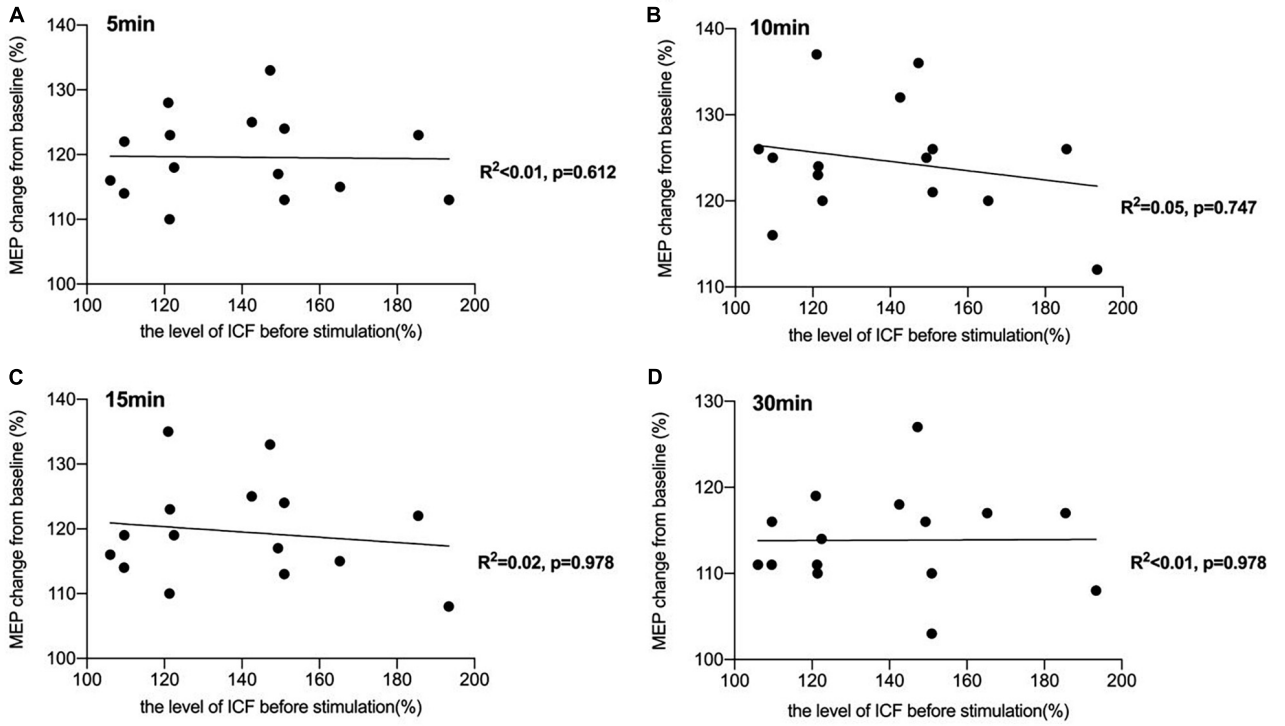

FIGURE 5 | Correlation between intracortical facilitation (ICF) and the after-effect of intermittent theta burst stimulation (iTBS)-induced long-term potentiation (LTP)-like plasticity. **(A)** No significant correlation was reported between the amount of ICF measured before iTBS and the iTBS after-effect at the time point of 5 min [$R^2 < 0.01$, $p = 0.612$, false discovery rate (FDR) corrected]. **(B)** There was also no significant correlation between the level of ICF and the after-effect of iTBS-induced LTP-like plasticity at the time point of 10 min ($R^2 = 0.05$, $p = 0.747$, FDR corrected). **(C)** A non-significant correlation was also reported between the amount of ICF before stimulation and the iTBS-induced effects at 15 min after stimulation ($R^2 = 0.02$, $p = 0.978$, FDR corrected). **(D)** There was no significant correlation between ICF before stimulation and iTBS-effect at 30 min ($R^2 < 0.01$, $p = 0.978$, FDR corrected).

TABLE 1 | Correlation between the level of short-interval intracortical inhibitory (SICI), long-interval intracortical inhibitory (LICI), and intracortical facilitation (ICF) measured before stimulation and the after-effect of intermittent theta burst stimulation (iTBS)-induced long-term potentiation (LTP)-like plasticity (all R^2 and *p*-values before and after applying the FDR correction).

ppTMS protocol	Time points after iTBS (min)	R^2	*p*-value before FDR correction	*p*-value after FDR correction	Results after FDR correction
SICI	5	0.44	0.005	0.030	Significant
	10	0.43	0.006	0.030	Significant
	15	0.45	0.008	0.030	Significant
	30	0.08	0.036	0.107	Not significant
LICI	5	0.28	0.078	0.170	Not significant
	10	0.22	0.085	0.170	Not significant
	15	0.18	0.118	0.202	Not significant
	30	0.31	0.317	0.476	Not significant
ICF	5	0.00036	0.459	0.612	Not significant
	10	0.05	0.623	0.747	Not significant
	15	0.02	0.916	0.978	Not significant
	30	0.000064	0.978	0.978	Not significant

by mediating long-lasting inhibitory postsynaptic potentials or involve presynaptic autoinhibition of interneurons through $GABA_A$ receptors to inhibit GABA release (McDonnell et al., 2006; McDonnell et al., 2007). The former postsynaptic inhibition hyperpolarizes target neurons and reduces LTP-like plasticity, whereas the latter one depolarizes target neurons and results in facilitation of LTP (Mott and Lewis, 1991; Stäubli et al., 1999). In the current study, LICI was used to measure $GABA_B$ receptor-mediated effects without distinguishing postsynaptic and presynaptic $GABA_B$ effects. On the other hand, McDonnell et al. (2006) and Cash et al. (2010) suggested that these two different $GABA_B$ effects should be measured using LICI protocol

and induce SICI in the presence of LICI in the human motor cortex. Therefore, although no significant correlation between postsynaptic $GABA_B$ effects measured by LICI- and iTBS-induced LTP was found in the present study, future studies need to further investigate the relationship between presynaptic $GABA_B$ effects and LTP-like plasticity.

Further, it is not consistent with our expectation that no significant correlation was found between iTBS after-effects and NMDA receptor-mediated activity before iTBS as assessed by ICF. Plentiful studies have shown that the NMDA receptor plays an important role in the development of rapid cortical plastic changes and activation of NMDA receptors is necessary to induce LTP-like plasticity (Hunt and Castillo, 2012; Hasan et al., 2013), while this phenomenon was not confirmed by others (Liao et al., 1995; Selig et al., 1995). Besides, previous work indicated that although LTP is induced by activation of NMDA receptors at synapses, these mechanisms are mediated by AMPA receptors trafficking in postsynaptic neurons (Park et al., 2018; Sumi and Harada, 2020). Further studies need to explore the role the AMPA receptor plays in iTBS-induced LTP-like plasticity and how to separate the effect of the NMDA and AMPA receptors on iTBS-induced after-effects. In addition, it may also be due to the fact that ICF is not an ideal measurement of NMDA receptor-mediated activities as more than one possible neural circuit contribute to ICF (Hanajima et al., 1998). Recent studies combining TMS–MRS methods showed that there was no significant relationship between the ICF protocol with ISI of 12 ms and MRS-glutamate, which questioned ICF as an effective tool to measure the level of NMDA-type glutamate receptor-mediated activity (Stagg et al., 2011; Dyke et al., 2017).

In conclusion, the present study found that $GABA_A$ receptor-mediated activity measured before stimulation is negatively correlated with the after-effect of cortical excitability induced by iTBS. SICI, as an index of $GABA_A$ receptor-mediated activity measured before stimulation, is a good predictor of iTBS-induced LTP-like plasticity for a period lasting 15 min following stimulation. However, there are several limitations in our study. First, we measured cortical excitability only within 30 min following iTBS protocols; it is unclear what happens after 30 min. In addition, a limited number of TMS pulses were applied to LM1, with only 10 trials for each condition (i.e., SICI, ICF, and LICI). Although we have ensured intraindividual reliability of cortical excitability by performing two sessions of single-pulse TMS with an interval of 5 min, the optimal number of trials was required to reduce interindividual differences in order to make the results more reliable. Furthermore, as a pilot study, the sample size is small and the sex of participants was not very balanced. Although no previous work has reported a sex difference in the iTBS-induced after-effects, further studies are still required to investigate sex differences in iTBS-induced LTP-like plasticity to make our findings more generalized to the entire population.

DATA AVAILABILITY STATEMENT

The raw data supporting the conclusions of this article will be made available by the authors, without undue reservation.

ETHICS STATEMENT

The studies involving human participants were reviewed and approved by the Ethics Committee of Affiliated Jiangsu Shengze Hospital of Nanjing Medical University. The patients/participants provided their written informed consent to participate in this study.

AUTHOR CONTRIBUTIONS

YS, T-FY, and CH had full access to all the data in the study, took responsibility for the integrity of the data and the accuracy of the data analysis, designed the trial, and provided critical revisions to the manuscript. XD wrote the original draft as well as review and editing of the current manuscript. QL performed the data analysis. QL, LQ, and XD performed the study procedures. YS was responsible for the funding acquisition. All authors contributed to the article and approved the submitted version.

FUNDING

This research was supported by the Introduced Project of Suzhou Clinical Medical Expert Team (Number SZYJTD201725), the Nanjing Municipal Science and Technology Bureau (Number 2019060002), and the National Key R&D Program of China (Numbers 2018YFC2001600 and 2018YFC2001603).

ACKNOWLEDGMENTS

We thank all volunteers for their participation in this study. We express our gratitude to Xinyu Zhang for assistance with recruitment and testing of study participants.

REFERENCES

Bachtiar, V., and Stagg, C. J. (2014). The role of inhibition in human motor cortical plasticity. *Neuroscience* 278, 93–104. doi: 10.1016/j.neuroscience.2014.07.059

Benjamini, Y., and Yekutieli, D. (2001). The control of the false discovery rate in multiple testing under dependency. *Ann. Statistics* 29, 1165–1188.

Blicher, J. U., Jakobsen, J., Andersen, G., and Nielsen, J. F. (2009). Cortical excitability in chronic stroke and modulation by training: a TMS study. *Neurorehabil. Neural Repair.* 23, 486–493. doi: 10.1177/1545968308328730

Bliss, T. V., and Lømo, T. (1973). Long-lasting potentiation of synaptic transmission in the dentate area of the anaesthetized rabbit following stimulation of the perforant path. *J. Physiol.* 232, 331–356. doi: 10.1113/jphysiol.1973.sp010273

Bulteau, S., Sébille, V., Fayet, G., Thomas-Ollivier, V., Deschamps, T., Bonnin-Rivalland, A., et al. (2017). Efficacy of intermittent Theta Burst Stimulation (iTBS) and 10-Hz high-frequency repetitive transcranial magnetic stimulation (rTMS) in treatment-resistant unipolar depression: study protocol for a randomised controlled trial. *Trials* 18, 1–10. doi: 10.1186/s13063-016-1764-8

Cash, R. F. H., Ziemann, U., Murray, K., and Thickbroom, G. W. (2010). Late cortical disinhibition in human motor cortex: a triple-pulse transcranial magnetic stimulation study. *J. Neurophysiol.* 103, 511–518. doi: 10.1152/jn.00782.2009

Castro-Alamancos, A., Donoghue, P., and Connors, W. (1995). Different forms of synaptic plasticity in somatosensory areas of the neocortex. *J. Neurosci.* 15(7 Pt 2), 5324–5333. doi: 10.1523/jneurosci.15-07-05324.1995

Chen, H., Epstein, J., and Stern, E. (2010). Neural plasticity after acquired brain injury: evidence from functional neuroimaging. *PMR* 2, S306–S312. doi: 10.1016/j.pmrj.2010.10.006

Cooke, S. F. (2006). Plasticity in the human central nervous system. *Brain* 129, 1659–1673. doi: 10.1093/brain/awl082

Cramer, S. C., Sur, M., Dobkin, B. H., O'brien, C., Sanger, T. D., Trojanowski, J. Q., et al. (2011). Harnessing neuroplasticity for clinical applications. *Brain* 134, 1591–1609.

Di Lazzaro, V., Pilato, F., Dileone, M., Profice, P., Oliviero, A., Mazzone, P., et al. (2008). The physiological basis of the effects of intermittent theta burst stimulation of the human motor cortex: Theta-burst rTMS of the human motor cortex. *J. Physiol.* 586, 3871–3879. doi: 10.1113/jphysiol.2008.152736

Di Lazzaro, V., Pilato, F., Dileone, M., Ranieri, F., Ricci, V., Profice, P., et al. (2006). GABAA receptor subtype specific enhancement of inhibition in human motor cortex. *J. Physiol.* 575, 721–726. doi: 10.1113/jphysiol.2006.114694

Dyke, K., Pépés, S. E., Chen, C., Kim, S., Sigurdsson, H. P., Draper, A., et al. (2017). Comparing GABA-dependent physiological measures of inhibition with proton magnetic resonance spectroscopy measurement of GABA using ultra-high-field MRI. *Neuroimage* 152, 360–370. doi: 10.1016/j.neuroimage.2017.03.011

Fujiki, M., Kawasaki, Y., and Fudaba, H. (2020). Continuous theta-burst stimulation intensity dependently facilitates motor-evoked potentials following focal electrical stimulation of the rat motor cortex. *Front. Neural Circuits* 14:585624. doi: 10.3389/fncir.2020.585624

Groppa, S., Oliviero, A., Eisen, A., Quartarone, A., Cohen, L. G., Mall, V., et al. (2012). A practical guide to diagnostic transcranial magnetic stimulation: report of an IFCN committee. *Clin. Neurophysiol.* 123, 858–882. doi: 10.1016/j.clinph.2012.01.010

Hamada, M., Murase, N., Hasan, A., Balaratnam, M., and Rothwell, J. C. (2013). The role of interneuron networks in driving human motor cortical plasticity. *Cereb. Cortex* 23, 1593–1605. doi: 10.1093/cercor/bhs147

Hanajima, R., Ugawa, Y., Terao, Y., Sakai, K., Furubayashi, T., Machii, K., et al. (1998). Paired-pulse magnetic stimulation of the human motor cortex: differences among I waves. *J. Physiol.* 509(Pt 2), 607–618. doi: 10.1111/j.1469-7793.1998.607bn.x

Hasan, M. T., Hernández-González, S., Dogbevia, G., Trevino, M., Bertocchi, I., Gruart, A., et al. (2013). Role of motor cortex NMDA receptors in learning-dependent synaptic plasticity of behaving mice. *Nat. Commun.* 4:2258. doi: 10.1038/ncomms3258

Hebb, D. O. (2005). *The Organization of Behavior: A Neuropsychological Theory*. Hove: Psychology Press.

Hess, G., Aizenman, C. D., and Donoghue, J. P. (1996). Conditions for the induction of long-term potentiation in layer II/III horizontal connections of the rat motor cortex. *J. Neurophysiol.* 75, 1765–1778. doi: 10.1152/jn.1996.75.5.1765

Hinder, M. R., Goss, E. L., Fujiyama, H., Canty, A. J., Garry, M. I., Rodger, J., et al. (2014). Inter- and intra-individual variability following intermittent theta burst stimulation: implications for rehabilitation and recovery. *Brain Stimulation* 7, 365–371. doi: 10.1016/j.brs.2014.01.004

Huang, Y. Z., Edwards, M. J., Rounis, E., Bhatia, K. P., and Rothwell, J. C. (2005). Theta burst stimulation of the human motor cortex. *Neuron* 45, 201–206.

Hunt, D. L., and Castillo, P. E. (2012). Synaptic plasticity of NMDA receptors: mechanisms and functional implications. *Curr. Opin. Neurobiol.* 22, 496–508. doi: 10.1016/j.conb.2012.01.007

Ilić, T. V., Meintzschel, F., Cleff, U., Ruge, D., Kessler, K. R., and Ziemann, U. (2002). Short-interval paired-pulse inhibition and facilitation of human motor cortex: the dimension of stimulus intensity. *J. Physiol.* 545, 153–167. doi: 10.1113/jphysiol.2002.030122

Kano, M., and Iino, K. (1991). Functional reorganization of adult cat somatosensory cortex is dependent on NMDA receptors. *NeuroReport* 2, 77–80. doi: 10.1097/00001756-199102000-00003

Kotak, V. C., Mirallave, A., Mowery, T. M., and Sanes, D. H. (2017). GABAergic inhibition gates excitatory LTP in perirhinal cortex. *Hippocampus* 27, 1217–1223. doi: 10.1002/hipo.22799

Kujirai, T., Caramia, M. D., Rothwell, J. C., Day, B. L., Thompson, P. D., Ferbert, A., et al. (1993). Corticocortical inhibition in human motor cortex. *J. Physiol.* 471, 501–519. doi: 10.1113/jphysiol.1993.sp019912

Larson, J., and Munkácsy, E. (2015). Theta-burst LTP. *Brain Res.* 1621, 38–50. doi: 10.1016/j.brainres.2014.10.034

Lefaucheur, J.-P., Aleman, A., Baeken, C., Benninger, D. H., Brunelin, J., Di Lazzaro, V., et al. (2020). Evidence-based guidelines on the therapeutic use of repetitive transcranial magnetic stimulation (rTMS): an update (2014–2018). *Clin. Neurophysiol.* 131, 474–528. doi: 10.1016/j.clinph.2019.11.002

Liao, D., Hessler, N. A., and Malinow, R. (1995). Activation of postsynaptically silent synapses during pairing-induced LTP in CA1 region of hippocampal slice. *Nature* 375, 400–404. doi: 10.1038/375400a0

Liuzzi, G., Hörniß, V., Lechner, P., Hoppe, J., Heise, K., Zimerman, M., et al. (2014). Development of movement-related intracortical inhibition in acute to chronic subcortical stroke. *Neurology* 82, 198–205. doi: 10.1212/WNL.0000000000000028

Llona, I., Farías, P., and Troc-Gajardo, J. L. (2017). Early postnatal development of somastostatinergic systems in brainstem respiratory network. *Plastic Brain* 1015, 131–144. doi: 10.1007/978-3-319-62817-2_8

Mancheva, K., Stephanova, D. I., Wolf, W., and Kossev, A. (2017). "Long-Latency intracortical inhibition during unilateral muscle activity," in *CMBEBIH 2017*, ed. A. Badnjevic (Singapore: Springer). doi: 10.1152/japplphysiol.01016.2017

Mateos-Aparicio, P., and Rodríguez-Moreno, A. (2019). The impact of studying brain plasticity. *Front. Cell. Neurosci.* 13:66. doi: 10.3389/fncel.2019.00066

McDonnell, M. N., Orekhov, Y., and Ziemann, U. (2006). The role of GABA B receptors in intracortical inhibition in the human motor cortex. *Exp. Brain Res.* 173, 86–93. doi: 10.1007/s00221-006-0365-2

McDonnell, M. N., Orekhov, Y., and Ziemann, U. (2007). Suppression of LTP-like plasticity in human motor cortex by the GABAB receptor agonist baclofen. *Exp. Brain Res.* 180, 181–186. doi: 10.1007/s00221-006-0849-840

Mott, D., and Lewis, D. (1991). Facilitation of the induction of long-term potentiation by GABAB receptors. *Science* 252, 1718–1720. doi: 10.1126/science.1675489

Oldfield, R. C. (1971). The assessment and analysis of handedness: the Edinburgh inventory. *Neuropsychologia* 9, 97–113. doi: 10.1016/0028-3932(71)90067-4

Ozdemir, Z., Sirin, G., Kayki, Y., Acar, E., and Soysal, A. (2017). P226 The effect of interstimulus interval between the conditioning and test stimulus on inhibition and fascilitation: a transcranial magnetic stimulation study. *Clin. Neurophysiol.* 128:e251.

Park, P., Kang, H., Sanderson, T. M., Bortolotto, Z. A., Georgiou, J., Zhuo, M., et al. (2018). The role of calcium-permeable AMPARs in long-term potentiation at principal neurons in the rodent hippocampus. *Front. Synaptic Neurosci.* 10:42. doi: 10.3389/fnsyn.2018.00042

Ridding, M. C., and Ziemann, U. (2010). Determinants of the induction of cortical plasticity by non-invasive brain stimulation in healthy subjects. *J. Physiol.* 588, 2291–2304. doi: 10.1113/jphysiol.2010.190314

Rossini, P. M., Burke, D., Chen, R., Cohen, L. G., Daskalakis, Z., Di Iorio, R., et al. (2015). Non-invasive electrical and magnetic stimulation of the brain, spinal cord, roots and peripheral nerves: basic principles and procedures for routine clinical and research application. an updated report from an IFCN Committee. *Clin. Neurophysiol.* 126, 1071–1107. doi: 10.1016/j.clinph.2015.02.001

Schilberg, L., Schuhmann, T., and Sack, A. T. (2017). Interindividual variability and intraindividual reliability of intermittent theta burst stimulation-induced neuroplasticity mechanisms in the healthy brain. *J. Cogn. Neurosci.* 29, 1022–1032. doi: 10.1162/jocn_a_01100

Schwenkreis, P., Maier, C., Pleger, B., Mansourian, N., Dertwinkel, R., Malin, J. P., et al. (2003). NMDA-mediated mechanisms in cortical excitability changes after limb amputation. *Acta Neurol. Scand.* 108, 179–184. doi: 10.1034/j.1600-0404.2003.00114.x

Selig, D. K., Hjelmstad, G. O., Herron, C., Nicoll, R. A., and Malenka, R. C. (1995). Independent mechanisms for long-term depression of AMPA and NMDA responses. *Neuron* 15, 417–426. doi: 10.1016/0896-6273(95)90045-4

Siebner, H., and Rothwell, J. (2003). Transcranial magnetic stimulation: new insights into representational cortical plasticity. *Exp. Brain Res.* 148, 1–16. doi: 10.1007/s00221-002-1234-1232

Stagg, C. J., Bestmann, S., Constantinescu, A. O., Moreno Moreno, L., Allman, C., Mekle, R., et al. (2011). Relationship between physiological measures of excitability and levels of glutamate and GABA in the human motor cortex. *J. Physiol.* 589, 5845–5855. doi: 10.1113/jphysiol.2011.216978

Stäubli, U., Scafidi, J., and Chun, D. (1999). GABA B receptor antagonism: facilitatory effects on memory parallel those on LTP induced by TBS but not HFS. *J. Neurosci.* 19, 4609–4615. doi: 10.1523/JNEUROSCI.19-11-04609.1999

Sumi, T., and Harada, K. (2020). Mechanism underlying hippocampal long-term potentiation and depression based on competition between endocytosis and exocytosis of AMPA receptors. *Sci. Rep.* 10:14711. doi: 10.1038/s41598-020-71528-3

Takeuchi, T., Duszkiewicz, A. J., and Morris, R. G. M. (2014). The synaptic plasticity and memory hypothesis: encoding, storage and persistence. *Philos. Trans. R. Soc. B: Biol. Sci.* 369:20130288. doi: 10.1098/rstb.2013.0288

Todd, G., Flavel, S. C., and Ridding, M. C. (2009). Priming theta-burst repetitive transcranial magnetic stimulation with low- and high-frequency stimulation. *Exp. Brain Res.* 195, 307–315. doi: 10.1007/s00221-009-1791-1798

Tran, D. M., Chowdhury, N. S., McNair, N. A., Harris, J. A., and Livesey, E. J. (2020). Linking cortical and behavioural inhibition: testing the parameter specificity of a transcranial magnetic stimulation protocol. *Brain Stimulation* 13, 1381–1383. doi: 10.1016/j.brs.2020.07.010

Trepel, C., and Racine, R. J. (2000). GABAergic modulation of neocortical long-term potentiation in the freely moving rat. *Synapse* 35, 120–128.

Wang, H., Wang, X., and Scheich, H. (1996). LTD and LTP induced by transcranial magnetic stimulation in auditory cortex. *Neuroreport* 7, 521–525. doi: 10.1097/00001756-199601310-00035

Wieloch, T., and Nikolich, K. (2006). Mechanisms of neural plasticity following brain injury. *Curr. Opin. Neurobiol.* 16, 258–264. doi: 10.1016/j.conb.2006.05.011

Yu, F., Tang, X., Hu, R., Liang, S., Wang, W., Tian, S., et al. (2020). The After-Effect of accelerated intermittent theta burst stimulation at different session intervals. *Front. Neurosci.* 14:576. doi: 10.3389/fnins.2020.00576

Ziemann, U., Corwell, B., and Cohen, L. G. (1998b). Modulation of plasticity in human motor cortex after forearm ischemic nerve block. *J. Neurosci.* 18, 1115–1123. doi: 10.1523/JNEUROSCI.18-03-01115.1998

Ziemann, U., Chen, R., Cohen, L. G., and Hallett, M. (1998a). Dextromethorphan decreases the excitability of the human motor cortex. *Neurology* 51, 1320–1324. doi: 10.1212/wnl.51.5.1320

Conflict of Interest: The authors declare that the research was conducted in the absence of any commercial or financial relationships that could be construed as a potential conflict of interest.

Publisher's Note: All claims expressed in this article are solely those of the authors and do not necessarily represent those of their affiliated organizations, or those of the publisher, the editors and the reviewers. Any product that may be evaluated in this article, or claim that may be made by its manufacturer, is not guaranteed or endorsed by the publisher.

frontiers in Neuroscience

CLINICAL TRIAL
published: 11 March 2022
doi: 10.3389/fnins.2022.808830

Sensorimotor Rhythm-Brain Computer Interface With Audio-Cue, Motor Observation and Multisensory Feedback for Upper-Limb Stroke Rehabilitation: A Controlled Study

Xin Li[1†], Lu Wang[2†], Si Miao[2†], Zan Yue[2], Zhiming Tang[1], Liujie Su[1], Yadan Zheng[1], Xiangzhen Wu[3], Shan Wang[4], Jing Wang[2*] and Zulin Dou[1*]*

[1] Department of Rehabilitation Medicine, The Third Affiliated Hospital of Sun Yat-sen University, Guangzhou, China, [2] Institute of Robotics and Intelligent Systems, School of Mechanical Engineering, Xi'an Jiaotong University, Xi'an, China, [3] Department of Rehabilitation Medicine, Shenzhen Hengsheng Hospital, Shenzhen, China, [4] Air Force Medical Center, PLA, Beijing, China

Several studies have shown the positive clinical effect of brain computer interface (BCI) training for stroke rehabilitation. This study investigated the efficacy of the sensorimotor rhythm (SMR)-based BCI with audio-cue, motor observation and multisensory feedback for post-stroke rehabilitation. Furthermore, we discussed the interaction between training intensity and training duration in BCI training. Twenty-four stroke patients with severe upper limb (UL) motor deficits were randomly assigned to two groups: 2-week SMR-BCI training combined with conventional treatment (BCI Group, BG, $n = 12$) and 2-week conventional treatment without SMR-BCI intervention (Control Group, CG, $n = 12$). Motor function was measured using clinical measurement scales, including Fugl-Meyer Assessment-Upper Extremities (FMA-UE; primary outcome measure), Wolf Motor Functional Test (WMFT), and Modified Barthel Index (MBI), at baseline (Week 0), post-intervention (Week 2), and follow-up week (Week 4). EEG data from patients allocated to the BG was recorded at Week 0 and Week 2 and quantified by mu suppression means event-related desynchronization (ERD) in mu rhythm (8–12 Hz). All functional assessment scores (FMA-UE, WMFT, and MBI) significantly improved at Week 2 for both groups ($p < 0.05$). The BG had significantly higher FMA-UE and WMFT improvement at Week 4 compared to the CG. The mu suppression of bilateral hemisphere both had a positive trend with the motor function scores at Week 2. This study proposes a new effective SMR-BCI system and demonstrates that the SMR-BCI training with audio-cue, motor observation and multisensory feedback, together with conventional therapy may promote long-lasting UL motor improvement.

Clinical Trial Registration: [http://www.chictr.org.cn], identifier [ChiCTR2000041119].

Keywords: stroke, motor imagery, brain computer interface, mu rhythm, rehabilitation

OPEN ACCESS

Edited by:
Surjo R. Soekadar, Charité – Universitätsmedizin Berlin, Germany

Reviewed by:
Pratik Yashvant Chhatbar, Duke University, United States
Pavel Bobrov, Institute of Higher Nervous Activity and Neurophysiology (RAS), Russia

***Correspondence:**
Shan Wang
ab0782@sina.com
Jing Wang
wangpele@gmail.com
Zulin Dou
douzul@163.com

† These authors have contributed equally to this work

Specialty section:
This article was submitted to Neuroprosthetics, a section of the journal Frontiers in Neuroscience

Received: *04 November 2021*
Accepted: *27 January 2022*
Published: *11 March 2022*

Citation:
Li X, Wang L, Miao S, Yue Z, Tang Z, Su L, Zheng Y, Wu X, Wang S, Wang J and Dou Z (2022) Sensorimotor Rhythm-Brain Computer Interface With Audio-Cue, Motor Observation and Multisensory Feedback for Upper-Limb Stroke Rehabilitation: A Controlled Study. Front. Neurosci. 16:808830. doi: 10.3389/fnins.2022.808830

INTRODUCTION

Stroke is a leading cause of mortality and disability worldwide (Johnson et al., 2019; Zhou et al., 2019). Up to 66% of stroke survivors experience upper limb (UL) motor impairments, which result in functional limitations in activities of daily living and decreased life quality (Kwah et al., 2013; Morris et al., 2013).

Electroencephalography (EEG)-based sensorimotor rhythm (SMR) brain computer interface (BCI) is a novel technology that can enhance activity-dependent neuroplasticity and restore motor function for stroke survivors (Ang et al., 2014a; Lazarou et al., 2018; Jeunet et al., 2019). SMRs can be measured over the sensorimotor cortex and modulated by actual movement, motor intention, or motor imagery (MI; Frenkel-Toledo et al., 2014; Yuan and He, 2014). Task-related modulation in EEG-based SMRs is usually manifested as event-related desynchronization (ERD) or event-related synchronization (ERS) in low-frequency components [mu rhythm (8–12 Hz) and beta rhythm (13–26 Hz)] (Pfurtscheller and Lopes da Silva, 1999), which forms the basis of neural control in EEG-based SMR-BCI (Yuan and He, 2014). Furthermore, patients with stroke or spinal cord lesions can control physical or virtual devices via SMR-BCI (Prasad et al., 2010; Caria et al., 2011; Ang et al., 2014a,b; Dodakian et al., 2014; McCrimmon et al., 2014; Ono et al., 2014; Yuan and He, 2014; Ang and Guan, 2015; Bartur et al., 2015; Pichiorri et al., 2015; Zich et al., 2015; Shu et al., 2017, 2018; Barsotti et al., 2018; Biasiucci et al., 2018; Lazarou et al., 2018; Lee et al., 2018; Norman et al., 2018; Jeunet et al., 2019; Song and Kim, 2019; Chen et al., 2020; Foong et al., 2020), which raises the possibility of SMR-BCI training for stroke rehabilitation.

Several clinical studies have investigated the effect of SMR-BCI systems and demonstrated the significantly positive outcomes on motor function improvement for stroke patients (Ang and Guan, 2015). Ramos-Murguialday et al. (2013) and Ang et al. (2014a,b) stated the BCI training had better efficacy than sham-BCI for stroke rehabilitation. Besides, Cantillo-Negrete et al. (2021) investigated the clinical and physiological effects of SMR-BCI intervention and conventional therapy for upper limb stroke rehabilitation and a revealed similar positive impact of the two therapy methods. Thus, SMR-BCI training, together with conventional therapy, is a suitable therapy option for stroke recovery.

To improve the efficacy of SMR-BCI, various SMR-BCI systems combined with sensory stimulation, motor observation (MO) have been proposed. Shu et al. (2017, 2018) and Ren et al. (2020) improved the SMR-BCI performance via proprioceptive stimulation before the motor imagery (MI) task. Choi et al. (2019), Nagai and Tanaka (2019), and Fujiwara et al. (2021) found users' ERD/ERS was enhanced when they performed MI task with motor observation. It is recognized that enhanced ERD/ERS of stroke patients, meaning enhanced motor-related cortical activation (Pfurtscheller and Lopes da Silva, 1999; Pfurtscheller et al., 2006b), can improve users' engagement and decoding accuracy for BCI system, which could help maximize brain plasticity and restore motor and cognitive function for stroke patients (Bundy et al., 2017; Nagai and Tanaka, 2019). Furthermore, Velasco-Álvarez et al. (2013) designed an audio-cued SMR-BCI system and showed its availability.

Besides, various neuro-feedback has been added to make SMR-BCI system a closed loop for better effect on stroke recovery. Ramos-Murguialday et al. (2013) and Ang et al. (2014a,b, 2015) demonstrated that SMR-BCI with robotic feedback was the most popular feedback method and had positive efficacy for stroke rehabilitation. Pichiorri et al. (2015) and Foong et al. (2020) observed that SMR-BCI with visual feedback showed its excellence for stroke recovery. Auditory feedback may also improve SMR-BCI performance (Nijboer et al., 2008; McCreadie et al., 2013, 2014). Several researchers found the users' ERD/ERS was improved via SMR-BCI with proprioceptive feedback (Vukelić and Gharabaghi, 2015; Barsotti et al., 2018).

For stroke patients, the ability to keep attention is weakened due to of brain damage. To enhance the ERD/ERS and maximize the efficacy of BCI training, we propose a new SMR-BCI system with audio-cue, MO, and multisensory (auditory, visual, and robotic) feedback and investigate the effectiveness of this system.

Another urgent investigation, which should be further explored, is optimal and safe exercise prescription (e.g., training intensity and duration) (Farrell et al., 2020; Luo et al., 2020). We used the definition of training intensity and duration in a review (Antje et al., 2020) as a reference: (1) training intensity (high: five times per week vs. moderate: 2–3 times per week), (2) training duration (short: 2–3 weeks vs. long: 4–8 weeks). Most of the SMR-BCI intervention proposed fell into the pattern of moderate training intensity with long training duration, involving 10 sessions (twice a week) (McCrimmon et al., 2014), 12 sessions (three times a week) (Ang et al., 2014a; Pichiorri et al., 2015; Chen et al., 2020), 18 sessions (three times a week) (Foong et al., 2020), 20 sessions (daily training exclude weekends) (Ramos-Murguialday et al., 2013; Wu et al., 2020) and 24 sessions (twice a week) (Sebastián-Romagosa et al., 2020), which have shown positive effects on stroke rehabilitation. Few studies have addressed the pattern of high training intensity with short training duration. One clinical trial involved 10 training sessions, but each session of BCI training lasted up to 40 min (Frolov et al., 2017). As our group suggests, motor function recovery and the brain networks of stroke patients could be improved significantly by 4-week SMR-BCI intervention combined with convention training compared to only conventional treatment (Wu et al., 2020), which leads us to ponder whether a high training intensity with short duration SMR-BCI intervention will get better influence. If that works, stroke patients will restore the ability to live independently faster.

As mentioned above, there are two purposes of this study. Firstly, to investigate the efficacy of non-invasive EEG-based SMR-BCI with audio-cue, MO, and multisensory (robotic, visual, and auditory) feedback, together with conventional therapy, for upper limb rehabilitation of stroke patients. Secondly, to discuss the influence of stroke rehabilitation after a high training intensity with short duration SMR-BCI intervention.

MATERIALS AND METHODS

Subjects

All patients were recruited from The Third Affiliated Hospital of Sun Yat-sen University.

The following inclusion criteria were applied: (1) age between 18 and 75 years; (2) hemiparesis resulting from a unilateral brain lesion, as confirmed by magnetic resonance imaging (MRI), with a time since stroke (TSS) of 6–24 weeks before study enrollment; (3) moderate to severe hand paralysis, as determined by a Brunnstrom score <IV; (4) sufficient cognition to follow simple instructions and understand the purpose of the study (Susanto et al., 2015).

The exclusion criteria were: (1) recurrent stroke; (2) other neurological, neuromuscular, orthopedic diseases; (3) shoulder or arm contracture/pain; (4) severe aphasia, dementia, psychotic symptoms, or a scalp deformity due to surgery, or those who could not undergo EEG recording for other reasons, such as involuntary movements; or (5) receiving other clinical central nervous system interventions (Susanto et al., 2015).

Based on experience, EEG acquisition devices used on women got poor signals because of their long hair, so we tried to select male patients.

From 79 potentially eligible patients, 24 stroke survivors were allocated to the intervention and received follow-up analysis (see **Figure 1**). Twenty-four patients were randomly assigned into one of the two groups: (1) the BCI therapy group (BCI Group, BG), and (2) the non-BCI group (Control Group, CG).

Study Design

All subjects were recruited to receive a total of 10 training sessions, lasting for 3 h per day, 5 days per week (excluding weekends). Each training session consisted of 1-h BCI therapy and 2-h conventional treatment for the BG, while only 3-h conventional treatment for the CG.

Each SMR-BCI intervention consisted of one calibration session and about ten BCI training sessions (1 h). Conventional treatment included physiotherapy and occupational therapy involving shoulder, elbow and hand training: neuromuscular electrical stimulation, passive joint activity, strength training, stretch and Activities of Daily Living (ADL) training. Specifically, for the patients who belonged to the BG, the hand training part in conventional treatment was excluded.

The clinical measure scales were measured at three time points: at baseline (Week 0), at post-intervention (Week 2), and at follow-up week (Week 4). Notably, the patients in both groups were still hospitalized after 2 weeks of intervention and received conventional therapy.

Sensorimotor Rhythm-Brain Computer Interface System Description

The SMR-BCI system is shown in **Figure 2**. Patients wore EEG caps with 16 active electrodes (g.Nautilus, g.tec medical engineering GmbH, Austria) and the affected hand wore an exoskeleton hand robot (RHB-III. Shenzhen Rehab Medical Technology Co., Ltd., China). The patients were advised to avoid blinking, coughing, chewing and minimize any body movements when performing tasks.

After undergoing a calibration session, including only one trial (described in the section "Sensorimotor Rhythm-Brain Computer Interface Session"), subjects performed MI training sessions according to the audio-cue and observed the corresponding video on the monitor. If the mu suppression was detected in the motor intention classification area (yellow shading), the exoskeleton hand would assist the paretic hand in grasping or opening action according to the MI task cued on the video. Once the robot was triggered, it would complete the movement regardless of the mu suppression during the motion. Then, the system provided audiovisual feedback with a training score (see **Figure 2**). In contrast, the robot would maintain the previous state and the BCI system would give corresponding audiovisual feedback (see **Figure 2**) if the mu suppression didn't reach the threshold (60%) and was in the rest area (blue area) within 12 s. During the time of performing MI task, the BCI system would detect the mu suppression of the subject three times, each time lasting 4 s. If the mu suppression was tested above the threshold in the first 4 s, the feedback meaning "successful" would be given. If not, the BCI system would monitor the mu suppression for the next 4 s, and so on, until 12 s.

The mu suppression (Oberman et al., 2008; Sun et al., 2017) of EEG SMR recorded by electrodes was used for a brain-controlled switch. EEG acquisition and processing details are described in section "Electroencephalography Acquisition, Processing, and Analysis."

Sensorimotor Rhythm-Brain Computer Interface Session

Before conducting MI sessions, patients first performed a calibration trial, to get the "Idle-state Potential," where subjects were instructed to keep still at resting state with eyes closed, called "idle task." A calibration trial lasted about 60 s. **Figure 3A** shows the timing of a calibration trial.

Each MI training session completed approximately 10 runs, each consisting of 10 trials. A break of 3–5 min was given after each run. **Figure 3B** shows the timing of a training trial. Each trial lasted 30 s. Subjects performed the MI task according to audio-cue and the video on the monitor. In addition, the video of three perspectives (first-person perspective, third-person perspective, and inverse first-person perspective) was played in turn. Once the mu suppression of the patient exceeded the threshold, the system would give the corresponding robotic, auditory, and visual feedback.

Electroencephalography Acquisition, Processing, and Analysis

Electroencephalography was recorded using g.Nautilus headset (g.tec medical engineering GmbH, Austria), which provided 16 active electrodes placed in the international 10–20 system positioning: FP1, FP2, FC3, FZ, FC4, C1, C2, CZ, C3, C4, CP3, PZ, CP4, PO7, PO8, and POz. The reference electrode and ground electrode were located on the right mastoid and left mastoid, respectively. Impedances for all electrodes were maintained at

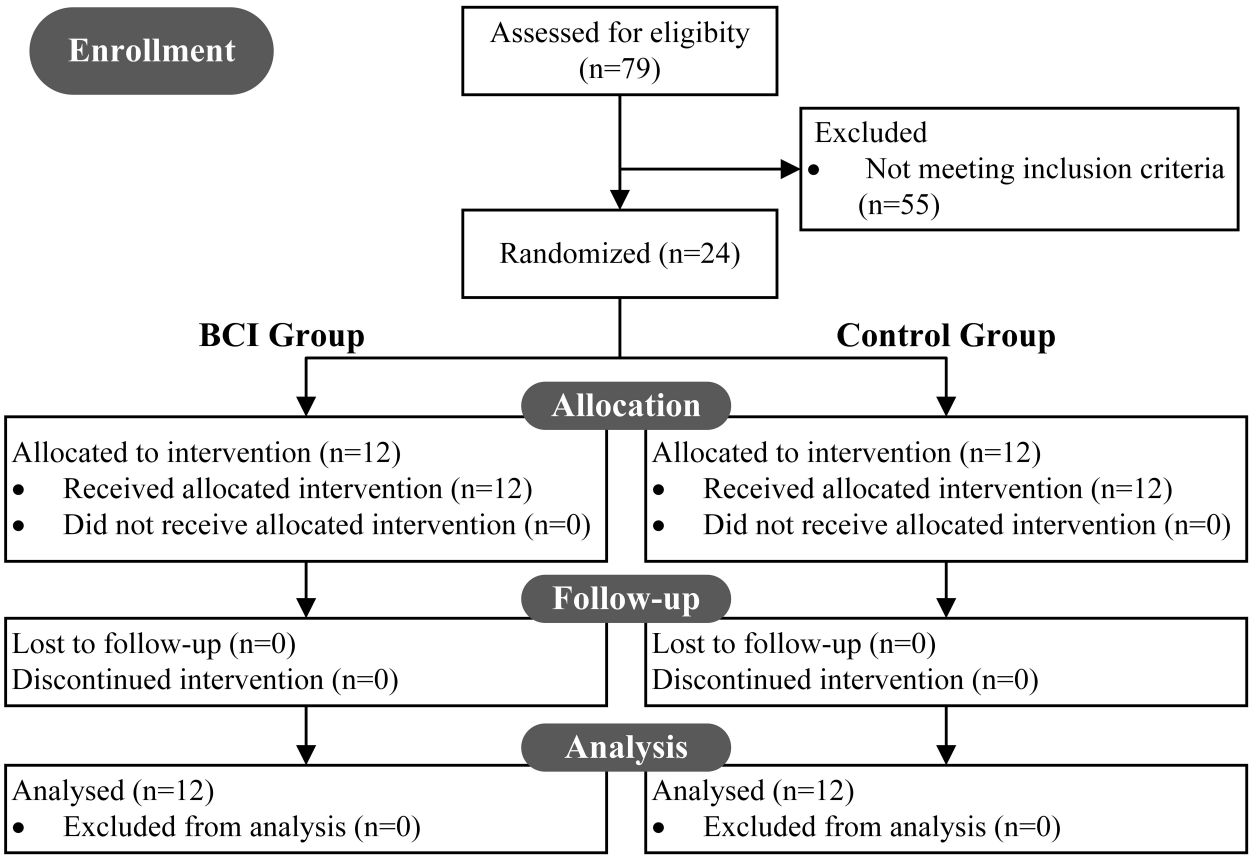

FIGURE 1 | CONSORT diagram: a flow from recruitment through follow-up and analysis. In all, 79 patients were screened to be eligible for the study, and 55 were excluded. 24 underwent intervention and were randomly assigned to two groups (BCI group, BG; control group, CG). All 24 recruited patients received follow-up analysis.

<5 kΩ throughout the experiment. Raw EEG recordings were sampled at 256 Hz. Signals were also processed in real-time by the amplifier using an analog bandpass filter (0.5–60 Hz) and a notch filter (48–52 Hz) to remove artifacts and power line interference.

After preprocessing, the EEG of C3/C4 electrodes covered over the primary motor cortex was used for BCI control. The signals were processed by a bandpass filtered (4th order Butterworth filter) between mu rhythm (8–12 Hz) with a Hamming window. Mu suppression reflects an ERD of the EEG caused by an increase in neural activity (Sun et al., 2017), which is used for the value of recognition in this BCI system. The mu suppression score was calculated according to the following equation (Braadbaart et al., 2013):

$$muSupp = -\frac{muP_{task} - muP_{idle}}{muP_{idle}} \times 100\% \quad (1)$$

where $muSupp$ represents the mu rhythm suppression value, muP_{task} represents the mu rhythm power of EEG while performing "MI task," and muP_{idle} is the mu rhythm power of EEG while performing "Idle task."

In the offline analysis, the EEG recorded by channel C3 and channel C4 was analyzed. The segments containing gross artifacts (identified by visual inspection) were excluded for further analysis. These EEG processes were carried out in MATLAB (The MathWorks, Inc., Natick, MA, United States).

Firstly, we analyzed the mu suppression as the equation (1) and its correlation with motor function scores. The following method was used to compute the mu suppression value:

1. Bandpass filtering of 8–12 Hz on the EEG recorded during 2-week SMR-BCI training session. While the EEG on time segment 5–45 s (see **Figure 3A**) was analyzed for idle-state, the EEG when performing MI tasks at Week 0 and Week 2 (see **Figure 3B**) was investigated for MI-state.
2. Squaring the bandpass-filtered samples to obtain power samples.
3. Computing the power value when performing "Idle task" by averaging the idle-state power samples.
4. Computing the power value when performing "MI task" by averaging the MI-state power samples in one session.
5. Computing the mu suppression using the equation (1).

Outcome Measures

Fugl-Meyer Assessment-Upper Extremities (FMA-UE) assessment scale was used as the primary motor function

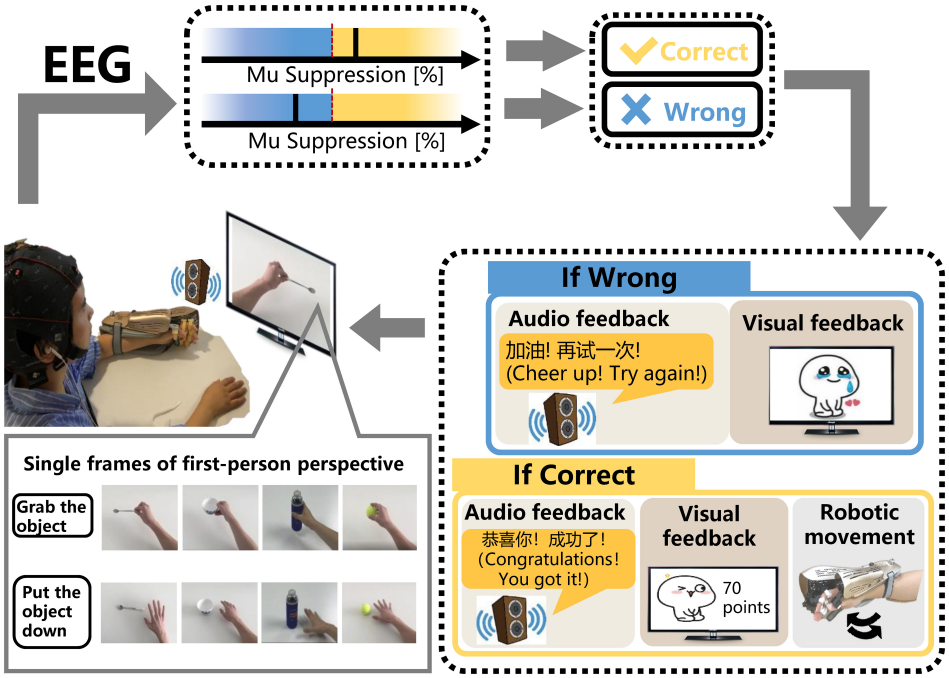

FIGURE 2 | The schematic diagram of the SMR-BCI system. According to audio-cue, subjects imagine "grabbing the object" or "putting the object down" accompanied by observing the video. BCI system calculates the mu suppression of subjects' EEG data and recognizes patients' intention via comparing the mu suppression value with the threshold. If the purpose is identified correctly, the system will give multisensory (robotic, auditory, and visual) feedback. On the contrary, the system will still provide corresponding auditory and visual feedback, but the robot will maintain the previous state.

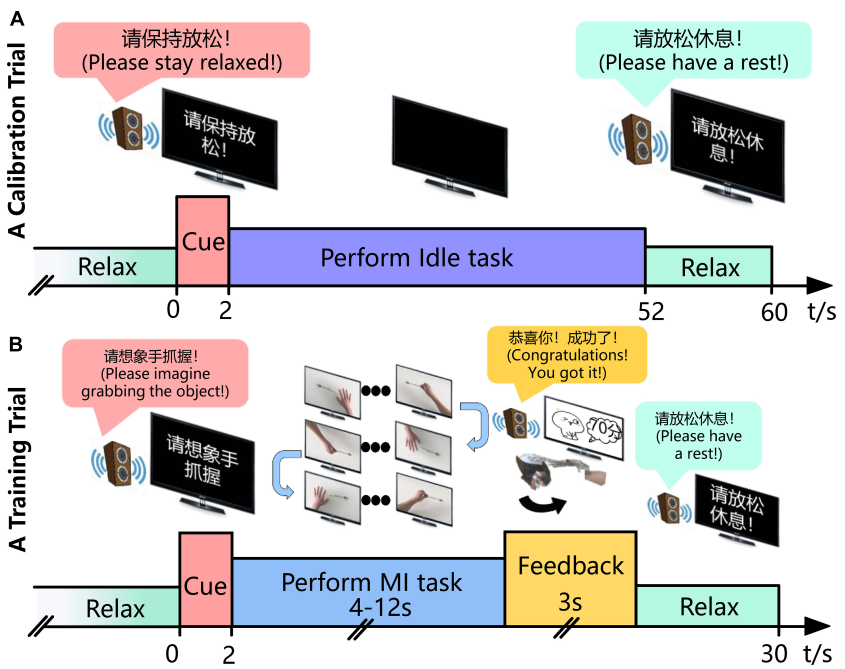

FIGURE 3 | Experimental time course of the BCI intervention for stroke patients' rehabilitation. **(A)** In the calibration trial, the patient gets an audio cue to keep still and eyes closed for 50 s and the EEG when performing the "Idle task" is collected. **(B)** In the training trial, the subject imagines, for instance, "grabbing the objects" according to the audio-cue and monitor from the first-person perspective, third-person perspective, or inverse first-person perspective in turn until his/her intention is recognized. Then, the system gives the corresponding auditory, visual and/or robotic feedback during the following 3 s. The MI task of "grabbing the object" and "putting the thing down" is cued alternatively if the intention is identified successfully, or it maintains the previous one.

outcome measure because of its high reliability. In this study, FMA-UE only referred to the upper extremity motor function part with a total score of 66 (Fuglmeyer et al., 1975; Page et al., 2012).

Secondary outcome measures were the Wolf Motor Function Test (WMFT; Wolf et al., 2001) and the Modified Barthel Index (MBI; Mahorney, 1965). The WMFT consists of 15 tasks (six joint-segment tasks, nine functional tasks; maximum score = 75), each of which should be performed within 120 s. The MBI is used to measure performance in ADL.

Mean change of FMA-UE and WMFT scores were compared with its estimated minimal clinically significant difference (MCID) values (Der Lee et al., 2001; Page et al., 2012) and estimated minimal detectable change (MDC) value (Lin et al., 2009), respectively.

Statistical Method

All demographic and clinical data were analyzed using SPSS version 23.0 (IBM Inc., Chicago, IL, United States). The variables tested normal (using Shapiro–Wilk test) were expressed as the mean ± standard deviation, and the two-tailed unpaired *t*-test was used for intergroup comparison while the two-tailed paired *t*-test was for intragroup comparison. Non-normally distributed data were expressed as the median with 25 and 75% quartile, and the Mann–Whitney *U* test was applied for intergroup comparison while the Wilcoxon ranked sum test was for intragroup comparison.

Two-way repeated measures ANOVA was performed for the functional scale scores (FMA-UE, WMFT, and MBI) with time (Week 0, Week 2, and Week 4) as the within-subject factor.

Associations between the clinical scores (at Week 2) and the mu suppression (at Week 2) were assessed using Pearson's (if the two variables are both normally distributed), or Spearman's correlation. Statistical significance was set at $p < 0.05$ for all analyses.

RESULTS

Demographics

The demographic information of the patients (at baseline) is shown in **Table 1**. For demographic information, standard variables, including age and clinical scale scores, were analyzed by the parametric tests while TSS was analyzed by the non-parametric test. The chi-square test was used to identify difference in rates among the groups.

There were no significant demographic differences in age (two-tailed unpaired *t*-test, $p = 0.054$), sex (all males), and affected hand (chi-square test, $p = 0.653$). Similarly, there were no significant differences in stroke type (chi-square test, $p = 0.386$), and TSS (Mann–Whitney *U* test, $p = 0.579$). In addition, patients in the two groups had similar levels of baseline clinical scores including FMA-UE (two-tailed unpaired *t*-test, $p = 0.795$), WMFT (two-tailed unpaired *t*-test, $p = 0.859$) and MBI (two-tailed unpaired *t*-test, $p = 0.397$).

Efficacy Measurements

Two-way repeated-measures ANOVA (FMA-UE, WMFT, and MBI, by Week 4, with time as the within-subjects factor and group as the between-subjects factor) showed a significant time × group interaction on FMA-UE ($F = 18.629$, $p < 0.01$) and WMFT ($F = 10.252$, $p = 0.001$) and no significant time × group interaction on MBI ($F = 0.500$, $p = 0.613$). The results showed that time had a significant effect on FMA-UE ($F = 120.626$, $p < 0.01$), WMFT ($F = 121.760$, $p < 0.01$), and MBI ($F = 17.228$, $p < 0.01$), but no significant effect for group on FMA-UE ($F = 0.005$, $p = 0.947$), WMFT ($F = 0.180$, $p = 0.675$), and MBI ($F = 1.614$, $p = 0.217$).

Fugl-Meyer Assessment-Upper Extremities, WMFT, and MBI scores of the BG and that of the CG were significantly improved in Week 2 and Week 4. The results are shown in the **Table 2**. No significant differences were found between groups for clinical scores at any measurement point.

As shown in **Table 3**, overall improvements of outcome measure scores of the BG were higher than that of the CG, and BG had significant improvement differences in FMA-UE and WMFT changes at Week 4 (Week 0-based change) compared to the CG.

Importantly, 5.25 points and 5.55 points have been estimated to represent the minimal clinically significant difference (MCID) of FMA-UE (Cervera et al., 2018) and minimal detectable change (MDC) of WMFT (Susanto et al., 2015), respectively. At Week 4, the increase of FMA-UE and WMFT surpassed MCID and MDC for all the patients in the BG (**Figure 4**).

Electroencephalography Results

The mu suppression values of bilateral cortex were compared before and after MI-BCI training (**Figure 5A**). No significant change in the bilateral hemisphere was found after BCI training [Ipsilesional hemisphere, $muSupp_{Week0} = 45.7735 \pm 28.0009$, $muSupp_{Week2} = 56.8294$ (47.9067, 60.6983), Wilcoxon ranked sum test, $p = 0.875$; Contralesional hemisphere, $muSupp_{Week0} = 62.4475$ (21.4197, 72.9325), $muSupp_{Week2} = 53.8142 \pm 25.9915$, Wilcoxon ranked sum test, $p = 0.388$]. Also, there was no significant difference in mu suppression between hemispheres (Week 0: Mann–Whitney *U* test, $p = 0.670$; Week 2: Mann–Whitney *U* test, $p = 0.768$).

Correlation analysis was performed to assess the relationship between the ranked mu suppression (Week 2) and the ranked clinical scale scores (Week 2) in the BG (**Figure 5B**). After 2-week comprehensive rehabilitation, including BCI and conventional interventions, the mu suppression of contralesional hemisphere had a significantly positive correlation with MBI scores (Pearson $r = 0.587$, $p = 0.045$). While there was no significant correlation between mu suppression of contralesional hemisphere and FMA-UE (Pearson $r = 0.273$, $p = 0.391$), or WMFT (Pearson $r = 0.105$, $p = 0.746$), they had a positive correlation trend. On the ipsilesional motor cortex, there was also a positive correlation trend between mu suppression and motor function (FMA-UE: Pearson $r = 0.385$, $p = 0.217$; WMFT: Pearson $r = 0.406$, $p = 0.191$; MBI: Pearson $r = 0.273$, $p = 0.391$). Pearson's *r* was used for all variables (two-tailed tests).

TABLE 1 | Demographic information of the patients.

Characteristic	Control group (n = 12)	BCI group (n = 12)	$t/Z/\chi^2$	P
Age (years)	55.0 ± 12.2	43.8 ± 14.7	−2.040[b]	0.054
Gender (male: female)	12:0	12:0		
Affected hand (right: left)	8:4	9:3	0.202[a]	0.653
Stroke type (isch: hemo)	9:3	7:5	0.750[a]	0.386
TSS (month)	4.3 ± 2.6	4.0 (2.0, 11.3)	−0.555[c]	0.579
STROKE PERIOD, N				
Subacute (1–6 months from onset)	10	7		
Chronic (>6 months from onset)	2	5		
LESION LOCALIZATION, N				
Cortical	4	3	0.202[a]	0.653
Subcortical	8	9		
MEASUREMENTS (baseline)				
FMA-UE	24.3 ± 17.1	22.6 ± 13.7	−0.264[b]	0.795
WMFT	27.8 ± 19.8	29.1 ± 16.6	0.179[b]	0.859
MBI	47.0 ± 32.9	57.9 ± 28.9	0.863[b]	0.397

hemo, hemorrhagic stroke; isch, ischemic stroke; TSS, time since Stroke onset; N, number; FMA-UE, Fugl-Meyer Assessment-Upper Extremities; WMFT, Wolf Motor Functional Test; MBI, Modified Barthel Index. [a]Chi-square test. [b]two-tailed unpaired t-test. [c]Mann–Whitney U test.

TABLE 2 | Efficacy measures by FMA-UE, WMFT, and MBI for BG and CG.

Outcome measures	Mean ± SD			p-value		
	Week 0	Week 2	Week 4	Week 0 vs. Week 2	Week 0 vs. Week 4	Week 2 vs. Week 4
BCI group						
FMA-UE	22.58 ± 13.71	27.67 ± 15.99	35.75 ± 14.26	0.003**	<0.001**	<0.001**
WMFT	29.08 ± 16.58	36.58 ± 18.35	44.50 ± 16.89	0.001**	<0.001**	<0.001**
MBI	57.92 ± 28.94	71.25 ± 20.53	76.50 ± 20.26	0.004**	0.001**	<0.001**
Control group						
FMA-UE	24.25 ± 17.08	28.92 ± 18.14	31.50 ± 17.79	0.002**	<0.001**	<0.001**
WMFT	27.75 ± 19.75	34.17 ± 22.90	38.08 ± 22.92	0.001**	<0.001**	<0.001**
MBI	47.00 ± 32.87	55.92 ± 29.18	61.33 ± 29.67	0.007**	0.003**	0.026*

*Measures with statistically significant ($p < 0.05$) changes are indicated with an *, $p < 0.01$ changes are indicated with an **.*

TABLE 3 | Intergroup comparison for outcome measure scores improvements.

Improvement		Control group (n = 12)	BCI group (n = 12)	$t/Z/\chi^2$	P
Week 2−Week 0	FMA-UE	4.7 ± 3.9	4.5 (2.0, 5.3)	−0.118[c]	0.906
	WMFT	6.0 (2.8, 7.3)	7.5 ± 5.5	−0.695[c]	0.487
	MBI	6.5 (4.8, 8.5)	9.0 (5.5, 16.8)	−0.955[c]	0.339
Week 4−Week 0	FMA-UE	6.0 (5.8, 7.5)	13.2 ± 3.0	−3.135[c]	0.002
	WMFT	10.3 ± 5.5	15.4 ± 5.1	2.346[b]	0.028
	MBI	10.0 (8.0, 13.8)	18.6 ± 14.6	−1.187[c]	0.235

FMA-UE, Fugl-Meyer Assessment-Upper Extremities; WMFT, Wolf Motor Functional Test; MBI, Modified Barthel Index. [b]two-tailed unpaired t-test. [c]Mann–Whitney U test.

DISCUSSION

This study presents the results from a clinical study investigating the efficacy of the SMR-BCI with audio-cue, motor observation, and multisensory (robotic, auditory, and visual) feedback compared with conventional therapy for upper limb stroke rehabilitation.

In terms of clinical scale scores (FMA-UE, WMFT, and MBI score), upper limb motor functional improvement was observed in both groups after 2-week intervention. This result is consistent with previous evidence demonstrating the effectiveness of BCI intervention for stroke patients' UL motor function recovery (Cervera et al., 2018; Wu et al., 2020) and a randomized controlled multicenter trial with post-stroke patients (in subacute and chronic phase), which showed significant improvements of FMA-UE scores in BCI and control group (Frolov et al., 2017). The clinical scale scores of the BG had a significantly greater motor function improvement than the CG at the follow-up week rather than Week 2. Similarly, the percentage of patients reaching MCID and MDC in the BG was greater than that in the CG at Week 4 instead of Week 2. This phenomenon may reflect the effectiveness of the long-term clinical effects of SMR-BCI intervention for post-stroke patients (Wu et al., 2020). BCI training added to conventional therapy may enhance

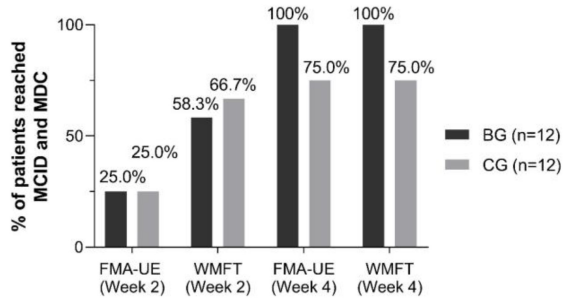

FIGURE 4 | Percent of patients reached minimal clinically important difference (MCID) and minimal detectable change (MDC) by FMA-UE and WMFT scores in each group at Week 2 and Week 4.

motor functioning of the upper extremity and brain function recovery in patients after a stroke (Kruse et al., 2020). Compared to conventional interventions, we suggest BCI-based training for motor recovery of the upper limbs in patients with stroke (Nojima et al., 2021).

Mu rhythms are suppressed, and their power is attenuated, when engaging in motor activity (Gastaut, 1952), observing actions executed by someone else (Muthukumaraswamy et al., 2004), or imagining performing an action (Pfurtscheller et al., 1996, 2006a, 2010). Thus, researchers usually link the mu suppression of motor cortex to the motor-relevant brain activation (Pineda, 2006). In this study, no significant difference in mu suppression value was found after 2-week BCI intervention. However, there was a positive trend between functional motor scores (FMA-UE, WMFT, and MBI) with mu suppression of bilateral hemisphere. This positive trend agrees with Bundy et al.'s (2017) study that suggests bilateral cortex activation, especially unaffected cortex activation, can contribute to the motor-relevant task of subacute stroke patients (Calautti et al., 2001). Neuronal reorganization may occur on both the ipsilesional and contralesional hemispheres during recovery to regain motor function and therefore bilateral activation for the hemiparetic side is often observed (Dodd et al., 2017). Meanwhile, this activation pattern gives a possible method to control the SMR-BCI system for stroke rehabilitation reliably via the bilateral cortex EEG-based information fusion (Bundy et al., 2017). Therefore, the unaffected hemisphere may play a role in motor recovery following stroke (Gould et al., 2021). However, there is an opinion that increased activation in the intact hemisphere may hinder reorganization in the lesioned hemisphere, which may have a negative impact on recovery. In response to the two contradictory views, a bimodal balance-recovery model that links interhemispheric balancing and functional recovery to the structural reverse was suggested (Di Pino et al., 2014). As our previous work has shown that motor function recovery and the brain networks of stroke patients could

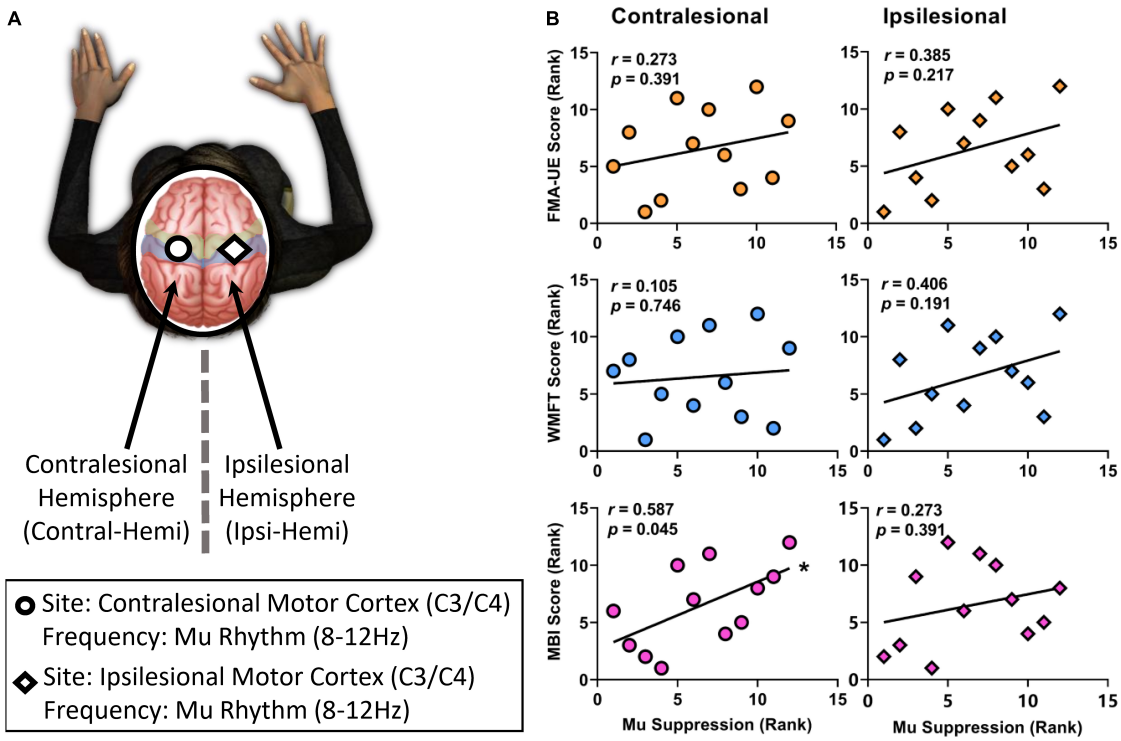

FIGURE 5 | The correlation between the ranked mu suppression value and the ranked clinical scale scores (FMA-UE, WMFT, MBI scores). **(A)** Analyses were performed using EEG activity at the frequency used for BCI control but an electrode in the contralesional hemisphere, at the frequency used for BCI control but an electrode in the ipsilesional hemisphere. **(B)** While there was a significantly positive correlation between mu suppression of contralesional hemisphere and MBI scores after 2-week BCI intervention, others showed no significantly positive trend. Significant ($p < 0.05$) changes are indicated with an *.

be improved significantly by 4-week SMR-BCI intervention. We conjecture that this bilateral activation, as well as the positive correlations between mu suppression and clinical scores, is a "middle state" for the patients in this study and may also mean that a 2-week training period would not be the optimal option for neurorehabilitation. This result is consistent with the conclusion that a BCI training with conventional therapy for a duration of 4 weeks or longer, with a high intensity training of five times per week, was recommend (Kruse et al., 2020). The influence of the training duration combined with the training intensity needs to be investigated further.

Several features distinguish this work from previous studies. Firstly, we developed a new SMR-BCI system for stroke rehabilitation. This BCI system showed a more vivid training experience for patients via audio-cue, motor observation, and multisensory (robotic, auditory, and visual) feedback to make subjects deeply involved in the training. Secondly, this study revealed the clinical efficacy of the SMR-BCI system we designed for post-stroke rehabilitation. Thirdly, the prescription (e.g., the intensity/frequency and the duration) of BCI training was discussed. We provided a training program (high training intensity, short training duration, and 1-h training session), which may help to develop a full picture of the clinical factor and the interaction between training duration and training intensity.

There were also several limitations to note. The small sample of participants and the absence of EEG data from the CG and follow-up week limited the further investigation of our findings on efficacy. Although the influence of patients' age and type of lesion in motor recovery of upper extremities of post-stroke patients need further analysis (Kruse et al., 2020), there are some views that relatively younger and more hemorrhagic stroke participants in the BG may tip off the outcome measures comparison between the groups.

CONCLUSION

In summary, this study showed the clinical efficacy of SMR-BCI with audio-cue, MO, and multisensory (robotic, auditory, and visual) feedback for post-stroke rehabilitation. Moreover, it discussed the impact of the high training intensity BCI training with short training duration.

Clinical efficacy was measured by three clinical measure scales (FMA-UE, WMFT, and MBI), and the results showed significant improvements at Week 2 and Week 4. Notably, there was a greater improvement for patients who belonged to the BG than the CG at Week 4.

Hence, in the future, more extensive clinical trials are warranted to verify the clinical efficacy and the role of this kind of BCI system has in the rehabilitation milieu. The discussion about the interaction between training intensity and duration also motivates further research.

DATA AVAILABILITY STATEMENT

The raw data supporting the conclusions of this article will be made available by the authors, without undue reservation.

ETHICS STATEMENT

The studies involving human participants were reviewed and approved by The Third Affiliated Hospital of Sun Yat-sen University, Guangzhou, China. The patients/participants provided their written informed consent to participate in this study.

AUTHOR CONTRIBUTIONS

XL, LW, SM, ZY, ZT, LS, YZ, XW, SW, JW, and ZD worked together to complete the manuscript. XL, LW, SW, JW, and ZD contributed to conception and design of the study. LW and SM carried out the data analysis. LS carried out the experiments. ZY and ZT provided statistical assistance and support. YZ and XW provided opinions on grammar and rhetoric. All authors contributed to manuscript revision, read and approved the submitted version.

FUNDING

This work was supported by the Key R&D Program of Guangdong Province, China under grant 2018B030339001 and Key Realm R&D Program of Guangzhou, China under grant 202007030007.

REFERENCES

Ang, K. K., Chua, K. S. G., Phua, K. S., Wang, C., Chin, Z. Y., Kuah, C. W. K., et al. (2014a). A randomized controlled trial of eeg–based motor imagery brain-computer interface robotic rehabilitation for stroke. *Clin. EEG Neurosci.* 46, 310–320. doi: 10.1177/1550059414522229

Ang, K. K., and Guan, C. (2015). Brain–computer interface for neurorehabilitation of upper limb after stroke. *Proc. IEEE* 103, 944–953. doi: 10.1109/JPROC.2015.2415800

Ang, K. K., Guan, C., Phua, K. S., Wang, C., Zhao, L., Teo, W. P., et al. (2015). Facilitating effects of transcranial direct current stimulation on motor imagery brain-computer interface with robotic feedback for stroke rehabilitation. *Arch. Phys. Med. Rehabil.* 96, S79–S87. doi: 10.1016/j.apmr.2014.08.008

Ang, K. K., Guan, C., Phua, K. S., Wang, C., Zhou, L., Tang, K. Y., et al. (2014b). Brain–computer interface–based robotic end effector system for wrist and hand rehabilitation: results of a three-armed randomized controlled trial for chronic stroke. *Front. Neuroeng.* 7:30. doi: 10.3389/fneng.2014.00030

Antje, K., Zorica, S., Jan, T., and Corina, S. A. (2020). Effect of brain–computer interface training based on non–invasive electroencephalography using motor imagery on functional recovery after stroke – a systematic review and meta-analysis. *BMC Neurol.* 20:385. doi: 10.1186/s12883-020-01960-5

Barsotti, M., Leonardis, D., Vanello, N., Bergamasco, M., and Frisoli, A. (2018). Effects of continuous kinaesthetic feedback based on tendon vibration on motor imagery BCI performance. *IEEE Trans. Neural Syst. Rehabil. Eng.* 26, 105–114. doi: 10.1109/tnsre.2017.2739244

Bartur, G., Pratt, H., Dickstein, R., Frenkel-Toledo, S., Geva, A., and Soroker, N. (2015). Electrophysiological manifestations of mirror visual feedback during manual movement. *Brain Res.* 1606, 113–124. doi: 10.1016/j.brainres.2015.02.029

Biasiucci, A., Leeb, R., Iturrate, I., Perdikis, S., Al-Khodairy, A., Corbet, T., et al. (2018). Brain–actuated functional electrical stimulation elicits lasting arm motor recovery after stroke. *Nat. Commun.* 9:2421. doi: 10.1038/s41467-018-04673-z

Braadbaart, L., Williams, J. H. G., and Waiter, G. D. (2013). Do mirror neuron areas mediate mu rhythm suppression during imitation and action observation? *Int. J. Psychophysiol.* 89, 99–105.

Bundy, D. T., Souders, L., Baranyai, K., Leonard, L., Schalk, G., Coker, R., et al. (2017). Contralesional brain–computer interface control of a powered exoskeleton for motor recovery in chronic stroke survivors. *Stroke* 48, 1908–1915.

Calautti, C., Leroy, F., Guincestre, J. Y., and Baron, J. C. (2001). Dynamics of motor network overactivation after striatocapsular stroke: a longitudinal PET study using a fixed-performance paradigm. *Stroke* 32:2534.

Cantillo-Negrete, J., Carino-Escobar, R. I., Carrillo-Mora, P., Rodriguez-Barragan, M. A., Hernandez-Arenas, C., Quinzaños-Fresnedo, J., et al. (2021). Brain–computer interface coupled to a robotic hand Orthosis for stroke patients' neurorehabilitation: a crossover feasibility study. *Front. Hum. Neurosci.* 15:656975. doi: 10.3389/fnhum.2021.656975

Caria, A., Weber, C., Brötz, D., Ramos, A., Ticini, L. F., Gharabaghi, A., et al. (2011). Chronic stroke recovery after combined BCI training and physiotherapy: a case report. *Psychophysiology* 48, 578–582. doi: 10.1111/j.1469-8986.2010.01117.x

Cervera, M. A., Soekadar, S. R., Ushiba, J., Millan, J. D. R., Liu, M., Birbaumer, N., et al. (2018). Brain–computer interfaces for post–stroke motor rehabilitation: a meta-analysis. *Ann. Clin. Transl. Neurol.* 5, 651–663. doi: 10.1002/acn3.544

Chen, S., Cao, L., Shu, X., Wang, H., Ding, L., Wang, S.-H., et al. (2020). Longitudinal electroencephalography analysis in subacute stroke patients during intervention of brain-computer interface with exoskeleton feedback. *Front. Neurosci.* 14:809. doi: 10.3389/fnins.2020.00809

Choi, H., Lim, H., Kim, J. W., Kang, Y. J., and Ku, J. (2019). Brain computer interface-based action observation game enhances mu suppression in patients with stroke. *Electronics* 8:1466.

Der Lee, J. H. V., De Groot, V., Beckerman, H., Wagenaar, R. C., Lankhorst, G. J., and Bouter, L. M. (2001). The intra- and interrater reliability of the action research arm test: a practical test of upper extremity function in patients with stroke. *Arch. Phys. Med. Rehabil.* 82, 14–19.

Di Pino, G., Pellegrino, G., Assenza, G., Capone, F., Ferreri, F., Formica, D., et al. (2014). Modulation of brain plasticity in stroke: a novel model for neurorehabilitation. *Nat. Rev. Neurol* 10, 597–608. doi: 10.1038/nrneurol.2014.162

Dodakian, L., Campbell Stewart, J., and Cramer, S. C. (2014). Motor imagery during movement activates the brain more than movement alone after stroke: a pilot study. *J. Rehabil. Med.* 46, 843–848. doi: 10.2340/16501977-1844

Dodd, K. C., Nair, V. A., and Prabhakaran, V. (2017). Role of the Contralesional vs. Ipsilesional Hemisphere in stroke recovery. *Front. Hum. Neurosci.* 11:469. doi: 10.3389/fnhum.2017.00469

Farrell, J. W. III, Merkas, J., and Pilutti, L. A. (2020). The effect of exercise training on gait, balance, and physical fitness asymmetries in persons with chronic neurological conditions: a systematic review of randomized controlled trials. *Front. Physiol.* 11:585765. doi: 10.3389/fphys.2020.585765

Foong, R., Ang, K. K., Quek, C., Guan, C., Phua, K. S., Kuah, C. W. K., et al. (2020). Assessment of the efficacy of EEG-Based MI-BCI with visual feedback and EEG correlates of mental fatigue for upper–limb stroke rehabilitation. *IEEE Trans. Biomed. Eng.* 67, 786–795. doi: 10.1109/TBME.2019.2921198

Frenkel-Toledo, S., Bentin, S., Perry, A., Liebermann, D. G., and Soroker, N. (2014). Mirror–neuron system recruitment by action observation: effects of focal brain damage on mu suppression. *Neuroimage* 87, 127–137.

Frolov, A. A., Mokienko, O., Lyukmanov, R., Biryukova, E., Kotov, S., Turbina, L., et al. (2017). Post–stroke rehabilitation training with a motor–imagery–based brain–computer interface (BCI)–controlled hand exoskeleton: a randomized controlled multicenter trial. *Front. Neurosci.* 11:400. doi: 10.3389/fnins.2017.00400

Fuglmeyer, A. R., Jaasko, L., Leyman, I., Olsson, S., and Steglind, S. (1975). The post–stroke hemiplegic patient. 1. A method for evaluation of physical performance. *Scand. J. Rehabil. Med.* 7, 13–31.

Fujiwara, K., Shibata, M., Awano, Y., Shibayama, K., Iso, N., Matsuo, M., et al. (2021). A method for using video presentation to increase the vividness and activity of cortical regions during motor imagery tasks. *Neural Regen. Res.* 16, 2431–2437. doi: 10.4103/1673-5374.313058

Gastaut, H. (1952). Electrocorticographic study of the reactivity of rolandic rhythm. *Rev. Neurologique* 87, 176–182.

Gould, L., Kress, S., Neudorf, J., Gibb, K., Persad, A., Meguro, K., et al. (2021). An fMRI, DTI and neurophysiological examination of atypical organization of motor cortex in ipsilesional hemisphere following post–stroke recovery. *J. Stroke Cerebrovasc. Dis.* 30:105593. doi: 10.1016/j.jstrokecerebrovasdis.2020.105593

Jeunet, C., Glize, B., McGonigal, A., Batail, J.-M., and Micoulaud-Franchi, J.-A. (2019). Using EEG–based brain computer interface and neurofeedback targeting sensorimotor rhythms to improve motor skills: theoretical background, applications and prospects. *Neurophysiol. Clin.* 49, 125–136. doi: 10.1016/j.neucli.2018.10.068

Johnson, C. O., Minh, N., Roth, G. A., Nichols, E., Alam, T., Abate, D., et al. (2019). Global, regional, and national burden of stroke, 1990-2016: a systematic analysis for the global burden of disease study 2016. *Lancet Neurol.* 18, 439–458. doi: 10.1016/s1474-4422(19)30034-1

Kruse, A., Suica, Z., Taeymans, J., and Schuster-Amft, C. (2020). Effect of brain–computer interface training based on non-invasive electroencephalography using motor imagery on functional recovery after stroke – a systematic review and meta-analysis. *BMC Neurol.* 20:385.

Kwah, L. K., Harvey, L. A., Diong, J., and Herbert, R. D. (2013). Models containing age and NIHSS predict recovery of ambulation and upper limb function six months after stroke: an observational study. *J. Physiother.* 59, 189–197. doi: 10.1016/S1836-9553(13)70183-8

Lazarou, I., Nikolopoulos, S., Petrantonakis, P. C., Kompatsiaris, I., and Tsolaki, M. (2018). EEG-based brain–computer interfaces for communication and rehabilitation of people with motor impairment: a novel approach of the 21st century. *Front. Hum. Neurosci.* 12:14. doi: 10.3389/fnhum.2018.00014

Lee, B. J. B., Williams, A., and Ben-Tzvi, P. (2018). Intelligent object grasping with sensor fusion for rehabilitation and assistive applications. *IEEE Trans. Neural. Syst. Rehabil. Eng.* 26, 1556–1565. doi: 10.1109/TNSRE.2018.2848549

Lin, K.-c, Hsieh, Y.-w, Wu, C.-y, Chen, C.-l, Jang, Y., and Liu, J.-s (2009).). Minimal detectable change and clinically important difference of the wolf motor function test in stroke patients. *Neurorehabil. Neural Repair* 23, 429–434. doi: 10.1177/1545968308331144

Luo, L., Meng, H., Wang, Z., Zhu, S., Yuan, S., Wang, Y., et al. (2020). Effect of high-intensity exercise on cardiorespiratory fitness in stroke survivors: a systematic review and meta-analysis. *Ann. Phys. Rehabil. Med.* 63, 59–68. doi: 10.1016/j.rehab.2019.07.006

Mahorney, F. (1965). Functional evaluation: the barthel index. *Md. State Med. J.* 14, 61–65.

McCreadie, K. A., Coyle, D. H., and Prasad, G. (2013). Sensorimotor learning with stereo auditory feedback for a brain–computer interface. *Med. Biol. Eng. Comput.* 51, 285–293. doi: 10.1007/s11517-012-0992-7

McCreadie, K. A., Coyle, D. H., and Prasad, G. (2014). Is sensorimotor BCI performance influenced differently by mono, stereo, or 3–D auditory feedback? *IEEE Trans. Neural. Syst. Rehabil. Eng.* 22, 431–440. doi: 10.1109/tnsre.2014.2312270

McCrimmon, C. M., King, C. E., Wang, P. T., Cramer, S. C., Nenadic, Z., and Do, A. H. (2014).). Brain-controlled functional electrical stimulation for lower–limb motor recovery in stroke survivors. *Annu. Int. Conf. IEEE Eng. Med. Biol. Soc.* 2014, 1247–1250. doi: 10.1109/embc.2014.6943823

Morris, J. H., van Wijck, F., Joice, S., and Donaghy, M. (2013). Predicting health related quality of life 6 months after stroke: the role of anxiety and upper limb dysfunction. *Disabil. Rehabil.* 35, 291–299. doi: 10.3109/09638288.2012.691942

Muthukumaraswamy, S. D., Johnson, B. W., and Mcnair, N. A. (2004). Mu rhythm modulation during observation of an object-directed grasp. *Cogn. Brain Res.* 19, 195–201.

Nagai, H., and Tanaka, T. (2019). Action observation of own hand movement enhances event–related desynchronization. *IEEE Trans. Neural Syst. Rehabil. Eng.* 27, 1407–1415. doi: 10.1109/tnsre.2019.2919194

Nijboer, F., Furdea, A., Gunst, I., Mellinger, J., McFarland, D. J., Birbaumer, N., et al. (2008). An auditory brain–computer interface (BCI). *J. Neurosci. Methods* 167, 43–50. doi: 10.1016/j.jneumeth.2007.02.009

Nojima, I., Sugata, H., Takeuchi, H., and Mima, T. (2021). Brain–computer interface training based on brain activity can induce motor recovery in patients with stroke: a meta–analysis. *Neurorehabil. Neural Repair* 36, 83–96. doi: 10.1177/15459683211062895

Norman, S. L., McFarland, D. J., Miner, A., Cramer, S. C., Wolbrecht, E. T., Wolpaw, J. R., et al. (2018). Controlling pre-movement sensorimotor rhythm can improve finger extension after stroke. *J. Neural Eng.* 15:14. doi: 10.1088/1741-2552/aad724

Oberman, L. M., Ramachandran, V. S., and Pineda, J. A. (2008). Modulation of mu suppression in children with autism spectrum disorders in response to familiar or unfamiliar stimuli: the mirror neuron hypothesis. *Neuropsychologia* 46, 1558–1565. doi: 10.1016/j.neuropsychologia.2008.01.010

Ono, T., Shindo, K., Kawashima, K., Ota, N., Ito, M., Ota, T., et al. (2014). Brain–computer interface with somatosensory feedback improves functional recovery from severe hemiplegia due to chronic stroke. *Front. Neuroeng.* 7:19. doi: 10.3389/fneng.2014.00019

Page, S. J., Fulk, G. D., and Boyne, P. (2012). Clinically important differences for the upper-extremity Fugl–Meyer scale in people with minimal to moderate impairment due to chronic stroke. *Phys. Ther.* 92, 791–798. doi: 10.2522/ptj.20110009

Pfurtscheller, G., Brunner, C., Schlögl, A., and Silva, F. (2006a). Mu rhythm (de)synchronization and EEG single–trial classification of different motor imagery tasks. *Neuroimage* 31, 153–159.

Pfurtscheller, G., Brunner, C., Schlogl, A., and da Silva, F. H. L. (2006b). Mu rhythm (de)synchronization and EEG single-trial classification of different motor imagery tasks. *Neuroimage* 31, 153–159. doi: 10.1016/j.neuroimage.2005.12.003

Pfurtscheller, G., and Lopes da Silva, F. H. (1999). Event–related EEG/MEG synchronization and desynchronization: basic principles. *Clin. Neurophysiol.* 110, 1842–1857. doi: 10.1016/s1388-2457(99)00141-8

Pfurtscheller, G., Scherer, R., Müller-Putz, G., and Silva, F. (2010). Short-lived brain state after cued motor imagery in naive subjects. *Eur. J. Neurosci.* 28, 1419–1426.

Pfurtscheller, G., Stancak, A. J., and Neuper, C. (1996). Event–related synchronization (ERS) in the alpha band – an electrophysiological correlate of cortical idling: a review. *Int. J. Psychophysiol.* 24, 39–46.

Pichiorri, F., Morone, G., Petti, M., Toppi, J., Pisotta, I., Molinari, M., et al. (2015). Brain–computer interface boosts motor imagery practice during stroke recovery. *Ann. Neurol.* 77, 851–865. doi: 10.1002/ana.24390

Pineda, J. A. (2006). The functional significance of mu rhythms: translating "seeing" and "hearing" into "doing". *Brain Res. Rev.* 50, 57–68.

Prasad, G., Herman, P., Coyle, D., McDonough, S., and Crosbie, J. (2010). Applying a brain–computer interface to support motor imagery practice in people with stroke for upper limb recovery: a feasibility study. *J. Neuroeng. Rehabil.* 7:60. doi: 10.1186/1743-0003-7-60

Ramos-Murguialday, A., Broetz, D., Rea, M., Läer, L., Yilmaz, Ö, Brasil, F. L., et al. (2013). Brain–machine interface in chronic stroke rehabilitation: a controlled study. *Ann. Neurol.* 74, 100–108. doi: 10.1002/ana.23879

Ren, S., Wang, W., Hou, Z. G., Liang, X., Wang, J., and Shi, W. (2020). Enhanced motor imagery based brain– computer interface via FES and VR for lower limbs. *IEEE Trans. Neural Syst. Rehabil. Eng.* 28, 1846–1855. doi: 10.1109/tnsre.2020.3001990

Sebastián-Romagosa, M., Cho, W., Ortner, R., Murovec, N., Von Oertzen, T., Kamada, K., et al. (2020). Brain computer interface treatment for motor rehabilitation of upper extremity of stroke patients—a feasibility study. *Front. Neurosci.* 14:591435. doi: 10.3389/fnins.2020.591435

Shu, X., Chen, S., Meng, J., Yao, L., Sheng, X., Jia, J., et al. (2018). Tactile stimulation improves sensorimotor rhythm-based bci performance in stroke patients. *IEEE Trans. Biomed. Eng.* 66, 1987–1995. doi: 10.1109/TBME.2018.2882075

Shu, X., Yao, L., Sheng, X., Zhang, D., and Zhu, X. (2017). Enhanced motor imagery–based BCI performance via tactile stimulation on unilateral hand. *Front. Hum. Neurosci.* 11:585. doi: 10.3389/fnhum.2017.00585

Song, M., and Kim, J. (2019). A paradigm to enhance motor imagery using rubber hand illusion induced by visuo–tactile stimulus. *IEEE Trans. Neural Syst. Rehabil. Eng.* 27, 477–486. doi: 10.1109/tnsre.2019.2895029

Sun, R., Wong, W.-W., Wang, J., and Tong, R. K.-Y. (2017). Changes in electroencephalography complexity using a brain computer interface-motor observation training in chronic stroke patients: a fuzzy approximate entropy analysis. *Front. Hum. Neurosci.* 11:444. doi: 10.3389/fnhum.2017.00444

Susanto, E. A., Tong, R. K., Ockenfeld, C., and Ho, N. S. (2015). Efficacy of robot-assisted fingers training in chronic stroke survivors: a pilot randomized-controlled trial. *J. NeuroEng. Rehabil.* 12:42.

Velasco-Álvarez, F., Ron-Angevin, R., da Silva-Sauer, L., and Sancha-Ros, S. (2013). Audio–cued motor imagery–based brain–computer interface: navigation through virtual and real environments. *Neurocomputing* 121, 89–98. doi: 10.1016/j.neucom.2012.11.038

Vukelić, M., and Gharabaghi, A. (2015). Oscillatory entrainment of the motor cortical network during motor imagery is modulated by the feedback modality. *NeuroImage* 111, 1–11. doi: 10.1016/j.neuroimage.2015.01.058

Wolf, S. L., Catlin, P. A., Ellis, M., Archer, A. L., Morgan, B., and Piacentino, A. (2001). Assessing wolf motor function test as outcome measure for research in patients after stroke. *Stroke* 32, 1635–1639. doi: 10.1161/01.Str.32.7.1635

Wu, Q., Yue, Z., Ge, Y., Ma, D., Yin, H., Zhao, H., et al. (2020). Brain functional networks study of subacute stroke patients with upper limb dysfunction after comprehensive rehabilitation including BCI training. *Front. Neurol.* 10:1419. doi: 10.3389/fneur.2019.01419

Yuan, H., and He, B. (2014). Brain-computer interfaces using sensorimotor rhythms: current state and future perspectives. *IEEE Trans. Biomed. Eng.* 61, 1425–1435. doi: 10.1109/tbme.2014.2312397

Zhou, M. G., Wang, H. D., Zeng, X. Y., Yin, P., Zhu, J., Chen, W. Q., et al. (2019). Mortality, morbidity, and risk factors in China and its provinces, 1990–2017: a systematic analysis for the global burden of disease study 2017. *Lancet* 394, 1145–1158. doi: 10.1016/s0140-6736(19)30427-1

Zich, C., Debener, S., Kranczioch, C., Bleichner, M. G., Gutberlet, I., and De Vos, M. (2015). Real–time EEG feedback during simultaneous EEG–fMRI identifies the cortical signature of motor imagery. *NeuroImage* 114, 438–447. doi: 10.1016/j.neuroimage.2015.04.020

Conflict of Interest: The authors declare that the research was conducted in the absence of any commercial or financial relationships that could be construed as a potential conflict of interest.

frontiers in Neuroscience

ORIGINAL RESEARCH
published: 15 March 2022
doi: 10.3389/fnins.2021.771056

Functional Connectivity Analysis and Detection of Mental Fatigue Induced by Different Tasks Using Functional Near-Infrared Spectroscopy

Yaoxing Peng[1†], Chunguang Li[1], Qu Chen[2*], Yufei Zhu[1] and Lining Sun[1†]*

[1] *The Key Laboratory of Robotics System of Jiangsu Province School of Mechanical Electric Engineering Soochow University, Suzhou, China,* [2] *Mathematics Teaching and Research Section, Basic Course Department, Communication Sergeant School of Army Engineering University, Chongqing, China*

OPEN ACCESS

Edited by:
Jinhua Zhang,
Xi'an Jiaotong University, China

Reviewed by:
Hong Zeng,
Southeast University, China
Dingguo Zhang,
University of Bath, United Kingdom

****Correspondence:***
Chunguang Li
lichunguang@suda.edu.cn
Qu Chen
7600685@qq.com

[†] These authors have contributed equally to this work

Specialty section:
This article was submitted to Neuroprosthetics, a section of the journal Frontiers in Neuroscience

Received: *05 September 2021*
Accepted: *21 December 2021*
Published: *15 March 2022*

Citation:
Peng Y, Li C, Chen Q, Zhu Y and Sun L (2022) Functional Connectivity Analysis and Detection of Mental Fatigue Induced by Different Tasks Using Functional Near-Infrared Spectroscopy. Front. Neurosci. 15:771056. doi: 10.3389/fnins.2021.771056

Objectives: The objective of this study was to investigate common functional near-infrared spectroscopy (fNIRS) features of mental fatigue induced by different tasks. In addition to distinguishing fatigue from non-fatigue state, the early signs of fatigue were also studied so as to give an early warning of fatigue.

Methods: fNIRS data from 36 participants were used to investigate the common character of functional connectivity network corresponding to mental fatigue, which was induced by psychomotor vigilance test (PVT), cognitive work, or simulated driving. To analyze the network reorganizations quantitatively, clustering coefficient, characteristic path length, and small worldness were calculated in five sub-bands (0.6–2.0, 0.145–0.600, 0.052–0.145, 0.021–0.052, and 0.005–0.021 Hz). Moreover, we applied a random forest method to classify three fatigue states.

Results: In a moderate fatigue state: the functional connectivity strength between brain regions increased overall in 0.021–0.052 Hz, and an asymmetrical pattern of connectivity (right hemisphere > left hemisphere) was presented. In 0.052–0.145 Hz, the connectivity strength decreased overall, the clustering coefficient decreased, and the characteristic path length increased significantly. In severe fatigue state: in 0.021–0.052 Hz, the brain network began to deviate from a small-world pattern. The classification accuracy of fatigue and non-fatigue was 85.4%. The classification accuracy of moderate fatigue and severe fatigue was 82.8%.

Conclusion: The preliminary research demonstrates the feasibility of detecting mental fatigue induced by different tasks, by applying the functional network features of cerebral hemoglobin signal. This universal and robust method has the potential to detect early signs of mental fatigue and prevent relative human error in various working environments.

Keywords: mental fatigue detection, functional near-infrared spectroscopy, functional network characteristics, functional connectivity, common signs of fatigue tasks

INTRODUCTION

Long-term cognitive tasks and attention tasks may lead to mental fatigue, which is usually manifested by decreased attention, slower reaction times, and increased aversion to tasks (Boksem et al., 2006). Mental fatigue and its related decline in brain physiological function represent an important social problem, leading to reduced productivity (Tanabe and Nishihara, 2004), impaired motor and cognitive task execution (Sharma et al., 2019), reduced risk alertness (Saxby et al., 2013), and an increased incidence of accidents (Nilsson et al., 1997). To cope with these adverse but preventable consequences caused by mental fatigue, a reasonable and accurate assessment of mental fatigue degree is required. Precise assessment of fatigue degree would allow developing better strategies to arrange the work intensity and reduce potential errors or work accidents.

It is noteworthy that the signs of mental fatigue will also be different under different task situations (Ream and Richardson, 1996). Due to the complexity of the human environment, a large number of internal or external causes can lead to mental fatigue. At the same time, mental fatigue and sleepiness are often difficult to distinguish. Although involving very different concepts, they are both related in the impairment of attention, vigilance and cognitive performance (Neu et al., 2011), high degree of internal consistency among different dimensions of subjective fatigue (Matthews and Desmond, 1998), and evolution that is parallel. This paper does not want to clearly distinguish the differences between mental fatigue and sleepiness, but to explore the universal character of mental fatigue in the realistic complex environment and improve the reliability of mental fatigue indication methods.

Mental fatigue is a complex process involving the changes in multiple brain regions related to tasks, including local and global scale changes (Sun et al., 2017). Therefore, functional connectivity analysis is one of the ideal methods used to research on the mechanism of mental fatigue. A lot of prior neuroimaging studies using EEG, fMRI, or fNIRS have shown that mental fatigue is related to the deviation and reorganization of functional connectivity (Esposito et al., 2014; Qi et al., 2019; Zhang et al., 2020). In addition, graph theoretical analysis methods have been widely used in quantitative research on connectivity network structure. Sun et al. (2014a) found that in a 20-min continuous attention task, the characteristic path length of the brain network was related to the decline in task performance, and the small worldness decreased during the task. Chua et al. (2017) induced mental fatigue through a simulated driving task and found that in a 1-h task, the clustering coefficient of the brain functional network increased, and the characteristic path length decreased. In short, local clustering and inter-regional connectivity will change according to mental fatigue. These characteristics may reflect cognitive performance during fatigue.

These studies have well summarized the mechanism of functional connectivity reorganization and evolution according to mental fatigue state and effectively identify fatigue state. However, these changes can distinguish fatigue from non-fatigue state, which is not enough to give an early warning before excessive fatigue. At the same time, most studies research mental fatigue under single induced task. Considering the complexity of realistic environment, it is not applicable in guiding a universal and robust mental fatigue detection method. Therefore, it is necessary to find the common change rules of brain activity concerning the development of mental fatigue in complex work environments and use them to provide scientific methods and theoretical support for fatigue monitoring and prevention.

The main purpose of this paper is to explore the common characteristics of the functional brain network corresponding to different mental fatigue states under complex fatigue-induced conditions. Therefore, we repeated three fatigue-inducing tasks, twice in the afternoon and evening, to simulate the complex state of mental fatigue that may occur in reality, and the fatigue may include the disturbance of drowsiness. Multidimensional Fatigue Inventory (MFI-20) was used to classify three mental fatigue levels: non-fatigue, moderate fatigue, and severe fatigue. The correlation between mental fatigue and cognitive decline was measured by behavioral test results. Functional near-infrared spectroscopy is a non-invasive neuroimaging technique allowing the measurement of variations in blood oxygenation in cortical areas (Borragán et al., 2019) with acceptable spatial and tolerance to movements. fNIRS is appropriate to track changes in brain connectivity and reliably reflect cognitive load (Herff et al., 2014). This study is based on the fNIRS method to detect the blood oxygen information of the cerebral cortex throughout the experimental process, construct a functional network in five frequency bands, and quantitatively analyze the structure of a fatigue-related functional network by the network analysis method, and at the same time, extracting the characteristics for fatigue classification, so as to provide reference for cross-task mental fatigue early warning method.

MATERIALS AND METHODS

Participants

The fatigue experiment recruited 36 undergraduate and graduate students (20 $\pm$ 2 years old, male:female = 27:9) from Soochow University. The participants were right-handed, in good health, and had no history of mental illness or cerebrovascular disease. Participants were not allowed to use medications, take a nap, and consume caffeine or stimulus drinks on the day of the experiment. All participants signed an informed consent before the experiment.

Experiment Procedure

Participants were randomly divided into three groups for different fatigue-inducing experiments, including Psychomotor Vigilance Test (PVT), cognitive work, or simulated driving. Participants were asked to respect normal sleep schedules before the experiment. Each participant repeated the test three times: before starting the day's work in the morning (7:00–8:00), in the afternoon (14:00–17:00), and before sleeping in the evening (20:00–23:00). The specific process is shown in **Figure 1**. In the morning, the n-back behavioral test was conducted, then the Multidimensional Fatigue Inventory (MFI-20) was filled out (8 min in total). In the afternoon and evening, the above

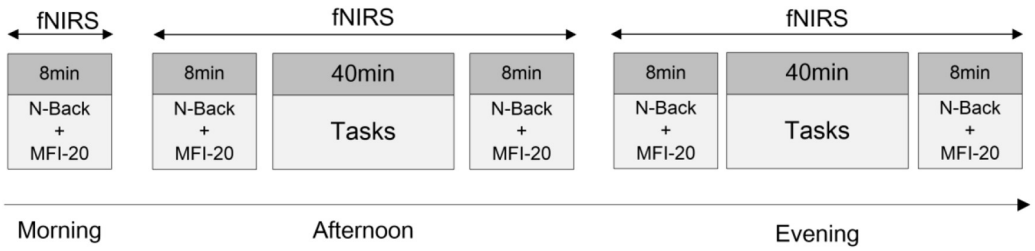

FIGURE 1 | Experimental procedure. About 8 min/person in the morning. The afternoon experiment and evening experiment are about 1 h/person.

behavioral tests and scale filling were carried out before and after the task. Cortical brain activity changes during the whole experiment were recorded using fNIRS.

Material and Tasks

Before and after the fatigue-inducing task, the participants filled in the Multidimensional Fatigue Inventory (Smets et al., 1995) and conducted the n-back (n = 1) behavioral test to evaluate cognition and vigilance performance associated with mental fatigue. The n-back task requires coordinated work across multiple brain regions (Cohen and D'Esposito, 2016). During the n-back test, the monitor displayed a blue square every 3S and broadcasted one random letter at the same time. Whenever a location of a square matched the location of the square presented one instance earlier, participants were asked to press the "W" key on a computer keyboard. Whenever an audio matched the last audio broadcast, participants were asked to press the "S" key on a computer keyboard. The schematic diagram of N-back is shown in **Figure 2**. The reaction time and accuracy of each comparison task were recorded as the basis for judging cognitive performance and vigilance.

Mental Fatigue Task

Mental fatigue induction tasks include psychomotor vigilance test (PVT), cognitive work, or simulated driving. PVT test is a simple reaction time test with high stimulus load. Participants were required to pay attention to the monitor. When the stimulus (red dot) was displayed in the middle of the monitor, they were supposed to respond with a button press on the keyboard as quickly as possible. In the test, inter-stimulus interval (ISI) was random and varied, ranging from 5 to 10 s. PVT task in this study was used to simulate passive mental fatigue caused by long-time simple attention tasks (Körber et al., 2015). Cognitive work included mathematical calculation tasks and foreign language reading tasks corresponding to the level of the participants, so as to simulate the mental fatigue state after the realistic learning task. A semi-immersive simulated driving task was designed. The route of the task included a motorway and a rural road. Simulated driving tasks were used to simulate passive fatigue caused by task underload under highly predictable and stable driving conditions (Larue et al., 2011; Li et al., 2016) and active fatigue caused by resource depletion due to high attention demand (Smit et al., 2004).

Functional Near-Infrared Spectroscopy Acquisition

This study used a multichannel fNIRS system (NirSmart, HuiChuang, Beijing, China) to record cortical brain activity. According to Brodmann's anatomical region system of cerebral cortex, a 4 * 4 headgear layout was designed, including 24 effective test channels composed of eight light emitters and eight light receivers, covering the prefrontal cortex (PFC), frontal eye field (FEF), supplementary motor cortex (SMA), and premotor cortex (PMC), four brain functional regions. In the experiment, the 10–20 system (Okamoto et al., 2004) was used as the positioning standard to locate the brain functional area. The channel distribution of specific brain imaging is shown in **Figure 3A**. The experimental environment is shown in **Figure 3B**. The sampling frequency was 16 Hz.

Data Analysis

Considering the different physiological information contained in different frequency bands of blood oxygen signal (Stefanovska et al., 1999), the Chebyshev bandpass filter was used to filter the original blood oxygen signal to (I, 0.005–0.021 Hz; II, 0.021–0.052 Hz; III, 0.052–0.145 Hz; IV, 0.145–0.600 Hz, V, 0.6–2.0 Hz) five frequency bands, corresponding to the physiological information of cardiac activity, respiratory activity, myogenic activity, neurogenic activity, and endogenic activity contained in hemoglobin signal. At the same time, the influence of high-frequency noise was eliminated.

In order to evaluate the changes in activity indicators in different cerebral cortex regions, this paper divides eight regions of interest (ROI) (as shown in **Table 1**) and calculates the overall blood oxygen concentration of each ROI brain region, which could reduce the individual difference caused by head size. Considering the differences in individual blood oxygen active channels, the weighted average method based on entropy weight was used to calculate the blood oxygen concentration of ROI. The calculation formula is as follows:

$$y = \sum_{j} X_{ij}\, \omega_j \; (i = 1, 2, \ldots, N,\; j = 1, 2, \ldots, M) \qquad (1)$$

X represents the N rows, M columns matrix composed of the original hemoglobin concentration, and ω_j represents the weight of each channel calculated by information entropy of channel blood oxygen concentration (Liu et al., 2017).

In order to study the dynamic interaction between regions in the process of cortical activity, Pearson correlation coefficient was

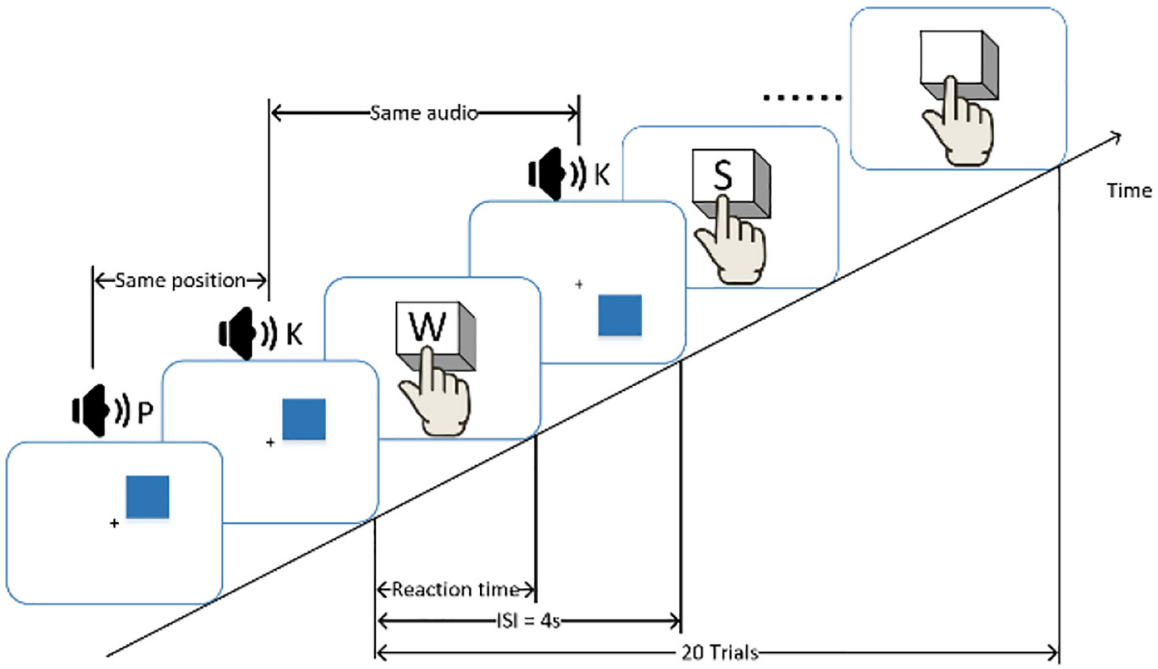

FIGURE 2 | A schematic diagram of the n-back experiment. Participants were required to respond to the same consecutive stimulus and press the button as quickly as possible. The inter-stimulus interval (ISI) of the stimulus is 3 s.

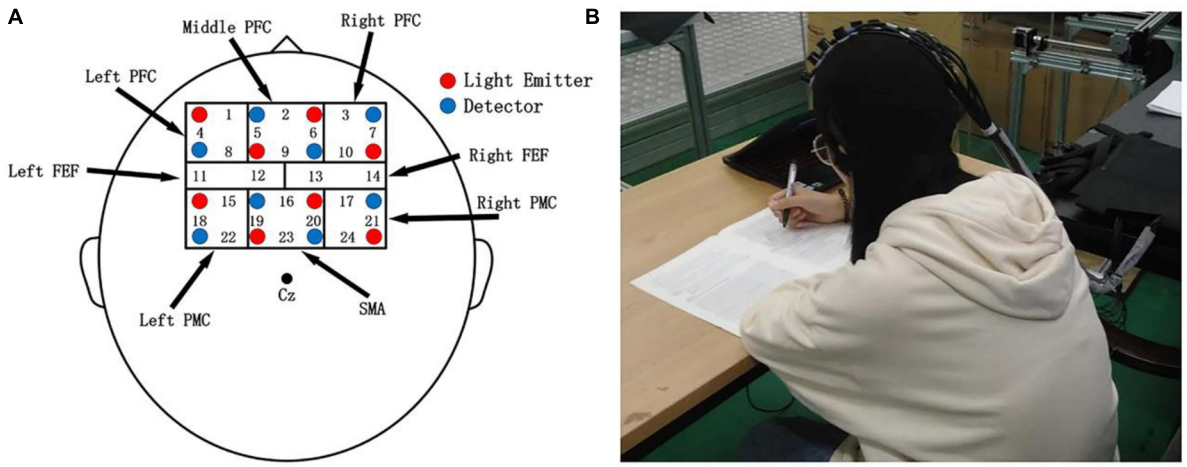

FIGURE 3 | (A) Probe and functional brain region distribution map; red and blue numbers represent sources and detectors, respectively. **(B)** Experimental environment.

used to calculate the correlation of blood oxygen concentration in each ROI during the task, and a weighted undirected network was constructed to quantitatively evaluate the changes in functional connectivity in brain-related regions corresponding to different fatigue levels. This paper calculated the clustering coefficient, characteristic path length, and small worldness. The clustering coefficient is the degree of local correlation of the network, characteristic path length is a measure of connectivity between the whole brain interval, and the small worldness reflects the unity of the overall information transmission of the network and the local high aggregation (Tononi et al., 1998; Watts and Strogatz, 1998).

In a weighted network, for node u, the node clustering coefficient is defined as:

$$C_u = \frac{1}{\deg(u)(\deg(u)-1)} \sum_{vw} (\widehat{w}_{uv}\widehat{w}_{uw}\widehat{w}_{vw})^{1/3} \quad (2)$$

where deg (u) is the degree of u. For weighted graphs, clustering coefficient is defined as the geometric average of the

TABLE 1 | The division of region of interest (ROI).

Name of ROI	Channels included
L-PFC	1, 4, 8
M-PFC	2, 5, 6, 9
R-PFC	3, 7, 10
L-FEF	11, 12
R-FEF	13, 14
SMA	15, 18, 22
L-PMC	16, 19, 20, 23
R-PMC	17, 21, 24

L, M, R represent left, medial, right, respectively. For example, L-PFC represents the left part of PFC.

subgraph edge weights. The edge weights $\widehat{w_{uv}}$ are normalized by the maximum weight in the network $\widehat{w_{uv}} = w_{uv}/\max(w)$ (Onnela et al., 2005).

The clustering coefficient of analyzed network is defined as the mean of the clustering coefficients of all nodes:

$$C = \frac{1}{n}\sum_{v \in G} C_v \tag{3}$$

The path length d_{ij} from the node i to node j is defined as the sum of the edge lengths along this path, where the length of each edge was obtained by computing the reciprocal of the edge weight. The characteristic path length of a weight directed graph was defined as the smallest sum of the edge lengths throughout all the possible paths (Sun et al., 2014a):

$$L = \frac{1}{n(n-1)}\sum_{i \neq j} d_{ij} \tag{4}$$

Small worldness:

$$\sigma = \frac{C_{real}}{C_{random}} / \frac{L_{real}}{L_{random}} \tag{5}$$

The small worldness could be summarized from the normalized clustering coefficient ($\gamma = C_{real}/C_{random}$) and the normalized characteristic path length ($\lambda = L_{real}/L_{random}$), where C_{real} and L_{real} are the clustering coefficient and characteristic path length of the analyzed network, C_{random} and L_{random} are the mean clustering coefficient and the mean characteristic path length of 100 matched random networks, respectively.

To compare the topological structure of functional connectivity without bias from different average connectivity difference (Sun et al., 2014a), the small worldness of unweighted network was calculated. Sparsity is defined as the ratio of the number of actual edges to the number of all possible edges in a fully connected network. A sparsity of 0.45 was adopted to convert the full connection matrix to a sparse network.

Three kinds of blood oxygen information, including oxyhemoglobin, deoxyhemoglobin, and total oxyhemoglobin, were recorded in the experiment. Characteristics of brain functional network were calculated under the three kinds of blood oxygen in this study.

Statistics

All statistical analyses were performed using SPSS version 25.0 (IBM Corp., Armonk, NY, United States). For MFI-20 scores, N-back test scores, functional connectivity strength, and network metrics, the primary result was analyzed by two-way analysis of variance (ANOVA) with three fatigue levels [L1 (non-fatigue), L2 (moderate fatigue), and L3 (severe fatigue)], and the three tasks (PVT, cognitive work, and simulated driving) as factors. If the significant main effects were on the fatigue level, but no interactions were detected, Tukey-Kramer's *post-hoc* test was used to locate differences between fatigue levels. For all analyses, the statistical significance was set at $p < 0.05$.

Mental Fatigue Classification

The levels of mental fatigue were defined by the score of MFI-20 scale and behavioral test. A clustering analysis of unsupervised k-means was performed on MFI-20 scale score, and the participants were grouped into non-fatigue and fatigue. According to the results of clustering analysis, taking the scale score of 2.57 as the threshold, the participants with a scale score less than 2.57 were classified as non-fatigue, and the participants with a score more than or equal to 2.57 were classified as fatigue. Then according to the score of n-back behavioral task (reaction time/accuracy) and MFI-20, the fatigue participants were further grouped into moderate fatigue and severe fatigue. This study took the scale score threshold from 2.57 to 5.00 with step of 0.01; the behavioral test scores of the grouped participants were statistically analyzed. When the threshold was 3.00, the statistical difference of behavioral test scores between moderate fatigue and severe fatigue participants was the largest, so the participants with a score more than or equal to 3.00 were divided into severe fatigue.

Machine Learning Method

To verify the feasibility of mental fatigue detection based on fNIRS data, we performed classification of mental fatigue states based on the functional connectivity strength and characteristics of brain functional network. This paper classified three mental fatigue levels: non-fatigue, moderate fatigue, and severe fatigue. The features include Pearson correlation coefficient (r) between eight ROI(3 hemoglobins * 5 frequency bands * 28 channel pairs), characteristic path length and clustering coefficient of brain functional network(3 hemoglobins * 5 frequency bands * 2 network characteristics), and 15 time-domain features(3 hemoglobins * 5 frequency bands * 8 ROI * 15 time-domain feature). The time-domain features include mean, standard deviation, coefficient of variation, energy, range, skewness, kurtosis and peak, Hjorth parameter, information entropy, root mean square, kurtosis factor, waveform factor, pulse factor, and margin factor. Considering the unbalanced number of three-level participants and high feature dimension, this study used the random forest algorithm based on Python library sklearn and random forest classifier. Because of the large number of available features, the key features were selected based on the Gini coefficient, and then the features were further screened,

and the parameters of random forest classifier were optimized by genetic algorithm.

RESULTS

Mental Fatigue Degree and Behavioral Task Performance

The MFI-20 scale scores corresponding to participants of three fatigue levels are shown in **Figure 4A**. The ANOVA results revealed a significant main effect of fatigue level (F = 305.584; $p < 0.001$; $\eta^2 = 0.795$) on MFI-20 scores, but no significant main effect of task ($p = 0.715$) or interaction between fatigue level and task ($p = 0.844$) was found. *Post-hoc* analyses indicated significant increases in MFI-20 score between non-fatigue and moderate fatigue ($p < 0.001$), between moderate fatigue and severe fatigue ($p < 0.001$), and between non-fatigue and severe fatigue ($p < 0.001$).

The N-back task scores corresponding to participants of three fatigue levels are shown in **Figure 4B**. The ANOVA results revealed a significant main effect of fatigue level (F = 15.759; $p < 0.001$; $\eta^2 = 0.166$) on N-back scores, and no main effect of task ($p = 0.286$) or interaction between fatigue level and task ($p = 0.259$) was significant. *Post-hoc* analyses indicated significant increases on N-back score between non-fatigue and severe fatigue ($p < 0.001$), and between moderate fatigue and severe fatigue ($p < 0.001$).

Functional Connectivity Network

In five frequency bands, the average functional connectivity network corresponding to the three mental fatigue levels are shown in **Figures 5–9**, respectively. In each band, two-way ANOVA was conducted on connectivity strength with the two factors: fatigue level (non-fatigue, moderate fatigue, and severe fatigue) and task (PVT, cognitive work, and simulated driving). When there was a significant main effect on fatigue level on one connectivity, there was no significant interaction between fatigue level and task; the ANOVA results of that connectivity will be shown below.

In frequency band I (0.005–0.021 Hz), the average functional connectivity network corresponding to the three mental fatigue levels are shown in **Figure 5**. The results of ANOVA revealed a significant main effect of fatigue level on the correlations of PFCM_PFCR (F = 4.655, p = 0.010, η^2 = 0.026) and FEFR_PMCR (F = 4.276, p = 0.015, η^2 = 0.024), and no significant interaction between fatigue level and task ($p > 0.311$) was found. *Post-hoc* analyses indicated a significant decrease in FEFR_PMCR connection between non-fatigue and moderate fatigue ($p = 0.029$), and a significant decrease in PFCM_PFCR connection between non-fatigue and severe fatigue ($p = 0.030$). From non-fatigue to moderate fatigue, the network connectivity decreased overall, especially between the regions of PFC and FEF, and between the regions of PFC and PMC. However, the connectivity strength remained relatively constant among PFCL, PFCM, and PFCR, as well as between the regions of SMA and PMC. From moderate fatigue to severe fatigue, the network connectivity increased overall, and a relatively compact connectivity was maintained between the left PFC and other brain regions, especially between PFC and FEF.

In frequency band II (0.021–0.052 Hz), the average functional connectivity network corresponding to the three mental fatigue levels are shown in **Figure 6**. The results of ANOVA revealed a significant main effect of fatigue level on the correlations of PFCL_FEFR (F = 5.994, p = 0.003, η^2 = 0.034) and PFCR_PMCR (F = 3.639, p = 0.027, η^2 = 0.021); no significant interaction between fatigue level and task ($p > 0.095$) was found. *Post-hoc* analyses indicated a significant increase in PFCL_FEFR connection between non-fatigue and moderate

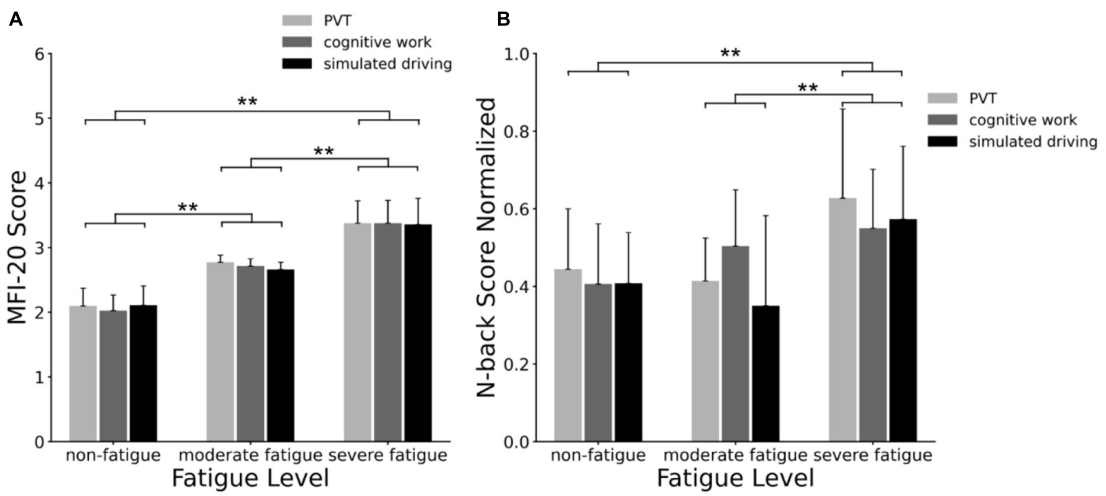

FIGURE 4 | (A) Multidimensional Fatigue Inventory (MFI-20) scale scores correspond to non-fatigue, moderate fatigue, and severe fatigue grade participants; the mean and standard deviation of each group were calculated; **(B)** behavioral task performance corresponded to non-fatigue, moderate fatigue, and severe fatigue participants. The behavioral task scores (reaction time/accuracy) were normalized, and the mean value and standard deviation of each group were calculated. $^{**}p < 0.01$.

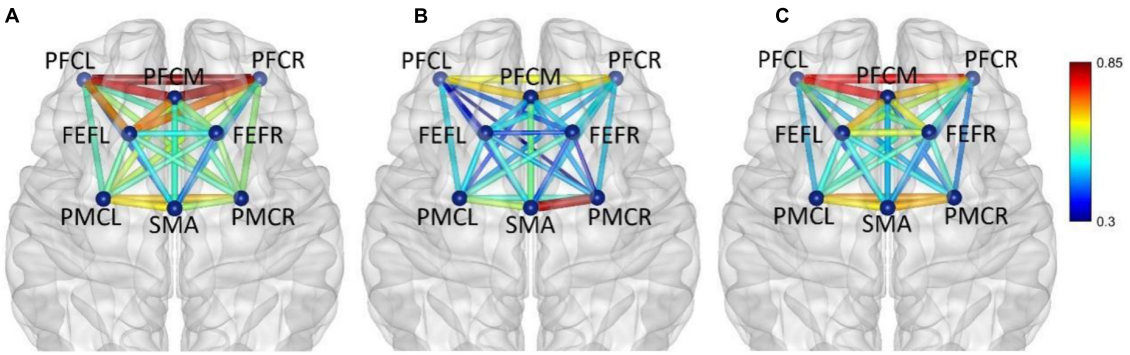

FIGURE 5 | Frequency band I (0.005–0.021 Hz), **(A)** non-fatigue, **(B)** moderate fatigue, and **(C)** severe fatigue. The average cortical functional connectivity network contains eight ROI brain regions. The width and color of the line represent the strength of the connectivity. Functional connectivity was visualized with the BrainNet Viewer (http://www.nitrc.org/project/bnv/).

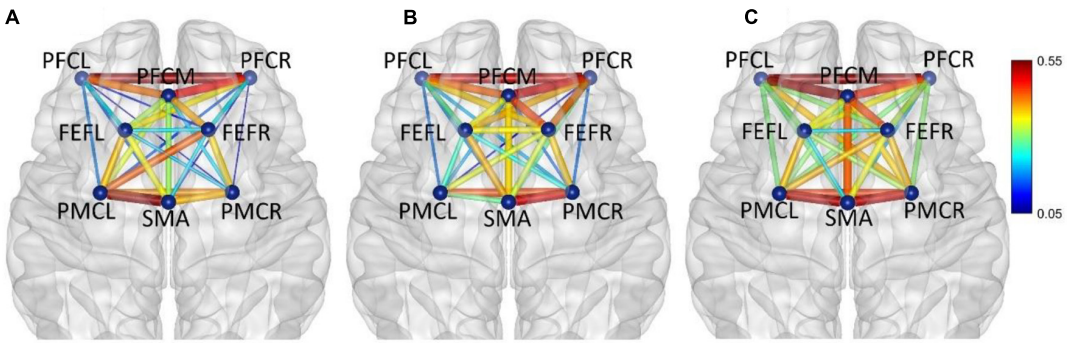

FIGURE 6 | In frequency band II (0.021–0.052 Hz), non-fatigue **(A,B)** moderate fatigue, and **(C)** severe fatigue. The average cortical functional connectivity network contains eight ROI brain regions. The width and color of the line represent the strength of the connectivity.

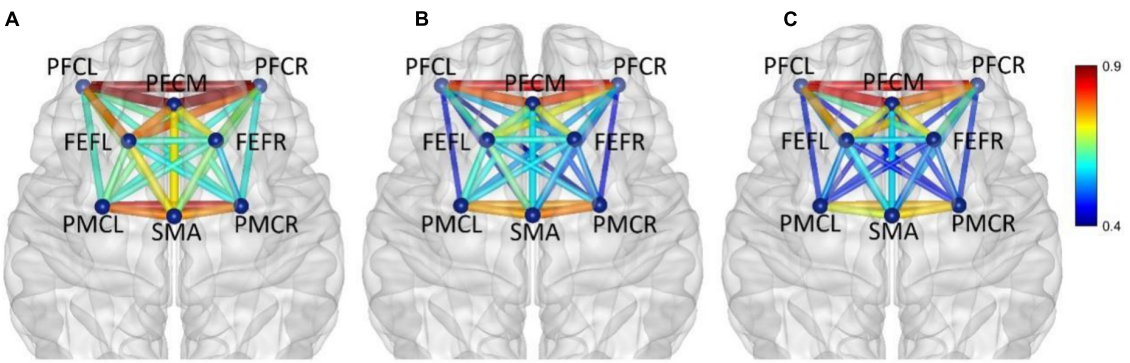

FIGURE 7 | In frequency band III (0.052–0.145 Hz), non-fatigue **(A,B)** moderate fatigue, **(C)** severe fatigue. The average cortical functional connectivity network contains 8 ROI brain regions. The width and color of the line represent the strength of the connectivity.

fatigue (p = 0.013), and between non-fatigue and severe fatigue (p = 0.049), and a significant increase in PFCR_PMCR connection between non-fatigue and severe fatigue (p = 0.029). From non-fatigue to moderate fatigue, the overall connectivity strength of the right hemisphere increased. The average functional connectivity strength of the left and right hemispheres was calculated. The connectivity strength of the right hemisphere is greater than that of the left hemisphere (p = 0.005). When severe fatigue occurred, there was no significant difference in the connectivity strength between the left and right hemispheres (p = 0.273).

In frequency band III (0.052–0.145 Hz), the average functional connectivity network corresponding to the three mental fatigue levels are shown in **Figure 7**. The results of ANOVA revealed

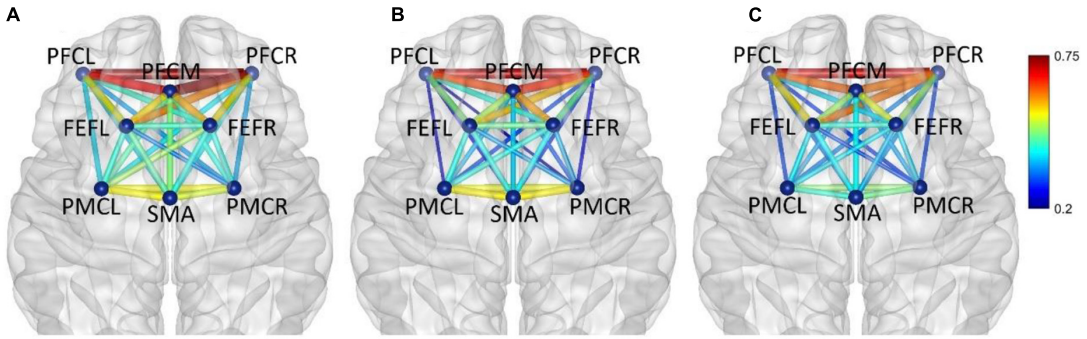

FIGURE 8 | In frequency band IV (0.145–0.600 Hz), non-fatigue **(A,B)** moderate fatigue, **(C)** severe fatigue. The average cortical functional connectivity network contains eight ROI brain regions. The width and color of the line represent the strength of the connectivity.

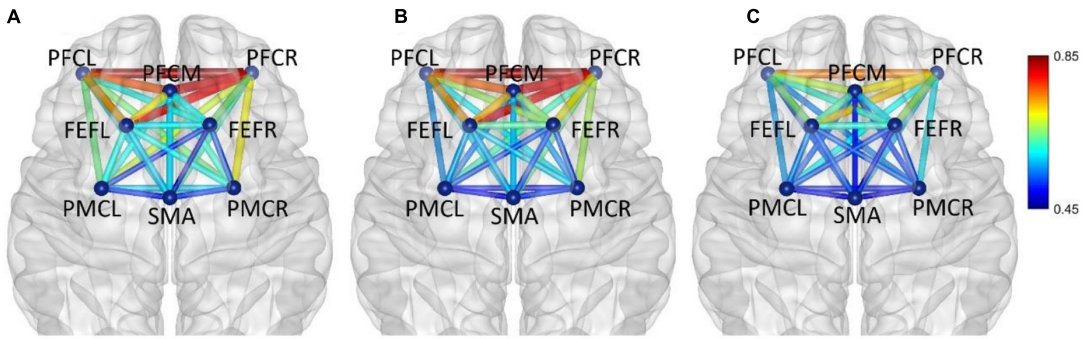

FIGURE 9 | In frequency band V (0.6–2.0 Hz), non-fatigue **(A,B)** moderate fatigue, and **(C)** severe fatigue. The average cortical functional connectivity network contains eight ROI brain regions. The width and color of the line represent the strength of the connectivity.

the significant main effect of fatigue level on the correlations of PFCL_PFCM, PFCL_PFCR, PFCL_FEFL, PFCL_PMCL, PFCL_PMCR, PFCM_PFCR, PFCM_PMCL, PFCR_SMA, PFCR_PMCL, PFCR_PMCR, FEFL_SMA, FEFL_PMCL, FEFL_PMCR, FEFR_PMCL, and PMCL_PMCR; no significant interaction between fatigue level and task ($p > 0.051$) was found. The details of ANOVA are shown in **Table 2**.

Post-hoc analyses indicated significant decreases in PFCL_PFCM, PFCL_FEFL, PFCL_PMCL, PFCL_PMCR, PFCM_PFCR, PFCR_SMA, PFCR_PMCR, and PMCL_PMCR connections between non-fatigue and moderate fatigue, decreases in PFCL_PFCR, PFCL_PMCR, PFCM_PFCR, PFCM_PMCL, PFCR_PMCL, FEFL_SMA, FEFL_PMCL, FEFL_PMCR, FEFR_PMCL connections between non-fatigue and severe fatigue, increase in PFCL_FEFL connection between moderate fatigue and severe fatigue, and a decrease in PFCM_PMCL, PMCL_PMCR connection between moderate fatigue and severe fatigue. The details of *post-hoc* analyses are shown in **Table 3**. From non-fatigue to moderate fatigue, the connectivity of the whole brain network decreased significantly. From moderate fatigue to severe fatigue, the whole network only maintained relatively strong connectivity between the regions of PFC and FEF.

In frequency band IV (0.145–0.600 Hz), the average functional connectivity network corresponding to the three mental fatigue levels are shown in **Figure 8**. The results of ANOVA revealed a significant main effect of fatigue level on the correlation of PFCM_PMCL ($F = 4.945$, $p = 0.008$, $\eta^2 = 0.028$); no significant interaction between fatigue level and task ($p = 0.165$)

TABLE 2 | Functional connectivity with significant main effect of fatigue level in band frequency III.

Functional connectivity	*F*	*p*-value	Partial eta squared (η^2)
PFCL_PFCM	5.835	0.003	0.033
PFCL_PFCR	5.013	0.007	0.028
PFCL_FEFL	10.848	<0.001	0.059
PFCL_PMCL	6.678	0.001	0.037
PFCL_PMCR	10.571	<0.001	0.058
PFCM_PFCR	10.452	<0.001	0.057
PFCM_PMCL	12.306	<0.001	0.067
PFCR_SMA	4.975	0.007	0.028
PFCR_PMCL	4.610	0.011	0.026
PFCR_PMCR	4.977	0.007	0.028
FEFL_SMA	7.640	0.001	0.042
FEFL_PMCL	4.068	0.018	0.023
FEFL_PMCR	3.901	0.021	0.022

No interaction was significant (all p > 0.05) on functional connectivity above.

TABLE 3 | *Post-hoc* analyses among fatigue levels in band frequency III.

Fatigue level	Fatigue level	Functional connectivity	Mean difference (I–J)	*p*-values
L1	L2	PFCL_PFCM	0.097	0.002
		PFCL_FEFL	0.168	<0.001
		PFCL_PMCL	0.137	0.016
		PFCL_PMCR	0.202	<0.001
		PFCM_PFCR	0.099	0.007
		PFCR_SMA	0.149	0.010
		PFCR_PMCR	0.137	0.021
		PMCL_PMCR	0.100	0.007
	L3	PFCL_PFCR	0.061	0.016
		PFCL_PMCR	0.157	0.002
		PFCM_PFCR	0.121	<0.001
		PFCM_PMCL	0.203	<0.001
		PFCR_PMCL	0.126	0.015
		FEFL_SMA	0.147	<0.001
		FEFL_PMCL	0.116	0.027
		FEFL_PMCR	0.119	0.019
		FEFR_PMCL	0.144	0.013
L2	L3	PFCL_FEFL	−0.141	0.001
		PFCM_PMCL	0.156	0.009
		PMCL_PMCR	0.116	<0.001

was found. *Post-hoc* analyses indicated a significant decrease in PFCM_PMCL connection between non-fatigue and severe fatigue ($p = 0.034$). From non-fatigue to moderate fatigue, the functional connectivity of the whole brain network was weakened. From moderate fatigue to severe fatigue, the whole network only maintained relatively strong connectivity between the regions of PFC and FEF.

In frequency band V (0.6–2.0 Hz), the average functional connectivity network corresponding to the three mental fatigue levels are shown in **Figure 9**. The functional connectivity of the whole brain network did not change significantly. From moderate fatigue to severe fatigue, the functional connectivity of the whole brain network decreased, especially between PFC and other regions of the brain.

Characteristics of Brain Functional Network

Comparison of clustering coefficient among three fatigue levels in five frequency bands are shown in **Figure 10A**. In frequency band III, the significant main effects of fatigue level on clustering coefficient ($F = 8.670$; $p < 0.001$; $\eta^2 = 0.048$) are presented, but no significant interaction between fatigue level and task ($p > 0.05$) was found, as shown in **Figure 10B**. *Post-hoc* analyses confirmed the decrease in clustering coefficient between non-fatigue and moderate fatigue ($p = 0.002$), and between non-fatigue and severe fatigue ($p = 0.002$).

Comparison of characteristic path length among three fatigue levels in five frequency bands is shown in **Figure 10C**. In frequency band III, the significant main effects of fatigue level on characteristic path length ($F = 8.670$; $p < 0.001$; $\eta^2 = 0.048$) are presented, but no significant interaction between fatigue level and task ($p > 0.05$) was found, as shown in **Figure 10D**. *Post-hoc* analyses confirmed the increase in characteristic path length between non-fatigue and moderate fatigue ($p = 0.006$), and between non-fatigue and severe fatigue ($p = 0.003$).

As for each fatigue level, average small worldness of weighted networks was larger than 1 in all the five frequency bands (as shown in **Figure 11A**), which indicated that all the connectivity networks in the three fatigue levels displayed small-world characteristics. In frequency band II, the significant main effect of fatigue level on small worldness was presented ($F = 4.290$; $p = 0.015$; $\eta^2 = 0.028$), but no significant main effect of task ($p = 0.059$) or interaction between fatigue level and task ($p = 0.120$) was found. As shown in **Figure 11B**. *Post-hoc* analyses confirmed the decrease in small worldness between non-fatigue and severe fatigue ($p = 0.042$).

Considering the possible influence of the difference average connectivity strength among the three fatigue levels on the network topological structure, a common sparsity has been considered in each weighted network through a dynamic threshold. In other words, all unweighted networks were guaranteed to have the same number of edges. The small worldness of unweighted networks are shown in **Figure 12B**. In frequency bands I and II, the significant main effect of fatigue level on unweighted small worldness was presented (band I: $F = 3.812$; $p = 0.023$; $\eta^2 = 0.030$; band II: $F = 4.064$; $p = 0.018$; $\eta^2 = 0.032$), but no significant main effect of task ($p > 0.419$) or interaction between fatigue level and task ($p > 0.101$) were found. In frequency band I, *post-hoc* analyses confirmed the decrease in small worldness between non-fatigue and moderate fatigue ($p = 0.037$). In frequency band II, *post-hoc* analyses confirmed the decrease in unweighted small worldness between non-fatigue and severe fatigue ($p = 0.010$).

Mental Fatigue Classification

In this study, the functional connectivity strength, characteristics of brain functional network, and time-domain characteristics of blood oxygen signal were used as features to classify the mental fatigue levels. The classification accuracy of non-fatigue and fatigue was 85.4%, the recall of fatigue was 89.3%, and the F1 score was 87.5% with a fivefold cross-validation. The classification accuracy of moderate fatigue and severe fatigue was 82.8%, the recall of severe fatigue was 90.5%, and the F1 score is 85.7% with a fivefold cross-validation.

DISCUSSION

In this study, there were three fatigue-inducing tasks: psychomotor vigilance test (PVT), cognitive work, and simulated driving. Based on fNIRS, cerebral hemoglobin information under different fatigue levels was recorded to construct the functional networks. Changes in functional connectivity and functional network reorganization under different fatigue levels were studied by graph theoretical analysis methods. The main findings are as follows:

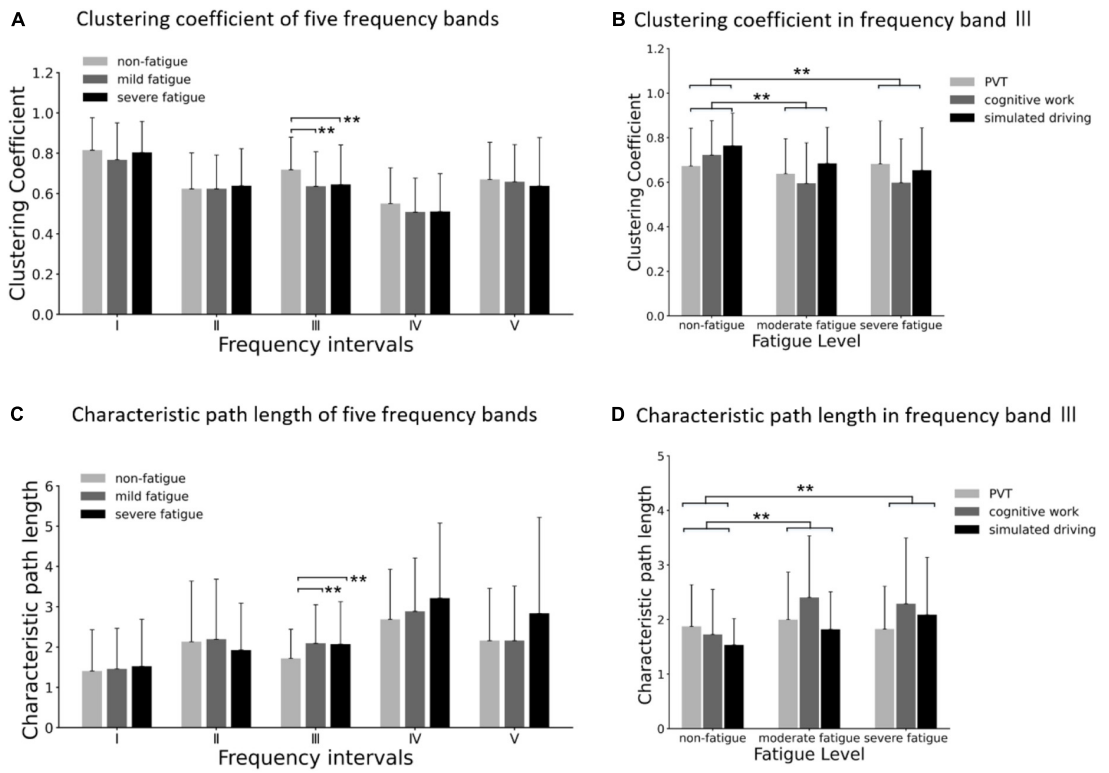

FIGURE 10 | (A) Comparison of clustering coefficient of three fatigue levels in five frequency bands. **(B)** Results of *post-hoc* analyses of clustering coefficient in frequency band III (0.052–0.14 5 Hz). **(C)** Comparison of characteristic path length of three fatigue levels in five frequency bands. **(D)** Results of *post-hoc* analyses of characteristic path length in frequency band III (0.052–0.145 Hz). Vertical bars are standard errors scores. $^{**}p < 0.01$.

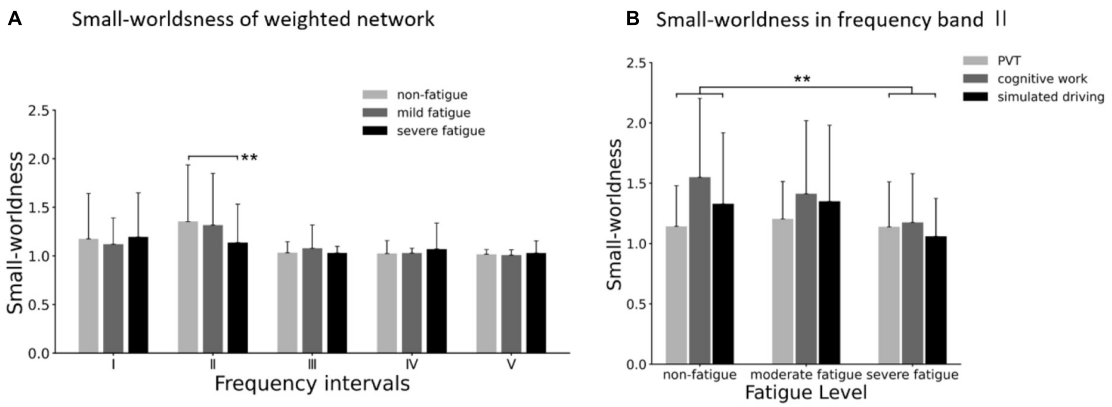

FIGURE 11 | (A) Comparison of small worldness in weighted network of three fatigue levels in five frequency bands. **(B)** Results of *post-hoc* analyses of small worldness in weighted network in frequency band II (0.021–0.052 Hz). Vertical bars are standard errors scores. $^{**}p < 0.01$.

As for moderate fatigue, the adequate behavioral task performances of participants were maintained, and there was no significant worsening in response time and accuracy. In frequency band II associated with neurogenic activity, the functional connectivity of the right hemisphere was generally enhanced; an asymmetrical pattern of connectivity (right hemisphere > left hemisphere) was presented. The most significant reorganization of functional connectivity network was in frequency band III associated with myogenic activity, the functional connectivity strength decreased overall, the clustering coefficient of brain network decreased, and the characteristic path length increased significantly.

As for severe fatigue, behavioral test performance decreased significantly. In frequency band II associated with neurogenic activity, the functional connectivity strength increased overall, and there was no significant difference in the connectivity

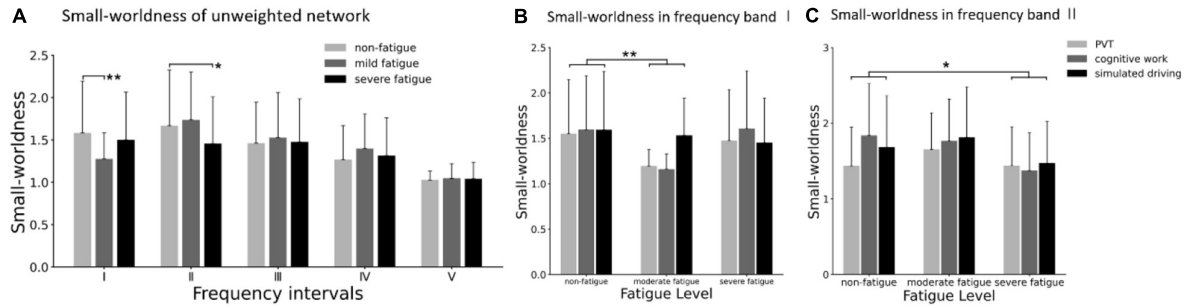

FIGURE 12 | (A) Comparison of small worldness in unweighted network of three fatigue levels in five frequency bands. **(B)** Results of *post-hoc* analyses of small worldness in unweighted network in frequency band I (0.005–0.021 Hz). **(C)** Results of *post-hoc* analyses of small worldness in unweighted network in frequency band II (0.021–0.052 Hz). Vertical bars are standard errors scores. $^{*}p < 0.05$; $^{**}p < 0.01$.

strength between the left and right hemispheres. Small worldness showed significant differences in frequency band II, and as fatigue deepened, the brain network structure began to deviate from the small-world pattern. In frequency band II associated with neurogenic activity, the small worldness decreased continuously, and the small worldness decreased significantly when severe fatigue occurred.

Moderate Mental Fatigue, Task Performance, and Changes in Functional Connectivity

Functional connectivity of the brain network based on regional cerebral blood flow (rCBF) plays an important role in information transmission across regions (Liang et al., 2013). There is a tight coupling between blood supply and brain functional topology. The functional connectivity strength showed a striking spatial correlation with rCBF (Liang et al., 2013). The oscillations in frequency bands I, II, and III reflect the influence of endothelial-related metabolic activity, intrinsic neuronal activity, and myogenic activity of the vascular smooth muscle (Shiogai et al., 2010; Li et al., 2012).

Compared with the non-fatigue state, the performance of the participants in the n-back test remained adequate in moderate fatigue, and there was no significant change in response to time and accuracy. In frequency band II associated with neurogenic activity, the strength of functional connectivity in the right hemisphere increased significantly, while the strength of connectivity between the left PMC and other brain regions decreased. There was an asymmetric network pattern between the left and right hemispheres in cortical connectivity. In previous studies, in the middle of the sleep deprivation experiment, the cortical activity of the right hemisphere increased mainly, while the bilateral activity increased in the later stage of the experiment (Borragán et al., 2019), and an increase in the frontal cortex oxygenation at the start of the driving task was found (Li et al., 2009); Asymmetric brain activation according to different types of mental fatigue was also reported (Shigihara et al., 2013). Other prior studies reported a major involvement of the right hemisphere during sustained attention tasks when tasks remained relatively easy or the participants remained alert. When the cognitive load increased, unilateral activation during the task was replaced by a bilateral activation (Klingberg et al., 1997; Helton et al., 2010), and the brain can obtain additional processing ability by activating both hemispheres (Scalf et al., 2009). Our results are similar to those studies. When the fatigue degree was mild, the same as the task load, the connectivity strength of the right hemisphere increased significantly; the connectivity pattern of the left and right hemispheres presented significant differences. The connectivity pattern of the left and right hemispheres tends to be the same in severe fatigue state.

In frequency band I, the functional connectivity strength decreased overall, and the clustering coefficient decreased significantly. That means that the connectivity strength between neighbor nodes decreased, and the degree of coordination in local brain regions decreased. The decreased clustering coefficient reflected the lower processing rate of local information. The oscillations in this frequency band reflect the myogenic activity of the vascular smooth muscle, and the substances related to metabolism have a direct effect on the state of contraction of the vascular musculature (Shiogai et al., 2010). In previous studies, higher fatigue would result in more endogenic regulation, and participants with regular exercise training showed less regulation related to endothelial cell metabolic activity in fatigue tasks (Lu et al., 2019). Similar to our study, the lower clustering coefficient may be the reflection of the lower demand for endogenous regulation in moderate fatigue.

The oscillations in frequency band III (0.052–0.145 Hz) reflect the myogenic activity of cerebrovascular smooth muscle, which plays an important role in the autoregulation of cerebral blood flow (Osol, 1995; Rowley et al., 2007). In the case of moderate fatigue, the overall functional connectivity strength of this frequency band decreased, and the corresponding clustering coefficient decreased significantly. Similar to our conclusion, previous studies have shown that the functional connectivity of myogenic frequency band decreases significantly in fatigue driving (Xu et al., 2017). It was observed in the early stage of the grip strength task that the brain directed phase transfer entropy, and the number of directional connectivity of the participants undergoing regular exercise were limited, and

the number of directional connectivity increased significantly when the fatigue increased in the later stage of the task (Osol, 1995). Similar to the endogenic frequency band, the availability of local resources may be the reason for the decreased connectivity strength between regions. At the same time, when the degree of fatigue deepened, the relevant areas must raise more resources from other areas to maintain task performance, which was also consistent with the increase in connectivity strength among PFC, FEF, and SMA observed in severe fatigue.

Severe Mental Fatigue, Task Performance, and Changes in Functional Connectivity

Compared with moderate fatigue, the behavior test performance of participants decreased significantly in severe fatigue. In the endogenic frequency band I and neurogenic frequency band II, the overall functional connectivity strength was maintained or increased, which reflected the additional activation of brain interval connection in response to resource depletion (Sun et al., 2014b; Li et al., 2019). The brain required more functional connectivity to complete the same tasks, which further exacerbates mental fatigue. At the same time, it was observed that the small worldness of the weighted network decreased significantly in neurogenic frequency band II. Considering the possible influence of the difference in average functional connectivity strength among three fatigue levels on the network structure characteristics, we maintain that each network has the same sparsity through a dynamic threshold. The small worldness calculated by this method showed a similar result (as shown in **Figure 12**). The small worldness reflects the balance of brain network in regional local cooperation and information transmission between regions and represents the best form of brain functional network structure. The decline in performance in fatigue state is related to the deviation of the brain network from small worldness (Sun et al., 2014a; Li et al., 2019). In previous pathological studies, the loss of small-world pattern has also been observed in the patient population, such as Alzheimer's disease (Stam et al., 2007), schizophrenia (Micheloyannis et al., 2006), etc. Small worldness is one of the key characteristics of health network. In severe fatigue, the decrease in small worldness reflected the decline in local specialized processing ability of brain network and information transmission efficiency between regions.

In frequency band IV, the overall connectivity strength decreased, only relatively weak connectivity remained between the regions of PFC and PMC, SMA. At the same time, the performance of the behavioral test decreased significantly. Anatomically, the prefrontal cortex is located at the top of the sensory and motor levels (Curtis and D'Esposito, 2003). The PFC can guide and regulate the functional connectivity pattern of brain regions by guiding attention, integrating sensory stimulation and motor planning, exert top–down influence on perceptual and sensorimotor areas (Hopfinger et al., 2000; Sarter et al., 2001). Sustained attention is a direct consequence of top-down signaling (Sun et al., 2014a). The decrease in connectivity strength between PFC, FEF, and PMC, SMA reflected that the depletion of brain resources led to the impairment of interregional information transmission efficiency, which reduced the ability of interregional cooperative problem solving and the accuracy of behavioral performance. Therefore, the behavioral task performance in severe fatigue declined.

Consistent with the decline in connectivity between regions, in terms of brain functional network characteristics, the characteristic path length in frequency band IV and frequency band V increased during severe fatigue. The change in clustering coefficient of the brain network is related to cognitive performance (Struck et al., 2021). In the state of mental fatigue, more isolation and less aggregation were observed (Li et al., 2016). Similar to our results, Sun et al. (2014a) found that the increase in the characteristic path length was related to the increase in reaction time caused by continuous attention tasks. Chen et al. (2019) induced mental fatigue through driving tasks. Significant differences in functional connectivity were observed between alert state and fatigue state. The frontal-to-parietal functional connectivity was weakened. Meanwhile, lower clustering coefficient values and higher characteristic path length values were observed in fatigue state in comparison with alert state. The characteristic path length is the embodiment of the overall connectivity of the brain network, which means that the information transmission efficiency of the cortical brain region is reduced (Watts and Strogatz, 1998). In high-frequency bands, functional connectivity mode was characterized by the decline in the overall functional connectivity strength and the limited connectivity between regions.

There are also some limitations in this study. The MFI-20 scale was used as the basis for defining the fatigue level, but there were deviations in the understanding of different people when filling in the scale. At the same time, the sensitivity of the scale to specific fatigue responses caused by different participants may be different (Di Stasi et al., 2012), which may be partially deviated from the real fatigue state of the participants. In future research, we can use a combination of a variety of subjective fatigue scales (Sun et al., 2017) or fatigue state judgment methods based on physiological signals and behavioral data.

CONCLUSION

This paper investigated the common character of functional connectivity network corresponding to mental fatigue induced by different tasks and classified the fatigue levels based on the common features. With the deepening of mental fatigue, the deviation and reorganization of functional connectivity were observed, and those changes reflected the unique forms of brain network functional connectivity under different fatigue levels.

In moderate fatigue, the overall functional connectivity of the neurogenic frequency band increased significantly, and the connectivity strength of the right hemisphere was greater than that of the left hemisphere. The connectivity strength of the endogenic frequency band and the myogenic frequency band

decreased, and the clustering coefficient decreased significantly; In severe fatigue, the overall functional connectivity strength of neurogenic frequency band increased, and the small worldness decreased. In the high-frequency band, only the PFC and FEF maintained close connectivity, and the characteristic path length increased.

Based on the common characteristics, the random forest classifier was used to distinguish the fatigue level induced by different tasks. The classification accuracy of non-fatigue and fatigue is 85.4%, and the recall of fatigue is 89.3%. The classification accuracy of moderate fatigue and severe fatigue was 82.8%, and the recall of severe fatigue was 90.5%. The common character of functional connectivity and preliminary fatigue discrimination results under each fatigue state prove that the findings of this study have potential application value for mental fatigue monitoring and early warning under complex conditions.

DATA AVAILABILITY STATEMENT

The raw data supporting the conclusions of this article will be made available by the authors, without undue reservation.

ETHICS STATEMENT

The studies involving human participants were reviewed and approved by the Ethics Committee of Soochow University (ECSU) approval No. SUDA20210909H01. The patients/participants provided their written informed consent to participate in this study.

AUTHOR CONTRIBUTIONS

YP: acquisition of data, analysis and interpretation of data, drafting the manuscript. CL: conception and design of study, analysis, and interpretation of data, review and editing. QC, YZ, and LS: review and editing. All authors contributed to the article and approved the submitted version.

FUNDING

This work was supported by the National Natural Science Foundation of China (Nos. 62073228 and U1713218).

REFERENCES

Boksem, M. A. S., Meijman, T. F., and Lorist, M. M. (2006). Mental fatigue, motivation and action monitoring. *Biol. Psychol.* 72, 123–132. doi: 10.1016/j.biopsycho.2005.08.007

Borragán, G., Guerrero-Mosquera, C., Guillaume, C., Slama, H., and Peigneux, P. (2019). Decreased prefrontal connectivity parallels cognitive fatigue-related performance decline after sleep deprivation. An optical imaging study. *Biol. Psychol.* 144, 115–124. doi: 10.1016/j.biopsycho.2019.03.004

Chen, J., Wang, H., Wang, Q., and Hua, C. (2019). Exploring the fatigue affecting electroencephalography based functional brain networks during real driving in young males. *Neuropsychologia* 129, 200–211. doi: 10.1016/j.neuropsychologia.2019.04.004

Chua, B. L., Dai, Z., Thakor, N., Bezerianos, A., and Sun, Y. (2017). "Connectome pattern alterations with increment of mental fatigue in one-hour driving simulation," in *Proceedings of the 2017 39th Annual International Conference of the IEEE Engineering in Medicine and Biology Society (EMBC)*, Jeju, 4355–4358. doi: 10.1109/EMBC.2017.8037820

Cohen, J. R., and D'Esposito, M. (2016). The segregation and integration of distinct brain networks and their relationship to cognition. *J. Neurosci.* 36, 12083–12094. doi: 10.1523/JNEUROSCI.2965-15.2016

Curtis, C. E., and D'Esposito, M. (2003). Persistent activity in the prefrontal cortex during working memory. *Trends Cogn. Sci.* 7, 415–423. doi: 10.1016/S1364-6613(03)00197-9

Di Stasi, L. L., Renner, R., Catena, A., Cañas, J. J., Velichkovsky, B. M., and Pannasch, S. (2012). Towards a driver fatigue test based on the saccadic main sequence: a partial validation by subjective report data. *Transp. Res. C Emerg. Technol.* 21, 122–133. doi: 10.1016/j.trc.2011.07.002

Esposito, F., Otto, T., Zijlstra, F. R. H., and Goebel, R. (2014). Spatially distributed effects of mental exhaustion on resting-state FMRI networks. *PLoS One* 9:e94222. doi: 10.1371/journal.pone.0094222

Helton, W. S., Warm, J. S., Tripp, L. D., Matthews, G., Parasuraman, R., and Hancock, P. A. (2010). Cerebral lateralization of vigilance: a function of task difficulty. *Neuropsychologia* 48, 1683–1688. doi: 10.1016/j.neuropsychologia.2010.02.014

Herff, C., Heger, D., Fortmann, O., Hennrich, J., Putze, F., and Schultz, T. (2014). Mental workload during n-back task-quantified in the prefrontal cortex using fNIRS. *Front. Hum. Neurosci.* 7:935. doi: 10.3389/fnhum.2013.00935

Hopfinger, J. B., Buonocore, M. H., and Mangun, G. R. (2000). The neural mechanisms of top-down attentional control. *Nat. Neurosci.* 3, 284–291. doi: 10.1038/72999

Klingberg, T., Sullivan, B. T. O., Roland, P. E., Prince, R., and Hospital, A. (1997). Bilateral activation of fronto-parietal networks by incrementing demand in a working memory task. *Cereb. Cortex* 7, 465–471. doi: 10.1093/cercor/7.5.465

Körber, M., Cingel, A., Zimmermann, M., and Bengler, K. (2015). Vigilance decrement and passive fatigue caused by monotony in automated driving. *Procedia Manuf.* 3, 2403–2409. doi: 10.1016/j.promfg.2015.07.499

Larue, G. S., Rakotonirainy, A., and Pettitt, A. N. (2011). Driving performance impairments due to hypovigilance on monotonous roads. *Accid. Anal. Prev.* 43, 2037–2046. doi: 10.1016/j.aap.2011.05.023

Li, G., Luo, Y., Zhang, Z., Xu, Y., Jiao, W., Jiang, Y., et al. (2019). Effects of mental fatigue on small-world brain functional network organization. *Neural Plast.* 2019:1716074. doi: 10.1155/2019/1716074

Li, J., Lim, J., Chen, Y., Wong, K., Thakor, N., Bezerianos, A., et al. (2016). Mid-task break improves global integration of functional connectivity in lower alpha band. *Front. Hum. Neurosci.* 10:304. doi: 10.3389/fnhum.2016.00304

Li, Z., Zhang, M., Xin, Q., Chen, G., Liu, F., and Li, J. (2012). Spectral analysis of near-infrared spectroscopy signals measured from prefrontal lobe in subjects at risk for stroke. *Med. Phys.* 39, 2179–2185. doi: 10.1118/1.3696363

Li, Z., Zhang, M., Zhang, X., Dai, S., Yu, X., and Wang, Y. (2009). Assessment of cerebral oxygenation during prolonged simulated driving using near infrared spectroscopy: its implications for fatigue development. *Eur. J. Appl. Physiol.* 107, 281–287. doi: 10.1007/s00421-009-1122-6

Liang, X., Zou, Q., He, Y., and Yang, Y. (2013). Coupling of functional connectivity and regional cerebral blood flow reveals a physiological basis for network hubs of the human brain. *Proc. Natl. Acad. Sci. U.S.A.* 110, 1929–1934. doi: 10.1073/pnas.1214900110

Liu, D., Chen, W., Chavarriaga, R., Pei, Z., and Millán, J. R. (2017). Decoding of self-paced lower-limb movement intention: a case study on the influence factors. *Front. Hum. Neurosci.* 11:560. doi: 10.3389/fnhum.2017.00560

Lu, K., Xu, G., Li, W., Huo, C., Liu, Q., Lv, Z., et al. (2019). Frequency-specific functional connectivity related to the rehabilitation task of stroke patients. *Med. Phys.* 46, 1545–1560. doi: 10.1002/mp.13398

Matthews, G., and Desmond, P. A. (1998). Personality and multiple dimensions of task-induced fatigue: a study of simulated driving. *Pers. Individ. Differ.* 25, 443–458. doi: 10.1016/S0191-8869(98)00045-2

Micheloyannis, S., Pachou, E., Stam, C. J., Breakspear, M., Bitsios, P., Vourkas, M., et al. (2006). Small-world networks and disturbed functional connectivity in schizophrenia. *Schizophr. Res.* 87, 60–66. doi: 10.1016/j.schres.2006.06.028

Neu, D., Kajosch, H., Peigneux, P., Verbanck, P., Linkowski, P., and Le Bon, O. (2011). Cognitive impairment in fatigue and sleepiness associated conditions. *Psychiatry Res.* 189, 128–134. doi: 10.1016/j.psychres.2010.12.005

Nilsson, T., Nelson, T. M., and Carlson, D. (1997). Development of fatigue symptoms during simulated driving. *Accid. Anal. Prev.* 29, 479–488. doi: 10.1016/s0001-4575(97)00027-4

Okamoto, M., Dan, H., Sakamoto, K., Takeo, K., Shimizu, K., Kohno, S., et al. (2004). Three-dimensional probabilistic anatomical cranio-cerebral correlation via the international 10-20 system oriented for transcranial functional brain mapping. *Neuroimage* 21, 99–111. doi: 10.1016/j.neuroimage.2003.08.026

Onnela, J. P., Saramäki, J., Kertész, J., and Kaski, K. (2005). Intensity and coherence of motifs in weighted complex networks. *Phys. Rev. E Stat. Nonlin. Soft Matter Phys.* 71(6 Pt 2):065103. doi: 10.1103/PhysRevE.71.065103

Osol, G. (1995). Mechanotransduction by vascular smooth muscle. *J. Vasc. Res.* 32, 275–292. doi: 10.1159/000159102

Qi, P., Ru, H., Gao, L., Zhang, X., Zhou, T., Tian, Y., et al. (2019). Neural mechanisms of mental fatigue revisited: new insights from the brain connectome. *Engineering* 5, 276–286. doi: 10.1016/j.eng.2018.11.025

Ream, E., and Richardson, A. (1996). Fatigue: a concept analysis. *Int. J. Nurs. Stud.* 33, 519–529. doi: 10.1016/0020-7489(96)00004-1

Rowley, A. B., Payne, S. J., Tachtsidis, I., Ebden, M. J., Whiteley, J. P., Gavaghan, D. J., et al. (2007). Synchronization between arterial blood pressure and cerebral oxyhaemoglobin concentration investigated by wavelet cross-correlation. *Physiol. Meas.* 28, 161–173. doi: 10.1088/0967-3334/28/2/005

Sarter, M., Givens, B., and Bruno, J. P. (2001). The cognitive neuroscience of sustained attention: where top-down meets bottom-up. *Brain Res. Rev.* 35, 146–160. doi: 10.1016/S0165-0173(01)00044-3

Saxby, D. J., Matthews, G., Warm, J. S., Hitchcock, E. M., and Neubauer, C. (2013). Active and passive fatigue in simulated driving: discriminating styles of workload regulation and their safety impacts. *J. Exp. Psychol. Appl.* 19, 287–300. doi: 10.1037/a0034386

Scalf, P. E., Banich, M. T., and Erickson, A. B. (2009). Interhemispheric interaction expands attentional capacity in an auditory selective attention task. *Exp. Brain Res.* 194, 317–322. doi: 10.1007/s00221-009-1739-z

Sharma, H. B., Panigrahi, S., Sarmah, A. K., and Dubey, B. K. (2019). Development and recovery time of mental fatigue and its impact on motor function. *Sci. Total Environ.* 161:135907. doi: 10.1016/j.biopsycho.2021.108076

Shigihara, Y., Tanaka, M., Ishii, A., Kanai, E., Funakura, M., and Watanabe, Y. (2013). Two types of mental fatigue affect spontaneous oscillatory brain activities in different ways. *Behav. Brain Funct.* 9:2. doi: 10.1186/1744-9081-9-2

Shiogai, Y., Stefanovska, A., and McClintock, P. V. E. (2010). Nonlinear dynamics of cardiovascular ageing. *Phys. Rep.* 488, 51–110. doi: 10.1016/j.physrep.2009.12.003

Smets, E. M., Garssen, B., Bonke, B., and De Haes, J. C. (1995). Pergamon fatigue inventory (MFI) psychometric qualities of an instrument to to assess fatigue. *J. Psychosom. Res.* 39, 315–325. doi: 10.1016/0022-3999(94)00125-o

Smit, A. S., Eling, P. A. T. M., and Coenen, A. M. L. (2004). Mental effort causes vigilance decrease due to resource depletion. *Acta Psychol.* 115, 35–42. doi: 10.1016/j.actpsy.2003.11.001

Stam, C. J., Jones, B. F., Nolte, G., Breakspear, M., and Scheltens, P. (2007). Small-world networks and functional connectivity in Alzheimer's disease. *Cereb. Cortex* 17, 92–99. doi: 10.1093/cercor/bhj127

Stefanovska, A., Bracic, M., and Kvernmo, H. D. (1999). Wavelet analysis of oscillations in the peripheral blood circulation measured by laser Doppler technique. *IEEE Trans. Biomed. Eng.* 46, 1230–1239. doi: 10.1109/10.790500

Struck, A. F., Boly, M., Hwang, G., Nair, V., Mathis, J., Nencka, A., et al. (2021). Regional and global resting-state functional MR connectivity in temporal lobe epilepsy: results from the Epilepsy Connectome Project. *Epilepsy Behav.* 117:107841. doi: 10.1016/j.yebeh.2021.107841

Sun, Y., Lim, J., Dai, Z., Wong, K., Taya, F., Chen, Y., et al. (2017). The effects of a mid-task break on the brain connectome in healthy participants: a resting-state functional MRI study. *Neuroimage* 152, 19–30. doi: 10.1016/j.neuroimage.2017.02.084

Sun, Y., Lim, J., Kwok, K., and Bezerianos, A. (2014a). Functional cortical connectivity analysis of mental fatigue unmasks hemispheric asymmetry and changes in small-world networks. *Brain Cogn.* 85, 220–230. doi: 10.1016/j.bandc.2013.12.011

Sun, Y., Lim, J., Meng, J., Kwok, K., Thakor, N., and Bezerianos, A. (2014b). Discriminative analysis of brain functional connectivity patterns for mental fatigue classification. *Ann. Biomed. Eng.* 42, 2084–2094. doi: 10.1007/s10439-014-1059-8

Tanabe, S., and Nishihara, N. (2004). Productivity and fatigue. *Indoor Air* 14(Suppl. 7), 126–133. doi: 10.1111/j.1600-0668.2004.00281.x

Tononi, G., Edelman, G. M., and Sporns, O. (1998). Complexity and coherency: integrating information in the brain. *Trends Cogn. Sci.* 2, 474–484. doi: 10.1016/S1364-6613(98)01259-5

Watts, D. J., and Strogatz, S. H. (1998). Collective dynamics of 'small-world' networks. *Nature* 393, 440–442.

Xu, L., Wang, B., Xu, G., Wang, W., Liu, Z., and Li, Z. (2017). Functional connectivity analysis using fNIRS in healthy subjects during prolonged simulated driving. *Neurosci. Lett.* 640, 21–28. doi: 10.1016/j.neulet.2017.01.018

Zhang, C., Sun, L., Cong, F., Kujala, T., Ristaniemi, T., and Parviainen, T. (2020). Optimal imaging of multi-channel EEG features based on a novel clustering technique for driver fatigue detection. *Biomed. Signal Process. Control* 62:102103. doi: 10.1016/j.bspc.2020.102103

Conflict of Interest: The authors declare that the research was conducted in the absence of any commercial or financial relationships that could be construed as a potential conflict of interest.

Publisher's Note: All claims expressed in this article are solely those of the authors and do not necessarily represent those of their affiliated organizations, or those of the publisher, the editors and the reviewers. Any product that may be evaluated in this article, or claim that may be made by its manufacturer, is not guaranteed or endorsed by the publisher.

frontiers in Neuroscience

ORIGINAL RESEARCH
published: 31 March 2022
doi: 10.3389/fnins.2022.810553

The Frequency Effect of the Motor Imagery Brain Computer Interface Training on Cortical Response in Healthy Subjects: A Randomized Clinical Trial of Functional Near-Infrared Spectroscopy Study

Qiang Lin[1,2,3†], Yanni Zhang[1,2†], Yajie Zhang[2], Wanqi Zhuang[2], Biyi Zhao[2], Xiaomin Ke[2], Tingting Peng[2], Tingting You[2], Yongchun Jiang[2], Anniwaer Yilifate[1,2], Wei Huang[2], Lingying Hou[1], Yaoyao You[1], Yaping Huai[4], Yaxian Qiu[1,2], Yuxin Zheng[1,2]* and Haining Ou[1,2,3]**

[1] Department of Rehabilitation, The Fifth Affiliated Hospital of Guangzhou Medical University, Guangzhou, China, [2] Fifth Clinical School, Guangzhou Medical University, Guangzhou, China, [3] Department of Rehabilitation, Guangzhou Key Laboratory of Enhanced Recovery After Abdominal Surgery, The Fifth Affiliated Hospital of Guangzhou Medical University, Guangzhou, China, [4] Department of Rehabilitation Medicine, Shenzhen Longhua District Central Hospital, Shenzhen, China

OPEN ACCESS

Edited by:
Jinhua Zhang,
Xi'an Jiaotong University, China

Reviewed by:
Zhiyuan Fang,
Guangdong University of Technology, China
Yan Zeng,
Shihezi University, China

***Correspondence:**
Haining Ou
ouhaining@gzhmu.edu.cn
Yuxin Zheng
zhengyx@gzhmu.edu.cn
Yaxian Qiu
2017687049@gzhmu.edu.cn

†These authors share first authorship

Specialty section:
This article was submitted to Neuroprosthetics, a section of the journal Frontiers in Neuroscience

Received: 07 November 2021
Accepted: 07 March 2022
Published: 31 March 2022

Citation:
Lin Q, Zhang Y, Zhang Y, Zhuang W, Zhao B, Ke X, Peng T, You T, Jiang Y, Yilifate A, Huang W, Hou L, You Y, Huai Y, Qiu Y, Zheng Y and Ou H (2022) The Frequency Effect of the Motor Imagery Brain Computer Interface Training on Cortical Response in Healthy Subjects: A Randomized Clinical Trial of Functional Near-Infrared Spectroscopy Study. Front. Neurosci. 16:810553. doi: 10.3389/fnins.2022.810553

Background: The motor imagery brain computer interface (MI-BCI) is now available in a commercial product for clinical rehabilitation. However, MI-BCI is still a relatively new technology for commercial rehabilitation application and there is limited prior work on the frequency effect. The MI-BCI has become a commercial product for clinical neurological rehabilitation, such as rehabilitation for upper limb motor dysfunction after stroke. However, the formulation of clinical rehabilitation programs for MI-BCI is lack of scientific and standardized guidance, especially limited prior work on the frequency effect. Therefore, this study aims at clarifying how frequency effects on MI-BCI training for the plasticity of the central nervous system.

Methods: Sixteen young healthy subjects (aged 22.94 ± 3.86 years) were enrolled in this randomized clinical trial study. Subjects were randomly assigned to a high frequency group (HF group) and low frequency group (LF group). The HF group performed MI-BCI training once per day while the LF group performed once every other day. All subjects performed 10 sessions of MI-BCI training. functional near-infrared spectroscopy (fNIRS) measurement, Wolf Motor Function Test (WMFT) and brain computer interface (BCI) performance were assessed at baseline, mid-assessment (after completion of five BCI training sessions), and post-assessment (after completion of 10 BCI training sessions).

Results: The results from the two-way ANOVA of beta values indicated that GROUP, TIME, and GROUP × TIME interaction of the right primary sensorimotor cortex had significant main effects [GROUP: $F_{(1,14)} = 7.251$, $P = 0.010$; TIME: $F_{(2,13)} = 3.317$, $P = 0.046$; GROUP × TIME: $F_{(2,13)} = 5.676$, $P = 0.007$]. The degree of activation was affected by training frequency, evaluation time point and interaction. The activation of

left primary sensory motor cortex was also affected by group (frequency) (P = 0.003). Moreover, the TIME variable was only significantly different in the HF group, in which the beta value of the mid-assessment was higher than that of both the baseline assessment (P = 0.027) and post-assessment (P = 0.001), respectively. Nevertheless, there was no significant difference in the results of WMFT between HF group and LF group.

Conclusion: The major results showed that more cortical activation and better BCI performance were found in the HF group relative to the LF group. Moreover, the within-group results also showed more cortical activation after five sessions of BCI training and better BCI performance after 10 sessions in the HF group, but no similar effects were found in the LF group. This pilot study provided an essential reference for the formulation of clinical programs for MI-BCI training in improvement for upper limb dysfunction.

Keywords: functional near infrared spectroscopy, cortical response, frequency effect, motor imagery, brain computer interface

INTRODUCTION

In recent years, brain computer interface (BCI) technology has matured into a potentially helpful tool. BCI technology establishes a direct real-time connection between the brain and external devices without relying on peripheral nerves or muscles to achieve human-computer interaction (Mane et al., 2020). There are different types of BCI, one of which is based on motor imagery (MI), called motor imagery-BCI (MI-BCI). This form of BCI is now available in a commercial product for the clinical rehabilitation of upper limb motor dysfunction after stroke, and has achieved positive results (Chaudhary et al., 2016).

Motor imagery brain computer interface converts the generated motor intention of the subject's motor imagery into motor instructions. It thus commands external devices such as robots to perform actual movement. It can also generate corresponding tactile, visual, and proprioceptive feedback, thus forming a central-peripheral-central active closed-loop control system (Potter et al., 2014). The MI-BCI system achieves repeated recruitment of motor neurons circuit during training to promote neural plasticity, thus repairing connections between damaged neurons and ultimately improving motor dysfunction. Floriana Pichiorri and Mattia (2020) found that compared with simple MI training, the Fugl-Meyer assessment scores of hemiplegic upper limbs in hospitalized patients with subacute stroke recovery and severe motor dysfunction using MI-BCI were significantly increased. Similar results can be seen in chronic stroke patients with severe hand weakness (Ramos-Murguialday et al., 2013).

Previous studies have also shown that active and repetitive reinforcement of functional activity is important for nerve remodeling and motor function recovery (Mane et al., 2020). Therefore, clarifying how the duration, frequency, and intensity of MI-BCI training affects the plasticity of the central nervous system and clinical function is crucial for developing MI-BCI rehabilitation programs. However, there is limited prior work on the frequency effect. Other neuromodulation studies have shown a correlation between neural plasticity and training frequency. Bai et al. (2020) found that repetitive transcranial magnetic stimulation (rTMS) training twice a day was more effective than once a day in promoting neuroplasticity in the language area of the brain, repairing or enhancing the connection between related neurons, and improving the language function of patients with aphasia after stroke. Accordingly, we assumed that there may also be a frequency effect in MI-BCI.

Current studies of the neural plasticity changes related to BCI mostly use the following neuroimaging methods: functional magnetic resonance imaging (fMRI) (Zhang et al., 2021), electroencephalography (EEG) (Abiri et al., 2019), and functional near-infrared spectroscopy (fNIRS) (Yang et al., 2019). Of these, fNIRS is reflects the neural activity of the brain indirectly via real-time monitoring of the concentration changes in hemoglobin and deoxyhemoglobin in the cerebral cortex under different stimulation tasks. Versus fMRI, fNIRS can be used in real environments for real-time monitoring. It is simple to use and has high temporal resolution. fNIRS has higher spatial resolution and is less affected by the head movement of subjects (Yang et al., 2019). Therefore, fNIRS has high application potential in the field of neuromodulation rehabilitation. Ding et al. (2021) found that BCI training improved brain functional connectivity between motor cortex and prefrontal cortex via fNIRS. Kaiser et al. (2014) also determined that MI-BCI training increased the cortical activation of the supplementary motor cortex (SMA) and the primary motor cortex. It also enhanced event-related desynchronization (ERD) through fNIRS testing.

However, MI-BCI is still a relatively new technology for commercial rehabilitation applications. It is crucial to understand the MI-BCI frequency effect for clinical standardized treatment. The heterogeneity of stroke patients is high and includes age and cognitive function: These both affect the therapeutic effect of MI-BCI. At the same time, because of the less use and less flexibility of the non-handedness (compared with the handedness), it was used to simulate the hemiplegic upper limbs of stroke patients and handedness stimulates the unaffected side. In this study, we evaluated the effect of MI-BCI frequency on the cortical function of non-handedness, and these numerical controls could help guide clinical application and future MI-BCI research. Therefore, to minimize the impact of the subject heterogeneity on the results, our study recruited young healthy subjects with right-handedness

to reduce the effects of brain injury in different regions and degrees as well as the effects of age, cognitive function, motor function, and lateralization of the brain. We also used non-handedness to simulate the improvement of upper limb function on the hemiplegic side to evaluate the regulation effect of MI-BCI frequency on cortical function of non-handedness. This data can help guide clinical applications and future MI-BCI research.

MATERIALS AND METHODS

Participants

This study recruited 22 young healthy subjects (age, 22.36 ± 3.53; males were 31.82%) from Guangzhou Medical University who met the following criteria: (a) right handedness as assessed by the Edinburgh Handedness Inventory; (b) no history of neurological diseases; (c) no history of brain and upper limb trauma, and (d) no cognitive impairment. Participants were excluded if they had one of the following exclusion criteria: (a) medications that reduce seizure thresholds or psychotropic medications; (b) any personal factors affected the EEG signal of the BCI leading to instability or making it impossible to collect fNIRS data; or (c) unable to finish the whole experimental. This study was approved by the Ethics Committee of the Fifth Affiliated Hospital of Guangzhou Medical University (No. KY01-2021-05-01) and had international clinical trial registration (ChiCTR2100050162).[1] All participants signed informed consent forms.

Study Design

In this randomized clinical trial (RCT) study, 22 subjects were randomly assigned to a high frequency group (HF group) and low frequency group (LF group) in a 1:1 ratio using computer-generated random numbers. The HF group performed BCI training once per day while the LF group performed once every other day. All subjects proceeded over 10 sessions in BCI training (30 min for one session) and assessed the clinical assessment and fNIRS testing at three time points: baseline, mid-assessment (after completion of five BCI training sessions), and post-assessment (after completion of 10 BCI training sessions) (**Figure 1**).

Intervention

Non-dominant hand function training was performed by the MI-BCI system (BCI-Hand with 24 EEG channels, Rehab Medical Technology Co., Ltd., Shenzhen, China), which consists of an EEG cap, a computer terminal (i.e., the control interface), an external manipulator, and a 23-inch computer monitor (**Figure 2A**). Subjects performed motor imagery by watching video cues about hand function (**Figure 2B**). The EEG cap was based on the International 10–20 System as a reference (**Figure 2C**), with 24-electrode conduction channels (including 22 recording electrodes and 2 reference electrodes) setting over the frontal and parietal regions. The EEG data were collected using the EEG amplifier with unipolar Ag/Ag-cl electrode channels, digitally sampled at 256 Hz with a 22-bit resolution for voltage ranges of ±130 mV. The real-time EEG signals collected were amplified by computer terminal according to the central processing control algorithm, and the mu ERD score (score from 0 to 100) during motor imagery was calculated. The external robotic arm would be driven when the score reaches 60 points. The non-dominant hand could perform the action while providing real-time feedback (both sensory and visual) (**Figure 2D**).

Preparation

Subjects were instructed on the experimental process and arranged in a comfortable sitting position. They were asked to minimize physical activity during BCI training. The researchers put EEG caps onto the subjects, instructed them to remain relaxed, and adjusted Electrodes to maintain waveform of the EEG signal smooth. The sampling frequency of the EEG system is 10–100 Hz. Finally, investigators placed manipulators on the subjects' non-dominant hand and adjusted them to be comfortable and ensure that they did not slip out during training.

Motor Imagery Brain Computer Interface Training

Motor imagery brain computer interface training included baseline acquisition phase and training phase. During the baseline acquisition phase, subjects were instructed to remain relaxed and collect a stable baseline EEG signal for 1 min. During the training phase, subjects performed 30 min of motor imagery tasks followed by pre-set video prompts on the computer screen. Each run was composed of one motor imagery task and one relaxation task. There were then 10 runs in one trial, and 6 to 8 trials were required for one session. The number of trials was mainly affected by the completion of the motor imagery task, and the difficulty of completing the task required more time.

Motor imagery tasks had various levels of difficulty. Different levels of difficulty had various requirements for motor imagery. The initial difficulty was set as 13 referring to the level of healthy subject. Upon completion of the last task, the system adjusted the difficulty level of the next task. The initial difficulty was set to 13. Each run has three chances to complete the MI task at this level per trial. If subjects failed to complete the MI task for three times, then the trial was considered a failure, and the difficulty level was automatically decreased in the next trial. If subjects completed all 10 runs in one trial, then the difficulty level was automatically upgraded in the next trial. The motor imagery tasks involved in the trial were all hand grasping motions, which could be divided into two categories: grasping and opening hand. Grasping action including but not limited to book, toothbrush, cups, chess, rubber, keys, etc. With the upgrading of difficulty, grasping objects tend to be small and exquisite.

Clinical Functional Assessment

The Wolf Motor Function Test (WMFT) was used to assess bilateral upper limb motor function with 17 items in total (Morris et al., 2001). Items 1–8 were used to assess isolated movement of the shoulder and elbow, and items 9–17 were used to assess the overall upper limb movement (shoulder, elbow and hand). Items 7 and 14 were strength measurements and only recorded

[1] https://www.chictr.org.cn

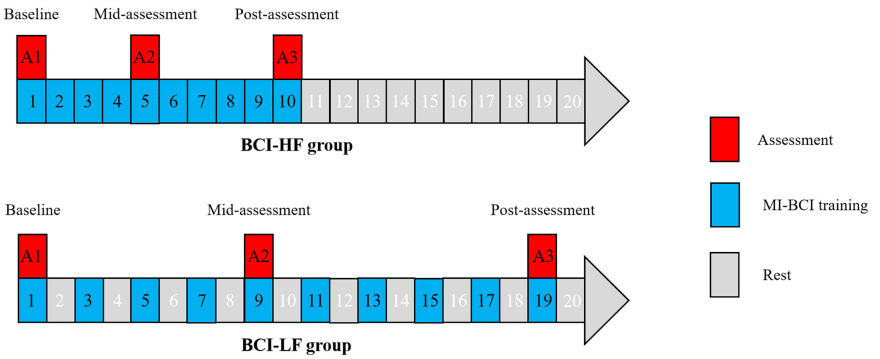

FIGURE 1 | Motor imagery brain computer interface (MI-BCI) training and assessment design in the High Frequency and Low Frequency groups.

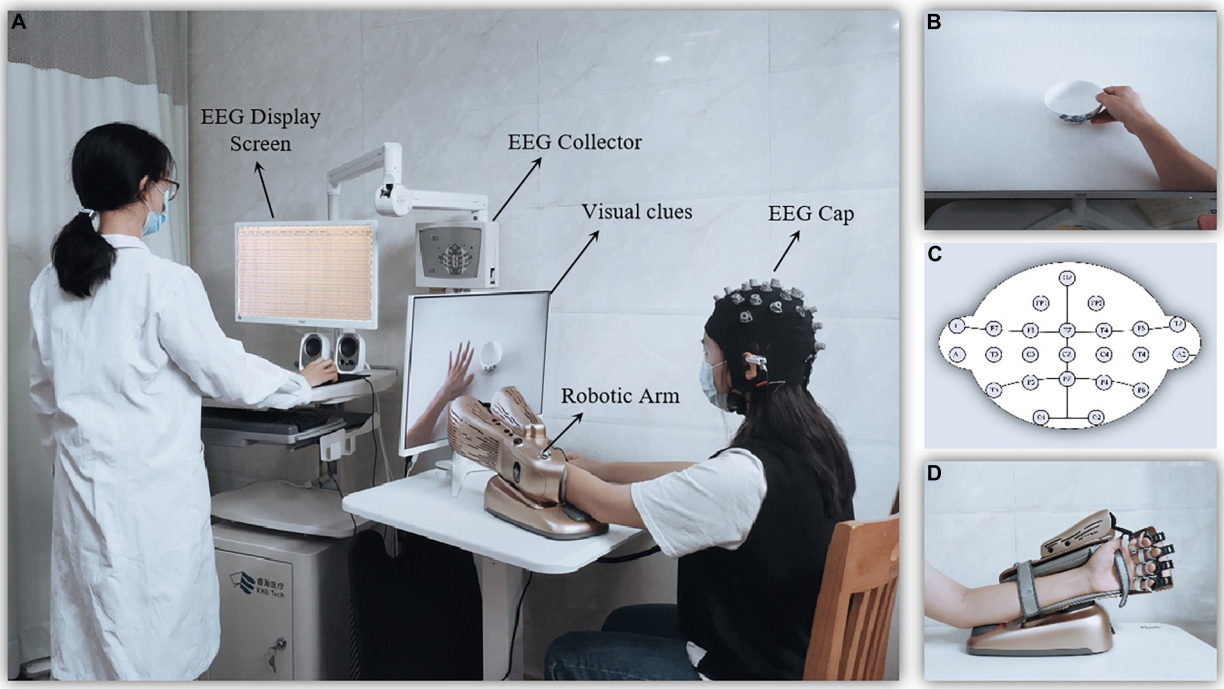

FIGURE 2 | Diagram of the motor imagery brain computer interface (MI-BCI) upper limb rehabilitation training system. **(A)** The MI-BCI training setting. **(B)** The screen providing visual clues for motor imagery. **(C)** The robotic arm for motion performing and feedback. **(D)** Electroencephalography (EEG) electrode placement.

the corresponding value but not the movement quality. The remaining items were scored in terms of movement quality using a 6-point scale (0 = does no attempt; 5 = normal movement) for a total of 75 scores. The ratio of grip strength was calculated based on Item 14 as the strength of non-dominant/left hand divided by the strength of dominant/right hand.

Brain Computer Interface Performance

The BCI performance was calculated via the MI task difficulty level and score using the specific formula: [Trial 1 (difficulty level × average score) + Trial 2 (difficulty level × average score) + … + Trial *n* (difficulty level × average score)]/the number of difficulty levels. Here, "*n*" is the number of trials completed for each session.

Functional Near-Infrared Spectroscopy Measurement and Data Processing

A 24-channel fNIRS device (Nirsmart, Danyang Huichuang Medical Equipment Co., Ltd., Jiangsu, China) was used with setting source probes and detectors according to a 10–20 system. Two source probes and two detectors were placed on the left and right frontal lobes, respectively. Four source probes and three detectors were placed on the left and right parietal lobes, respectively. The channel

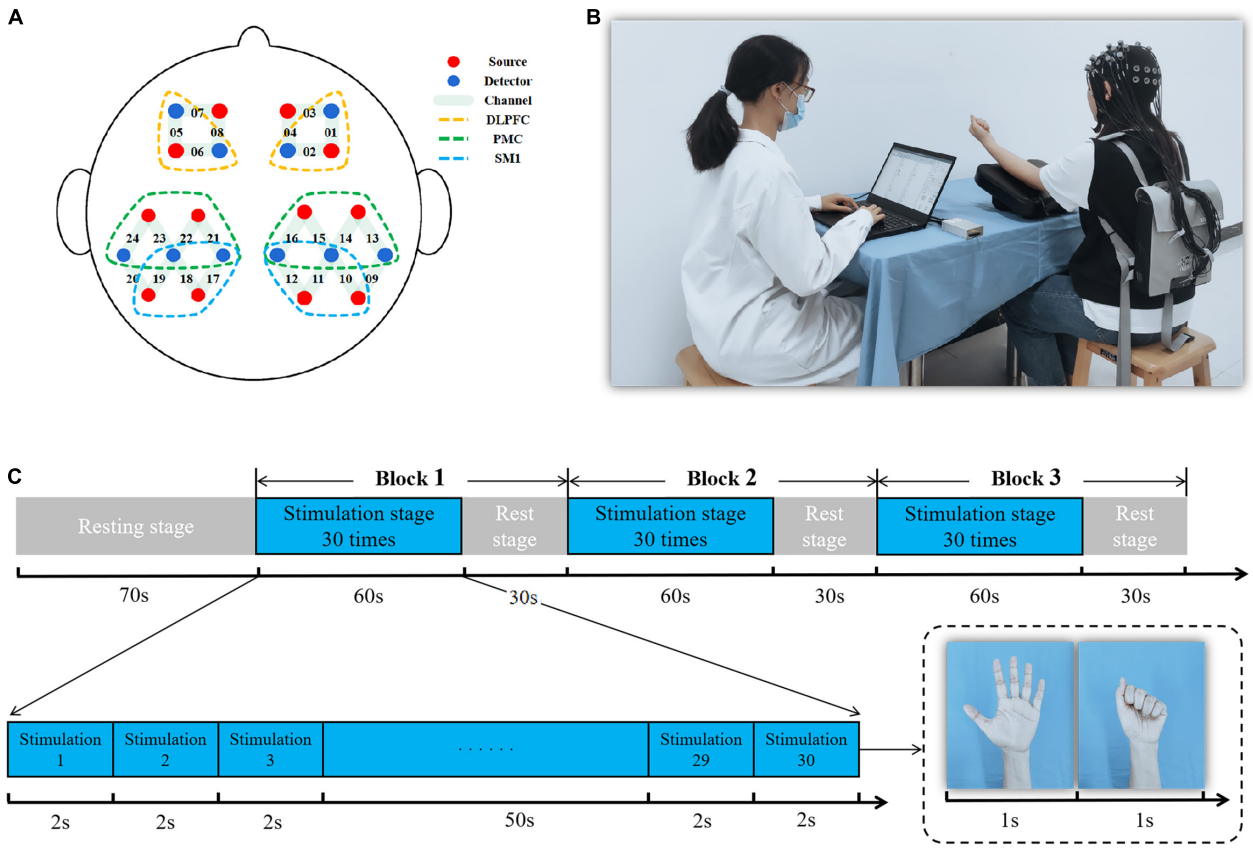

FIGURE 3 | Diagram of the functional near-infrared spectroscopy (fNIRS) measurement. **(A)** Regions of interest and the channel setting; **(B)** fNIRS measurement presentation; **(C)** fNIRS experimental paradigm.

setting is shown in **Figure 3A**. We recorded data with wavelengths of 730 and 850 nm. The fNIRS device converts the optical signals into the concentration changes of oxygenated hemoglobin (HbO_2) and deoxygenated hemoglobin (HbR) according to the modified Beer-Lambert Law to investigate the effects of different stimulus conditions on cortical activation (Pinti et al., 2020).

The motor task paradigm of fNIRS was a non-dominant grasping task at a frequency of 0.5 Hz that included a 70-s rest stage and a 270-s stimulation stage for 340 s of fNIRS testing. Of these, the stimulation stage consisted of three trials (60-s stimulation and 30-s rest for one trial) (**Figures 3B,C**).

There were six regions of interest: bilateral primary sensorimotor cortex (SM1), bilateral promotor cortex (PMC), and bilateral dorsolateral prefrontal cortex (DLPFC). Bilateral SM1 were covered by channels 10, 11, 12, 17, 18, and 19. These mainly included primary somatosensory cortex (S1) and primary motor cortex (M1) and achieved motor learning through sensory and motor input (Gomez et al., 2021). Bilateral PMC were covered by channels 13, 14, 15, 16, 21, 22, 23, and 24 and involved motor planning (Li et al., 2015). Bilateral DLPFC were covered by channels 1, 2, 5, and 6 and were mainly responsible for cognitive, emotional, and sensory processing (Seminowicz and Moayedi, 2017; **Figure 3A**). The average value of the channels that overlapped more than 50% in the regions-of-interest were used as an outcome value of the cortex (Wan et al., 2018).

The original data collected by fNIRS were pre-processed by NIRSPARK software including artifact processing, filtering, segmentation, and baseline comparison. We converted optical density into blood oxygen concentration data—these data were block averaged and statistically analyzed to calculate the beta values for the region-of-interest. Thus, the differences of the cortical activation from GROUP (HF group and LF group) and TIME (baseline, mid-assessment, and post-assessment) could be compared. The general linear model (GLM) for was used to estimate of the hemodynamic response at individual-level fNIRS data statistical analysis individual-level statistical analysis. For GLM specification, the canonical hemodynamic response function was used to construct the reference time series representation from task variables. The estimation of GLM parameters on a channel-by-channel basis, which calculated the activation beta value (weight coefficient in the linear model) for each experimental condition (Hou et al., 2021).

Statistical Analysis

Statistical analysis used SPSS25.0 software. Measurement data confirmed a normal distribution via mean ± standard deviation; count data were represented by rate or constituent ration.

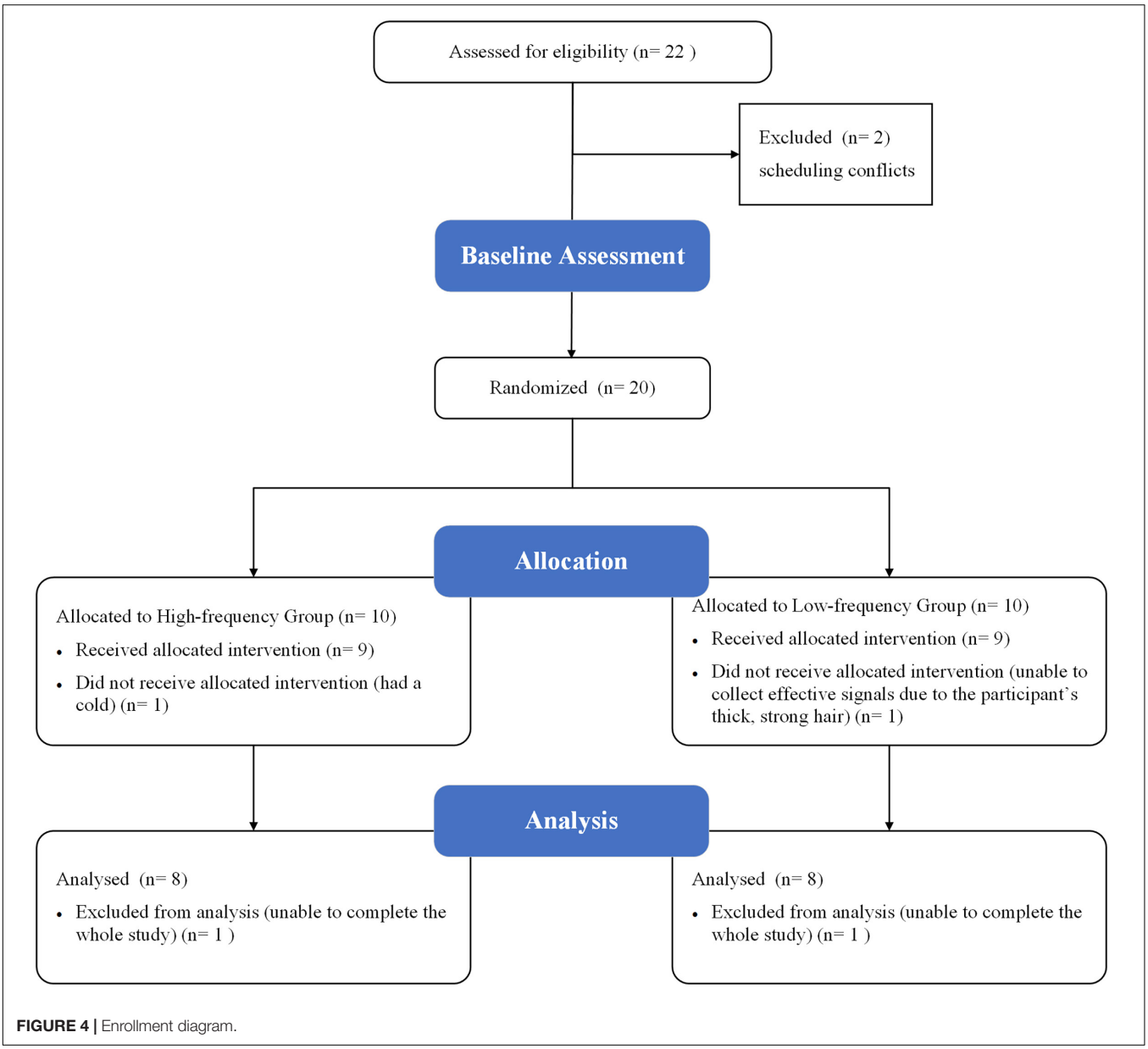

FIGURE 4 | Enrollment diagram.

Two independent sample *t*-tests were used to compare the baseline measurement data between the two groups including homogeneity of variance and normal distribution. The parameters (beta values, BCI performance, and WMFT scores) of GROUP effect (HF and LF), TIME effect (baseline, mid-assessment and post-assessment) and GROUP × TIME interaction effects were analyzed by two-way analysis of variance. *Post-hoc* tests used multiple comparison Bonferroni corrections. Statistical significance was defined as $P < 0.05$.

RESULTS

This study originally enrolled 22 participants; however, only 16 completed all MI-BCI training and assessments. Of the six participants who dropped out of the study, two were attributed to scheduling conflicts for the baseline assessment; one was unable to collect effective signals from fNIRS due to the participant's thick, strong hair; one was due to having a cold during MI-BCI training; and the remaining two were unable to complete the whole study. No participant reported any adverse events or results during the MI-BCI training and assessments (**Figure 4**). Ultimately, 16 subjects (aged 22.94 ± 3.86 years; 31.25% males) were equally randomly assigned to either the HF or LF group. At baseline, no significant differences were found in age, sex ratio, WMFT scores, BCI performance, and beta values of ROIs between the two groups (all $P > 0.05$).

The results from the two-way ANOVA of WMFT scores and the grip strength ratio showed no significant main effect in GROUP, TIME, and GROUP × TIME interaction. The results

from the two-way ANOVA of MI-BCI performance revealed a significant main effect [$F_{(1,16)} = 8.210$, $P = 0.006$] in frequencies. However, no significant main effect was found for TIME, and GROUP × TIME interaction (**Table 1**).

The results from the two-way ANOVA of beta values in ROIs indicated that GROUP, TIME, and GROUP × TIME interaction of the right SM1 had significant main effects [GROUP: $F_{(1,14)} = 7.251$, $P = 0.010$; TIME: $F_{(2,13)} = 3.317$, $P = 0.046$; GROUP × TIME: $F_{(2,13)} = 5.676$, $P = 0.007$] (**Table 2** and **Figures 5**, **6**). The *post-test* results showed a significant difference between the groups at mid-assessment ($P < 0.001$) (**Table 3**). Moreover, the TIME variable was only significantly different in the HF group, in which the beta value of the mid-assessment was higher than that of both the baseline assessment ($P = 0.027$) and post-assessment ($P = 0.001$), respectively (**Table 4**). The beta value trend of the baseline assessment was higher than that of the post-assessment; however, this result was not statistically significant. The two-way ANOVA of the left SM1 results showed that only GROUP variable had a significant main effect [$F_{(1,14)} = 9.849$, $P = 0.003$] and that no significant main effect was found for TIME and GROUP × TIME interaction (**Table 1**). The *post-test* revealed that significant differences were only found between groups in the mid-assessment ($P = 0.040$) (**Table 3**). The two-way ANOVA of bilateral PMC and DLPFC results revealed no significant main effect of GROUP, TIME, and GROUP × TIME interaction (**Table 1**).

DISCUSSION

In recent years, the MI-BCI system based on the closed-loop control theory has become a research hotspot due to its great potential application prospect in rehabilitation filed for upper limb dysfunction caused by the central nervous system (Ang and Guan, 2015). However, no relevant guideline is available on the clinical parameter setting of this novel technology (Mane et al., 2020), which restricts BCI clinical application. Our study used fNIRS to explore the frequency effect of MI-BCI training for non-dominant hand functions and cortical activation in normal subjects. To our knowledge, this study is the first RCT on the frequency-response of the MI-BCI upper limb rehabilitation system. In this study, all subjects in the HF and LF groups received ten sessions of non-dominant hand MI-BCI training. The clinical evaluation results of WMFT were not affected by the training frequency. The possible reason was that in order to exclude the heterogeneity of the subjects, the

TABLE 1 | Results of analysis of variance (ANOVA) conducted on GROUP, TIME, and interaction effect on wolf motor function test (WMFT) and brain computer interface (BCI) performance.

Assessment indicators	Main effect (GROUP)		Main effect (TIME)		Interaction effect (GROUP*TIME)	
	F	*P*-values	F	*P*-values	F	*P*-values
WMFT scores						
Dominant/right hand	2.000	0.165	0.500	0.610	0.500	0.610
Non-dominant/left hand	2.032	0.161	1.581	0.218	0.677	0.513
The ratio of grip strength (%)	2.704	0.108	0.689	0.508	0.390	0.680
BCI performance (scores)	8.210	**0.006**	0.549	0.582	0.069	0.934

GROUP factor refers to the combination of the high frequency and low frequency groups. TIME factor refers to baseline, mid-assessment, or post-assessment. The ratio of grip strength was calculated as the strength of the non-dominant/left hand divided by the strength of the dominant/right hand. The calculation formula of BCI performance is described in the methodology section. P-values less than 0.05 indicate statistically significant differences and are marked in bold.
WMFT, Wolf motor function test; BCI, brain computer interface.

TABLE 2 | Results of analysis of variance (ANOVA) conducted on GROUP, TIME, and interaction effect for beta values of regions of interest.

Regions of interest	Main effect (GROUP)		Main effect (TIME)		Interaction effect (GROUP*TIME)	
	F	*P*-values	*F*	*P*-values	*F*	*P*-values
SM1						
Right	7.251	**0.010**	3.317	**0.046**	5.676	**0.007**
Left	9.849	**0.003**	0.123	0.884	0.077	0.926
PMC						
Right	2.704	0.108	0.689	0.508	0.390	0.680
Left	0.000	0.994	1.096	0.344	1.597	0.215
DLPFC						
Right	1.810	0.186	0.154	0.857	0.680	0.512
Left	0.422	0.519	0.363	0.698	0.552	0.580

GROUP factor refers to the combination of the high frequency and low frequency groups. TIME factor refers to baseline, mid-assessment, or post-assessment. P-values less than 0.05 indicate statistically significant differences and are marked in bold.
SM1, primary sensorimotor cortex; PMC, primary motor cortex; DLPFC, dorsolateral prefrontal cortex.

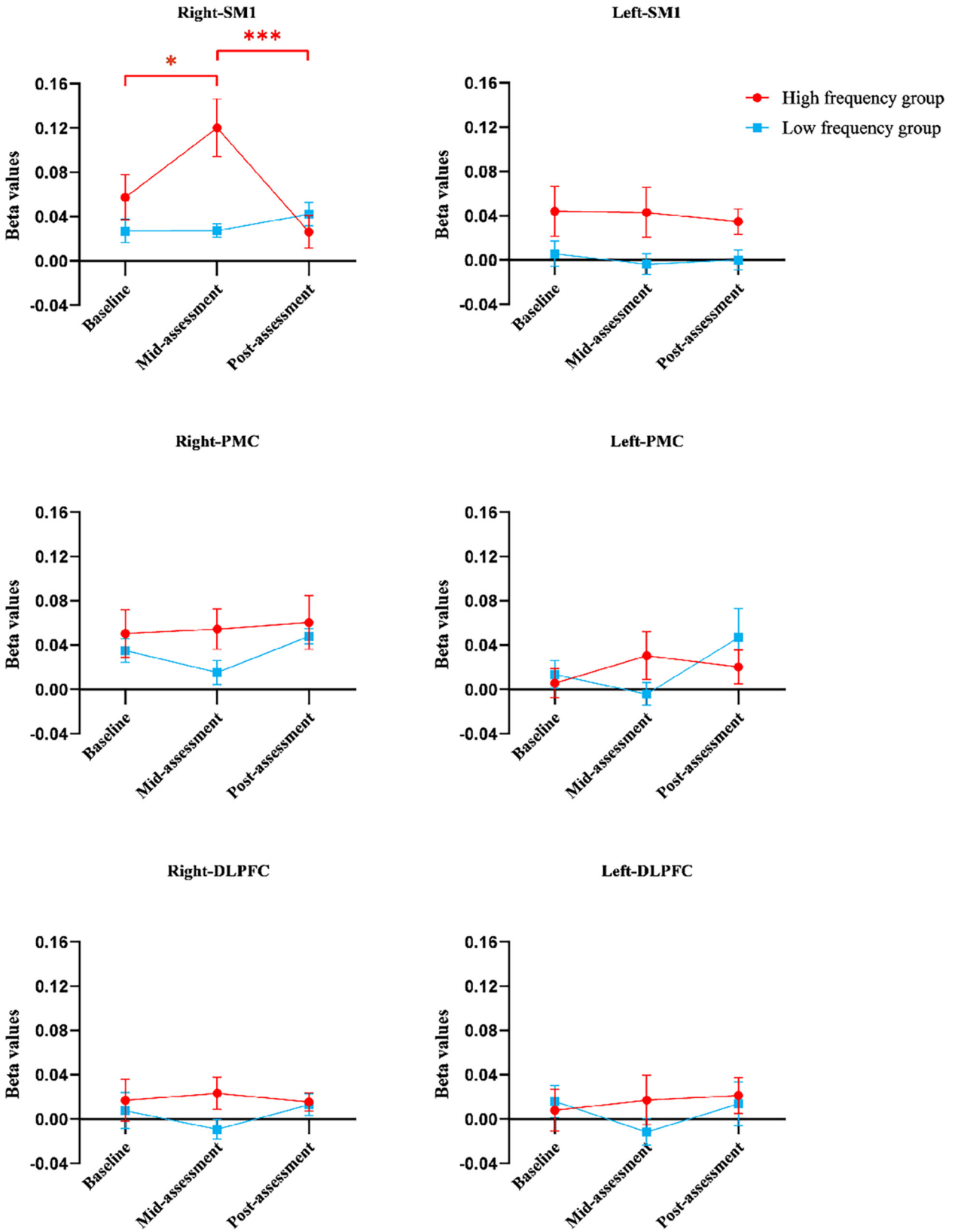

FIGURE 5 | The beta values of regions of interests in different groups at three assessment time-points. Error bars represent standard errors. *Indicates statistical significance $P < 0.05$ and ***indicates statistical significance $P < 0.001$. DLPFC, dorsolateral prefrontal cortex; PMC, promoter cortex; SM1, primary sensory-motor cortex.

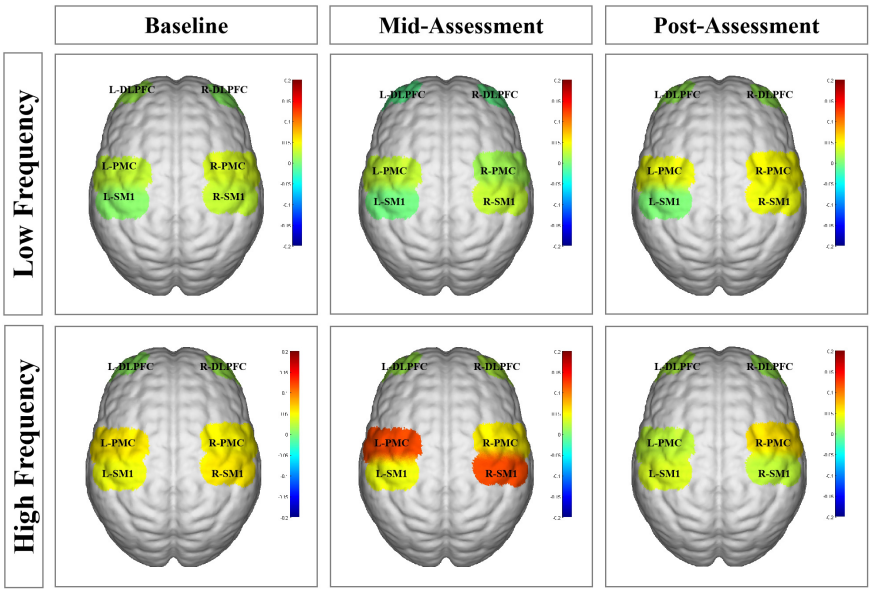

FIGURE 6 | Functional near-infrared spectroscopy (fNIRS) activation maps in different groups at three assessment time-points. The beta values are indicated by color. L-DLPFC, left dorsolateral prefrontal cortex; R-DLPFC, right dorsolateral prefrontal cortex; L-PMC, left promoter cortex; R-PMC, right promoter cortex; L-SM1, left primary sensory-motor cortex; R-SM1, right primary sensory-motor cortex; L, left; R, right.

TABLE 3 | The beta values of SM1 in the Bonferroni correction for multiple comparisons between high frequency group and low frequency group.

TIME	Right SM1			Left SM1		
	Mean difference	Standard error	*P*-values	Mean difference	Standard error	*P*-values
Baseline	0.030	0.023	0.195	0.038	0.022	0.089
Mid-assessment	0.093	0.023	**<0.001**	0.047	0.022	**0.040**
Post-assessment	−0.016	0.023	0.488	0.035	0.022	0.122

TIME factor refers to baseline, mid-assessment, or post-assessment. P-values less than 0.05 indicate statistically significant differences and are marked in bold.
SM1, primary sensorimotor cortex.

TABLE 4 | The beta values of SM1 in the Bonferroni correction for multiple comparisons within high frequency group and low frequency group, respectively.

GROUP	Right SM1			Left SM1		
	Mean difference	Standard error	*P*-values	Mean difference	Standard error	*P*-values
High frequency group						
Baseline vs. Mid-assessment	-0.063	0.023	**0.027**	0.001	0.022	1.000
Baseline vs. Post-assessment	0.031	0.023	0.547	0.009	0.022	1.000
Mid-assessment vs. Post-assessment	0.094	0.023	**0.001**	0.008	0.022	1.000
Low frequency group						
Baseline vs. Mid-assessment	0.000	0.023	1.000	0.010	0.023	1.000
Baseline vs. Post-assessment	-0.015	0.023	1.000	0.006	0.023	1.000
Mid-assessment vs. Post-assessment	-0.015	0.023	1.000	-0.004	0.023	1.000

GROUP factor refers to the combination of the high frequency and low frequency groups. P-values less than 0.05 indicate statistically significant differences and are marked in bold.
SM1, primary sensorimotor cortex.

selected subjects were all healthy young individuals, and the upper limbs were not affected, and there was not much room for improvement. Therefore, the clinical evaluation of Wolf failed to reflect the subtle changes in the upper limb function of the subjects. Although no statistically significant differences were found between these two groups in WMFT performance, the fNIRS evaluation results showed that frequency (GROUP effect) presented a main effect on the contralateral SM1 activation.

Furthermore, compared with baseline values, contralateral SM1 activation increased in the HF group after five consecutive sessions of BCI training. Meanwhile, BCI performance in the HF group was better than that in LF group after 10 consecutive sessions of BCI training. Several possible explanations and mechanisms are presented below.

First, brain neuroplasticity, including the reorganization of brain structure and function, occurs throughout the human lifespan (Dimyan and Cohen, 2011). Meanwhile, a previous study has confirmed the positive correlation between functional improvement after stroke and enhanced neuroplasticity following rehabilitative interventions (Draaisma et al., 2020). The BCI system based on the closed-loop principle is used to compensate for the absent feedback information due to peripheral limb motor dysfunction by external devices (Potter et al., 2014), such as robotic arms, visual feedback system, or functional electrical stimulation (FES). Therefore, BCI training has aroused new interest for rehabilitative purposes—especially for patients with moderate-to-severe motor dysfunction who are limited to other conventional treatment measures (Young et al., 2014). Moreover, previous small sample BCI studies have also shown positive effect for stroke patients not only in the subacute stage, but also in the chronic stage (Cervera et al., 2018). However, given that the clinical application of BCI remains relatively new, the effect of frequency as one of the important parameters has not yet been studied. Among relevant publications to date, the frequency of BCI training was inconsistent. For example, some studies scheduled BCI training at a frequency of twice per week (Johnson et al., 2018), while others had a seven time-per-week schedule (Nishimoto et al., 2018). Considering the critical recovery and neural plasticity stage spanning the first 6 months post-stroke (Hendricks et al., 2002), great significance must be placed on clarifying the frequency parameter setting of BCI training to maximize rehabilitation and the ultimate functional outcomes. In order to eliminate the heterogeneity in patient subjects and explore in isolation the frequency effect of BCI training on neuroplasticity, young and healthy subjects were enrolled to perform non-dominant hand MI-BCI training in our study. The cortical response was found to be more visible after 5 sessions of BCI training in the HF group, but not in the LF group. On the other hand, other clinical BCI training studies on stroke patients found functional improvement after BCI training at a frequency of five times per week (Ramos-Murguialday et al., 2013; Mukaino et al., 2014). Based on the perspectives of cortical modulation and functional improvement, all of the results indicated the potential of HF BCI training to yield positive effects, which may constitute important references for future treatment in patient populations. Nevertheless, Young et al. mainly explored the dose-response on BCI training and incidentally involved in the frequency effect. The relevant results of this clinical retrospective study with a small sample size suggested no significant difference in frequency effect, which was inconsistent with the results of our study (Young et al., 2015). Two major reasons were considered, one of which may be related to the differing populations studied (stroke patients recruited in the study by Young et al.; normal subjects recruited in our study). The other reason may be related to the differing total number and frequency of BCI training sessions for each subject in Young's study. Furthermore, in the study by Young et al., LF treatment was defined as $\leq$2 times per week, whereas HF treatment was defined as $>$2 times per week, in which the range of HF group was considerably broad (Young et al., 2015). For example, the three times per week schedule identified as HF in the study by Young et al. was still considered as the LF BCI intervention in our study. Therefore, additional studies on frequency response in patients are needed. Furthermore, the MI-BCI training procedure requires relatively high cognitive ability (Carelli et al., 2017). For example, sufficient cognitive ability is needed to understand the content of BCI training and to cooperate with the demands of the MI task. Furthermore, attention must be sustained over the 30-min training session. All participants recruited for our study were college students enrolled in Guangzhou Medical University. The heterogeneity of such samples, including cognitive and attention levels, has been well-controlled. However, in real clinical settings, the patient's cognition and attentional capacity are not only affected by various diseases, but also by other confounding factors such as age and education level. Thus, future research is needed to better delineate the frequency effects of BCI training in different populations. In addition, after ten sessions of MI-BCI training, the BCI performance of the HF group in our study was improved relative to the LF group. The BCI performance score was considered more related to the MI performance and attentional level during the training sessions. Previous studies have reported that BCI training could improve motor function and cognitive function concurrently (Ali et al., 2020). Furthermore, BCI has also been designed for use in children with attention deficit hyperactivity disorder (ADHD) (Qian et al., 2018). We also found improvement in BCI performance in the HF group relative to the LF group, which suggested that HF training may be more beneficial to cognitive improvement than LF training. These findings could also be used to guide the formulation of future clinical BCI training programs.

Finally, compared within HF group, more contralateral cortical activation was found after five training sessions than in baseline data, whereas no difference was found after ten training sessions. Moreover, as shown in **Figure 5A**, the beta value of right/contralateral SM1 was the highest after five-session training and then decreased back to baseline levels after ten training sessions in HF group. A possible explanation might be that non-dominant gripping is considered as relatively simple to master for healthy, young subjects. So, the increased contralateral SM1 activation from baseline to after five training sessions might involve in a process of neural recruitment during motor learning, whereas the decreased contralateral SM1 activation seen between the 5- to the 10-session training might involve in motor acquisition, which indicated that the brain operated in the most economical tendency (Paparella et al., 2020). However, although this decrease was seen in the HF group, it was not seen in the LF group, which also suggested that HF MI-BCI training may have a greater potential on motor relearning than LF MI-BCI training. Thus, MI-BCI training tasks whose difficulty level can be tailored should be considered for clinical application, and corresponding MI-BCI modules should be generated for improved clinical rehabilitation.

Limitation

This study was a pilot study of frequency-response for the MI-BCI training system. There were two main limitations to this study. First, only healthy young subjects were included in an effort to control for heterogeneity. Future studies should extend research populations to include, for example, healthy elderly subjects or stroke patients with varying degrees of brain damage and functional levels to further explore frequency-response and provide more evidence for guiding clinical application. Second, this study only explored a single type of external MI-BCI equipment (i.e., a robotic arm) for providing feedback in the MI-BCI system. Future research efforts are encouraged to assess different external equipment, such as virtual reality and FES, and explore different frequency effects based on comprehensive factors.

CONCLUSION

In this study, healthy young participants underwent ten sessions at varying frequencies of MI-BCI training on non-dominant hand function. The results showed that more cortical activation and better BCI performance were found in the HF group relative to the LF group. Moreover, the within-group results also showed more cortical activation after five sessions of BCI training and better BCI performance after ten sessions in the HF group, but no similar effects were found in the LF group. These results indicated that a 30-min session duration once per day for five consecutive days may be the minimum effective dose of MI-BCI training for evoking cortical activation modulation in healthy subjects, which could be deduced to the population with central nervous system disease, such as stroke patients, in the future. This pilot RCT study provides an important theoretical basis for the clinical application of MI-BCI training for improving upper limb dysfunction.

DATA AVAILABILITY STATEMENT

The raw data supporting the conclusions of this article will be made available by the authors, without undue reservation.

ETHICS STATEMENT

The studies involving human participants were reviewed and approved by the Ethics Committee of the Fifth Affiliated Hospital of Guangzhou Medical University. The patients/participants provided their written informed consent to participate in this study.

AUTHOR CONTRIBUTIONS

HO, YxZ, YQ, and QL designed the study. QL, YnZ, and YJZ drafted the manuscript. WZ, BZ, and XK performed data analysis. TP, TY, and YJ wrote sections of the manuscript. AY drew the figures. WH, LH, YY, and YH collected the data. HO, YxZ, and YQ approved the final version of the manuscript. All authors contributed to manuscript revision, read, and approved the submitted version.

FUNDING

This study was supported by the National Science Foundation of China (No. 81902281), Natural Science Foundation of Guangdong Province (No. 2021A1515012197), Guangdong Province Department of Education (No. 2021ZDZX2063), the General Guidance Program of Guangzhou Municipal Health and Family Planning (Nos. 20191A011091, 20221A011109, 20221A011106, 20221A011104, and 20211A010079), Guangzhou Key Medical Disciplines (2021–2023), and Basic Research Project of Shenzhen Science, Technology and Innovation Commission (No. JCYJ20210324123414039).

ACKNOWLEDGMENTS

We would like to thank Jiahui Zhang, Yawen Liu, Wenxi Luo, Rongwei Du, Xinru Zhang, Aijia Chen, Zechun Chen (the undergraduates of Guangzhou Medical University), and Mingyuan Guo (employee of the Fifth Affiliated Hospital of Guangzhou Medical University) for data collection.

REFERENCES

Abiri, R., Borhani, S., Sellers, E. W., Jiang, Y., and Zhao, X. (2019). A comprehensive review of EEG-based brain-computer interface paradigms. *J. Neural Eng.* 16:011001. doi: 10.1088/1741-2552/aaf12e

Ali, J. I., Viczko, J., and Smart, C. M. (2020). Efficacy of neurofeedback interventions for cognitive rehabilitation following brain injury: systematic review and recommendations for future research. *J. Int. Neuropsychol. Soc.* 26, 31–46. doi: 10.1017/S1355617719001061

Ang, K. K., and Guan, C. (2015). Brain–computer interface for neurorehabilitation of upper limb after stroke. *Proc. IEEE* 103, 944–953. doi: 10.1109/jproc.2015.2415800

Bai, G., Jiang, L., Ma, W., Meng, P., Li, J., Wang, Y., et al. (2020). Effect of low-frequency rTMS and intensive speech therapy treatment on patients with nonfluent aphasia after stroke. *Neurologist* 26, 6–9. doi: 10.1097/NRL.0000000000000303

Carelli, L., Solca, F., Faini, A., Meriggi, P., Sangalli, D., Cipresso, P., et al. (2017). Brain-computer interface for clinical purposes: cognitive assessment and rehabilitation. *Biomed. Res. Int.* 2017:1695290. doi: 10.1155/2017/1695290

Cervera, M. A., Soekadar, S. R., Ushiba, J., Millan, J. D. R., Liu, M., Birbaumer, N., et al. (2018). Brain-computer interfaces for post-stroke motor rehabilitation: a meta-analysis. *Ann. Clin. Transl. Neurol.* 5, 651–663. doi: 10.1002/acn3.544

Chaudhary, U., Birbaumer, N., and Ramos-Murguialday, A. (2016). Brain-computer interfaces for communication and rehabilitation. *Nat. Rev. Neurol.* 12, 513–525. doi: 10.1038/nrneurol.2016.113

Dimyan, M. A., and Cohen, L. G. (2011). Neuroplasticity in the context of motor rehabilitation after stroke. *Nat. Rev. Neurol.* 7, 76–85. doi: 10.1038/nrneurol.2010.200

Ding, Q., Lin, T., Wu, M., Yang, W., Li, W., Jing, Y., et al. (2021). Influence of iTBS on the acute neuroplastic change after BCI training. *Front. Cell Neurosci.* 15:653487. doi: 10.3389/fncel.2021.653487

Draaisma, L. R., Wessel, M. J., and Hummel, F. C. (2020). Neurotechnologies as tools for cognitive rehabilitation in stroke patients. *Expert Rev. Neurother.* 20, 1249–1261. doi: 10.1080/14737175.2020.1820324

Gomez, L. J., Dooley, J. C., Sokoloff, G., and Blumberg, M. S. (2021). Parallel and serial sensory processing in developing primary somatosensory and motor cortex. *J. Neurosci.* 41, 3418–3431. doi: 10.1523/JNEUROSCI.2614-20.2021

Hendricks, H. T., van Limbeek, J., Geurts, A. C., and Zwarts, M. J. (2002). Motor recovery after stroke: a systematic review of the literature. *Arch. Phys. Med. Rehabil.* 83, 1629–1637. doi: 10.1053/apmr.2002.35473

Hou, X., Zhang, Z., Zhao, C., Duan, L., Gong, Y., Li, Z., et al. (2021). NIRS-KIT: a MATLAB toolbox for both resting-state and task fNIRS data analysis. *Neurophotonics*. 8:010802. doi: 10.1117/1.NPh.8.1.010802

Johnson, N. N., Carey, J., Edelman, B. J., Doud, A., Grande, A., Lakshminarayan, K., et al. (2018). Combined rTMS and virtual reality brain-computer interface training for motor recovery after stroke. *J. Neural Eng.* 15:016009. doi: 10.1088/1741-2552/aa8ce3

Kaiser, V., Bauernfeind, G., Kreilinger, A., Kaufmann, T., Kubler, A., Neuper, C., et al. (2014). Cortical effects of user training in a motor imagery based brain-computer interface measured by fNIRS and EEG. *Neuroimage* 85(Pt 1), 432–444. doi: 10.1016/j.neuroimage.2013.04.097

Li, N., Chen, T. W., Guo, Z. V., Gerfen, C. R., and Svoboda, K. (2015). A motor cortex circuit for motor planning and movement. *Nature* 519, 51–56. doi: 10.1038/nature14178

Mane, R., Chouhan, T., and Guan, C. (2020). BCI for stroke rehabilitation: motor and beyond. *J. Neural Eng.* 17:041001. doi: 10.1088/1741-2552/aba162

Morris, D. M., Uswatte, G., Crago, J. E., Cook, E. W. III, and Taub, E. (2001). The reliability of the wolf motor function test for assessing upper extremity function after stroke. *Arch. Phys. Med. Rehabil.* 82, 750–755. doi: 10.1053/apmr.2001.23183

Mukaino, M., Ono, T., Shindo, K., Fujiwara, T., Ota, T., Kimura, A., et al. (2014). Efficacy of brain-computer interface-driven neuromuscular electrical stimulation for chronic paresis after stroke. *J. Rehabil. Med.* 46, 378–382. doi: 10.2340/16501977-1785

Nishimoto, A., Kawakami, M., Fujiwara, T., Hiramoto, M., Honaga, K., Abe, K., et al. (2018). Feasibility of task-specific brain-machine interface training for upper-extremity paralysis in patients with chronic hemiparetic stroke. *J. Rehabil. Med.* 50, 52–58. doi: 10.2340/16501977-2275

Paparella, G., Rocchi, L., Bologna, M., Berardelli, A., and Rothwell, J. (2020). Differential effects of motor skill acquisition on the primary motor and sensory cortices in healthy humans. *J. Physiol.* 598, 4031–4045. doi: 10.1113/JP279966

Pichiorri, F., and Mattia, D. (2020). Brain-computer interfaces in neurologic rehabilitation practice. *Handb. Clin. Neurol.* 168, 101–116. doi: 10.1016/B978-0-444-63934-9.00009-3

Pinti, P., Tachtsidis, I., Hamilton, A., Hirsch, J., Aichelburg, C., Gilbert, S., et al. (2020). The present and future use of functional near-infrared spectroscopy (fNIRS) for cognitive neuroscience. *Ann. N. Y. Acad. Sci.* 1464, 5–29. doi: 10.1111/nyas.13948

Potter, S. M., El Hady, A., and Fetz, E. E. (2014). Closed-loop neuroscience and neuroengineering. *Front. Neural Circuits* 8:115. doi: 10.3389/fncir.2014.00115

Qian, X., Loo, B. R. Y., Castellanos, F. X., Liu, S., Koh, H. L., Poh, X. W. W., et al. (2018). Brain-computer-interface-based intervention re-normalizes brain functional network topology in children with attention deficit/hyperactivity disorder. *Transl. Psychiatry* 8:149. doi: 10.1038/s41398-018-0213-8

Ramos-Murguialday, A., Broetz, D., Rea, M., Laer, L., Yilmaz, O., Brasil, F. L., et al. (2013). Brain-machine interface in chronic stroke rehabilitation: a controlled study. *Ann. Neurol* 74, 100–108. doi: 10.1002/ana.23879

Seminowicz, D. A., and Moayedi, M. (2017). The dorsolateral prefrontal cortex in acute and chronic pain. *J. Pain* 18, 1027–1035. doi: 10.1016/j.jpain.2017.03.008

Wan, N., Hancock, A. S., Moon, T. K., and Gillam, R. B. (2018). A functional near-infrared spectroscopic investigation of speech production during reading. *Hum. Brain Mapp.* 39, 1428–1437. doi: 10.1002/hbm.23932

Yang, M., Yang, Z., Yuan, T., Feng, W., and Wang, P. (2019). A systemic review of functional near-infrared spectroscopy for stroke: current application and future directions. *Front. Neurol.* 10:58. doi: 10.3389/fneur.2019.00058

Young, B. M., Nigogosyan, Z., Walton, L. M., Remsik, A., Song, J., Nair, V. A., et al. (2015). Dose-response relationships using brain-computer interface technology impact stroke rehabilitation. *Front. Hum. Neurosci.* 9:361. doi: 10.3389/fnhum.2015.00361

Young, B. M., Williams, J., and Prabhakaran, V. (2014). BCI-FES: could a new rehabilitation device hold fresh promise for stroke patients? *Expert Rev. Med. Devices* 11, 537–539. doi: 10.1586/17434440.2014.941811

Zhang, Y., Le, S., Li, H., Ji, B., Wang, M. H., Tao, J., et al. (2021). MRI magnetic compatible electrical neural interface: from materials to application. *Biosens. Bioelectron.* 194:113592. doi: 10.1016/j.bios.2021.113592

Conflict of Interest: The authors declare that the research was conducted in the absence of any commercial or financial relationships that could be construed as a potential conflict of interest.

Publisher's Note: All claims expressed in this article are solely those of the authors and do not necessarily represent those of their affiliated organizations, or those of the publisher, the editors and the reviewers. Any product that may be evaluated in this article, or claim that may be made by its manufacturer, is not guaranteed or endorsed by the publisher.

frontiers | Frontiers in Neuroscience

ORIGINAL RESEARCH
published: 08 April 2022
doi: 10.3389/fnins.2022.809657

Brain–Computer Interface-Robot Training Enhances Upper Extremity Performance and Changes the Cortical Activation in Stroke Patients: A Functional Near-Infrared Spectroscopy Study

Lingyu Liu[1], Minxia Jin[1], Linguo Zhang[1], Qiuzhen Zhang[1], Dunrong Hu[1], Lingjing Jin[1] and Zhiyu Nie[2]**

[1] Department of Neurorehabilitation, Shanghai Yangzhi Rehabilitation Hospital, Shanghai Sunshine Rehabilitation Center, School of Medicine, Tongji University, Shanghai, China, [2] Department of Neurology, Tongji Hospital, School of Medicine, Tongji University, Shanghai, China

OPEN ACCESS

Edited by:
Jing Wang,
Xi'an Jiaotong University, China

Reviewed by:
Guoyuan Yang,
Shanghai Jiao Tong University, China
Olesya Mokienko,
Research Center of Neurology of RAMS, Russia

***Correspondence:**
Lingjing Jin
lingjingjin@163.com
Zhiyu Nie
nzhiyu2002@sina.com

Specialty section:
This article was submitted to Neuroprosthetics, a section of the journal Frontiers in Neuroscience

Received: 05 November 2021
Accepted: 11 March 2022
Published: 08 April 2022

Citation:
Liu L, Jin M, Zhang L, Zhang Q, Hu D, Jin L and Nie Z (2022) Brain–Computer Interface-Robot Training Enhances Upper Extremity Performance and Changes the Cortical Activation in Stroke Patients: A Functional Near-Infrared Spectroscopy Study. Front. Neurosci. 16:809657. doi: 10.3389/fnins.2022.809657

Introduction: We evaluated the efficacy of brain–computer interface (BCI) training to explore the hypothesized beneficial effects of physiotherapy alone in chronic stroke patients with moderate or severe paresis. We also focused on the neuroplastic changes in the primary motor cortex (M_1) after BCI training.

Methods: In this study, 18 hospitalized chronic stroke patients with moderate or severe motor deficits participated. Patients were operated on for 20 sessions and followed up after 1 month. Functional assessments were performed at five points, namely, pre1-, pre2-, mid-, post-training, and 1-month follow-up. Wolf Motor Function Test (WMFT) was used as the primary outcome measure, while Fugl-Meyer Assessment (FMA), its wrist and hand (FMA-WH) sub-score and its shoulder and elbow (FMA-SE) sub-score served as secondary outcome measures. Neuroplastic changes were measured by functional near-infrared spectroscopy (fNIRS) at baseline and after 20 sessions of BCI training. Pearson correlation analysis was used to evaluate functional connectivity (FC) across time points.

Results: Compared to the baseline, better functional outcome was observed after BCI training and 1-month follow-up, including a significantly higher probability of achieving a clinically relevant increase in the WMFT full score (ΔWMFT score = 12.39 points, $F = 30.28$, and $P < 0.001$), WMFT completion time (ΔWMFT time = 248.39 s, $F = 16.83$, and $P < 0.001$), and FMA full score (ΔFMA-UE = 12.72 points, $F = 106.07$, and $P < 0.001$), FMA-WH sub-score (ΔFMA-WH = 5.6 points, $F = 35.53$, and $P < 0.001$), and FMA-SE sub-score (ΔFMA-SE = 8.06 points, $F = 22.38$, and $P < 0.001$). Compared to the baseline, after BCI training the FC between the ipsilateral M_1 and the contralateral M_1 was increased ($P < 0.05$), which was the same as the FC between the ipsilateral M_1 and the ipsilateral frontal lobe, and the FC between the contralateral M_1 and the contralateral frontal lobe was also increased ($P < 0.05$).

Conclusion: The findings demonstrate that BCI-based rehabilitation could be an effective intervention for the motor performance of patients after stroke with moderate or severe upper limb paresis and represents a potential strategy in stroke neurorehabilitation. Our results suggest that FC between ipsilesional M_1 and frontal cortex might be enhanced after BCI training.

Clinical Trial Registration: www.chictr.org.cn, identifier: ChiCTR2100046301.

Keywords: stroke rehabilitation, brain–computer interface, upper extremity, functional connectivity, functional near-infrared spectroscopy

INTRODUCTION

Stroke is one of the most prevalent pathologies which causes devastating consequences in most of the survivors worldwide (Benjamin et al., 2017). Rehabilitation is often operated early to minimize disability and to improve the quality of patients' daily life. Most patients reach a functional plateau, especially 6 months after the onset. Previous research findings have suggested that some neural plasticity, which may hamper functional recovery, might occur, and gradually persist during this plateau, has been approaching (Miller et al., 2013). This promotes many uses of alternative, non-conventional treatments such as constraint-induced movement therapy (Varkuti et al., 2013), robot-assisted movement therapy (Pinter et al., 2013), and brain–computer interface (BCI) (Tariq et al., 2018). Recently, with the advancements in neurotechnology, BCI has become the emergence in stroke rehabilitation. It is an innovative intervention that records and decodes neural signals by real-time electroencephalogram (EEG) and transfers them into digital signals. Then assistive devices, such as prostheses or robots, can be triggered by specific signals. The EEG-based BCI has emerged as a potentially effective therapeutic scheme in motor recovery in the chronic stroke stage. Neural signals are detected and inputted to provide real-time feedback, which effectively enables patients to modulate their brain activity (Cervera et al., 2018). Several research studies have recently provided evidence that BCI promotes functional recovery in upper limb or hand function (Ang et al., 2015a; Kasashima-Shindo et al., 2015), although others have found no changes when compared to robots in the chronic stage (Ang et al., 2014).

In order to increase the BCI performance accuracy, stroke survivors carry out motor imagery (MI) exercises or motor watching during EEG recording (Cervera et al., 2018). MI induced the decoded brain oscillations, which is used to trigger a robotic device to reproduce the real movement with the paretic limb (Irimia et al., 2016). These types of multimodal feedback, including visual, haptic, and kinesthetic feedback, provide a closed-loop feedback system for patients. Numerous neurophysiological studies have demonstrated the effect of MI on motor function and neuroplasticity. In these findings, it has been shown that the MI-based BCI rehabilitation system could activate the primary motor cortex (M_1) and other brain structures involved in motor planning and control of voluntary movements (Ramos-Murguialday et al., 2013; Ono et al., 2014).

Previous studies have demonstrated that motor recovery has been related to modulating changes in neuroplasticity in the adult human brain (Wander et al., 2013). A growing number of studies have shown that specific regional activation in the cortex and motor recovery after stroke are closely related processes (Grefkes et al., 2008). The changes beyond the motor network after BCI is unclear, especially the functional connectivity (FC) or neural reorganization of cortical regions between the motor network and the sensor network. FC and basic reorganization changes of the motor recovery can be investigated using many neuroimaging techniques, including functional magnetic resonance imaging (fMRI), electroencephalography (EEG), and functional near-infrared spectroscopy (fNIRS) (Sun et al., 2017; Yang et al., 2019).

Functional near-infrared spectroscopy is an emerging technology that measures the concentration changes in oxy-Hb and deoxy-Hb caused by brain activity. It has been known that the requirement for oxygen during brain activation generates the dilatation of arterioles and capillaries, which is called neurovascular coupling (NVC) during the process of the local neural activity and metabolism between neurons and other tissues. Based on the NVC mechanism, cerebral oxygenation fluctuation signals can be recorded by fNIRS, and the coherence and phase-locking value (PLV) be calculated, by which the FC of the brain networks could be assessed (Briels et al., 2020). By performing the PLV, we could identify the consistent phase differences that indicate high phase synchronization. The better the consistency of the hemodynamic changes in a specific frequency domain in different cortical regions, the stronger the connectivity of the neural activity between these regions will be. Previous studies have provided strong evidence that stroke plays a causal role in impairing cerebral blood flow (CBF) regulation during brain activation, which depends on NVC. Real-time adjustment of CBF to neuronal activity *via* NVC has an essential role in the maintenance of normal brain function (Tarantini et al., 2017). Simultaneously, this response reduces the resistance of the vascular bed to guarantee adequate cerebral blood perfusion to activate neurons. The development of fNIRS has greatly advanced the understanding of the underlying behavior of neural mechanisms and remodeling after brain lesions in humans. It provides real-time sensitivity of the brain's oxygenation state.

Additionally, compared with fMRI, fNIRS measurement can be taken in an upright position with a higher temporal resolution (∼10 Hz) and in a task state without physical restraint. Several studies using fNIRS have successfully observed FC during both the rest and the task state in healthy volunteers (Lu et al., 2010). Recently, this method has gradually become a well-established neuroimaging tool in scientific studies.

In this study, we explored the efficacy of rehabilitation in upper extremity motor recovery after BCI training and the neuroplastic changes in cortical organization. In this single pre-post intervention group study, we designed a task-related and clinical setting by using fNIRS to evaluate whether the brain activation for M_1 can be assessed routinely after BCI training in chronic stroke. We hypothesized an improvement in motor performance and a strengthening of the FC between ipsilateral M_1 and the frontal cortex after BCI training.

MATERIALS AND METHODS

Participants and Study Design

The study was conducted and approved by the Human Ethics Committee of Shanghai Yangzhi Rehabilitation Hospital (#SBKT-2021-044), at which all participants had completed inpatient rehabilitation and had received standard medical care and traditional rehabilitation for 4 weeks, which consisted of routine physiotherapy and occupational therapy focused on rehabilitation of functional transfer. Any activities involving arm and hand movements were avoided. All participants provided written informed consent before the beginning of the study. The inclusion criteria for these patients were as follows: (1) First-time onset stroke patients diagnosed by computed tomography or brain MRI (poststroke time ≥6 months); (2) stable neurological status with unilateral residual hemiplegia; (3) functional restriction in the upper extremities and Brunnstrom stage ≥II; (4) right-handed individuals, who were confirmed by the Edinburgh Handedness Inventory; (5) with the ability to understand the therapists' direction and MMSE score ≥21 according to the education level. Those excluded were (1) with medical instability such as heart/respiratory failure, deep venous thrombosis, acute myocardial infarction, non-compensated diabetes, active liver disease, or/and kidney dysfunction; (2) with the severe cognitive disorder or/and MMSE score <21 that the patient cannot follow and perform tasks; (3) with severe aphasia; (4) with limitation of passive range of motion in the paretic upper limb (dorsal wrist flexion $< 20^{\circ}$, limitation of elbow flexion $> 30^{\circ}$, and shoulder abduction $< 60^{\circ}$); (5) with upper limb muscular-skeletal diseases such as a fracture; (6) with a mental illness history or taking any antipsychotic drugs that are not suitable for this study; and (7) those who had received antispastic therapy (including any antispastic medicine or botulinum toxin injection) within the 6 months prior to the study.

Patients accepted the BCI-robot training system. Each patient performed 20 sessions (one session per day and 5 days per week) and followed up after 1 month. The sessions were conducted every day except weekends and holidays. Functional assessments were performed at five points, namely, pre1, pre2, mid-, post-, and 1-month follow-up (FU). fNIRS assessments were measured at two time points, namely, pre1 and post BCI training. Two qualified therapists performed all training and another researcher in the team conducted the evaluations. Pre1 and Pre2 were scheduled within 3 days before the intervention, respectively, while mid-, post-, and 1-month FU were carried out, respectively, after 10 sessions of training, 20 sessions of training, and 1 month after the intervention (see **Figure 1**).

Participants' Baselines

A total of 21 hemiplegic patients were recruited and 18 completed this study. Altogether, there were 14 men and 4 women (mean age = 45.33 years, SD = 15.07). The stroke duration ranged from 6 to 20 months [median time = 6.5 months, IQR = 6–8 months]. Notably, nine patients had a stroke in the right hemisphere (50%), and 9 in the left hemisphere (50%). None of them had brain-stem involvement (**Table 1**).

Motor and Cognitive Assessments

Functional and behavioral scales were performed to measure the motor improvements. The Wolf Motor Function Test (WMFT, score from 0 to 75) was used as the primary outcome measure, while Fugl-Meyer Assessment (FMA, score from 0 to 66), its wrist and hand (FMA-WH) sub-score, and shoulder and elbow (FMA-SE) sub-score served as secondary outcome measures. To detect the baseline stability, the clinical assessments were done two times in 3 days in the beginning of the training. The different scores reflect different extents of impairment in upper limb functions. The lower scores correspond to greater impairment. The Brunnstrom stage (from stage I to stage VI) was also used to measure baseline impairment for this clinical trial. The activities of daily living recovery were evaluated using the Barthel index (BI, score from 0 to 100), which includes 10 items (a score of 100 corresponding to complete independence). In addition, we used the Mini-Mental State Examination (MMSE, score from 0 to 30) for cognitive assessment. Higher scores indicate better cognitive function, and a score below 25 points is considered to be abnormal. Those above 21 points (according to the education level) are anticipated.

BCI-Robot System Description

MI-based BCI-robot training system (RHB-III with 16 EEG channels; Shenzhen Rehab Medical Technology Co., Ltd., China) is shown in **Figure 2A**. The whole system consisted of the collection system of real-time EEG signals, a central processing control algorithm, and a manus robot feedback. In all patients, EEG was recorded using 16 active electrodes within the 10–20 system of electrode locations over the frontal and parietal regions. Recording locations were channel positions F1, Fz, F3, FC3, FC1, FCz, FC2, FC4, C3, C1, Cz, C2, C4, CP1, CPz, and CP2 (**Figure 2B**). The real-time EEG signals were amplified and processed by the central processing control algorithm. Video clips on the computer screen were played to guide the participants to execute MI tasks. An exoskeleton robot hand was used to help the paretic hand perform the real movement in grasping/opening tasks. A mu event-related desynchronization (ERD) (score from 0 to 100) was displayed to provide real-time visual feedback.

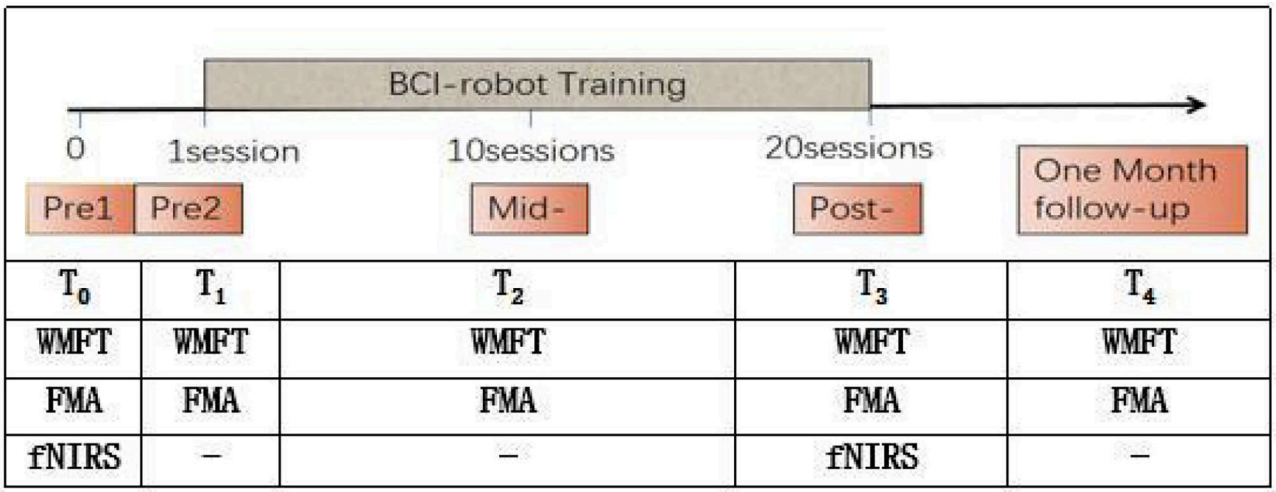

FIGURE 1 | Timing of assessments.

TABLE 1 | Demographic, clinical, and neuropsychological characteristics of the patients.

Number	Age	Gender	Hemisphere lesion	Type of lesion	Days after stroke (m)	BI	Brunnstrom
1	40	M	L basal ganglia	IS	8	98	II
2	53	M	L lateral ventricle	IS	6	93	IV
3	72	M	L MCAO	IS	6	85	IV
4	35	M	L internal capsule	H	6	92	III
5	43	M	L basal ganglia	H	6	92	III
6	23	M	L corona radiate	H	8	77	II
7	28	M	L basal ganglia	H	6	69	II
8	29	F	L basal ganglia	H	9	78	II
9	73	M	R lateral ventricle	IS	7	73	II
10	39	M	R basal ganglia	H	6	74	II
11	39	M	R MCAO	IS	9	67	II
12	51	F	R corona radiate	H	6	73	II
13	29	M	R hemisphere	H	20	79	II
14	39	M	L basal ganglia	H	7	59	II
15	44	M	R temporal lobe	H	6	61	II
16	67	F	R internal capsule	H	6	77	II
17	55	F	R corona radiate	H	7	98	II
18	57	M	R basal ganglia	IS	7	71	III

M, male; F, female; R, right; L, left; MCAO, middle cerebral artery occlusion; BI, Barthel index; IS, ischemic; H, hemorrhagic.

Participants could modify their MI strategy to achieve MI-triggered robotic feedback more successfully (Sun et al., 2017).

Electroencephalogram signals from the C3 and C4 electrodes were used for BCI control. A voice clue was used before each trial began to help the participant on the MI task. The system presented the instruction on the screen after 2 s. Then, a text and voice cue of "hand grasp"/"hand open" was displayed and lasted for 2 s. Meanwhile, a hand movement video clip with a duration of 6 s was then displayed. Participants can watch the video and perform the same MI processing in their brains. EEG signal measurements were collected with unipolar Ag/Ag-Cl electrode channels and digitally sampled at 256 Hz with a resolution of 22 bits for voltage ranges of $\pm$130 mV. In terms of ensuring the transmission impedance was below 1 kΩ, all electrodes were immersed in saltwater for preparation.

In this study, the paretic hand was strapped to the manus robotic exoskeleton. Participants were instructed to watch the actions displayed in the video and guided to imagine they were performing the same movement with the paretic hand. According to the real-time EEG signals, the calculation of the mu ERD score was conducted. When the score was above 60, the robot would be triggered and assist the paretic hand to accomplish the

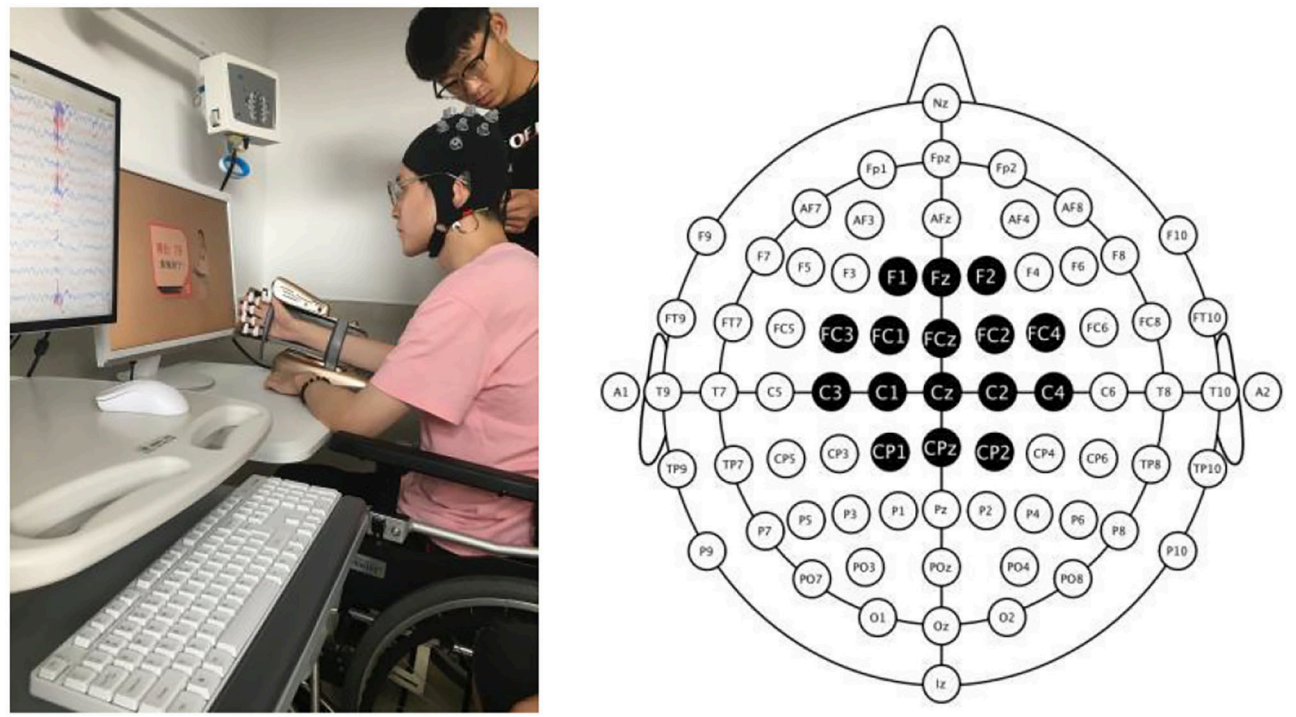

FIGURE 2 | Photograph of the BCI-robot training system. **(A)** The whole system includes an EEG amplifier collecting real-time EEG, a PC processing EEG signal providing visual and auditory feedback, and a triggered-robot hand supporting sensory and movement feedback. **(B)** The montage of real-time EEG electrodes. There were 16 active electrodes placed on the frontal and parietal cortex.

grasp/open task for the next 3 s. But if the mu ERD score was below 60, the robot would not be triggered to move, which was considered a failed trial. The mu ERD score was then shown for 2 s. Participants were encouraged to instruct MI until successful or unsuccessful detection was indicated on the video screen. If MI was successfully detected, visual and movement feedback were provided by the robot through the real movement of the paretic hand. The BCI-robot therapy session included 4 runs of 40 trials each, for a total of 160 trials, and an interrun break of 3 min. It took about 40–50 min for each BCI training session in total.

Functional Near-Infrared Spectroscopy

In this study, we utilized the multichannel fNIRS system (NirScan, NirScan-6000, USA) to measure the changes in concentration of oxygenated hemoglobin (oxy-Hb) and deoxygenated hemoglobin (deoxy-Hb). Channels between each transmitter and receiver were placed according to the international 10–20 system, in which the distance was set at 3–5 mm. The sampling rate of the NIRS system was set to 10 Hz, and the wavelengths used were 740 and 850 nm. The probe layout consisted of 12 channels (30 mm spacing interval). The channel montage configuration of the NIRS probe set is shown in **Figure 3**. The optodes were positioned over the primary motor cortex area (LMC: L1–L4; RMC: R5–R8) and the frontal cortex area (LF: L9 and L10; RF: R11 and R12). Prior to each recording, a NIR gain quality check was performed to ensure data acquisition was moderate, namely, neither under-gained nor over-gained. To place the probes in a fixed position on the scalp, the participant's head was covered with a cap and fixed with a trap to adjust and fixate the transmitters and receivers. In order to attain maximum efficiency of light coupling to the tissue, hairs were carefully swept away to ensure the optodes touched the participant's skin tightly (see **Figure 3**).

As shown in **Figure 4**, the experimental design in the fNIRS testing comprised two periods, namely, the resting state (RS) and task state (TS). The RS required the subjects to sit quietly for 10 s to become ready. The participants were requested to close their eyes, relax, and avoid any movements except those needed for the motor tasks to avoid affecting the blood oxygen data. Before measurement, participants were taught to rehearse the motor task to comprehend the task instructions. For the TS, the participants were instructed to perform a repetitive three-time grip-and-rest task for a total of 180 s by using a dynamometer as accurately as possible. During this TS, the relax duration was set to 30 s for NIRS signals reaching the baselines. Then, the participants were required to sit for at least 30 s as the RS. The total trial time of one session was thus 220 s.

Functional near-infrared spectroscopy data processing was operated as follows. First, a proficient expert made a preliminary examination of the raw data, and the signals with poor quality

were marked and removed. Second, signals containing motion artifacts were labeled and excluded for calculating task-related changes. Subsequently, further analysis on only the oxy-Hb and deoxy-Hb data of non-marked channels covering functionally involved areas, namely, the four regions of interest (ROIs), was performed. Third, according to the modified Beer-Lambert law, data processing was made using a MATLAB script. A high pass filter with a cutoff frequency at 0.01 Hz was used to make the baseline removal, such as the physiological signals, and the low pass filter with a cutoff frequency at 0.8 Hz was applied to the signals. Transfer function models were applied for artifact reduction of the systemic influences (Bauernfeind et al., 2014). Then the baseline correction on each trial was performed to make the task state stable and the baseline signal began at approximately zero. The average time for hemodynamic response function (HRF) in each ROI was measured for each participant over each recorded trial at task state. The averaged amplitude of each HRF was also calculated for statistical analysis. FC was calculated in terms of both time and frequency. We utilized the correlation approach to estimate the strength of the pairwise Pearson's correlation between ROIs for the time aspect (Pannunzi et al., 2017). In terms of frequency, coherence and phase-locking value (PLV) were applied to analyze the level of synchronization of the fNIRS signals, which indicated the stability of the phase difference between the two time series (Briels et al., 2020). We performed Welch's averaged, modified periodogram method to calculate the squared coherence between ROIs. All connectivity matrices were made to be Fisher's *z*-transformed for statistical analysis (Arun et al., 2020).

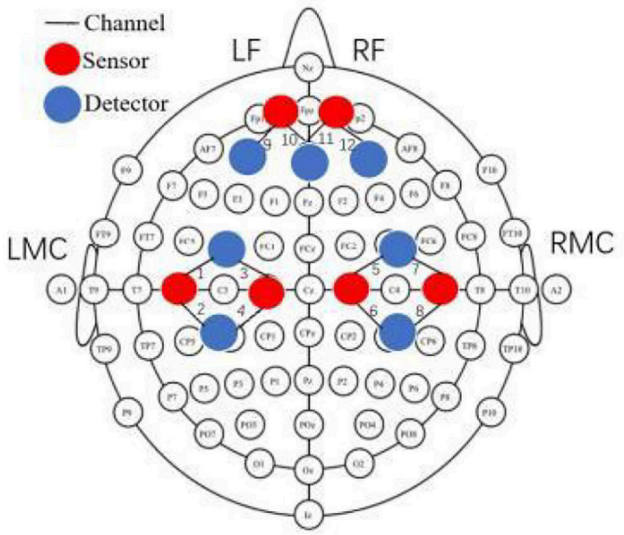

FIGURE 3 | Functional near-infrared spectroscopy (fNIRS) 12-channel montage configuration. The probes were located over the frontal cortex (left frontal cortex and right frontal cortex near FP_Z), the primary motor cortex (M_1) (left M_1 and right M_1). The red circles represent the positions of sensors (S) and the blue circles represent the positions of detectors (D). The line between them is the channel. LMC, left M_1 cortex; RMC, right M_1 cortex; LF, left frontal cortex; RF, right frontal cortex.

Statistical Analysis

Measurement data were expressed by mean and standard deviation. All data analyses and statistics were performed in MATLAB. All data were tested for normal distribution using Shapiro–Wilk test. The mean comparison after the intervention was performed using a one-sample *t*-test or Kruskal–Wallis test. Repeated measures ANOVA with the Bonferroni *post-hoc* test was utilized to measure the differences in the clinical assessments at five different time points (two pre-assessments, a mid-assessment, a post-assessment, and a 1-month FU assessment). Repeated measures of ANOVA were also used to compare FC matrices at baseline and after BCI training. Pearson correlation analysis was utilized between the FC. The statistically significant level was 0.05 in this study.

RESULTS

Functional Improvement After BCI-Robot Therapy

Totally, 21 participants were recruited and received the screen learning control. Two participants were unable to achieve control over the BCI, and one was discharged earlier than expected due to non-medical reasons. Finally, 18 participants completed

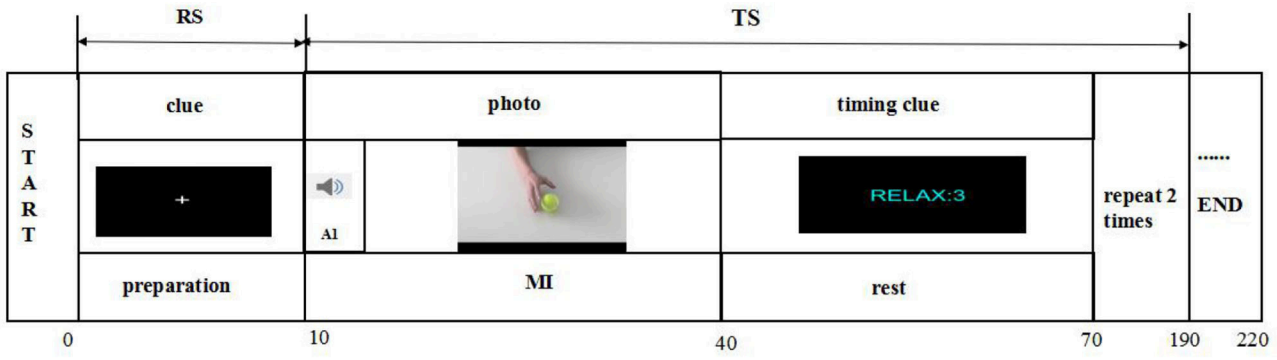

FIGURE 4 | Illustration of fNIRS testing. There are two states of fNIRS testing, namely, the rest state (RS) and the task state (TS). The RS is 10 s, and the TS is a 180-s grasping task. The grasping task consists of three trials, and each trial is followed by a 30-s intertrial break.

20 sessions of BCI-robot training and a 1-month FU, with all participants completing the clinical assessments and fNIRS measurements. No adverse effects were reported.

Clinical Functional Assessments

Motor improvements measured by clinical scores, including the WMFT and FMA-UE scores, are summarized in **Table 2**. Significant increases were observed in the WMFT full score ($P < 0.001$, ΔWMFT score = 12.39 points, $F = 30.28$, one-way ANOVA with the Bonferroni *post-hoc* test), FMA full score ($P < 0.001$, ΔFMA-UE = 12.72 points, $F = 106.07$, one-way ANOVA with the Bonferroni *post-hoc* test), and WMFT completion time score ($P < 0.001$, ΔWMFT time = 248.39 s, $F = 16.83$, one-way ANOVA). As depicted in **Table 2**, a statistically significant mean FMA-UE increase of 12.72 points has been observed. Importantly, as recommended in the literature (Page et al., 2015), the minimal clinically important difference (MCID) for the FMA-UE scale is accepted to be a 5-point increase in chronic stroke survivors. **Table 2** lists all the clinical scores measured in this study (i.e., means and 95% confidence intervals of each clinical assessment as well as the one-way ANOVA probabilities for evaluation with respect to the assessment sessions). As shown in **Table 2**, FMA-WH sub-score ΔFMA-WH = 5.6 points, $F = 35.53$, and $P < 0.001$) and FMA-SE sub-score (ΔFMA-SE = 8.06 points, $F = 22.38$, and $P < 0.001$) have also increased significantly, respectively.

Hemodynamic Response Function

Compared to the baseline, the averaged amplitude of HbO_2 concentration increased after BCI training in the four ROIs significantly during the grasping task (**Figure 5**). Compared to the baseline, there was a significant increase in average Oxy-Hb amplitude at any time point in the whole four ROIs after BCI training during the grasping task.

Resting-State FC Analysis

For resting-state FC, the increased correlation between the ipsilateral motor cortex and ipsilateral frontal lobe was observed after BCI training ($Z = 0.5835$, $P = 0.024$; **Figure 6B**). Increased coherence between the ipsilateral motor cortex and contralateral motor cortex was also observed after BCI training ($Z = 0.7964$, $P = 0.035$; **Figure 6C**). Additionally, increased FC was measured between the contralateral motor cortex and contralateral frontal lobe after BCI training ($Z = 0.7934$, $P = 0.028$; **Figure 6C**). There was no significant difference in FC between the ipsilateral motor cortex and contralateral frontal lobe measured after BCI training ($Z = 0.64$, $P = 0.067$; **Figure 6C**).

DISCUSSION

This study evaluated the effects of a closed-loop neurofeedback BCI-robot system on the improvement of the motor functional recovery of the upper extremities, which was measured by the WMFT and FMA-UE test, as well as the FC between the motor and sensory systems in the brain. The findings on the neuroplastic effects of BCI training showed FC changes involving the contralateral hemisphere in task-related brain activation

TABLE 2 | Means and 95% confidence intervals for each assessment at five time points, as well as the probabilities and *F*-value of the statistical analyses.

	Pre1-	Pre2-	Mid-	Post-	1-month FU	One-way ANOVA	
Evaluation	**Mean (95% confidence interval)**					***P*-value**	***F*-value**
WMFT							
Score	24.89 (16.97–32.81)	26.22 (18.22–34.23)	30.22 (21.03–39.41)	34.17 (24.63–43.70)	37.28*** (27.14–47.41)	<0.001	30.38
Time	1,076.44 (856.41–1,296.48)	1,040.39 (825.35–1,255.43)	986.78 (768.13–1,205.43)	899.61 (676.29–1,122.93)	828.06*** (619.152–1,036.96)	<0.001	16.83
FMA-UE							
Full score	28.06 (21.26–34.85)	29.61 (22.937–36.29)	32.89 (26.25–39.53)	36.50 (29.75–43.25)	40.78*** (34.00–47.56)	<0.001	106.07
Wrist/hand	9.83 (7.05–12.62)	9.55 (7.21–11.65)	11.83 (8.78–14.89)	13.78 (10.67–16.89)	15.44*** (12.38–18.51)	<0.001	35.53
Shoulder/elbow	17.67 (13.10–22.24)	18.24 (12.41–21.43)	21.83 (17.11–26.56)	22.50 (17.86–27.14)	25.72*** (21.07–30.38)	<0.001	22.38

*Significant levels are demonstrated as *** for $p < 0.001$. WMFT, Wolf Motor Function Test; FMA, Fugl-Meyer Assessment; Pre1, first pre-training assessment; Pre2, second pre-training assessment; Mid-, ten-training assessment; Post-, post-training assessment; 1-month FU, 1-month follow-up.*

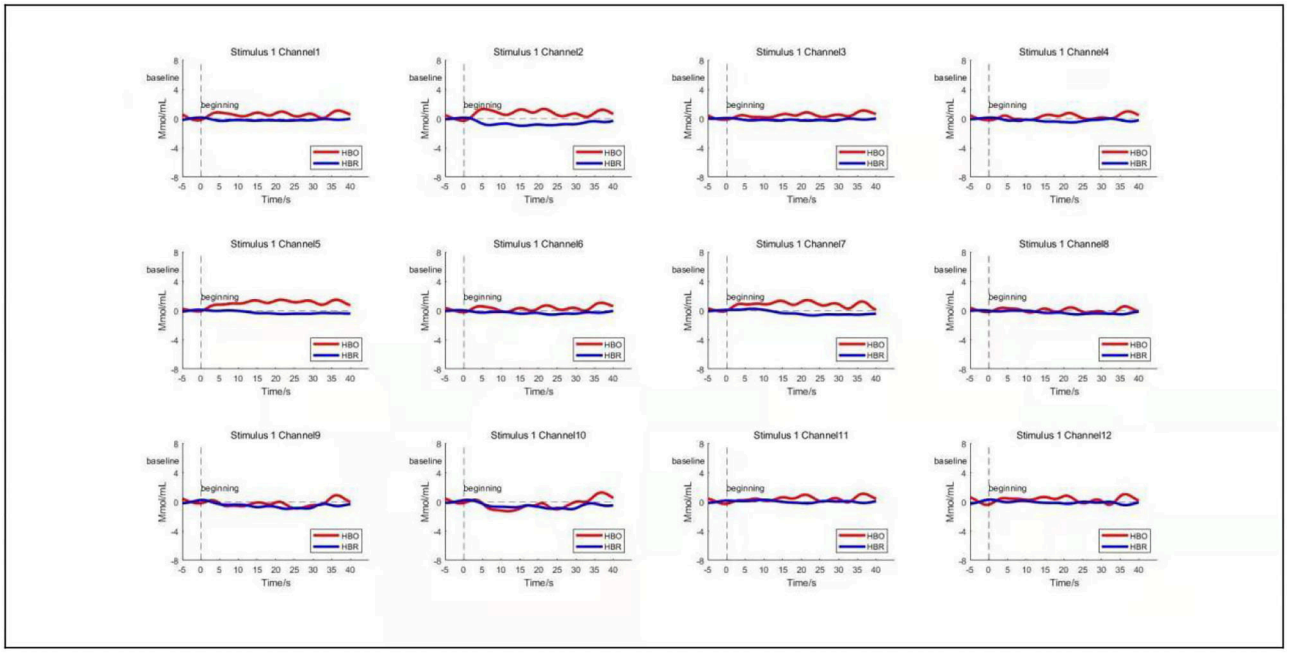

Before BCI

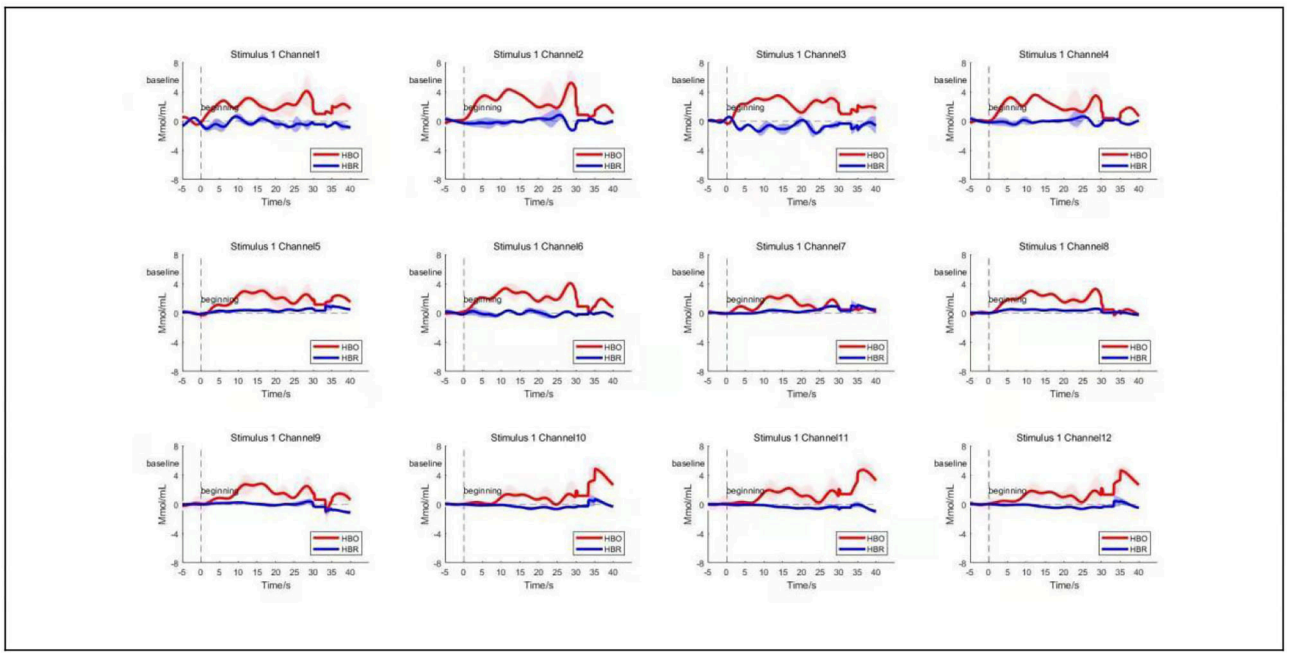

After BCI

FIGURE 5 | Average time series of HRF. Changes in average oxy-Hb amplitude increased at any time point in the whole four ROIs after BCI training during the grasping task (bottom panel). Channels 1–4 located in left M_1, and channels 5–8 located in right M_1. Channels 9 and 10 located in the left frontal polar cortex, and channels 11 and 12 located in the right frontal polar cortex. Top three panels show the HRF change before BCI training, bottom three panels show the HRF change after BCI training. HBO refers to oxy-Hb. HBR refers to deoxy-Hb.

induced by BCI training rehabilitative therapy. Specifically, the examination of the fNIRS showed changes in the patterns of brain activation associated with the paralyzed hand grasping were observed with the administration of BCI therapy. The grasp of the impaired hand was accompanied by a more increasing connectivity pattern after BCI therapy between the ipsilesional

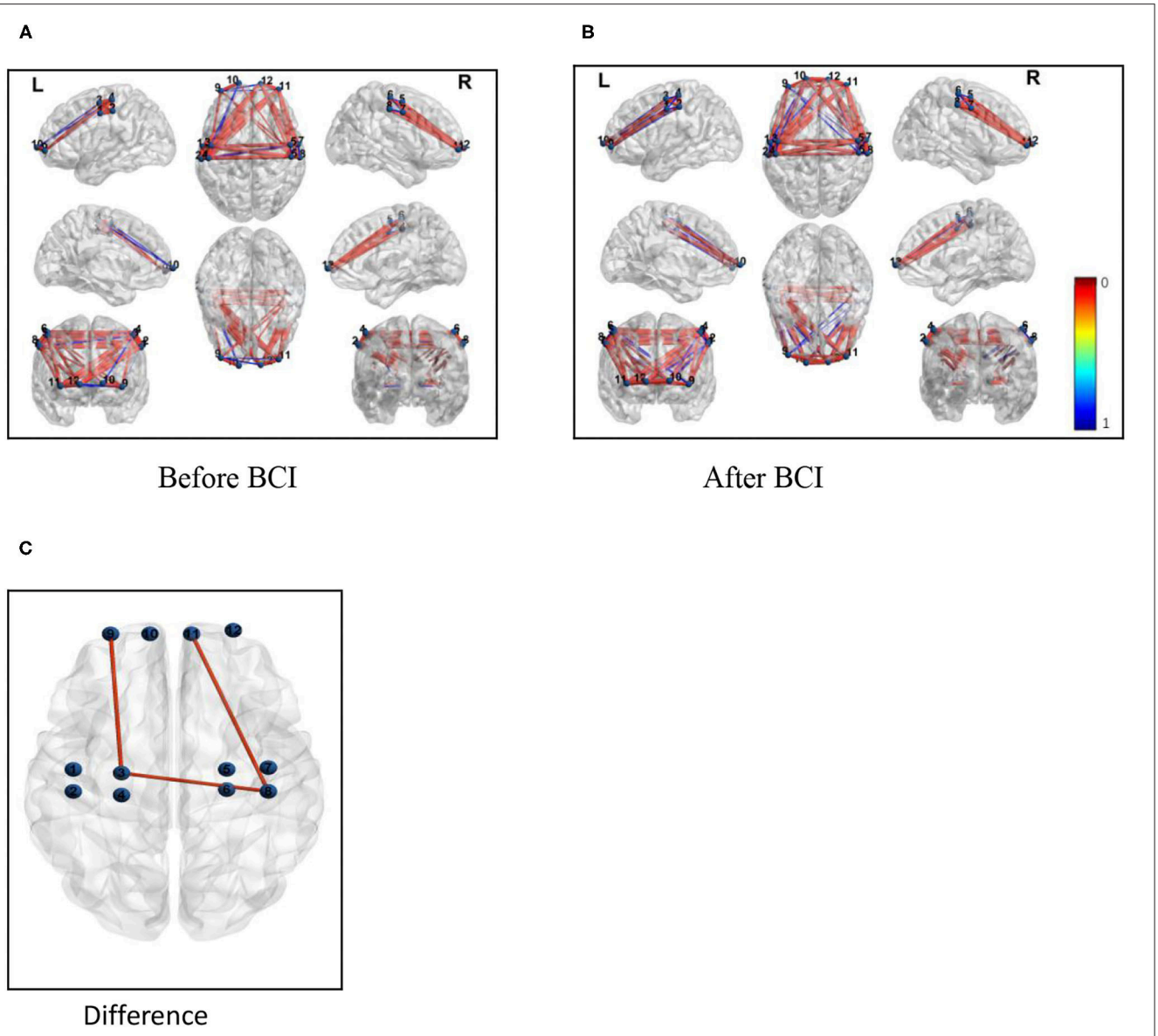

FIGURE 6 | Functional connectivity (correlation) change measured after BCI training. Channels with differences in FC at baseline and the 1-month follow-up (Pearson correlation). **(A)** Correlations between each channel before BCI training. **(B)** Correlations between each channel after BCI training. **(C)** Correlations between the ipsilateral M_1 and the ipsilateral frontal lobe and the contralateral M_1 increased and the FC between the contralateral M_1 and the contralateral frontal lobe was also increased.

primary motor cortex (M_1) and the ipsilesional frontal cortex (**Figure 6**).

In this study, both the WMFT and the FMA scores were found to be significant using one-way ANOVA on this data after the BCI therapy. In controlled trials, when compared with control interventions, the results showed that BCIs had a significant effect on the improvement of upper extremity function (Ono et al., 2014). When comparing to standard robotic rehabilitation, it showed in the experimental group the average motor improvement was slightly more than in controls (Ang et al., 2014; Ono et al., 2014; Remsik et al., 2016). In single-group studies, all of them indicated significant improvements in the scores of the FMA-UE and other functional scales (Halder et al., 2011), and we obtained the similar research results. We noted that in this preliminary study, we did not design a control group, which used a pre- and post-intervention comparison to observe differences in clinical outcomes, which, first, could be sources of significant biasTo reduce bias, we optimized the BCI system used in this study, which removed the instruction automatically of the robotic hand and quantified the control recognition ability of the BCI system when the patient performed motion observation and motion imagery. In addition, we noted that the participants in

the studies were at chronic stages, in which spontaneous recovery was less likely to occur (Soekadar et al., 2015; Remsik et al., 2016). However, some scholars suggested that different lengths of the BCI intervention might be another confounding factor (Ang et al., 2015b). In our study, all subjects completed these behavioral assessments, including post-therapy and 1-month FU assessments after 20 sessions of interventions. It may also be taken into consideration that both WMFT and FMA-UE are objective measurements of clinical function.

According to BCI system studies, patients in the chronic stage have the accuracy to perform MI with diverse feedback, including visual, kinesthetic, and/or proprioceptive feedback, even in those severe cases in whom volitional isolated finger movement is not possible. Serious movement dysfunction in the upper extremity requires more help, such as a robotic device to achieve hand functional movement (Pichiorri et al., 2015). Recently, more evidence has demonstrated that the motor function of patients with severe stroke could be promoted by BCI, in particular, distal hand function (Frolov et al., 2017). Compared with the sham group, the clinical performance above MCID in the BCI group could be observed. Another study (Ramos-Murguialday et al., 2013) included severely impaired subjects and designed a homogeneous sample with a good match by age, gender, paretic side, and motor impairment scores in the controlled trial. Subjects in both groups had a similar amount of BCI training, and the experimental group had higher muscle activity and showed a significant improvement in hand function. Furthermore, research work made by Shindo demonstrated that finger function and surface EMG activity have been improved without motor function (Shindo et al., 2011). All these findings suggest that BCI can be a promising strategy in the rehabilitation of chronic stroke.

Motor recovery after stroke relies on neural plasticity at both structural and functional levels. Rehabilitation training after stroke may strengthen neural connections in existing ones and/or lead to the formation of new neural pathways (Rathee et al., 2017). Some randomized controlled trials mentioned the mechanisms of neural responses to BCI training. One previous EEG study showed that desynchronization over the ipsilesional central area during MI tasks after BCI training has a greater response than pre-intervention, indicating higher activation of the motor area in the ipsilesional brain through BCI training (Mihara et al., 2013; Li et al., 2014). The changes in FC patterns during the grasp of the impaired hand associated with the intervention of BCI therapy suggest that there may be a neuroplastic response to the treatment between the motor system and the sensory system. Several previous studies showed neuroplasticity changes due to BCI intervention, including increasing activity in pre-motor cortex (PMC) or enhancement of ipsilesional connectivity in hemispheric EEG activity (Cervera et al., 2018). Particularly, an fNIRS study of patients with subcortical stroke also showed the activation of the PMC, which was considered to be associated with motor planning and the execution of goal-oriented actions (Sugawara et al., 2013). In addition, research work proved that BCI might activate some special brain cortex, including the prefrontal cortex, PMC, and posterior parietal cortex in some pre-post single-group designs (Halder et al., 2011). By using structural equation modeling of resting-state fMRI data, an investigation was made to explore the effective connectivity between motor control and motor execution. Connectivity from frontoparietal guidance systems to the motor network is diminished in stroke survivors (Inman et al., 2012). In our study, we found FC between ipsilesional M1 and frontal cortex might be enhanced after BCI training. This might improve the overall BCI performance. This result indicates an enhancement of synchronization during the neurological activity among the different cerebral regions after stroke (**Figure 6**). The increased FC in the brain regions supported that BCI training could improve the degree of the disturbance of the neurovascular activities of the brain. The brain activity changes examined by fNIRS may be a response to an objective measurement that is proven by standardized motor function tests.

Recently, a study has described the relevance between neuroplasticity and functional improvement in the MI-based BCI training system (Varkuti et al., 2013). The authors concluded that BCI training might strengthen neuroplasticity and lead to better recovery, due to MI-based BCI might control voluntary movement of the hand in the same neural mechanisms (Orihuela-Espina et al., 2013; Remsik et al., 2016). Additionally, the persistence of these changes up to 1-month FU after the intervention of BCI therapy indicated the possibility for lasting effects under the conditions of this rehabilitative approach. The brain has a certain degree of plasticity, which could be strengthened by using feedback information such as punishment or reward. By decoding and outputting the patient's neural information, BCI could control peripheral muscles and provide feedback to form a new "closed-loop pathway" between the central nervous system and the peripheral nervous system, and then promote the remodeling and recovery of brain function after stroke. Relying on the direct central intervention of the brain, it can further activate functional neuroplasticity and promote cortical remodeling (Birbaumer, 2006). Several studies have shown that (Hummel and Cohen, 2006) 63% of patients with hemiplegia have functional asymmetry after damage to the brain, which has widely been considered to have an unbeneficial effect on the patient's functional recovery. The more the asymmetry is, the worse the recovery of movement will be. A meta-analysis shows (Tang et al., 2015) that the asymmetric performance of the brain after stroke could be improved to a certain extent by BCI intervention. In the next study, we will focus on the inter-hemispheric and intra-hemispheric connections. BCI combined with external robots (e.g., exoskeletons and orthosis) or FES formed the closed-loop intervention mode and promoted better hand function recovery through inducing the activation of specific brain regions.

Nevertheless, the specific mechanisms of the BCI system underlying functional improvements remain largely unknown. In our study, BCI might promote the activation of ipsi or peri-lesional cortex, which effectively results in functional motor activity in the lesioned hemisphere, as was observed in the previous study through the BCI-FES system by scalp EEG analysis (Biasiucci et al., 2018). A meta-analysis of the effect of the BCI system in stroke recovery suggested movement intention and

movement-dependent approaches of ipsilesional reorganization caused by BCI coinciding with better recovery in the chronic phases of stroke (Bai et al., 2020). Additionally, the heterogeneity of current BCI systems complicates attempts to elucidate their mechanisms, because it is likely that functional improvements rely on different strategies that target different aspects of neural circuitry. Besides, BCI improvement may also be influenced by effects from "non-motor" mechanisms (Simon et al., 2021), such as sustained exertion of effort, senses of achievement from controls of the BCI, or improvements in the mood by engaging with a challenging task.

This study has shown the effect on motor performance after BCI-hand robotic training. Additionally, we conducted an examination of neural activities by fNIRS. Changes in neural FC patterns were observed with BCI therapy in both motor and sensory areas in the ipsilesional cerebral in this population of patients with stroke. But there were some limitations and challenges to BCI research work. First, we must be careful of the small sample ($n = 18$) and heterogeneity of stroke survivors, including the different levels of motor impairment (moderate to severe) and lesions (cortical to subcortical). BCI might induce the consistent brain changes of pre-post intervention in these patients over the time course. We noted that although these research findings were promising, the scope of the conclusions was limited by the lack of a control group. Further randomized controlled trials with larger samples should also be designed strictly and performed in the next step to further verify this hypothesis. Second, though most studies about the BCI system tended to be efficient in the movement recovery for patients in the chronic stage after stroke, it is impossible that patients had the whole motivation to continue investing effort into trying to control the BCI without the therapist's assistance, which made it difficult to utilize this rehabilitative technology at home. Third, we assumed the non-motor mechanisms that contributed to the functional recovery during the control of the BCI system. In the further study, we attempt to improve scientific rigor and reproducibility in neurofeedback research.

In summary, BCI training is safe for patients after chronic stroke. More standardized studies should be done to better demonstrate and elucidate the effects of the BCI system therapy and to identify which protocols are the best therapy for different types of stroke. In particular, patients with severe motor deficits show greater recruitment of motor and non-motor areas such as the frontal areas of both the affected and unaffected hemispheres to strive for a full recovery.

DATA AVAILABILITY STATEMENT

The raw data supporting the conclusions of this article will be made available by the authors, without undue reservation.

ETHICS STATEMENT

The studies involving human participants were reviewed and approved by the Human Ethics Committee of Shanghai Yangzhi Rehabilitation Hospital (#SBKT-2021-044). The patients/participants provided their written informed consent to participate in this study. Written informed consent was obtained from the individuals for the publication of any potentially identifiable images or data included in this article.

AUTHOR CONTRIBUTIONS

LL, LJ, and ZN designed the experiment. MJ and LZ conducted the measurements. LL, QZ, and DH participated in the data acquisition. LL supervised the whole process, data acquisition, analysis, manuscript revision, provided the scientific input, and contributed to the manuscript writing. LJ and ZN participated in the manuscript revision, supervised the whole process, and provided clinical input. All authors contributed to the article and approved the submitted version.

FUNDING

This study was supported by the Shanghai Municipal Science and Technology Major Project (2021SHZDZX0100) and the Fundamental Research Funds for the Central Universities.

REFERENCES

Ang, K. K., Chua, K. S., Phua, K. S., Wang, C., Chin, Z. Y., Kuah, C. W., et al. (2015a). A randomized controlled trial of EEG-based motor imagery brain-computer interface robotic rehabilitation for stroke. *Clin. EEG Neurosci.* 46, 310–320. doi: 10.1177/1550059414522229

Ang, K. K., Guan, C., Phua, K. S., Wang, C., Zhao, L., Teo, W. P., et al. (2015b). Facilitating effects of transcranial direct current stimulation on motor imagery brain-computer interface with robotic feedback for stroke rehabilitation. *Arch. Phys. Med. Rehabil.* 96(3 Suppl.), S79–S87. doi: 10.1016/j.apmr.2014.08.008

Ang, K. K., Guan, C., Phua, K. S., Wang, C., Zhou, L., Tang, K. Y., et al. (2014). Brain-computer interface-based robotic end effector system for wrist and hand rehabilitation: results of a three-armed randomized controlled trial for chronic stroke. *Front. Neuroeng.* 7, 30–42. doi: 10.3389/fneng.2014.00030

Arun, K. M., Smitha, K. A., Sylaja, P. N., and Kesavadas, C. (2020). Identifying resting-state functional connectivity changes in the motor cortex using fNIRS during recovery from stroke. *Brain Topogr.* 33, 710–719. doi: 10.1007/s10548-020-00785-2

Bai, Z. F., Fong, K. N. K., Zhang, J. J., Chan, J., and Ting, K. H. (2020). Immediate and long-term effects of BCI-based rehabilitation of the upper extremity after stroke: a systematic review and meta-analysis. *J. Neuroeng. Rehabil.* 17, 57–66. doi: 10.1186/s12984-020-00686-2

Bauernfeind, G., Wriessnegger, S. C., Daly, I., and Müller-Putz, G. R. (2014). Separating heart and brain: on the reduction of physiological noise from multichannel functional near-infrared spectroscopy (fNIRS) signals. *J. Neural Eng.* 11, 056010. doi: 10.1088/1741-2560/11/5/056010

Benjamin, E. J., Blaha, M. J., Chiuve, S. E., Cushman, M., Das, S. R., Deo, R., et al. (2017). Heart disease and stroke statistics-2017 update: a report from the American Heart Association. *Circulation* 135, e229–e445. doi: 10.1161/CIR.0000000000000485

Biasiucci, A., Leeb, R., Iturrate, I., Perdikis, S., Al-Khodairy, A., Corbet, T., et al. (2018). Brain-actuated functional electrical stimulation elicits

lasting arm motor recovery after stroke. *Nat. Commun.* 9, 2421. doi: 10.1038/s41467-018-04673-z

Birbaumer, N. (2006). Breaking the silence: brain-computer interfaces (BCI) for communication and motor control. *Psychophysiology* 43, 517–532. doi: 10.1111/j.1469-8986.2006.00456.x

Briels, C. T., Schoonhoven, D. N., Stam, C. J., De Waal, H., Scheltens, P., and Gouw, A. A. (2020). Reproducibility of EEG functional connectivity in Alzheimer's disease. *Alzheimers Res. Ther.* 12, 68. doi: 10.1186/s13195-020-00632-3

Cervera, M. A., Soekadar, S. R., Ushiba, J., Millán, J. D. R., Liu, M., Birbaumer, N., et al. (2018). Brain-computer interfaces for post-stroke motor rehabilitation: a meta-analysis. *Ann. Clin. Transl. Neurol.* 5, 651–663. doi: 10.1002/acn3.544

Frolov, A. A., Mokienko, O., Lyukmanov, R., Biryukova, E., Kotov, S., Turbina, L., et al. (2017). Post-stroke rehabilitation training with a motor-imagery-based brain-computer interface (bci)-controlled hand exoskeleton: a randomized controlled multicenter trial. *Front. Neurosci.* 11, 400. doi: 10.3389/fnins.2017.00400

Grefkes, C., Nowak, D. A., Eickhoff, S. B., Dafotakis, M., Küst, J., Karbe, H., et al. (2008). Cortical connectivity after subcortical stroke assessed with functional magnetic resonance imaging. *Ann. Neurol.* 63, 236–246. doi: 10.1002/ana.21228

Halder, S., Agorastos, D., Veit, R., Hammer, E. M., Lee, S., Varkuti, B., et al. (2011). Neural mechanisms of brain-computer interface control. *Neuroimage* 55, 1779–1790. doi: 10.1016/j.neuroimage.2011.01.021

Hummel, F. C., and Cohen, L. G. (2006). Non-invasive brain stimulation: a new strategy to improve neurorehabilitation after stroke? *Lancet Neurol.* 5, 708–712. doi: 10.1016/S1474-4422(06)70525-7

Inman, C. S., James, G. A., Hamann, S., Rajendra, J. K., Pagnoni, G., and Butler, A. J. (2012). Altered resting-state effective connectivity of fronto-parietal motor control systems on the primary motor network following stroke. *Neuroimage* 59, 227–237. doi: 10.1016/j.neuroimage.2011.07.083

Irimia, D., Sabathiel, N., Ortner, R., Poboroniuc, M., Coon, W., Allison, B. Z., et al. (2016). "recoveriX: a new BCI-based technology for persons with stroke," in *Proceedings of the 2016 38th Annual International Conference of the IEEE Engineering in Medicine and Biology Society EMBC* (Piscataway, NJ: IEEE), 1504–1507.

Kasashima-Shindo, Y., Fujiwara, T., Ushiba, J., Matsushika, Y., Kamatani, D., Oto, M., et al. (2015). Brain-computer interface training combined with transcranial direct current stimulation in patients with chronic severe hemiparesis: proof of concept study. *J. Rehabil. Med.* 47, 318–324. doi: 10.2340/16501977-1925

Li, M., Liu, Y., Wu, Y., Liu, S., Jia, J., and Zhang, L. (2014). Neurophysiological substrates of stroke patients with motor imagery-based brain-computer Interface training. *Int. J. Neurosci.* 124, 403–415. doi: 10.3109/00207454.2013.850082

Lu, C. M., Zhang, Y. J., Biswal, B. B., et al. (2010). Use of fNIRS to assess resting state functional connectivity. *J. Neurosci. Methods* 186, 242–249. doi: 10.1016/j.jneumeth.2009.11.010

Mihara, M., Hattori, N., Hatakenaka, M., Yagura, H., Kawano, T., Hino, T., et al. (2013). Near-infrared spectroscopy-mediated neurofeedback enhances efficacy of motor imagery-based training in poststroke victims: a pilot study. *Stroke* 44, 1091–1098. doi: 10.1161/STROKEAHA.111.674507

Miller, K. K., Combs, S. A., Van Puymbroeck, M., Altenburger, P. A., Kean, J., Dierks, T. A., et al. (2013). Fatigue and pain: relationships with physical performance and patient beliefs after stroke. *Top. Stroke Rehabil.* 20, 347–355. doi: 10.1310/tsr2004-347

Ono, T., Shindo, K., Kawashima, K., Ota, N., Ito, M., Ota, T., et al. (2014). Brain-computer interface with somatosensory feedback improves functional recovery from severe hemiplegia due to chronic stroke. *Front. Neuroeng.* 7, 19. doi: 10.3389/fneng.2014.00019

Orihuela-Espina, F., Fernandez Del Castillo, I., Palafox, L., Pasaye, E., Sanchez-Villavicencio, I., Leder, R., et al. (2013). Neural reorganization accompanying upper limb motor rehabilitation from stroke with virtual reality-based gesture therapy. *Top. Stroke Rehabil.* 20, 197–209. doi: 10.1310/tsr2003-197

Page, S. J., Hade, E., and Persch, A. (2015). Psychometrics of the wrist stability and hand mobility subscales of the Fugl-Meyer assessment in moderately impaired stroke. *Phys. Ther.* 95, 103–108. doi: 10.2522/ptj.20130235

Pannunzi, M., Hindriks, R., Bettinardi, R. G., Wenger, E., Lisofsky, N., Martensson, J., et al. (2017). Resting -state fMRI correlations: from linkwise unreliability to whole brain stability. *Neuroimage* 157, 250–262. doi: 10.1016/j.neuroimage.2017.06.006

Pichiorri, F., Morone, G., Petti, M., Toppi, J., Pisotta, I., and Molinari, M. (2015). Brain-computer interface boosts motor imagery practice during stroke recovery. *Ann. Neurol.* 77, 851–865. doi: 10.1002/ana.24390

Pinter, D., Pegritz, S., Pargfrieder, C., Reiter, G., Wurm, W., Gattringer, T., et al. (2013). Exploratory study on the effects of a robotic hand rehabilitation device on changes in grip strength and brain activity after stroke. *Top. Stroke Rehabil.* 20, 308–316. doi: 10.1310/tsr2004-308

Ramos-Murguialday, A., Broetz, D., Rea, M., Laer, L., Yilmaz, O., Brasil, F. L., et al. (2013). Brain-machine interface in chronic stroke rehabilitation: A controlled study. *Ann. Neurol.* 74, 100–108. doi: 10.1002/ana.23879

Rathee, D., Cecotti, H., and Prasad, G. (2017). Single-trial effffective brain connectivity patterns enhance discriminability of mental imagery tasks. *J. Neural Eng.* 14, 056005. doi: 10.1088/1741-2552/aa785c

Remsik, A., Young, B., Vermilyea, R., Kiekoefer, L., Abrams, J., Elmore, S. E., et al. (2016). A review of the progression and future implications of brain-computer interface therapies for restoration of distal upper extremity motor function after stroke. *Expert. Rev. Med. Devices* 13, 445–454. doi: 10.1080/17434440.2016.1174572

Shindo, K., Kawashima, K., Ushiba, J., Ota, N., Ito, M., and Ota, T. (2011). Effects of neurofeedback training with an electroencephalogram-based brain-computer interface for hand paralysis in patients with chronic stroke: a preliminary case series study. *J. Rehabil. Med.* 43, 951–957. doi: 10.2340/16501977-0859

Simon, C., Bolton, D. A. E., Kennedy, N. C., Soekadar, S. R., and Ruddy, K. L. (2021). Challenges and opportunities for the future of brain-computer interface in neurorehabilitation. *Front. Neurosci.* 15:699428. doi: 10.3389/fnins.2021.699428

Soekadar, S. R., Birbaumer, N., Slutzky, M. W., and Cohen, L. G. (2015). Brain-machine interfaces in neurorehabilitation of stroke. *Neurobiol. Dis.* 83, 172–179. doi: 10.1016/j.nbd.2014.11.025

Sugawara, K., Onishi, H., Yamashiro, K., Kirimoto, H., Tsubaki, A., Suzuki, M., et al. (2013). Activation of the human premotor cortex during motor preparation in visuomotor tasks. *Brain Topogr.* 26, 581–590. doi: 10.1007/s10548-013-0299-5

Sun, R., Wong, W. W., Wang, J., and Tong, R. K. (2017). Changes in electroencephalography complexity using a brain computer interface-motor observation training in chronic stroke patients: a fuzzy approximate entropy analysis. *Front. Hum. Neurosci.* 11, 444. doi: 10.3389/fnhum.2017.00444

Tang, Q., Li, G., Liu, T., Wang, A., Feng, S., Liao, X., et al. (2015). Modulation of interhemispheric activation balance in motor- related areas of stroke patients with motor recovery: systematic review and meta-analysis of fMRI studies. *Neurosci. Biobehav. Rev.* 57, 392–400. doi: 10.1016/j.neubiorev.2015.09.003

Tarantini, S., Tran, C. H. T., Gordon, G. R., Ungvari, Z., and Csiszar, A. (2017). Impaired neurovascular coupling in aging and Alzheimer s disease: contribution of astrocyte dysfunction and endothelial impairment to cognitive decline. *Exp. Gerontol.* 94, 52–58. doi: 10.1016/j.exger.2016.11.004

Tariq, M., Trivailo, P. M., and Simic, M. (2018). EEG-based BCI control schemes for lower-limb assistive-robots. *Front. Hum. Neurosci.* 12, 312. doi: 10.3389/fnhum.2018.00312

Varkuti, B., Guan, C., Pan, Y., Phua, K. S., Ang, K. K., Kuah, C. W., et al. (2013). Resting state changes in functional connectivity correlate with movement recovery for BCI and robot-assisted upper-extremity training after stroke. *Neurorehabil. Neural Repair* 27, 53–62. doi: 10.1177/1545968312445910

Wander, J. D., Blakely, T., Miller, K. J., Weaver, K. E., Johnson, L. A., Olson, J. D., et al. (2013). Distributed cortical adaptation during learning of a brain-computer interface task. *Proc. Natl. Acad. Sci. U. S. A.* 110, 10818–10823. doi: 10.1073/pnas.1221127110

Yang, M., Yang, Z., Yuan, T., Feng, W., and Wang, P. (2019). A systemic review of functional near-infrared spectroscopy for stroke: current application and future directions. *Front. Neurol.* 10, 58. doi: 10.3389/fneur.2019.00058

Conflict of Interest: The authors declare that the research was conducted in the absence of any commercial or financial relationships that could be construed as a potential conflict of interest.

Publisher's Note: All claims expressed in this article are solely those of the authors and do not necessarily represent those of their affiliated organizations, or those of the publisher, the editors and the reviewers. Any product that may be evaluated in this article, or claim that may be made by its manufacturer, is not guaranteed or endorsed by the publisher.

frontiers | Frontiers in Neuroscience

SYSTEMATIC REVIEW
published: 22 April 2022
doi: 10.3389/fnins.2022.854219

Transcranial Magnetic Stimulation for Improving Dysphagia After Stroke: A Meta-Analysis of Randomized Controlled Trials

Yu-lei Xie[1,2†], *Shan Wang*[1,2,3†], *Jia-meng Jia*[1,2†], *Yu-han Xie*[4], *Xin Chen*[1,2], *Wu Qing*[1,2*] and *Yin-xu Wang*[1,2*]

[1] Department of Rehabilitation Medicine, Affiliated Hospital of North Sichuan Medical College, Nanchong, China, [2] North Sichuan Medical College, Nanchong, China, [3] Department of Rehabilitation Medicine, Chengdu Second People's Hospital, Chengdu, China, [4] University of South China, Hengyang, China

OPEN ACCESS

Edited by:
Jinhua Zhang,
Xi'an Jiaotong University, China

Reviewed by:
Marcello Romano,
Azienda Ospedaliera Ospedali Riuniti Villa Sofia Cervello, Italy
Martin Lotze,
University of Greifswald, Germany

***Correspondence:**
Yin-xu Wang
34089681@qq.com
Wu Qing
cbkf2017@126.com

[†] These authors have contributed equally to this work and share first authorship

Specialty section:
This article was submitted to Neuroprosthetics, a section of the journal Frontiers in Neuroscience

Received: 13 January 2022
Accepted: 21 March 2022
Published: 22 April 2022

Citation:
Xie Y-l, Wang S, Jia J-m, Xie Y-h, Chen X, Qing W and Wang Y-x (2022) Transcranial Magnetic Stimulation for Improving Dysphagia After Stroke: A Meta-Analysis of Randomized Controlled Trials. Front. Neurosci. 16:854219. doi: 10.3389/fnins.2022.854219

Background: Rehabilitation of post-stroke dysphagia is an urgent clinical problem, and repetitive transcranial magnetic stimulation (rTMS) has been widely used in the study of post-stroke function. However, there is no reliable evidence-based medicine to support the effect of rTMS on post-stroke dysphagia. This review aims to evaluate the effectiveness and safety of rTMS on post-stroke dysphagia.

Methods: English-language literature published before December 20, 2021, were searched in six electronic databases. Identified articles were screened, data were extracted, and the methodological quality of included trials was assessed. Meta-analysis was performed using RevMan 5.3 software. The GRADE method was used to assess the quality of the evidence.

Results: A total of 10 studies with 246 patients were included. Meta-analysis showed that rTMS significantly improved overall swallowing function (standardized mean difference [SMD]−0.76, 95% confidence interval (CI)−1.07 to−0.46, $p < 0.0001$, $n = 206$; moderate-quality evidence), Penetration Aspiration Scale (PAS) (mean difference [MD]−1.03, 95% CI−1.51 to−0.55, $p < 0.0001$, $n = 161$; low-quality evidence) and Barthel index scale (BI) (MD 23.86, 95% CI 12.73 to 34.99, $p < 0.0001$, $n = 136$; moderate-quality evidence). Subgroup analyses revealed that (1) rTMS targeting the affected hemisphere and targeting both hemispheres significantly enhanced overall swallowing function and reduced aspiration. (2) Low-frequency rTMS significantly enhanced overall swallowing function and reduced aspiration, and there was no significant difference between high-frequency rTMS and control group in reducing aspiration ($p = 0.09$). (3) There was no statistical difference in the dropout rate (low-quality evidence) and adverse effects (moderate-quality evidence) between the rTMS group and the control group.

Conclusion: rTMS improved overall swallowing function and activity of daily living ability and reduced aspiration in post-stroke patients with good acceptability and mild adverse effects.

Keywords: deglutition disorders, transcranial magnetic stimulation, stroke, meta-analysis, systematic review

INTRODUCTION

Stroke, as a common cerebrovascular disease, is the primary cause of disability worldwide (Gorelick, 2019). About 19-81% of survivors after stroke are left with dysphagia, which is characterized by varing degree of eating disorders, choking cough, salivation and abnormal pronunciation (Martino et al., 2005; Suntrup et al., 2015). Dysphagia is associated with increased risk of malnutrition and pneumonia, and leads to prolonged hospital stay, poor prognosis and mortality (Park et al., 2017; Pandian et al., 2018; Alamer et al., 2020). Therefore, the rehabilitation of post-stroke dysphagia is still an urgent clinical problem.

Repetitive transcranial magnetic stimulation (rTMS), as a non-invasive neuromodulation technique, is an emerging choice for post-stroke dysphagia (Lefaucheur et al., 2020). In general, rTMS can be divided into two main treatment protocols according to the stimulation frequency: low frequency ($\leq$1 Hz) and high frequency (>1 Hz). Low frequency rTMS (LF-rTMS) inhibits cortical excitability, while high frequency rTMS (HF-rTMS) activates cortical excitability (Lin et al., 2019). It is now recognized that rTMS can inhibit maladaptive cortical plasticity, improve adaptive cortical activity, and promote neurological recovery after stroke (Kobayashi and Pascual-Leone, 2003). According to the latest evidence-based guidelines for rTMS, rTMS has been proved to show the efficacy of A grade in treatment of depression, neuropathic pain, and upper limb dysfunction after stroke (Lefaucheur et al., 2020).

In recent years, several meta-analyses (Yang et al., 2015, 2021; Liao et al., 2017; Lin et al., 2019; Cheng et al., 2021; Li et al., 2021)

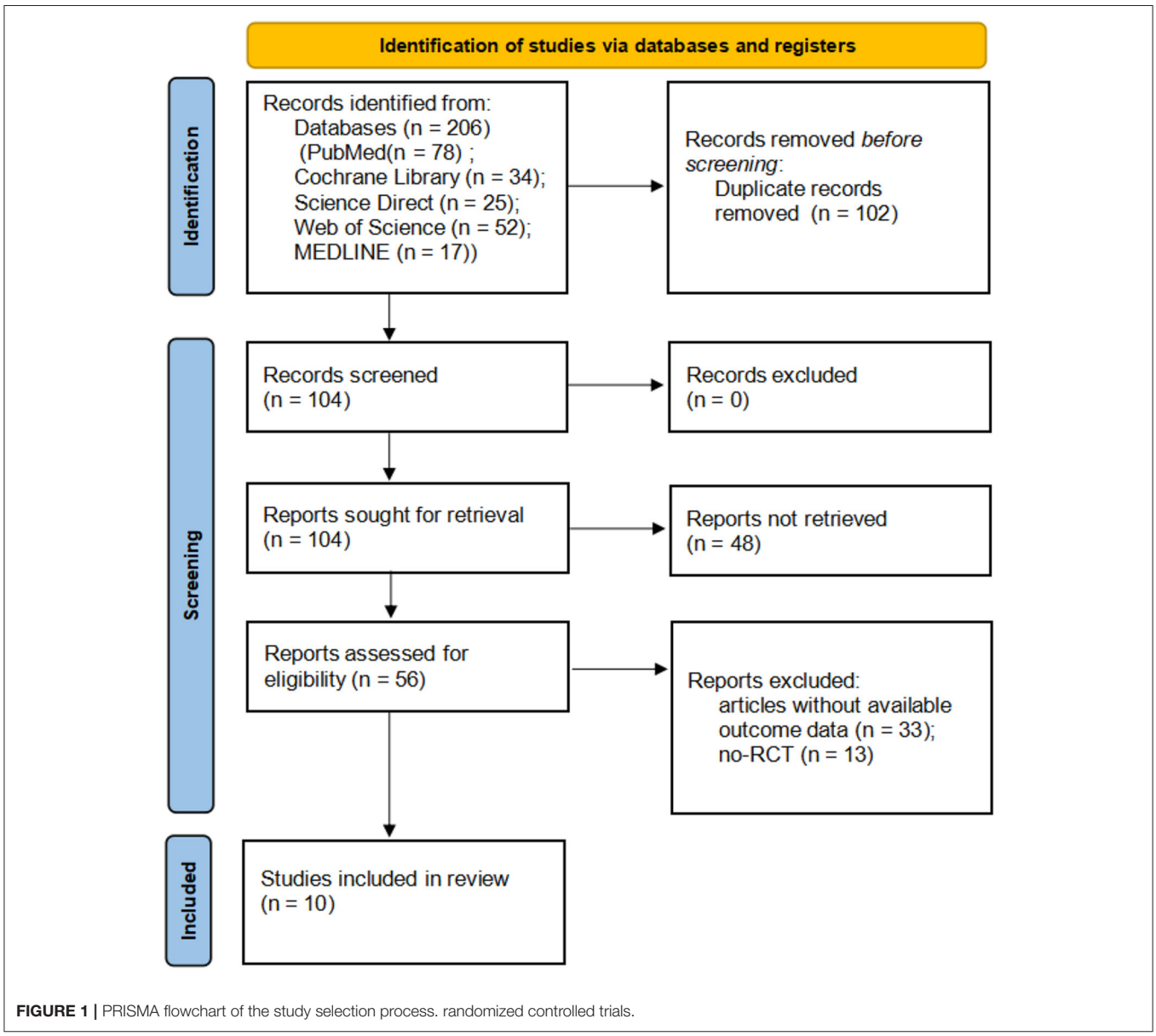

FIGURE 1 | PRISMA flowchart of the study selection process. randomized controlled trials.

TABLE 1 | Characteristics of the randomized controlled studies.

References	Intervention	Age (M ± SD)	Sample size (M/F)	Site for stimulation (esophageal cortical)	Stimulation parameters	Outcomes/ measure
Khedr et al. (2009)	Active rTMS	58.9 (11.7)	14	The ipsilesional hemisphere, esophageal motor cortex;	3 Hz, 120%MT, 10 min, 5 times	DD, BI, MEP, dropout rate
	Sham rTMS	56.2 (13.4)	12			
Khedr and Abo-Elfetoh (2010)	Active rTMS	LMI: 56.7 (16)	6/0	The bilateral hemisphere, esophageal motor cortex;	3 Hz, 130%MT, 10 min, 5 times	DD, BI
		Other: 55.4 (9.7)	2/3			
	Sham rTMS	LMI: 58 (17.5)	5/0			
		Other: 60.5 (11)	3/3			
Kim et al. (2011)	Sham rTMS	68.2 (12.6)	6/4	The ipsilesional hemisphere, mylohyoid motor cortex;	5 Hz, 100%MT, 20 min, 10 times	FDS, PAS, ASHA NOMS
	High-frequency rTMS	69.8 (8.0)	5/5			
	Low-frequency rTMS	66.4 (12.3)	6/4	The contralesional side, mylohyoid motor cortex;	1 Hz, 100%MT, 20 min, 10 times	
Park et al. (2013)	Active rTMS	73.7 (3.8)	5/4	The contralesional side, pharyngeal motor cortex;	5 Hz, 90%MT, 10 min, 10 times	VDS, PAS
	Sham rTMS	68.9 (9.3)	5/4			
Lim et al. (2014)	Active rTMS	62.5 (8.2)	14	The contralesional side, pharyngeal motor cortex;	1 Hz, 100%MT, 20 min, 10 times	FDS, PAS, PTT, ASHA NOMS, adverse effects, dropout rate
	Conventional dysphagia therapy	59.8 (11.8)	15			
Park et al. (2017)	Sham rTMS	69.6 (8.6)	7/4	The bilateral hemisphere, mylohyoid motor cortex;	10 Hz, 90%MT, 10 min, 10 times	VDS, PAS
	Bilateral rTMS	60.2 (13.8)	8/3			
	Unilateral rTMS	67.5 (13.4)	8/3	The ipsilesional hemisphere, mylohyoid motor cortex;		
Du et al. (2016)	Sham rTMS	58.83 (3.35)	6/6	The ipsilesional hemisphere, mylohyoid motor cortex;	3 Hz, 90%MT, 1200 pulses, 5 times	SSA, BI, DD, adverse effects, dropout rate
	High-frequency rTMS	58.2 (2.78)	13/2			
	Low-frequency rTMS	57.92 (2.47)	7/6	The contralesional side, mylohyoid motor cortex;	1 Hz, 100%MT, 1200 pulses, 5 times	
Unluer et al. (2019)	Active rTMS	67.8 (11.88)	9/6	The contralesional side, mylohyoid motor cortex;	1 Hz, 90%MT, 1200 pulses, 5 times	PAS, adverse effects, dropout rate
	Conventional dysphagia therapy	69.31 (12.89)	7/6			
Tarameshlu et al. (2019)	Active rTMS	55.33 (19.55)	4/2	The contralesional side, mylohyoid motor cortex;	1 Hz, 120%MT, 1200 pulses, 5 times	MASA, FOIS
	Conventional dysphagia therapy	76.67 (5.92)	5/1			
Cabib et al. (2020)	Active rTMS	70 (8.6)	12	The contralesional side, pharyngeal sensory cortex;	5 Hz, 90%MT, 250 pulses, 1 time	PAS, MEP, adverse effects
	Sham rTMS	70 (8.6)	12			

BI, Barthel Index Scale; DD, The degree of dysphagia; MEP, motor-evoked potential; LMI, Lateral medullary infarction; FDS, the Functional Dysphagia Scale; PAS, the Penetration Aspiration Scale; ASHA NOMS, the American Speech-Language Hearing Association National Outcomes Measurements System Swallowing Scale; VDS, the videofluoroscopic dysphagia scale; PTT, the pharyngeal transit time; SSA, the Standardized Swallowing Assessment; MASA, the Mann Assessment of Swallowing Ability; FOIS, the Functional Oral Intake Scale; IPES, intra-pharyngeal electrical stimulation.

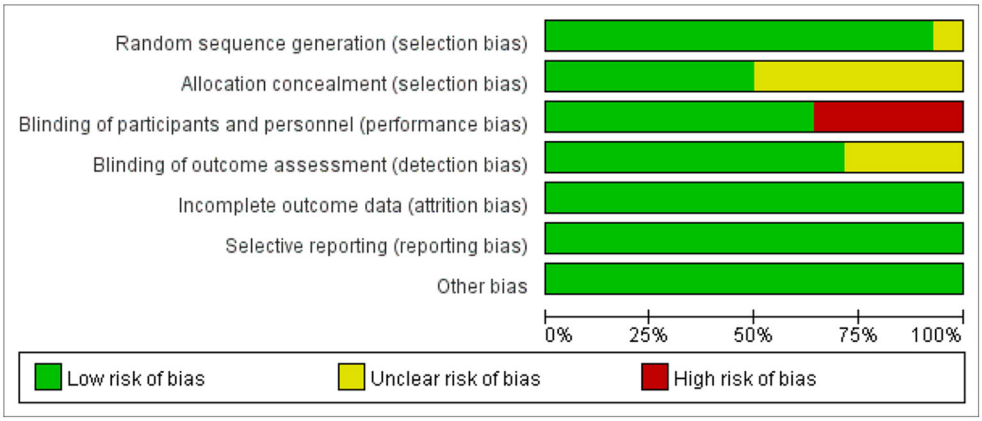

FIGURE 2 | Performance of each type of bias in all studies.

have investigated the effects of rTMS on post-stroke dysphagia, suggesting that rTMS may have beneficial effects on swallowing disorders. However, some of reviews focused on non-invasive brain stimulation (NIBS), including rTMS, transcranial Direct Current Stimulation (tDCS) and other kinds of stimulation, while few of reviews further analyzed the effects of stimulation site, frequency and stimulation time on dysphagia. A recent meta-analysis (Yang et al., 2021), partially affirming the effects of rTMS on post-stroke dysphagia, concluded in its subgroup analysis of intervention frequency that there was no statistically significant difference between either the high-frequency and low-frequency groups or the conventional training group, which may be related to incorrect data extraction and exclusion of some studies that met their inclusion criteria. A growing body of evidence supports the beneficial effects of transcranial magnetic stimulation on post-stroke dysphagia (Lefaucheur et al., 2020), but the relationship between transcranial magnetic stimulation and factors such as target, parameter settings, and treatment course remains to be further investigated. Therefore, this meta-analysis aims to provide the latest evidence on the effects of transcranial magnetic stimulation on post-stroke swallowing disorders.

MATERIALS AND METHODS

This work adhered to the Preferred Reporting Items for Systematic Reviews and Meta-Analyses (PRISMA) guidelines (Ardern et al., 2021).

Search Strategies

The following databases were searched to identify studies on the effect of rTMS on post-stroke dysphagia, published before December 20, 2021: PubMed, Cochrane Library, ScienceDirect, MEDLINE, and Web of Science for relevant studies. The English keywords used for the database searches were "stroke," "transcranial magnetic stimulation," "repetitive transcranial magnetic stimulation," "TMS," "rTMS," "deglutition disorders," and "dysphagia." The reference lists of identified articles were checked for other potential studies.

Inclusion and Exclusion Criteria

Two review authors independently assessed the methodological quality of the included studies. We recorded and resolved any disagreements through discussions with a third reviewer.

Clinical studies that meet the following criteria were included:

(1) All patients with ischemic or hemorrhagic stroke displayed definitive radiographic evidence of relevant pathology on magnetic resonance imaging (MRI) or computed tomography (CT);

(2) All participants were identified as having dysphagia;

(3) No participants had swallowing disorders caused by other diseases;

(4) Randomized controlled trials compared rTMS with sham stimulation or other routine rehabilitation training.

If data were repeated or shared in multiple studies, the study that best met the above criteria were considered. All published or unpublished studies were investigated. If the information required for the analysis could not be obtained from the publication, the author was contacted to obtain the necessary details.

Risk of Bias and Quality of Outcomes Assessment

Two review authors independently assessed the methodological quality of the included studies. A third reviewer recorded and resolved any disagreements. Each RCT used Cochrane's collaborative tools to assess the risk of bias, including adequacy of sequence generation, concealment of allocation, blinding of participants and personnel, blinding of result evaluators, incomplete results' data, selective reporting, and other biases (Higgins et al., 2011; Corbett et al., 2014). The Grading of Recommendations Assessment, Development and Evaluation (GRADE) guidelines for systematic reviews were used to evaluate the quality of outcomes (Guyatt et al., 2008).

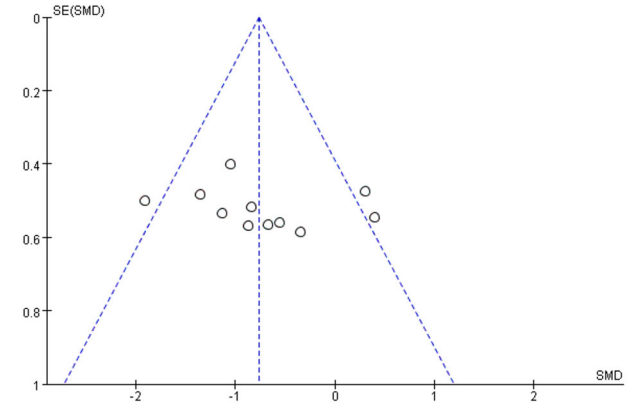

FIGURE 3 | Funnel plot for the publication bias of overall swallowing function.

Data Extraction

All searches and included studies were conducted by two independent reviewers. If there was any objection, a third reviewer made the final decision. The following data were extracted from the final included researches: basic study information (study authors, year of publication), participant characteristics (age, and sample size), rTMS parameters [stimulus site, true stimulus frequency, stimulus intensity (% of motor threshold (MT)), and treatment regimen], overall swallowing function and activity of daily living outcome measures, dropout rate, and adverse effects.

Outcome Indicators

Outcome measures for the efficacy of therapy were as follows: (1) DD (Dysphagia Grade); (2) Functional Dysphagia Scale (FDS); (3) Videofluoroscopic Dysphagia Scale (VDS); (4) Penetration Aspiration Scale (PAS); (5) Barthel index scale (BI); (6) dropout rate; (7) adverse effects.

The DD is a four-level score for the swallowing function according to patients' clinical manifestations (Khedr and Abo-Elfetoh, 2010). The FDS is a scale quantifying dysphagia severity (Han et al., 2001). The VDS, with a sum of 100 points, is a reliable, objective, and quantifiable predictor of long-term dysphagia after stroke (Kim et al., 2014). The PAS is an 8 point multidimensional indicator of airway invasion that measures selected aspects such as penetration and inhalation, depth of invasion into the delivery airway, and whether substances entering the airway are expelled (Martin-Harris et al., 2005). The higher the score of the above 4 scales, the worse the swallowing function. If dysphagia outcomes were reported from multiple time points, those from immediately after the intervention were obtained for meta-analysis.

Statistical Analyses

All statistical analysis used the RevMan 5.3 statistical software (The Nordic Cochrane Center, The Cochrane Collaboration, Copenhagen, Denmark), and the heterogeneity of different research results was tested by the overlap of confidence intervals and chi-square tests. When there was no heterogeneity in the test results, fixed-effect model was used for the meta-analysis, and when the test results were heterogeneous, the random-effect model was used. For enumeration data, the risk ratio (RR) and 95% confidence intervals (CIs) were used as the statistical tool for the efficacy analysis and the effect size, respectively. If substantial heterogeneity was detected ($I^2 > 50\%$), subgroup analysis or sensitivity analysis was conducted to determine the source of heterogeneity.

RESULTS

Search and Selection of Studies

The study selection process is shown in **Figure 1**. A total of 206 potential relevant studies were screened from six English-language databases using a relevant search strategy. Of these relevant studies, 102 duplicates were removed and the remaining 104 studies were further evaluated for eligibility. An additional 48 articles were removed after screening the title and abstract. Finally, after reviewing the full text of the remaining 56 articles, 46 articles were excluded, and a total of 10 studies were included.

Characteristics of the Included Studies

Table 1 shows the characteristics of the 10 studies included in this meta-analysis with a total of 246 participants (149 in the rTMS group and 109 in the control group). Participants all were identified dysphagia according to either the videofluoroscopic swallowing study (VFSS) or Fiberoptic endoscopic evaluation of swallowing (FEES). Four studies (Lim et al., 2014; Tarameshlu et al., 2019; Unluer et al., 2019; Cabib et al., 2020) used LF-rTMS; 4 studies (Khedr et al., 2009; Khedr and Abo-Elfetoh, 2010; Park et al., 2013, 2017) used HF-rTMS; and 2 studies (Kim et al., 2011; Du et al., 2016) compared the efficacy of LF-rTMS and HF-rTMS. rTMS stimulation sites included the ipsilesional hemisphere, the contralesional hemisphere, and the bilateral hemisphere. The interventions of control group included sham rTMS stimulation among 7 studies (Khedr et al., 2009; Khedr and Abo-Elfetoh, 2010; Kim et al., 2011; Park et al., 2013, 2017; Du et al., 2016; Cabib et al., 2020), and 3 studies (Lim et al., 2014; Tarameshlu et al., 2019; Unluer et al., 2019) with conventional therapy.

In terms of outcome measures, different dysphagia measurement tools were used to assess swallowing function within the same study or between studies. Overall swallowing function measures included DD [4 studies (Khedr et al., 2009; Khedr and Abo-Elfetoh, 2010; Du et al., 2016; Tarameshlu et al., 2019)], FDS [2 studies (Kim et al., 2011; Lim et al., 2014)], VDS [2 studies (Park et al., 2013, 2017)]. Aspiration was assessed by PAS [6 studies (Kim et al., 2011; Park et al., 2013, 2017; Lim et al., 2014; Unluer et al., 2019; Cabib et al., 2020)]. BI was used to assess activity of daily living.

Research Quality

In all included literature, some of articles designed two experimental groups based on parameters such as lesion site and stimulation frequency. According to this review, the two experimental groups did not interfere with each other in the same literature. Therefore, we treated each study in these three articles as a randomized controlled experiment. There was also one study that divided the patients into two randomized controlled

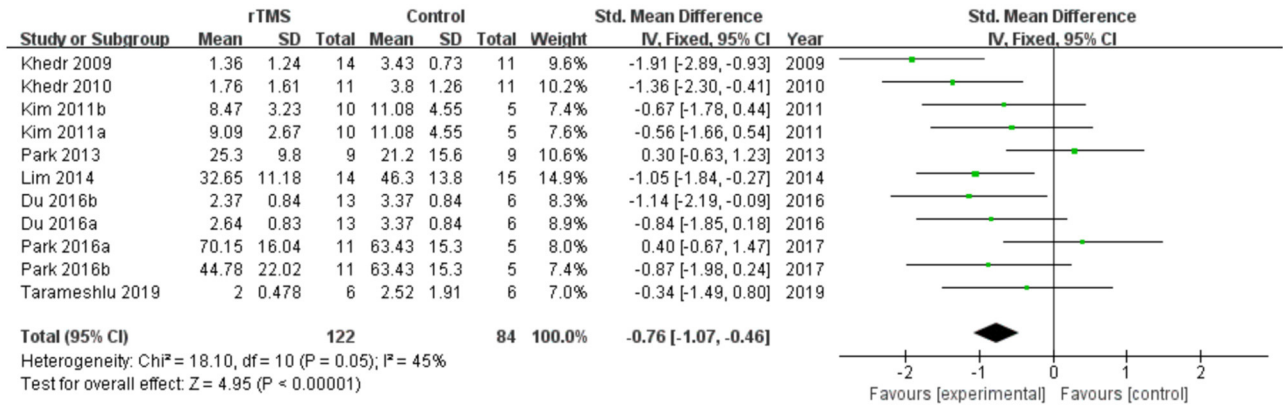

FIGURE 4 | Forest plot for overall swallowing function.

TABLE 2 | GRADE quality of evidence assessment of individual outcome indicators for the efficacy of repetitive transcranial magnetic stimulation in the treatment of dysphagia.

Outcome indicator	Number of participants	Heterogeneity		Model of analysis	Group effect value		Estimated value	95% CI	Grade
		I^2	*P*		Z	*P*			
Overall swallowing function	206 (11 RCT)	45%	0.05	Fixed effect	4.95	<0.0001	−0.76 (SMD)	−1.07,−0.46	Moderate
PAS	161 (8 RCT)	23%	0.24	Fixed effect	4.18	<0.0001	−1.03 (MD)	−1.51,−0.55	Low
BI	85 (3 RCT)	0%	0.89	Fixed effect	4.2	<0.0001	23.86 (MD)	12.73, 34.99	Moderate
Dropout rate	136 (4 RCT)	0%	0.53	Fixed effect	0.33	0.74	0.87 (RR)	0.38, 2.00	Low
Adverse effects	121 (4 RCT)	0%	0.91	Fixed effect	1.41	0.16	2.61 (RR)	0.69, 9.86	Moderate

RCT, randomized controlled trials; SMD, standardized mean difference; RR, relative risk; CI, confidence interval; PAS, Penetration Aspiration Scale; BI, Barthel index scale; GRADE, Grading of Recommendation Assessment, Development and Evaluation.

trials based on the site of the disease, and we combined and merged the data. We selected 13 studies from 10 articles. Two researchers assessed the quality of the 13 included studies. Data completeness was assured in a large extent, but 4 studies (Park et al., 2013; Lim et al., 2014; Unluer et al., 2019; Cabib et al., 2020) had performance bias (complete blinding of subjects was not achieved) (**Figure 2**). The number of this meta-analysis included is very small, so we could not use funnel plots to assess publication bias. Therefore, publication bias could not be completely eliminated.

Meta-Analysis of Treatment Effect

Overall Swallowing Function

Ten studies involving a total of 206 patients with post-stroke dysphagia evaluated the effect of rTMS on overall swallowing function. Heterogeneity of included studies was low ($I^2 = 45\%$), and therefore a fixed-effect model was used for meta-analysis. The funnel plot revealed significant symmetry (**Figure 3**). The simulated results showed that the rTMS significantly improved overall swallowing function compared to the control group (standard mean difference [SMD]−0.76, 95% confidence interval (CI)−1.07 to−0.46, $p < 0.0001$) (**Figure 4**). According to the GRADE, the overall level of evidence for the effect of rTMS on global swallowing function was "Moderate" (**Table 2**).

Subgroup Analysis of Overall Swallowing Function

Subgroup analyses were performed according to stimulus site (the ipsilesional hemisphere, the contralesional hemisphere, and the bilateral hemisphere). Subgroup analysis showed that the SMD for trials involving the "the ipsilesional hemisphere" stimulus was−0.74 (95% CI−1.69 to 0.20, $p = 0.12$) and for trials involving the "the contralesional hemisphere" stimulus was−0.59 (95% CI−1.14 to−0.05, $p = 0.03$). The mean effect size for trials involving "the bilateral hemisphere" stimulus was−1.15 (95% CI−1.87 to−0.43) (**Figure 5**). Stimulation of the bilateral hemisphere may produce better therapeutic effects on overall swallowing function. Subgroup analyses were performed according to stimulation frequency (LF-rTMS, HF-rTMS). Subgroup analysis showed a SMD of−0.70 (95% CI−1.33 to -−0.06) for the studies of HF-rTMS. The study of LF-rTMS showed a SMD of−0.86 (95% CI−1.16 to - 0.34). These results suggested that LF-rTMS treatment produced better effects on overall swallowing function than HF-rTMS treatment (**Figure 6**).

PAS

Seven studies involving a total of 161 patients with post-stroke dysphagia evaluated the effect of rTMS on PAS. Heterogeneity of included studies was low ($I^2 = 23\%$), and therefore a fixed-effect model was used. The simulated

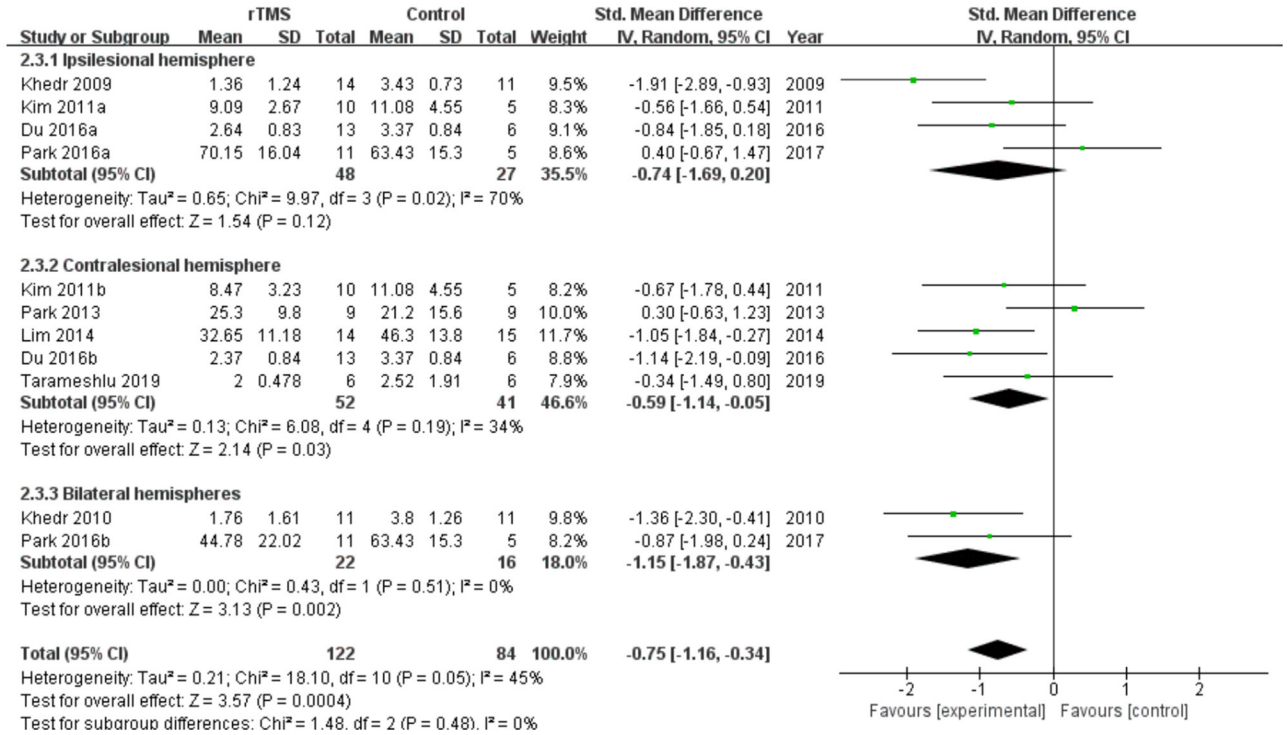

FIGURE 5 | Forest plot for subgroup analysis for overall swallowing function: ipsilesional hemisphere vs. contralesional hemisphere vs. bilateral hemispheres.

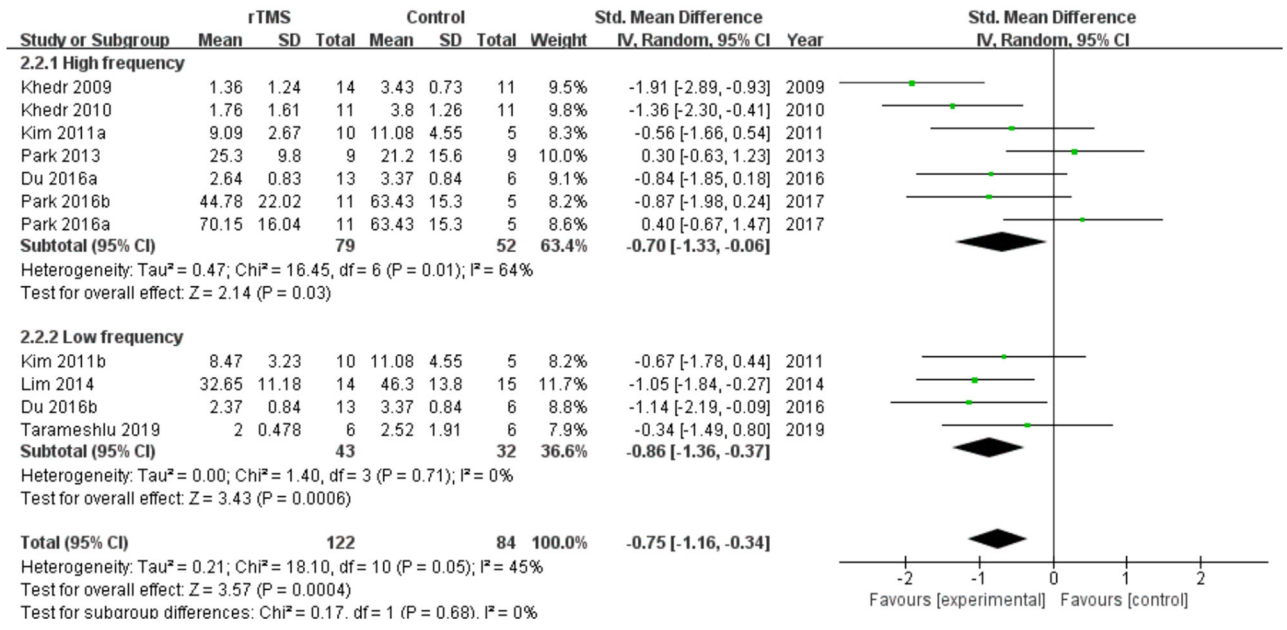

FIGURE 6 | Forest plot for subgroup analysis for overall swallowing function: low frequency transcranial magnetic stimulation vs. high frequency transcranial magnetic stimulation.

results showed that the rTMS significantly reduced accidental aspiration compared to the control group (mean difference [MD]−1.03, 95% CI−1.51 to−0.55, $p < 0.0001$) (**Figure 7**). According to the GRADE, the overall level of evidence for the effect of rTMS on PAS was "Low" (**Table 2**).

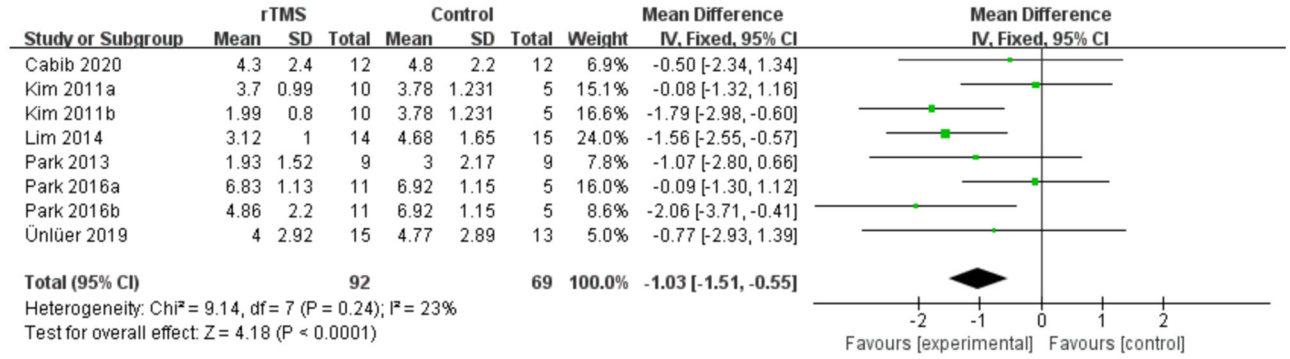

FIGURE 7 | Forest plot for subgroup analysis for Penetration Aspiration Scale.

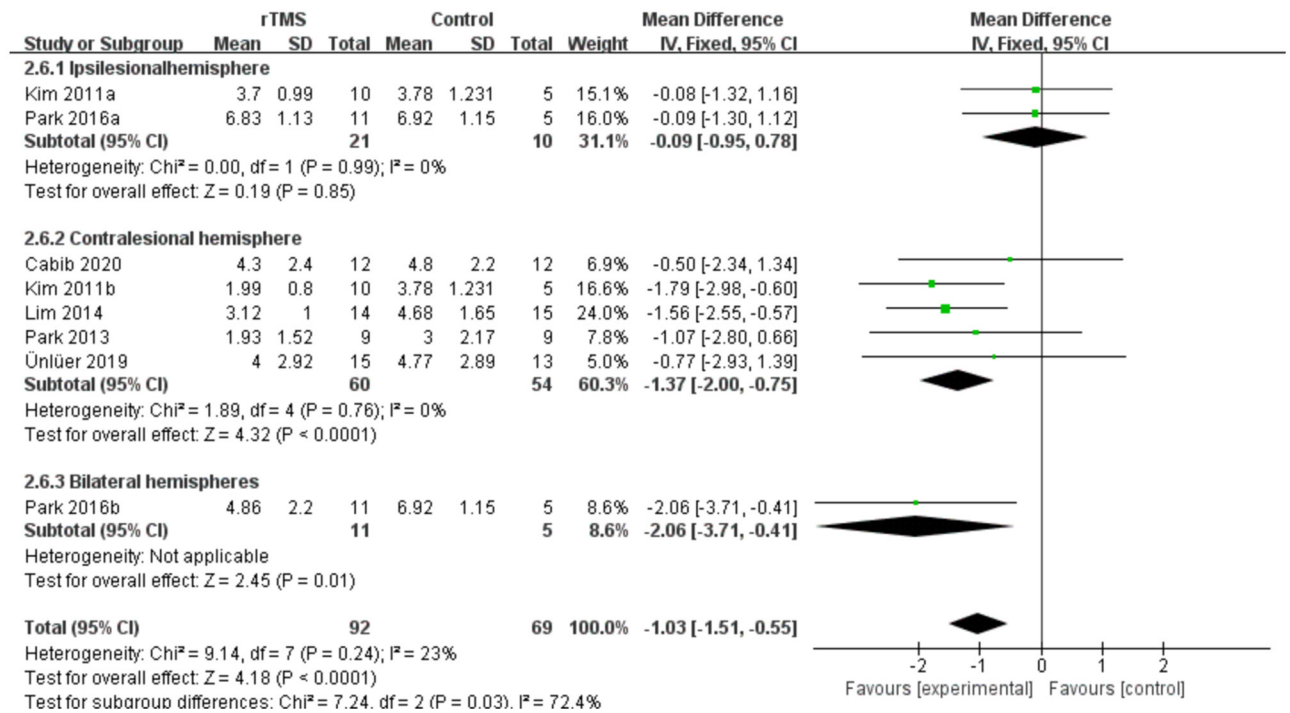

FIGURE 8 | Forest plot for subgroup analysis for Penetration Aspiration Scale: ipsilesional hemisphere vs. contralesional hemisphere vs. bilateral hemispheres.

Subgroup Analysis of PAS

Subgroup analyses were performed according to stimulus site (the ipsilesional hemisphere, the contralesional hemisphere, and the bilateral hemisphere). Subgroup analysis showed that the MD for trials involving the "the ipsilesional hemisphere" stimulus was−0.09 (95% CI−0.95 to 0.78, $p = 0.85$) and for trials involving the "the contralesional hemisphere" stimulus was−1.37 (95% CI−2.00 to−0.75, $p < 0.0001$). The MD for trials involving "the bilateral hemisphere" stimulus was−2.06 (95% CI−3.71 to−0.41) (**Figure 8**). Stimulation of the bilateral hemisphere may produce better therapeutic effects on overall swallowing function. Subgroup analyses were performed according to stimulation frequency (LF-rTMS, HF-rTMS). Subgroup analysis showed a MD of−0.60 (95% CI−1.31 to -−0.10) for the studies of HF-rTMS. The studies of LF-rTMS showed a SMD of−1.42 (95% CI−2.09 to - 0.75). These results suggest that LF-rTMS treatment produced better effects on overall swallowing function than HF-rTMS treatment (**Figure 9**).

BI

Four studies involving a total of 137 patients with post-stroke dysphagia evaluated the effect of rTMS on BI. Heterogeneity of included studies was low ($I^2 = 0\%$), and therefore a fixed-effect model was used for meta-analysis. The simulated results showed that the rTMS significantly improved activity of daily living compared to the control group (MD 23.86, 95% CI 12.73

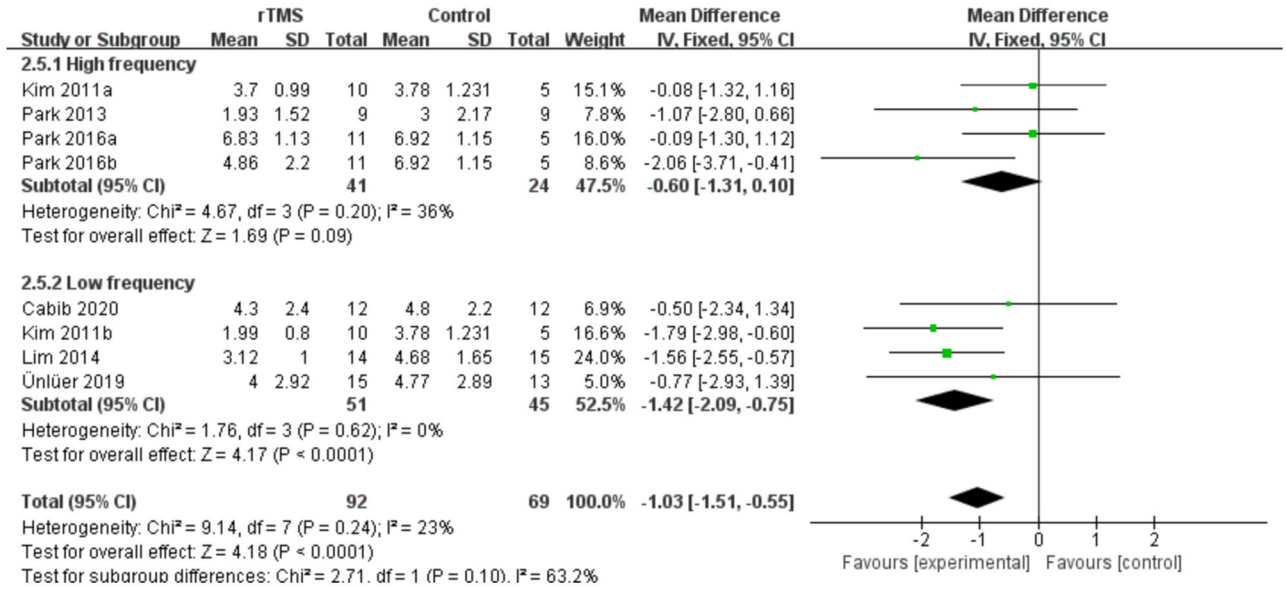

FIGURE 9 | Forest plot for subgroup analysis for Penetration Aspiration Scale: low frequency Transcranial Magnetic Stimulation vs. high frequency Transcranial Magnetic Stimulation.

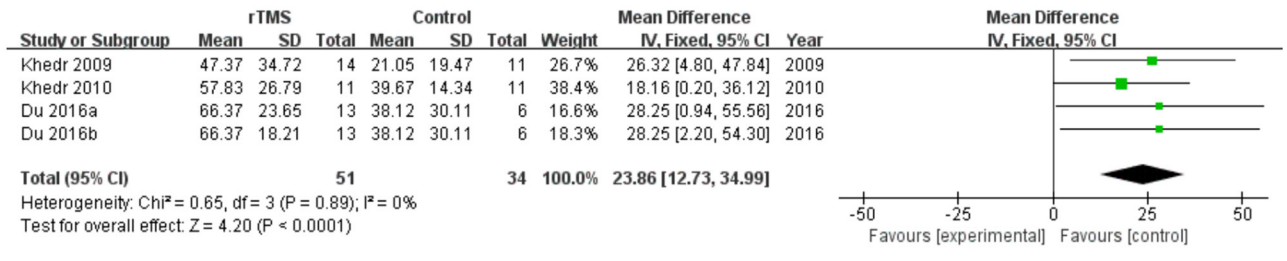

FIGURE 10 | Forest plot for subgroup analysis for Barthel index scale.

to 34.99, $p < 0.0001$) (**Figure 10**). According to the GRADE, the overall level of evidence for the effect of rTMS on BI was "Moderate" (**Table 2**).

Meta-Analysis of Dropout Rate

Four studies involving a total of 136 patients with post-stroke dysphagia evaluated the effect of rTMS on dropout rate. Heterogeneity of included studies was low ($I^2 = 0\%$), and therefore a fixed-effect model was used for meta-analysis. The results showed no differences in dropout rate between the rTMS group and the control group (RR 0.87, 95% CI 0.38 to 2.00, $p = 0.74$) (**Figure 11**). According to the GRADE, the overall level of evidence for the effect of rTMS on dropout rate was "Low" (**Table 2**).

Meta-Analysis of Adverse Effects

No serious adverse reactions were reported in any of the included studies. Four studies reported minor adverse reactions. Seven of 67 patients in the rTMS group and 1 of 54 patients in the control group reported discomfort. Other adverse reactions included headache, dizziness, pain at the site of irritation, and tinnitus. There was no heterogeneity between studies ($I^2 = 0\%$). The results showed no differences in adverse effects between the rTMS group and the control group (RR 2.61, 95% CI 0.69 to 9.86, $p = 0.16$) (**Figure 12**). According to the GRADE, the overall level of evidence for the effect of rTMS on adverse effects was "Moderate" (**Table 2**).

DISCUSSION

This meta-analysis identified 10 studies including a total of 246 patients with post-stroke dysphagia, 149 of whom received 5 to 10 sessions of active rTMS and 109 of whom received sham rTMS or swallowing training. Overall, the results of our meta-analysis supported the benefits of rTMS on overall dysphagia function (moderate-quality evidence) and which reduced instances of aspiration (low-quality evidence) and improved activity of daily living (moderate-quality evidence) for patients with post-stroke dysphagia. rTMS was found to be safe and have no serious adverse effects reported.

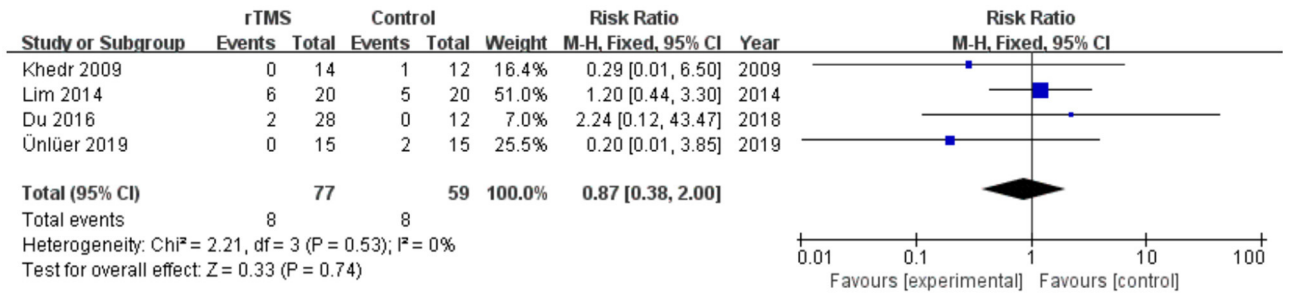

FIGURE 11 | Forest plot for subgroup analysis for Dropout Rate.

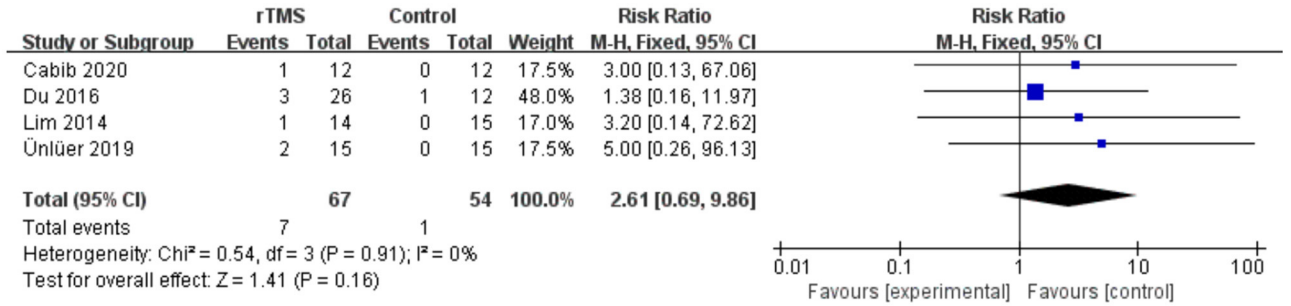

FIGURE 12 | Forest plot for subgroup analysis for Adverse Effects.

Our meta-analysis suggested that rTMS improved swallowing function in post-stroke patients and the heterogeneity of all outcome indicators remained small (I^2 < 50%). The funnel plot was symmetrical, suggesting no publication bias in the included studies. The pooled results were generally consistent with previous reviews (Liao et al., 2017; Cheng et al., 2021; Wang et al., 2021), which reported a positive effect of rTMS on recovery from post-stroke dysphagia. The difference from the above studies was that we included only studies in which rTMS was compared with sham stimulation or conventional swallowing treatment, excluding the effect of other types such as NIBS on post-stroke dysphagia.

To reduce potential heterogeneity, we further performed subgroup analysis based on stimulation site and stimulation frequency. Stimulation location subgroup analysis showed that rTMS of the bilateral hemisphere and the contralesional hemisphere significantly improved swallowing function after stroke. In contrast, rTMS of the ipsilesional hemisphere produced lower effect values and the results of the meta-analysis suggested that stimulation of the ipsilesional hemisphere was ineffective, in agreement with the results of the meta-analysis by Liao et al. (2017) and Cheng et al. (2021). Momosaki et al. (2014) reported that 3 Hz rTMS of the bilateral pharyngeal motor cortex resulted in significant recovery on post-stroke dysphagia. Tarameshlu et al. (2019) and Unluer et al. (2019) found that rTMS was effective in improving post-stroke dysphagia and swallowing coordination after stimulation of the unaffected hemisphere. In a randomized controlled trial (Park et al., 2017), Park et al. showed no effect of high-frequency rTMS of the affected hemisphere on swallowing function. However, Du et al. (2016) observed a positive effect of rTMS of the affected hemisphere on swallowing disorders. Therefore, more studies are needed to further validate the effects of rTMS on the affected hemisphere.

Within-frequency subgroup analysis showed that LF-rTMS produced greater effect values than HF-rTMS, suggesting that LF-rTMS is more effective than HF-rTMS on swallowing disorders, which is consistent with the results of Cheng et al. (2021). Kim et al. (2011) conducted a RCT comparing LF-rTMS and HF-rTMS in improving post-stroke dysphagia and found that the effect of LF-rTMS was significant compared with HF-rTMS. In contrast, a meta-analysis by Liao et al. (2017) concluded that the effect size of the HF-rTMS subgroup was greater than that of the LF-rTMS subgroup. This may be related to its early publication and the inclusion of only six studies. Also, we found that the results of our subgroup analysis were not fully consistent with the results of some meta-analyses. Yang et al. (2021) found a simulated effect size SMD = 0.65 (95% CI = 0.04 - 1.26, p = 0.04) for rTMS, suggesting that rTMS treatment was superior to conventional treatment. However, subgroup analysis showed no statistical difference between LF-rTMS and HF-rTMS and the conventional training group. This is slightly different from our results, that rTMS showed a significant improvement in overall swallowing function in our pooled analysis, and was also effective in both groups in the subgroup analysis. This may be related to the fact that the review by Yang et al. missed some of the studies that met their inclusion criteria.

Recovery of impaired swallowing function after stroke is complex. Functional magnetic resonance imaging studies suggest

that swallowing function may be associated with primary motor sensory cortex, insula, cingulate gyrus, prefrontal cortex, temporal lobe and occipital areas (Mihai et al., 2014, 2016). After stroke, if the injury involves the cortical brainstem tract, medulla oblongata reticular structure or nerve nucleus, the swallowing muscles will not work properly, thus affecting swallowing function (Wilmskoetter et al., 2020). The corticomedullary is the bridge between the brainstem and the swallowing cortex, and a study by Michou et al. confirmed that increased excitability of the corticomedullary was associated with improved swallowing safety (Mihai et al., 2014). Hamdy et al. shown the human swallowing system is bilaterally innervated and is asymmetric (Hamdy et al., 1996). The bilateral cerebral hemispheres maintain normal swallowing function by inhibiting homeostasis through the interaction of the corpus callosum (Lefaucheur et al., 2020). Hamdy et al. also suggested that reorganization of the contralateral pharyngeal cortex was associated with recovery of swallowing function, which demonstrates the role of intact hemispheric reorganization in the recovery of swallowing function after stroke (Hamdy et al., 1998; Fraser et al., 2002).

Therefore, different stimulation protocols will improve post-stroke swallowing disorders through different pathways. First, in unilateral cortical stimulation protocols, current mainstream studies are generally based on the interhemispheric inhibition model, such as Tarameshlu et al. (2019) and Khedr and Abo-Elfetoh (2010) included in our meta-analysis. This theory suggests that the damaged hemisphere decreases excitatory output after brain injury, while the unaffected hemisphere produces excessive inhibition on the affected hemisphere, resulting in various functional impairments (Alia et al., 2017). LF-rTMS stimulates the contralesional hemisphere to produce a long-term depression effect or HF-rTMS stimulates the ipsilesional hemisphere to produce a long-term potentiation effect, thus bringing the rebalance. The long term potentiation effect of HF-rTMS of the ipsilesional hemisphere can bring the imbalanced cortical excitability back to balance, thus improving the function (Lefaucheur et al., 2020). This theory has been widely applied to various types of NIBS, but it can only partially explain the results obtained from our subgroup analysis.

Again, in the compensatory model it was noted that the recovery of dysfunction after brain injury may be related to compensatory reorganization in the unaffected hemisphere, and stimulation of the unaffected hemisphere with HF-rTMS may facilitate the emergence of this compensation and contribute to the recovery of swallowing function (Hamdy et al., 1998). However, our results in the subgroup analysis of overall swallowing function showed that the SMD of HF-rTMS (-0.70, $P = 0.03$) was smaller than LF-rTMS (-0.86, $P = 0.0006$); the subgroup analysis in PAS showed no significant effect of HF-rTMS ($P = 0.09$). At the same time, some of the studies (Park et al., 2013, 2017) included in this review used this model and did not observe any significant improvement in swallowing disorders. Therefore, it's rational to suspect that the mechanism of recovery from dysphagia after stroke is more complex than the interhemispheric inhibition model or the compensatory model.

In addition to this, a bimodal balance-recovery model has recently been proposed to describe the process of neuroplastic changes after stroke. This model incorporates the concept of "structural reserve"; if the brain has extensive damage and low structural reserve, then input from the unaffected hemisphere will be critical to replace the lost function; and conversely, if the structural reserve is high, then neural stimulation based on the interhemispheric inhibition model may be more appropriate (Sankarasubramanian et al., 2017). This provides a possible explanation for our conclusion. We found that bilateral stimulation was more effective than unilateral stimulation in some studies, and we considered that the use of transcranial magnetic stimulation in both hemispheres could produce a significant swallowing recovery effect by promoting plasticity in both hemispheres. We have found similar results in rTMS to improve other types of post-stroke dysfunction. For example, Jiang et al. (2020) observed higher effect values for the bilateral hemisphere compared to unilateral hemisphere stimulation in a meta-analysis of rTMS improvement of cognitive dysfunction. However, few studies have done the subgroup analyse according to degree of injury because the recruited patients had different degrees of brain injury. Raw data were also very difficult to obtain, so it was difficult for us to analyze them in subgroups according to different levels of injury. Future studies should be conducted in further subgroups according to different injury levels and time of stroke onset to explore the development of individualized treatment plans for patients.

In activity of daily living ability, we found significant improvement in the rTMS group, which is consistent with the studies of Liu et al. (2021) and Sui et al. (2021) rTMS can further improve hand function and cognitive function after stroke, thus further improving patients' motor ability and activity of daily living ability (Lefaucheur et al., 2020; Sharma et al., 2020).

In terms of treatment acceptability, the results of this study suggest that rTMS treatment was well-tolerated and there was no significant difference in the dropout rate between the rTMS treatment group and the control group. The reasons for follow-up failure were not mainly related to rTMS treatment, and no serious adverse effects were reported in any of the included trials. On the other hand, adverse reactions associated with rTMS were rare and mild, although patients in the rTMS-treated group were more likely to experience adverse reactions than the control group. The most common were transient headache and dizziness.

LIMITATIONS

Several limitations should be considered when interpreting the results of the current study. First, the small sample size (12–29) of the included studies may limit the statistical power to detect the effects of rTMS on swallowing function in patients with post-stroke dysphagia. Second, there was considerable heterogeneity in the stimulation parameters (frequency, intensity and pulse) in the included studies. Therefore, the optimal stimulation parameters for rTMS are not clear. Third, our paper only performed subgroup analyses for frequency and stimulation site, but there was heterogeneity in the results of some of the subgroup analyses. The efficacy of rTMS may also be influenced by other parameters, such as brain injury severity and time to stroke onset.

CONCLUSION

In conclusion, this meta-analysis study suggests that rTMS has a favorable effect on swallowing function in patients with post-stroke dysphagia. However, there are many parameters that can influence the efficacy, such as the frequency and the site of stimulation. Further research on the mechanism of rTMS and the setting of optimal parameters will be important for the development of this novel intervention in clinical practice.

DATA AVAILABILITY STATEMENT

The original contributions presented in the study are included in the article/supplementary material, further inquiries can be directed to the corresponding author/s.

AUTHOR CONTRIBUTIONS

Y-lX and SW were responsible for the literature screening and data extraction. SW, J-mJ, and Y-hX were responsible for risk of bias assessment. Y-lX and XC were responsible for statistical analysis and writing up the article. WQ and Y-xW were responsible for planning and guidance on this paper. All authors contributed to the article and approved the submitted version.

FUNDING

This work was supported by Sichuan Medical Research Project Plan [Q18038]; Research and Development Project of Affiliated Hospital of North Sichuan Medical College [2021ZD014] and China Nanchong City-School Cooperative Scientific Research Special Fund [19SXHZ0103].

REFERENCES

Alamer, A., Melese, H., and Nigussie, F. (2020). Effectiveness of neuromuscular electrical stimulation on post-stroke dysphagia: a systematic review of randomized controlled trials. *Clin. Interv. Aging.* 15, 1521–1531. doi: 10.2147/CIA.S262596

Alia, C., Spalletti, C., Lai, S., Panarese, A., Lamola, G., Bertolucci, F., et al. (2017). Neuroplastic changes following brain ischemia and their contribution to stroke recovery: novel approaches in neurorehabilitation. *Front. Cell. Neurosci.* 11, 76. doi: 10.3389/fncel.2017.00076

Ardern, C. L., Buttner, F., Andrade, R., Weir, A., Ashe, M. C., Holden, S., et al. (2021). Implementing the 27 PRISMA 2020 Statement items for systematic reviews in the sport and exercise medicine, musculoskeletal rehabilitation and sports science fields: the PERSiST (implementing Prisma in Exercise, Rehabilitation, Sport medicine and SporTs science) guidance. *Br. J. Sports Med.* 56:e103987. doi: 10.1136/bjsports-2021-103987

Cabib, C., Nascimento, W., Rofes, L., Arreola, V., Tomsen, N., Mundet, L., et al. (2020). Short-term neurophysiological effects of sensory pathway neurorehabilitation strategies on chronic poststroke oropharyngeal dysphagia. *Neurogastroenterol. Motil.* 32:e13887. doi: 10.1111/nmo.13887

Cheng, I., Sasegbon, A., and Hamdy, S. (2021). Effects of neurostimulation on poststroke dysphagia: a synthesis of current evidence from randomized controlled trials. *Neuromodulation* 24, 1388–1401. doi: 10.1111/ner.13327

Corbett, M. S., Higgins, J. P., and Woolacott, N. F. (2014). Assessing baseline imbalance in randomised trials: implications for the Cochrane risk of bias tool. *Res. Synth. Methods* 5, 79–85. doi: 10.1002/jrsm.1090

Du, J., Yang, F., Liu, L., Hu, J., Cai, B., Liu, W., et al. (2016). Repetitive transcranial magnetic stimulation for rehabilitation of poststroke dysphagia: A randomized, double-blind clinical trial. *Clin. Neurophysiol.* 127, 1907–1913. doi: 10.1016/j.clinph.2015.11.045

Fraser, C., Power, M., Hamdy, S., Rothwell, J., Hobday, D., Hollander, I., et al. (2002). Driving plasticity in human adult motor cortex is associated with improved motor function after brain injury. *Neuron* 34, 831–840. doi: 10.1016/s0896-6273(02)00705-5

Gorelick, P. B. (2019). The global burden of stroke: persistent and disabling. *Lancet Neurol.* 18, 417–418. doi: 10.1016/S1474-4422(19)30030-4

Guyatt, G. H., Oxman, A. D., Vist, G. E., Kunz, R., Falck-Ytter, Y., Alonso-Coello, P., et al. (2008). GRADE: an emerging consensus on rating quality of evidence and strength of recommendations. *BMJ* 336, 924–926. doi: 10.1136/bmj.39489.470347.AD

Hamdy, S., Aziz, Q., Rothwell, J. C., Power, M., Singh, K. D., Nicholson, D. A., et al. (1998). Recovery of swallowing after dysphagic stroke relates to functional reorganization in the intact motor cortex. *Gastroenterology* 115, 1104–1112. doi: 10.1016/s0016-5085(98)70081-2

Hamdy, S., Aziz, Q., Rothwell, J. C., Singh, K. D., Barlow, J., Hughes, D. G., et al. (1996). The cortical topography of human swallowing musculature in health and disease. *Nat. Med.* 2, 1217–1224. doi: 10.1038/nm1196-1217

Han, T. R., Paik, N. J., and Park, J. W. (2001). Quantifying swallowing function after stroke: A functional dysphagia scale based on videofluoroscopic studies. *Arch. Phys. Med. Rehabil.* 82, 677–682. doi: 10.1053/apmr.2001.21939

Higgins, J. P., Altman, D. G., Gotzsche, P. C., Juni, P., Moher, D., Oxman, A. D., et al. (2011). The Cochrane Collaboration's tool for assessing risk of bias in randomised trials. *BMJ.* 343:d5928. doi: 10.1136/bmj.d5928

Jiang, L., Cui, H., Zhang, C., Cao, X., Gu, N., Zhu, Y., et al. (2020). Repetitive transcranial magnetic stimulation for improving cognitive function in patients with mild cognitive impairment: a systematic review. *Front. Aging Neurosci.* 12, 593000. doi: 10.3389/fnagi.2020.593000

Khedr, E. M., and Abo-Elfetoh, N. (2010). Therapeutic role of rTMS on recovery of dysphagia in patients with lateral medullary syndrome and brainstem infarction. *J. Neurol. Neurosurg. Psychiatry.* 81, 495–499. doi: 10.1136/jnnp.2009.188482

Khedr, E. M., Abo-Elfetoh, N., and Rothwell, J. C. (2009). Treatment of post-stroke dysphagia with repetitive transcranial magnetic stimulation. *Acta Neurol. Scand.* 119, 155–161. doi: 10.1111/j.1600-0404.2008.01093.x

Kim, J., Oh, B. M., Kim, J. Y., Lee, G. J., Lee, S. A., and Han, T. R. (2014). Validation of the videofluoroscopic dysphagia scale in various etiologies. *Dysphagia* 29, 438–443. doi: 10.1007/s00455-014-9524-y

Kim, L., Chun, M. H., Kim, B. R., and Lee, S. J. (2011). Effect of repetitive transcranial magnetic stimulation on patients with brain injury and Dysphagia. *Ann. Rehabil. Med.* 35, 765–771. doi: 10.5535/arm.2011.35.6.765

Kobayashi, M., and Pascual-Leone, A. (2003). Transcranial magnetic stimulation in neurology. *Lancet Neurol.* 2, 145–156. doi: 10.1016/s1474-4422(03)00321-1

Lefaucheur, J. P., Aleman, A., Baeken, C., Benninger, D. H., Brunelin, J., Di Lazzaro, V., et al. (2020). Evidence-based guidelines on the therapeutic use of repetitive transcranial magnetic stimulation (rTMS): An update (2014-2018). *Clin. Neurophysiol.* 131, 474–528. doi: 10.1016/j.clinph.2019.11.002

Li, L., Huang, H., Jia, Y., Yu, Y., Liu, Z., Shi, X., et al. (2021). Systematic review and network meta-analysis of noninvasive brain stimulation on dysphagia after stroke. *Neural Plast.* 2021:3831472. doi: 10.1155/2021/3831472

Liao, X., Xing, G., Guo, Z., Jin, Y., Tang, Q., He, B., et al. (2017). Repetitive transcranial magnetic stimulation as an alternative therapy for dysphagia after stroke: a systematic review and meta-analysis. *Clin. Rehabil.* 31, 289–298. doi: 10.1177/0269215516644771

Lim, K. B., Lee, H. J., Yoo, J., and Kwon, Y. G. (2014). Effect of low-frequency rTMS and NMES on subacute unilateral hemispheric stroke with dysphagia. *Ann. Rehabil. Med.* 38, 592–602. doi: 10.5535/arm.2014.38.5.592

Lin, Y., Jiang, W. J., Shan, P. Y., Lu, M., Wang, T., Li, R. H., et al. (2019). The role of repetitive transcranial magnetic stimulation (rTMS) in the treatment of cognitive impairment in patients with Alzheimer's disease: A systematic review and meta-analysis. *J. Neurol. Sci.* 398, 184–191. doi: 10.1016/j.jns.2019.01.038

Liu, Y., Li, H., Zhang, J., Zhao, Q. Q., Mei, H. N., and Ma, J. (2021). A meta-analysis: whether repetitive transcranial magnetic stimulation improves dysfunction caused by stroke with lower limb spasticity. *Evid. Based Complement. Alternat. Med.* 2021:7219293. doi: 10.1155/2021/7219293

Martin-Harris, B., Brodsky, M. B., Michel, Y., Ford, C. L., Walters, B., and Heffner, J. (2005). Breathing and swallowing dynamics across the adult lifespan. *Arch. Otolaryngol. Head Neck Surg.* 131, 762–770. doi: 10.1001/archotol.131.9.762

Martino, R., Foley, N., Bhogal, S., Diamant, N., Speechley, M., and Teasell, R. (2005). Dysphagia after stroke: incidence, diagnosis, and pulmonary complications. *Stroke* 36, 2756–2763. doi: 10.1161/01.STR.0000190056.76543.eb

Mihai, P. G., Otto, M., Domin, M., Platz, T., Hamdy, S., and Lotze, M. (2016). Brain imaging correlates of recovered swallowing after dysphagic stroke: A fMRI and DWI study. *Neuroimage Clin.* 12, 1013–1021. doi: 10.1016/j.nicl.2016.05.006

Mihai, P. G., Otto, M., Platz, T., Eickhoff, S. B., and Lotze, M. (2014). Sequential evolution of cortical activity and effective connectivity of swallowing using fMRI. *Hum. Brain Mapp.* 35, 5962–5973. doi: 10.1002/hbm.22597

Momosaki, R., Abo, M., and Kakuda, W. (2014). Bilateral repetitive transcranial magnetic stimulation combined with intensive swallowing rehabilitation for chronic stroke Dysphagia: a case series study. *Case Rep. Neurol.* 6, 60–67. doi: 10.1159/000360936

Pandian, J. D., Gall, S. L., Kate, M. P., Silva, G. S., Akinyemi, R. O., Ovbiagele, B. I., et al. (2018). Prevention of stroke: a global perspective. *Lancet* 392, 1269–1278. doi: 10.1016/S0140-6736(18)31269-8

Park, E., Kim, M. S., Chang, W. H., Oh, S. M., Kim, Y. K., Lee, A., et al. (2017). Effects of bilateral repetitive transcranial magnetic stimulation on post-stroke dysphagia. *Brain Stimul.* 10, 75–82. doi: 10.1016/j.brs.2016.08.005

Park, J. W., Oh, J. C., Lee, J. W., Yeo, J. S., and Ryu, K. H. (2013). The effect of 5Hz high-frequency rTMS over contralesional pharyngeal motor cortex in post-stroke oropharyngeal dysphagia: a randomized controlled study. *Neurogastroenterol. Motil.* 25, 324–e250. doi: 10.1111/nmo.12063

Sankarasubramanian, V., Machado, A. G., Conforto, A. B., Potter-Baker, K. A., Cunningham, D. A., Varnerin, N. M., et al. (2017). Inhibition versus facilitation of contralesional motor cortices in stroke: Deriving a model to tailor brain stimulation. *Clin. Neurophysiol.* 128, 892–902. doi: 10.1016/j.clinph.2017.03.030

Sharma, H., Vishnu, V. Y., Kumar, N., Sreenivas, V., Rajeswari, M. R., Bhatia, R., et al. (2020). Efficacy of low-frequency repetitive transcranial magnetic stimulation in ischemic stroke: a double-blind randomized controlled trial. *Arch. Rehabil. Res. Clin. Transl.* 2:100039. doi: 10.1016/j.arrct.2020.100039

Sui, Y. F., Tong, L. Q., Zhang, X. Y., Song, Z. H., and Guo, T. C. (2021). Effects of paired associated stimulation with different stimulation position on motor cortex excitability and upper limb motor function in patients with cerebral infarction. *J. Clin. Neurosci.* 90, 363–369. doi: 10.1016/j.jocn.2021.06.028

Suntrup, S., Kemmling, A., Warnecke, T., Hamacher, C., Oelenberg, S., Niederstadt, T., et al. (2015). The impact of lesion location on dysphagia incidence, pattern and complications in acute stroke. Part 1: dysphagia incidence, severity and aspiration. *Eur. J. Neurol.* 22, 832–838. doi: 10.1111/ene.12670

Tarameshlu, M., Ansari, N. N., Ghelichi, L., and Jalaei, S. (2019). The effect of repetitive transcranial magnetic stimulation combined with traditional dysphagia therapy on poststroke dysphagia: a pilot double-blinded randomized-controlled trial. *Int. J. Rehabil. Res.* 42, 133–138. doi: 10.1097/MRR.0000000000000336

Unluer, N. O., Temucin, C. M., Demir, N., Serel, A. S., and Karaduman, A. A. (2019). Effects of low-frequency repetitive transcranial magnetic stimulation on swallowing function and quality of life of post-stroke patients. *Dysphagia.* 34, 360–371. doi: 10.1007/s00455-018-09965-6

Wang, T., Dong, L., Cong, X., Luo, H., Li, W., Meng, P., et al. (2021). Comparative efficacy of non-invasive neurostimulation therapies for poststroke dysphagia: A systematic review and meta-analysis. *Neurophysiol. Clin.* 51, 493–506. doi: 10.1016/j.neucli.2021.02.006

Wilmskoetter, J., Daniels, S. K., and Miller, A. J. (2020). Cortical and subcortical control of swallowing-can we use information from lesion locations to improve diagnosis and treatment for patients with stroke? *Am. J. Speech Lang. Pathol.* 29, 1030–1043. doi: 10.1044/2019_AJSLP-19-00068

Yang, S. N., Pyun, S. B., Kim, H. J., Ahn, H. S., and Rhyu, B. J. (2015). Effectiveness of non-invasive brain stimulation in dysphagia subsequent to stroke: a systemic review and meta-analysis. *Dysphagia.* 30, 383–391. doi: 10.1007/s00455-015-9619-0

Yang, W., Cao, X., Zhang, X., Wang, X., Li, X., and Huai, Y. (2021). The effect of repetitive transcranial magnetic stimulation on dysphagia after stroke: a systematic review and meta-analysis. *Front. Neurosci.* 15, 769848. doi: 10.3389/fnins.2021.769848

Conflict of Interest: The authors declare that the research was conducted in the absence of any commercial or financial relationships that could be construed as a potential conflict of interest.

frontiers | Frontiers in Neuroscience

ORIGINAL RESEARCH
published: 02 June 2022
doi: 10.3389/fnins.2022.732156

Evaluation of Methods for the Extraction of Spatial Muscle Synergies

Kunkun Zhao[1†], Haiying Wen[1,2†], Zhisheng Zhang[1*], Manfredo Atzori[3,4], Henning Müller[3,5], Zhongqu Xie[1] and Alessandro Scano[6]*

[1] School of Mechanical Engineering, Southeast University, Nanjing, China, [2] Engineering Research Center of New Light Sources Technology and Equipment, Ministry of Education, Nanjing, China, [3] Information Systems Institute, University of Applied Sciences Western Switzerland (HES-SO Valais), Sierre, Switzerland, [4] Department of Neuroscience, University of Padova, Padua, Italy, [5] Medical Faculty, University of Geneva, Geneva, Switzerland, [6] UOS STIIMA Lecco – Human-Centered, Smart and Safe, Living Environment, Italian National Research Council (CNR), Lecco, Italy

Muscle synergies have been largely used in many application fields, including motor control studies, prosthesis control, movement classification, rehabilitation, and clinical studies. Due to the complexity of the motor control system, the full repertoire of the underlying synergies has been identified only for some classes of movements and scenarios. Several extraction methods have been used to extract muscle synergies. However, some of these methods may not effectively capture the nonlinear relationship between muscles and impose constraints on input signals or extracted synergies. Moreover, other approaches such as autoencoders (AEs), an unsupervised neural network, were recently introduced to study bioinspired control and movement classification. In this study, we evaluated the performance of five methods for the extraction of spatial muscle synergy, namely, principal component analysis (PCA), independent component analysis (ICA), factor analysis (FA), nonnegative matrix factorization (NMF), and AEs using simulated data and a publicly available database. To analyze the performance of the considered extraction methods with respect to several factors, we generated a comprehensive set of simulated data (ground truth), including spatial synergies and temporal coefficients. The signal-to-noise ratio (SNR) and the number of channels (NoC) varied when generating simulated data to evaluate their effects on ground truth reconstruction. This study also tested the efficacy of each synergy extraction method when coupled with standard classification methods, including K-nearest neighbors (KNN), linear discriminant analysis (LDA), support vector machines (SVM), and Random Forest (RF). The results showed that both SNR and NoC affected the outputs of the muscle synergy analysis. Although AEs showed better performance than FA in variance accounted for and PCA in synergy vector similarity and activation coefficient similarity, NMF and ICA outperformed the other three methods. Classification tasks showed that classification algorithms were sensitive to synergy extraction methods, while KNN and RF outperformed the other two methods for all extraction methods; in general, the classification accuracy of NMF and PCA was higher. Overall, the results suggest selecting suitable methods when performing muscle synergy-related analysis.

Keywords: autoencoder (AE), muscle synergy, non-negative matrix factorization (NMF), independent component analysis (ICA), factor analysis (FA), principal component analysis (PCA)

OPEN ACCESS

Edited by:
Haoyong Yu,
National University of Singapore, Singapore

Reviewed by:
Toshihiro Kawase,
Tokyo Denki University, Japan
Shi Xiaohua,
Shanghai Jiao Tong University, China

****Correspondence:***
Zhisheng Zhang
oldbc@seu.edu.cn
Haiying Wen
wenhy@seu.edu.cn

† These authors have contributed equally to this work

Specialty section:
This article was submitted to Neuroprosthetics, a section of the journal Frontiers in Neuroscience

Received: *28 June 2021*
Accepted: *04 May 2022*
Published: *02 June 2022*

Citation:
Zhao K, Wen H, Zhang Z, Atzori M, Müller H, Xie Z and Scano A (2022) Evaluation of Methods for the Extraction of Spatial Muscle Synergies. Front. Neurosci. 16:732156. doi: 10.3389/fnins.2022.732156

INTRODUCTION

Muscle synergy theory assumes that the central nervous system (CNS) achieves a variety of motor tasks by combining a few sets of synergies rather than controlling each muscle individually. Although the hypothesis is debated, an increasing number of studies in human and animals using stimulation and behavior experiments have verified the theory in the last decades (d'Avella et al., 2003; Cheung, 2005; Torres-Oviedo et al., 2006). Muscle synergies are usually estimated from electromyogram (EMG) recordings according to corresponding models. Several synergy models have been proposed, such as the time-invariant model (Tresch et al., 2006), the time-varying model (D'Avella et al., 2006), and the space-by-time model (Delis et al., 2018; Hilt et al., 2018), while most studies extracted muscle synergies based on the time-invariant spatial model (Clark et al., 2010; Israely et al., 2018; Scano et al., 2019; Cheung et al., 2020) using the non-negative matrix factorization (NMF) (Lee and Seung, 2001), in which time-invariant synergies with fixed weights among muscles were modulated by time-varying activation coefficients. Commonly used factorization methods to extract spatial muscle synergies also include principal component analysis (PCA) (Ranganathan and Krishnan, 2012), factor analysis (FA) (Tresch et al., 2006; Kieliba et al., 2018), and independent component analysis (ICA) (Rasool et al., 2016). A few variants of ICA such as a combination of PCA and ICA (ICAPCA), fast ICA (fICA) and probabilistic ICA (pICA), and second-order blind identification (SOBI) were also applied in some studies (Tresch et al., 2006; Steele et al., 2015; Ebied et al., 2018).

Despite the availability of these factorization methods in the literature, the most appropriate method for muscle synergy extraction was not clearly defined (Rabbi et al., 2020). Several studies have compared the performance of factorization methods for the identification of spatial muscles or kinematic synergies under various scenarios. Tresch et al. (2006) evaluated the performance of five matrix factorization methods (i.e., FA, ICA, NMF, ICAPCA, and pICA) using simulated data. The results showed that the performance of factorization methods was affected by the signal characteristics and the noise type. They reported that ICAPCA and pICA were the best methods; FA, ICA, and NMF had similar performance, followed by PCA. By comparing the performance of three factorization methods (i.e., PCA, ICA, and NMF) in identifying kinematic and muscle synergies in human reaching data, Lambert-Shirzad and Van der Loos (2017) found that PCA and NMF had a comparable performance on both EMG and joint motion data and both outperformed ICA. When FA, ICA, and NMF were used to extract muscle synergies in locomotor tasks (Ivanenko et al., 2005), similar weighting coefficients and temporal structures were reported among the three methods. Ebied et al. (2018) evaluated three factors [i.e., muscle synergy sparsity, level of the noise, and the number of channels (NoC)] on the effects of factorization methods (i.e., PCA, ICA, NMF, and SOBI) in the extraction of spatial muscle synergy. They found that, although SOBI had a better performance when a limited NoC was available, NMF had the best performance when the NoC was higher. Furthermore, Rabbi et al. (2020) reported that NMF was the most appropriate extraction method in walking and running conditions by comparing four extraction methods (i.e., NMF, PCA, ICA, and FA). By comparing the results of previous studies, we learned that the performance of factorization methods was not always consistent under various settings and scenarios. Although these methods can reconstruct a high variance accounted for (VAF) with a proper number of synergies, they cannot represent non-linear relations between muscles in the extracted synergies, such as the agonist-antagonist relationships (Spüler et al., 2016). Besides, the studies were limited to synergy extraction analysis (input space); other desired tasks (task space), such as synergy-based classification, were less explored.

In the past decades, neural networks and deep learning-based methods have used surprisingly well in physiological and biomedical applications (Buongiorno et al., 2019b). Autoencoders (AEs) as a type of unsupervised neural network have also been used in myoelectric control and pattern recognition. Lv et al. (2018) reported that the AE was not sensitive to the electrode shift compared with time-domain and autoregressive features in classification tasks and achieved a lower classification error. Muhammad et al. also found that the stacked sparse AE outperformed the linear discriminant analysis (LDA) in hand motion classification whether in within-day or between-day analysis (Zia ur Rehman et al., 2018). In myoelectric control, Yu et al. (2019) achieved a promising wrist torque estimation under isometric contraction based on a stack-AE, with the potential of providing intuitive and dexterous control of artificial limbs (Vujaklija et al., 2018). In terms of synergy extraction, Spüler et al. (2016) first used AEs to extract muscle synergies and described the agonist-antagonist relationships among muscles using simulated data and real EMG data. They found that AEs had a significantly better fit to the data than other methods, including NMF, ICA, and PCA. De Feudis et al. (2021) used AEs to extract kinematic synergies and reported a comparable result with the PCA. By comparing with the NMF, the most frequently used method for muscle synergy extraction in the literature, Buongiorno et al. (2019a, 2020) showed that the AEs outperformed the state-of-art synergy-based force/moment estimation methods at the expense of the EMG reconstruction quality. These studies described the potential of the AEs in myoelectric control as a bioinspired approach (Camardella et al., 2019) for muscle synergy extraction. To the best of our knowledge, few articles systematically compared and analyzed the performance of the AEs in muscle synergy extraction with other commonly used methods.

From the preliminary studies comparing several methods for extracting synergies (Tresch et al., 2006; Ebied et al., 2018), we noted a growing interest in the identification of the most suitable methods for extracting synergies and their properties also in the recent literature. These approaches include recent algorithms such as AEs (Spüler et al., 2016) and mixed-matrix factorization (Scano et al., 2022). In this study, we focused on comparing the capabilities of five factorization methods (i.e., PCA, ICA, FA, NMF, and AE) used for the extraction of spatial muscle synergy. Specifically, we evaluated the performance of AE in synergy extraction to the other four commonly used methods in

the literature. We further explored the influence of the signal-to-noise ratio (SNR, i.e., noise) and the NoC on synergy extraction methods based on simulated data. Considering the wide usage of the synergy-based methods in myoelectric control, robotic control, and rehabilitation, we expanded toward comparisons between extraction methods to evaluate their performance in classification tasks. Muscle synergies extracted from a publicly available NinaPro dataset (Atzori et al., 2014, 2015), already employed previously for synergy extraction (Pale et al., 2020), were input into four classification algorithms, namely, K-nearest neighbor (KNN), LDA, support vector machine (SVM), and random forest (RF). Classification accuracy was used to assess the performance of each extraction method in the task space.

MATERIALS AND METHODS

An overview of the study design is reported in **Figure 1**. In this study, simulated data were generated to represent the ground truth of synergy vectors W and temporal coefficients c according to specific criteria (see "Simulated Data" section). Ground truth data also spanned across varying NoC and SNR. Then, the performance analysis was performed. We first evaluated the performance of synergy extraction methods with simulated data. In this step, synergies extracted using five methods were compared with the original ground truth (simulated synergies and temporal coefficients). The VAF and similarity were used as indices to assess the performance. Then, we assessed the performance of extraction methods in classification tasks using a publicly available dataset (NinaPro). Similarly, we first extracted the synergies from public data using five extracting methods. Extracted synergies were then input into four classification algorithms (i.e., KNN, LDA, SVM, and RF) to identify movements. Classification accuracy was used to assess the performance.

Simulated Data

Simulated data were generated to evaluate the performance of the synergy extraction methods (**Figure 1**). According to previous studies, EMG activations are the combination of synergy vectors and activation coefficients, as shown in the following equation:

$$M = g\left(\sum_{i=1}^{k} w_i c_i + e\right), \tag{1}$$

where M is an m-by-n matrix, indicating m muscles and n samples, w_i (m-by-1) is the ith synergy vector, and c_i (1-by-n) is the corresponding activation coefficient. e is the Gaussian noise matrix. $y = g(x)$ is a threshold function with $y = 0$ for $x < 0$ and $y = x$ for $x \geq 0$, which ensures the non-negativity of the simulated data.

Our simulation began with the generation of the ground truth W and c. Synergy vectors W were randomly drawn from an exponential distribution [with a mean value of 10, similar to a previous study that reported that synergy vectors were roughly similar to the distribution observed in previous experimental data (Tresch et al., 2006)]. To hold the statistical properties of the EMG signals, the activation coefficients c were selected from the real EMG envelope signals randomly assigned from a set of reaching movements, in which ten upper limb muscle activities were recorded (Zhao et al., 2019). The raw EMG signals were preprocessed by moving the root mean square with a window size of 100 samples with 75% overlap, resampled to 1,000 sample points, and normalized to [0, 1] ($y = (x - x_{min})/(x_{max} - x_{min})$). Each synergy vector was also normalized to have a unit norm. Then, we obtained simulated muscle activations according to Eq. 1, which were later used to evaluate the performance of extraction methods.

Meanwhile, to evaluate the performance of extraction methods in different settings, two types of constraints were set when generating simulated data. We first randomly generated a set of synergies with varying dimensions [NoC, i.e., number of muscles (m)] by fixing the number of synergies (n), i.e., a matrix with dimension m-by-n. This setting was used to evaluate the performance of extraction methods when a limited number of EMG signals were recorded. In this study, four types of channels (i.e., Ch6, Ch8, Ch10, and Ch12) were evaluated. This setting covered the studies in which 8–12 muscle recordings were measured in their experiments. When generating the ground truth, four synergies were fixed in this study because previous studies in upper limb reaching movements reported that four synergies were sufficient to explain most of the variability of muscle activations (Israely et al., 2017). We, in this study, remark that any reasonable number of synergies could be chosen in principle. Then, Gaussian noise was added to the original signal with a specified the signal-to-noise ratio [$SNR = 10 \cdot lg(P_s/P_n)$, P_s and P_n are signal and noise power, respectively] when each dataset was generated. Three types of noise (with SNR 10, 15, and 20 dB) were covered in this study. We finally generated 24,000 ($20 \times 4 \times 3 \times 100$) trials that consisted of 20 datasets, and each dataset consisted of 100 trials for each setting.

Extraction Methods

Although the computation process of these extraction methods is different, they can be represented by the linear combination of a set of synergy vectors and corresponding activation coefficients as follows:

$$M = c \cdot W + e, \tag{2}$$

where M represents muscle activations (the processed EMG) and W and c are muscle synergies and activation coefficients, respectively. Although sharing the same model, each extraction method imposes different constraints on the input signals and extracted synergies. PCA constrains W to be orthogonal, and the first component has the largest variance. Both PCA and FA assume that the data are from Gaussian distributions, while ICA is designed to analyze non-Gaussian data. The number of common factors that can be assessed using FA is limited by the degrees of freedom in the model, that is $\left[(m-k)^2 - (m+k)\right] > 0$ (e.g., when four common factors are identified, the data have at least eight dimensions). NMF can be used for both Gaussian and non-Gaussian data but imposes a non-negativity constraint on the components of the extracted synergies. PCA, FA, and NMF were performed using the Matlab functions *pca*,

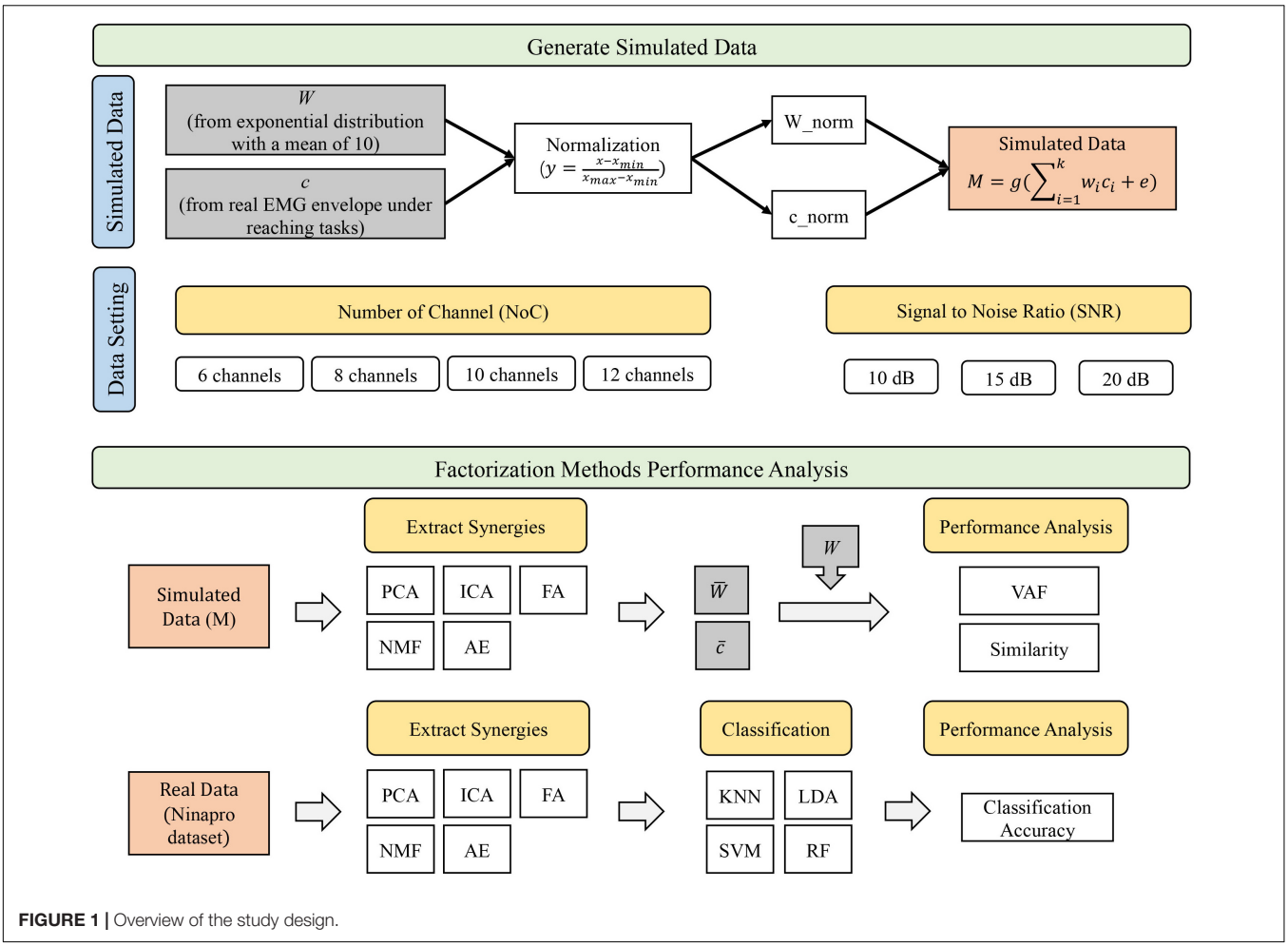

FIGURE 1 | Overview of the study design.

factoran, and *nnmf*, respectively. Singular value decomposition was used to identify the components in PCA. For FA, the weighted least-squares method was used to estimate the factor scores. Multiplication update rules proposed by Lee and Seung (2001) were applied in NMF. ICA was performed using the function *fastica* in the FastICA package (Hyvärinen and Oja, 1997; Hyvarinen, 1999).

Autoencoders consists of two main parts, namely, an encoder that captures the representative features contained in the input data and a decoder that reconstructs the input. According to different internal structures, five types of AEs are proposed, namely, undercomplete AE, regularized AE, sparse AE, denoising AE, and variational AE (De Feudis et al., 2021). In this study, an undercomplete AE (denoted as AE below) was used to learn some non-linear coupling information among muscles. The topology structure of the undercomplete AE is shown in **Figure 2**.

The Matlab function *trainscg* was used to train the AE. The training process was based on the optimization of a cost function, *msesparse*, which measured the error between the input and the output. The transfer functions of encode and decode were *satlin* and *purelin*, respectively (Buongiorno et al., 2019a, 2020).

We defined the weights and biases of the encoder (i.e., IW and Ib) and decoder (i.e., OW and Ob) (**Figure 2**). Muscle synergies are defined as OW, and activation coefficients c and reconstructed muscle activation $\tilde{M}$ are as follows:

$$\begin{cases} c = IW \times M + Ib \\ \tilde{M} = OW \times c + Ob \end{cases} \tag{3}$$

Performance Analysis

Two indices were used to assess the performance of the employed extraction methods, i.e., (1) variance accounted for calculated by each extraction method under various settings and (2) the similarity between original synergy vectors (and activation coefficients) and the synergies identified using the extraction methods.

First, we decided to extract four synergies from the simulated data using each extraction method. This choice was followed based on a previous study: when comparing several algorithms for synergy extraction, Tresch et al. (2006) reported that, in all cases, the algorithms were examined using four basis vectors to reconstruct each data set. More recently, Ebied et al. (2018) also reported that, in all settings, the number of synergies was fixed to four. This choice was also in line with the ground truth dimensionality. Moreover, fixing the number of synergies allowed us to compare synergies that have low influence from

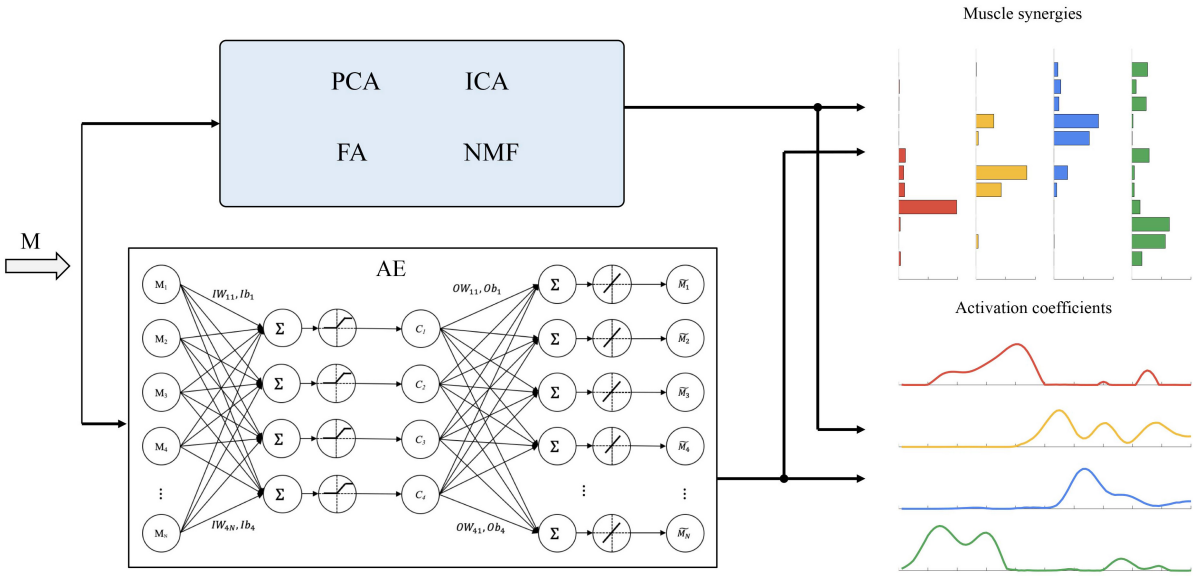

FIGURE 2 | Schematic representation of the extraction methods considered in this study. Principal component analysis (PCA), independent component analysis (ICA), factor analysis (FA), and non-negative matrix factorization (NMF) follow a similar procedure for synergy extraction, which factorizes muscle activations (M) into a set of muscle synergies and corresponding activation coefficients. The topology structure of the autoencoders used in this study is also shown.

merging or fractionation. The VAF from each extraction method was compared to assess the difference caused due to the varying settings.

Then, we matched the synergy vectors between the original simulated and the extracted ones by pairing together the two vectors from the original ground truth synergy vectors and the extracted, which has the largest absolute value of the dot product. In case that the largest value was negative, we reversed the sign of the synergy vectors identified using the extracting methods as in a previous study (Tresch et al., 2006). Then, the synergy vector similarity (SVS) and activation coefficient similarity (ACS) were computed by averaging the dot products among all matched synergy vectors and activation coefficients. We further calculated the principal angle (PA), which quantified the similarity between subspaces identified by original synergy vectors and the extracting methods. If the two subspaces are identical, the PAs between them will be zero.

Finally, to evaluate the influence of chance, 24,000 sets of synergy vectors and activation coefficients were randomly generated according to the same constraints used to generate the simulated data. We calculated and compared the similarity between the randomly generated synergy vectors and activation coefficients and the extracted ones.

Classification Tasks

As a further step in our study that is linked to the promising results of muscle synergy-based applications in classification and intuitive prosthetic control (Jiang et al., 2009, 2012, 2014; Ma et al., 2015), we were interested in quantifying the classification accuracy that can be achieved with classification algorithms when synergies extracted with different methods were used as inputs. We questioned which synergy extraction method can be suggested for classification problems when using standard classification algorithms. The NinaPro dataset 1 (Atzori et al., 2014, 2015) was used as the dataset for this study. It includes 53 movements from 27 intact subjects with ten muscles from the upper limb. Eight electrodes were uniformly placed beneath the elbow at a fixed distance from the radio-humeral joint, labeled incrementally counterclockwise starting from the flexor carpi ulnaris muscle (Pale et al., 2020), while the other two were placed on the flexor and extensor muscles (Atzori et al., 2012). These muscles cover the main forearm muscle groups involved in upper limb reach-to-grasp movements. Considering the importance of wrist movements in daily living and implementation in prosthesis control (Ma et al., 2015), a set of wrist-related movements (Ninapro dataset 1, Exercise B, Movement 11–16) were considered as classification movements in this study (Atzori et al., 2014), i.e., wrist supination/pronation, wrist flexion/extension, and wrist radial/ulnar deviation.

We first separated the EMG signals for each movement and each trial from the dataset for each subject. In this study, each trial represents the movement in the positive or negative direction of one degree of freedom, such as wrist flexion or extension. According to previous studies (Jiang et al., 2014; Vujaklija et al., 2018), thus, one synergy was extracted from each trial, while a total of two synergies were extracted for each degree of freedom, basically representing flexion and extension. Then, all extracted synergies were used to train four commonly used classification algorithms, namely, KNN (with five nearest neighbors and Euclidean distance was used for distance measurement; Matlab function, *fitcknn*) (Ebied et al., 2018), LDA (Matlab function, *fitcdiscr*) (Zia ur Rehman et al., 2018), SVMs (with linear kernel function; Matlab function, *fitcecoc*) (Atzori et al., 2012), and RFs (with 50 weak learners; Matlab function, *TreeBagger*)

(Atzori et al., 2014). The program performed a 5-fold cross-validation. The classification accuracy was computed to evaluate the performance of synergy extracting methods in the task space.

Statistical Analysis

To test if extraction methods and different settings affected the VAF and the similarity of synergies and activation coefficients, a statistical analysis was conducted. One-way ANOVA was first used to test the effect of SNR and NoC on VAF identified by each extraction method. A *post hoc* test (*t*-test) was run to quantify the statistical difference among settings (three types of SNR and four types of NoC).

Furthermore, one-way ANOVA and the Tukey-Kramer *post hoc* test were used to examine statistically significant differences of similarity obtained with different settings. We then used one-way ANOVA and the Tukey-Kramer *post hoc* test to test if classification algorithms had a significant influence on the classification accuracy for each extraction method. Matlab R2020b was used for statistical analysis. The significance level was set at $p = 0.05$.

RESULTS

Variance Accounted for Analysis

Figure 3 shows the VAF of five extraction methods under different SNR and NoC. We observed that NMF and ICA had a higher VAF value under both settings (i.e., SNR and NoC), followed by PCA. AE and FA both had an average VAF lower than 0.8. Statistical analysis showed that both SNR and NoC had a significant influence on VAF ($p < 0.001$). The VAF of four commonly used methods (i.e., PCA, ICA, FA, and NMF) showed an increasing trend with the increase of the SNR (i.e., the decrease in the noise level) while the VAF of AE decreased with the increase of the SNR. In contrast, the VAF of PCA, ICA, NMF, and AE decreased with the increase of the NoC. VAF of FA showed an apparent increase with the increase of both factors.

In terms of SNR, the *post hoc* test showed that the difference was significant ($p < 0.001$) for any two different SNR settings except AE, in which the significance level between 10 and 15 dB was $p = 0.128$. In contrast, for different NoC settings, there was no significant difference when the NoC was 10Ch and 12Ch for PCA, ICA, and NMF. In terms of FA and AE, statistical differences were observed for any two different NoC settings.

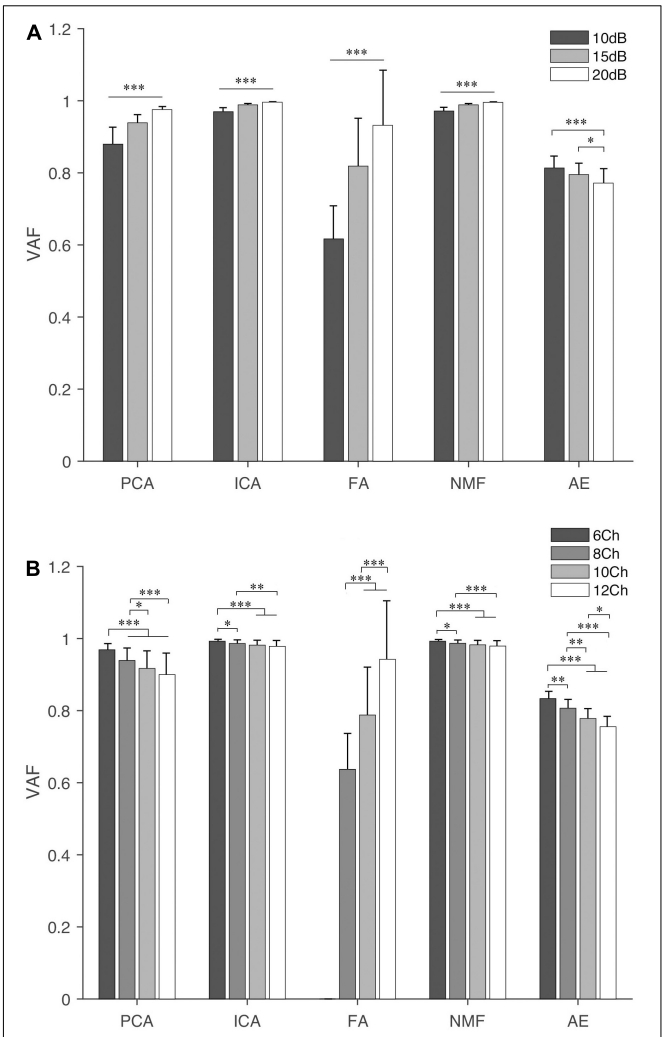

FIGURE 3 | The variance accounted for (VAF) of the five extraction methods under different settings: SNR **(A)** and NoC **(B)**. For FA, when four synergies are extracted, at least eight muscles should be included. Thus, three bars are shown for FA. "*", "**", and "***" indicate the significance levels are 0.05, 0.01, and 0.001, respectively.

Synergy Similarity Analysis

Similarity analysis among extraction methods is shown in **Figures 4–7**. First, SVS, ACS, and PA were significantly better ($p < 0.001$) than those obtained by random generation (**Figure 4**) except for the SVS calculated by PCA, which was significantly lower than the chance level (0.58 ± 0.016 vs. 0.63 ± 0.009).

The influence of different settings on the similarity and PA is shown in **Figures 5–7**. NMF and FA had higher SVS under both settings, followed by ICA and AE, while PCA had the lowest similarity value (**Figure 5**). Besides, SVS increased with the increase of SNR and NoC for each extraction method. The SNR had a significant influence ($p < 0.001$) on the SVS. The *post hoc* test showed that, when SNR was larger than 10 dB, there was no statistical difference in SVS for FA ($p = 0.209$) and AE ($p = 0.283$). In terms of the influence of NoC on SVS, a significant difference was observed among settings for FA. In contrast, there was no statistical difference among NoC settings for ICA ($p = 0.801$) and AE ($p = 0.454$). For PCA and NMF, when the NoC was higher than 6Ch, there was also no significant difference in SVS.

Similar results were observed in the ACS (**Figure 6**). NMF and FA had higher ACS under both settings, followed by ICA and AE, and PCA had the lowest similarity value. The SNR had a significant influence ($p < 0.001$) on the ACS. In contrast, the NoC had a different influence on ACS among extraction methods. ACS of FA was significantly influenced by the NoC ($p < 0.001$). For the other four extraction methods (i.e., PCA, ICA, NMF, and AE), in general, when the NoC was higher than 6Ch, there was

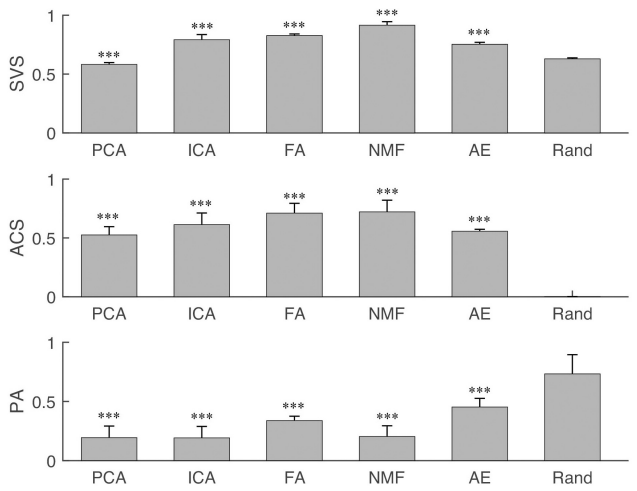

FIGURE 4 | The synergy similarity of the extraction methods and random data. Three panels from top to bottom are synergy vector similarity (SVS), activation coefficient similarity (ACS), and principal angle (PA). The last bar in each panel "Rand" is the similarity between randomly generated data and the simulated data. The star shows the significance level between methods and Rand. "***" indicate the significance levels are 0.05, 0.01, and 0.001, respectively.

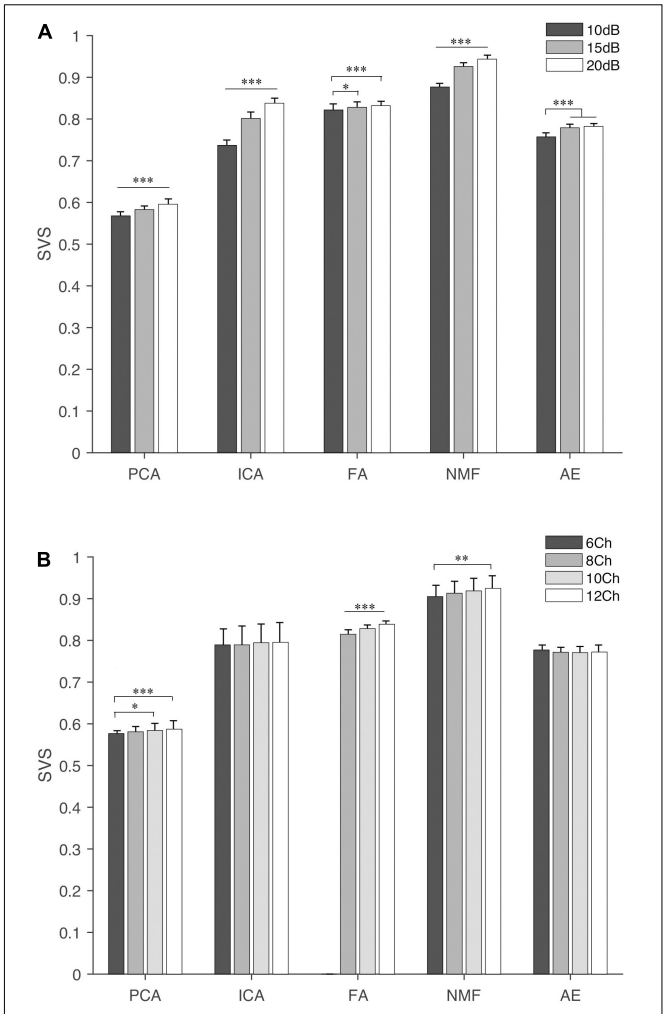

FIGURE 5 | The SVS of extraction methods under different settings, **(A)** SNR and **(B)** NoC. The fine line on the bar is the standard error between trials. "*", "**", and "***" indicate the significance levels are 0.05, 0.01, and 0.001, respectively.

no significant difference among different settings, while the ACS between 8Ch and 12Ch of NMF was $p = 0.04$.

For the PA (**Figure 7**), in general, FA and AE had a larger PA under both settings, followed by NMF, PCA, and ICA. SNR had a significant influence on five extraction methods ($p < 0.001$). NoC had no statistical influence on PA calculated by PCA ($p = 0.142$) and ICA ($p = 0.159$). The *post hoc* test showed that the PA of NMF was not affected by the NoC, while it affected the results of FA and AE.

Classification Accuracy

The results of the classification accuracy of different classification algorithms based on the extracted synergies from five extracting methods are shown in **Figure 8**. In general, synergies extracted by NMF and PCA had higher classification accuracy. This was followed by FA and AE, and ICA had the lowest classification accuracy. For each extraction algorithm, RF and KNN had higher classification accuracy than LDA and SVM. Statistical analysis showed that classification algorithms had a significant influence ($p < 0.001$) on the classification accuracy for each extraction method. The *post hoc* test showed that the classification accuracy obtained by KNN and RF was significantly higher than that by LDA and SVM. When the synergies extracted by ICA were as input, LDA and SVM showed a statistically different classification accuracy.

DISCUSSION

In this study, we evaluated the performance of five synergy extraction methods using a set of simulated and experimental data. With respect to previous studies, this study introduced several novel aspects, including the performance analysis of an AE with the other four well-established synergy extraction methods under different settings and the coupling with classification tasks to link our results to real applications.

Several studies have used simulated and real data to evaluate the performance of commonly used factorization methods in spatial synergy extraction (Tresch et al., 2006; Ebied et al., 2018). However, these commonly used methods not only had specific constraints on input signals but also considered the variable reconstruction rate of the EMG signals as the only performance index. Besides, these methods did not incorporate the knowledge of the mechanical actions of muscles (Tresch et al., 2006), such as the agonist/antagonist activities and task performance (Spüler et al., 2016).

Among these methods, NMF is usually the most popular method for synergy extraction used in the majority of the studies. NMF imposes a non-negative constraint on the inputs (processed

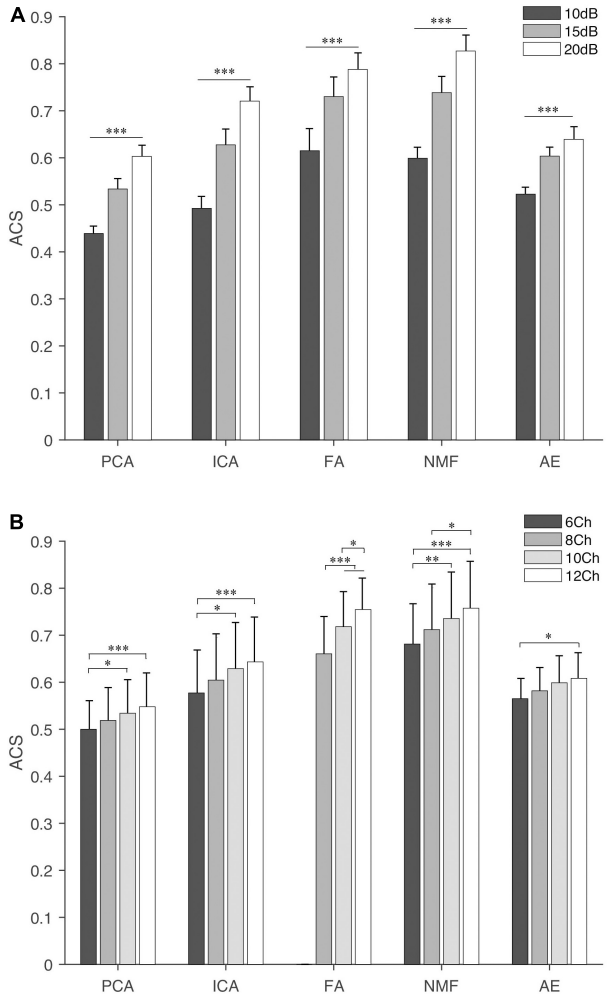

FIGURE 6 | Activation coefficient similarity of extraction methods under different settings, **(A)** SNR and **(B)** NoC. The fine line on the bar is the standard error between trials. "*", "**", and "***" indicate the significance levels are below 0.05, 0.01, and 0.001, respectively.

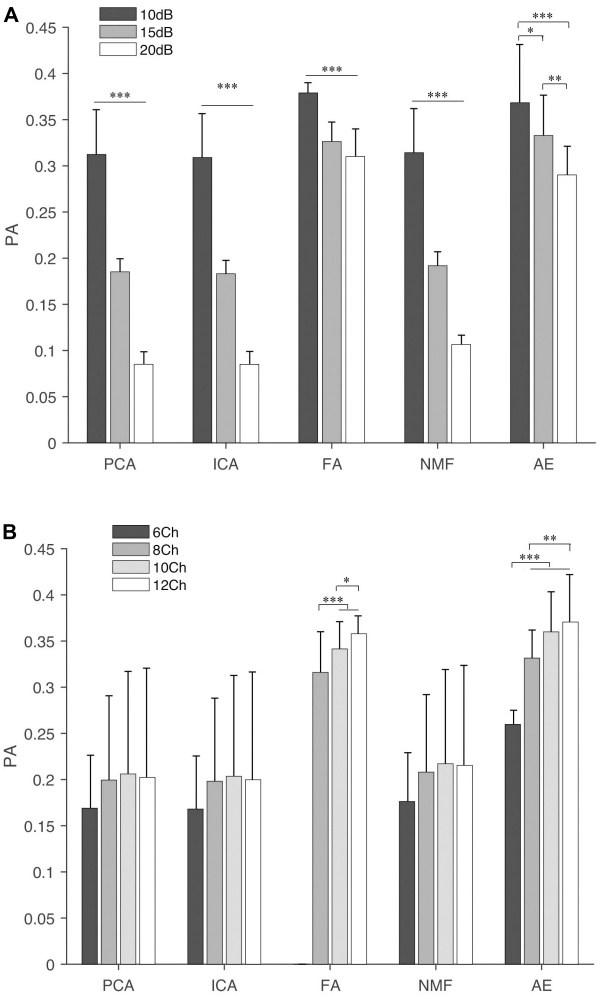

FIGURE 7 | Principal angles of extracting methods under different settings, **(A)** SNR and **(B)** NoC. The fine line on the bar is the standard error between trials. "*", "**", and "***" indicate the significance levels are 0.05, 0.01, and 0.001, respectively.

EMG signals) and outputs (synergies and activation coefficients). In a non-negative space, the basis vectors (extracted synergies) are not constrained to be orthogonal but are constrained to be independent (Lambert-Shirzad and Van der Loos, 2017). The non-negative property makes the extracted synergies particularly appropriate for clinical explanations because it reflects the non-negative nature of neural commands and muscle contraction.

Independent component analysis decomposes a multivariate signal into independent non-Gaussian signals by maximizing the statistical independence of the estimated components (Hyvärinen and Oja, 2000). ICA is designed to analyze non-Gaussian data and is substantially affected by the noise structure. Tresch et al. (2006) showed that ICA had a better performance when the signals were corrupted by constant variance Gaussian noise. However, the results of ICA depend heavily on the independency and data distribution of the latent variables (muscle synergies). Due to the difference of the simulated or experimental data in the current study from previous studies, this study showed a better performance using ICA. Besides, some studies (Tresch et al., 2006; Steele et al., 2015) compared the performance of several variants of the ICA such as pICA and PCAICA and reported that PCAICA was one of the most computationally efficient methods (Tresch et al., 2006). However, if the datasets with different muscle activations correlations were considered, similarity analysis dramatically changed (Steele et al., 2015). Thus, the results were limited to this study, and extensions to other implementations are required in future studies.

Both NMF and ICA extract independent components from the input data and have specific constraints on the inputs. Other methods employed in this study such as PCA and FA have instead different constraints on the inputs and outputs. PCA uses the muscle activation matrix covariance to identify components that best describe the variance of the input data while minimizing the covariance of the basis vectors and

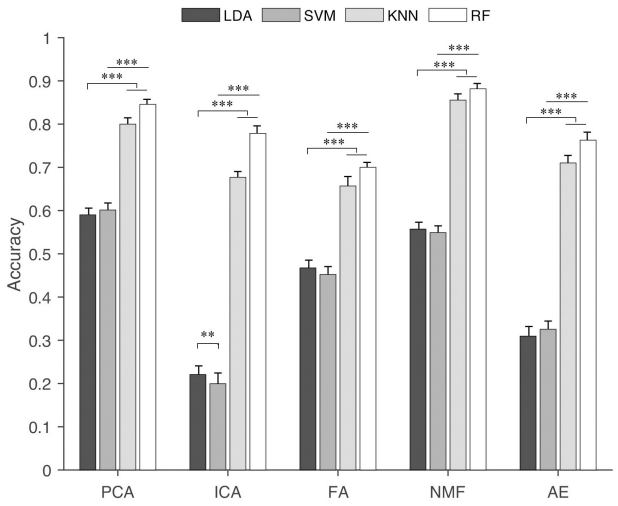

FIGURE 8 | Classification accuracy of different classification algorithms for each synergy extraction method. "**" and "***" indicate the significance levels are 0.01 and 0.001, respectively.

constrains the components to be orthogonal (Abdi and Williams, 2010). While PCA accepts negative inputs, it constrains the synergies to be orthogonal, and this is not supported at any level in previous findings in experimentations with physiological systems that were modeled with PCA. This makes PCA very versatile and adaptable to negative data (such as kinematics) but probably not the best algorithm to describe neural control at the muscle level (Weiss and Flanders, 2004) because the components yielded using PCA impose a constrain that is not found at the physiological organization level and may not represent underlying "constructs." In contrast, the underlying constructs can be labeled and readily interpreted using FA (Suhr, 2005). In a way similar to PCA, which tries to reproduce the total variable variance by a transformation of the input data, FA is also modeled as linear combinations of the factors and latent variables. However, FA is designed to identify a set of unobservable factors from the observed variables and attempts to reproduce the intercorrelations among variables, and the results were affected by the dependencies among activation coefficients (Tresch et al., 2006). In this study, the activation coefficients were from a set of experimental data that were randomly selected and grouped, which made the simulated muscle activations more independent and with few correlations among muscles. This might be one explanation that FA had a worse performance in reconstructing the variance of the muscle activations (VAF analysis) and quantifying spanned subspace (PA).

For the AEs, if only a single sigmoid hidden layer is used, the optimal solution is strongly related to PCA (Bourlard and Kamp, 1988; Chicco et al., 2014). The weights of AEs with a single hidden layer of size p (where p is less than the size of the input) span the same vector subspace as the one spanned by the first p principal components, and the output of the AE is an orthogonal projection onto this subspace. The potential of the AEs is their non-linearity, which allows the model to learn more powerful generalizations compared with PCA and FA and to reconstruct the input data with significantly lower information loss (Hinton and Salakhutdinov, 2006). From this perspective, the AEs are more appropriate for physiological signals analysis because they are usually non-linear and non-stationary.

In general, this study reported that NMF and ICA have better performance than the other methods. This finding is consistent with the abovementioned technical analysis of extraction methods. EMG signals are usually non-Gaussian data and exist with large non-linear and non-stationary components, which makes the NMF and ICA (non-Gaussian data input) outperform the PCA and FA (Gaussian data input) in muscle synergy extraction. Therefore, higher performance was observed when NMF and ICA were used to extract muscle synergies. Furthermore, our simulated data lack correlations among signals, thus FA lost priority in reproducing intercorrelations among variables. For the AEs, although some studies reported promising results in synergy extraction and force estimation using AEs (Spüler et al., 2016; Buongiorno et al., 2020), our results did not confirm this conclusion. One explanation is that AEs can achieve a trade-off between input space (muscle synergy extraction) and task space (force/moment reconstruction), while this study focused on synergy extraction not exploiting all the potential of this method. Moreover, several setups and design choices can be adopted for an AE, and the study did not test systematically all the possible configurations. Thus, even though AEs outperform FA and PCA in some settings, in our specific scenarios, NMF and ICA perform better.

Four synergies account for over 90% of the variability for NMF, ICA, and PCA in this study. Furthermore, 90% is often used as a "high" threshold to identify the optimal number of synergies in previous large studies, even though lower VAF values are used in some studies. Further analysis showed that VAF computed using FA was variable among different settings, and FA had the smallest VAF (78.91%) followed by AE (79.35%). This implies that, in our simulation, AE and FA could not capture the variance of muscle activation as well as the other methods when extracting the same number of synergies. On the contrary, NMF, ICA, and PCA had larger VAF among the five methods (98.53, 98.48, and 93.13%, respectively). The results were consistent with previous studies (Tresch et al., 2006; Ebied et al., 2018).

Similarity analysis first showed that all extraction methods had a better performance than random level except SVS of PCA. This exception can be explained as the structureless of the simulated data. In this study, randomly generated data were used to assess the performance of extraction methods, while muscles usually were activated in coordination manners. Some studies have used PCA to extract synergies from muscle activities and reported meaningful coordinated patterns among muscles.

Furthermore, the results showed that SNR and NoC had different influences on the performance of the extraction methods. In terms of SNR, all extraction methods performed better with the decrease of the noise (the increase of the SNR), i.e., SVS and ACS increased but PA decreased with the increase of the SNR, and differences were statistically significant. Similar results were reported in the previous work (Ebied et al., 2018; Kieliba et al., 2018). However, extraction methods had

different performances when varying the NoC. First, SVS and ACS increased with the increase of the NoC for each extraction method. Similar results were observed for PA, especially for FA and AE. However, a high PA means worse performance. This indicates that PA has opposite performance with another two similarity indices. Remarkably, there was no statistical difference in the PA under different NoC settings for PCA, ICA, and NMF. Thus, we concluded that the performance of these three extraction methods (PCA, ICA, and NMF) is consistent under varying NoC. Second, the results showed that, when NoC was larger than 6Ch, SVS, ACS, and PA were less affected by NoC for PCA, ICA, NMF, and AE. The results suggest that, in the future muscle synergy analysis, it is not that more muscles are better. A limited number of muscles (eight muscles in this study) are enough to depict the variability of synergy structure.

In general, the results revealed that the noise and NoC affected the outputs of muscle synergy analysis, especially for noise. This has been proven by previous studies (Steele et al., 2013; Banks et al., 2017; Kieliba et al., 2018). They showed that signal preprocessing methods, synergy extraction methods, and the number and choice of muscles all affected the output of muscle synergies. AEs though showed better performance than FA in VAF and PCA in SVS and ACS, while losing priority compared with NMF and ICA. For the classification tasks, the results showed that synergies extracted from NMF and PCA had a higher classification accuracy, which indicates that these two extraction methods are suitable for classification tasks. In contrast, classification algorithms were sensitive to extraction methods. KNN and RF outperformed LDA and SVM in the current study for each extraction method. It suggests selecting the most suitable combinations of extraction methods and classification algorithms under different scenarios in future studies.

We did not investigate the influence of cross talk among muscles in this study. Cross talk influences the EMG signals and alters the components of muscle synergies. In this study, a publicly available dataset was used, in which the EMG signals were measured with Delsys double-differential EMG electrodes, and particular care was taken when placing the electrodes on the muscles (Atzori et al., 2014), which both reduce the influence of cross talk (Hug, 2011). Otherwise, previous studies showed that the number of independent motor command signals is not affected by cross talk, and muscle synergy analysis can identify whether a muscle is activated independently from an adjacent muscle even in the presence of cross talk (Chvatal and Ting, 2013). Besides, other synergy-related studies seldom considered the influence of cross talk while achieving simultaneous and intuitive myoelectric prosthetic control (Jiang et al., 2009, 2012, 2014; Zhang et al., 2017) and higher classification accuracy (Ma et al., 2015; Afzal et al., 2017). Thus, the results are limitedly influenced by cross talk in this study, so further studies are needed in the future.

Some limitations are worth noting. The study fixed the number of synergies to four. It is appropriate to study the dimension reduction capability of the extraction methods, and previous research pointed out that the number and choice of muscles impact the muscle synergy analyses (Steele et al., 2013). However, we also wish to mention that selecting a different number of synergies may lead to other sources of bias. In fact, if the very same method would be used for all algorithms to select the number of synergies (linear fit with a selected RMSE or selected VAF threshold), one may compare more "dense synergies" (when fewer synergies are extracted) to "more sparse ones," leading to inconsistent matching because a different number of synergies were selected due to a very small amount of reconstruction of the overall variation. Finally, the transfer function and type of AEs may influence the performance of AEs in synergy extraction. In future studies, these problems will be further explored. We also plan to consider more settings to verify the feasibility and strength of these extracting methods in spatial synergy extraction.

CONCLUSION

This article compared the performance of five muscle synergy extraction methods by the simulation analysis and classification tasks of a publicly available dataset. The results showed that the performance of synergy extraction methods was affected by the noise and NoC, and classification algorithms were sensitive to the extraction methods. Even though AEs outperformed FA and PCA in some settings, in general, NMF and ICA had better performance in the current research.

DATA AVAILABILITY STATEMENT

The original contributions presented in the study are included in the article/supplementary material, further inquiries can be directed to the corresponding author.

AUTHOR CONTRIBUTIONS

KZ, HW, and AS: conceptualization and methodology. KZ: software, validation, formal analysis, visualization, and writing-original draft. KZ and AS: investigation. KZ, MA, and HM: resources and data curation. HW, ZZ, MA, HM, and ZX: writing-review and editing. ZZ, HW, and AS: supervision and project administration. KZ, ZZ, and HW: funding acquisition. All authors provided intellectual contributions.

FUNDING

This work was supported by the National Natural Science Foundation of China (Grant no. 51775108), Natural Science Foundation of Jiangsu Province (Grant no. BK20190368), Postgraduate Research and Practice Innovation Program of Jiangsu Province (Grant no. KYCX19_0061), Fundamental Research Funds for the Central Universities, and ZhiShan Scholar Program of Southeast University.

REFERENCES

Abdi, H., and Williams, L. J. (2010). Principal component analysis. *WIREs Comp. Stat.* 2, 433–459. doi: 10.1002/wics.101

Afzal, T., Iqbal, K., White, G., and Wright, A. B. (2017). A Method for Locomotion Mode Identification Using Muscle Synergies. *IEEE Trans. Neural Syst. Rehabil. Eng.* 25, 608–617. doi: 10.1109/TNSRE.2016.2585962

Atzori, M., Gijsberts, A., Castellini, C., Caputo, B., Hager, A.-G. M., Elsig, S., et al. (2014). Electromyography data for non-invasive naturally-controlled robotic hand prostheses. *Sci. Data* 1:140053. doi: 10.1038/sdata.2014.53

Atzori, M., Gijsberts, A., Heynen, S., Hager, A.-G. M., Deriaz, O., van der Smagt, P., et al. (2012). "Building the Ninapro database: A resource for the biorobotics community," in *2012 4th IEEE RAS & EMBS International Conference on Biomedical Robotics and Biomechatronics (BioRob)*, (Rome: IEEE), 1258–1265. doi: 10.1109/BioRob.2012.6290287

Atzori, M., Gijsberts, A., Kuzborskij, I., Elsig, S., Mittaz Hager, A.-G., Deriaz, O., et al. (2015). Characterization of a Benchmark Database for Myoelectric Movement Classification. *IEEE Trans. Neural Syst. Rehabil. Eng.* 23, 73–83. doi: 10.1109/TNSRE.2014.2328495

Banks, C. L., Pai, M. M., McGuirk, T. E., Fregly, B. J., and Patten, C. (2017). Methodological Choices in Muscle Synergy Analysis Impact Differentiation of Physiological Characteristics Following Stroke. *Front. Comput. Neurosci.* 11:78. doi: 10.3389/fncom.2017.00078

Bourlard, H., and Kamp, Y. (1988). Auto-association by multilayer perceptrons and singular value decomposition. *Biol. Cybern.* 59, 291–294. doi: 10.1007/BF00332918

Buongiorno, D., Camardella, C., Cascarano, G. D., Pelaez Murciego, L., Barsotti, M., De Feudis, I., et al. (2019a). "An undercomplete autoencoder to extract muscle synergies for motor intention detection," in *2019 International Joint Conference on Neural Networks (IJCNN)*, (Budapest: IEEE), ,1–8. doi: 10.1109/IJCNN.2019.8851975

Buongiorno, D., Cascarano, G. D., Brunetti, A., De Feudis, I., and Bevilacqua, V. (2019b). "A Survey on Deep Learning in Electromyographic Signal Analysis," in *Intelligent Computing Methodologies Lecture Notes in Computer Science*, eds D.-S. Huang, Z.-K. Huang, and A. Hussain (Cham: Springer International Publishing), 751–761. doi: 10.1007/978-3-030-26766-7_68

Buongiorno, D., Cascarano, G. D., Camardella, C., De Feudis, I., Frisoli, A., and Bevilacqua, V. (2020). Task-Oriented Muscle Synergy Extraction Using An Autoencoder-Based Neural Model. *Information* 11:219. doi: 10.3390/info11040219

Camardella, C., Barsotti, M., Murciego, L. P., Buongiorno, D., Bevilacqua, V., and Frisoli, A. (2019). "Evaluating Generalization Capability of Bio-inspired Models for a Myoelectric Control: A Pilot Study," in *Intelligent Computing Methodologies Lecture Notes in Computer Science*, eds D.-S. Huang, Z.-K. Huang, and A. Hussain (Cham: Springer International Publishing), 739–750. doi: 10.1007/978-3-030-26766-7_67

Cheung, V. C. K. (2005). Central and Sensory Contributions to the Activation and Organization of Muscle Synergies during Natural Motor Behaviors. *J. Neurosci.* 25, 6419–6434. doi: 10.1523/JNEUROSCI.4904-04.2005

Cheung, V. C. K., Cheung, B. M. F., Zhang, J. H., Chan, Z. Y. S., Ha, S. C. W., Chen, C.-Y., et al. (2020). Plasticity of muscle synergies through fractionation and merging during development and training of human runners. *Nat. Commun.* 11:4356. doi: 10.1038/s41467-020-18210-4

Chicco, D., Sadowski, P., and Baldi, P. (2014). "Deep autoencoder neural networks for gene ontology annotation predictions," in *Proceedings of the 5th ACM Conference on Bioinformatics, Computational Biology, and Health Informatics*, (New YorkNY: Association for Computing Machinery), 533–540. doi: 10.1145/2649387.2649442

Chvatal, S. A., and Ting, L. H. (2013). Common muscle synergies for balance and walking. *Front. Comput. Neurosci.* 7:48. doi: 10.3389/fncom.2013.00048

Clark, D. J., Ting, L. H., Zajac, F. E., Neptune, R. R., and Kautz, S. A. (2010). Merging of Healthy Motor Modules Predicts Reduced Locomotor Performance and Muscle Coordination Complexity Post-Stroke. *J. Neurophysiol.* 103, 844–857. doi: 10.1152/jn.00825.2009

D'Avella, A., Portone, A., Fernandez, L., and Lacquaniti, F. (2006). Control of Fast-Reaching Movements by Muscle Synergy Combinations. *J. Neurosci.* 26, 7791–7810. doi: 10.1523/JNEUROSCI.0830-06.2006

d'Avella, A., Saltiel, P., and Bizzi, E. (2003). Combinations of muscle synergies in the construction of a natural motor behavior. *Nat. Neurosci.* 6, 300–308. doi: 10.1038/nn1010

De Feudis, I., Buongiorno, D., Cascarano, G. D., Brunetti, A., Micele, D., and Bevilacqua, V. (2021). "A Nonlinear Autoencoder for Kinematic Synergy Extraction from Movement Data Acquired with HTC Vive Trackers," in *Progresses in Artificial Intelligence and Neural Systems Smart Innovation, Systems and Technologies*, eds A. Esposito, M. Faundez-Zanuy, F. C. Morabito, and E. Pasero (Singapore: Springer Singapore), 231–241. doi: 10.1007/978-981-15-5093-5_22

Delis, I., Hilt, P. M., Pozzo, T., Panzeri, S., and Berret, B. (2018). Deciphering the functional role of spatial and temporal muscle synergies in whole-body movements. *Sci. Rep.* 8:8391. doi: 10.1038/s41598-018-26780-z

Ebied, A., Kinney-Lang, E., Spyrou, L., and Escudero, J. (2018). Evaluation of matrix factorisation approaches for muscle synergy extraction. *Med. Eng. Phys.* 57, 51–60. doi: 10.1016/j.medengphy.2018.04.003

Hilt, P. M., Delis, I., Pozzo, T., and Berret, B. (2018). Space-by-Time Modular Decomposition Effectively Describes Whole-Body Muscle Activity During Upright Reaching in Various Directions. *Front. Comput. Neurosci.* 12:20. doi: 10.3389/fncom.2018.00020

Hinton, G. E., and Salakhutdinov, R. R. (2006). Reducing the Dimensionality of Data with Neural Networks. *Science* 313, 504–507. doi: 10.1126/science.1127647

Hug, F. (2011). Can muscle coordination be precisely studied by surface electromyography? *J. Electromyogr. Kinesiol.* 21, 1–12. doi: 10.1016/j.jelekin.2010.08.009

Hyvarinen, A. (1999). Fast and robust fixed-point algorithms for independent component analysis. *IEEE Trans. Neural Netw.* 10, 626–634. doi: 10.1109/72.761722

Hyvärinen, A., and Oja, E. (1997). A Fast Fixed-Point Algorithm for Independent Component Analysis. *Neural Computation* 9, 1483–1492. doi: 10.1162/neco.1997.9.7.1483

Hyvärinen, A., and Oja, E. (2000). Independent component analysis: algorithms and applications. *Neural Netw.* 13, 411–430. doi: 10.1016/S0893-6080(00)00026-5

Israely, S., Leisman, G., Machluf, C., Shnitzer, T., and Carmeli, E. (2017). Direction Modulation of Muscle Synergies in a Hand-Reaching Task. *IEEE Trans. Neural Syst. Rehabil. Eng.* 25, 2427–2440. doi: 10.1109/TNSRE.2017.2769659

Israely, S., Leisman, G., Machluf, C. C., and Carmeli, E. (2018). Muscle Synergies Control during Hand-Reaching Tasks in Multiple Directions Post-stroke. *Front. Comput. Neurosci.* 12:10. doi: 10.3389/fncom.2018.00010

Ivanenko, Y. P., Cappellini, G., and Dominici, N. (2005). Coordination of Locomotion with Voluntary Movements in Humans. *J. Neurosci.* 25, 7238–7253. doi: 10.1523/JNEUROSCI.1327-05.2005

Jiang, N., Englehart, K. B., and Parker, P. A. (2009). Extracting Simultaneous and Proportional Neural Control Information for Multiple-DOF Prostheses From the Surface Electromyographic Signal. *IEEE Trans. Biomed. Eng.* 56, 1070–1080. doi: 10.1109/TBME.2008.2007967

Jiang, N., Rehbaum, H., Vujaklija, I., Graimann, B., and Farina, D. (2014). Intuitive, Online, Simultaneous, and Proportional Myoelectric Control Over Two Degrees-of-Freedom in Upper Limb Amputees. *IEEE Trans. Neural Syst. Rehabil. Eng.* 22, 501–510. doi: 10.1109/TNSRE.2013.2278411

Jiang, N., Vest-Nielsen, J. L., Muceli, S., and Farina, D. (2012). EMG-based simultaneous and proportional estimation of wrist/hand kinematics in uni-lateral trans-radial amputees. *J. NeuroEngineering Rehabil.* 9:42. doi: 10.1186/1743-0003-9-42

Kieliba, P., Tropea, P., Pirondini, E., Coscia, M., Micera, S., and Artoni, F. (2018). How are Muscle Synergies Affected by Electromyography Pre-Processing? *IEEE Trans. Neural Syst. Rehabil. Eng.* 26, 882–893. doi: 10.1109/TNSRE.2018.2810859

Lambert-Shirzad, N., and Van der Loos, H. F. M. (2017). On identifying kinematic and muscle synergies: a comparison of matrix factorization methods using experimental data from the healthy population. *J. Neurophysiol.* 117, 290–302. doi: 10.1152/jn.00435.2016

Lee, D. D., and Seung, H. S. (2001). Algorithms for Non-negative Matrix Factorization. *Adv. Neural Inf. Process. Syst.* 13, 556–562.

Lv, B., Sheng, X., and Zhu, X. (2018). "Improving Myoelectric Pattern Recognition Robustness to Electrode Shift by Autoencoder," in *2018 40th Annual International Conference of the IEEE Engineering in Medicine and Biology*

Society (EMBC), (Honolulu, HI: IEEE), 5652–5655. doi: 10.1109/EMBC.2018.8513525

Ma, J., Thakor, N. V., and Matsuno, F. (2015). Hand and Wrist Movement Control of Myoelectric Prosthesis Based on Synergy. *IEEE Trans. Human-Mach. Syst.* 45, 74–83. doi: 10.1109/THMS.2014.2358634

Pale, U., Atzori, M., Müller, H., and Scano, A. (2020). Variability of Muscle Synergies in Hand Grasps: Analysis of Intra- and Inter-Session Data. *Sensors* 20:297. doi: 10.3390/s20154297

Rabbi, M. F., Pizzolato, C., Lloyd, D. G., Carty, C. P., Devaprakash, D., and Diamond, L. E. (2020). Non-negative matrix factorisation is the most appropriate method for extraction of muscle synergies in walking and running. *Sci. Rep.* 10:8266. doi: 10.1038/s41598-020-65257-w

Ranganathan, R., and Krishnan, C. (2012). Extracting synergies in gait: using EMG variability to evaluate control strategies. *J. Neurophysiol.* 108, 1537–1544. doi: 10.1152/jn.01112.2011

Rasool, G., Iqbal, K., Bouaynaya, N., and White, G. (2016). Real-Time Task Discrimination for Myoelectric Control Employing Task-Specific Muscle Synergies. *IEEE Trans. Neural Syst. Rehabil. Eng.* 24, 98–108. doi: 10.1109/TNSRE.2015.2410176

Scano, A., Dardari, L., Molteni, F., Giberti, H., Tosatti, L. M., and d'Avella, A. (2019). A Comprehensive Spatial Mapping of Muscle Synergies in Highly Variable Upper-Limb Movements of Healthy Subjects. *Front. Physiol.* 10:1231. doi: 10.3389/fphys.2019.01231

Scano, A., Mira, R. M., and d'Avella, A. (2022). Mixed matrix factorization: a novel algorithm for the extraction of kinematic-muscular synergies. *J. Neurophysiol.* 127, 529–547. doi: 10.1152/jn.00379.2021

Spüler, M., Irastorza-Landa, N., Sarasola-Sanz, A., and Ramos-Murguialday, A. (2016). "Extracting Muscle Synergy Patterns from EMG Data Using Autoencoders," in *Artificial Neural Networks and Machine Learning – ICANN 2016 Lecture Notes in Computer Science*, eds A. E. P. Villa, P. Masulli, and A. J. Pons Rivero (Cham: Springer International Publishing), 47–54. doi: 10.1007/978-3-319-44781-0_6

Steele, K. M., Tresch, M. C., and Perreault, E. J. (2013). The number and choice of muscles impact the results of muscle synergy analyses. *Front. Comput. Neurosci.* 7:105. doi: 10.3389/fncom.2013.00105

Steele, K. M., Tresch, M. C., and Perreault, E. J. (2015). Consequences of biomechanically constrained tasks in the design and interpretation of synergy analyses. *J. Neurophysiol.* 113, 2102–2113. doi: 10.1152/jn.00769.2013

Suhr, D. D. (2005). "Principal Component Analysis vs. Exploratory Factor Analysis," in *SUGI 30 Proceeding*(Cary, North Carolina: sas institute), 203–230.

Torres-Oviedo, G., Macpherson, J. M., and Ting, L. H. (2006). Muscle Synergy Organization Is Robust Across a Variety of Postural Perturbations. *J. Neurophysiol.* 96, 1530–1546. doi: 10.1152/jn.00810.2005

Tresch, M. C., Cheung, V. C. K., and d'Avella, A. (2006). Matrix Factorization Algorithms for the Identification of Muscle Synergies: Evaluation on Simulated and Experimental Data Sets. *J. Neurophysiol.* 95, 2199–2212. doi: 10.1152/jn.00222.2005

Vujaklija, I., Shalchyan, V., Kamavuako, E. N., Jiang, N., Marateb, H. R., and Farina, D. (2018). Online mapping of EMG signals into kinematics by autoencoding. *J. NeuroEngineering Rehabil.* 15:21. doi: 10.1186/s12984-018-0363-1

Weiss, E. J., and Flanders, M. (2004). Muscular and Postural Synergies of the Human Hand. *J. Neurophysiol.* 92, 523–535. doi: 10.1152/jn.01265.2003

Yu, Y., Chen, C., Sheng, X., and Zhu, X. (2019). "Continuous estimation of wrist torques with stack-autoencoder based deep neural network: A preliminary study," in *2019 9th International IEEE/EMBS Conference on Neural Engineering (NER)*, (San Francisco, CA: IEEE), 473–476. doi: 10.1109/NER.2019.8716941

Zhang, S., Zhang, X., Cao, S., Gao, X., Chen, X., and Zhou, P. (2017). Myoelectric Pattern Recognition Based on Muscle Synergies for Simultaneous Control of Dexterous Finger Movements. *IEEE Trans. Human Mach. Syst.* 47, 576–582. doi: 10.1109/THMS.2017.2700444

Zhao, K., Zhang, Z., Wen, H., Wang, Z., and Wu, J. (2019). Modular Organization of Muscle Synergies to Achieve Movement Behaviors. *J. Healthcare Engineering* 2019:8130297. doi: 10.1155/2019/8130297

Zia ur Rehman, M., Gilani, S., Waris, A., Niazi, I., Slabaugh, G., Farina, D., et al. (2018). Stacked Sparse Autoencoders for EMG-Based Classification of Hand Motions: A Comparative Multi Day Analyses between Surface and Intramuscular EMG. *Appl. Sci.* 8:1126. doi: 10.3390/app8071126

Conflict of Interest: The authors declare that the research was conducted in the absence of any commercial or financial relationships that could be construed as a potential conflict of interest.

Publisher's Note: All claims expressed in this article are solely those of the authors and do not necessarily represent those of their affiliated organizations, or those of the publisher, the editors and the reviewers. Any product that may be evaluated in this article, or claim that may be made by its manufacturer, is not guaranteed or endorsed by the publisher.

Advantages of publishing in Frontiers

OPEN ACCESS
Articles are free to read for greatest visibility and readership

FAST PUBLICATION
Around 90 days from submission to decision

HIGH QUALITY PEER-REVIEW
Rigorous, collaborative, and constructive peer-review

TRANSPARENT PEER-REVIEW
Editors and reviewers acknowledged by name on published articles

Frontiers
Avenue du Tribunal-Fédéral 34
1005 Lausanne | Switzerland

Visit us: www.frontiersin.org
Contact us: frontiersin.org/about/contact

REPRODUCIBILITY OF RESEARCH
Support open data and methods to enhance research reproducibility

DIGITAL PUBLISHING
Articles designed for optimal readership across devices

FOLLOW US
@frontiersin

IMPACT METRICS
Advanced article metrics track visibility across digital media

EXTENSIVE PROMOTION
Marketing and promotion of impactful research

LOOP RESEARCH NETWORK
Our network increases your article's readership